

Lecture Notes in Electrical Engineering 365

Felix Pasila

Yusak Tanoto

Resmana Lim

Murtiyanto Santoso

Nemuel Daniel Pah

*Editors*

# Proceedings of Second International Conference on Electrical Systems, Technology and Information 2015 (ICESTI 2015)

# Lecture Notes in Electrical Engineering

Volume 365

## Board of Series editors

Leopoldo Angrisani, Napoli, Italy  
Marco Arteaga, Coyoacán, México  
Samarjit Chakraborty, München, Germany  
Jiming Chen, Hangzhou, P.R. China  
Tan Kay Chen, Singapore, Singapore  
Rüdiger Dillmann, Karlsruhe, Germany  
Haibin Duan, Beijing, China  
Gianluigi Ferrari, Parma, Italy  
Manuel Ferre, Madrid, Spain  
Sandra Hirche, München, Germany  
Faryar Jabbari, Irvine, USA  
Janusz Kacprzyk, Warsaw, Poland  
Alaa Khamis, New Cairo City, Egypt  
Torsten Kroeger, Stanford, USA  
Tan Cher Ming, Singapore, Singapore  
Wolfgang Minker, Ulm, Germany  
Pradeep Misra, Dayton, USA  
Sebastian Möller, Berlin, Germany  
Subhas Mukhopadhyay, Palmerston, New Zealand  
Cun-Zheng Ning, Tempe, USA  
Toyoaki Nishida, Sakyo-ku, Japan  
Bijaya Ketan Panigrahi, New Delhi, India  
Federica Pascucci, Roma, Italy  
Tariq Samad, Minneapolis, USA  
Gan Woon Seng, Nanyang Avenue, Singapore  
Germano Veiga, Porto, Portugal  
Haitao Wu, Beijing, China  
Junjie James Zhang, Charlotte, USA

### *About this Series*

“Lecture Notes in Electrical Engineering (LNEE)” is a book series which reports the latest research and developments in Electrical Engineering, namely:

- Communication, Networks, and Information Theory
- Computer Engineering
- Signal, Image, Speech and Information Processing
- Circuits and Systems
- Bioengineering

LNEE publishes authored monographs and contributed volumes which present cutting edge research information as well as new perspectives on classical fields, while maintaining Springer’s high standards of academic excellence. Also considered for publication are lecture materials, proceedings, and other related materials of exceptionally high quality and interest. The subject matter should be original and timely, reporting the latest research and developments in all areas of electrical engineering.

The audience for the books in LNEE consists of advanced level students, researchers, and industry professionals working at the forefront of their fields. Much like Springer’s other Lecture Notes series, LNEE will be distributed through Springer’s print and electronic publishing channels.

More information about this series at <http://www.springer.com/series/7818>

Felix Pasila · Yusak Tanoto  
Resmana Lim · Murtiyanto Santoso  
Nemuel Daniel Pah  
Editors

Proceedings of Second  
International Conference  
on Electrical Systems,  
Technology and Information  
2015 (ICESTI 2015)

*Editors*

Felix Pasila  
Department of Electrical Engineering  
Petra Christian University  
Surabaya  
Indonesia

Murtiyanto Santoso  
Department of Electrical Engineering  
Petra Christian University  
Surabaya  
Indonesia

Yusak Tanoto  
Department of Electrical Engineering  
Petra Christian University  
Surabaya  
Indonesia

Nemuel Daniel Pah  
University of Surabaya  
Surabaya  
Indonesia

Resmana Lim  
Department of Electrical Engineering  
Petra Christian University  
Surabaya  
Indonesia

ISSN 1876-1100                      ISSN 1876-1119 (electronic)  
Lecture Notes in Electrical Engineering  
ISBN 978-981-287-986-8              ISBN 978-981-287-988-2 (eBook)  
DOI 10.1007/978-981-287-988-2

Library of Congress Control Number: 2015960766

© Springer Science+Business Media Singapore 2016

This work is subject to copyright. All rights are reserved by the Publisher, whether the whole or part of the material is concerned, specifically the rights of translation, reprinting, reuse of illustrations, recitation, broadcasting, reproduction on microfilms or in any other physical way, and transmission or information storage and retrieval, electronic adaptation, computer software, or by similar or dissimilar methodology now known or hereafter developed.

The use of general descriptive names, registered names, trademarks, service marks, etc. in this publication does not imply, even in the absence of a specific statement, that such names are exempt from the relevant protective laws and regulations and therefore free for general use.

The publisher, the authors and the editors are safe to assume that the advice and information in this book are believed to be true and accurate at the date of publication. Neither the publisher nor the authors or the editors give a warranty, express or implied, with respect to the material contained herein or for any errors or omissions that may have been made.

Printed on acid-free paper

This Springer imprint is published by SpringerNature  
The registered company is Springer Science+Business Media Singapore Pte Ltd.

# Contents

## Part I Invited Speaker

<b>1 Computational Intelligence Based Regulation of the DC Bus in the On-grid Photovoltaic System</b> . . . . .	3
Mauridhi Hery Purnomo, Iwan Setiawan and Ardyono Priyadi	
<b>2 Virtual Prototyping of a Compliant Spindle for Robotic Deburring</b> . . . . .	17
Giovanni Berselli, Marcello Pellicciari, Gabriele Bigi and Angelo O. Andrisano	
<b>3 A Concept of Multi Rough Sets Defined on Multi-contextual Information Systems</b> . . . . .	31
Rolly Intan	

## Part II Technology Innovation in Robotics Image Recognition and Computational Intelligence Applications

<b>4 Coordinates Modelling of the Discrete Hexapod Manipulator via Artificial Intelligence</b> . . . . .	47
Felix Pasila and Roche Alimin	
<b>5 An Object Recognition in Video Image Using Computer Vision</b> . . . . .	55
Sang-gu Kim, Seung-hoon Kang, Joung Gyu Lee and Hoon Jae Lee	
<b>6 Comparative Study on Mammogram Image Enhancement Methods According to the Determinant of Radiography Image Quality</b> . . . . .	65
Erna Alimudin, Hanung Adi Nugroho and Teguh Bharata Adji	

<b>7</b>	<b>Clustering and Principal Feature Selection Impact for Internet Traffic Classification Using K-NN.</b> . . . . .	75
	Trianggoro Wiradinata and P. Adi Suryaputra	
<b>8</b>	<b>Altitude Lock Capability Benchmarking: Type 2 Fuzzy, Type 1 Fuzzy, and Fuzzy-PID with Extreme Altitude Change as a Disturbance</b> . . . . .	83
	Hendi Wicaksono, Yohanes Gunawan, Cornelius Kristanto and Leonardie Haryanto	
<b>9</b>	<b>Indonesian Dynamic Sign Language Recognition at Complex Background with 2D Convolutional Neural Networks</b> . . . . .	91
	Nehemia Sugianto and Elizabeth Irenne Yuwono	
<b>10</b>	<b>Image-Based Distance Change Identification by Segment Correlation</b> . . . . .	99
	Nemuel Daniel Pah	
<b>11</b>	<b>Situation Awareness Assessment Mechanism for a Telepresence Robot</b> . . . . .	107
	Petrus Santoso and Handry Khoswanto	
<b>12</b>	<b>Relevant Features for Classification of Digital Mammogram Images.</b> . . . . .	115
	Erna Alimudin, Hanung Adi Nugroho and Teguh Bharata Adji	
<b>13</b>	<b>Multi-objective Using NSGA-2 for Enhancing the Consistency-Matrix.</b> . . . . .	123
	Abba Suganda Girsang, Sfenrianto and Jarot S. Suroso	
<b>14</b>	<b>Optimization of AI Tactic in Action-RPG Game</b> . . . . .	131
	Kristo Radion Purba	
<b>15</b>	<b>Direction and Semantic Features for Handwritten Balinese Character Recognition System</b> . . . . .	139
	Luh Putu Ayu Prapitasari and Komang Budiarta	
<b>16</b>	<b>Energy Decomposition Model Using Takagi-Sugeno Neuro Fuzzy</b> . . . . .	149
	Yusak Tanoto and Felix Pasila	
<b>17</b>	<b>Odometry Algorithm with Obstacle Avoidance on Mobile Robot Navigation.</b> . . . . .	155
	Handry Khoswanto, Petrus Santoso and Resmana Lim	

**Part III Technology Innovation in Electrical Engineering,  
Electric Vehicle and Energy Management**

**18 Vision-Based Human Position Estimation and Following Using an Unmanned Hexarotor Helicopter . . . . . 165**  
Jung Hyun Lee and Taeseok Jin

**19 The Role of Renewable Energy: Sumba Iconic Island, an Implementation of 100 Percent Renewable Energy by 2020 . . . . . 173**  
Abraham Lomi

**20 Electromechanical Characterization of Bucky Gel Actuator Based on Polymer Composite PCL-PU-CNT for Artificial Muscle . . . . . 185**  
Yudan Whulanza, Andika Praditya Hadiputra, Felix Pasila and Sugeng Supriadi

**21 A Single-Phase Twin-Buck Inverter . . . . . 193**  
Hanny H. Tumbelaka

**22 Performance Comparison of Intelligent Control of Maximum Power Point Tracking in Photovoltaic System. . . . . 203**  
Daniel Martomanggolo Wonohadidjojo

**23 Vehicle Security and Management System on GPS Assisted Vehicle Using Geofence and Google Map . . . . . 215**  
Lanny Agustine, Egber Pangaliela and Hartono Pranjoto

**24 Security and Stability Improvement of Power System Due to Interconnection of DG to the Grid . . . . . 227**  
Ni Putu Agustini, Lauhil Mahfudz Hayusman, Taufik Hidayat and I. Made Wartana

**25 Solar Simulator Using Halogen Lamp for PV Research . . . . . 239**  
Aryuanto Soetedjo, Yusuf Ismail Nakhoda, Abraham Lomi and Teguh Adi Suryanto

**26 Artificial Bee Colony Algorithm for Optimal Power Flow on Transient Stability of Java-Bali 500 KV . . . . . 247**  
Irrine Budi Sulistiawati and M. Ibrahim Ashari

**27 Sizing and Costs Implications of Long-Term Electricity Planning: A Case of Kupang City, Indonesia. . . . . 257**  
Daniel Rohi and Yusak Tanoto

**28 Dynamic Simulation of Wheel Drive and Suspension System in a Through-the-Road Parallel Hybrid Electric Vehicle . . . . . 263**  
Mohamad Yamin, Cokorda P. Mahandari and Rasyid H. Sudono



<b>29</b>	<b>A Reliable, Low-Cost, and Low-Power Base Platform for Energy Management System</b> . . . . .	271
	Henry Hermawan, Edward Oesnawi and Albert Darmaliputra	
<b>30</b>	<b>Android Application for Distribution Switchboard Design</b> . . . . .	279
	Julius Sentosa Setiadji, Kevin Budihargono and Petrus Santoso	
<b>Part IV Technology Innovation in Electronic, Manufacturing, Instrumentation and Material Engineering</b>		
<b>31</b>	<b>Adaptive Bilateral Filter for Infrared Small Target Enhancement</b> . . . . .	289
	Tae Wuk Bae and Hwi Gang Kim	
<b>32</b>	<b>Innovative Tester for Underwater Locator Beacon Used in Flight/Voyage Recorder (Black Box)</b> . . . . .	299
	Hartono Pranjoto and Sutoyo	
<b>33</b>	<b>2D CFD Model of Blunt NACA 0018 at High Reynolds Number for Improving Vertical Axis Turbine Performance</b> . . . . .	309
	Nu Rhahida Arini, Stephen R. Turnock and Mingyi Tan	
<b>34</b>	<b>Recycling of the Ash Waste by Electric Plasma Treatment to Produce Fibrous Materials</b> . . . . .	319
	S.L. Buyantuev, A.S. Kondratenko, E.T. Bazarsadaev and A.B. Khmelev	
<b>35</b>	<b>Performance Evaluation of Welded Knitted E-Fabrics for Electrical Resistance Heating</b> . . . . .	327
	Senem Kursun Bahadir, Ozgur Atalay, Fatma Kalaoglu, Savvas Vassiliadis and Stelios Potirakis	
<b>36</b>	<b>IP Based Module for Building Automation System</b> . . . . .	337
	J.D. Irawan, S. Prasetyo and S.A. Wibowo	
<b>37</b>	<b>Influence of CTAB and Sonication on Nickel Hydroxide Nanoparticles Synthesis by Electrolysis at High Voltage</b> . . . . .	345
	Yanatra Budipramana, Suprpto, Taslim Ersam and Fredy Kurniawan	
<b>38</b>	<b>Waste Industrial Processing of Boron-Treated by Plasma Arc to Produce the Melt and Fiber Materials</b> . . . . .	353
	S.L. Buyantuev, Ning Guiling, A.S. Kondratenko, Junwei Ye, E.T. Bazarsadaev, A.B. Khmelev and Shuhong Guo	
<b>39</b>	<b>Design of Arrhythmia Detection Device Based on Fingertip Pulse Sensor</b> . . . . .	363
	R. Wahyu Kusuma, R. Al Aziz Abbie and Purnawarman Musa	

**40 Analysis of Fundamental Frequency and Formant Frequency for Speaker ‘Makhraj’ Pronunciation with DTW Method . . . . . 373**  
 Muhammad Subali, Miftah Andriansyah and Christanto Sinambela

**41 Design and Fabrication of “Ha (ʌm)” Shape-Slot Microstrip Antenna for WLAN 2.4 GHz . . . . . 383**  
 Srisanto Sotyhadi, Sholeh Hadi Pramono and Moechammad Sarosa

**42 Investigation of the Electric Discharge Machining on the Stability of Coal-Water Slurries . . . . . 393**  
 S.L. Buyantuev, A.B. Khmelev, A.S. Kondratenko and F.P. Baldynova

**43 A River Water Level Monitoring System Using Android-Based Wireless Sensor Networks for a Flood Early Warning System . . . . 401**  
 Riny Sulistyowati, Hari Agus Sujono and Ahmad Khamdi Musthofa

**44 The Influence of Depth of Cut, Feed Rate and Step-Over on Surface Roughness of Polycarbonate Material in Subtractive Rapid Prototyping . . . . . 409**  
 The Jaya Suteja

**45 Adaptive Cars Headlamps System with Image Processing and Lighting Angle Control . . . . . 415**  
 William Tandy Prasetyo, Petrus Santoso and Resmana Lim

**46 Changes in the Rheological Properties and the Selection of a Mathematical Model of the Behavior of Coal-Water Slurry During Transport and Storage . . . . . 423**  
 S.L. Buyantuev, A.B. Khmelev and A.S. Kondratenko

**47 Design of a Fetal Heartbeat Detector . . . . . 429**  
 Nur Sultan Salahuddin, Sri Poernomo Sari, Paulus A. Jambormias and Johan Harlan

**Part V Technology Innovation in Internet of Things and Its Applications**

**48 Network Traffic and Security Event Collecting System . . . . . 439**  
 Hee-Seung Son, Jin-Heung Lee, Tae-Yong Kim and Sang-Gon Lee

**49 Paper Prototyping for BatiKids: A Technique to Examine Children’s Interaction and Feedback in Designing a Game-Based Learning . . . . . 447**  
 Hestiasari Rante, Heidi Schelhowe and Michael Lund

<b>50</b>	<b>Tracing Related Scientific Papers by a Given Seed Paper Using Parscit . . . . .</b>	<b>457</b>
	Resmana Lim, Indra Ruslan, Hansin Susatya, Adi Wibowo, Andreas Handojo and Raymond Sutjiadi	
<b>51</b>	<b>Factors Affecting Edmodo Adoption as Online Learning Medium. . . . .</b>	<b>465</b>
	Iwa Sungkono Herlambanggoro and Trianggoro Wiradinata	
<b>52</b>	<b>Principal Feature Selection Impact for Internet Traffic Classification Using Naïve Bayes. . . . .</b>	<b>475</b>
	Adi Suryaputra Paramita	
<b>53</b>	<b>Study on the Public Sector Information (PSI) Service Model for Science and Technology Domain in South Korea . . . . .</b>	<b>481</b>
	Yong Ho Lee	
<b>54</b>	<b>Digital Natives: Its Characteristics and Challenge to the Library Service Quality . . . . .</b>	<b>487</b>
	Siana Halim, Felecia, Ingrid, Dian Wulandari and Demmy Kasih	
<b>55</b>	<b>Web-Based Design of the Regional Health Service System in Bogor Regency. . . . .</b>	<b>495</b>
	B. Sundari, Revida Iriana and Bertilia Lina Kusrina	
<b>56</b>	<b>Security Handwritten Documents Using Inner Product . . . . .</b>	<b>501</b>
	Syaifudin and Dian Pratiwi	
<b>57</b>	<b>Augmented Reality Technique for Climate Change Mitigation . . . .</b>	<b>511</b>
	Ruswandi Tahrir	
<b>58</b>	<b>Cyber Security for Website of Technology Policy Laboratory . . . .</b>	<b>521</b>
	Jarot S. Suroso	
<b>59</b>	<b>TAM-MOA Hybrid Model to Analyze the Acceptance of Smartphone for Pediatricians in Teaching Hospital in Indonesia. . . . .</b>	<b>529</b>
	Oktri Mohammad Firdaus, Nanan Sekarwana, T.M.A. Ari Samadhi and Kah Hin Chai	
<b>60</b>	<b>Development of the Remote Instrumentation Systems Based on Embedded Web to Support Remote Laboratory . . . . .</b>	<b>537</b>
	F. Yudi Limpraptono and Irmalia Suryani Faradisa	
<b>61</b>	<b>Enhancing University Library Services with Mobile Library Information System . . . . .</b>	<b>545</b>
	Singgih Lukman Anggana and Stephanus Eko Wahyudi	

**62 Multi Level Filtering to Classify and Block Undesirable Explicit Material in Website . . . . . 553**  
 Mohammad Iqbal, Hifshan Riesvicky, Hasma Rasjid and Yulia Charli

**63 Query Rewriting and Corpus of Semantic Similarity as Encryption Method for Documents in Indonesian Language. . . . . 565**  
 Detty Purnamasari, Rini Arianty, Diana Tri Susetianingias and Reni Diah Kusumawati

**64 Securing Client-Server Application Design for Information System Inventory . . . . . 573**  
 Ibnu Gunawan, Djoni Haryadi Setiabudi, Agustinus Noertjahyana and Yongky Hermawan

**Part VI Technology Innovation in Information, Modelling and Mobile Applications**

**65 Analyzing Humanitarian Logistic Coordination for Disaster Relief in Indonesia. . . . . 583**  
 Tanti Octavia, I. Gede Agus Widyadana and Herry Christian Palit

**66 Surakarta Cultural Heritage Management Based on Geographic Information Systems . . . . . 589**  
 Ery Dewayani and M. Viny Christanti

**67 Gray Code of Generating Tree of *n* Permutation with *m* Cycles . . . . . 599**  
 Sulistyo Puspitodjati, Henny Widowati and Crispina Pardede

**68 Android and iOS Hybrid Applications for Surabaya Public Transport Information. . . . . 607**  
 Djoni Haryadi Setiabudi and Lady Joanne Tjahyana

**69 Games and Multimedia Implementation on Heroic Battle of Surabaya: An Android Based Mobile Device Application. . . . . 619**  
 Andreas Handojo, Resmana Lim, Justinus Andjarwirawan and Sandy Sunaryo

**70 Streamlining Business Process: A Case Study of Optimizing a Business Process to Issue a Letter of Assignment for a Lecturer in the University of Surabaya. . . . . 631**  
 S.T. Jimmy

**71 Design of Adventure Indonesian Folklore Game . . . . . 639**  
 Kartika Gunadi, Liliana and Harvey Tjahjono

**72 Measuring the Usage Level of the IE Tools in SMEs  
Using Malcolm Baldrige Scoring System . . . . . 649**  
I. Nyoman Sutapa, Togas W.S. Panjaitan and Jani Rahardjo

**73 Enumeration and Generation Aspects of Tribonacci Strings . . . . . 659**  
Maukar, Asep Juarna and Djati Kerami

**74 A Leukocyte Detection System Using Scale Invariant  
Feature Transform Method . . . . . 669**  
Lina and Budi Dharmawan

**75 The Diameter of Enhanced Extended Fibonacci Cube  
Interconnection Networks . . . . . 675**  
Ernastuti, Mufid Nilmada and Ravi Salim

**76 Prototype Design of a Realtime Monitoring System of a Fuel  
Tank at a Gas Station Using an Android-Based Mobile  
Application . . . . . 685**  
Riny Sulityowati and Bayu Bhahtra Kurnia Rafik

# Introduction

This book includes the original, peer-reviewed research papers from the 2nd International Conference on Electrical Systems, Technology and Information (ICESTI 2015), held during 9–12 September 2015, at Patra Jasa Resort & Villas Bali, Indonesia.

The primary objective of this book is to provide references for dissemination and discussion of the topics that have been presented in the conference. This volume is unique in that it includes work related to Electrical Engineering, Technology and Information towards their sustainable development. Engineers, researchers as well as lecturers from universities and professionals in industry and government will gain valuable insights into interdisciplinary solutions in the field of Electrical Systems, Technology and Information, and its applications.

The topics of ICESTI 2015 provide a forum for accessing the most up-to-date and authoritative knowledge and the best practices in the field of Electrical Engineering, Technology and Information towards their sustainable development. The editors selected high quality papers from the conference that passed through a minimum of three reviewers, with an acceptance rate of 50.6 %.

In the conference there were three invited papers from keynote speakers, whose papers are also included in this book, entitled: “Computational Intelligence based Regulation of the DC bus in the On-Grid Photovoltaic System”, “Virtual Prototyping of a Compliant Spindle for Robotic Deburring” and “A Concept of Multi Rough Sets Defined on Multi-Contextual Information Systems”.

The conference also classified the technology innovation topics into five parts: “Technology Innovation in Robotics, Image Recognition and Computational Intelligence Applications”, “Technology Innovation in Electrical Engineering, Electric Vehicle and Energy Management”, “Technology Innovation in Electronic, Manufacturing, Instrumentation and Material Engineering”, “Technology Innovation in Internet of Things and Its Applications” and “Technology Innovation in Information, Modeling and Mobile Applications”.

In addition, we are really thankful for the contributions and for the valuable time spent in the review process by our Advisory Boards, Committee Members and Reviewers. Also, we appreciate our collaboration partners (Petra Christian

University, Surabaya; Gunadarma University, Jakarta; UBAYA, Surabaya, University of Ciputra, Surabaya, Institute of National Technology, Malang and LNEE Springer, Germany), our supporting institution (Oulu University, Finland, Widya Mandala Catholic University, Surabaya and Dongseo University, Korea) and our sponsors (Continuing Education Centre, Petra Christian University, Surabaya and Patrajasa Resort Hotel, Bali).

On behalf of the editors

Felix Pasila

**Part I**  
**Invited Speaker**



# Chapter 1

## Computational Intelligence Based Regulation of the DC Bus in the On-grid Photovoltaic System

Mauridhi Hery Purnomo, Iwan Setiawan and Ardyono Priyadi

**Abstract** This paper presents a bidirectional DC/AC converter control system based on the vector control method for regulating the DC bus in On-grid photovoltaic systems. In this control scheme, the main task of the DC/AC converter is to control the power flow between the DC bus and the electrical grid. To avoid conventional controller parameter tuning problems and in addition to enhance transient performances of the DC bus voltage response that caused by abrupt changes of local DC loads that directly connected to DC bus system, in this work, the DC/AC converter control system is designed by utilizing radial basis function neural networks, that is a kind of the computational intelligence method. By combining with simple proportional control, the overshoot and undershoot of the DC bus voltage that caused by sudden connections and disconnections of the local DC loads can be damped more quickly and better than the standard optimal PI control system, so the overvoltage condition of the DC bus capacitor could be avoided. The effectiveness of the proposed control system is proved by simulation results.

**Keywords** Bidirectional DC/AC converter · Computational intelligence · Radial basis function neural networks · Vector control

### 1.1 Introduction

In the last decades, the development of distributed power generation systems based on renewable distributed generators like Photovoltaic, wind turbine, and fuel cell have grown rapidly [1–4]. To efficiently supply electrical power to local DC loads,

---

M.H. Purnomo (✉) · I. Setiawan · A. Priyadi  
Institut Teknologi Sepuluh Nopember, Surabaya, Indonesia  
e-mail: hery@ee.its.ac.id

I. Setiawan  
Universitas Diponegoro, Semarang, Indonesia

the combination of the On grid DG system with DC microgrid recently also has attract a lot of attention [5].

In the control system point of view, there are at least two independent controlled converters in On-grid renewable power systems that connected via DC link: (1) an AC/DC or a DC/DC renewable power source side converter and (2) a bidirectional DC/AC grid side converter. The major task of the renewable power source side converter generally is to extract maximum power from green power source, i.e. by using Maximum Power Point Tracking (MPPT) algorithm, whereas the DC/AC grid side converter is to regulate DC bus voltage in a certain reference such that the flow of the electrical power between the DC link and the grid could be guaranteed.

In the On-grid green power systems combined with local DC loads, the dynamic of the DC bus capacitor voltage basically is not only influenced by power dynamic generated using the green power sources but also the change of the load that directly connected to DC bus. If the DC/AC grid side converter is not controlled properly, the sudden connection and disconnection of the local DC loads could make overvoltage in the DC link capacitor.

Based on the type of the controller, up until now, Proportional Integral (PI) based controller is one of the most popular techniques generally utilized for DC/AC converter to regulate DC bus capacitor. However to get the optimal parameter of the control system, the parameter of the plant model practically should be known accurately. Several papers proposed intelligence techniques such as Fuzzy logic control and Sliding Mode Controller [6–8] to avoid conventional controller parameter tuning problems and to enhance the control performances.

The main focus of this work is to design a controller of bidirectional DC/AC converters for regulating DC bus voltage in On-grid photovoltaic system combined with DC micro grid by using Radial Basis Function Neural Networks (RBFNN). RBFNN is one of the intelligence computation technique that has been widely adopted and implemented for off-line and on-line modelling and control application [9, 10]. The utilizing of the RBFNN as a control component in this case is to dampen overshoot and undershoot of the DC bus voltage that caused by sudden connections and disconnections of the local DC loads so the overvoltage condition of the DC bus capacitor could be avoided. Some simulations using Matlab Simulink software have been drawn to show the effectiveness of the proposed controller. Based on the simulation results, the performance of the RBFNN is better than the optimum PI controller.

The remainder of this paper is organized as follows. Section 1.2 describes the system model of the On-grid photovoltaic system combined with DC micro grid and the short theories of the RBFNN. The proposed control design is discussed in Sect. 1.3. Section 1.4 discusses some RBFNN simulation results, and finally, the conclusions are drawn in Sect. 1.5.

## 1.2 System Model

Figure 1.1 shows the topology of the On-Grid photovoltaic power system combined with DC microgrid under study. As shown in Fig. 1.1, there are two converters and its associated controller that operated independently.

The DC/DC buck-boost converter connected to the PV module is used to pump maximum electric power generated from the PV panel to the intermediate storage of the DC bus capacitor. Whereas the DC/AC converter injects surplus energy from the DC bus capacitor to the electrical grid. In this case, the PV power production is lower than the DC load consumption. The converter is able to transfer energy from the electrical grid to supply power shortages to the local DC load.

### 1.2.1 Photovoltaic Module and Its Converter

The main tasks of the DC/DC buck-boost converter as shown at Fig. 1.2 are to extract maximum electrical power from the PV module by means of the MPPT algorithm and at the same time the converter amplify the output voltage of the PV module to the DC bus voltage level. The PV module itself basically can be modeled as a circuit that contains current source parallel with diode. The typical characteristic of the V-I and V-P relations of the PV module is shown in Fig. 1.3. For the detail model of the PV module, the readers could refer to [11].

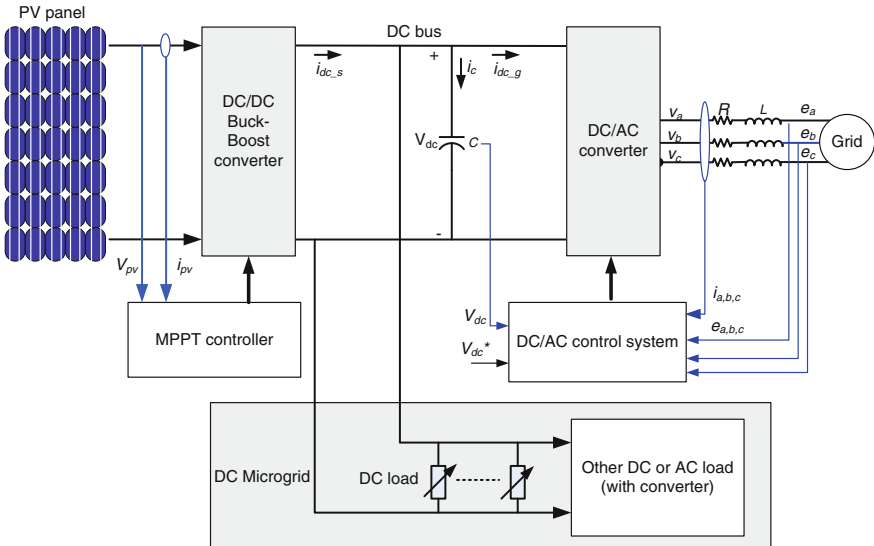
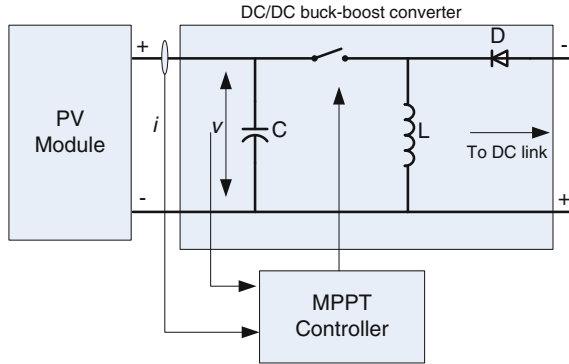
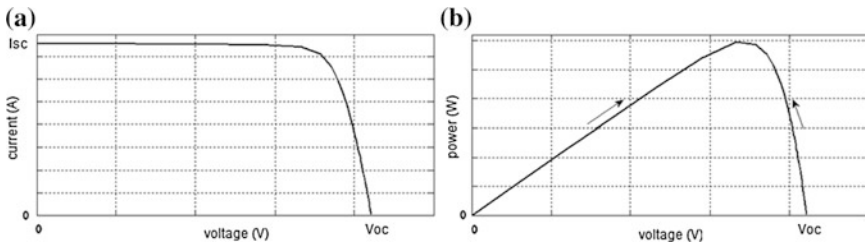


Fig. 1.1 Topology of the On Grid PV system combined with DC loads



**Fig. 1.2** DC-DC buck-boost converter circuit model



**Fig. 1.3** The typical characteristic of V-I and V-P of a PV module

Although there several sophisticated MPPT algorithms proposed in the literature [12], in this works, the Perturb and observe (P&O) algorithm is used to extract maximum power from PV module. P&O basically, due to the dynamic of the solar irradiation, is far slower compared to the dynamic of the DC load connected to DC bus.

**1.2.2 The Bidirectional DC/AC Converter Control Model**

The main task of the DC/AC converter control system (Fig. 1.4) is to control the flow of the active power between DC bus and the electrical grid bidirectionally. This bidirectional control of the electrical power is accomplished indirectly by regulating the DC link voltage at a certain level.

In this proposed scheme there are two main factors that determine the direction of the power flow in the DC/AC converter: (1) The power generated from the PV module and (2) The total DC loads connected to DC bus. If the total DC loads

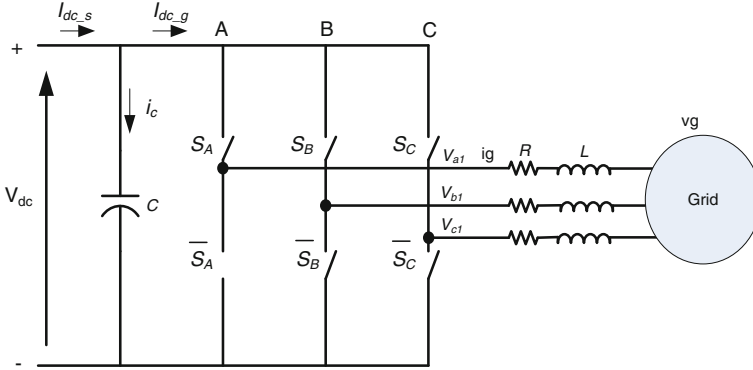


**Fig. 1.4** The DC/AC Converter Model

power is less than the power of the PV module, the DC/AC converter will inject the surplus energy to the electrical grid (inverter mode), and conversely if consumption of the DC load power is higher than the power production of the PV module, the DC/AC converter will transfer some power from the electrical grid (rectifier mode). So in this case, the balance of the power will be maintained.

For the converter circuit model in Fig. 1.4, the mathematical relations in the standard rotated  $dq$  model is represented in (1.1) and (1.2) [13].

$$v_{df} = Ri_{df} + L \frac{di_{df}}{dt} + v_{dg} - \omega_s Li_{qf} \tag{1.1}$$

$$v_{qf} = Ri_{qf} + L \frac{di_{qf}}{dt} + v_{qg} + \omega_s Li_{df} \tag{1.2}$$

where  $R$  and  $L$  are a resistance and an inductance of the filter, whereas  $i_{df}$ ,  $i_{qf}$ ,  $v_{df}$ ,  $v_{qf}$ ,  $v_{dg}$ ,  $v_{qg}$  respectively are currents and voltages of the inverter and the grid in  $dq$ -axes model, and  $\omega_s$  is a grid frequency. For ease of the design of feedback controllers, the two relations could be represented in the standard differential equation below [14]:

$$\frac{di_{df}}{dt} = -\frac{R}{L}i_{df} + \frac{1}{L}v_{df} + \frac{1}{L}d_{df} \tag{1.3}$$

$$\frac{di_{qf}}{dt} = -\frac{R}{L}i_{qf} + \frac{1}{L}v_{qf} + \frac{1}{L}d_{qf} \tag{1.4}$$

where:

$$d_{df} = (-v_{dg} + \omega_s L i_{qf}) \quad (1.5)$$

$$d_{qf} = (-\omega_s L i_{df}) \quad (1.6)$$

In this case,  $d_{df}$  and  $d_{qf}$  could be regard as measurable disturbances that can be easily compensated by its negation. If the rotated  $dq$ -axes perfectly aligned with the rotated grid voltage vector, the grid active and reactive power respectively could be represented in (1.7) and (1.8).

$$P_g = \frac{3}{2} (v_{dg} i_{df}) \quad (1.7)$$

$$Q_g = \frac{3}{2} (-v_{dg} i_{qf}) \quad (1.8)$$

From (1.7) to (1.8), it is clear that the active and the reactive grid power respectively could be controlled by the regulation of the  $d$ -axis and the  $q$ -axis current component independently. In the DC/AC control system, the reference of the  $d$ -axis current component is derived from the output of the DC bus voltage loop control.

By using SPWM with 3th harmonic injection, The dynamic capacitor voltage itself is represented by (1.9) [14].

$$\frac{V_{dc}}{dt} = -\frac{3}{2} \frac{m_a}{\sqrt{3}C} i_{df} + \frac{1}{C} i_{dc-} \quad (1.9)$$

### 1.2.3 The RBFNN Model

The RBFNN basically can be categorized as associative memory network that is fit used for on-line adaptive controller. This attribute basically come from the RBFNN properties: local generalization, simple learning rule and just have three-layer networks architecture [15]. Mathematically, The output of the RBFNN could be formulated as:

$$y = \sum_{i=1}^p G_i(\|c_i - X\|) w_i \quad (1.10)$$

where  $X$ ,  $G_i(\cdot)$ ,  $w_i$  and  $c_i$  are input vector, Gaussian function weight and centers respectively. The RBFNN Weight updating can be computed easily by using least mean square algorithm that is showed in (1.11).

$$w(k+1) = w(k) + \alpha e(k) G(k) \quad (1.11)$$

### 1.3 Control Design

By using vector control technique, there are two loop controls that should be to designed: (1) The inner current loop control that related with the grid active and reactive power injection/absorption, and (2) the outer DC bus voltage loop control that related with regulation of the capacitor voltage.

Due to the capacitor voltage level is directly determined by active power that flow via DC bus, then the control output of the DC bus control in this case is used as reference of the  $d$ -axis current component. Figure 1.5 shows the complete block diagram of the proposed DC/AC converter control system.

#### 1.3.1 Current Loop Control Design

As shown by (1.3) and (1.4), the dynamic of the  $dq$ -axis current component of the converter circuit basically is coupled first order system. To control of those current, in this work, we just utilize PI control plus Feedforward control:

$$u_{d(q)} = u_{PI} - d_{d(q)}f \tag{1.12}$$

where  $u_{dq}$  and  $u_{PI}$  respectively are total control output and PI control output, whereas  $d_{dff}$  is current coupling terms as represented by (1.5) and (1.6). By using

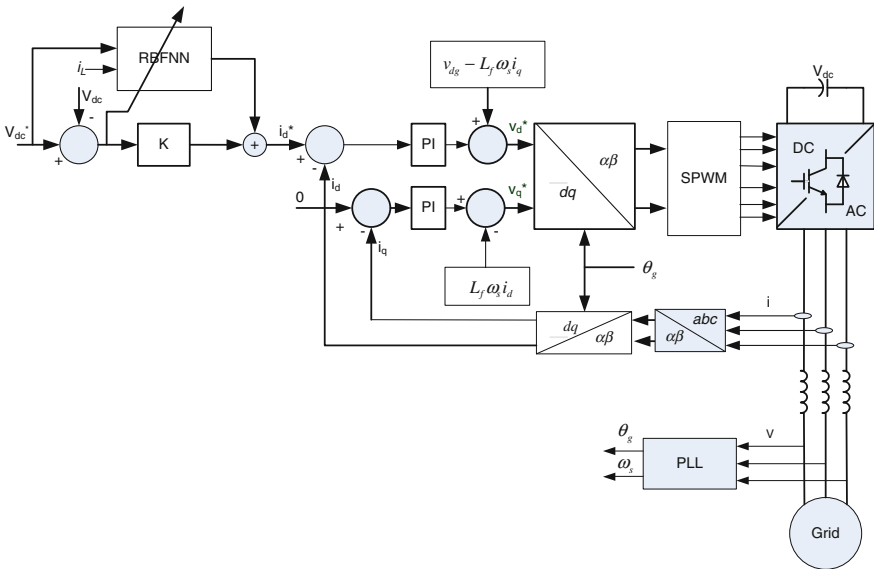


Fig. 1.5 Diagram block of the DC/AC Converter control system

the control strategy (1.12), the dynamic of the  $dq$ -axis current model dynamic could be simply represented by transfer function form:

$$H_{d(q)}(s) = \frac{I_{d(q)}(s)}{V_{d(q)f}(s)} = \frac{(1/R)}{(L/R)s + 1} \quad (1.13)$$

Utilizing pole placement technique, the PI control parameters can be obtained easily by using (1.14):

$$\begin{aligned} K_i &= R/T_{cl} \\ K_p &= \frac{L}{T_{cl}} \end{aligned} \quad (1.14)$$

where  $K_i$ ,  $K_p$  and  $T_{cl}$  are the integrator gain, the proportional gain and the desired closed loop time constant, respectively. Equation (1.15) shows the final transfer function of the  $dq$ -axis current component closed loop system by using pole placement technique.

$$H_{d(q)cl}(s) = \frac{I_{d(q)}(s)}{I_{d(q)ref}(s)} = \frac{1}{T_{cl} + 1} \quad (1.15)$$

### 1.3.2 DC Bus Voltage Control Design

By substituting  $I_d(s)$  from (1.15) to the transfer function  $V_{dc}(s)/I_d(s)$  from (1.9), we can obtain dynamic the DC bus capacitor voltage to the change of the  $d$ -axis current component reference (1.16).

$$V_{dc}(s) = -\frac{3m_a}{s2\sqrt{3}C} \frac{1}{(T_{cl} + 1)} I_{d\_ref}(s) + \frac{1}{Cs} i_{dc\_s} \quad (1.16)$$

by referring to the DC/AC control topology in the Fig. 1.5 the  $d$ -axis current component reference  $I_{d\_ref}(s)$  basically is the simple proportional gain output plus the RBFNN output:

$$I_{d\_ref} = K_P(V_{dc} - V_{dc\_ref}) + U_{RBFNN} \quad (1.17)$$

Substituting (1.17) to (1.16), we will derive (1.18)

$$V_{dc}(s) = \frac{HK_p}{(s + HK_p)} V_{dc\_ref}(s) + \frac{U_{RBFNN}}{(HK_p/s + 1)} + \frac{1}{(HK_p/s + 1)Cs} i_{dc\_s} \quad (1.18)$$



If the weight updating of the RBFNN in Eq. (1.11) is stable such that:

$$U_{RBFNN} = -\frac{1}{C_S} i_{dc\_s}(s) \quad (1.19)$$

Then (1.18) could be simplified as:

$$V_{dc}(s) = \frac{HK_p}{(s + HK_p)} V_{dc\_ref}(s) \quad (1.20)$$

by using the final limit teorema of the Laplace transform, it is clear that from (1.20), the output of DC bus capacitor voltage in the steady state will always equal to its reference.

## 1.4 Simulation Result and Discussion

In this Section, some simulations based on the Matlab Simulink software packet have been done to show the performance of the proposed control system and comparing the results with the PI base control system. For the simulation purpose, the parameter of the plant and the RBFNN model is chosen as shown in Table 1.1. Whereas Table 1.2 shows the PI control parameter for both the inner current loop and the DC bus voltage loop control. The PI parameter for the inner loop is obtained by using the pole placement technique, where the desired closed loop time constant is 0.001 s. The outer loop PI controller parameters is derived using the symmetrical optimum method. As shown in Tables 1.1 and 1.2, for fair comparison, the simple gain proportional at the RBFNN controller is the same with the proportional gain of the optimal PI controller.

In this simulation, the power of the PV module is extracted using the simple P&O MPPT algorithm where the output of this algorithm is used directly to drive a semiconductor switch of the DC/DC buck-boost converter. Figure 1.6a shows the output power of the PV module in 1 s time duration for solar irradiance 1000 W/m<sup>2</sup> that is delivered to DC bus system that have reference 350 V.

**Table 1.1** Plant and RBFNN control parameter

Plant parameter	Value	Plant parameter	Value
Pv nominal power (W)	2000	L DC/AC filter (H)	0.01
DC bus voltage ref. (V)	350	C- DC link (uF)	1200
Grid voltage (rms) (V)	110	SPWM frequency (KHz)	10
Grid frequency (Hz)	50	RBFNN MF number	6
Time sampling (s)	0.0001	Alpha	0.0000025
R DC/AC filter (ohm)	0.02	Simple gain	0.560

**Table 1.2** The optimal PI parameters

Inner Loop Control parameter	Value	Outer Loop Control parameter (for comparison)	Value
Kp	10.0	Kp	0.560
Ki	20.0	Ki	62.22

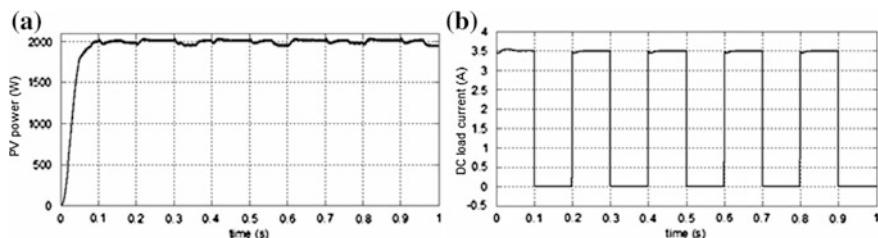


**Fig. 1.6** The PV Power output delivered to DC bus (a) the change of DC load current caused by connection and disconnection DC load (b)

To test the transient performance of the DC/AC converter control system in the capability of the voltage regulation and the grid power injection in response to the abrupt changes of the DC load, in this work, we do by connecting/disconnecting 100 ohm resistor in the DC microgrid bus suddenly every 0.1 s. Figure 1.6b shows the current flowing into the microgrid caused by such action.

In view of the control system, this DC load changes can basically be considered as disturbance that cause the output control system deviates from the reference. Figure 1.7 shows the changes of some important variables in the on grid PV system in response to the DC load changes: (a) the DC bus voltage, (b) the grid active power, (c) the grid reactive power, and (d) the grid current.

For comparison purposes, the response of the RBFNN control system and the standard PI control system is plotted in the same axis as shown in Fig. 1.7. From Fig. 1.7a, we can see that in response to the changes of DC load current, the voltage of the DC bus in a while will deviate from its reference. However it is clear from Fig. 1.7a that at any time the DC load is changed, the output response of the RBFNN control system in the transient state is more damped compared to the response of the PI control system. The superiority of the RBFNN control system over the PI control can also be seen from performance indexes ITAE showed in Fig. 1.7a.

With the constant solar irradiance and the changing load, the profile of the surplus electrical power that is injected to the grid is shown in Fig. 1.7b. From Fig. 1.7b, it could be seen that the power injection resulted from the RBFNN control system has settling time faster compared to the response of the PI control system. We can also see the bidirectional nature of the DC/AC converter system at

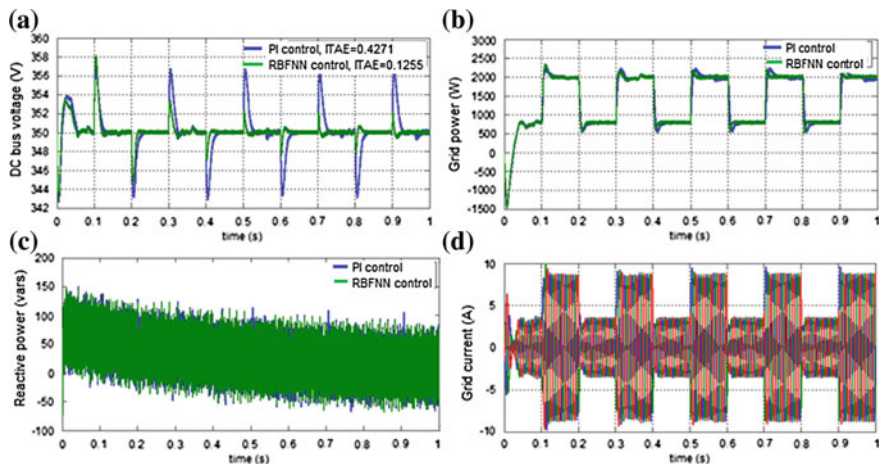


**Fig. 1.7** The System response: The DC bus voltage (a) Active power injected to Grid (b) Reactive power (c) AC current (d)

that figure. The negative value of the grid power in the first 0.4 s of the simulation showed that the converters is in the rectifier mode, this is due to the PV power is still in transient state and the power that generated by the PV module is not sufficient to supply the DC load.

Due to the reactive power is directly controlled by q-axis current component, then the response of the RBFNN control system and the PI control system virtually the same as shown by Fig. 1.7c. While Fig. 1.7d shows the three phases current that injected to the electrical grid resulted from the RBFNN control system.

Finally, to guarantee the stability of the control system, we should determine the RBFNN parameters (i.e.  $K_p$  and  $\alpha$ ) appropriately. Figure 1.8 shows the influence of the chosen RBFNN parameter on the controlled output in response to the step change of the generated green power.

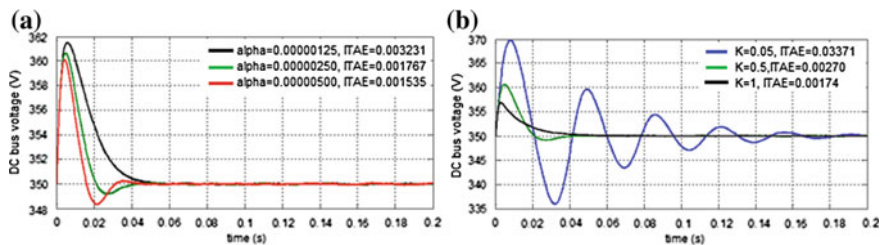


**Fig. 1.8** The DC bus voltage response to the change of the DC load current change for several value of alpha (a) and proportional gain (b)

## 1.5 Conclusion

In this work, we present the RBFNN control system design for the DC bus voltage regulation in the on-grid PV system. The effectivity and the performance of the proposed controller in the response to the disturbance, i.e. response to the sudden connection and disconnection of the DC load is proved by the simulation study. The simulation results show that compared to the Optimal PI control system, the overshoot of DC bus voltage caused by the abrupt change of the DC load for the RBFNN control system is more damped and the controlled output is more quickly to settled.

In the future work, the investigation of the optimal RBFNN parameter, i.e. the proportional gain and the learning rate will be done further by utilizing optimization method such as PSO and Genetic Algorithm.

## References

1. Guido, P., et al.: Distributed generation: definition, benefits and issues. *Energy policy* **33**(6), 787–798 (2005)
2. Frede, B., et al.: Overview of control and grid synchronization for distributed power generation systems. *IEEE Trans. Ind. Electron.* **53**(5), 1398–1409 (2006)
3. Bo, Y., et al.: Design and analysis of a grid-connected photovoltaic power system. *IEEE Trans. Power Electron.* **25**(4), 992–1000 (2010)
4. Manuel, C.J., et al.: Power-electronic systems for the grid integration of renewable energy sources, a survey. *IEEE Trans. Ind. Electron.* **53**(4), 1002–1016 (2006)
5. Wu, T-F., et al., Dc-bus voltage regulation and power compensation with bi-directional inverter in dc-microgrid applications, Energy Conversion Congress and Exposition (ECCE), 2011 IEEE (2011)
6. Deepak, N., Pillai, C.N., Gupta, H.O.: Particle swarm optimization approach for controller design in WECS equipped with DFIG. *J. Electr. Syst.* **6**(2), 01–17 (2010)
7. Mishra, S., Mishra, Y., Fangxing, Li, Dong, Z.Y.: TS-fuzzy controlled DFIG based wind energy conversion systems. In *Power and Energy Society General Meeting, PES'09*. IEEE, pp. 1–7 (2009)
8. Bekakra, Y., Djilani, B.A.: Speed and flux control for DFOC of doubly fed induction machine using sliding mode controller. *Acta Electrotech. Inf.* **10**(4), 75–81 (2010)
9. Chen, S., Billing, S.A.: Neural networks for nonlinear dynamic system modelling and identification. In: Harris, C.J. (ed.): *Advances in Intelligent Control*. Taylor and Francis, London (1992)
10. Hunt and Sbarbaro-Hofer: Neural networks for nonlinear internal model control. *IEE Proc. D* **138**(5), 431–438 (1991)
11. Tsai, H.-L., Tu, C.-S., Su, Y.-J.: Development of generalized photovoltaic model using MATLAB/SIMULINK. In: *Proceedings of the World Congress on Engineering and Computer Science*, Citeseer (2008)
12. De Brito, Gomes, M.A.G., et al.: Evaluation of the main MPPT techniques for photovoltaic applications. *IEEE Trans. Ind. Electron.* **60**(3), 1156–1167 (2013)
13. Abad, G., et al.: *Doubly Fed Induction Machine: Modeling and Control for Wind Energy Generation*, vol. 86. Wiley, New York (2011)

14. Setiawan, I., Priyadi, A., Purnomo, M.H.: Adaptive B-Spline neural network-based vector control for a grid side converter in wind turbine-DFIG systems. *IEEJ Power Energy* **10**(6) (2015)
15. Brown, M., Christopher, J.H.: *Neurofuzzy adaptive Modelling and Control*. Prentice Hall, Hertfordshire (1994)

# Chapter 2

## Virtual Prototyping of a Compliant Spindle for Robotic Deburring

Giovanni Berselli, Marcello Pellicciari, Gabriele Bigi  
and Angelo O. Andrisano

**Abstract** At the current state-of-the-art, Robotic Deburring (RD) has been successfully adopted in many industrial applications, but it still needs improvements in terms of final quality. In fact, the effectiveness of a RD process is highly influenced by the limited accuracy of the robot motions and by the unpredictable variety of burr size/shape. Tool compliance partially solves the problem, although dedicated engineering design tools are strictly needed, in order to identify those optimized parameters and RD strategies that allow achieving the best quality and cost-effectiveness. In this context, the present paper proposes a CAD-based Virtual Prototype (VP) of a pneumatic compliant spindle, suitable to assess the process efficiency in different case scenarios. The proposed VP is created by integrating a 3D multi-body model of the spindle mechanical structure with the behavioural model of the process forces, as adapted from previous literature. Numerical simulations are provided, concerning the prediction of both cutting forces and surface finishing accuracy.

**Keywords** CAD-based tools · Compliant spindle · Robotic deburring · Virtual prototyping

### 2.1 Introduction

The process of finishing mechanical parts with complex shapes and narrow tolerances generally involves the use of five axes CNC machines, namely extremely expensive devices that require large set-up times. As a potential alternative for the same task, industrial robots offer greater flexibility along with a lower initial

---

G. Berselli (✉)

University of Genova, Via All'Opera Pia, 15/A, 16145 Genova, Italy  
e-mail: giovanni.berselli@unige.it

M. Pellicciari · G. Bigi · A.O. Andrisano

University of Modena and Reggio Emilia, Via Vignolese, 905/B, 41125 Modena, Italy

© Springer Science+Business Media Singapore 2016

F. Pasila et al. (eds.), *Proceedings of Second International Conference on Electrical Systems, Technology and Information 2015 (ICESTI 2015)*,

Lecture Notes in Electrical Engineering 365, DOI 10.1007/978-981-287-988-2\_2

investment, but are characterized by an inferior process quality. In the last few years, several efforts have been devoted to the developments of engineering methods and tools for improving the effectiveness of Robotic Deburring (RD) and, more in general, of robotic machining [1].

Focusing on deburring operations, the offline programming of an ideal robot trajectory cannot achieve the best end-product quality, the reasons being the limited motion accuracy of any industrial manipulator and the uneven/unpredictable process condition (i.e.: different burr thickness and varying material properties [2, 3]). In practice, a RD process may lead to either *partial* or *excessive* deburring (where part of the workpiece is accidentally removed). In addition, in case very strict tolerances and good surface roughness are required, a uniform contact pressure between the tool and the workpiece must be guaranteed at all times, despite the burr thickness. In these instances, either an active force feedback [4] or a passive compliant tool are usually adopted, the passive solution being more industrially common thanks to its cost-effectiveness, ease of use and seamless/faster adaptation to unexpected process variations or collisions. Nonetheless, the tuning of the system parameters (e.g. choice of the tool shape, feed-rate, overall compliance) is rather time consuming and requires several physical tests which actually reduce the robotic cell productivity. Therefore, a virtual engineering approach is needed, in order to predict the RD performance without any on-field testing, possibly leading to a “first-time-right”, “plug-and-produce” technology application.

For what concerns past literature dealing with deburring processes, a review of several models for the prediction of the cutting forces is reported in [5] (e.g. linear models by Altintas [6] and exponential model by Kienzle [7]), whereas CAD/CAM-assisted methods have been recently proposed in [8]. In any case, most of the previous works simply neglects the influence of the tool compliance, whose complex interaction with the deburring process is experienced only on the physical test rig. Owing to the above mentioned considerations, the present work addresses the development of a CAD-based Virtual Prototype (VP) of a compliant tool coupled with the cutting process, which should allow for the offline optimization of the RD operations. In particular, the behavior of the spindle mechanical structure is modeled by means of a commercial multibody software (*Recurdyn*), whereas the process forces are concurrently co-simulated in a mathematical simulation environment (*Simulink*).

### ***2.1.1 Description of the Compliant Spindle***

Several commercially available compliant spindles are commonly employed in RD and are usually characterized by pneumatic actuation and radial compliance [3]. The tool considered in this paper, whose detailed description can be found in [9], has been chosen for its widespread adoption and its classical architecture. With

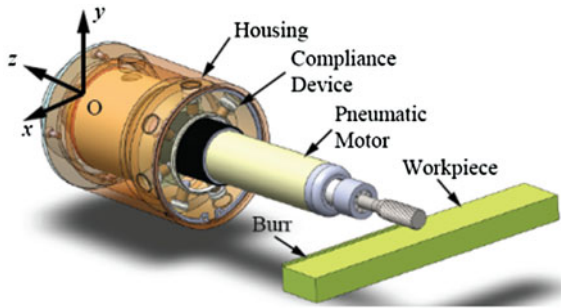


Fig. 2.1 Cad drawing of the deburring tool

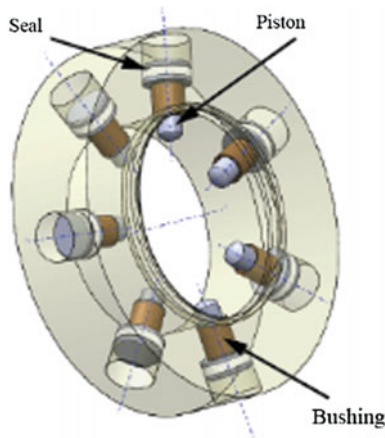


Fig. 2.2 Compliance device

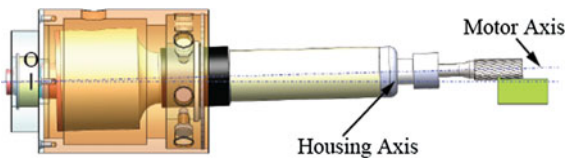


Fig. 2.3 Deburring tool in deflected configuration

reference to the CAD drawing of Fig. 2.1, the device comprises a pneumatic motor inserted into a housing and supported by a spherical joint (located on point O) and by a *Compliance Device*. The compliance device (Fig. 2.2) is composed of seven pistons, having limited stroke, and connected to a common chamber with a common air inlet. Initially, as also reported in Sect. 3.3, all the pistons are in direct contact with the pneumatic motor. On the other hand, as depicted in Fig. 2.3, the



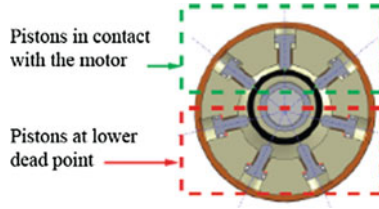


Fig. 2.4 Piston contacts

pneumatic motor can deflect during interaction with the environment. In this case, some of the pistons may reach their lower dead point, thus losing contact with the motor (see Fig. 2.4).

## 2.2 Mechanics of Milling Processes: Background Theory

Let us first neglect the influence of the system compliance. In this case, the mechanics of milling processes has been extensively treated in [7, pp. 35–46], whose nomenclature is hereafter preserved. With reference to Fig. 2.5, let us consider an end mill having diameter  $D$ , helix angle  $\beta$  and number of teeth (or flutes)  $N$ . Let us define  $c$  as the process feed rate,  $\phi_j$  as the instantaneous angle of immersion of the  $j$ -th tooth within the work piece,  $\phi_p = 2\pi/N$  as the tooth spacing angle,  $\phi_{st}, \phi_{ex}, \phi_s = (\phi_{ex} - \phi_{st})$  as the cutter entry, exit, and swept angles. Although helical mills are usually employed, let us first assume  $\beta = 0$  and let us consider the  $j$ -th tooth only.

In this case, the instantaneous chip thickness,  $h_j$ , can be approximated as  $h_j(\phi_j) = c \sin \phi_j$ , whereas tangential,  $F_{t,j}$ , radial,  $F_{r,j}$ , and axial,  $F_{a,j}$ , cutting forces can be expressed as function of edge contact length,  $a$ , and uncut chip area,  $ah(\phi_j)$ , such that:

$$F_{q,j}(\phi_j) = K_{q,c}ah(\phi_j) + K_{q,e}ea, \quad \text{for } q = t, r, a \text{ and } j = 0, \dots, N - 1 \quad (2.1)$$

Fig. 2.5 Geometry of milling process [7]

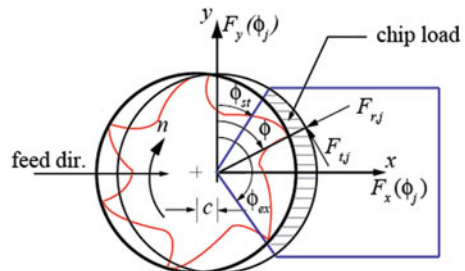
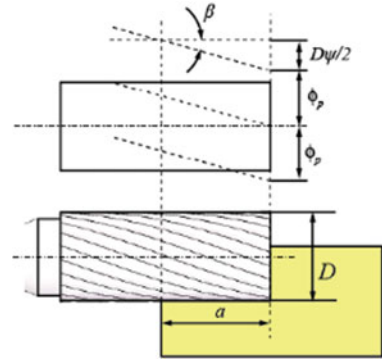


**Fig. 2.6** Geometry of helical end milling [7]



where  $K_{t,c}$ ,  $K_{r,c}$ , and  $K_{a,c}$  are respectively defined as the cutting force coefficients due to the shearing action in tangential, radial, and axial directions, whereas  $K_{t,e}$ ,  $K_{r,e}$ , and  $K_{a,e}$  are the edge constants.

Naturally, cutting forces are produced only when the tool is in the cutting (immersion) zone, that is  $F_{q,j}(\phi_j) > 0$  if  $\phi_{st} \leq \phi_j \leq \phi_{ex}$ . In addition, multiple teeth will be cutting simultaneously if  $\phi_s > \phi_p$ , the overall force being given by the summation of the single  $j$ -th contribution.

In case an helical mill is used (i.e.  $\beta > 0$ ), the cutting edge will be lagging behind the tool end point (see Fig. 2.6). The lag angle,  $\psi$ , at the axial cut depth,  $z$ , is  $\psi = 2zD^{-1}\tan\beta$ . In particular, as stated in [7], when the bottom point of a reference flute is at immersion angle  $\phi$ , a cutting edge point axially located at a distance  $z$  above the reference flute will have an immersion angle of  $(\phi - \psi)$ . Assuming that the bottom end of one flute is designated as the reference immersion angle  $\phi$ , the immersion being measured clockwise from the normal  $y$  axis, the bottom end points of the remaining flutes are at angles  $\phi_j(0) = \phi + j\phi_p$  for  $j = 0, \dots, N - 1$ . The immersion angle for the  $j$ -th flute at an axial cut depth  $z$  is:

$$\phi_j(z) = \phi + j\phi_p - k_\beta z \quad \text{where } k_\beta = 2D^{-1}\tan\beta \quad (2.2)$$

The chip thickness,  $h_j$ , is now approximated as  $h_j(\phi_j, z) = c \sin\phi_j(z)$ . Similarly to Eq. 2.1, the contribution of the elemental tangential,  $dF_{t,j}$ , radial,  $dF_{r,j}$ , and axial,  $dF_{a,j}$ , forces on a differential flute element with height  $z$  can be written as:

$$dF_{q,j}(\phi_j, z) = [K_{q,c}h_j(\phi_j(z)) + K_{q,e}]dz, \quad \text{for } q = t, r, a \text{ and } j = 0, \dots, N - 1 \quad (2.3)$$

From the equilibrium conditions, the radial and tangential elemental forces can be resolved into feed,  $x$ , and normal,  $y$ , directions using the following transformations:

$$\begin{aligned} dF_{x,j} &= -dF_{t,j}\cos\phi_j(z) - dF_{r,j}\sin\phi_j(z); \\ dF_{y,j} &= dF_{t,j}\sin\phi_j(z) - dF_{r,j}\cos\phi_j(z) \end{aligned} \quad (2.4)$$

The total force produced by the  $j$ -th flute can be obtained by integrating the differential cutting forces:

$$F_{p,j}(\phi_j(z)) = \int_{z_{j,1}}^{z_{j,2}} dF_{p,j}(\phi_j(z))dz, \quad \text{for } p = x, y, z \quad (2.5)$$

where  $z_{j,2}(\phi_j(z))$  and  $z_{j,1}(\phi_j(z))$  are the lower and upper axial engagement limits of the in-cut portion of the  $j$ -th flute. The integrations are carried out by noting that  $d\phi_j(z) = -k_\beta z$ , so that:

$$\begin{aligned} F_{x,j}(\phi_j(z)) &= \left\{ \frac{c}{4k_\beta} [-K_{tc} \cos 2\phi_j(z) + K_{rc}(2\phi_j(z) - \sin 2\phi_j(z))] + \frac{1}{k_\beta} [K_{te} \sin \phi_j(z) - K_{re} \cos \phi_j(z)] \right\}_{z_{j,1}(\phi_j(z))}^{z_{j,2}(\phi_j(z))} \\ F_{y,j}(\phi_j(z)) &= \left\{ \frac{-c}{4k_\beta} [-K_{tc}(2\phi_j(z) - \sin 2\phi_j(z)) + K_{rc} \cos 2\phi_j(z)] + \frac{1}{k_\beta} [K_{te} \cos \phi_j(z) + K_{re} \sin \phi_j(z)] \right\}_{z_{j,1}(\phi_j(z))}^{z_{j,2}(\phi_j(z))} \\ F_{z,j}(\phi_j(z)) &= \frac{1}{k_\beta} [K_{ac} \cos \phi_j(z) - K_{ae} \phi_j(z)]_{z_{j,1}(\phi_j(z))}^{z_{j,2}(\phi_j(z))}. \end{aligned} \quad (2.6)$$

Note that the lag angle at full axial depth of cut (i.e. when  $z = a$ ) is  $\psi_a = k_\beta a$ . With reference to Fig. 2.7, the computer algorithm proposed in [7] to determine the axial integration boundaries is as follows:

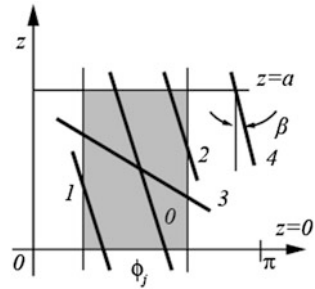
- If  $\phi_{st} < \phi_j(z=0) < \phi_{ex}$ , then  $z_{j,1} = 0$ ;  
If  $\phi_{st} < \phi_j(z=a) < \phi_{ex}$ , then  $z_{j,2} = a$ ;  
If  $\phi_j(z=a) < \phi_{ex}$ , then  $z_{j,2} = (1/k_\beta)(\phi + j\phi_p - \phi_{st})$ ;
- If  $\phi_j(z=0) > \phi_{ex}$  and  $\phi_j(z=a) < \phi_{ex}$  then  $z_{j,1} = (1/k_\beta)(\phi + j\phi_p - \phi_{ex})$ ;  
If  $\phi_j(z=a) > \phi_{st}$  then  $z_{j,2} = a$ ;  
If  $\phi_j(z=a) < \phi_{st}$ , then  $z_{j,2} = (1/k_\beta)(\phi + j\phi_p - \phi_{st})$ ;
- If  $\phi_j(z=0) > \phi_{ex}$  and  $\phi_j(z=a) > \phi_{ex}$  then the flute is out of cut.

Note that these expressions can be used if flute  $j = 0$  is aligned at  $\phi = 0$  in the beginning of the algorithm.

The total instantaneous forces on the cutter at immersion  $\phi$  are finally computed as follows:

$$F_x(\phi) = \sum_{j=0}^{N-1} F_{xj}; F_y(\phi) = \sum_{j=0}^{N-1} F_{yj}; F_z(\phi) = \sum_{j=0}^{N-1} F_{zj}. \quad (2.7)$$

**Fig. 2.7** Helical flute-part face integration zones [7]



### 2.3 Virtual Prototype of the Compliant Spindle

The spindle VP can be conceptually divided in three subsystems arranged in a loop structure, the output of one subsystem being the input of the following one. With reference to Fig. 2.8, the model subsystems are used to compute: (1) radial burr,  $p_{rb}$ , and work piece,  $p_{rp}$ , cut depths; (2) cutting forces; (3) cutting tool position and velocity via co-simulation with a CAD-based multi-body software.

#### 2.3.1 Computation of Radial Burr and Workpiece Cut Depth

With reference to Fig. 2.9, let us define a spatial coordinate  $w$  and let us suppose to conceptually unroll a 3D burr profile along that same coordinate. The burr height

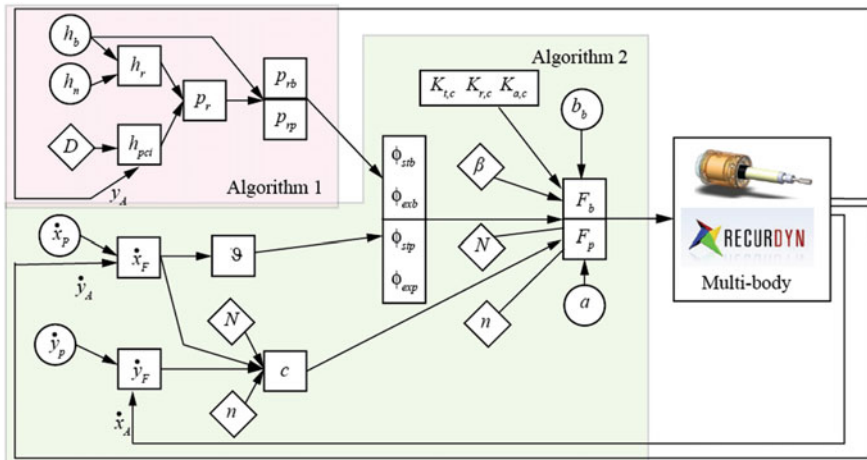


**Fig. 2.8** Spindle VP: integration between CAD-based multi-body software and process models

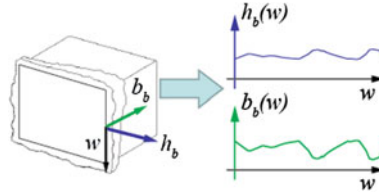


Fig. 2.9 Definition of burr height and width

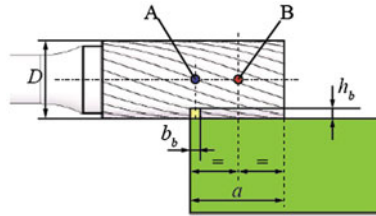


Fig. 2.10 Burr and workpiece geometry

and width can then be defined as function of  $w$ , that is  $h_b = h_b(w)$  and  $b_b = b_b(w)$ , respectively. With reference to Figs. 2.1 and 2.10, let us now define a fixed reference systems, located on point O, the  $z$  axis being aligned with the housing symmetry axis, and the  $x$  axis indicating the feed direction. Similarly, let us locate the application points of the process forces (as computed in the next algorithm) in A and B. These points lie at the intersections between the mill longitudinal axis (Fig. 2.10) and the two lines parallel to the  $y$  axis and respectively passing through the midpoints of  $b_b$  and  $a$  (the latter being the edge contact length between workpiece and cutter). Note that the position of both points A and B, with respect to O, can vary due to the spindle compliance. In particular, Fig. 2.11 depicts a condition where the deburring process is incomplete, whereas Fig. 2.12 depicts a condition where the mill is cutting both burr and workpiece. With reference to these same figures, let us define, for each time instant,  $t$ , the variables  $x_A$  and  $y_A$  as the  $x$  and  $y$  coordinates of point A in the fixed reference systems located on point O,  $h_{pci}$  as the  $y$  coordinate of the mill/workpiece inferior contact point (point C), that defines the workpiece profile after deburring (i.e.  $h_{pci} = y_A - D/2$ ),  $h_r$  and  $h_n$  as the real and desired (nominal) workpiece height with respect to O (i.e.  $h_r = h_n - h_b$ ),  $p_r$  as the radial deburring depth  $p_r = h_r - h_{pci}$ . Three cases are possible:

- **Ideal deburring:**  $p_r = h_b$ , so that  $p_{rb} = h_b$  and  $p_{rp} = 0$ ;
- **Partial deburring:**  $p_r < h_b$ , so that  $p_{rb} = p_r$  and  $p_{rp} = 0$ ;
- **Excessive deburring:**  $p_r > h_b$ , so that  $p_{rb} = h_b$  and  $p_{rp} = p_r - h_b$ ;

Fig. 2.11 Partial deburring

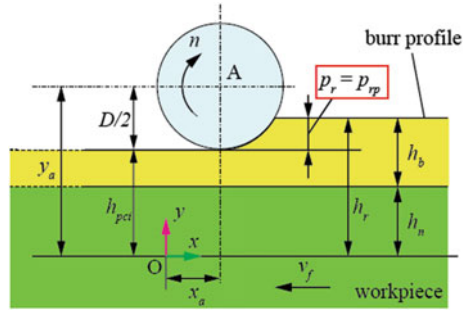
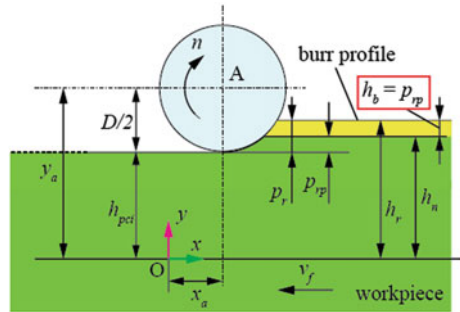


Fig. 2.12 Excessive deburring

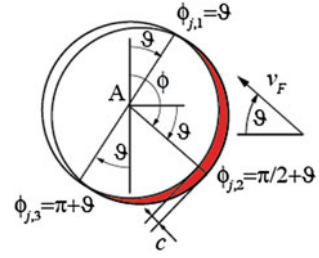


Owing to the above mentioned considerations, the process forces considered hereafter,  $F_b$  and  $F_p$ , are respectively due to either the mill-burr or the mill-workpiece interaction. The force  $F_b$ , (hereafter named burr force), is applied on point A, whereas the force  $F_p$ , (hereafter named workpiece force), is applied on point B.

### 2.3.2 Computation of the Deburring Forces

Due to the presence of a compliant structure, the feed velocity vector will be inclined with respect to the horizontal axis of the workpiece. Let us define  $v_P = [\dot{x}_P, \dot{y}_P, \dot{z}_P]^T$  and  $v_A = [\dot{x}_A, \dot{y}_A, \dot{z}_A]^T$  as the relative velocities of workpiece and point A with respect to the fixed O-frame. The feed velocity vector of the workpiece with respect to the mill is  $v_F = v_P - v_A = [\dot{x}_F, \dot{y}_F, \dot{z}_F]^T$ . Note that, due to the spindle compliance,  $\dot{z}_F \neq 0$ . Nonetheless, as long as  $\dot{z}_F$  is always an order of magnitude lower than  $\dot{x}_F$  and  $\dot{y}_F$ , its contribution is neglected for application purposes (that is  $v_F \approx [\dot{x}_F, \dot{y}_F, 0]^T$ ). The angle of inclination,  $\vartheta$ , of the spindle velocity with respect to

**Fig. 2.13** Computation of  $h(\phi_j, \vartheta)$



the horizontal axis can be evaluated as  $\vartheta = \text{atan}(\dot{y}_F/\dot{x}_F)$ . The process feed rate,  $c$ , is then given by:

$$c = (Nn)^{-1} (\dot{x}_F^2 + \dot{y}_F^2)^{\frac{1}{2}} \quad (2.8)$$

$$h_j(\phi_j) = c \sin(\phi_j - \vartheta) \quad (2.9)$$

For instance, with reference to Fig. 2.13, if  $\phi_j = \phi_{j,1} = \vartheta$ , then  $h(\phi_{j,1}, \vartheta) = 0$ . In the same way, if  $\phi_j = \phi_{j,2} = \pi/2 + \vartheta$ , then  $h(\phi_{j,2}, \vartheta) = c$ . At last, if  $\phi_j = \phi_{j,3} = \pi + \vartheta$ , then  $h(\phi_{j,3}, \vartheta) = 0$ .

Naturally, if the spindle compliance is neglected and, consequently  $\dot{y}_F = 0$ , both Eqs. 2.8 and 2.9 simplifies into the relations given by the standard model from Altintas [7] (recalled in Sect. 2.2), namely  $c = \dot{x}_F$  and  $h_j(\phi_j) = c \sin \phi_j$ .

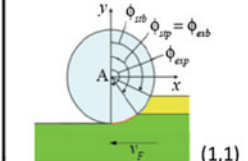
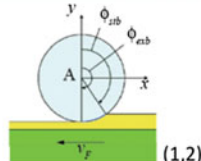
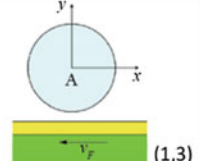
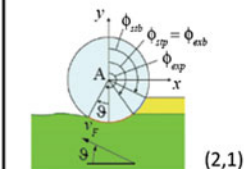
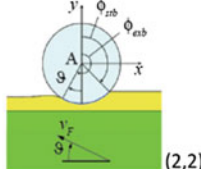
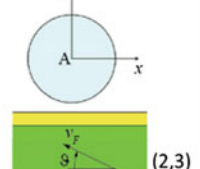
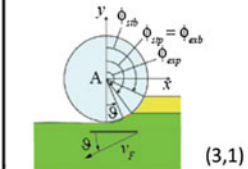
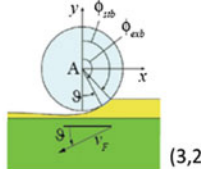
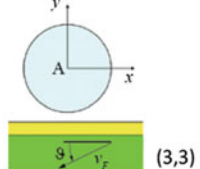
The cutting forces can then be found by inserting Eqs. 2.8–2.9 into Eq. 2.3 and performing the necessary calculations for the integration of the elemental forces (Eq. 2.5). The following expressions are found:

$$\begin{aligned} F_{x,j}(\phi_j(z)) &= \left\{ \frac{c}{k_\beta} \left[ K_{tc} \left( -\frac{\phi_j(z) \sin(\vartheta)}{2} - \frac{\cos(2\phi_j(z) - \vartheta)}{4} \right) + K_{rc} \left( \frac{\phi_j(z) \cos(\vartheta)}{2} - \frac{\sin(2\phi_j(z) - \vartheta)}{4} \right) \right] \right\}_{z_{j,1}(\phi_j(z))}^{z_{j,2}(\phi_j(z))} \\ F_{y,j}(\phi_j(z)) &= \left\{ \frac{c}{k_\beta} \left[ K_{tc} \left( -\frac{\phi_j(z) \sin(\vartheta)}{2} - \frac{\cos(2\phi_j(z) - \vartheta)}{4} \right) + K_{rc} \left( \frac{\phi_j(z) \cos(\vartheta)}{2} - \frac{\sin(2\phi_j(z) - \vartheta)}{4} \right) \right] \right\}_{z_{j,1}(\phi_j(z))}^{z_{j,2}(\phi_j(z))} \\ F_{z,j}(\phi_j(z)) &= \frac{1}{k_\beta} [K_{ac} c \cos(\phi_j(z) - \vartheta)]_{z_{j,1}(\phi_j(z))}^{z_{j,2}(\phi_j(z))} \end{aligned} \quad (2.10)$$

Also in this case, if  $\vartheta = 0$ , Eq. 2.10 reduces to Eq. 2.6. As the last step for the calculation of the cutting forces, the integral limits must be computed. In particular, four integral limits can be defined,  $\phi_{stb}$ ,  $\phi_{stp}$ ,  $\phi_{exb}$ ,  $\phi_{exp}$ , which represent the angular immersion of the mill within either the burr or the workpiece.

In case there exists a velocity component in  $y$  direction,  $\dot{y}_F$ , the possible instantaneous cases are depicted in Table 2.1, according to the value of  $\vartheta$  (either zero, positive or negative) or to the values of  $p_{rp}$  and  $p_{rb}$  (Figs. 2.11 and 2.12).

**Table 2.1** Possible cases for the deburring process

	$p_{rp} > 0 \in p_{rb} > 0$	$p_{rp} = 0 \in p_{rb} > 0$	$p_{rp} = 0 \in p_{rb} = 0$
$\vartheta = 0$	 (1,1)	 (1,2)	 (1,3)
$\vartheta > 0$	 (2,1)	 (2,2)	 (2,3)
$\vartheta < 0$	 (3,1)	 (3,2)	 (3,3)

For what concerns the cases depicted in the third column, it is not necessary to compute any integral limit, the mill not being in contact with either burr or workpiece (i.e.  $F_b = F_p = 0$ ). In parallel, the cases portrayed in the second column depict a situation where the mill is in contact with the burr only, so that  $\phi_{stp}$  and  $\phi_{exp}$  are not defined (i.e.  $F_p = 0$ ). In summary, the overall algorithm for the computation of the integral limits, which requires  $p_{rp}$ ,  $p_{rb}$ , and  $h_b$  as inputs, is formulated as follows:

$$\begin{aligned}
 \varphi_{stb} &= \pi - \arccos\left(1 - \frac{2p_r}{D}\right), \text{ always,} \\
 \varphi_{exb} &= \begin{cases} \pi - \arccos\left(1 - \frac{2p_{rp}}{D}\right), & p_r > h_b \\ \pi + \vartheta, & 0 < p_r < h_b \end{cases} \\
 \varphi_{stp} &= \pi - \arccos\left(1 - \frac{2p_{rp}}{D}\right), \text{ if } p_r > h_b; \\
 \varphi_{exp} &= \pi + \vartheta, \text{ if } p_r > h_b
 \end{aligned} \tag{2.11}$$



### 2.3.3 CAD-Based Multibody Model

As depicted in Fig. 2.8, the CAD-based multi-body model of the spindle mechanical structure computes mill position and velocity (specifically of point A and B) for given workpiece,  $F_p$ , and burr,  $F_b$ , forces. The multi-body model describes the kinematic structure of the spindle, the dynamics of every moving body, and the internal forces due to frictions, contacts, and internal pressure in the chamber of the compliant device. As for the spindle kinematic structure, the housing is considered as fixed (connected to the ground), the pneumatic motor is connected to the housing via a spherical joint on point O, the mill rotates with a given velocity  $n$ . The seven pistons can translate along their axis. Three possible contacts are imposed to each piston, namely contact with the pneumatic motor (point C), and possible contacts with the chamber at either the lower or the upper dead-points, see Figs. 2.2, 2.4 and 2.16. At the initial (undeflected) spindle configuration, all the pistons are in contact with the motor. Concerning the internal forces, two forces have been included:

- Pressure on the piston dome,  $F_{pst}$ , simply given as  $F_{pst} = A_{pst}p$ , the parameter  $A_{pst}$  and  $p$  being piston dome area and chamber pressure.
- Friction force on the piston rubber seals,  $F_{sln}$ . Note that, as depicted in Fig. 2.14, the seals present a hollow structure subjected to a pressure  $p$ . The force,  $F'_{sln}$ , having direction perpendicular to that of the piston motion and due to the chamber-seal interaction, is computed as  $F'_{sln} = A_{sln}p + P$ , the parameter  $A_{sln}$  and  $P$  being the seal lateral area and preload. The force,  $F_{sln}$ , having direction parallel to that of the piston motion and due to friction, is given by  $F_{sln} = \mu F'_{sln}$ , the parameter  $\mu$  being either the static or dynamic coefficient of friction.

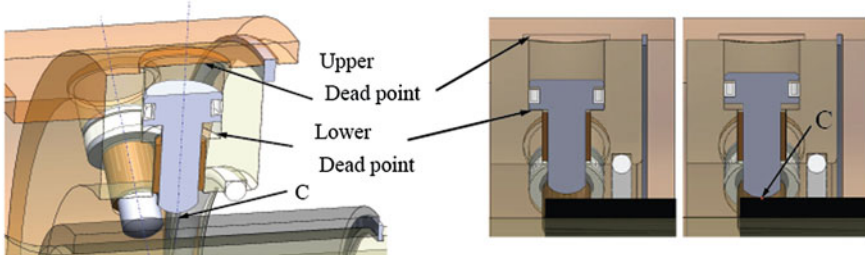


Fig. 2.14 Contact points

### 2.4 Numerical Simulations

At this stage, the VP is validated via a set of numerical simulations. The following parameters have been used:  $K_{t,c} = 2000 \text{ N/mm}^2$ ,  $K_{r,c} = 1200 \text{ N/mm}^2$ ,  $K_{a,c} = 800 \text{ N/mm}^2$ ,  $K_{t,e} = K_{r,e} = K_{a,e} = 0$ ,  $N = 20$ ,  $n = 40.000 \text{ rpm}$ ,  $D = 8 \text{ mm}$ ,  $a = 10 \text{ mm}$ ,  $h_b = b_b = 1 \text{ mm}$ ,  $h_n = 5 \text{ mm}$ ,  $v_f = 80 \text{ mm/s}$ ,  $p = 5 \text{ bar}$ ,  $\beta = 20^\circ$ ,  $F_{pst} = 7.70 \text{ N}$ ,  $F_{sln} = 3.90 \text{ N}$  (static friction) or  $F_{sln} = 2.80 \text{ N}$  (dynamic friction). Let us define the process error as;

$$e = \min(h_{pci} - h_n, h_b) \tag{2.12}$$

A positive error indicates a partial deburring, whereas a negative error indicates an excessive deburring. As an example, Fig. 2.15 depicts a graph of the burr force components  $F_{b,x}$ ,  $F_{b,y}$ ,  $F_{b,z}$  which underlines how the process forces stabilize after

**Fig. 2.15** Burr force components

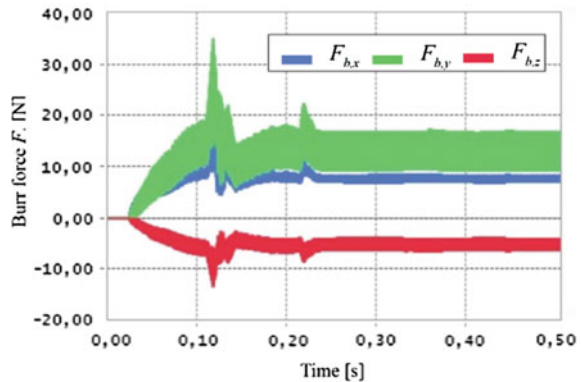
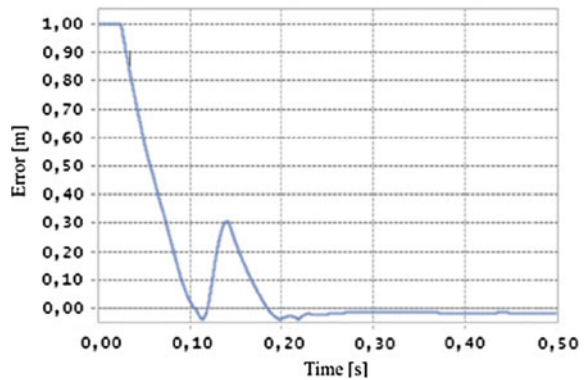


**Fig. 2.16** Surface finishing error



an initial transient. Figure 2.16 depicts the process error, which stabilizes on a sufficiently low negative value.

## 2.5 Conclusions

A CAD-based Virtual Prototype (VP) of a pneumatic compliant spindle has been presented, which is based on a co-simulation model employing a commercial-multibody software along with a mathematical simulation environment. The VP can effectively predict both deburring forces and finishing errors, thus enabling for a virtual test of the process quality. In addition, the versatility of the CAD environment allows to easily evaluate the influence of several design (and control) parameters, such as the overall spindle compliance and the influence of friction in the sliding pairs. Future research will be devoted to the experimental validation of the proposed VP.

**Acknowledgments** This research was funded by the Italian Ministry of research within the project “Adaptive and modular approaches for the digital enabled factory”, CTN01\_00163\_216730.

## References

1. Pandremenos, J., Doukas, C., Stavropoulos, P., Chryssolouris, G.: Machining with robots: a critical review. In: Proceedings of DET2011, 7th International Conference on Digital Enterprise Technology, pp. 1–8. 28–30 Sept (2011)
2. Mohammad, M., Babriya, V., Sobh, T.: Modeling A Deburring Process, Using DELMIA V5, Technological Developments in Education and Automation, pp 549–558 2010
3. Ryuh, B., Pennock, G.R.: Robot automation systems for deburring, industrial robotics: programming, simulation and applications. In: Huat, L.K. (Ed.) InTech (2006). ISBN:3-86611-286-6
4. Liang, L., Xi, F., Liu, K.: Modeling and control of automated polishing/deburring process using a dual-purpose compliant toolhead. *Int. J. Mach. Tools Manuf.* **48**(12–13) (2008)
5. Denkena, B., Hollmann, F.: Process Machine Interactions—Prediction and Manipulation of Interactions between Manufacturing Processes and Machine Tool Structures, Springer (2013)
6. Altintas, Y.: Manufacturing automation, Metal Cutting Mechanics, Machine Tool Vibrations, and CNC Design. Cambridge University Press, New York (2012)
7. Kienzle, O., Victor, H., Spezifische Shnittkraeftebei der Metall-bearbeitung’, *Werkstattstechnik und Maschinenbau*, Bd. 47, H.5, (1957)
8. Schützer, K., Abele, E., Güth, S.: Simulation-based deburring tool and process development. *CIRP Ann. Manuf. Technol.* **64**(1), 357–360 (2015)
9. Lawson, D.K.: Deburring tool, U.S. Patent 6,974,286 B2, filed Jul 25, 2003, and issued Dec 13 (2005)

# Chapter 3

## A Concept of Multi Rough Sets Defined on Multi-contextual Information Systems

Rolly Intan

**Abstract** Rough set theory, introduced by Pawlak in 1982 [1], is an important concept in constructing many applications of Data Mining and Knowledge Discovery. Rough set as a generalization of crisp set, deals with crisp granularity of objects by providing an alternative to formulate a given crisp set with imprecise boundaries. In rough set theory, a given crisp set of object is approximated into two different subsets derived from a crisp partition defined on the universal set of objects. The universal set of objects is characterized by a non-empty finite set of attributes, called data table or information system. The information system is formally represented by a pair  $(U, A)$  in which  $U$  is a universal set of objects and  $A$  is a finite set of attributes. In the real application, depending on the context, a given object may have different values of attributes. Thus, a given set of objects might be approximated based on multi-context of attributes, called multi-contextual information systems. Here,  $n$  context of attributes will provide  $n$  partitions. Clearly, a given set of object,  $X \subseteq U$ , may then be represented by  $n$  pairs of lower and upper approximations. The  $n$  pairs of lower and upper approximations are denoted as *multi rough sets* of  $X$  as already proposed in [2, 3]. This paper extends the concept of multi rough sets by providing more properties and examining more set operations.

**Keywords** Rough sets · Multi rough sets · Granular computing · Multi-context of attributes

### 3.1 Introduction

In the real application, depending on the context, a given object may be characterized by different values of attributes or different set of attributes. In this case, different set of attributes are considered as different contexts in which they may also

---

R. Intan (✉)  
Department of Informatics Engineering, Petra Christian University,  
Surabaya, Indonesia  
e-mail: rintan@petra.ac.id

provide different values of attributes for a given object based on different perceptions. Here, context may be viewed as background or situation by which somehow it is necessary to group some attributes as a subset of attributes and consider the subset as a certain context. For instance, considering human beings as a universal set of objects, every person (object) might be characterized by several sets of attributes corresponding to some contexts such as his or her status as employee, student, club member, family member, etc. In the context of student, student's set of attributes might be regarded as  $\{ID\text{-Number}, Name, Address, Supervisor, Major, \text{etc.}\}$ . We may consider different sets of attributes in the relation to the contexts of both employee and family member. Using the same example of human beings as universal set of objects, in the relation to perception-based data especially for fuzzy data, attributes such as *weight*, *age* and *height* might have different fuzzy values in describing a given certain object depending on contexts (perceptions) of Japanese, American and so on. For instance, Japanese may consider height of 175 cm as  $\{high\}$ , but American may consider it as  $\{medium\}$ . Therefore, it is necessary to consider multi-contextual information systems as an extension of information system (see Sect. 3.3). Here, every context as represented by a certain set of attributes may provide a certain partition of objects. Consequently,  $n$  contexts ( $n$  subsets of attributes) will provide  $n$  partitions. A given set of object,  $X$ , may then be approximated into  $n$  pairs of lower and upper approximations, called *multi rough sets* of  $X$  as already proposed in [4, 5]. In the relation to the concept of multi rough sets, more properties and more set operations are proposed and examined. Primary concern is also given to the generalization of contexts in the presence of multi-contextual information systems. Furthermore, three general contexts, namely AND-general context, OR-general context and  $OR^+$  general context, are recalled. It can be proved that AND-general context and  $OR^+$ -general context provide (disjoint) partitions. On the other hand,  $OR^+$ -general context provides covering of the universe. Then, a summarized rough set of a given crisp set of objects is able to be derived from partitions as well as covering of the general contexts. Finally, relations among three general contexts are examined and summarized.

## 3.2 Concept of Rough Sets

Rough set theory, introduced by Pawlak in 1982 [6], plays essential roles in many applications of Data Mining and Knowledge Discovery. The theory offers mathematical tools to discover hidden patterns in data, recognize partial or total dependencies in data bases, remove redundant data, and others [7]. Rough set generalizes classical (crisp) set by providing an alternative to formulate sets with imprecise boundaries. A rough set is basically an approximate expression of a given crisp set in terms of two crisp subsets derived from a crisp partition defined on the universal set involved [3]. Two subsets are denoted as the lower and upper approximation. Every elements in the crisp partition is related based on equivalence relation. Thus, an element belongs to the only one equivalence class and two distinct equivalence

classes are disjoint. Formally, the concept of rough sets is defined precisely as follows. Let  $U$  denotes a non-empty universal set, and let  $R$  be an equivalence relation on  $U$ . The partition of the universe is referred to as the quotient set and is denoted by  $U/R$ , where  $[x]_R$  represents the equivalence class in  $U/R$  that contains  $x \in U$ . A rough set of subset  $A \subseteq U$  is represented by a pair of lower and upper approximation. The lower approximation [6],

$$\begin{aligned} Lo(A) &= \{x \in U | [x]_R \subseteq A\}, \\ &= \{[x]_R \in U/R | [x]_R \subseteq A\}, \end{aligned} \quad (3.1)$$

is the union of all equivalence classes in  $U/R$  that are contained in  $A$ . The upper approximation [6],

$$\begin{aligned} Up(A) &= \{x \in U | [x]_R \cap A = \emptyset\}, \\ &= \{[x]_R \in U/R | [x]_R \cap A = \emptyset\}, \end{aligned} \quad (3.2)$$

is the union of all equivalence classes in  $U/R$  that overlap with  $A$ .

### 3.3 Multi-contextual Information Systems

A *Multi Rough Sets* is considered as a generalized concept of rough set. A multi rough sets is constructed when a given set of objects is approximated into several partitions of objects in which every partition is constructed by a certain context of attributes. Every context of attributes is represented by a set of attributes. Clearly, multi-contexts of attributes may provide partitions of multi-contexts that are generated from multi-contextual information systems. Here, multi-contextual information systems [4, 5] is formally defined by a pair  $I = (U, \mathbf{A})$ , where  $U$  is a universal set of objects and  $\mathbf{A}$  is a non-empty set of contexts such as  $\mathbf{A} = \{A_1, \dots, A_n\}$ .  $A_i \in \mathbf{A}$  is a certain set of attributes and denoted as a context. Every attribute,  $a \in A_i$ , is associated with a set of  $V_a$  as its attribute values called domain of  $a$ . It is not necessary for  $i \neq j \Rightarrow A_i \cap A_j = \emptyset$ . Attributes such as *weight* and *height* might be represented by different contexts (i.e. context of Japanese and context of American) in which they may provide different perceptions or values of a certain attribute concerning a given object. Therefore, for all  $x \in U$ ,  $a(x)^i \in V_a$  is denoted as the value of objects  $x$  in terms of attribute  $a$  based on the context  $a \in A_i$ . An equivalence relation (indiscernibility relation) is then defined in terms of context  $A_i$  as follows.

For  $x, y \in U$  [4],

$$R_{A_i}(x, y) \Leftrightarrow a(x)^i = a(y)^i, \quad a(x)^i, a(y)^i \in V_a, \quad \forall a \in A_i. \quad (3.3)$$

Equivalence class of  $x \in U$  in the context  $A_i$  is given by [4]

$$[x]_{A_i} = \{y \in U | R_{A_i}(x, y)\}. \quad (3.4)$$

It should be proved that for  $i \neq j$ ,  $\exists x \in U$ ,  $[x]_{A_i} \neq [x]_{A_j}$ , otherwise  $A_i$  and  $A_j$  are redundants in terms of providing similar crisp partitions. By eliminating all redundant contexts, the number of contexts in the relation to the number of objects satisfies the following equation [4].

$$\text{For } |U| = m, \quad |\mathbf{A}| \leq B(m), \quad B(m) = \sum_{i=0}^{m-1} C(m-1, i) \times B(i), \quad (3.5)$$

where  $B(0) = 1$  and  $C(n, k)$  is combination of size  $k$  from  $n$  elements given by:

$$C(n, k) = \frac{n!}{k!(n-k)!}.$$

$|U|$  and  $|\mathbf{A}|$  are cardinalities of  $U$  and  $\mathbf{A}$  representing the number of objects and the number of contexts, respectively. It can be clearly seen that a set of contexts  $\mathbf{A}$  derives set of partitions of universal objects as given by  $\{U/A_1, \dots, U/A_n\}$ , where  $U/A_i$  expresses a partition of the universe based on context  $A_i$ . Here,  $U/A_i$  contains all equivalence classes of  $[x]_{A_i}$ ,  $x \in U$ .

### 3.4 Concept of Multi Rough Set

A multi rough set is introduced as an approximation of a given crisp set in the presence of a set of partitions derived from multi-contextual information systems providing set of rough sets corresponding to the set of partitions. Here, the multi rough sets may be provided regardless of redundant contexts in multi-contextual information systems. Clearly, every element of the multi rough set is a pair of lower and upper approximation in the relation to a given context of attributes. Formally, multi rough set is given by the following definition.

**Definition 3.1** Let  $U$  be a non-empty universal set of objects.  $R_{A_i}$  and  $U/R_{A_i}$  represent equivalence relation and partition with respect to set of attributes in the context of  $A_i$ , respectively. For  $X \subseteq U$ , in the relation to a set of contexts,  $\mathbf{A} = \{A_1, A_2, \dots, A_n\}$ ,  $\mathbf{X}$  is multi rough set of  $X$  as given by the following equation [4, 5].

$$X = \{(Lo(X_1), Up(X_1)), (Lo(X_2), Up(X_2)), \dots, (Lo(X_n), Up(X_n))\}. \quad (3.6)$$

Thus, a pair of lower and upper approximations,  $(Lo(X_i), Up(X_i))$  is an element of multi rough set in terms of context  $A_i$ . Similar to the definition of classical rough set,  $Lo(X_i)$  and  $Up(X_i)$  are then defined by following equations [4]

$$Lo(X_i) = \{u \in U \mid [u]_{A_i} \subseteq X\} = \bigcup \{[u]_{A_i} \in U/A_i \mid [u]_{A_i} \subseteq X\}, \quad (3.7)$$

and

$$Up(X_i) = \{u \in U \mid [u]_{A_i} \cap X \neq \emptyset\} = \bigcup \{[u]_{A_i} \in U/A_i \mid [u]_{A_i} \cap X \neq \emptyset\}, \quad (3.8)$$

respectively. Similar to crisp multi-set (*bags*) as discussed in [8], a multi rough set,  $\mathbf{X}$  is characterized by a counting function  $\Sigma_{\mathbf{X}}$  as given by:

$$\sum_{\mathbf{X}} \mathbf{P}(U)^2 \rightarrow \mathbf{N}, \quad (3.9)$$

where  $P(U)$  is power set of  $U$  and  $\mathbf{N}$  is a set of non-negative integers. Here,  $\Sigma_{\mathbf{X}}((M, N))$  counts number of occurrences the pair  $(M, N)$  in the multi rough set  $\mathbf{X}$  for any pair of lower and upper approximations  $(M, N) \in P(U)^2$ . It should be verified that

$$(M, N) \notin \mathbf{X} \Rightarrow \sum_{\mathbf{X}} ((M, N)) = 0$$

Also,  $\mathbf{X}^*$  denotes a support set of  $\mathbf{X}$ . In its definition,  $\mathbf{X}^*$  satisfies the following equation:

$$(M, N) \in \mathbf{X}^* \Leftrightarrow \sum_{\mathbf{X}} ((M, N)) > 0, \quad (3.10)$$

where  $\forall (M, N) \in \mathbf{X}^*, \sum_{\mathbf{X}^*} ((M, N)) = 1$ . It can be also verified that if  $\mathbf{X} = \mathbf{X}^*$  then there is no redundancy in the set of contexts  $\mathbf{A}$ , not vice versa. It is necessary to define some basic relations and operations concerning sets of pair lower and upper approximations as elements of multi rough set. For  $\mathbf{X}$  and  $\mathbf{Y}$  are two multi rough sets on  $U$  drawn from multi-contextual information systems  $\mathbf{A}$ , where  $|\mathbf{A}| = n$  [4, 5]:

- i. Containment:  $\mathbf{X} \subseteq \mathbf{Y} \Leftrightarrow (Lo(X_i) \subseteq Lo(Y_i), Up(X_i) \subseteq Up(Y_i)), \forall i \in \mathbf{N}_n$ ;
- ii. Equality:  $\mathbf{X} = \mathbf{Y} \Leftrightarrow (Lo(X_i) = Lo(Y_i), Up(X_i) = Up(Y_i)), \forall i \in \mathbf{N}_n$ ;
- iii. Complement:  
 $\mathbf{Y} = \neg \mathbf{X} \Leftrightarrow (Lo(Y_i) = U - Up(X_i), Up(Y_i) = U - Lo(X_i)), \forall i \in \mathbf{N}_n$ ;
- iv. Union:  $\mathbf{X} \cup \mathbf{Y} \Leftrightarrow \{(Lo(X_i) \cup Lo(Y_i), Up(X_i) \cup Up(Y_i)) \mid \forall i \in \mathbf{N}_n\}$ ;
- v. Intersection:  $\mathbf{X} \cap \mathbf{Y} \Leftrightarrow \{(Lo(X_i) \cap Lo(Y_i), Up(X_i) \cap Up(Y_i)) \mid \forall i \in \mathbf{N}_n\}$ ;

where  $\mathbf{N}_n$  is a non-negative set of integers which is less or equal to  $n$ . Obviously, the operations given in (i)–(v) are strongly related to the order of elements corresponding to set of contexts. In the relation to the occurrences of elements with regardless of the order of elements in the multi rough set, some more basic operations are defined as follows.



- (a) Containment:  $\mathbf{X} \prec \mathbf{Y} \Leftrightarrow \sum_{\mathbf{X}}((M, N)) \leq \sum_{\mathbf{Y}}((M, N)), \forall(M, N)$ ;  
 (b) Equality:  $\mathbf{X} \equiv \mathbf{Y} \Leftrightarrow \sum_{\mathbf{X}}((M, N)) = \sum_{\mathbf{Y}}((M, N)), \forall(M, N)$ ;  
 (c) Union:  $\sum_{\mathbf{X} \oplus \mathbf{Y}}((M, N)) = \mathbf{max}[\sum_{\mathbf{X}}((M, N)), \sum_{\mathbf{Y}}((M, N))], \forall(M, N)$ ;  
 (d) Intersection:  $\sum_{\mathbf{X} \otimes \mathbf{Y}}((M, N)) = \mathbf{min}[\sum_{\mathbf{X}}((M, N)), \sum_{\mathbf{Y}}((M, N))], \forall(M, N)$ ;  
 (e) Insertion:  $\sum_{\mathbf{X} + \mathbf{Y}}((M, N)) = \sum_{\mathbf{X}}((M, N)) + \sum_{\mathbf{Y}}((M, N)), \forall(M, N) \in \mathbf{X} \oplus \mathbf{Y}$ ;  
 (f) Minus:  $\sum_{\mathbf{X} - \mathbf{Y}}((M, N)) = \mathbf{max}[\sum_{\mathbf{X}}((M, N)) - \sum_{\mathbf{Y}}((M, N)), 0], \forall(M, N) \in \mathbf{X}$ ;

It can be proved that the above basic operations satisfy the following properties:

1. Idempotent laws:

$$\mathbf{X} \cup \mathbf{X} = \mathbf{X}, \quad \mathbf{X} \cap \mathbf{X} = \mathbf{X}, \quad \mathbf{X} \oplus \mathbf{X} = \mathbf{X}, \quad \mathbf{X} \otimes \mathbf{X} = \mathbf{X};$$

2. Commutative laws:

$$\begin{aligned} \mathbf{X} \cup \mathbf{Y} &= \mathbf{Y} \cup \mathbf{X}, & \mathbf{X} \cap \mathbf{Y} &= \mathbf{Y} \cap \mathbf{X}, & \mathbf{X} \oplus \mathbf{Y} &= \mathbf{Y} \oplus \mathbf{X}, \\ \mathbf{X} \otimes \mathbf{Y} &= \mathbf{Y} \otimes \mathbf{X}, & \mathbf{X} + \mathbf{Y} &= \mathbf{Y} + \mathbf{X}; \end{aligned}$$

3. Associative laws:

$$\begin{aligned} \mathbf{W} \cup (\mathbf{X} \cup \mathbf{Y}) &= (\mathbf{W} \cup \mathbf{Y}) \cup \mathbf{X}, & \mathbf{W} \cap (\mathbf{X} \cap \mathbf{Y}) &= (\mathbf{W} \cap \mathbf{X}) \cap \mathbf{Y}, \\ \mathbf{W} \oplus (\mathbf{X} \oplus \mathbf{Y}) &= (\mathbf{W} \oplus \mathbf{Y}) \oplus \mathbf{X}, & \mathbf{W} \otimes (\mathbf{X} \otimes \mathbf{Y}) &= (\mathbf{W} \otimes \mathbf{Y}) \otimes \mathbf{X}, \\ \mathbf{W} + (\mathbf{X} + \mathbf{Y}) &= (\mathbf{W} + \mathbf{Y}) + \mathbf{X}; \end{aligned}$$

4. Absorption laws:

$$\begin{aligned} \mathbf{X} \cap (\mathbf{X} \cup \mathbf{Y}) &= \mathbf{X}, & \mathbf{X} \cup (\mathbf{X} \cap \mathbf{Y}) &= \mathbf{X}, \\ \mathbf{X} \otimes (\mathbf{X} \oplus \mathbf{Y}) &= \mathbf{X}, & \mathbf{X} \oplus (\mathbf{X} \otimes \mathbf{Y}) &= \mathbf{X}, \\ \mathbf{X} \otimes (\mathbf{X} + \mathbf{Y}) &= \mathbf{X}, & \mathbf{X} \oplus (\mathbf{X} + \mathbf{Y}) &= \mathbf{X} + \mathbf{Y}; \end{aligned}$$

5. Distributive laws:

$$\begin{aligned} \mathbf{W} \cup (\mathbf{X} \cap \mathbf{Y}) &= (\mathbf{W} \cup \mathbf{X}) \cap (\mathbf{W} \cup \mathbf{Y}), \\ \mathbf{W} \cap (\mathbf{X} \cup \mathbf{Y}) &= (\mathbf{W} \cap \mathbf{X}) \cup (\mathbf{W} \cap \mathbf{Y}), \\ \mathbf{W} \oplus (\mathbf{X} \otimes \mathbf{Y}) &= (\mathbf{W} \oplus \mathbf{X}) \otimes (\mathbf{W} \oplus \mathbf{Y}), \\ \mathbf{W} \otimes (\mathbf{X} \oplus \mathbf{Y}) &= (\mathbf{W} \otimes \mathbf{X}) \oplus (\mathbf{W} \otimes \mathbf{Y}), \\ \mathbf{W} + (\mathbf{X} \otimes \mathbf{Y}) &= (\mathbf{W} + \mathbf{X}) \otimes (\mathbf{W} + \mathbf{Y}), \\ \mathbf{W} + (\mathbf{X} \oplus \mathbf{Y}) &= (\mathbf{W} + \mathbf{X}) \oplus (\mathbf{W} + \mathbf{Y}); \end{aligned}$$

6. Additive laws:

$$\mathbf{X} \oplus \mathbf{Y} = \mathbf{X} + \mathbf{Y} - (\mathbf{X} \otimes \mathbf{Y});$$

7. Double negation law:

$$\neg\neg\mathbf{X} = \mathbf{X};$$

8. De Morgan laws:

$$\neg(\mathbf{X}\cap\mathbf{Y}) = \neg\mathbf{X}\cup\neg\mathbf{Y}, \quad \neg(\mathbf{X}\cup\mathbf{Y}) = \neg\mathbf{X}\cap\neg\mathbf{Y};$$

9. Maximum multi rough sets ( $\mathbf{U} = \{(U, U), \dots\}$ ,  $|\mathbf{U}| = |\mathbf{X}|$ ):

$$\mathbf{X}\cap\mathbf{U} = \mathbf{X}, \quad \mathbf{X}\cup\mathbf{U} = \mathbf{U};$$

10. Minimum multi rough sets ( $\mathbf{E} = \{(\emptyset, \emptyset), \dots\}$ ,  $|\mathbf{E}| = |\mathbf{X}|$ ):

$$\mathbf{X}\cap\mathbf{E} = \mathbf{E}, \quad \mathbf{X}\cup\mathbf{E} = \mathbf{X};$$

11. Kleene's laws:

$$(\mathbf{X}\cap\neg\mathbf{X})\cap(\mathbf{Y}\cup\neg\mathbf{Y}) = (\mathbf{X}\cap\neg\mathbf{X}), \quad (\mathbf{X}\cap\neg\mathbf{X})\cup(\mathbf{Y}\cup\neg\mathbf{Y}) = (\mathbf{Y}\cup\neg\mathbf{Y});$$

Since basic operations defined in (iii)–(v) do not satisfy complementary laws ( $(\mathbf{X}\cap\neg\mathbf{X}) \neq \mathbf{E}$  and  $(\mathbf{X}\cup\neg\mathbf{X}) \neq \mathbf{U}$ ), they do not satisfy Boolean algebra but just Kleene algebra instead. We may apply operations of union and intersection to all pair elements of multi rough sets  $\mathbf{X}$  in order to achieve a summary of the multi rough set as given by the following definition [4, 5]:

$$\Gamma(\mathbf{X}) = \bigcup_i Up(X_i), \quad (3.11)$$

$$\Theta(\mathbf{X}) = \bigcap_i Up(X_i), \quad (3.12)$$

$$\Phi(\mathbf{X}) = \bigcup_i Lo(X_i), \quad (3.13)$$

$$\Psi(\mathbf{X}) = \bigcap_i Lo(X_i), \quad (3.14)$$

where  $Lo(\mathbf{X}) = \{(\Phi(\mathbf{X}), \Psi(\mathbf{X}))\}$  and  $Up(\mathbf{X}) = \{(\Gamma(\mathbf{X}), \Theta(\mathbf{X}))\}$  are summarized multi rough set by which they have only one pair elements. It can be easily proved that their relationship satisfies the following equation:

$$\Psi(\mathbf{X}) \subseteq \Phi(\mathbf{X}) \subseteq \mathbf{X} \subseteq \Theta(\mathbf{X}) \subseteq \Gamma(\mathbf{X}).$$

Here, pair of  $(\Phi(\mathbf{X}), \Theta(\mathbf{X}))$  may be considered as a finer approximation of  $\mathbf{X} \subseteq \mathbf{U}$ . On the other hand, pair of  $(\Psi(\mathbf{X}), \Gamma(\mathbf{X}))$  is a worse approximation of  $\mathbf{X} \subseteq \mathbf{U}$ .

Moreover, it can be followed that the definition of summary multi rough set satisfies some properties such as [4]:

- (1)  $X \subseteq Y \Leftrightarrow [\Psi(X) \subseteq \Psi(Y), \Phi(X) \subseteq \Phi(Y), \Theta(X) \subseteq \Theta(Y), \Gamma(X) \subseteq \Gamma(Y)],$
- (2)  $\Psi(X) = \neg\Gamma(\neg X), \Phi(X) = \neg\Theta(\neg X), \Theta(X) = \neg\Phi(\neg X), \Gamma(X) = \neg\Psi(\neg X),$
- (3)  $\Psi(U) = \Phi(U) = \Theta(U) = \Gamma(U) = U, \Psi(\emptyset) = \Phi(\emptyset) = \Theta(\emptyset) = \Gamma(\emptyset) = \emptyset,$
- (4)  $\Psi(X \cap Y) = \Psi(X) \cap \Psi(Y), \Phi(X \cap Y) = \Phi(X) \cap \Phi(Y), \Theta(X \cap Y) \leq \Theta(X) \cap \Theta(Y),$   
 $\Gamma(X \cap Y) \leq \Gamma(X) \leq \Gamma(Y),$
- (5)  $\Psi(X \cup Y) \geq \Psi(X) + \Psi(Y) - \Psi(X \cap Y), \Phi(X \cup Y) \geq \Phi(X) + \Phi(Y) - \Phi(X \cap Y),$   
 $\Phi(X \cup Y) \leq \Phi(X) + \Phi(Y) - \Phi(X \cap Y), \Gamma(X \cup Y) \leq \Gamma(X) + \Gamma(Y) - \Gamma(X \cap Y).$

Furthermore, we may consider two special characteristics of context, namely *total ignorance* and *identity*, as follows.

1.  $A_i$  is called *total ignorance* ( $\tau$ ) if  $x \in U, [x]_\tau = U.$   
 Therefore  $\forall X \subseteq U, X \neq \emptyset \Rightarrow Lo(X_\tau) = \emptyset, Up(X_\tau) = U.$
2.  $A_i$  is called *identity* ( $\iota$ ) if  $\forall x \in U, [x]_\iota = \{x\}.$   
 Therefore,  $\forall X \subseteq U \Rightarrow Lo(X_\iota) = Up(X_\iota) = X.$

Clearly, in the relation to intersection and union operations, it is also satisfied some properties as follows.  $\forall A_i \in \mathbf{A}, X \subseteq U$  [4],

- Union:  $X \neq \emptyset \Rightarrow Up(X_i) \cup Up(X_\tau) = U, Lo(X_i) \cup Lo(X_\tau) = Lo(X_i),$

$$Up(X_i) \cup Up(X_\tau) = Up(X_i), Lo(X_i) \cup Lo(X_\tau) = X.$$

- Intersection:  $Up(X_i) \cap Up(X_\tau) = Up(X_i), Lo(X_i) \cap Lo(X_\tau) = \emptyset,$

$$Up(X_i) \cap Up(X_\tau) = X, Lo(X_i) \cap Lo(X_\tau) = Lo(X_i).$$

From the above relations dealing with union and intersection operations,  $\iota$  is considered as identity context for intersection operation of lower approximation as well as for union operation of upper approximation. On the other hand,  $\tau$  is considered as an identity context for intersection operation of upper approximation as well as for union operation of lower approximation.

Moreover, it is necessary to define two count functions in order to characterize multi rough sets based on the number of objects (elements of  $U$ ) as follows:

**Definition 3.2**  $\eta_{\mathbf{X}}: U \rightarrow \mathbb{N}_n$  and  $\sigma_{\mathbf{X}}: U \rightarrow \mathbb{N}_n$  are defined as two functions to characterize multi rough set by counting total number of copies of a given element of  $U$  in upper and lower sides of multi rough set  $\mathbf{X}$ , respectively, as given by:

$$\eta_{\mathbf{X}}(x) = \sum_i^n \theta_{Up(X_i)}(x), \quad (3.15)$$

$$\sigma_X(x) = \sum_i^n \theta_{Lo(X_i)}(x), \quad (3.16)$$

where  $|\mathbf{A}| = n$  and  $\theta_M(x) = 1 \Leftrightarrow x \in M$ , otherwise  $\theta_M(x) = 0$ .

These count functions are similar to one proposed in (Yager 1990) talking about *bags* (multi-set). Similar results will be found by firstly taking *insertion operation* to all lower side yielding a multi-set of lower side as well as all upper side yielding a multi-set of upper side. Then, the counting function is used to calculate number of copies each element in both multi-sets. In the relation to summary rough sets as discussed before, these two count functions,  $\eta$  and  $\sigma$ , satisfy some properties such as for  $X, Y \in U$ ,  $|\mathbf{A}| = n$  [4]:

1.  $\eta_{\mathbf{X}}(y) \geq \sigma_{\mathbf{X}}(y), \forall y \in U$ ,
2.  $\sigma_{\mathbf{X}}(y) > 0 \Rightarrow y \in X$ ,
3.  $y \in X \Rightarrow \eta_{\mathbf{X}}(y) = n$ ,
4.  $y \in \Theta(X) \Leftrightarrow \eta_{\mathbf{X}}(y) = n$ ,
5.  $y \in \Psi(X) \Leftrightarrow \sigma_{\mathbf{X}}(y) = n$ ,
6.  $\eta_{\mathbf{X}}(y) > 0 \Leftrightarrow \Gamma(X)$ ,
7.  $\sigma_{\mathbf{X}}(y) > 0 \Leftrightarrow \Phi(X)$ ,
8.  $\mathbf{X} \subseteq \mathbf{Y} \Rightarrow \eta_{\mathbf{X}}(y) \leq \eta_{\mathbf{Y}}(y), \sigma_{\mathbf{X}}(y) \leq \sigma_{\mathbf{Y}}(y), \forall y \in U$ ,
9.  $\mathbf{X} = \mathbf{Y} \Rightarrow \eta_{\mathbf{X}}(y) = \eta_{\mathbf{Y}}(y), \sigma_{\mathbf{X}}(y) = \sigma_{\mathbf{Y}}(y), \forall y \in U$ ,
10.  $\eta_{\mathbf{X} \cup \mathbf{Y}}(y) = \eta_{\mathbf{X}}(y) + \eta_{\mathbf{Y}}(y) - \eta_{\mathbf{X} \cap \mathbf{Y}}(y)$ ,
11.  $\sigma_{\mathbf{X} \cup \mathbf{Y}}(y) = \sigma_{\mathbf{X}}(y) + \sigma_{\mathbf{Y}}(y) - \sigma_{\mathbf{X} \cap \mathbf{Y}}(y)$ ,
12.  $\eta_{\mathbf{X} \otimes \mathbf{Y}}(y) = \eta_{\mathbf{X}}(y) + \eta_{\mathbf{Y}}(y) - \eta_{\mathbf{X} \otimes \mathbf{Y}}(y)$ ,
13.  $\sigma_{\mathbf{X} \otimes \mathbf{Y}}(y) = \sigma_{\mathbf{X}}(y) + \sigma_{\mathbf{Y}}(y) - \sigma_{\mathbf{X} \otimes \mathbf{Y}}(y)$ ,

Simply, two membership functions denoted by  $\mu_{\mathbf{X}}(y): U \rightarrow [0,1]$  and  $\nu_{\mathbf{X}}(y): U \rightarrow [0,1]$  might be defined by dividing two previous count functions with total number of contexts ( $|\mathbf{A}| = n$ ) as follows [4].

$$\mu_X(y) = \frac{\eta_X(y)}{n}, \quad (3.17)$$

$$\nu_X(y) = \frac{\sigma_X(y)}{n}, \quad (3.18)$$

where  $\mu_X(y)$  and  $\nu_X(y)$  represent membership value of  $y$  in upper and lower multi set  $\mathbf{X}$ , respectively. Actually,  $\mu$  and  $\nu$  are nothing but another representation of the count functions. However,  $(\nu_X(y), \mu_X(y))$  might be considered as pair of an *interval membership function* of  $y \in U$  in the presence of multi-contexts of attributes. Similarly, by changing  $n$  to 1 in Property (3)–(5),  $\mu$  and  $\nu$  have exactly the same properties as given by  $\eta$  and  $\sigma$ , respectively.

### 3.5 Generalization of Contexts

The objective behind generalization of contexts is to combine all contexts of attributes into one general context. In this case, three kinds of general context are introduced, namely AND-general context, OR-general context and OR<sup>+</sup>-general context.

First, *AND-general context* is a general context which is provided by AND logic operator to all attributes of all contexts. It is simply built by unifying all elements of attributes of all contexts into one general context as given by the following definition.

**Definition 3.3** Let  $A = \{A_1, A_2, \dots, A_n\}$  be set of contexts.  $A_\wedge$  is defined as AND-general context by  $A_\wedge = A_1 \wedge A_2 \wedge \dots \wedge A_n$ , where  $A_\wedge$  is a result of summation of all conditions as given by all attributes of  $A_i$ ,  $\forall i \in N_n$  or simply,

$$A_\wedge = A_1 + A_2 + \dots + A_n \quad (3.19)$$

Similar to what has been discussed in Sect. 3.3, In Definition 3.3, it is also not necessary  $i \neq j \Rightarrow A_i \cap A_j = \emptyset$ . In this case, every attribute is assumed to provide unique and independent value of the attribute in the relation to a given object in terms of a certain context of attribute. It can be verified that  $A_\wedge$  satisfies  $|A_\wedge| = \sum_{i=1}^n |A_i|$ . Also,  $\forall [u]_{A_\wedge}, \forall i \in N_n, \exists [u]_{A_i}$  such that  $[u]_{A_\wedge} \subseteq [u]_{A_i}$ .

For a given  $X \subseteq U$ ,  $Lo(X_\wedge)$  and  $Up(X_\wedge)$  are denoted as lower and upper approximation of  $X$  based on set of attributes,  $A_\wedge$ . Approximation space constructed by AND-general context is considered as the finest disjointed partition by combining all partition of contexts and considering every possible area of intersection among equivalence classes as a equivalence class of AND-general context (see Fig. 3.1c). It can be clearly seen that AND-general context provides the finest approximation of rough set.

Second, the independency of every context persists in the process of generalization, if relationships among contexts are related by OR logic operator. Obviously, instead of a disjoint partition, it may provide a covering of the universal objects. Since OR-general context provides a covering [9, 1], it is also called *Cover-general context* (*C-general context*, for short) as given by the following definition.

**Definition 3.4** Let  $A = \{A_1, A_2, \dots, A_n\}$  be set of contexts.  $A_\vee$  is defined as C-general context as given by:  $A_\vee = A_1 \vee A_2 \vee \dots \vee A_n$ , such that [4]

$$U/A_\vee = \bigcup_{i=1}^n U/A_i \quad (3.20)$$

where  $U/A_\vee$  is a covering of the universe as union of all equivalence classes in  $U/A_i$ ,  $i \in N_n$ .

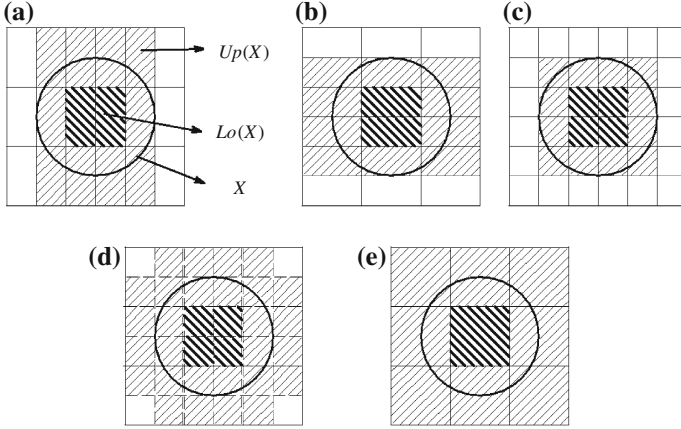


**Fig. 3.1** Generalization contexts [4]. **a**  $U/A_1$ , **b**  $U/A_2$ , **c**  $U/A_\wedge$ , **d**  $U/A_\vee$ , **e**  $U/A_\vee^+$

Consequently,  $|U/A_\vee| \leq \sum_{i=1}^n |U/A_i|$  and  $\forall C \in U/A_\vee, \forall i \in \mathbb{N}_n, \exists [u]_{A_i}$  such that  $C = [u]_{A_i}$ , where  $C$  is a *similarity class* in covering and  $[u]_{A_i}$  is an equivalence class in the partition of  $U/A_i$ . Here  $C$  is called similarity class in order to distinguish it from equivalence class provided by equivalence relation as usually used in partition. Here, every similarity class may take overlap one to each other in providing a covering. Therefore, a given object  $u \in U$  is possibly a member or an element of more than one similarity classes. It can be proved that for  $X \subseteq U$ ,  $Lo(X_\vee)$  and  $Up(X_\vee)$ , as a pair of lower and upper approximations of  $X$  in terms of  $A_\vee$ , are calculated by the following equations [4],

$$Lo(X_\vee) = \bigcup_{i=1}^n Lo(A_i), \tag{3.21}$$

$$Up(X_\vee) = \bigcup_{i=1}^n Up(A_i), \tag{3.22}$$

where  $Lo(X_i)$  and  $Up(X_i)$  are lower and upper approximation of  $X$  dealing with the context  $A_i$ . It can be easily verified that iterative operation is applied in operation of the upper approximation as given by  $Up(X_\vee) \subseteq Up(Up(X_\vee))$ . In this case,  $M(Up(X_\vee))$  is then considered as a maximum upper approximation as given by  $Up(X_\vee) \subseteq Up(Up(X_\vee)) \subseteq \dots \subseteq M(Up(X_\vee))$  in which the iterative operation is no longer applied in the maximum upper approximation as shown in the following relation:  $Up(M(Up(X_\vee))) = M(Up(X_\vee))$ . In the relation to the covering of the universal objects, some properties have been already given and discussed in [2]. Furthermore, related to summary of multi rough set as discussed in the previous section, it can be verified that  $Up(X_\vee) = \Gamma(X)$  and  $Lo(X_\vee) = \Phi(X)$ .

The third general context is called  $OR^+$ -general context. In  $OR^+$ -general context, transitive closure operation is applied to the covering as provided by  $OR$ -general context or  $C$ -general context. In other words, similarity classes of  $OR^+$ -general context are constructed by union of all equivalence classes of all partitions (of all contexts) that overlap one to each other. Similarity classes of  $OR^+$ -general context is then defined by the following definition.

**Definition 3.5** Let  $A = \{A_1, A_2, \dots, A_n\}$  be set of contexts.  $A_{\downarrow}^+$  is defined as  $OR^+$ -general context by:  $A_{\downarrow}^+ = A_1 \circ A_2 \circ \dots \circ A_n$ , such that  $y \in [x]_{A_{\downarrow}^+}$  iff [4]

$$(\exists C_i \in U/A_{\downarrow}, x, y \in C_i) \quad OR \quad (\exists C_{i_1}, C_{i_2}, \dots, C_{i_m} \in U/A_{\downarrow}, \quad (3.23)$$

$$x \in C_{i_1}, C_{i_k} \cap C_{i_{k+1}} \neq \emptyset, k = 1, \dots, m-1, y \in C_{i_m}).$$

where  $m \leq n$  and  $[x]_{A_{\downarrow}^+}$  is an equivalence class containing  $x$  in terms of  $A_{\downarrow}^+$ .

For  $U/A_{\downarrow}$  be a set of equivalence classes provided by all contexts, equivalence classes generated by  $A_{\downarrow}^+$  are able to be constructed by the following algorithm [4, 5]:

```

 $S_i \in U / A_{\downarrow}^+, i \in N$ : Equivalence classes of  $OR^+$ -general context.
 $p = 0$ ;  $SC = U / A_{\downarrow} U / A_{\downarrow}$ ;
while  $SC = \emptyset$  do {
 $p = p + 1$ ;  $S_p = \emptyset$ ;
 $SC = SC - \{M\}$ ;  $M$  is an element (similarity class) of  $SC$ .
 $S_p = M$ ;
 $SS = SC$ ;
while  $SS \neq \emptyset$  do {
     $SS = SS - \{M\}$ ;  $M$  is an element (similarity class) of  $SS$ .
    if  $S_p \cap M \neq \emptyset$  then {
         $S_p = S_p \cup M$ ;
         $SC = SC - \{M\}$ ;
    }
}
}

```

Finally, algorithm in Definition 3.5 shows that there will be  $p$  equivalence classes. Possibly,  $p$  might be equal to 1 in case all elements in  $U/A_{\downarrow}$  transitively join each other. It can be verified that all equivalence classes in  $U/A_{\downarrow}^+$  are disjoint. Also,  $\forall S \in U/A_{\downarrow}^+$  such that  $\forall i \in N_n, \exists M \in U/A_i, M \subseteq S$ . For a given  $X \subseteq U$ ,  $Lo(A_{\downarrow}^+)$  and  $Up(A_{\downarrow}^+)$  are defined as lower and upper approximation of  $X$ , respectively provided by set of attributes,  $A_{\downarrow}^+$ . It can be easily seen that  $OR^+$ -general context will construct the worst disjointed partition. Hence, it will provide the worst approximation of rough set. In the relation to the maximum upper approximation based on  $OR$ -general context, it can be easily proved that apr

$Up(A_{\downarrow}^+) = M(Up(A_{\downarrow}))$ . Compare to summary multi rough set in previous discussion and approximation based on AND-general context, we have the following relation [4].

$$Lo(A_{\downarrow}^+) \subseteq \Psi(X) \subseteq \Phi(X) \subseteq Lo(A_{\wedge}) \subseteq X \subseteq Up(A_{\wedge}) \subseteq \Theta(X) \subseteq \Gamma(X) \subseteq Up(A_{\downarrow}^+)$$

To be more clearly understandable how generalization of contexts applied in the approximation of  $X$ , they are illustrated by Fig. 3.1. To simplify the problem, two contexts are given,  $A_1$  and  $A_2$ , such as approximation of  $X$  is represented in Fig. 3.1a, b. Approximations of  $X$  based on AND, OR and  $OR^+$ -general context are given in Fig. 3.1c–e, respectively.

### 3.6 Conclusion

The concept of multi rough sets based on multi contextual information systems was proposed by Intan et al. (2003) [4, 5]. Here, context can be viewed as situation or background by which somehow it is necessary to group some attributes as a subset of attributes and consider the subset as a certain context. Multi rough sets were considered as a generalization of rough sets. This paper was an extended work by exploring more properties and set operations of the concept of multi rough sets based on multi-contextual information systems. Basic operations and some properties were examined. Two count functions as well as their properties were defined and examined to characterize multi rough sets. Finally, three types of general contexts, namely AND-general context, C-general context and  $OR^+$ -general context were proposed and discussed in order to aggregate contexts into one general context. This paper also discussed briefly relation among all approximations provided by the general contexts. In the future work, it is necessary to apply and implement the concept of multi rough sets in the real world application.

### References

1. Yao, Y.Y., Zhang, J.P.: Interpreting fuzzy membership functions in the theory of rough sets. In: Proceedings of RSCTC'00, pp. 50–57 (2000)
2. Intan, R., Yao, Y.Y., Mukaidono, M.: Generalization of rough sets using weak fuzzy similarity relations. In: Inuiguchi, M., Tsumoto, S., Hirano, S. (eds.) Rough Set Theory and Granular Computing, Studies in Fuzziness and Soft Computing, vol. 125, pp. 37–46. Physica-Verlag, Heidelberg (2003)
3. Klir, G.J., Yuan, B.: Fuzzy Sets and Fuzzy Logic: Theory and Applications. Prentice Hall, Upper Saddle River (1995)
4. Intan, R., Mukaidono, M.: Multi rough sets based on multi-contexts of attributes. In: Wang, G., Liu, Q., Yao, Y., Skowron, A. (eds.) Proceedings of the 9th International Conference on Rough Sets, Fuzzy Sets, Data Mining and Granular Computing (RSFDGrC). Lecture Notes in Artificial Intelligence, vol. 2639, pp. 279–282. Springer, Heidelberg (2003)



5. Intan, R., Mukaidono, M.: Multi rough sets and generalizations of contexts in multi-contexts information system. In: Zhong, N., Raś, Z.W., Tsumoto, S., Suzuki, E. (eds.) Foundations of Intelligent Systems, Proceedings of the 14th International Symposium on Methodologies for Intelligent Systems (ISMIS). Lecture Notes in Artificial Intelligence, vol. 2871, pp. 174–178. Springer, Heidelberg (2003)
6. Pawlak, Z.: Rough sets. *Int. J. Comput. Inf. Sci.* **11**, 341–356 (1982)
7. Komorowski, J., Pawlak, Z., Polkowski, L., Skowron, A.: Rough sets: a tutorial (1999)
8. Yager, R.R.: On the theory of bags. *Int. J. Gen. Syst.* **13**, 23–37 (1986)
9. Intan, R., Mukaidono, M., Yao, Y.Y.: Generalization of rough sets with  $\alpha$  coverings of the universe induced by conditional probability relations. In: Terano, T., Nishida, T., Namatame, A., Tsumoto, S., Ohsawa, Y., Washio, T. (eds.) Proceedings of the International Workshop on Rough Sets and Granular Computing. Lecture Notes in Artificial Intelligence, vol. 2253, pp. 311–315. Springer, Heidelberg (2001)

**Part II**  
**Technology Innovation in Robotics Image**  
**Recognition and Computational**  
**Intelligence Applications**

# Chapter 4

## Coordinates Modelling of the Discrete Hexapod Manipulator via Artificial Intelligence

Felix Pasila and Roche Alimin

**Abstract** This paper will present how to model the XYZ coordinates of a Discrete Manipulator with two-six discrete pneumatic actuators via artificial intelligence algorithm (AI) efficiently. The XYZ model is said efficient if mathematical calculation of the discrete states of manipulator related to XYZ coordinates, with the inverse static analysis (ISA) problem, can be approximately done via AI. The research method used simulation software and hardware implementation with the case of massive manipulator with two level discrete actuators. Simulations with typical desired displacement inputs are presented and a good performance of the results via AI is obtained. The comparison showed that the parallel manipulator has the Root Mean Squared (RMS) error less than 2 %.

**Keywords** Discrete manipulator · Artificial intelligence algorithm · Inverse static analysis problem

### 4.1 Introduction

Discrete manipulator (DM) is a manipulator that consists of a number of actuators which are arranged in serial and/or parallel. In general, DM mechanism consists of a combination of joints, where the actuators can move and serve the manipulator like a prismatic joint. DM has been developed for a wide range of applications such as motion simulators and bio-mechanic applications.

To achieve variation range and accuracy, the architecture of DM practically requires a large number of discrete actuators that can be arranged in a hybrid series-parallel configuration. In designing a DM, the Jacobian matrix method is proposed in determining actuator states of the DM. However, this method has its

---

F. Pasila (✉) · R. Alimin  
Department of Electrical Engineering, Petra Christian University,  
Surabaya, Indonesia  
e-mail: felix@petra.ac.id

disadvantages because Jacobian matrix can only control a few number of actuators. One method to overcome the complexity of the solutions that have been proposed to overcome the limitations of the Jacobian matrix in designing DM is using Inverse Static Analysis (ISA) [1], where one of the ISA solution is using AI [2].

A DM, which the actuators are assigned with a limited number of state, is intended to reduce the complexity of the mechanism and to develop a manipulator without sensors [1]. Several solution of using DM in the sense of ISA Problem, such as: exhaustive search mechanism via brute-force [3]; differential geometry and variation of calculus [4]; combinatorial of heuristics computation [5, 6]; genetic algorithm methods [7]; probability theory and computation [8]; Hopfield networks and Boltzmann machines algorithms [3]. Even though most of the proposed solution methods are relatively effective in reducing problem complexity (from exponential to polynomial time), the resulting of proposed solutions still have slow calculations in terms of real-time computation.

Previous studies which are closely linked to the control of DM using artificial intelligence was conducted by Pasila [2]. This study focused on controlling the 6 DOF parallel manipulator using neuro-fuzzy method. The parallel manipulators used in this research have more than six prismatic actuator with Spherical-Prismatic-Spherical -3D mechanism. Results obtained from this study is that the parallel manipulator twisted due to the way the actuators are arranged and still have big error in terms of RMS.

The goal of this research is to design a two-level discrete manipulator for bio-mechanical purposes with 12 discrete actuator. Here, the ISA solution uses Neuro-Fuzzy network. The second objective is to obtain a state approximation for each actuator to obtain efficient results with Root Mean Square (RMS) error of less than 5 %.

## 4.2 Research Methodology

### 4.2.1 *Design of the Discrete Manipulator*

The discrete manipulator model used in this paper consists of three parts of body, the upper and the medium platform that serve as moving body, and the lower platform that serves as a fixed body. All bodies are connected to the two-six pneumatic actuators. The bodies are circular and have similar diameters. Moreover, the simulation software used Solidworks Motion Study (SW) in order to determine the dimensions of the fixed and the moving platforms for the DM, as well as the location of each actuator. This trial and error method was done to obtain dimensions of the fixed and the moving platforms that accommodate the actuator arrangement. By doing this, the manipulator will not go to an unexpected twist. In this paper, the minimum number of actuators required in order to prevent a twist in the manipulator is 6 actuators for each level. This gives the number of actuator used was

determined to be double-six or 12 actuators. In order to determine the position of each actuator, a novel parallel manipulator was implemented which based on hexapod Stewart-Gough platform [9].

### 4.2.2 Generating Data via SW Software

Data gathering was done via software simulation SW software, by measuring the position of a selected point on the upper platform. The motion simulation generates 1596 data, where each the data consists of coordinates along X, Y, and Z axis along with the combined states on the moving platform. Some of the extracted data can be seen in Table 4.1.

### 4.2.3 Neuro-Fuzzy network as AI Method

This sub-section presents the diagram of the considered model, like shown in Fig. 4.1. The architecture, has three inputs (desired axes) and 12 outputs (actuator states), is called as feedforward Neuro-Fuzzy type Takagi-Sugeno [10].

In particular, the control method presents the Gaussian membership functions  $G_j^n$  ( $j = 1, 2, 3; n = 1, \dots, 12$ ), as a fuzzyfication variable for input pairs  $Z = [R_x, R_y, R_z]$ ,

**Table 4.1** Selected data of two-six hexapod mechanism (1 = extend, 0 = floating, -1 = retract)

Lower Manipulator States						Upper Manipulator States						Axis Coordinates		
S1	S2	S3	S4	S5	S6	S7	S8	S9	S10	S11	S12	X	Y	Z
0	0	1	1	0	0	1	0	-1	-1	0	1	6	24	627
0	0	1	1	0	0	1	1	0	-1	-1	0	6	27	623
0	0	0	1	1	0	1	0	-1	-1	0	1	-85	-83	574
0	0	0	0	1	1	0	1	1	0	-1	-1	-18	-4	628
0	1	1	0	-1	-1	0	1	0	1	0	0	50	15	707
-1	-1	0	1	1	0	1	0	-1	-1	0	1	-9	19	623
-1	-1	0	1	1	0	-1	0	1	1	0	-1	9	51	574
1	1	0	-1	-1	0	1	0	-1	-1	0	1	10	-22	627
-1	0	1	1	0	-1	1	1	0	-1	-1	0	-11	-12	619
0	-1	-1	0	1	1	1	0	0	0	0	0	15	-2	728

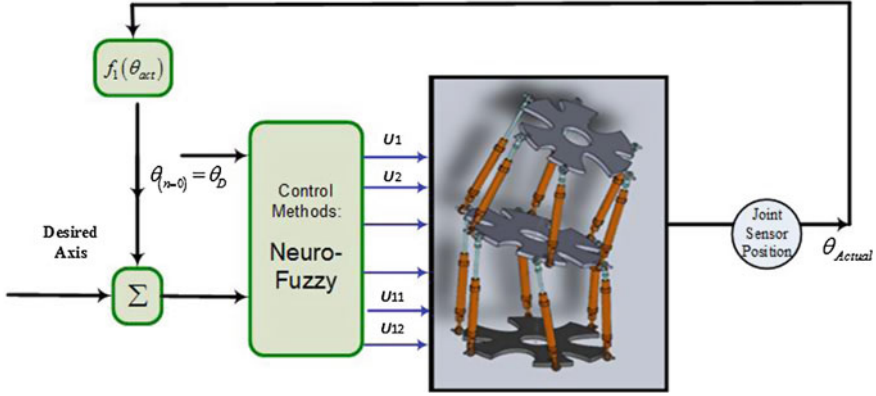


**Fig. 4.1** Control mechanism via Neuro-Fuzzy network, No. of set input = 3, No. output = 12, No. optimal membership function 6, training method: LMA

where  $R_x$ ,  $R_y$ ,  $R_z$  are the input set of the orientations with respect to the XYZ Euler coordinates,

$$G_j^n(Z_j = \exp \left[ - \left( Z_j - C_j^n / \sigma_j^n \right)^2 \right] \quad (4.1)$$

with  $C_j^n$  and variance  $\sigma_j^n$  together with the corresponding fuzzy rules  $FR^n$  can be written as:

$$\begin{aligned} FR^n &: IF Z_1 \text{ is } G_1^n \text{ AND } Z_2 \text{ is } G_2^n \\ THEN y_i^n &= w_{0i}^n + w_{1i}^n Z_1 + w_{2i}^n Z_2 \end{aligned} \quad (4.2)$$

where  $w_{0i}^n$ ,  $w_{1i}^n$  and  $w_{2i}^n$  (for  $i = 1, \dots, 10$ , and  $n = 1, \dots, M$ ,  $M$  is the number of optimized rules for the model, here  $M = 6$ ) being the Takagi-Sugeno parameters.

$$\bar{u}_i = \sum_{n=1}^M y_i^n \left[ \frac{\prod_{j=1}^3 G_j^n(Z_j)}{\sum_{n=1}^M \prod_{j=1}^3 G_j^n(Z_j)} \right] \quad (4.3)$$

$$U_{State\_i} = \text{round}(\bar{u}_i) \quad (4.4)$$

Equations (4.3), (4.4) are derived by approximating the actuator activation states  $u_i$  through possible states (+1, 0 or -1) via threshold processes. These give the actuator states as approximated solution.

### 4.3 Results and Discussions

In this paper, the data simulation is generated from the 3D SW software. At this point, Figs. 4.2 and 4.3 show the implementation of the discrete manipulator with 12 actuators along with the graphs of data simulation results and their neuro-fuzzy model respectively. The total dataset for model use 1596 data which are already selected and sorted from the smallest to the largest value.

Moreover, Fig. 4.3 describes the comparison between the simulation results obtained with the SW software, which shows the approximate value when the actuator is discretely controlled. In addition, it can be seen that the position along X, Y and Z axis closely have generated similar value compared to the continuous controller form. As a result, the RMS error of coordinates modeling in X, Y and Z are 1.43, 1.34 and 1.75 % respectively. The total performance has, in average, 1.51 % of RMS error.

**Fig. 4.2** Implementation of Discrete Manipulator with 12 Discrete Actuators



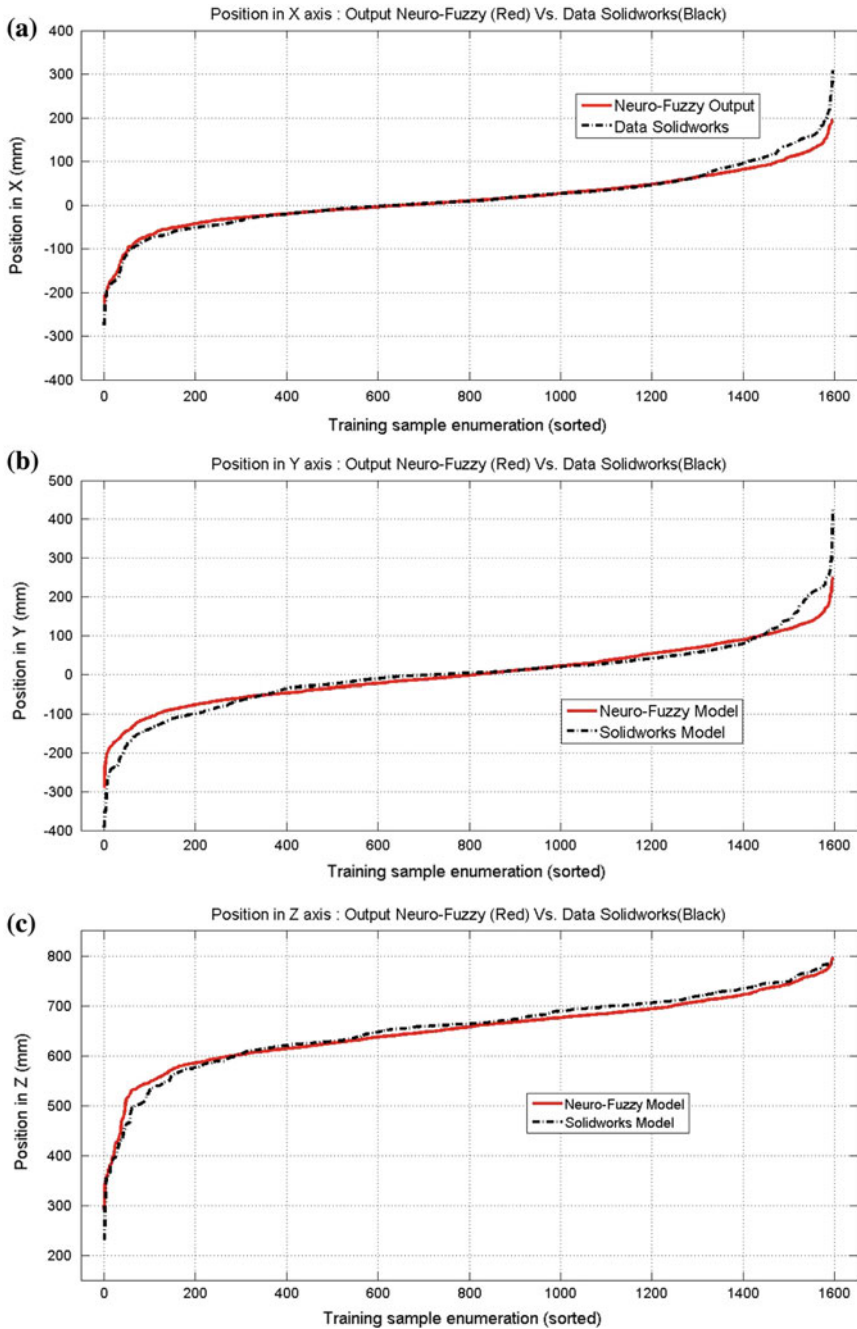


**Fig. 4.3** Data graph showing comparison between software simulation result and manipulator measurement process result. **a** Position along the X axis, **b** Y axis, **c** Z axis



## 4.4 Conclusions

As conclusion, this paper presented: (1) twelve discrete actuators two-six three-state discrete actuators with six DOF; (2) Neuro-Fuzzy methods type Takagi Sugeno for the solution of inverse static analysis of the considered manipulator. The prediction of the XYZ coordinates and its relevant states via neuro-fuzzy methods is used as control mechanism for the 12 actuators manipulator. The simulation result obtained using SW software shows that the reference point on the moving platform can move along the X, Y, and Z axis, which indicated the position of the point along each axis. RMS error of the manipulator obtained by comparing software simulation data and the results of neuro-fuzzy method shows quite small values on the X, Y and Z axis, which are less than 2 % Therefore it is most likely that neuro-fuzzy network can be used as an ISA solution on this manipulator.

**Acknowledgments** We would like to thank Ministry of Research, Technology and Higher Education of Indonesia for supporting this research under two years Research Grant 2014-2015, with the Number: 25/SP2H/LPPM-UKP/IV/201.

## References

1. Pasila, F.: Inverse static analysis of massive parallel arrays of three-state actuators via artificial intelligence. PhD Dissertation, University of Bologna (2013)
2. Pasila, F., Alimin, R.: Neuro-fuzzy architecture of the 3D model of massive parallel actuators. *ARPN J. Eng. Appl. Sci.* **9**(12) (2014)
3. Yang, P., Waldron, K.J.: Massively parallel actuation. In: 2001 IEEE/ASME International Conference on Advanced Intelligent Mechatronics, pp. 868–873 (2001)
4. Chirikjian, G.S.: Inverse kinematics of binary manipulators using a continuum model. *J. Intell. Rob. Syst.* **19**, 5–22 (1997)
5. Lees, D.S., Chirikjian G.S.: A combinatorial approach to trajectory planning for binary manipulators. In: Proceedings of the 1996 IEEE International Conference on Robotics and Automation, pp. 2749–2754 (1996)
6. Sujan, V.A., Lichter D., Dubowsky S.: Lightweight hyper-redundant binary elements for planetary exploration robots. In: 2001 IEEE/ASME International Conference on Advanced Intelligent Mechatronics, pp. 1273–1278 (2001)
7. Lichter, D., Sujan V.A., Dubowsky S.: Computational issues in the planning and kinematics of binary robots. In: Proceedings of the 2002 IEEE International Conference on Robotics and Automation, pp. 341–346 (2002)
8. Suthakorn, J., Chirikjian, G.S.: A new inverse kinematic algorithm for binary manipulators with many actuators. *Adv. Robot.* **15**(2), 225–244 (2001)
9. Ioannis, D., Papadopoulos, E.: Model-based control of a 6-dof electrohydraulic Stewart-Gough platform. *Mech. Mach. Theory* **43**, 1385–1400 (2008)
10. Sugeno, T.: Fuzzy identification of systems and its applications to modeling and control. *IEEE Trans. Syst. Man Cybern.* **SMC-15**, 116–132 (1985)

# Chapter 5

## An Object Recognition in Video Image Using Computer Vision

Sang-gu Kim, Seung-hoon Kang, Joung Gyu Lee and Hoon Jae Lee

**Abstract** This paper examines a variety of algorithms and techniques for image processing in the intention of the development of a face recognition program that operates itself on CAM in both still images and video images, through using detection, tracking and recognition technologies. Moreover, we implement various tracking and detection algorithms, while additionally enabling recognition function of face images from detected frames. Finally, we analyze the proposed performances of the implemented result.

**Keywords** Image processing · Computer vision · Face recognition · Algorithm · Recognition

### 5.1 Introduction

It is not an exaggeration to state that magnificent advancement in IT industry and commercialization of information communications and network environments have led people's daily activities into cyberspaces. Along with the rising, development and commercialization of new technology in IT industry, various issues regarding privacy and information securities of personal information comes up to the surface as well. As some previous identification processes relying upon passwords, verification code and PIN fail to ensure securities due to problems like losses, identity disguise, theft, and hacking, an alternative technology in biometrics is applied widely today, using people's fingerprint/iris or face recognition, pulse, body temperature, or footsteps, for checking online and electronic payment system. Even smart phone mobile industries have begun to employ this technology, so multiple forms of adaptation are taking place [1].

---

S. Kim · S. Kang · J.G. Lee · H.J. Lee (✉)

Division of Computer Information Engineering, Dongseo University, Busan, South Korea  
e-mail: hjlee@dongseo.ac.kr

© Springer Science+Business Media Singapore 2016

F. Pasila et al. (eds.), *Proceedings of Second International Conference on Electrical Systems, Technology and Information 2015 (ICESTI 2015)*,

Lecture Notes in Electrical Engineering 365, DOI 10.1007/978-981-287-988-2\_5

Today, Computer Vision is a more popular technology in facilitating bio-recognition. Previously used in military, satellite and medical fields exclusively by the experts, the technology is expanding its realm of application, while being actively studied in multi-faceted fashion for phone users to benefit from it as well, along with the commercialization of smart phones. Computer Vision, also known as image processing and analysis technology that makes computers self-operate functions as human's eyes. An application program for detection, emphasis, transformation and compression of visual images. It is prevalently applied in robotics and IoT fields; in fact, Microsoft has revealed its agenda to equip security systems based on face, fingerprints and iris recognition on Windows 10, instead of traditional password system.

This paper examines a variety of algorithms and techniques for image processing and intends to develop a face recognition program that operates itself on CAM in both still image and video images, through using detection, tracking and recognition technologies [2]. Furthermore, we implement a recognition function additionally by using face images from detected frames. Finally, we analyze proposed performances for an implemented result.

## 5.2 Related Studies

### 5.2.1 *Application of Computer Vision Technology*

#### 5.2.1.1 **Detecting Drivers Falling Asleep Behind the Wheel by Using Image Processing**

Modern automobile industry develops future-oriented, robotized automobiles combined with IT technologies as demonstrated in Fig. 5.1. It is currently developing a system that warns the drivers of the dead zone with rear, side, frontal and driver's surveillance camera that prevents the accidents through analyzing the data received from live frontal and driver's cameras, based on a big data related to sleep driving.

#### 5.2.1.2 **Context Aware CCTV**

Compared to numbers of CCTV for preventing crimes and disasters, as well as security maintenance, the number of control personnel lacks, which provides difficulty in surveying over all videos. To compensate this challenge, a smart CCTV system is being studied, to inform of crime or disaster beforehand, through the usage of image processing/recognition technologies.

**Fig. 5.1** Example of image processing applied simulation



## 5.2.2 Image Processing Algorithms

Smart image processing system employs a variety of algorithms for detection, classification, tracking and recognition of objects in the video. The paper elaborates on algorithms used for object detection and tracking, which are the core pieces of the system.

### 5.2.2.1 Algorithm for Tracking

**Optical Flow:** Optical flow represents the movement of pixels between previous and present frames in vector form. Like in Fig. 5.2, measuring all movements of pixels in the video is known as optical flow, as shown by Lucas Kanade's algorithm proposed in 1981, a way of calculating the optical flow [3].

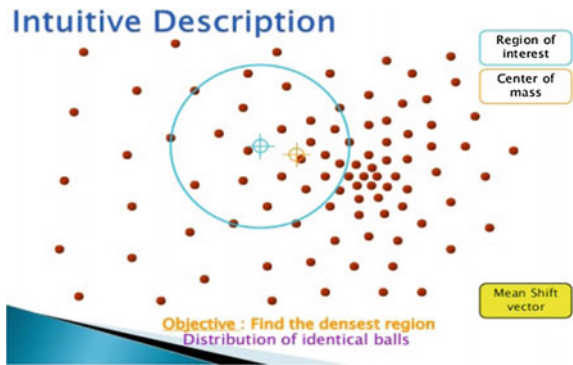
**Mean-shift:** It is also called mean-shift algorithm. It is a tenacious way to find local extrema in density distribution of a data set. In other words, since it tracks the object based on density distribution (corner points, color model), it runs effectively in continuous distribution and is appropriate for high-speed tracking. It operates through a determined search window, as shown in Fig. 5.3 and attaining center of mass of all data within the search window. Next, it shifts the center of window into the center of the data, and repeats the process until the window stops.

**Cam-shift:** An algorithm involving mean-shift as well, it differs from the mean-shift algorithm, for its search window controls the range by itself. This

**Fig. 5.2** Vector arrangements of optical flow



**Fig. 5.3** Mean-Shift Algorithm operation mechanism



technique is also an improvement for streaming environment, because it has more general and simple application.

Kalman Filter: First introduced in 1960, Kalman Filter is a widely used algorithm in the field of signal processing. It collects and analyzes past and present data, to remove interferences and estimate new results. It is used in rockets, satellites and missiles.

### 5.2.2.2 Object Detection Algorithm

Detecting an object means detecting a keypoint. For comprehensive function of video, such as object tracking and recognition, an object detection procedure must take place first. A frame, conspicuously differing from other frames during object detection within a photo or video, is referred to a keypoint (corner point). Most

prominent example of keypoint detection method is SIFT < HOG, and Haar Like Classifier. Figure 5.4 demonstrates operation mechanism of SIFT, first selection will easily distinguish key points in a video and extracting key vectors of Local Patch, based on those key points.

Figure 5.5 shows HOG algorithm, which divides the cells of target areas in regular sizes, draws histogram of each edge pixel's direction in each cell, and connects these histogram values in a single row.

Lastly, Haar was initially developed as an application program for face recognition. As Fig. 5.6 demonstrates, there exist multiple characteristics of forms using variations in the area and brightness, while it extracts characteristics of the object by combining hundreds or thousands of characteristics.

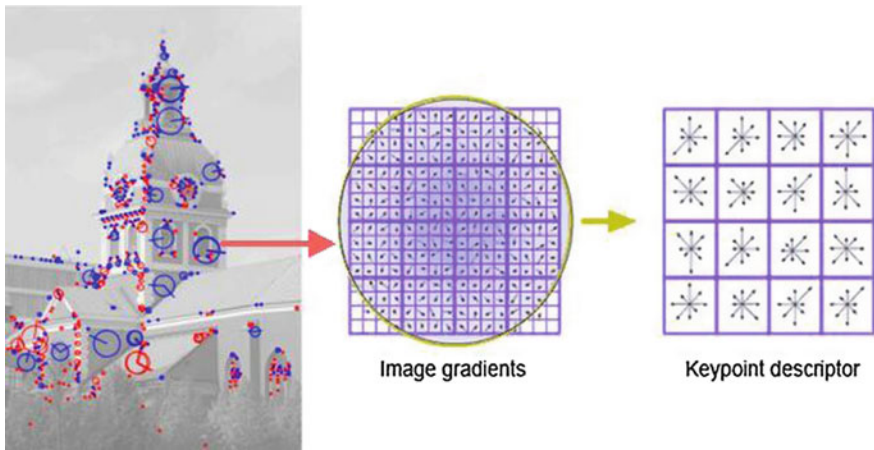
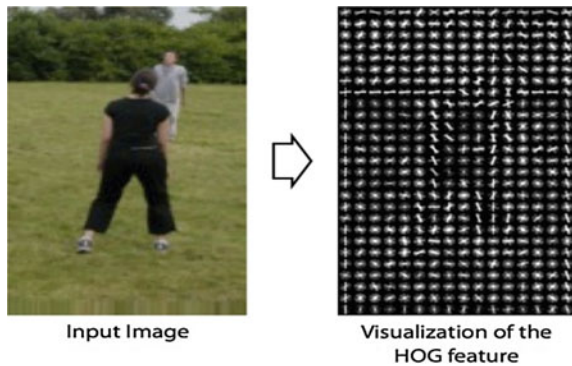


Fig. 5.4 Algorithm operation mechanism of SIFT

Fig. 5.5 Algorithm operation mechanism of HOG



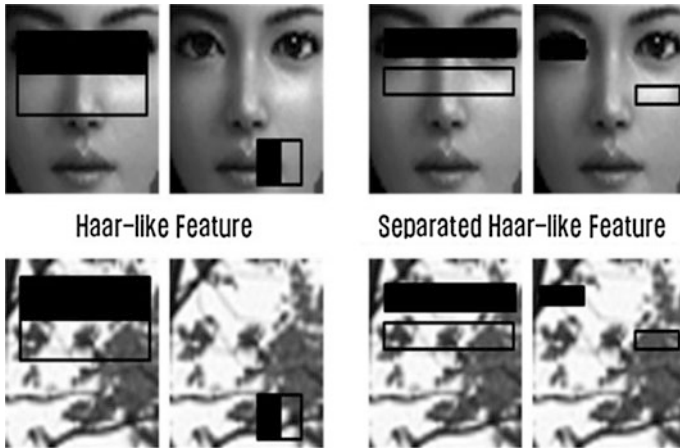


Fig. 5.6 Algorithm operation mechanism of Haar

### 5.3 Implementation

The program we used during the project was a MFC, Visual-Control Program, written with C++. The screen projects CAM video image when it opens, and it detects and tracks faces in real time.

Like in Fig. 5.7, it distinguishes face, eyes, nose, and mouth into separate colored rectangles of red, blue, green and yellow, and runs tracking on each of them independently. It detects and tracks multiple faces simultaneously, and it even captures and saves targeted parts as image files after detection.

Open CV, since it is written with C and C++, it is optimized for C++. Thus, it requires few modifications in settings in order to build and use C, C++ based modules on Android. Primarily, once construction of basic Android development environment is in place, Cygwin corresponding to the operating system is launched. Cygwin is an emulator devised for Windows to be able to run series with Unix and

Fig. 5.7 Open visual-control running screen [4]

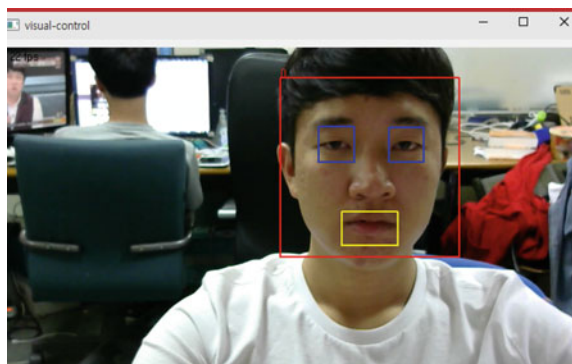




**Fig. 5.8** Camera and SIFT Algorithm interconnection

Linux operating system. Next, NDK for Android should be launched. NDK is a tool that fulfills a part of application program through using a library or module, written in native code language like C and C++ [5].

Figure 5.8 shows a printed image of rectangle on a screen, by running camera on Android and using drawing function `cvRectangle()` provided by OpenCV, after proper setting is done.

In actual practice, we used SIFT key point extraction algorithm to find the key points, marked rectangles on key point locations as shown in (1) and (2) in Fig. 5.9,

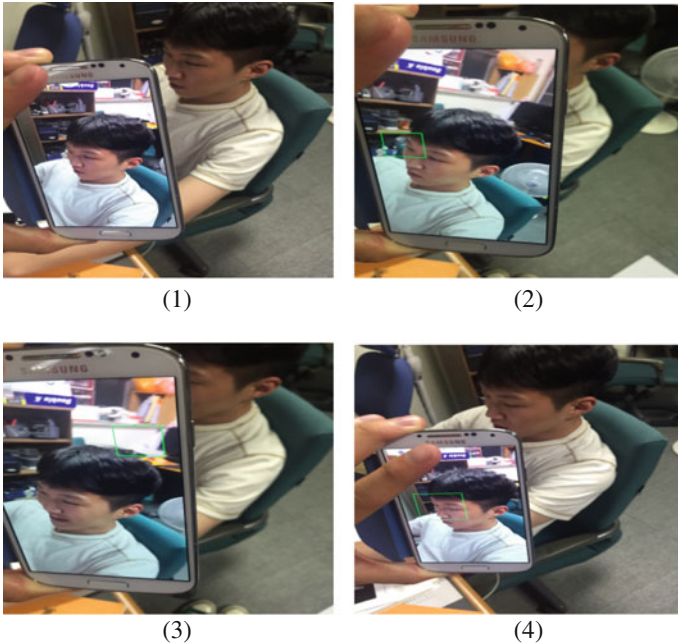


**Fig. 5.9** Haar classifier face detection



and ran tracking using Mean-shift algorithm. SIFT and Mean-shift algorithms detected and tracked the object at fast speed on a photo or non-moving image, but in real time videos like CAM, the detection rate decreased, while it took significant time for them to track and rediscover key points. As it is mentioned in Chap. 2 about related studies, applying Cam-shift algorithm, will be a much better fit for live streaming, because it could refine and track key points rapidly, when the targeted key point is lost like in Fig. 5.9 (3). Also, Haar classification method provides higher facial detection rate than SIFT algorithm (4) of Fig. 5.9 shows how rectangle marks the face on a camera screen when one tries to use Haar classifier by Open CV to detect the face.

Due to the difference in movement of screen and operation speed of tracking key points, mainly because of algorithm's heaviness, we proceeded the experiment at slow moving speed. Shooting the lateral side of the face, that projects the windows on eyes, forehead and cheek around facial borderline. We are planning on an upgrade version, to enable construction of servers to save streaming and images, matching and recognition of faces through saving the captured images on a data base, in addition to object detection and tracking.

## 5.4 Conclusion

We have implemented computer vision technology by using image processing algorithm, and we mainly focused on Mean-shift and Haar classification method out of multiple algorithm. However, as Mean-shift algorithm fails to match the tracking speed with screen moving speed because of complicated calculation processes, we solved this problem with Cam-shift algorithm that is not only fast, but also light and appropriate for streaming environment. Moreover, tracking algorithm operates based on density distribution (key point, corner, color) of data set, so there is a need of an application of color based model for more successful detection of key point. Using a image processing algorithm with color based model allow object detection through brightening the dark spots on the screen, and this may contribute the prevention of crimes with its application on CCTVs.

**Acknowledgments** This paper was supported by the Ministry of Education, (MOE) through the fostering project of the Innovation for Engineering Education.

## References

1. Chi, Y.J., Jong, W.H.: Technological trends in smart image analysis & event detection. Electronics and Telecommunications Trends, Electronics and Telecommunications Research Institute ETRI (2012)
2. Clement, F., et al.: Learning hierarchical features for scene labeling. IEEE Trans. Pattern Anal. Mach. Intell. **35**(8) (2013)

3. Jong-wook, G., et al.: Trends of video big data analysis technics. 2014 Electronics and Telecommunications Trends, Electronics and Telecommunications Research Institute (ETRI) (2014)
4. Jin, H.K.: Trends of Pattern Recognition Technology. KAIST Artificial Intelligence and Pattern Recognition Lab
5. Gary, R.B., Adrian, K.: Learning OpenCV. O'Reilly Media, Inc., Sebastopol (2008)

# Chapter 6

## Comparative Study on Mammogram Image Enhancement Methods According to the Determinant of Radiography Image Quality

Erna Alimudin, Hanung Adi Nugroho and Teguh Bharata Adji

**Abstract** Breast cancer diagnosis by analysing the mammogram becomes difficult for the low quality of X-ray image. It therefore requires a mammogram image enhancement, thus leading the extracted features to more accurate classification result. When conducting an enhancement process, it is deemed essential to consider a number of factors those are contrast sensitivity, blurring, visual noise, spotting, and detail sections that determine the quality of radiography image. This research work used 60 mammogram images from Oncology Clinic Kotabaru Yogyakarta. The images were processed by some enhancement methods based on five determinants of radiography image quality, these are smoothing by Median Filter, filtering by Butterworth Filter and Wiener Filter, denoising by Mean Filter, and histogram equalization by CLAHE. The highest PSNR was obtained by CLAHE method. Further step was to compare between Median Filter—CLAHE and Mean Filter—CLAHE. Results showed that Median Filter—CLAHE became the best enhancement method among the compared methods. This method had the lowest MSE value and the highest PSNR value. It indicated that CLAHE method able to improve the contrast of mammogram image which required high contrast sensitivity due to low contrast in chest soft tissues. The Median Filter meanwhile, was able to reduce noise and blur, thus making the mammogram image clearer. Overall, both these methods were able to enhance image quality and eligible to the determinants of radiography image quality.

**Keywords** CLAHE · Enhancement · Filter · Mammogram

---

E. Alimudin (✉) · H.A. Nugroho · T.B. Adji  
Faculty of Engineering, Department of Electrical Engineering  
and Information Technology, Universitas Gadjah Mada,  
Jl. Grafika 2, 55281 Yogyakarta, Indonesia  
e-mail: [ernaalimudin@gmail.com](mailto:ernaalimudin@gmail.com)

## 6.1 Introduction

Women breast cancer is among the top 5 mortality-rate caused by cancer in thirteen of the fifteen Asian countries [1]. Based on pathology breast cancer places at second rank among other cancers in women [2]. It can be successfully treated if it can be detected at an early stage [3]. Detection can be done by screening mammography. It is used to evaluate the presence of certain diseases in humans [4].

Doctors recommend mammography with low doses as the safest examination of several screening methods and more accurate than self-examination in which a tumour can be detected before it is realised by the patient. In other words, mammography so far is the only effective procedure for breast cancer screening. Mammogram image has to be viewed in an optimal lighting condition and the films must be checked whether the label identity is correct and eligible for the determinants of the radiography image quality. Whole breast parenchymal patterns are assessed. The standard picture of mediolateral oblique projection (MLO) and cranio-caudal (CC) are studied properly on the left and right breast 'back to back' enabling the symmetry of the breast tissue to be examined [5].

One of the major advantages of using mammography is its low cost in use for many patients. Hundreds of film, on the other hand, are cultivated by radiologists everyday so it is not easy to maintain the consistence and accuracy of the diagnosis. A radiologist might be able to misinterpret some disorders [6, 7]. Considering this, Computer Aided Diagnosis (CAD) system has the greatest hope to improve the breast cancer detection and reduce the disease morbidity.

Breast cancer diagnosis from a mammogram becomes difficult due to the low quality of X-ray images. It may lead to misinterpretation. It can be avoided by using CAD. Like an expert, the computer is used to classify mammogram images into normal and abnormal based on the presence of abnormalities. From the mammogram images, some features will be extracted to distinguish between normal or abnormal. This research work compares some enhancement methods to find an appropriate method that leads to more accurate classification.

Nowadays, medical image has been recognised as a way to identify the inside of the human body. The image can be produced in various ways and modalities of medical imaging either using ionising or using non-ionising radiation. Quality and detail should be considered in making medical image useful for diagnosis.

The quality of the resulting image includes all factors capable of clearly and precisely showing the inner structure of the human body. This is the general objective of the imaging procedure that is capability. In addition, if there found anatomical abnormalities, then five determinants of the radiography image quality has to be considered. So the image quality and appearance of anatomic structures in the inside can be shown clearly. These factors are:

1. Contrast sensitivity.
2. Blurring.
3. Visual noise.
4. Spotting.
5. Detail Section (spatial/geometric) [8].

The first thing that determines the characteristic and quality of the radiography image is imaging method and technology which are used to generate radiography image. Medical imaging technology is an extension of the human eye visual power. Medical image and imaging technology become tools in observing object and organ inside the human body that is not visible by eye. Ability to capture the smallest structures and subtle of human body parts is needed in medical imaging. It is influenced by contrast sensitivity.

Mammography technique requires high contrast sensitivity due to very low physical contrast in chest soft tissue. There are several factors that determine the contrast sensitivity of the radiography or mammography. Either blur or noise is a common feature of undesirable elements in the medical image because it can reduce the visibility of certain objects. Object is designed according to a decrease in the size (detailed) from left to right, and according to a decrease in contrast from the bottom to up. Noise and blur are two elements that decrease the visibility image. Noise reduces the visibility of object with low contrast. While blur reduces the visibility of object whose size is small. Typically, most of the object with small anatomical size would have a relatively low contrast value and visibility decreases due to noise and blur [8]. Unlike ultrasound images that have known type of noise that often interfere is speckle noise, mammogram images have not known yet what kind of noise that interfere them.

Previous studies have conducted several methods to enhance mammogram images [9]. However, it did not compare several methods based on its relationship to the five factors that determines the radiography image quality. Comparison of methods is needed to determine the most appropriate method is used for image enhancement. Because, enhancement method on CAD system for digital mammogram image classification is an early stage which would greatly affect the classification accuracy. CAD system for digital mammogram image classification is designed to assist radiologists in mammography screening. Comparing enhancement methods based on their relationship to the five determinants of radiography image quality, i.e.: Contrast, blurring, visual noise, spotting and detail parts, is important because the abnormality signs in mammogram images will be influenced by these five factors. The purpose of this research is to investigate at the most influential factor in improving mammogram image quality and find the most appropriate enhancement method to solve the problems which affecting these factors. Moreover, consider that mammogram image has not known yet what is special kind of noise that interfere it, then try several methods will be a good choice.

## 6.2 Methods

Data used in this research were mammogram digital images. This data were taken from the database of Oncology Clinic Kotabaru Yogyakarta which collecting from 60 patients. Each patient had two mammogram images, i.e. right and left breasts that were based on the viewpoint of the CC (cranio caudal). Two images were called as right cranio caudal (RCC) and left cranio caudal (LCC). Sixty patients consisted of 20 normal patient and 40 abnormal patients (20 abnormal benign and 20 abnormal malignant). The resolution of each image was  $\pm 1400 \times 1850$  pixels with .tif format.

The whole images were input then converted into grayscale format, and then input to enhancement process to undergo five enhancement methods. The whole images that had been through enhancement process were then inputted to the calculation process of mean square error (MSE) and peak signal-to-noise ratio (PSNR) of each method.

Enhancement methods that related to the five determinants of radiography image quality were:

- a. Smoothing, that was aimed to reduce noise, less blurring, result cleaner image of pixelated. One of these methods was Median Filter.
- b. Filtering that was used for noise removal.
  - LPF can be performed with Butterworth Filter
  - HPF can be performed with Wiener Filter
- c. Denoising that was aimed to overcome the problem of poor image display as well as the bad compression. One of the methods is the Average Harmonic Filter.
- d. Histogram equalisation for contrast setting by obtaining the histogram intensity uniformly distributed in the image. The method used was Contrast Limited Adaptive Histogram Equalization (CLAHE).

The ability of enhancement method can also be measured by visual techniques, which only by looking at the image and comparing image result with image contained noise. However, it is not easy to see the disorders without having an excellent knowledge base in medical image. Thus, the measurement by visual technique has different interpretations for each observer. MSE and PSNR are parameters to measure ability of enhancement methods. PSNR are used to comparing the squared error between the original image and the reconstructed image. PSNR value is determined by a large or small MSE value that occurred in image. The larger the PSNR value, the better the display of result image will be. Conversely, the smaller the value of PSNR, the worse the display of result image will be. Unit value of PSNR and MSE is decibel (dB). If PSNR value becomes greater, then MSE value becomes smaller. PSNR is commonly used to measure the quality of the image rearrangements. MSE value obtained by comparing the difference of the pixels on the original image and result

image on the same pixel position. The greater MSE value, the worse the display image will be. Conversely, the smaller MSE value, the better the display of result image will be [10]. This will be the parameters for comparison of each method. MSE and PSNR value are formulated in Eqs. (1) and (2).

$$MSE = \left( \frac{1}{MN} \sum_{x=0}^{M-1} \sum_{y=0}^{N-1} (g'(x,y) - g(x,y))^2 \right) \tag{1}$$

$$PSNR = 20 \log_{10} \left( \frac{2^n}{MSE} \right) \tag{2}$$

where  $x$  is size of row,  $y$  is size of column,  $g'(x, y)$  is matrix of image processing result,  $[M N]$  is size of image, and  $n$  is bit/pixel.

### 6.3 Result and Discussion

Figure 6.1 shows calculation of MSE and PSNR value for each method. The minimum error value of the method shows good image quality after experiencing an image enhancement. If MSE value order from smallest to largest to, then the order is Mean Filter, Median Filter, CLAHE, Wiener Filter, and Butterworth Filter. The maximum PSNR value of the method shows good image quality after experiencing an image enhancement. If order from largest to smallest, then the order is CLAHE, Mean Filter, Median Filter, Wiener Filter, and Butterworth Filters. More details can be seen in Fig. 6.1.

Remarks:

- The X axis is filled by five enhancement methods. The methods are Median Filter, Butterworth Filter, Wiener Filter, Mean Filter, and CLAHE.
- The Y axis is filled by (a) MSE and (b) PSNR value of each method after applied to 60 mammogram images which used in the research.

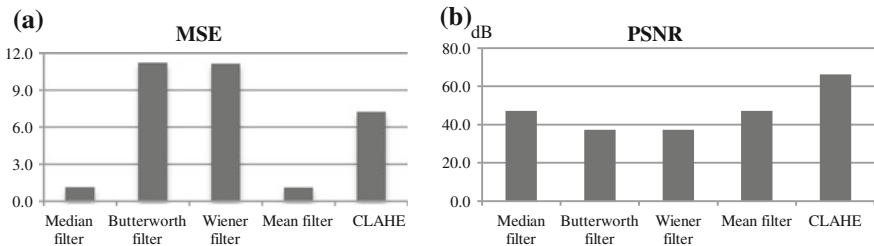


Fig. 6.1 Result of a MSE and b PSNR calculation

After experiment with enhancement methods found CLAHE method obtained the highest PSNR value. Mammography technique requires a high contrast sensitivity due to physical contrast is very low. Adaptive Histogram Equalization (AHE) is a contrast of image enhancement method by increasing local contrast of the image. The problem of excessive contrast enhancement at AHE can be overcome by using CLAHE, which gives the limit value on the histogram [11]. It shows that the contrast factor becomes an important point in deciding the mammogram image quality and CLAHE method can improve image quality of mammogram because it managed to enhance contrast image.

The Median Filter and Mean Filter have MSE and PSNR values that slightly same. The second highest PSNR value after CLAHE owned by Median Filter and Mean Filter. Median Filter is a method of smoothing while the Mean Filter is a method of denoising. Smoothing is used to reduce noise, less blurring, and produce a cleaner image of pixelated with the same size without modifying the size of the data image. An image can be smoothed through up average the neighbouring pixels. Noise is unwanted components in the image. Denoising process can overcome this problem. Denoising is used to overcome the problem of poor display image and poor compression [12]. It proves that blurring and visual noise factors also become important points in determine mammogram image quality. The Median Filter and Mean Filter which are methods of smoothing and denoising can enhance mammogram image quality because it managed to improve blur and reduce noise.

Filtering in image enhancement has function to noise removal. It can be done with linear and nonlinear approach. Removal linearly noise can be done either in spatial and frequency area. Filtering methods are categorized into two, namely low pass filtering (LPF) and high pass filtering (HPF). One of LPF method commonly used is Butterworth Filter and one of HPF method commonly used is the Wiener Filter. After experiment, the Butterworth Filter and Wiener Filter have the lowest PSNR value compared with other methods. It shows that filtering with Butterworth Filter and Wiener Filter is less appropriate for used to enhance mammogram image. The filters have some disadvantages, one of disadvantages is sometimes required information is lost during the process of filtering.

Butterworth Filter is possible to get the original image with great results. However, if the frequency threshold is not exactly the result becomes no longer appropriate. Wiener Filter or also called as the minimum mean square error filter able to reduce the noise sensitivity of the Butterworth Filter. However, the variance value of the image must be known to obtain a constant value [12]. Appropriate constant value needed to get good quality image of the filtering result. It shows that the usage of Butterworth Filter and Wiener Filter are risk.

After seeing the results in Fig. 6.1 then proposed to try another method which is by combine several methods based on the MSE and PSNR values. The purpose of combine some methods is to reach all factors that determine the quality of radiography image by enhancement process. Thus, the enhancement process does not just solve contrast problem but also noise and blur problem. CLAHE method has maximum PSNR value and third order based on the minimum MSE value. From Fig. 6.1 can be seen that the MSE and PSNR values of the Mean Filter and Median



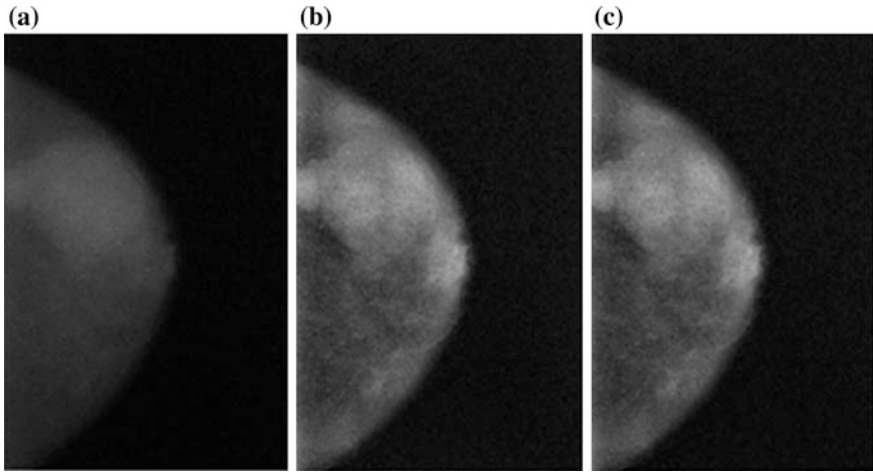


**Fig. 6.2** a Raw image, b Result image by *Mean Filter* + CLAHE, c Result image by *Median Filter* + CLAHE

Filter has a slightly difference in value. Both are listed first and the second order is based on the value of the minimum MSE value. Then, for the PSNR value, both are second and third based on the maximum value. By considering these results, it is proposed to try two models of image enhancement stages, the first one using the Mean Filter followed by CLAHE and the second using a Median Filter which is also followed by CLAHE. The result can be seen in Fig. 6.2.

More detail about MSE and PSNR calculation results can be seen in Fig. 6.3.

From the graph in Fig. 6.3 can be seen that the value of MSE and PSNR with Median Filter method followed by CLAHE showed lower and higher values than the Mean Filter method followed by CLAHE, those are 12.19 and 37.28 dB.

MSE and PSNR value of Median Filter is greater when compared with the Mean Filter. It indicates Median Filter is better than Mean Filter method. Pixel values in the image that has been processed by Mean Filter has not big difference between one pixel with the neighbour pixel when compared to the image that has been processed by Median Filter, because the Mean Filter taking the average value while Median Filter taking the middle value. It shows that the Median Filter and Mean

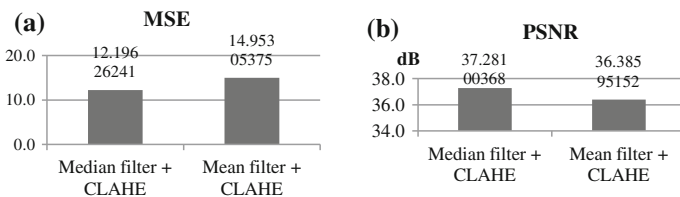


**Fig. 6.3** a MSE and b PSNR calculation of median filter + CLAHE and Mean Filter + CLAHE

Filter can reduce noise, but the image result from Mean Filter will more blur when compared with the Median Filter. MSE and PSNR value of Median Filter is greater when compared with the Mean Filter. It indicates that Median Filter is better than Mean Filter method.

## 6.4 Conclusions

Mammogram image enhancement is an important stage to get a good quality image by appropriated feature extraction to obtain more precise classification results. Mammogram image enhancement has to consider the determinants of radiography image quality, those are contrast sensitivity, blurring, visual noise, spotting, and detail sections (spatial/geometric). Enhancement methods that related to the five determinants of radiography image quality are smoothing by Median Filter, filtering by Butterworth Filter and Wiener Filter, de-noising by Mean Filter, and histogram equalization by CLAHE. After conducting an experiment with five mammogram image enhancement methods, the highest PSNR obtained from CLAHE method. It shows that the contrast factor becomes an important point in determine mammogram image quality and CLAHE method can enhance mammogram image which requires a high contrast sensitivity due to physical contrast is very low.

Combination method of Median Filter and CLAHE that proposed in this research is the best method to enhance mammogram image compared to the other comparison method in this research. This method has the lowest MSE value and the highest PSNR value. It shows CLAHE method capable of improving image contrast mammogram and Median Filter can reduce noise and reduce blur so that the image is becoming more clearly. Both methods are able to increase image quality and meet the determinants of the radiography image quality.

## References

1. Merel, K., et al.: The burden of cancer in member countries of the Association of Southeast Asian Nations (ASEAN). *Asian Pacific J. Cancer* **13**, 411–420 (2012)
2. Aziz, M.F.: Gynecological cancer in Indonesia. *Gynecol. Oncol.* **20**(1), 8–10 (2009)
3. Luo, Z.L.Z., Wu, X.W.X., Guo, S.G.S., Ye, B.Y.B.: Diagnosis of breast cancer tumor based on PCA and fuzzy support vector machine classifier. In: 2008 Fourth International Conference on Natural Computation, vol. 4, pp. 437–441 (2008)
4. Rosenberg, G.A., Kieper, D.A., Williams, M.B., Johnson, N., Lanzkowsky, L., *The Role of Molecular Imaging Technologies in Breast Cancer Diagnosis and Management* (2002)
5. Taplin, S., Rutter, C., Finder, C., Mandelson, M.T., Houn, F., White, E.: Screening mammography: clinical image quality and the risk of interval. *Am. J. Roentgonol.* **178**(4), 797–803 (2002)
6. Bird, R.E., Wallace, T.W., Yankaskas, B.C.: Analysis of cancers missed at screening mammography. *Radiology* **184**(3), 613–617 (1992)

7. Birdwell, R.L., Ikeda, D.M., O'Shaughnessy, K.F., Sickles, E.: Mammographic characteristics of 115 missed cancers later detected with screening mammography and the potential utility of computer-aided detection. *Radiology* **219**(1), 192–202 (2001)
8. Kanal, K.M., Krupinski, E., Berns, E.A., Geiser, W.R., Rubin, D.L., Shepard, J.D., Siegel, E. L., Wolfman, J.A., Mian, T.A., Mahoney, M.C., ACR—AAPM—SIIM practice guideline for determinants of image quality in digital mammography. *J. Digit. Imaging*, 10–25 (2013)
9. Gowri, D.S., A Review on Mammogram Image Enhancement Techniques for Breast Cancer Detection (2014)
10. Wang, Z., Bovik, A.C., A universal image quality index. *IEEE Signal Process. Lett.* **XX**, 1–4 (2002)
11. Wang, X., Wong, B.S., Tui, C.G., Khoo, K.P., Foo, F.: Image enhancement for radiographic non-destructive inspection of the aircraft. *A-PCNDT* **12**, 3–8 (2006)
12. Gonzalez, R.C., *Digital Image Processing* (2007)

# Chapter 7

## Clustering and Principal Feature Selection Impact for Internet Traffic Classification Using K-NN

Trianggoro Wiradinata and P. Adi Suryaputra

**Abstract** K-NN is a classification algorithm which suitable for large amounts of data and have higher accuracy for internet traffic classification, unfortunately K-NN algorithm has disadvantage in computation time because K-NN algorithm calculates the distance of all data in some dataset. This research provide alternative solution to overcome K-NN computation time, the alternative solution is to implement clustering process before the classification process. Clustering process does not require high computation time. Fuzzy C-Mean algorithm is implemented in this research. The Fuzzy C-Mean algorithm clusters the based datasets that be entered. Fuzzy C-Mean has disadvantage of clustering, that is the results are often not the same even though the input data are same, and the initial dataset that of the Fuzzy C-Mean is not optimal, to optimize the initial datasets, in this research, feature selection algorithm is used, after selecting the main feature of dataset, the output from fuzzy C-Mean become consistent. Selection of the features is a method that is expected to provide an initial dataset that is optimum for the algorithm Fuzzy C-Means. Algorithms for feature selection in this study used is Principal Component Analysis (PCA). PCA reduced nonsignificant attribute to created optimal dataset and can improve performance clustering and classification algorithm. Results of this research is clustering and principal feature selection give significant impact in accuracy and computation time for internet traffic classification. The combination from this three methods have successfully modeled to generate a data classification method of internet bandwidth usage.

**Keywords** Classification · Clustering · Feature · Internet · K-NN

---

T. Wiradinata · P. Adi Suryaputra (✉)  
University of Ciputra, UC Town Citraland, Surabaya, Indonesia  
e-mail: adi.suryaputra@ciputra.ac.id

© Springer Science+Business Media Singapore 2016  
F. Pasila et al. (eds.), *Proceedings of Second International Conference on Electrical Systems, Technology and Information 2015 (ICESTI 2015)*,  
Lecture Notes in Electrical Engineering 365, DOI 10.1007/978-981-287-988-2\_7

## 7.1 Introduction

The purpose of this research is to investigate how to improve the K-Nearest Neighbor (K-NN) classification accuracy and computation time for internet bandwidth usage classification process. K-NN algorithm calculates all distances distribution of existing data, so the results of the classification are more accurate because it considers all the possibilities that exist, the process of rigorous computational algorithms K-NN finally have a weakness in terms of performance that is the slow process of classification.

In addressing the weakness of K-NN algorithm in this research, an experiment study has been conducted by firstly forming the ready-classified datasets, which is done by clustering beforehand. Clustering process is done so that the spread of the data occurs naturally based on similarity of existing data, as the data is scattered then carried out a process of classification, clustering process is expected to accelerate the performance of K-NN algorithm. This clustering algorithm is an algorithm that meets the Fuzzy C Mean. At Algorithm Fuzzy C Mean, number of clusters to be formed does not need to be determined in advance, so the number of clusters that formed later would show the grouping of data occurs. In a recent study in 2012 conducted by LOU Xiaojun, LI Junying, and Haitao LIU still stated that the Fuzzy C Mean generally have a weakness for the output partition/cluster for the same dataset [1].

Based on these previous research there are some opportunity to develop an Internet traffic classification model using machine learning algorithms. In this research K-NN algorithm is used for that classification, Fuzzy C Mean algorithm for clustering process and Principal Feature Selection for principal feature selection. One advantage of Fuzzy C-Mean algorithm is the number of classification does not need to be specified from the beginning such as in Fuzzy K Mean algorithm. It is expected that the classification is formed to represent real data. However Fuzzy C Mean requires a feature of selection for data to be used that Internet traffic with the same correlation could fit into the same classification. Another thing that could be the development on these studies is how the process of finding the features and precise fit.

## 7.2 Literature Review

### 7.2.1 *K-Nearest Neighbor*

Algorithm k-nearest neighbor (k-NN or KNN) is an algorithm used for the classification of the object based on the distance between the objects. The data used for the classification process in the K-NN projected into multiple dimensions, where each dimension represents the features of the data [2]. The space is divided into sections based on the classification of data that are classified. A point in this space marked class C if class C is the most common classification of the k nearest neighbors of the dot. Near or far neighbors Euclidean are usually calculated based

on the distance learning phase, the algorithm is simply to store the vectors of features and classification of the learning data. In the classification phase, the same features are calculated for test data (which classification is not known). The distance of this new vector of all learning data vector is calculated, and the number  $k$  closest is retrieved [3]. K-NN algorithm accuracy is greatly influenced by the presence or absence of features that are not relevant, or if the weight of such features is not equivalent to its relevance to the classification. Research on these algorithms largely discusses how to choose and give weight to the feature, in order to become a better classification performance.

### ***7.2.2 Fuzzy C-Mean***

Fuzzy C-Means clustering is a technique to clustering of each data point in dataset which determined by the degree of membership. This technique was first introduced by Jim Bezdek in 1981. First step of Fuzzy C-Means is to determine cluster centers, which marked the average location for each cluster. In the initial condition, the center of the cluster is still not accurate. Each data point has a degree of membership for each cluster. By improving the cluster centers and the degree of membership of each data point repeatedly, it will be seen that the center cluster will move towards the right location. This loop is based on minimization of an objective function that describes the distance from the given data point to the center of the cluster that is weighted by the degrees of membership of data points. Output of Fuzzy C-Means is a row of cluster centers and some degree of membership for each data point. First of all, the method provides membership values, which can be useful for assessing the validity of the cluster structure obtained. Second, the method has a simple and efficient algorithm which makes it applicable in a broad class of situations [4].

### ***7.2.3 Principal Feature Selection***

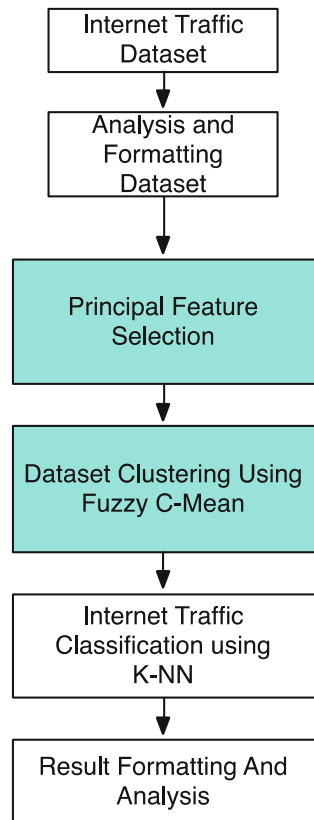
Principal Component Analysis (PCA) is the principal feature selection method used in this research. Esbensen [5], explained that the main component analysis (PCA) is a multivariate data analysis method mostly used for exploratory analysis of data, outlier detection, rank (dimension) reduction, graphical clustering, classification, and regression. The proper understanding of PCA is a prerequisite for the controlling other latent variable methods, including Principal Component Analysis regression, multivariate calibration and classification. Current use of PCA is associated with the latent data structure visualization with a graphical plot. Since PCA allows interpretation based on all variables simultaneously, then PCA is mostly used as the first data analysis conducted on multivariate data sets, although further data analysis with other methods even more advanced one may be required [6].

### 7.3 Research Methodology

The purpose of this study is to investigate the impact of clustering and principal feature selection for K-NN Classification accuracy and computation time by using Fuzzy C-Mean as clustering algorithm and Principal Component Analysis (PCA) as principal feature selection. PCA is first technique implement in this research for analyzing internet traffic dataset and to find the discriminant feature [7]. Fuzzy C-Mean is a technique for improving the K-NN computation time, Fuzzy C-Mean is the solution to help K-NN in data clustering, Fuzzy C-Mean will make the distribution and grouping of data so as to make the K-NN does not need to perform the calculation of all distances between existing data. The research methodology to achieve these research objectives, as shown in Fig. 7.1.

The contribution in this research shown in the blue box on Fig. 7.1. This research dataset is collecting from mooreset dataset which used in another internet traffic classification research, this data is collected from <http://www.cl.cam.ac.uk/research/srg/netos/nprobe/data/papers/sigmetrics/> [8].

Fig. 7.1 Research methodology



## 7.4 Experimental Result

This research used dataset 10 for experimental dataset, the dataset class and number of flow is present in Table 7.1. The experimental result is present in Table 7.2 until Tables 7.3 and 7.4.

Table 7.1 shows that dataset 10 has a 65036. Fuzzy C-Mean clustering the data before classified by K-NN, Fuzzy C-Mean clustering is expected to improve the computation time of the algorithm K-NN. Principal Feature Selection done by PCA via transform the dataset into new dataset, the new dataset is create by dimensional reduction from PCA. Table 7.2 shown that Fuzzy C-Mean gave significant impact for K-NN Classification in execution time, K-NN execution time decreases almost 400 s. The feature reduction which done by PCA shows the most significant impact, Table 7.2 shown execution time improvement is more less 70 %, unfortunately

**Table 7.1** Number of data flow

Class	Number of flow
WWW	54436
Mail	6592
FTP-control (fc)	81
FTP-pasv (fp)	257
Attack	446
P2p	624
Database (db)	1773
Ftp-data (fd)	592
Multimedia (mm)	0
Services (srv)	212
Interactive (int)	22
Games (gm)	1
Total	65036

**Table 7.2** Execution time result

Algorithm	Times (s)
Traditional K-NN	1232
Traditional K-NN + Fuzzy C-Mean	839
Traditional K-NN + Fuzzy C-Mean + PCA	249

**Table 7.3** Accuracy result

Algorithm	Accuracy (%)
Traditional K-NN	98.41
Traditional K-NN + Fuzzy C-Mean	96.70
Traditional K-NN + Fuzzy C-Mean + PCA	98.06



**Table 7.4** Classification summary

	Traditional K-NN	Traditional K-NN + Fuzzy C-Mean	Traditional K-NN + Fuzzy C-Mean + PCA
Max precision value	99.77 %	99.09 %	99.60 %
Min precision value	0 %	0 %	0 %
Number of class in dataset	11	11	11
Number of class figure out in classification	10	10	9

K-NN classification accuracy is decline when Fuzzy C-Mean and PCA implement in classification model as shown in Table 7.3. In Table 7.4 also shown that Max Precision value is decline when Fuzzy C-Mean and PCA implement in this classification model.

## 7.5 Conclusion

K-NN has great accuracy in internet traffic classification. K-NN disadvantage is its high execution time. To improve the execution of K-NN algorithms needed to carry out the reduction features PCA and Fuzzy C-Mean algorithm to form a cluster prior to the classification process, with the combination of two algorithm. K-NN algorithm would have a shorter execution time and but unfortunately the classification accuracy declining. In the future, work will be conducted on how to figure out number of class in dataset and improving accuracy from K-NN but still have short execution time.

**Acknowledgments** We would like to thank to Indonesian Higher Education and Research for this opportunity and research grant, and also for University Of Ciputra for research facility.

## References

1. Lou, X., Li, J., Liu, H.: Improved fuzzy C-means clustering algorithm based on cluster density related work. *J. Comput. Inf. Syst.* **2**(January), 727–737 (2012)
2. Zhang, L., Liu, Q., Yang, W., Wei, N., Dong, D.: An improved k-nearest neighbor model for short-term traffic flow prediction. In: *Procedia—Social and Behavioral Sciences*, vol. 96 (Cictp), pp. 653–662 (2013). doi:[10.1016/j.sbspro.2013.08.076](https://doi.org/10.1016/j.sbspro.2013.08.076)
3. Lee, Y.-H., Wei, C.-P., Cheng, T.-H., Yang, C.-T.: Nearest-neighbor-based approach to time-series classification. *Decis. Support Syst.* **53**(1), 207–217 (2012). doi:[10.1016/j.dss.2011.12.014](https://doi.org/10.1016/j.dss.2011.12.014)
4. Berget, I., Mevik, B.-H., Næs, T.: New modifications and applications of fuzzy-means methodology. *Comput. Stat. Data Anal.* **52**(5), 2403–2418 (2008). doi:[10.1016/j.csda.2007.10.020](https://doi.org/10.1016/j.csda.2007.10.020)

5. Esbensen, K.H.: *Principal Component Analysis: Concept, Geometrical Interpretation, Mathematical Background, Algorithms, History, Practice*. Elsevier, New York (2009)
6. Wang, F.: *Factor Analysis and Principal-Component Analysis*. Elsevier, New York (2009)
7. Paramita, A.S.: Feature selection technique using principal component analysis for improving fuzzy C-mean internet traffic classification. *Aust. J. Basic Appl. Sci.* **8**(14), 13–18 (2014)
8. Antonio, T., Paramita, A.S.: Full paper feature selection technique impact for internet traffic classification using naïve Bayesian. *JurnalTeknologi* **20**, 85–88 (2014)

# Chapter 8

## Altitude Lock Capability Benchmarking: Type 2 Fuzzy, Type 1 Fuzzy, and Fuzzy-PID with Extreme Altitude Change as a Disturbance

Hendi Wicaksono, Yohanes Gunawan, Cornelius Kristanto  
and Leonardie Haryanto

**Abstract** In the past three years, our research developed a low cost QuadRotor. QuadRotor are built from four brushless motors with four Electronic Speed Controllers (ESC) and four propellers in one carbon frame of QuadRotor. KK2 board is added as a flight controller of QuadRotor. This KK2 board has been completed only to deal with altitude stabilization. Our research focused on altitude locking development using several control methods implemented on YoHe board. This paper presents altitude lock capability, to be benchmark between Type2 Fuzzy controller and Type1 Fuzzy controller, also with Fuzzy-PID. The benchmark focuses on their flight analysis performance with extreme altitude change (50 cm) as a disturbance. From that three control methods that have applied, and overall tested, Type2 Fuzzy shows better result than others.

**Keywords** Type2 fuzzy · Type1 fuzzy · Fuzzy-PID · Altitude lock

### 8.1 Introduction

QuadRotor is one of a popular Unmanned Aerial Vehicle (UAV). QuadRotor have four rotors to spin symmetrically. This fast growing QuadRotor had been become a popular research's object more than any other UAVs. Many controllers was develop to complete a Quadrotor maneuver. Type2 Fuzzy with Fast Geometric Defuzzification was introduced by Simon [2]. This method shows very important concept to make us able to apply it in the Type2 Fuzzy in a real time. Type1 Fuzzy

---

H. Wicaksono (✉) · Y. Gunawan · C. Kristanto · L. Haryanto  
Electrical Engineering Department, University of Surabaya,  
Raya Kalirungkut, Surabaya, Indonesia  
e-mail: hendi@staff.ubaya.ac.id

which can be called as Ordinary Fuzzy is a Fuzzy method which was introduced by Zadeh 1965. The comparison of those Fuzzy's structure was well described in [1]. PID Controller was used decades years ago, and now days many researchers combine PID Controller with auto tuning from as an output of Fuzzy. It is called a Fuzzy-PID which was explained in [4] and also [3]. Type2 Fuzzy, Type1 Fuzzy, and Fuzzy-PID was designed in our research and have been published. In the past publication, we analyzed the performance of each control method to lock an altitude of QuadRotor. The best control method seen from error percentage is Type2 Fuzzy Control.

The body of this paper is organized as follow. Section 8.2 explains QuadRotor specification which is used in this paper. The control method designs of Type2 Fuzzy, Type1 Fuzzy, and also Fuzzy-PID will be described in Sect. 8.3. The experiment results are given in Sect. 8.4, and finally a conclusion is given in Sect. 8.5.

## 8.2 QuadRotor Specification and Design

The QuadRotor used in this research was built from scratch. There are eight main parts that should be combined piece by piece to build a one QuadRotor. First, Whirlwind FY450 as a frame was chosen. This frame is made from plastic with several thicknesses so it is strong enough to make it flies. For the motor, four Brushless Motors DC (BLDC) Sunny Sky X2212 which has 980 kV are used. DJI 10 × 4.7 is a propeller installed on BLDC motors. Four DJI 10 × 4.7 with two types direction are installed on the four BLDC motors. As a driver, ZTW Spider 30 A Electronic Speed Controller (ESC) with Pulse Width Modulation (PWM) as an output, is used QuadRotor is shown in Fig. 8.1 and the detail of the parts are shown in Fig. 8.2.

Fig. 8.1 QuadRotor





Fig. 8.2 QuadRotor parts

All control methods were built and processed from YoHe Board. In this application, YoHe Board’s functions are:

1. YoHe Board recognizes the manual or auto conditions from a pulse generated from RX Orange when the toggle button is active in TX Orange.
2. In the manual mode, YoHe Board gets and recognizes the throttle signal and makes a pulse signal with sharp as same as the input throttle signal, then sent it to KK2.0 Board.
3. In the auto mode, YoHe Board will activate a sonar sensor and get the current altitude, after that it will calculate an error signal
4. Continue from number 3, YoHe Board is then running a control method coding, whose output is throttle value. After that as it was explained in item number 2, YoHe Board will generate a pulse signal as big as the throttle value and then sent it to KK2.0 Board.

The block connecting all of parts of QuadRotor in general use compare with block connection for altitude lock system with YoHe Board shown in Figs. 8.3 and 8.4. We put in a YoHe Board connection between RX and KK2.0 board. Beside that the system completed with Bluetooth V3 as a media to transfer a data flight from QuadRotor to ground station (laptop).



Fig. 8.3 Block connection parts of QuadRotor in general use

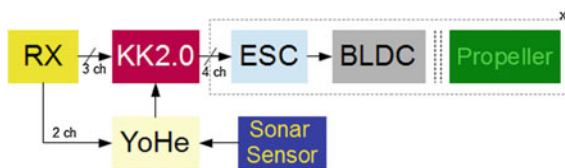


Fig. 8.4 Block connection parts of QuadRotor for altitude lock system

### 8.3 Control Method Design

In this paper, there are three control methods to compare the altitude lock capability to handle the extreme altitude change disturbance. There are Type2 Fuzzy, Type1 Fuzzy, and Fuzzy-PID. Each control method was published in several publications for their performance analysis. In it's common structure, the design of Type2 Fuzzy and Type1 Fuzzy are quietly similar.

Structure of Type2 Fuzzy is shown in Fig. 8.7, while Fig. 8.8 shows structure of Type1 Fuzzy. The difference between both structures lay at the end of the process. Type2 Fuzzy have Type Reducer step before defuzzifier step. In this paper, we don't apply a general form of Type2 Fuzzy because it is too hard to make a microcontroller code running at a real time. For that reason, Fast Geometric Defuzzification used in a real time running. We have been trying to make coding with a selection mode to change from one control method to another control method. Because of that mission, YoHe Board completed with ATmega 2560 with 256 KB memory. After Type2 was coded into the board, we decided not to put in all code to the microcontroller because the only Type2 Fuzzy code was taken around 80 % memory capacity.

Both of Type2 Fuzzy and Type1 Fuzzy have a same control process like is shown in Fig. 8.5. In this system have a value defined to height desired and the height (n) getting from sonar sensor measurement. Both of Fuzzy have two inputs, they are an error which calculates from the difference between the desired height and height (n) and a second input is a delta error which calculates from the difference between an error (n) and an error (n - 1). As an output is the throttle value which will be converted to pulse and sent to KK2.0 board. And whereas Fuzzy-PID control process shown in Fig. 8.6. In that figure we can see that an output of Fuzzy

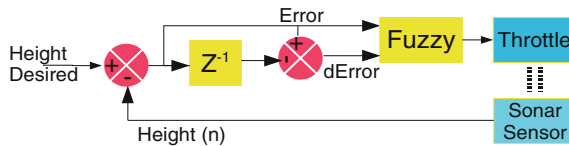


Fig. 8.5 Fuzzy control process

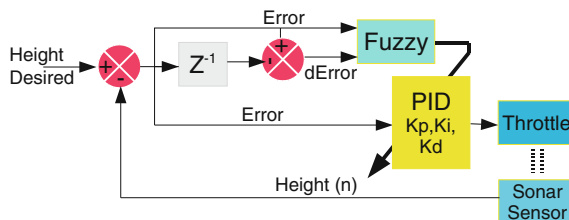


Fig. 8.6 Fuzzy-PID control process

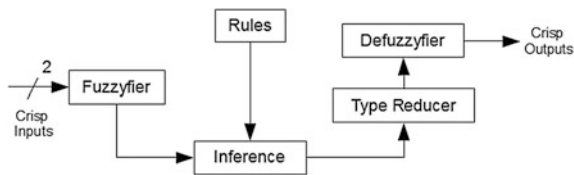


Fig. 8.7 Type2 fuzzy structure

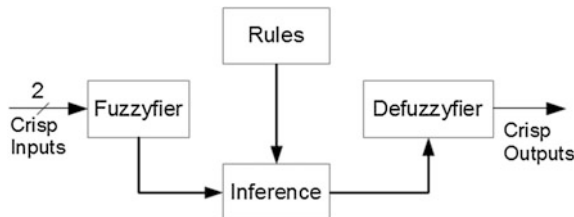


Fig. 8.8 Type1 fuzzy structure

form is a Proportional, Derivative, and Integral constant which will be used by a PID controller.

The structure of Type2 Fuzzy compares to Type1 Fuzzy shown Figs. 8.7 and 8.8. The difference between Type2 Fuzzy Structure and Type1 Fuzzy lies on almost the end of the block. In Type2 Fuzzy there is a type reducer block, which change from Type2 Fuzzy 3 dimensional back to Type1 Fuzzy 2 dimensional so the output can become crisp output. Type2 Fuzzy in general form very difficult to running at a real time. So, Fast Geometric Defuzzification used in this paper. The theory and the calculations of crisp input until became to an output explained more detail in other our publications [5, 6, 7, 8].

### 8.4 Experiments Results and Discussions

In the experiments, we got flight data through Bluetooth that sent data to our laptop in ground station. We had 1 experiment with five times of flight to get validate data. In this paper, we only gave just one flight data from five data that we had. To simulate an extreme altitude change as a disturbance, our pilot make a + pitch and - pitch maneuver which in the middle there is a box with 50 cm height. The results can be shown in Fig. 8.9.

The disturbance is shown as a red circle. After the extreme altitude change, around 50 cm, we tested how the control method will draw back to the desired height. Because in the real applications it can be happened suddenly. For the quick response after getting a disturbance Type1 Fuzzy and follow with Fuzzy-PID

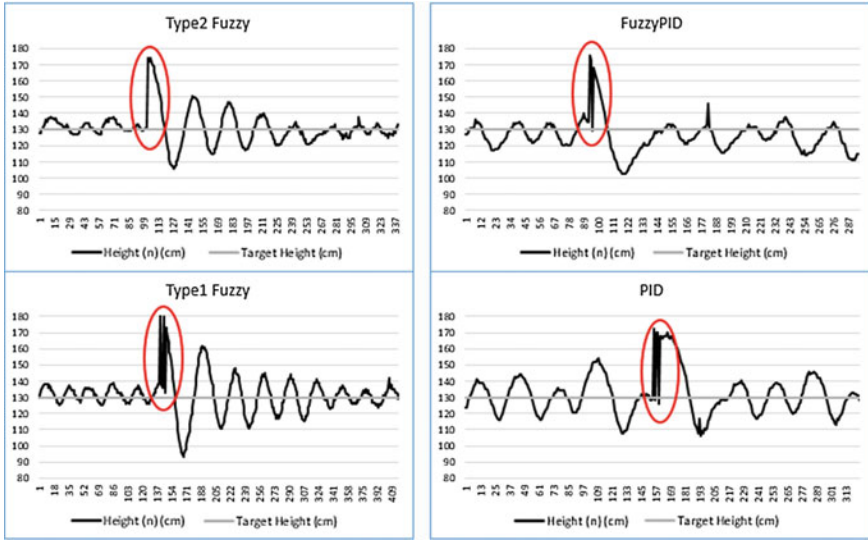


Fig. 8.9 Experiments results

showed a better performance than the Type2 Fuzzy. But, for that quick response, both controllers suffered with bigger oscillations before it came back to it’s desired height. They also took longer time than the Type2 Fuzzy. In overall, Type2 Fuzzy is better than the others. Thus this experiment is actually strongly confirmed the other research about Type2 Fuzzy controller which can solve high order non-linearity systems.

### 8.5 Conclusion

This paper describes a benchmarking between three control methods are Type2 Fuzzy, Type1 Fuzzy, and Fuzzy-PID. There are two important parameters in this benchmarking paper, such as the response of QuadRotor to get the height target, and oscillation happened while the QuadRotor maintain their height target. In a fast response to get their height target, a Type1 Fuzzy is the best one, then followed by Fuzzy-PID, and then Type2 Fuzzy. And for the an oscillation while maintain the height target, Type2 Fuzzy is the best one, then Type1 Fuzzy, and the last is Fuzzy-PID. For future works, a still going re-search is using the camera as a height sensor.



## References

1. Cazarez-Castro, N., Aguilar, L., Castillo, O.: Designing type-1 and type-2 fuzzy logic controllers via fuzzy Lyapunov synthesis for nonsmooth mechanical systems. *Eng. Appl.* **25**(5), 971–979 (2012)
2. Coupland, S., John, R.: A fast geometric method for defuzzification of Type-2 fuzzy sets. *IEEE Trans. Fuzzy Syst.* **16**(4), 929–941 (2008)
3. Meza, J.L., Santibanez, V., Soto, R., Llama, M.A.: Fuzzy self-tuning PID semiglobal regulator for robot manipulators. *IEEE Trans. Ind. Electron.* **59**(6), 2709–2717 (2012)
4. Sanchez, E.N., Becerra, H.M., Velez, C.M.: Combining fuzzy, PID and regulation control for an autonomous mini-helicopter. *Inf. Sci. (Ny)* **177**(10), 1999–2022 (2007)
5. Wicaksono, H., Christophorus, B.: T1-Fuzzy vs T2-Fuzzy stabilize Quadrotor Hover with payload position disturbance. *Int. J. Appl. Eng. Res.* **9**(22), 17883–17894 (2014)
6. Wicaksono, H.: Fast geometric T2-Fuzzy based improved lower extremities stimulation Response. *Telkomnika*, 207–216 (2010)
7. Wicaksono, H., Gunawan, Y., Olifianto, B., Haryanto, L.: Neural Network Backpropagation vs Fuzzy-PID controller based on Quadcopter altitude lock using sonar sensor. In: *Seminar Nasional Teknologi Terapan*, No. 5, issue no. 8, pp. 4–7 (2014)
8. Wicaksono, H., Yusuf, Y.G., Yodinata, A.: Altitude lock design for QuadCopter using sonar based on fuzzy controller. In: *Digital Information System Conference* (2014)

# Chapter 9

## Indonesian Dynamic Sign Language Recognition at Complex Background with 2D Convolutional Neural Networks

Nehemia Sugianto and Elizabeth Irenne Yuwono

**Abstract** As the media of communication for people with hearing and speech disabilities, the importance to bridge the communication gap between them and normal people using sign language has become significance. This research proposed a model for the development of sign language recognition technology using Microsoft Kinect and convolutional neural network (CNNs). The proposed model succeeds in recognizing 10 dynamic Indonesian sign language words on complex background. There are total of 100 gesture image sequences containing color and depth data, perform by different users. The classifier consists of two CNNs and one ANN. The first CNN is to extract hand feature from color data, while the other is to extract hand feature from depth data. The training consists of three modes by applying drop-out and data augmentation and achieves the highest validation rate on 81.60 % and test result on 73.00 %.

**Keywords** Computer vision · Convolutional neural network · Deep learning · Hand gesture recognition · Indonesian sign language recognition

### 9.1 Introduction

According to World Health Organization (WHO) Media Centre, over 5 % of world population have disabling hearing loss worldwide, approximately 360 million people consisting of 328 million adults and 32 million children [1]. Currently there are some assistive method for hearing loss, such as hearing aids, implants or assistive device, and sign language. Despite the high number of people with hearing loss, the current production of hearing aids only meets less than 10 % of them. Sign language has been the media of communication for deaf and people with speech impairments. Sign language relies heavily on visual representation based on hand

---

N. Sugianto (✉) · E.I. Yuwono  
Universitas Ciputra, UC Town Citraland, Surabaya 60219, Indonesia  
e-mail: nsugianto@ciputra.ac.id

shape, pose, or gesture. Therefore research related to sign language recognition is concentrated in computer vision and language understanding.

Despite its great demand, there are still many people with disability who do not understand sign language since they never receive any education about sign language. Besides there are communication gap between people with disability and normal people, since normal people mostly do not understand sign language. This research is focusing on the development of sign language recognition technology for communication and education purpose.

## 9.2 Related Works

Currently researches related to sign language is divided into two concentration, they are for recognition of static and dynamic sign language. Static sign language is defined as sign language using hand pose, finger shape as representation. While dynamic sign language uses gestures as representation. Currently researches related to static sign language recognition have progressed to various method, they are based on skin color, custom made color gloves, and finger detection [2].

Dynamic sign language recognition is related to gesture recognition, latest researches used various method based on gesture videos. We uses Microsoft Kinect as sensor device as the approach of [3] in extracting appearance-based hand features and track the hand position in 2D and 3D. The features were classified by comparing Hidden-Markov Model and sequential pattern boosting. The accuracy result on isolated gestures was 99.9 and 85.1 % on more realistic gestures. The depth data from Kinect could be used to improve data validity as [4], where they used spatio-temporal features on images from RGB camera and depth map for gesture analysis. Using Convolutional Neural Network for classification as [5, 6] has proven to give successive result. The first used two Convolutional Neural Network each with 3 layers deep for hand and upper body extraction from gray scaled images. They applied dropout and data augmentation in training to reduce overfitting and result in 91.7 % validation accuracy. While the latter used three-dimensional Convolutional Neural Network on normalized gesture videos. There are two subnetworks with 4 layers each; one is for high resolution network (HRN) and the other is for low resolution network (LRN). The classification rates on VIVA Challenge dataset is 77.5 %.

## 9.3 Method

This research used Convolutional Neural Network classifier for dynamic sign language recognition based on Indonesian Sign Language System (Sistem Bahasa Isyarat Indonesia—SIBI). Section 9.3.1 described the data set used based on pre-recorded video samples of SIBI. Section 9.3.2 described the preprocessing steps

of video data set for classifier. Section 9.3.3 described the classification process using Convolutional Neural Network (Fig. 9.1).

### 9.3.1 Data Set

The data set was recorded by Microsoft Kinect sensor version 1 to obtain the RGB image sequences, depth data, and skeleton data. There are total of 100 images sequences containing 10 dynamic sign language words with different variations in gesture movement. The gestures were performed by 2 users (one man and one woman) within age range of 20-30 years with different height. The users were given simple training in performing sign language before data collecting to meet SIBI quality standard. From 100 images sequences obtained, 80 % were used for training while the other 20 % were used for classifier experiment.

### 9.3.2 Preprocessing

There are four phases in preprocessing the dataset before classified. The first phase is system initialization to prepare the suitable environment. Using the skeleton data

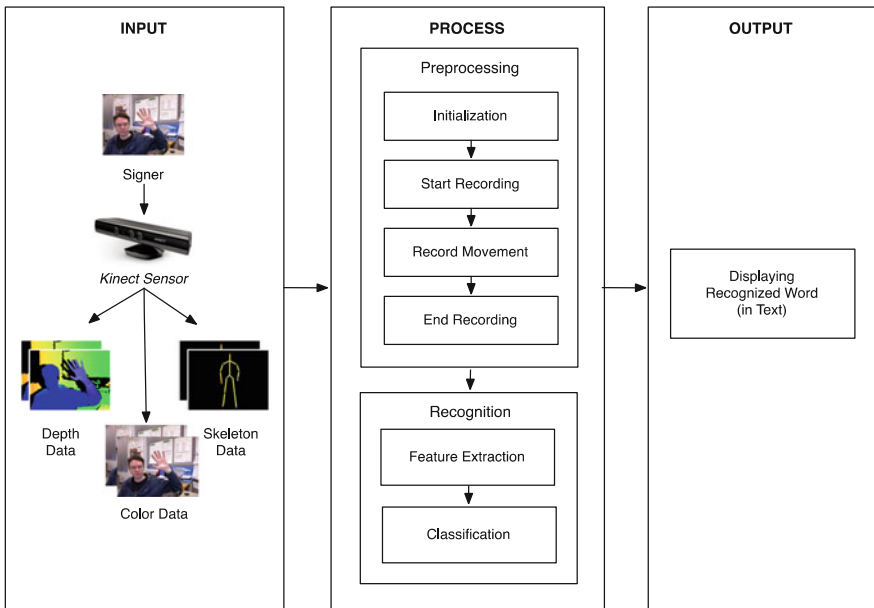


Fig. 9.1 Model Architecture of Indonesian sign language recognition system

obtained from Kinect sensor, system detected user existence and their number. System only continued if only one user is detected. Then system checked whether user hands are not blocked by anything and detected by Kinect sensor. When user is ready to start recording, system will validate by ensuring that both hands are in front of user body. The first phase of data preprocessing is shown by Fig. 9.2.

The second phase is the beginning of gesture recording as shown in Fig. 9.3. On the beginning of recording, system save the position of user left hand and right hand to be used as pivot for the gesture. Figure 9.4 shows the next phase; gesture recording. In this phase there are two kinds of images saved. First is from RGB camera of Kinect and the other is depth data from Kinect infrared camera. These two data are save consequently until both hands stop moving.

The next phase is preparing the image sequences to be ready for classifier as shown in Fig. 9.5. Both Color Data and Depth Data receive the same treatments for the first 4 processes. They were normalized into 32 frames each by eliminating image if the difference between current and previous hand position is too close. And

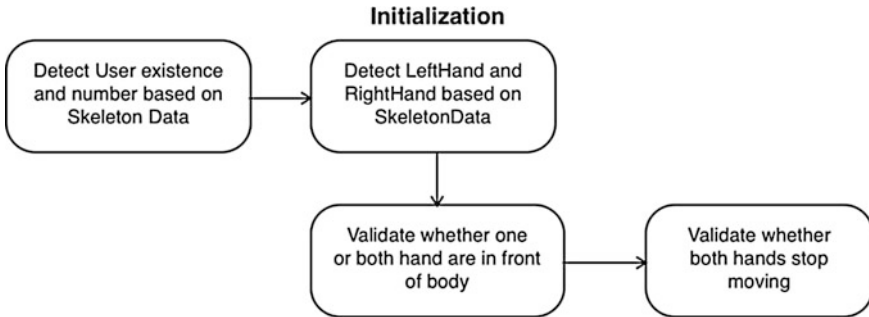


Fig. 9.2 Preprocessing phase: initialization



Fig. 9.3 Preprocessing phase: start recording

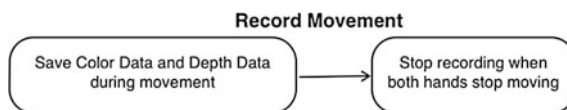
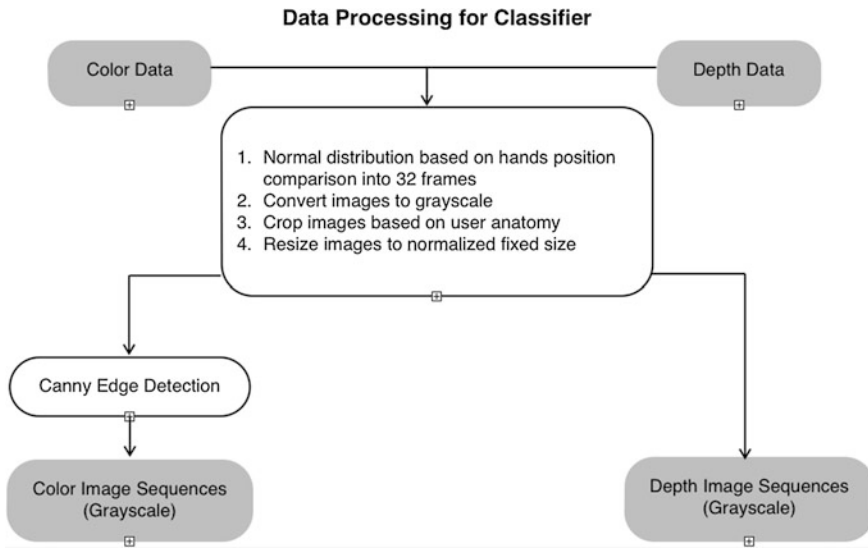


Fig. 9.4 Preprocessing phase: record movement



**Fig. 9.5** Preprocessing Phase—Image Processing for Classifier

then they were converted to gray scaled images. Each image is cropped around gesture area. The width is calculated from the widest area between left and right hand among gestures, and the height is obtained from the highest head position and lowest hip center position among gestures. After that, all images is resize to fixed size of  $256 \times 256$  pixels. The result is 32 gray scaled images from Color Data and 32 gray scaled images from Depth Data.

### 9.4 Proposed Architecture

The architecture of model consists of two CNNs and one ANN. CNNs are used to extract features and ANN is used to classify the features into classes. The architecture is depicted in Fig. 9.6.

First CNN is for extracting hand features from color data and second CNN is for extracting hand features from depth data with network parameter  $W_C$  and  $W_D$ , respectively. Each network, with parameters  $W$ , produced class-membership probabilities  $(P(C|x,W))$  for classes  $C$  given the gesture’s observation  $x$ . We multiplied the class-membership probabilities from the two CNN element-wise to compute the final class-membership probabilities for the gesture classifier as described in Eq. 9.1:

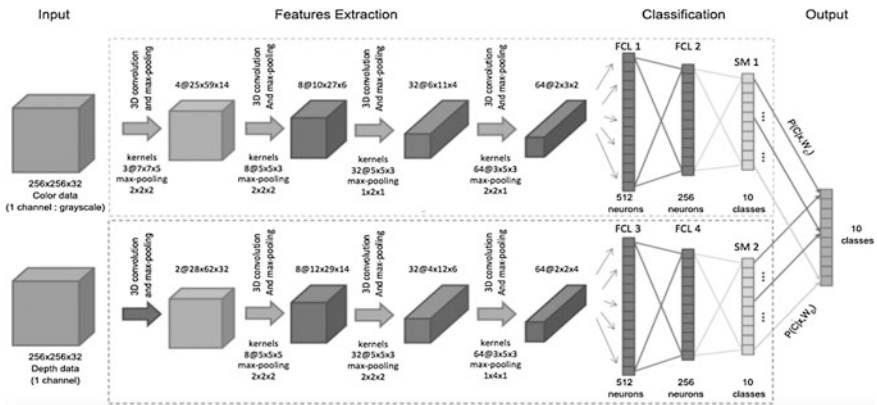


**Fig. 9.6** The proposed architecture of Indonesian sign language recognition system using two CNNs and one ANN. This figure only shows one of two identical CNNs

$$P(C|x) = P(C|x, W_L) \times P(C|x, W_H) \tag{9.1}$$

The first CNN consists of four 2D convolution layers which each layer is followed by the max-pooling operator, two fully connected layers and an output softmax layer that estimates the class-membership probability  $P(C|x, W_C)$ . The input of this CNN is images sequences in color data (256 pixels  $\times$  256 pixels  $\times$  32 frames). In Fig. 9.6 shows the sizes of the convolutional kernels, volumes at each layer and the max-pooling operator.

The second CNN consists of four 2D convolution layers which each layer is followed by the max-pooling operator, two fully connected layers and an output softmax layer that estimates the class-membership probability  $P(C|x, W_C)$ . Two fully connected layers and an output softmax layer are called ANN. The input of this CNN is images sequences in depth data (256 pixels  $\times$  256 pixels  $\times$  32 frames). In Fig. 9.6 shows the sizes of the convolutional kernels, volumes at each layer and the max-pooling operator.

The ANN is used to provide classification after concatenating the outcomes of both CNNs. ANN has three layers: one input layer, one hidden layer and one output layer. Input layer has 512 neurons. Hidden layer has 256 neurons (is obtained from two-thirds of number of neurons in input layer and output layer). The activation function that is used in this layer is sigmoid biner. The output value range of the activation function is from 0 to 1. Output layer has 10 neurons which is the number of gestures that can be recognized by the model. The activation function that is used in this layer is sigmoid biner. The output value range of the activation function is from 0 to 1. We used threshold function to produce the final value in range of 0–1. If the output value is smaller than 0.8 then the final value is 0. If the output value is equal and larger than 0.8 then the final value is 1. The neuron which has value of 1 is selected as the recognized gesture.

## 9.5 Results and Discussion

To reduce overfitting, data augmentation is used to produce additional data samples. Data augmentation is performed in real time on the CPU during collecting data samples. There are six methods used in data augmentation: spatial translation up to 10 pixels in x and y directions (-10 and +10), rotation up to 10° (-10° and +10°), scaling up to 10 % (-10 % and +10 %).

We used 20 images sequences (20 %) from 100 images sequences as training data set (20 in color and depth data, respectively). Each images sequence has 32 frames. Using data augmentation, we had 140 images sequences as training data set (140 in color and depth data, respectively).

The two CNNs used Nesterov’s accelerated gradient descent (NAG) with a fixed momentum coefficient 0.9, mini batches of size 20 and learning rate is initialized at 0.003 with a 5 % decrease after each epoch. The weights are randomly initialized with a normal distribution. The biases are initialized at 0.2.

Experiments are conducted on one machine with a processor (2.4 GHz Intel Core i5), 4 GB DDR3 and Intel HD Graphics 3000 384 MB. The models are implemented using MatConvNet—Convolutional Neural Networks for MATLAB by A. Vedaldi and K. Lenc [7].

We evaluated the performance of the model using several scenarios of training dataset in order to prevent over fitting. Data augmentation and drop-out method were used to get successful generalization of the classifier. First scenario was using existing training dataset collected. Second scenario was using existing training dataset collected and drop-out. Third scenario was using existing training dataset collected, drop-out and data augmentation.

The validation results of the experiments are shown in Table 9.1. The accuracy rate of the model using existing training dataset was 71.90 % (28.10 % error rate). The accuracy rate of the model using existing training dataset and drop-out was 74.40 % (25.60 % error rate). The accuracy rate of the model using existing training dataset, dropout and data augmentation was 81.60 % (18.40 % error rate). The highest accuracy (81.60 %) was obtained when the model was trained using existing dataset, dropout and data augmentation. The accuracy on the test data set is 73.00 % (Table 9.2).

**Table 9.1** Validation results

Training scenario	Accuracy rate (%)	Error rate (%)
Existing training dataset	71.90	28.10
Existing training dataset + Drop-out	74.40	25.60
Existing training dataset + Drop-out + Data Augmentation	81.60	18.40



**Table 9.2** The confusion matrix of proposed final model

Class Output	Almari	Analisis	Biola	Bola	Buka	Dasi	Kayu	Namun	Rumah	Voli
Almari	7	2	0	1	0	0	0	0	0	0
Analisis	1	6	0	1	2	0	0	0	0	0
Biola	0	0	9	0	0	0	1	0	0	0
Bola	1	0	0	8	0	0	0	0	1	0
Buka	0	2	0	0	8	0	0	0	0	0
Dasi	0	0	0	0	0	6	0	2	2	0
Kayu	0	0	1	0	0	0	8	0	1	0
Namun	0	0	0	0	0	2	0	7	0	1
Rumah	0	0	0	0	0	2	1	0	6	1
Voli	1	0	0	0	0	0	0	1	0	8

## 9.6 Conclusion

The proposed model has proven to demonstrate considerable result for the recognition of dynamic Indonesian sign language. The highest validation result is achieved from training model that used existing training dataset with drop-out and data augmentation applied, it is 81.6 %. The test result is 73 %. The model used convolutional neural network to analyze gestures in complex background and quite robust in terms of user variants.

## References

1. World Health Organization.: Media Centre Fact Sheets on Deafness and Hearing Loss (2015)
2. Kyatanavar, R.D., Futane, P.R.: Comparative study of sign language recognition systems. *Int. J. Sci. Res. Publ.* **2**(16) (2012)
3. Cooper, H., Ong, E.J., Pugeault, N., Bowden, R.: Sign language recognition using sub-units. *J. Mach. Learn. Res.* **13**(1), 2205–2231 (2012)
4. Memis, A., Albaryak. S.: A kinect based sign language recognition system using spatio-temporal features. In: *Proceedings of SPIE (The International Society for Optical Engineering)* (2013)
5. Pigou, L., Dieleman, S., Kindermans, P., Schrauwen, B.: Sign language recognition using convolutional neural networks. *Lect. Notes Comput. Sci.* **8925**, 572–578 (2015)
6. Molchanov, P., Gupta, S., Kim, K., Kautz, J.: Hand gesture recognition with 3D convolutional neural network. *IEEE Comput. Vis. Pattern Recognit. (CVPR)* (2015)
7. Vedaldi, A., Lenc, K.: MatConvNet—Convolutional Neural Networks for MATLAB. *CoRR*, vol. abs/1412.4564 (2014)

# Chapter 10

## Image-Based Distance Change Identification by Segment Correlation

Nemuel Daniel Pah

**Abstract** Image-based distance identification is an interesting topic in image processing. It can be classified into three methods. The parallax approaches, the method with marker and the method with a priori knowledge of an object's physical size. The above methods are not easily implemented in an embedded system. This paper reports the development of an efficient image-based algorithm to identify the change of distance between camera and the captured object by measuring the movement of objects in the image. The algorithm is designed to work on a single camera without the aid of image markers such as laser beams. The algorithm calculates the correlation of predefined segments in the image to detect object movements, and therefore identify the direction and magnitude of distance change. The algorithm was designed to be implemented in a quadcopter to identify its change of altitude. The performance of the algorithm was examined using a simulated environment, and is reported in this paper.

**Keywords** Image processing · Distance measurement · Segment correlation

### 10.1 Introduction

The research that is reported in this paper was conducted to develop image-based algorithm that is able to sense the change of distance between a camera and the captured object. The algorithm was developed to be applied in a quadcopter as a sensor to provide information about altitude change to its controller.

The algorithm of image-based distance measurement system can be grouped into three main methods. The parallax method [1–3] uses two cameras or a combination of mirrors to capture two or more images from different perspectives. The second method measures object distance with an aid of markers. Barreto [4] and

---

N.D. Pah (✉)

Electrical Engineering, University of Surabaya, Surabaya, Indonesia  
e-mail: nemuelpah@staff.ubaya.ac.id

Muljowidodo [5] developed distance measurement algorithm based on triangulation of a single laser beam, while Deng [1] and Lu [6] used two parallel laser beams projected to the object. The other methods [7, 8] based their calculation on the knowledge of the physical size of objects in image. Such requirements are not easily implemented in a quadcopter due to its limitation in weight and computational capability. In [9], the author reported an algorithm to identify distance (altitude) change by observing the shift of gray level function in ten preselected rows in the image. The algorithm was able to identify distance change with an accuracy of more than 96 % but with a success rate of only 76 %.

This paper reports the development of another efficient image-based algorithm to identify the change of distance by calculating the correlation of predefined segments in the image to identify object's movement near the left and right edges of the image's frame. The current development of the algorithm reported in this paper shows a promising result. The algorithm can identify altitude change with an accuracy of above 97 %.

## 10.2 The Proposed Algorithm for Distance Change Identification

This section elaborates the proposed image-based algorithm to identify distance change between a camera and the captured object. The algorithm is based on image frames captured from a single facing down camera, mounted on the body of a quadcopter. The algorithm is designed to be simple and efficient in terms of computational complexity, computational time, and memory usage.

The fundamental principle of the algorithm is to detect the movement of objects in the captured frames. It is assumed that objects in the image move to the edge of the frame if the camera gets closer to the ground, and vice versa.

### 10.2.1 Preprocessing

The algorithm calculates object's movement by comparing images of two consecutive frames, i.e. the reference frame,  $I(x,y)$ , and the comparing frame,  $I'(x,y)$ . The image frames are grayscale image captured from an 8-bit RGB camera ( $460 \times 640$  pixels at 30 fps).

The algorithm only calculates the movement of objects inside two selected segments located near the left and right edges of the image frame, where object movements due to distance change are more observable. The segments,  $R_L$  and  $R_R$ , are sub-images of the reference frame,  $I(x,y)$ , with a size of  $15 \times 15$  pixels, as illustrated in Fig. 10.1a.

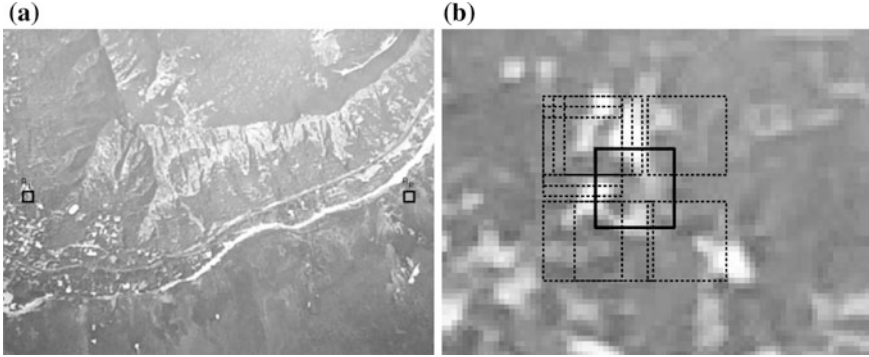


**Fig. 10.1** **a** The boxes,  $R_L$  and  $R_R$ , indicate the location of the referenced segments. **b** An illustration of some neighboring segments,  $R'_L$ , in the comparing frame,  $I'(x,y)$

$$R_L(m,n) = \{I(37+r, 247+s) \mid -7 < r < 7 \text{ and } -7 < s < 7\} \quad (10.1)$$

$$R_R(m,n) = \{I(602+r, 247+s) \mid -7 < r < 7 \text{ and } -7 < s < 7\} \quad (10.2)$$

## 10.2.2 Object Movement Identification

The direction and magnitude of object's movement is calculated by searching the relative location of  $R_L$  and  $R_R$  in the comparing image frame,  $I'(x,y)$ . The search is performed by calculating the correlation function between the reference segment ( $R_L$  or  $R_R$ ) and its neighboring segments,  $R'_R$  or  $R'_L$ , in the comparing frame,  $I'(x,y)$ .

$$C_L(i,j) = \langle R_L, R'_{Li,j} \rangle \text{ and } C_R(i,j) = \langle R_R, R'_{Ri,j} \rangle \quad (10.3)$$

The algorithm uses 400 neighboring segments on each side. The neighboring segments are the overlapping segments around the location of  $R_R$  or  $R_L$  with a size of  $15 \times 15$  pixels (as shown in Fig. 10.1b). The segments are expressed with:

$$R'_L(m,n)_{i,j} = \{I'(x+i, y+j) \mid i = 20:40, \text{ and } j = 230:250\} \quad (10.4)$$

$$R'_R(m,n)_{i,j} = \{I'(x+i, y+j) \mid i = 585:605, \text{ and } j = 230:250\} \quad (10.5)$$

The movement vector is the vector from the centroid of  $R_R$  or  $R_L$  to the centroid of the local maxima in  $C_L(i,j)$  or  $C_R(i,j)$ . By assuming that the centroid of  $R_R$  or  $R_L$  is at the origin, the movement vector is defined by:

$$v_R = \arg \max_{i,j} C_R(i,j) \text{ and } v_L = \arg \max_{i,j} C_L(i,j) \quad (10.6)$$

### 10.2.3 Distance Change Identification

The altitude change is identified by analyzing the two movement vectors,  $v_L$  and  $v_R$ . The direction of the vectors may indicate four basic movements of the camera, as illustrated in Fig. 10.2.

To identify the direction and amount of distance change, the algorithm calculates only the projection of the vectors along the x-axis,  $v_{Lx}$  and  $v_{Rx}$ . The distance increases if both vectors are pointing inward, vice versa. The amount of change,  $d$ , is proportional to the average of the two vectors. The distance change is considered to be absent if both vectors are pointing to the same direction, or having zero magnitude. The proportional coefficient,  $k$ , is determined by the initial altitude,  $h$ , and the horizontal size of the image frame (640 pixels).

$$d = k \frac{v_{Lx} + v_{Rx}}{2} \quad \text{with} \quad k = \frac{2h}{640} \quad (10.7)$$

If the initial altitude,  $h$ , is unknown, the change of distance,  $d$ , is expressed as the proportion or percentage of  $h$ .

The algorithm is designed to be simple in terms of computational complexity, computational time, and memory usage. The complexity of the algorithm is due to the correlation function,  $O(N^2)$ . However, the algorithm consumes a relatively large memory space. In total, the algorithm needs almost 3 kbytes of memory space.

## 10.3 Experimental Results and Discussions

The algorithm was examined using a simulated environment as that in [9]. The images were captured using Live Cam VX-800, 8-bit RGB web camera with a resolution of  $480 \times 640$  pixels. The camera was mounted on a moveable platform

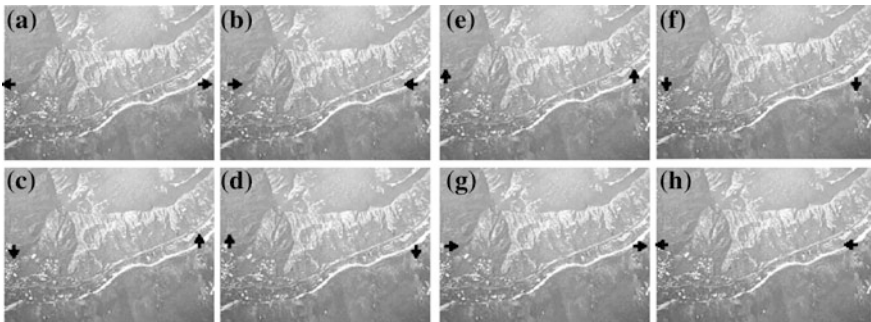


**Fig. 10.2** The direction of the vectors  $v_L$  and  $v_R$  that indicates camera movement, i.e. **a** decrement of distance, **b** increment of distance, **c** clockwise rotation, **d** anti-clockwise rotation, **e** downward, **f** upward, **g** left, and **h** right

that was able to simulate some movements of the quadcopter. The simulated movements were the change of altitude (representing change of distance) along the z-axis, rotation of camera while maintaining its distance, and horizontal translation to both the x-axis and y-axis. A poster of aerial view was placed in front of the camera at a predetermined distance (altitude) to simulate ground view.

### 10.3.1 Experiments with Various Change of Distance

In the first experiment, 20 frames were recorded from the camera at various different distances (z-axis) that represent distance changes from  $\pm 0.00$  to  $\pm 0.04$  m. The frames were recorded while maintaining the camera rotation and translation. The first frame was recorded at an altitude of  $h = 0.70$  m. The experiment was conducted to investigate the ability of the algorithm to identify the change of distance. The results are shown in Fig. 10.3.

The results show that the algorithm could predict distance change accurately (with an error below 0.005 m) from frame 1 to 11 when the distance change was below 0.02 m. As the distance change was increased to a value above 0.02 m, the algorithm failed to identify this change. The error increased to an unacceptable rate.

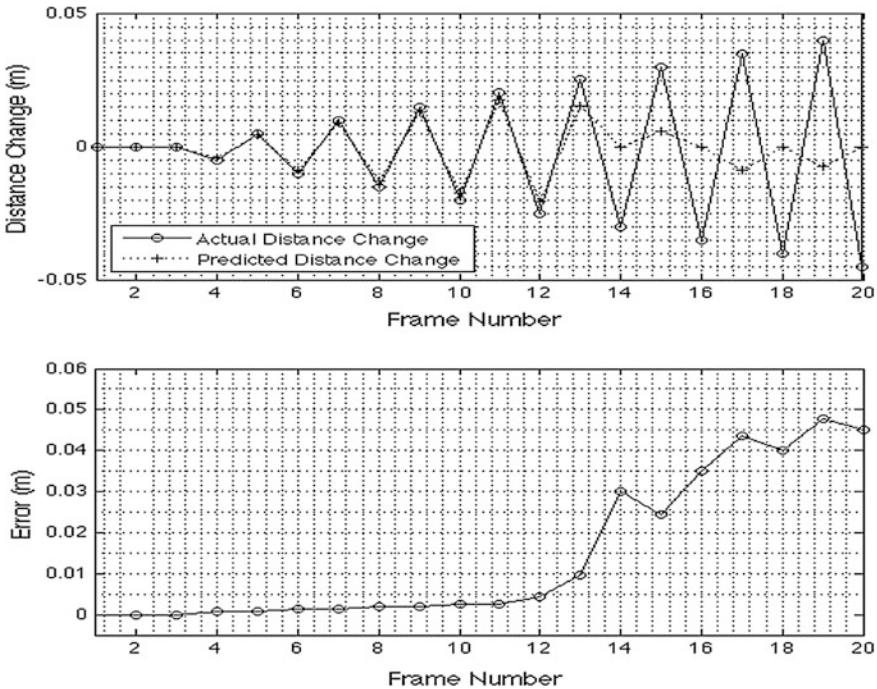


Fig. 10.3 The predicted distance change and error of experiment with variation of distance

The limitation of the algorithm was caused by the distribution of the neighboring searching segments as explained in Sect. 10.2.2. The algorithm is only sensitive to a distance change of up to 0.0219 m (equivalent to 3.12 % of its original distance).

### 10.3.2 Experiments with Translational Movement

The second experiment was conducted to investigate the algorithm’s ability to compensate horizontal translation to both x-axis and y-axis. In the experiment, 25 frames were recorded from the camera at a constant altitude (z-axis) of 0.60 m, while translated along the x-axis and y-axis as shown in Table 10.1. The results, shown in Fig. 10.4, confirm that the algorithm was able to compensate the

**Table 10.1** The x-axis and y-axis (in cm) translations of the frames in Fig. 10.5

Frame	1	2	3	4	5	6	7	8	9	10	11	12	13
x-axis	0.0	0.0	0.5	1.0	1.5	2.0	2.0	1.5	1.0	0.5	0.0	-0.5	-1.0
y-axis	0.0	0.0	0.0	0.0	0.0	0.0	0.0	0.0	0.0	0.0	0.0	0.0	0.0
Frame	14	15	16	17	18	19	20	21	22	23	24	25	
x-axis	-1.5	-2.0	-2.0	-1.5	-1.0	-0.5	0.0	0.0	0.0	0.0	0.0	0.0	
y-axis	0.0	0.0	0.0	0.0	0.0	0.0	0.0	1.0	2.0	0.0	-1.0	-2.0	

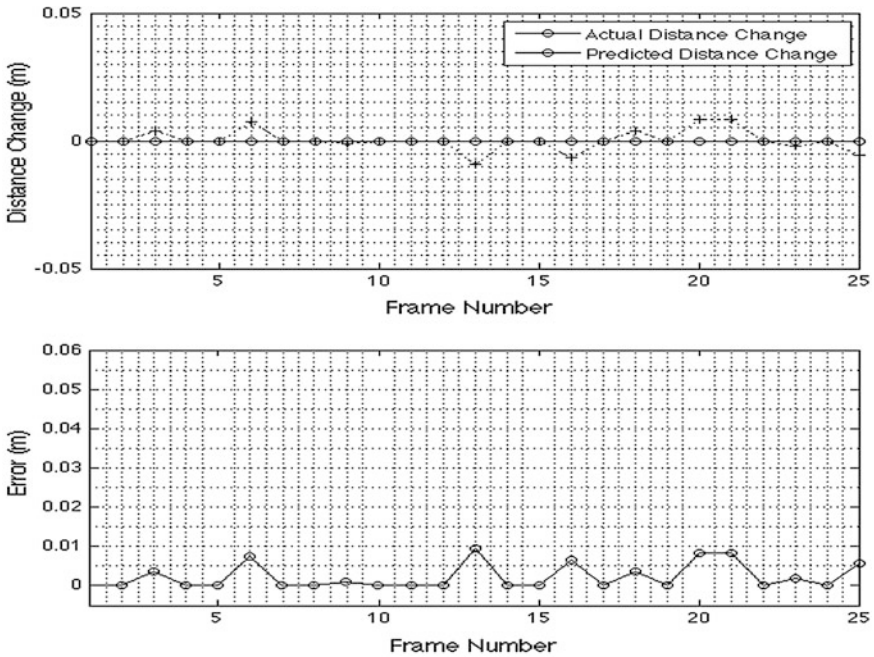


**Fig. 10.4** The predicted distance change and error of experiment with translational movement

translational movement with the maximum error of less than 0.01 m (equivalent to 1.67 % of the initial distance). The error was due to the algorithm’s misinterpretation of other objects as if it was the shift of the original object in  $R_R$  or  $R_L$ . The misinterpretation may occur if the captured images consist of flat, monotone, or periodic texture.

### 10.3.3 Experiments with Rotational Movement

This experiment was conducted to investigate the algorithm’s ability to compensate rotation movement. In this experiment, 9 frames were recorded from the camera at a constant altitude (z-axis) of 0.50 m, while rotating around z-axis. The results, shown in Fig. 10.5, confirm that the algorithm was able to compensate the rotational movement with the maximum error of less than 0.015 m (equivalent to 3 % of the initial distance). The error was also due to the algorithm’s misinterpretation of other object as if it was the shift of the original object in  $R_R$  or  $R_L$ . As with the

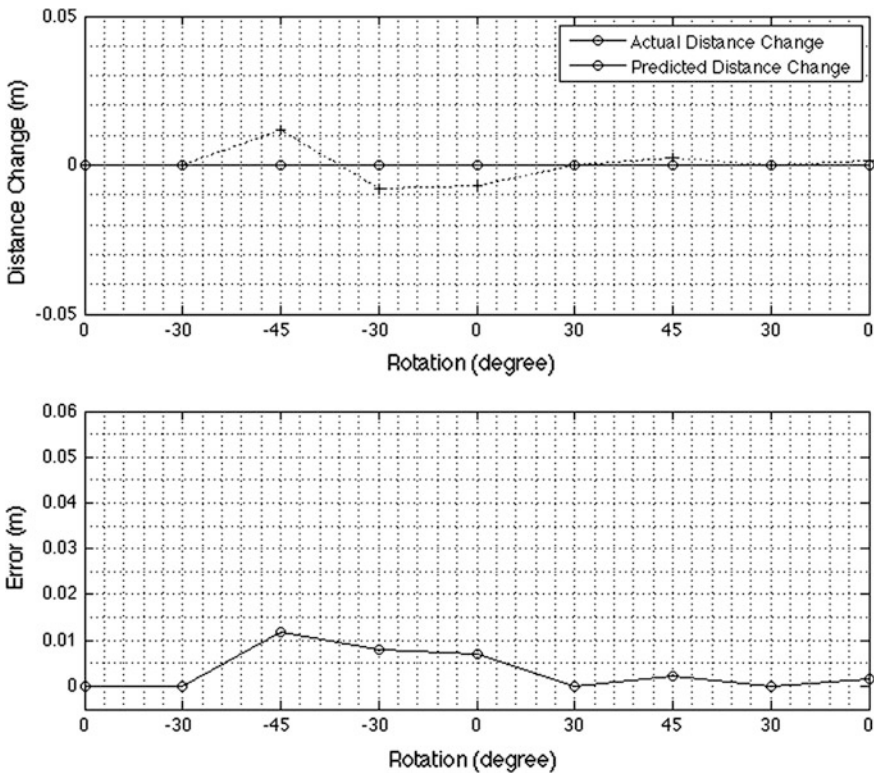


Fig. 10.5 The predicted distance change and error of experiment with rotational movement



translational case, the misinterpretation may occur if the captured images consist of flat, monotone, or periodic texture.

## 10.4 Conclusion

This paper presents an image-based algorithm to identify the change of distance based on correlation of reference segments. The algorithm was able to identify distance change of up to 3.12 % of its initial distance with inaccuracy of more than 97 %, and is able to compensate horizontal and rotational movement. The future suggested development of the algorithm would be the simplification of computational complexity from  $O(N^2)$  to  $O(N)$ , the approach to reduce the number of needed memory, and the improvement of the algorithm accuracy.

## References

1. Deng, L.Y., Tang, N.C., Shih, T.K., Lee, D.L., Cheng, Y.H., Lo, K.Y.: The development of image-based distance measurement system. *J. Internet Technol.* **10**(1) (2009)
2. Kim, H., Lin, C., Song, J., Chae, H.: Distance measurement using a single camera with a rotating mirror. *Int. J. Control Autom. Syst.* **3**(4), 542–551 (2005)
3. Hsu, T., Wang, T.: An improvement stereo vision images processing for object distance measurement (2013)
4. Barreto, S.V.F., Sant'Anna, R.E., Feitosa, M.: A method for image processing and distance measuring based on laser distance triangulation. In: *IEEE 20th International Conference on Electronics, Circuits, and Systems (ICECS)*, pp. 695–698 (2013)
5. Muljowidodo, K., Mochammad Rasid, A., Budiyo, A.: Distance measurement, laser spot identification, innovative measuring system. *Indian J. Mar. Sci.* **38**(3), 324–331 (2009)
6. Lu, M.C., Wang, W.Y., Chu, C.Y.: Image-based distance and area measuring systems. *IEEE Sens. J.* **6**(2), 495–503 (2006)
7. Deshmukh, M.P.D., Dhok, P.G.P.: Analysis of distance measurement system of leading vehicle. *Int. J. Instrum. Control Syst.* **2**(1), 11–23 (2012)
8. Rahman, A., Salam, A., Islam, M., Sarker, P.: An image based approach to compute object distance. *Int. J. Comput. Intell. Syst.* **1**(4), 304–312 (2008)
9. Pah, N.D., Hermawan, H.: The development of image-based algorithm to identify altitude change of a quadcopter. In: *Accepted to be presented in the 7th International Conference on Information Technology and Electrical Engineering (ICITEE)* (2015)

# Chapter 11

## Situation Awareness Assessment Mechanism for a Telepresence Robot

Petrus Santoso and Handry Khoswanto

**Abstract** There are several metrics to evaluate about the sophistication of a telepresence robot. One of them is concerning operator performance especially about Situation Awareness (SA). There are many ways to enhance their awareness about situation and environment in the remote side. To do an evaluation, this paper want to propose a mechanism to do an SA assessment on a telepresence robot. The proposed mechanism is basically based on a query that randomly displayed to the operator. The operator will quickly respond to the query on the telepresence robot user interface. The query is used to assess SA, therefore all SA requirements from perception to prediction will be accommodated. The mechanism is developed and implemented on the telepresence robot prototype. Some users tried to operate and respond to the assessment queries. The user response can be stored and retrieved to be processed further to do an SA assessment. The mechanism seems to be working and can be easily deployed to another telepresence robot as long as the protocol is compatible.

**Keywords** Telepresence · Robotic · Situation awareness

### 11.1 Introduction

To implement a functionally working telepresence robot, there are several metrics that need to be taken care of. Three groups of common metrics have been elaborated by Steinfeld et al. [1] namely: System Performance, Operator Performance and Robot Performance. System performance assessment concern with how well the human(s) and the robot(s) perform as a team. Operator Performance concern with situation awareness, workload and accuracy of mental models of device operation. Robot performance deal with robot self-awareness, human awareness and autonomy.

---

P. Santoso (✉) · H. Khoswanto  
Department of Electrical Engineering, Petra Christian University,  
JL. Siwalankerto 121-131, Surabaya 60236, Indonesia  
e-mail: petrus@petra.ac.id

This paper wants to focus on the situation awareness (SA) aspect of operator performance. By definition, SA is an understanding of the environment state (not ignoring the relevant system parameters) [2]. It is critical to subsequent decision making, operator performance and workload in many dynamic control tasks [3, 4]. Basically SA is a very important metric for controlling dynamic system. In this case, it is very important for a telepresence robot.

There are three defined levels of SA, namely perception, comprehension and projection [2]. Perception also called SA level 1. This level is achieved if the human operator is able to perceive the information needed to do the task via the interface. This is the basic level of SA. Comprehension is the next level, it is also called SA level 2. The human operator can interpret the perceived information correctly, alone or combined with other information at hand. Projection is the highest level, it is also called SA level 3. It is the ability to predict future event based on the current situation. To achieve the highest level of SA, the user interface must be designed to facilitate the acquisition of all the needed information.

To evaluate SA, there is a common query-based tool known as “Situation Awareness Global Assessment Technique” (SAGAT) [2]. The important aspect of using SAGAT is to do a detailed task analysis. The result of task analysis is used to formulate appropriate operator queries. These queries are used to measure SA [1]. The usual scenario using SAGAT is performed using a simulator. At a certain point of interest, the simulator is frozen randomly then the operator is directed to quickly answer queries about their current perception of the situation. All the queries should contain all SA requirements from level 1 (perception), level 2 (comprehension) and level 3 (projection).

In the case of telepresence robot, it is possible to use simulator to assess SA. In the other hand, the idea of this paper is to assess SA in real world scenario. Therefore there is a need to develop a mechanism to assess SA that enable the user to respond as fast as possible and not quite intrusive. The work presented in this paper focuses on the development of mechanism to assess SA, specifically for a telepresence robot.

## 11.2 System Design

The prototype of telepresence robot used in the development of SA assessment mechanism is implemented based on the ASP framework as depicted on Fig. 11.1.

The first step of the framework is defining an architecture based on a requirement analysis. Architecture design will be followed by the service design. Service design presents all of the Service Elements needed by the system. The last step is outlined the whole system protocol. The protocol will implement all of the Service Primitives on each Service Elements [5].

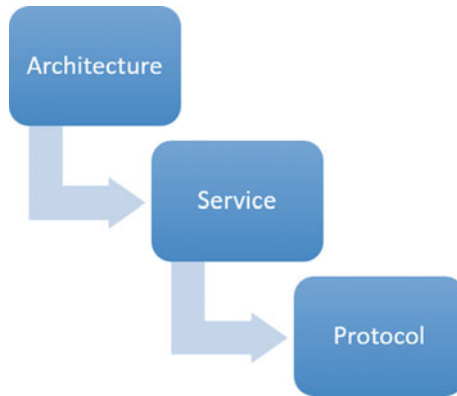


Fig. 11.1 ASP framework

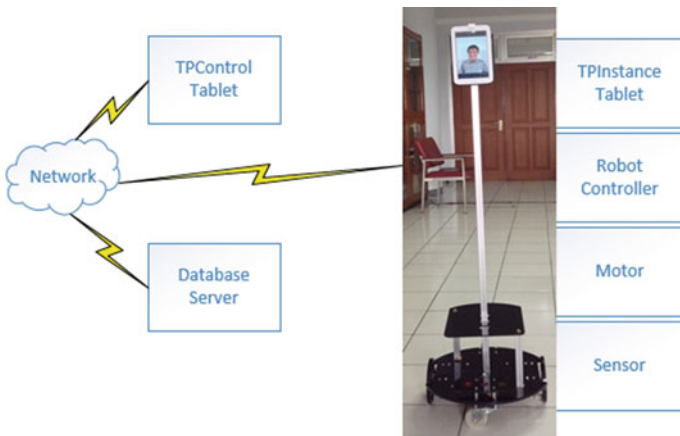


Fig. 11.2 Architecture of telepresence robot

The architecture of the telepresence robot are shown on Fig. 11.2. The system mainly consist of three entities, namely: TPControl Tablet, Telepresence Robot controlled by TPInstance Tablet and a database server. All three are connected through a computer network, whether it is local or global.

TPControl Tablet is the main control unit held by telepresence operator. This tablet is used to give command to telepresence robot and receive information given by telepresence robot. TPInstance Tablet is used as the receiving unit. It receives command from TPControl Tablet, interprets the received command and drives the robot accordingly. It also collects information from the available sensors and sends

**Table 11.1** Service primitive

Service element	Service primitive (SP)
Movement	Forward_Req
	Backward_Req
	Left_Req
	Right_Req
	Stop_Req
	Move_Ack
Monitoring	Video_Req
	Video_Ack
Video Call	Call_Req
	Disc_Req
	Add_Recipient_Req
	Remove_Recipient_Req
Auxiliary	Send_Robot_Status
	Send_Aux_Req
	Get_Aux_Req
	Aux_Ack
SA Assessment	SAQuery_Begin
	SAQuery_Req
	SAQuery_Respond
	SAQuery_Store
	SAQuery_Ack
	SAQuery_End

the information to the TPControl Tablet. The Database server is added to the system to collect user's responds concerning SA Query.

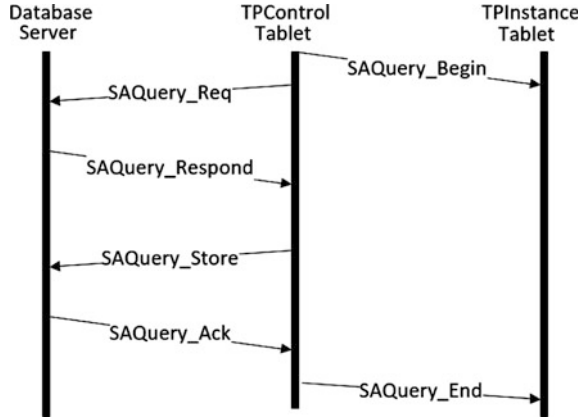
Focusing on the additional service for SA assessment, the revised service design from [5] is shown in the service primitives list on Table 11.1. The additional service element is printed in bold.

The SA Assessment service element deals with SA assessment mechanism. It is a sequence of SPs represent notification to the TPInstance Tablet and information exchange between TPControl Tablet and database server.

As for the protocol, a time sequence diagram for SA Assessment service is outlined at Fig. 11.3. The involved entities are TPControl Tablet, TPInstance Tablet and the database server.

The depicted time sequence diagram depicted the flow of SPs throughout SA Query process.

**Fig. 11.3** SAQuery time sequence diagram



### 11.3 SA Assessment Mechanism

The proposed SA Assessment tool is the SAGAT query tool. Some discussions have been done to do a detailed task analysis of telepresence robot. A database of SA Query has been developed. Some sample questions can be seen on Fig. 11.4.

The detailed SA Assessment mechanism can be seen also on Fig. 11.3. SAQuery\_Begin tells the TPInstance Tablet to pause all operations during SA Assessment. TPControl then retrieves SA questions from database server with

**(a)**

<p>Robot situation is:</p> <input type="checkbox"/> Normal <input type="checkbox"/> Cautionary <input type="checkbox"/> Troubled <input type="checkbox"/> I don't know	<p>Distance to Nearest object:</p> <input type="checkbox"/> < 1 m <input type="checkbox"/> 1 – 2 m <input type="checkbox"/> 2 – 5 m <input type="checkbox"/> > 5 m <input type="checkbox"/> I don't know
<p>Environment situation is:</p> <input type="checkbox"/> Normal <input type="checkbox"/> Cautionary <input type="checkbox"/> Dangerous <input type="checkbox"/> I don't know	<p>How many people are around:</p> <input type="checkbox"/> None <input type="checkbox"/> 1 <input type="checkbox"/> 2 – 5 <input type="checkbox"/> More than 5 <input type="checkbox"/> I don't know

**(b)**

Check all that apply:

 Crowded situation  
 At the intersection  
 Exit from the room  
 Entering a room  
 Nearby obstacles:  
      Ahead  
      Behind  
      Beside  
 Nearest People  
      In the left side  
      In the right side  
      Facing the robot  
      In the same direction

**(c)**

Is it safe to drive forward?

 Yes  
 No  
 I don't know

Write a short observation about robot situation:

**Fig. 11.4** SA Query examples **a** SA Level 1. **b** SA Level 2. **c** SA Level 3

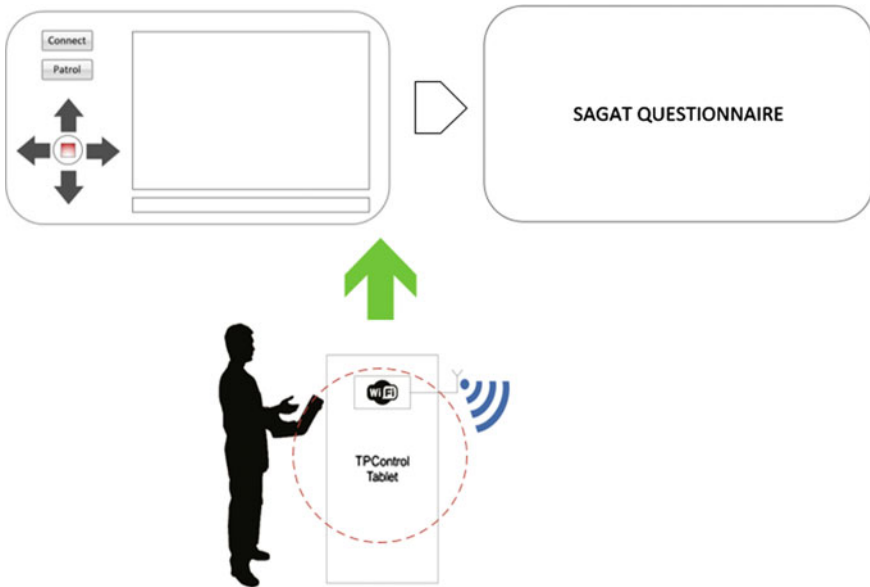


**Fig. 11.5** Interface of the SAGAT query

SAQuery\_Req. It is responded by SAQuery\_Respond. SA questions then displayed on TPControl Tablet. The operator responds, the result is sent to the database server by SAQuery\_Store. Acknowledge given by database server and TPControl Tablet tells TPInstance Tablet to resume all operations.

All the depicted mechanisms are mainly happened on the TPControl Tablet. An illustration of the interface as seen by telepresence operator is shown on Fig. 11.5.

## 11.4 Result and Discussion

The SA assessment mechanism has been implemented and deployed to a working telepresence robot. Several operators have been doing beta testing toward the SA assessment mechanism. After several beta testing, the implemented mechanism is considered suitable for real SA assessment process.

The result of beta testing can be summarized as follows. The designed mechanism is work as expected, TPInstance can be paused during SA assessment, SA query and response works, normal operation can be resumed after SA assessment. The time taken for a single SA assessment can be done below 5s for each displayed query. Most of the operators considered that the assessment method is still intrusive, but in the other hand can give a good insight on SA performance.

Further improvement can be made to make the mechanism less intrusive. SA query and respond can be stored locally and later synchronized to the database

server when the situation is possible. This mechanism will reduce the time needed to do an SA query and can be considered less intrusive.

## 11.5 Conclusion

The depicted mechanism in this paper can be considered working without problem. It is easily deployed to all our current prototypes of telepresence robot. It is a useful assessment mechanism to evaluate the performance of telepresence robot, therefore it will be used in all the next iteration of our telepresence robot development.

**Acknowledgments** This Research is funded by Competitive Research Grants fund of Indonesian Higher Education Directorate under contract No. 30/SP2H/PDSTRL\_PEN/LPPM-UKP/IV/2015.

## References

1. Steinfeld, A., Fong, T., Lewis, M., Scholtz, J., Schultz, A., Kaber, D., Goodrich, M.: Common metrics for human-robot interaction (2006)
2. Endsley, M.R.: Measurement of situation awareness in dynamic systems. *J. Hum. Factors Ergon. Soc.* **37**(1), 65–84 (1995)
3. Kaber, D.B., Onal, E., Endsley, M.R.: Design of automation for telerobots and the effect on performance, operator situation awareness, and subjective workload. *Hum. Factors Ergon. Manuf.* **10**(4), 409–430 (2000)
4. Scholtz, J., Antonishek, B., Young, J.: Evaluation of a human-robot interface: development of a situational awareness methodology. In: 37th Annu. Hawaii Int. Conf. Syst. Sci. 2004. Proc. no. C, 1–9 (2004)
5. Santoso, P., Khoswanto, H.: Open protocol framework for telepresence robot. *ARNP J. Eng. Appl. Sci.* **9**(12), 2437–2440 (2014)



# Chapter 12

## Relevant Features for Classification of Digital Mammogram Images

Erna Alimudin, Hanung Adi Nugroho and Teguh Bharata Adji

**Abstract** Breast cancer incident in Indonesia reaches 26 per 100,000 women. An early detection of breast cancer is a helpful effort for reaching a successful treatment. Mammography is the best tool for such detection, especially by means of Computer Aided Diagnosis (CAD). The systems of CAD are used to assist the radiologist to determine the benign or malignant abnormalities in the breast. Mammogram image processing system generally consists of mammogram image acquisition, pre-processing, segmentation, feature extraction, feature selection and classification. The features used in feature extraction should be able to represent the characteristics of mammogram image. A feature extraction process uses some texture features based on Gray Level Co-occurrence Matrix (GLCM) and histogram. This study used 60 mammogram images, left and right, from Clinical Oncology Kotabaru Yogyakarta. After passing through the enhancement process, mammogram images were extracted with 11 features of GLCM and histogram. The result then showed that the texture features could be used for the mammogram image feature extraction, but not all of the features were relevant. Thus, for knowing the effects of using irrelevant features, the classification results by using all features and selected features were compared. The highest accuracy was obtained from the selected features reaching at 86.67 %. High accuracy was determined by the relevant features used as input classifier. The selected features here included IDM, ASM, Energy, Contrast, Entropy-based GLCM, Histogram-based Entropy, and Skewness.

**Keywords** Feature extraction · GLCM · Histogram · Mammogram

---

E. Alimudin (✉) · H.A. Nugroho · T.B. Adji  
Department of Electrical Engineering and Information Technology,  
Faculty of Engineering, Universitas Gadjah Mada, Jl. Grafika 2, 55281,  
Yogyakarta, Indonesia  
e-mail: [ernaalimudin@gmail.com](mailto:ernaalimudin@gmail.com)

## 12.1 Introduction

Breast cancer is a malignant tumor that starts in the breast cells. A malignant tumor is a group of cancer cells that can grow into surrounding tissues or spread to distant areas of the body. Though this disease occurs almost entirely in women, it can occur in men as well [1]. As reported by the International Agency on Research in Cancer, breast cancer is the commonest female malignancy in Indonesia in which the age standardized rates in Indonesia is 36.2 per 100,000 in Indonesia, whereas mortality is 18.6 per 100,000 in Indonesia [2].

Early detection of breast cancer is important for a successful treatment. Here, mammography could be the best tool for early detection, especially with CAD. CAD generally refers to computer-assisted detection and diagnosis supported by a computer. Computer aided detection refers to searching or finding some abnormalities and computer-aided diagnosis refers to the evaluation or assessment mammogram abnormalities. The technology of computer-aided detection can be used as a second opinion to review the results of x-ray films of patients after a radiologist has made an initial interpretation. CAD system here highlights the presence of breast abnormalities detected on a digital mammogram.

CAD systems are used to help the radiologist determine the benign or malignant abnormalities in the breast [3]. Generally, the mammogram image processing system consists of a mammogram image acquisition, pre-processing, segmentation, feature extraction, feature selection and classification [4]. The final result of classification is determined by processes that run earlier. Using relevant features will determine the classification results.

Features used as input classifier determine the accuracy of classification. The accuracy will increase with the relevant features that are able to represent the characteristics of mammogram image. Mammography technique requires high contrast sensitivity due to the very low physical contrast in chest soft tissue. Blur and noise are the common undesirable elements in the medical image as they can reduce the visibility of certain objects. Object is designed based upon the decreasing size (detail) from left to right, and decreasing contrast from bottom to top. Noise and blur are two things that together produce the decreasing visibility of the image [5]. It shows that the enhancement method needed here is a method that can enhance or restore a mammogram image texture. Hence, the features used in feature extraction must be able to describe the characteristic of mammogram image texture.

Several previous researches examined a feature extraction stage. Some features were used as an input classifier in the final research stages. Previously there were some studies that used features based Gray Level Co-occurrence Matrices (GLCM). One of them was made by Herwanto [6]. In his research, four features were used; those are contrast, correlation, energy and homogeneity. Mammogram images which had been in ROI were extracted using four features before being classified as normal or abnormal. Here, accuracy was obtained at 87.6 %. Liu [7] also used GLCM features in his research. All features extracted were used as input classifier. Classifier was trained by using 30 training images and tested by using 30 testing

images. The obtained accuracy in classifying the image into two categories of benign and malignant was approximately at 59 %. In addition to use GLCM based texture features, other texture features used in previous research were intensity and intensity histogram based texture features. A comparative study of those features has ever been undertaken by Nithya [8] extracting the features of normal and abnormal mammogram images. His research tried GLCM, histogram and histogram intensity but did not attempt to combine those features. Then, this research attempted to combine those features to find out which features were the most relevant to extract mammogram images. Mammogram images as radiography image have several factors such as contrast, blurring, visual noise, spotting, and detail section [9], which determine the image quality. Thus, in this research mammogram images would be extracted by GLCM features and histogram based features known as texture based features. From a previous research, it has been found that the texture features based on histogram and GLCM were able to extract the features of mammogram images and can be used as input classifier. However, the research had not performed a feature selection. Thus, this research would like to perform feature selection. Then, at the end of this research, classification result would be compared by using all features and selected features. The purpose of this stage was to observe the influence of using selected features. Moreover, feature selection method used here was a method that could rank the most relevant feature to the less relevant feature or irrelevant feature. Hence, from this research, the most relevant features to extract mammogram images could be identified. The features should be appropriate to describe several factors which determine an image quality on mammogram images.

## 12.2 Methods

Data used in this research was mammogram digital images taken from the private database of Oncology Clinic Kotabaru Yogyakarta and consisting of 60 patients. Each patient had two mammogram images, right and left breast, based on the viewpoint of the CC (cranio caudal). Two images are called right cranio caudal (RCC) and left cranio caudal (LCC). 60 patients consisted of 20 normal patients and 40 abnormal patients (20 abnormal benign and 20 abnormal malignant). The size of each image was  $\pm 1400 \times 1850$  pixels with .tif format.

The purpose of this research was to observe the most relevant features for classification of digital mammogram images. The first stage was inputting the image prior to be transformed into gray scale format. The second stage was enhancement process and in the third stage, image enhancement results were extracted by texture-based features. Six histogram-based features include the mean intensity, standard deviation, skewness, energy, entropy, and smoothness. Meanwhile, five GLCM based features include ASM, contrast, IDM, Entropy, and correlation. Eventually, the features values of left mammogram and right mammogram of normal and abnormal patient were compared to obtain the representative

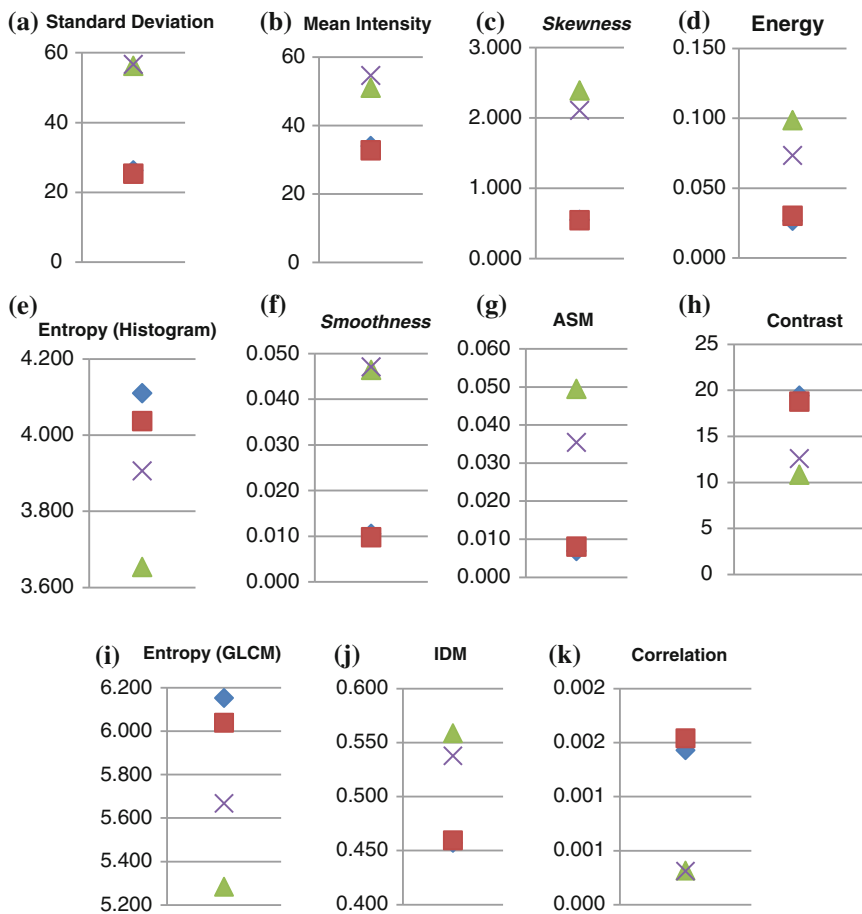
features. At the fourth stage, the entire images were classified into normal and abnormal. Furthermore, the results of classification using all features were compared with results of classification using the selected features. Method used to obtain subset of selected feature is Ranker search method by Gain Info Attribute Evaluation with decision tree algorithm. This method was chosen in view of its ability to compile these features from the most relevant to less relevant. Hence, the research purpose could be achieved.

### 12.3 Result and Discussion

The first thing in the results of the study refers to the result of feature extraction. Figure 12.1 presents the features values of the left and right mammogram images of normal patients and abnormal patients. In normal patients, both the left and the right mammogram images were categorized normal, while in abnormal patients, one mammogram image between the left and right images was categorized abnormal. Therefore, to facilitate the visualization of patient, the data of one normal and one abnormal patient would be used as sample in which each patient had left and right mammogram image.

From the graphic image of the 11 extracted features in Fig. 12.1a–k it can be seen the pattern of each feature. Features that can well represent the class image show the value point of left and right mammogram image in almost the same value point at the feature graphic image of normal patient. Thus, the points will look overlap or nearly overlap on the graph. It shows the symmetry between the left and right mammogram image indicating patient in the normal class. Furthermore, the graphic image of abnormal patient showed the value point of left and right mammogram image in a different point, so the points would separate or had a distance at the graph. It shows the asymmetry between the left and right mammogram images indicating patient in the abnormal class. Features that could not represent a class image would show the spreading points at the graph in both normal and abnormal patient. It means that the feature was not appropriate to classify the image of the normal patients because the obtained features value of the left and right image are not the same or close. Conversely, if the value point of feature graphic image looks concentrate in one value point for normal and abnormal patient, both of them look alike. It means that the feature is not relevant to classify abnormal patient because left and right mammogram image feature values approaching or almost same. It can be seen in Fig. 12.1.

Features that have a significant or insignificant influence can be seen by looking at the distribution pattern on the graph. Some graphic images which show the value point of left and right mammogram image extracted features of normal patient are almost same, thus the value point shown in the graph overlap, and show dissimilarity of the value point of left and right mammogram image extracted features of abnormal patient so that the value point shown in the graph apart are Skewness, Energy, Entropy-based histogram, ASM, Contrast, IDM, and Entropy-based



Note :

- ◆ Left Mammogram of Normal Patient
- Right Mammogram of Normal Patient
- ▲ Left Mammogram of Abnormal Patient
- ✕ Right Mammogram of Abnormal Patient

Fig. 12.1 Feature extraction of Left and Right mammogram from normal and abnormal patient

GLCM. Whereas, features which show the value point of left and right mammogram image extracted features of abnormal patient are overlap or almost same, then making difficult to categorize mean intensity, standard deviation, smoothness, and correlation.

It suggests that there are some relevant features in use in feature extraction capable of distinguishing the classes of mammogram image of the patient's left and right. However, other features also are irrelevant for classification. Furthermore, a

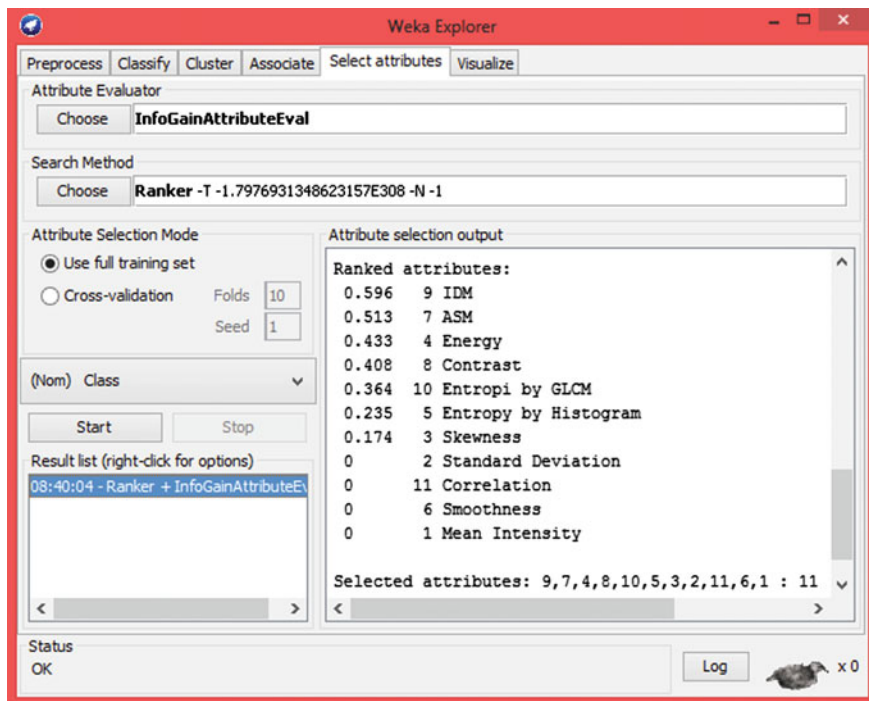


Fig. 12.2 Selected attributes result

testing needs to see its effect on the classification. Then, testing will be attempted by using the entire features as input classifier and compared by using the selected features. The selected attributes result by Ranker search methods with Info Gain attribute valuator are shown in Fig. 12.2.

Figure 12.2 shows the selected attributes result ranking the features from the most relevant feature to the less relevant or irrelevant one. 7 top rank feature selected as the most relevant feature have info gain value over zero and are used as the subset features of selected features. The subset features of selected features results used in this research included IDM, ASM, Energy, Contrast, Entropy-based GLCM, Histogram-based Entropy, and Skewness. Then, the classification result by using all features was compared with the classification using selected features. Table 12.1 shows the result of classification using the Error Back Propagation (EBP) 2 layer that has been trained with 30 training images and tested with 30 testing images.

Table 12.1 Comparison of classification results

Features	Accuration	Sensitivity	Specificity
All features	66,67	72,72	50
Selected features	86,67	90	80

From Table 12.1 it can be seen that the values of accuracy, sensitivity, and specificity of the classification using selected features are higher than using all features. Ranker search method produces a subset features-consisting of 7 features. Despite all features have more number of features compared to the selected ones, accuracy by using all features in fact is lower than selected ones. It shows that number of features used an in not more influential than relevant features used and irrelevant features will just lower accuracy in classification results.

Ranker search method has an order of features from the most relevant to the less or not relevant that is IDM, ASM, Energy, Contrast, Entropy-based GLCM, Histogram-based Entropy, and Skewness, Standard Deviation, Correlation, Smoothness, and Mean Intensity. Four most bottom features in order had zero information gain value indicating that they are irrelevant. As a consequence, these four features were not used and seven most top features in order of ranker search method results used as selected features and used as input classifier. The result used selected features that had higher accuracy, sensitivity, and specificity. It shows that the number of relevant selected features as input greatly affect the result of classifier performance. These features are IDM, ASM, Energy, Contrast, Entropy-based GLCM, Histogram-based Entropy, and Skewness. Moreover, Fig. 12.1 shows that these features can well represent and describe the class of mammogram images which consist of normal or abnormal.

## 12.4 Conclusions

Texture features can be used to extract features mammogram image. However, not all features are relevant in use as the number of features used does not always provide high accuracy in the classification. High accuracy could be obtained from the use of relevant features. Also, the relevant features are able to represent the image class. Thus, it will deliver the appropriate classification results. Some selected features are used as input classifier consisting of IDM, ASM, Energy, Contrast, Entropy-based GLCM, Histogram-based Entropy, and Skewness. In classification results, these selected features obtained the high value of accuracy, sensitivity, and specificity at 86, 67, 90, and 80 %, respectively. A feature selection stage was made to select a subset of features to improve accuracy. Moreover, it can reduce the size or classifier complexity but without reducing the accuracy by using all features.

## References

1. American Cancer Society: Breast cancer. (2014)
2. Ng, C.H., Pathy, N.B., Taib, N.A., Teh, Y.C., Mun, K.S., Amiruddin, A., Evlina, S.: Comparison of breast cancer in Indonesia and Malaysia—A clinico-pathological study between Dharmais Cancer Centre Jakarta and University Malaya medical centre. Kuala Lumpur **12**, 2943–2946 (2011)

3. Jalalian, A., Mashohor, S.B.T., Mahmud, H.R., Saripan, M.I.B., Ramli, A.R.B., Karasfi, B.: Computer-aided detection/diagnosis of breast cancer in mammography and ultrasound: a review. *Clin. Imaging* **37**(3), 420–426 (2013)
4. Velayutham, C.: A novel feature extraction method using spectral shape in digital mammogram image. In: *World Congress Informational Communication Technology*, pp. 835–840 (2011)
5. Taplin, S.H., Rutter, C.M., Finder, C., Mandelson, M.T., Houn, F., White, E.: Screening mammography: clinical image quality and the risk of interval. *Am. J. Roentgonology* **178**(4), 797–803 (2002)
6. Arymurthy, A.M.: A system for computer aided diagnosis of breast cancer based on mass analysis, pp. 247–253 (2013)
7. Liu, J., Chen, J., Huang, Z., Liu, X.: Design and implementation of content-based medical image retrieval system on mammograms. *Int. Conf. Biomed. Eng. Informatics* **4**, 237–240 (2011)
8. Nithya, R., Santhi, B.: Comparative study on feature extraction method for breast cancer classification. *J. Theor. Appl. Inf. Technol.* **33**(2) (2011)
9. Alimudin, E., Nugroho, H.A., Adji, T.B.: Comparative study on mammogram image enhancement methods according to determinant of radiography image quality (2015)



# Chapter 13

## Multi-objective Using NSGA-2 for Enhancing the Consistency-Matrix

Abba Suganda Girsang, Sfenrianto and Jarot S. Suroso

**Abstract** The problem of consistency matrix in Analytic Hierarchy Process (AHP) is an interesting issue. For achieving consistency in the inconsistent matrix, researchers usually change the consistent ratio (CR) and the deviation matrix. The pursuit of a minimal CR is important, since this index directly measures the consistency matrix in the AHP. While the deviation matrix should be minimal such that the original opinion of the decision makes is preserved. Ideally, the both value of CR and deviation matrix should be minimal. However, in fact those two objectives will be conflicted if both of them are optimized simultaneously. Therefore, a non-dominated Sorting Genetic Algorithm-2 (NSGA-2) for solving the multi-objective problems is considered as an appropriate approach for solving this problem. Six inconsistent AHP matrices are successfully repaired using NSGA-2.

**Keywords** AHP · Consistent ratio · Genetic algorithm · NSGA-2

### 13.1 Introduction

In solving multi criteria decision making (MCDM), the analytic hierarchy process (AHP) is a decision making tool to obtain a priority alternative. In AHP, a comparison matrix is generated to reveal the opinion of decision makers (DMs) [1–4]. One of the interesting issues of comparison matrix in AHP is the consistency. AHP matrix can be used if it satisfies the consistency requirement. This issue takes

---

A.S. Girsang (✉)

Master Information Technology, Bina Nusantara University, Jakarta, Indonesia  
e-mail: agirsang@binus.edu

Sfenrianto · J.S. Suroso

Master Management Information System, Bina Nusantara University, Jakarta, Indonesia  
e-mail: sfenrianto@binus.edu

J.S. Suroso

e-mail: jsembodo@binus.edu

attention for researchers to alleviate the inconsistency of pairwise comparison preference.

In a single objective problem, some researches use metaheuristic algorithm to solve the inconsistent matrix problem. Lin et al. [5] used genetic algorithm to solve the inconsistent in the comparison matrix. Yang et al. [6] continues this research to solve the inconsistent comparison matrix by combining particle swarm optimization PSO and Taguchi method. Girsang et al. [3, 4] used ant colony optimization to solve the inconsistent matrix. Although those metaheuristic methods are successfully solved that problem, the variations of the implemented metaheuristic, is rarely achieved. Girsang et al. [7] implemented multi-objective approach using PSO to solve this problem. Implementing NSGA-2 as one of the algorithm using genetic algorithm is interesting research in this area.

### 13.2 Multi-objective for Repairing the Inconsistent Matrix

The main purpose of multi-objective algorithm is to find a set of solutions which optimally balances the weakness among objectives of a multi-objective problems [8]. This problem uses two functions objective ( $F_1$  and  $F_2$ ) to point out each objective. The first objective is to minimize CR as shown Eq. (13.1). In order to obtain the consistent comparison matrix, the threshold CR must be less than 0.1.

$$\begin{aligned} \text{Min } F_1 &= \text{CR} \\ 0 < F_1 &< 0.1. \end{aligned} \quad (13.1)$$

Saaty [1] defined the threshold of CR is 0.1. Suppose the CR is defined in Eqs. (13.2)–(13.4).

$$A \times W = \lambda_{\max} \times W, \quad (13.2)$$

$$CI = (\lambda_{\max} - n)/(n - 1), \quad (13.3)$$

$$CR = CI/RI, \quad (13.4)$$

where  $A$  is a comparison matrix,  $\lambda_{\max}$  is the largest eigenvalue,  $W$  is the eigenvector of the matrix.

Further,  $CI$  is consistent index,  $n$  represents number criteria or size matrix, and  $RI$  (random consistency index) is the average index of randomly generated weights. Value  $RI$  on each size matrices can be described on Table 13.1. Eigenvector  $W$  can be represented as a set of the weight of each criteria of matrix  $A$ , while  $\lambda$  can be represented as a set of scalar corresponding to eigenvector  $W$  as Eq. (13.2).

**Table 13.1** Random consistency index (*RI*)

Number criteria	1	2	3	4	5	6	7	8	9	10	11
RI	0	0	0.58	0.9	1.12	1.24	1.32	1.41	1.45	1.49	1.51

The second objective is to minimize deviation matrix as shown Eq. (13.5). *Di* is used to define the deviation matrix.

$$\text{Min } F_2 = Di \tag{13.5}$$

Difference index (*Di*) is defined as the real difference between the same gene values in two genotypes. *Di* is defined in Eq. (13.6).

$$Di = \frac{\sum(G'./G) + (G./G')}{n^2 - 1} - 1, \tag{13.6}$$

where *G'* and *G* are row vectors comprising the lower triangular elements of the substitute matrix *A'* and of the original matrix *A*, respectively; “./” means element-to-element division. Smaller *Di* indicates more similar between two matrices. *Di* will be 0 if two matrices are same.

### 13.3 Implement Algorithm NSGA-2 for Repairing the Matrix

The encoding of matrix can be assembled by picking all elements in the matrix. However, due to the elements of multiplicative preference matrix have a relation such that  $a_{ij} = 1/a_{ji}$ ;  $a_{ii} = 1$ , an encoding node can only encodes the lower triangular elements of the matrix as nodes. It can be encoded by picking row by row sequentially in the elements of the lower triangular matrix. Take matrix *A* ( $n = 4$ ) for example and its encoding shown in Fig. 13.1. The number element of encode *A* can be determined ( $n^2 - n/2$ ). All elements in the inconsistent matrix should be changed into new value to achieve the consistent matrix. The new values are generated by fractioned from original values into several candidate values. This strategy makes that although fraction data changes the origin value, it only changes the weight of judgment without changing the tendency judgment.

$$A = \begin{bmatrix} 1 & 1/5 & 4 & 1/3 \\ 5 & 1 & 3 & 1/5 \\ 1/4 & 1/3 & 1 & 1/8 \\ 3 & 5 & 8 & 1 \end{bmatrix} \quad \text{Encode } A = 5-1/4-1/3-3-5-8$$

**Fig. 13.1** Matrix *A* with  $n = 4$  and its encoding

Second, if the origin element is 1 (neutral), the data should not be fractioned. It is performed to maintain the neutrality of judgment. The third, each candidate value is built from minimal to maximal based on the interval of fraction factor ( $\psi$ ). The different value  $\psi$  will set the different number of candidate values. For example, if  $\psi = 0.2$  then number candidate value of each element will be 40 ( $= \frac{9-1}{0.2}$ ). Suppose  $g_r$  is the origin value on node  $r$  and  $n$  is the size matrix, thus  $G_B$  can be described in Eq. (13.7)

$$G_B = g_1 - g_2 - g_3, \dots, g_{\frac{n-2}{2}} \tag{13.7}$$

Each elements of  $g_r$  is fractioned into several candidate element  $g_{rs}$ . Value  $s$  indicates the index of candidate element. The candidate element can be produced by following the role in Eq. (13.8).

$$g_{rs} = \begin{cases} g_{rs-1} + \psi, & \text{if } 1 < g_r \leq 9 \\ \frac{1}{g_{rs-1} + \psi}, & \text{if } 1/9 \leq g_r < 1 \end{cases} \tag{13.8}$$

There are some steps to implement NSGA-2 to repair the inconsistent matrix.

- (a) Generating the populations. There are 100 populations in each generations. Each population consists of chromosomes which represent the candidate elements.  
The candidate elements are came from fractioning the original element. In this first step, the candidate element is chosen randomly. Figure 13.2 shows one sample chromosome of encoding matrix  $A$  on Fig. 13.1.
- (b) Generated populations are sorted based on non-dominated which depicts the level front. The first front dominates the second front, and the second front dominates the third front, and so forth.
- (c) Each chromosomes as representing solution has crowding distance. Crowding distance states the distribution solution in its front. The longer crowding distance is more distribution solution. Therefore, the longer crowding distance is better.
- (d) To generate the parent individual, process “the tournament based selection” is used. In this process the parent is chosen as the best fitness. The better fitness is based on the small front and the long crowding distance. If there are two solutions have the different rank front, the small rank front is chosen, however if they have the same rank front, the longer crowded distance is chosen.
- (e) Crossover is performed in process of generating two parents,  $P_{Cr} = 0.9$
- (f) Mutation is performed,  $P_{Mu} = 0.1$

Chromosome1	4.8	1/4.8	1/2.2	5.2	4.8	6.4
-------------	-----	-------	-------	-----	-----	-----

Fig. 13.2 Chromosome1 as sample chromosome of Fig. 13.1

**Table 13.2** The inconsistency matrices

Matrix	Value element of inconsistent matrix	CR
$A_1$	$5 - 5 - \frac{1}{5}$	0.254
$A_2$	$9 - \frac{1}{3} - \frac{1}{5} - 5 - \frac{1}{2} - 2$	0.172
$A_3$	$3 - \frac{1}{2} - \frac{1}{7} - 6 - 9 - 9 - 2 - 4 - 4 - \frac{1}{5}$	0.139
$A_4$	$\frac{1}{2} - 9 - 3 - 1 - 4 - \frac{1}{5} - 5 - 5 - 7 - 7 - 3 - 3 - \frac{1}{3} - 3 - \frac{1}{7}$	0.136
$A_5$	$7 - 3 - 9 - 1 - 2 - \frac{1}{5} - \frac{1}{2} - 3 - \frac{1}{4} - 2 - 3 - 4 - \frac{1}{3} - 3 - 9 - \frac{1}{2} - \frac{1}{7} - \frac{1}{3} - \frac{1}{4} - \frac{1}{5}$	0.21
$A_6$	$\frac{1}{5} - \frac{1}{3} - 3 - \frac{1}{7} - \frac{1}{5} - \frac{1}{6} - \frac{1}{6} - \frac{1}{6} - \frac{1}{3} - \frac{1}{3} - \frac{1}{3} - 3 - \frac{1}{6} - \frac{1}{4} - 4 - 2 - 3 - 5 - \frac{1}{6} - 7 - 5 - 5 - 4 - 7 - 5 - 8 - 6 - 6 - 2$	0.169 [9]

**Table 13.3** Matrices repaired with the best CR and  $D_i$

Matrix	Best CR			Best $D_i$		
	Elements of lower triangular matrix	CR	$D_i$	Elements of lower triangular matrix	CR	$D_i$
$A_1$	0.4.4-0.625	$3.1 \cdot 10^{-6}$	0.262	5.8-4.0-0.25	0.099	0.146
$A_2$	8-0.625-0.132-2.4-0.455-3.8	$3.10^{-4}$	0.166	7.8-0.357-0.156-4.2-0.385-2.4	0.099	0.018
$A_3$	0.714-0.227-5.8-2.0-8.8-5.6-2.4-8.6-0.833	0.003	0.464	3.4-0.5-0.2-5.8-7.4-9.0-1.6-2.8-5.6-0.263	0.088	0.027
$A_4$	714-7.0-8.8-1.0-1.8-0.208-8.8-8.2-1.6-7.0-1.2-2.0-0.147-1.2-0.122	0.009	0.228	0.5-7.8-3.4-1.0-4.6-0.312-7.6-6.2-5.0-6.8-2.4-3.8-0.312-2.0-0.172	0.095	0.026
$A_5$	2-6-2-7.8-1.0-2.6-0.294-0.833-2.8-0.238-1.2-4-0-5-4-0-5-2.8-4-6-0-455-0.714-0.2-0-5-0.714-0.152	0.032	0.189	3.0-4.6-4.6-1.0-2.0-0.25-0.833-2.8-0.156-2.0-4-4-4-4-0-263-2.6-3-4-0-417-0-333-0.132-0-455-0-227-0-294	0.089	0.088
$A_6$	385-0.833-2.4-0.132-0.135-0.116-0.227-0.333-0.217-1.2-0.238-0.625-0.238-4.6-2.8-1.2-1.2-0.556-7.6-9.0-2.0-1.6-8.4-1.4-7.4-8.6-4-6-2.4	0.043	0.228	0.2-0.625-2.8-0.25-0.217-0.119-0.208-0.455-0.312-3.8-0.25-0.714-0.263-5.2-2.0-1.2-6.8-0.625-7.4-4.6-4.6-3.0-6.6-8.6-8.8-7.6-3.0-2.2	0.090	0.105

## 13.4 Experimental Results

To see the performance of NSGA-2 in repairing some inconsistent matrix, there are six inconsistent matrices which need to be modified as shown in Table 13.2. When the CR is lowest (good consistent ratio), it leads to the highest (the worst) deviation, and vice versa, as seen on Table 13.3.

However, in order to get the acceptable matrix, the CR of modified matrix is limited below 0.1. It makes the solution consist of some relations “CR-deviation” which can be identified as non-dominated solutions.

## 13.5 Conclusion

This paper presents a study to use the NSGA-2, multi-objective algorithm using GA, to solve the inconsistent problem on comparison matrix in AHP. There are two objectives (consistent ratio and deviation matrix) considered in rectifying the matrix in order to be consistent. However they are conflicting in that process. This algorithm offers some non-dominated solutions which are also satisfied the acceptable consistent matrices. To see the performance, six inconsistent comparison matrices with varying size are repaired by the NSGA-2. Besides repairing inconsistent comparison matrices, the NSGA-2 also can generate some non-dominated solution which can be classified as optimal solutions.

## References

1. Saaty, T.L.: The Analytic Hierarchy Process. McGraw-Hill, New York (1980)
2. Saaty, T.L., Decision Making for Leaders, vol. 7, Esf Editeur (1984)
3. Girsang, A.S., Tsai, C.-W., Yang, C.-S.: Ant algorithm for modifying an inconsistent pairwise weighting matrix in an analytic hierarchy process. *Neural Comput. Appl.*, 1–15 (2014)
4. Girsang, A.S., Tsai, C.-W., Yang, C.-S., Ant Colony Optimization for Reducing the Consistency Ratio in Comparison Matrix. In: International Conference on Advances in Engineering and Technology (ICAET'2014) Singapore (2014)
5. Lin, C.C., Wang, W.C., Yu, W.D.: Improving AHP for construction with an adaptive AHP approach ( $A^3$ ). *Autom. Constr.* **17**, 180–187 (2008)
6. Yang, I., Wang, W.C., Yang, T.I.: Automatic repair of inconsistent pairwise weighting matrices in analytic hierarchy process. *Autom. Constr.* **22**, 290–297 (2012)
7. Girsang, A.S., Tsai, C.-W., Yang, C.-S., Multi-objective particle swarm optimization for repairing inconsistent comparison matrices. *Int. J. Comput. Appl.* **36** (2014)
8. Engelbrecht, A.P., Fundamentals of Computational Swarm Intelligence. Wiley (2006)
9. Saaty, T.L., Vargas, L.G., Models, Methods, Concepts & Applications Of The Analytic Hierarchy Process. Kluwer (2001)

# Chapter 14

## Optimization of AI Tactic in Action-RPG Game

**Kristo Radion Purba**

**Abstract** In an Action RPG game, usually there is one or more player character. Also, there are many enemies and bosses. Player should kill as many as possible to get more experience. A smart AI is needed to increase the game challenge. In this research, a method is proposed to optimize the enemy AI strategy, by implementing enemy units grouping, and attacking in group using hit and run strategy against the player. The grouping is done using clustering, while the behavior picking is using Fuzzy Logic. If the player is approaching a group, most likely the group will retreat and the others start attacking. The units' formation is also maintained using clustering and distance calculation to player character. From the testing, this method can slightly increasing the game difficulty because of the enemies are trickier.

**Keywords** Artificial intelligence · Fuzzy logic · Clustering · Hit and run · Action RPG game

### 14.1 Introduction

RPGs have their origins in the paper and pen role-playing games pioneered by Dungeons & Dragons. These were defined games with rules [1]. In computer games, RPG is where player and enemy character have certain statistics, and have quests. Hybrid game genre like Action RPG game becomes common nowadays.

In an Action RPG game, usually there is one or more player character. Also, there are many enemies and some bosses. Player should kill as many as possible to get more experience. The effectiveness of AI in video games depends on how well game characters are able to cooperate and react to the opponent player [2].

---

K.R. Purba (✉)  
Petra Christian University, Surabaya, Indonesia  
e-mail: kristo@petra.ac.id; kristoradion@live.com



The enemies' AI can be really smart or dull. A dull AI causes a boring game playing, although it can help the player to reach higher experience because player can kill more enemies easily. But a smart AI is needed to increase the challenge.

This research result can create an AI that is more difficult to fight in action RPG game, thus increasing the game's challenge, and contributes in the field of game artificial intelligence.

### ***14.1.1 Related Works***

Hit and run is a common strategy used in a RTS (Real Time Strategy) games. A Research has been done to create an AI that controls enemies to do the hit and run tactic against player [3]. This research is implemented in Warcraft 2 game. In this game, unit can dodge enemy attacks by moving away, so the hit and run is mainly used to dodge. The difference between [3] and this research, is the hit and run will be used to avoid enemy from attacking.

Neural network is also common to optimize the AI reactivity against the player, which for example implemented in [4], the aims of the research are to develop controllers capable of defeating opponents of varying difficulty levels.

A research is also done to optimize the AI units in StarCraft game (a real time strategy game) in which the enemies can do micromanagement, terrain analysis, picking up strategies, and controlling attack timing to do maximum damage on player [5]. This research will be different from [4, 5] because of the type of game, and [4] is using neural network to control units globally.

## **14.2 Literature Review**

In this section, we will explain about K-Means Clustering and Fuzzy Logic, which will be used in this research.

### ***14.2.1 K-Means Clustering***

K-Means clustering is an algorithm to classify or to group your objects based on attributes/features into K number of group. The grouping is done by minimizing the sum of squares of distances between data and the corresponding cluster centroid [6]. The distance between data are calculated using Pythagoras formula, that takes x and y as the parameter.

## 14.2.2 Fuzzy Logic in Game

Fuzzy logic is a generalization of the classical set theory [7]. A research is conducted in [8] that optimizes the behavior of enemy in Pacman game. It uses distance (against player character), pellet/bullet time, and average lifetime as the membership function. It has several fuzzy rules grouped into hunting behavior, defense, shy ghost, and random behavior. In general, the enemy will attack the player if it has a good skill and good pellet time. It will defense if the enemy is not so good, shy ghost if worse, and random behavior is worst.

## 14.3 Methodology

Enemies will attack player mainly using grouped hit and run strategy. The grouping will be done using K-Means clustering, while the strategy is picked using Fuzzy Logic. The whole process is shown in Fig. 14.1.

### 14.3.1 Units' Grouping

The distance used in the clustering process is done by considering a unit X and Y position, and unit's strength. Unit's strength is determined by remaining HP (hit points/life), attack, speed, defense and range. The formula is shown in Eq. 14.1.

$$strength = \frac{remaining\ HP}{10} + \left( \frac{speed}{100} \times attack \right) + defense + \frac{range}{10} \quad (14.1)$$

With the strength and unit's position (X and Y coordinate), we can calculate the unit's distance that will be used in the clustering, the formula is shown in Eq. 14.2.

$$distance = strength + \sqrt{(x_2 - x_1)^2 + (y_2 - y_1)^2} \quad (14.2)$$

So the distance term used here is not the actual distance. The process of units grouping is shown in flowchart in Fig. 14.2.

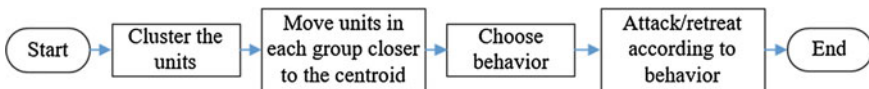


Fig. 14.1 Enemy AI strategy

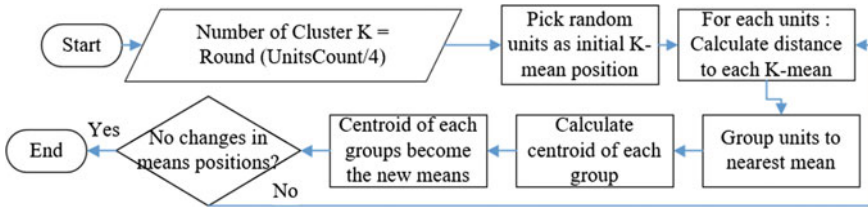


Fig. 14.2 Units' grouping

### 14.3.2 Picking the Behavior

The behavior is determined by fuzzy membership functions, calculated using average of group units' statistics, i.e.:

a. Group strength

Each unit in the group has strength (Eq. 14.1). Each group will calculate its average units' strength, to be used in the membership function, shown in Fig. 14.3.

b. Player direction

Player direction determines whether the player is currently going toward a group or not. This is calculated by the angular difference (degree), illustrated in Fig. 14.4.

The membership function is shown in Fig. 14.5.

c. Distance to player

Each group will calculate its centroid distance to the player. The membership function is shown in Fig. 14.6. oR defines whether the group is in the optimum range, based on the mean of attack range of every units. For example, if the mean of range is 350, and distance of group's centroid to player is 350, we say that the oR is 1, calculated using Eq. 14.4.

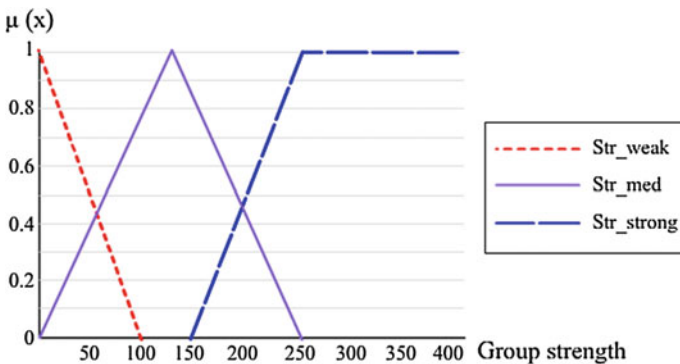


Fig. 14.3 Group strength membership function

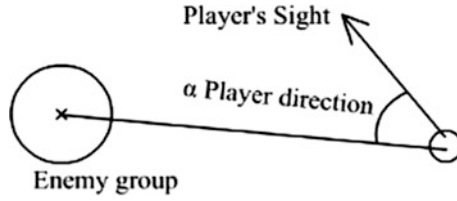


Fig. 14.4 Player direction

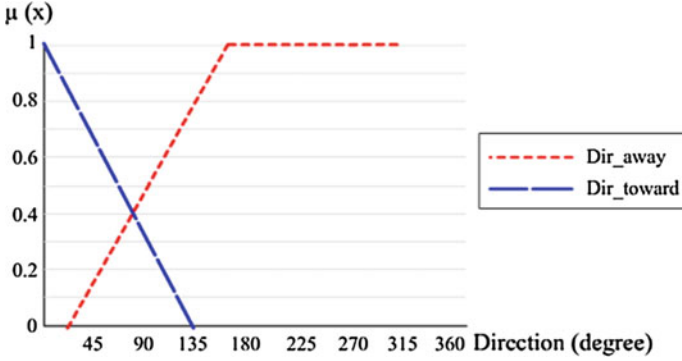


Fig. 14.5 Player direction membership function

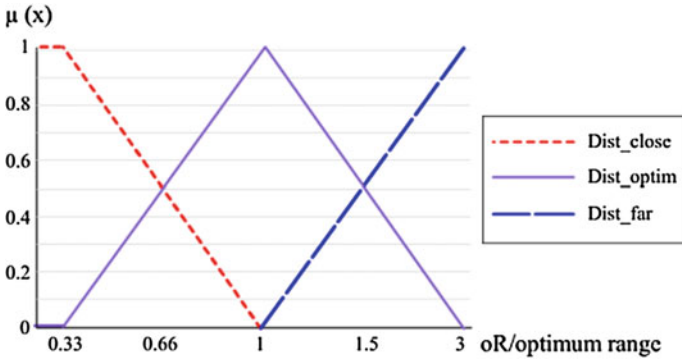


Fig. 14.6 Distance to player membership function

$$oR = distance\ To\ Player : \frac{\sum_{i=1}^N range(i)}{N} \tag{14.4}$$

The behavior that will be used in the defuzzification is divided into 4, i.e. Attack ( $z = 100$ ), Hold ( $z = 70$ ), Retreat ( $z = 40$ ), Retreat far ( $z = 10$ ). The fuzzy output will

be calculated using the following rules, and will result a floating number between 0 and 100:

- IF str\_strong AND dir\_away AND dist\_far THEN attack
- IF str\_strong AND dir\_away AND dist\_med THEN attack
- IF str\_strong AND dir\_away AND dist\_close THEN hold
- IF str\_strong AND dir\_toward AND dist\_far THEN attack
- IF str\_strong AND dir\_toward AND dist\_med THEN hold
- IF str\_strong AND dir\_toward AND dist\_close THEN hold
- IF str\_med AND dir\_away AND dist\_far THEN attack
- IF str\_med AND dir\_away AND dist\_med THEN attack
- IF str\_med AND dir\_away AND dist\_close THEN hold
- IF str\_med AND dir\_toward AND dist\_far THEN hold
- IF str\_med AND dir\_toward AND dist\_med THEN hold
- IF str\_med AND dir\_toward AND dist\_close THEN hold
- IF str\_weak AND dir\_away AND dist\_far THEN hold
- IF str\_weak AND dir\_away AND dist\_med THEN hold
- IF str\_weak AND dir\_away AND dist\_close THEN retreat
- IF str\_weak AND dir\_toward AND dist\_far THEN retreat
- IF str\_weak AND dir\_toward AND dist\_med THEN retreat far
- IF str\_weak AND dir\_toward AND dist\_close THEN retreat far

The executed behavior will be a crisp behavior, i.e.: Attack (if the fuzzy output is 80–100), hold (60–79), retreat (40–59), retreat far (20–39), random behavior (0–19).

## 14.4 Testing and Result

This research is tested using a simple battle simulator program by applying generic unit statistics available in most RPG games. In this section we will compare the methods implemented (MI) to random behavior of enemies (RB) in terms of game

**Table 14.1** Method testing

Enemies test case	Game Dur. (RB) (s)	Game Dur. (MI) (s)	Life Rem. (RB)	Life Rem. (MI)
5 Archer, 5 Marksman, 5 Catapult	12.5	17.3	720	601
15 Catapult	18.8	20.1	522	355
15 Marksman	14.2	15.7	641	556
15 Archer	16.1	22.4	748	590
10 Marksman, 5 Catapult	13.1	15.4	691	614
10 Archer, 5 Catapult	17.9	21.8	709	652
7 Archer, 8 Marksman	15.7	16.2	662	611
5 Marksman, 10 Catapult	19.2	23.3	531	342
Average	15.9375	19.025	653	540.125

duration (seconds) and how many player's life remains after killing all enemies, displayed in Table 14.1. From Table 14.1, It can be seen that the game duration increases, from average of 15.93 to 19.025 s (19 %). It is also seen that the life remaining is increasing, from average of 653 to 540.12 (-21 %). It means, the enemies are trickier.

## 14.5 Conclusion

It can be concluded that the enemies grouping, and hit and run strategy works well to create a trickier enemy. It is also seen that the methods implemented (MI) gives the better result than random behavior of enemies in terms of game duration and remaining life after battle. The methods also can be applied to other RPG games using the generic unit's statistics and game rules that are used in this research.

## References

1. Janssen, C.: Role-Playing Game (RPG) (2015). Accessed 1 Sept 2015
2. van der Marcel, H., Sander, B., Pieter, S.: Dynamic formations in real-time strategy games. In: IEEE Symposium on Computational Intelligence and Games (2008)
3. Weber, B.: Reactive planning for micromanagement in RTS games. Department of Computer Science, University of California, Santa Cruz (2014)
4. Tong, C.K. et. al.: Game AI generation using evolutionary multi-objective optimization. In: IEEE Congress on Evolutionary Computation (CEC) (2012)
5. Weber, B. et. al.: Building human-level ai for real-time strategy games. In: Proceedings of the AAAI Fall Symposium on Advances in Cognitive Systems (2011)
6. Teknomo, K.: K-Means clustering tutorial (2007)
7. Demonecourt, F.: Introduction to fuzzy logic. MIT, Cambridge (2013)
8. Adnan, S., Brady, K., Luke, R.: Real-Time game design of Pac-Man using fuzzy logic. Int. Arab J. Inf. Technol. **3**(4), 315–325 (2006)

# Chapter 15

## Direction and Semantic Features for Handwritten Balinese Character Recognition System

Luh Putu Ayu Prapitasari and Komang Budiarta

**Abstract** This research presents a new work on feature extraction methods for handwritten and isolated Balinese character recognition system. Balinese script has different difficulties compared to other scripts and its uniqueness makes it very interesting yet challenging in the development of this system. The goal of this work is to achieve good performance on Balinese character recognition by comparing more than one feature extractor methods. Based on the experimentations, the direction and semantic features have shown better performance when both are paired as feature extractors. For the classifier, we employed Backpropagation Neural Network with 50 nodes in hidden layer and chosen the Lavenberg-Marquardt as the training algorithm. The overall performance accuracy is 90 %.

**Keywords** Optical character recognition · Balinese script · Direction feature · Semantic feature · Backpropagation Neural Network

### 15.1 Introduction

Balinese language has its own script, namely Balinese script (Aksara Bali). From the total of 47 characters, this research is limited to the recognition of 18 basic consonants, called AkṣaraWreṣāstra as shown in Fig. 15.1.

The focus of this work is to find the best yet simple feature extraction method for the Balinese Character Recognition System. In general, there are three groups of features, such as geometrical, structural and space-transformation feature. We compared the features from geometrical group, called direction feature, with another feature that is belong to structural group, namely semantic feature. The detail of this work is explained in the next sections.

---

L.P.A. Prapitasari (✉) · K. Budiarta  
STMIK STIKOM Bali, Jl. Raya Puputan Renon no. 86, Bali, Indonesia  
e-mail: prapita@stikom-bali.ac.id

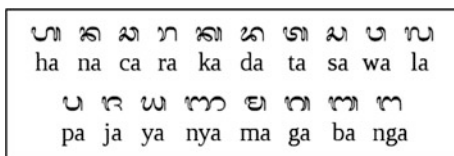


**Fig. 15.1** Akṣara Wreṣāstra

This paper is organized as follows. Section 15.2 contains a brief summary of the related works on this subject. In Sect. 15.3, we present the proposed method including all the results for comparison. In Sect. 15.4, we present the implemented method and the results. Section 15.5 contains some brief conclusions and future direction of this work.

## 15.2 Related Works

Undoubtedly there are many extensive works that have already done in Optical Character Recognition (OCR) system all over the world until now. A report of the development in handwriting recognition has been published in [1]. Earlier report in [2] explained about methodologies used in character recognition based on local features. Those features such as: end points and angles or corners, vertical or horizontal lines, curvatures analysis and structural methods. The importance of descriptive approach is mentioned in [3].

The world heritages of languages and scripts have given a lot of chances for exploiting researches in this field. Some of the examples are the work in Chinese characters [4], Devanagari [5], Arabic [6] and Japanese [7]. Although the works on those characters or scripts have already started in decades, but in contrast, the work on Indonesian's ancient scripts just started not long ago. For example, a recent publication on the script of Javanese can be seen in [8, 9]. Some publications of researches on Balinese script are available such as in [10, 11] including a work on pre-processing task for the scripts which are written on palm leaves [12].

One of the keys in OCR is in the selection of feature extraction methods and in most cases, a single feature is not sufficient to describe the uniqueness of the character in order to differentiate one character from another [13]. Directional features are also of interest, such as in [14, 15]. The zoning method is surveyed in [16] and as proven to work very well in OCR system. Furthermore, in [17] has implemented the use of semantic features, such as the head and end point of the stroke of the character for better OCR system.

From the all mentioned methods in feature extractions, we then picked two which are quite popular: the direction and semantic features.



### 15.3 Proposed Method

There are three main phases of Balinese character recognition system, for instance: pre-processing, feature extraction and classification. As mentioned in the earlier section, this research is focusing on the second phase. The detail process is illustrated in Fig. 15.2.

The input image is pre-processed manually, including removing the noises, and segmenting the images to isolate the characters. At last on this phase, the image is then resized into  $48 \times 48$  pixels. After skeletoning, the image is then saved as a vector based on its binary information. On the next phase, there are two features extraction methods used. Firstly is the direction feature, which is used to detect the stroke of the character by giving a value based on the pixel direction. The assumption is that the white color as the background and given the value 0, and black is defined as the character and is given a specific value based on its direction, as displayed in Table 15.1.

Value designation for each direction is done by: (1) defining the starting point of the stroke of the character and assuming the position to be at the most bottom left of

Fig. 15.2 Framework of Balinese OCR system

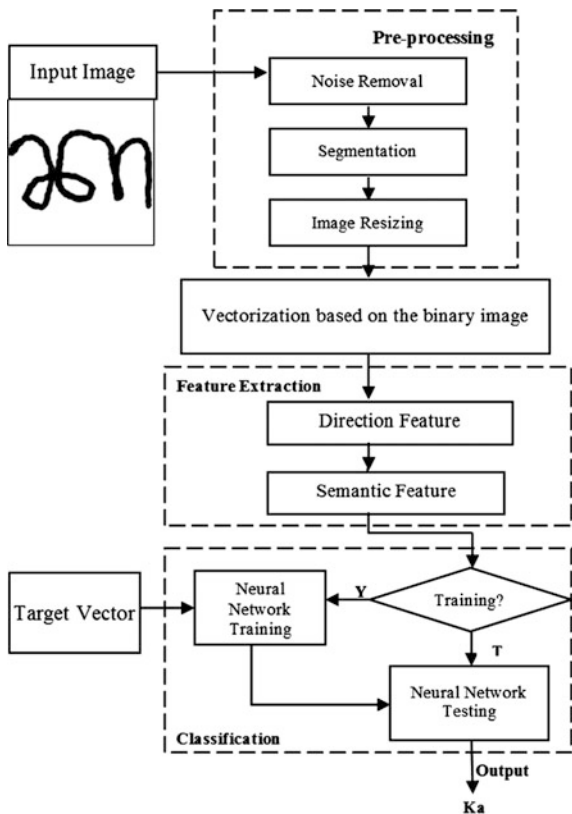


**Table 15.1** Directions and its value

Shape	Value	Direction
	2	Vertical
—	4	Horizontal
/	3	Right diagonal
\	5	Left diagonal

the stroke, and then the next new starting point is assumed when the position of the next pixel is differ to previous pixels. For every starting point found, the temporary value is set to 8, (2) after the iteration completed and all values have been set to 8, then come the normalization for all the values. All the values are grouped together and changed to the information contains in this group. This is the 4-directional feature, or simply we call as directional feature. Zoning is done after the all value is assigned to each pixel on the skeleton. The result is as shown in Fig. 15.3.

Secondly, after direction feature detection is done, the semantic features of each character are then extracted. The information of the height and weight, number of loops, number of horizontal and vertical lines and number of end points are stacked together in a vector, as can be seen in Fig. 15.4.

The last phase is the classification phase. It classifies each of the input character based on its features. The classifier used in this system is Backpropagation Neural Network (BNN). Detailed description of this method are available (and can be referred further) in [18, 19] and also in the recent book [20]. The input for BNN is a vector of size  $28 \times 1$ , where the first 12 rows are for keeping the information of semantic features and the remaining rows holding the direction features. This phase is illustrated in Fig. 15.5.

Hidden layer is tested with 10 and 50 nodes for comparison. The BNN implemented two algorithms for the training process: Lavenberg-Marquardt and Gradient Descent algorithm with adaptive momentum, again for comparison. The output is also a vector of size  $18 \times 1$  which is holding information of the recognized character in Latin alphabet.

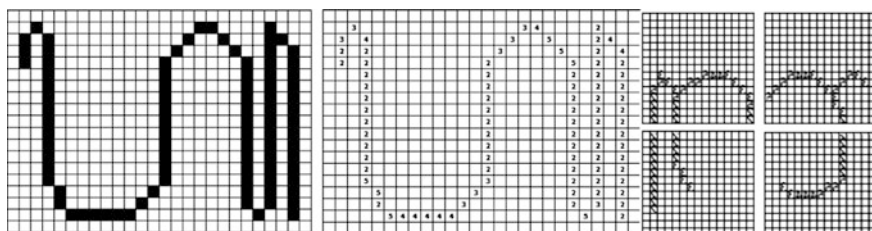


**Fig. 15.3** Direction feature. Setting up value for character ‘ha’, where (left) binary input in black and white color after skeletoning, (middle) value assigned for each pixel based on its direction, and (right) showing the 4 zones after the direction values are given to skeleton of character ‘nga’

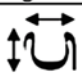
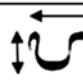
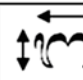








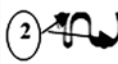


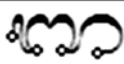
Height and Width		
		
1 row 1 cols	1 row 2 cols	1 row 2 cols
Loops		
		
No loop	1 loop	2 loops
Number of horizontal lines		
		
3	3	5
Number of vertical lines		
		
1	1	2
End points		
		

Fig. 15.4 Semantic features based on height and width, number of loops, number of horizontal and vertical lines and number of end points

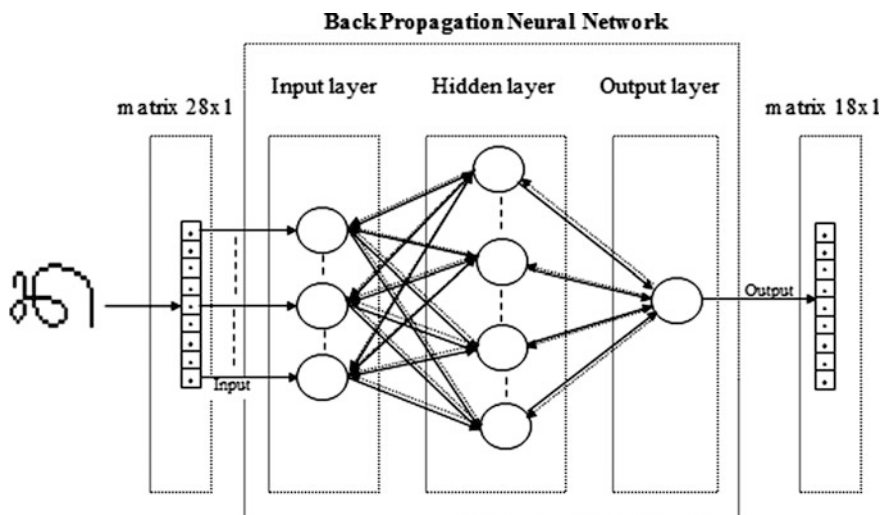


Fig. 15.5 Classification phase using BNN

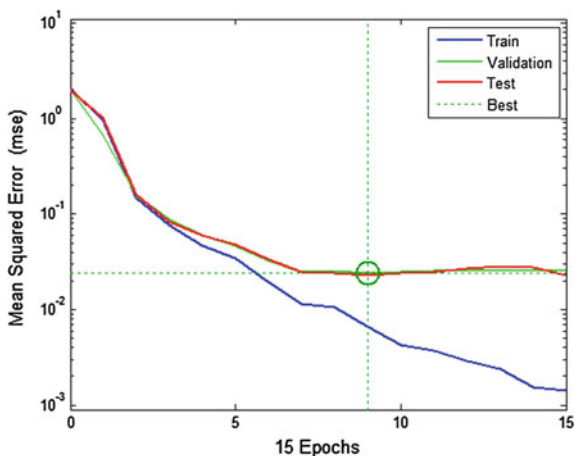
### 15.4 Implementation and Results

Before the interface is designed, the total 900 samples of handwritten characters are fed into the system by comparing the performances of only direction feature, only semantic feature and then both direction and semantic features. And in the training step of BNN, the two algorithms are employed. The result is listed in Table 15.2 below. The best result with 90 % of accuracy is achieved when the system is fed by using both direction and semantic features, the training algorithm used is Lavenberg-Marquardt and when the number of hidden nodes is set to 50. Figure 15.6 shows the performance of the trial system and the best testing result,

**Table 15.2** Results of implemented BNN training algorithms

Features	Training algorithm	No. of nodes on hidden layer	Results (%)
Direction	Tramlm	10	68
		50	85
	Tramedx	10	42
		50	49
Semantic	Tramlm	10	61
		50	74
	Tramgdx	10	32
		50	38
Direction and semantic	Tramlm	10	71
		50	90
	Traingdx	10	40
		50	49

**Fig. 15.6** Performance of BNN based on number of iterations (epochs) versus mse



which is reached where the Mean Squared Error (MSE) close to 0.01, while at the same time the training phase having lower MSE, which is close to 0.001.

Based on the above result, the interface is then designed as depicted in Fig. 15.7. It is developed in Matlab R2008b under Microsoft Windows 7 operating system. Hardware configuration is a personal computer with processor type: Intel Dual Core 2.8 Hz. In Table 15.3, we can see some of the outputs of the system. For comparison, we have provided both successful and un-successful recognition. The sign ‘\*’ is for the input that is failed to be recognized (un-successful).

Fig. 15.7 Interface of Balinese OCR system

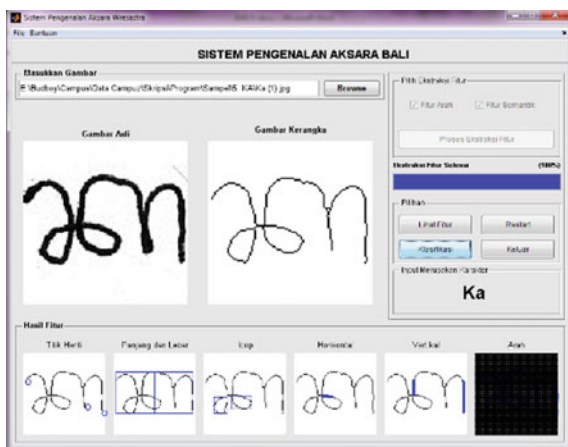


Table 15.3 Some of Balinese OCR results

Input	Direction Feature																Semantic Feature												OCR output
	1	2	3	4	5	6	7	8	9	10	11	12	13	14	15	16	17	18	19	20	21	22	23	24	25	26	27	28	
ᮊ	4	10	3	8	5	1	9	6	9	7	4	9	23	3	3	0	3	1	0	0	2	2	1	0	2	3	0	3	Ha
ᮊᮓ	6	9	4	3	4	10	6	9	19	14	0	9	19	17	0	2	3	1	0	0	2	2	1	0	0	3	0	3	Ha
ᮊᮔ	16	14	5	23	12	21	0	12	11	12	7	12	15	10	4	9	2	1	0	0	1	1	1	2	0	2	1	1	Na
ᮊᮕ	9	4	2	10	2	19	7	14	7	5	8	22	6	13	7	4	3	2	0	0	1	1	1	3	3	1	1	0	Sa *
ᮊᮖ	7	11	6	13	8	26	8	11	16	14	5	12	14	9	1	14	3	1	1	0	1	1	1	1	1	2	0	1	Ca
ᮊᮗ	11	13	3	10	7	13	3	0	7	2	4	12	21	2	0	0	3	1	0	1	1	1	1	0	0	2	1	1	Ra
ᮊᮘ	13	14	1	10	4	14	7	17	13	2	8	14	12	6	2	5	5	2	1	0	2	2	1	2	1	2	0	2	Sa *
ᮊᮙ	2	14	3	10	1	20	13	13	12	8	7	10	15	4	2	6	3	1	0	0	2	2	1	2	2	2	0	2	Ka
ᮊᮚ	1	11	7	7	7	6	3	5	12	11	6	20	7	19	2	0	3	2	0	0	1	1	1	0	2	2	0	2	Wa
ᮊᮛ	0	17	6	13	1	6	6	13	23	10	3	6	12	10	4	6	5	1	2	6	2	1	1	1	0	1	0	1	Ma
ᮊᮜ	9	25	14	17	7	2	1	17	23	5	6	6	9	12	2	2	6	1	1	3	1	1	1	2	1	3	1	2	Na *

## 15.5 Conclusion and Future Direction

From the implementation and experiments, it can be concluded that the designed system recognizes most of the input characters with the accuracy of 90 % with employing both direction and semantic features. While, implementing only one feature detection method gave us lower accuracy with 85 and 74 % for direction and semantic feature, respectively. Based on the input that we fed, the system worked much better when there is no broken stroke available on the data samples.

Future direction of this research would be: (1) pairing the geometrical or structural features with space-transformation features such as PCA features for better achievement, and (2) improving the pre-processing phase. Because, so far all the pre-processing tasks have been done manually. The task will be much easier if it can be done by a system automatically.

## References

1. Sebastiano, I.: More than twenty years of advancements on frontiers in handwriting recognition. *Pattern Recogn.* **47**(3), 916–928 (2014)
2. Mantas, J.: An overview of character recognition methodologies. *Pattern Recogn.* **19**(6), 425–430 (1986)
3. Govindan, V.K., et al.: Character recognition—a review. *Pattern Recogn.* **23**(7), 671–683 (1990)
4. Cheng-Lin, L., Sako, H., Fujisawa, H.: Handwritten chinese character recognition: alternatives to nonlinear normalization. In: *ICDAR* (2003)
5. Hariharan, S., et al.: Online handwritten character recognition of devanagari and telugu characters using support vector machines. In: *Tenth international workshop on Frontiers in handwriting recognition* (2006)
6. Nawaz, S.N., et al.: An approach to offline arabic character recognition using neural networks. *Electronics, circuits and systems, 2003. ICECS 2003*. In: *Proceedings of the 2003 10th IEEE international conference on*. IEEE (2003)
7. Kawamura, A., et al.: Online recognition of freely handwritten japanese characters using directional feature densities. *pattern recognition methodology and systems*. In: *11th IAPR international conference on IEEE* (1992)
8. Rudy A., et al.: *Feature Extraction for Java Character Recognition*. *Intelligence in the Era of Big Data*, pp. 278–288. Springer, Berlin, (2015)
9. Budhi, G., et al.: Comparison of bidirectional associative memory, counter propagation and evolutionary neural network for java characters recognition. In: *Advanced informatics: concept, theory and application (ICAICTA)*, (2014)
10. Luh P.A.: Offline balinese handwritten character recognition based on Backpropagation Neural Networks. In: *Proceeding of national seminar on computer and intelligent system-KOMMIT 6*, pp. 114–118, Bali (2010)
11. Kadek, A.D.I., Luh P.A.: Character segmentation for balinese script using canny edge detection algorithm. In: *Proceedings of national conference of system & informatics*, pp. 402–406, Bali (2011)
12. Luh, P.A.: Noise removal for ancient palm leaf manuscript of Bali. In: *Proceedings of National Conference of Information System, KNSI*, 1514–1518, Bali (2012)

13. Trier, Ø., et al.: Feature extraction methods for character recognition-a survey. *Pattern Recogn.* **29**(4), 641–662 (1996)
14. Zhen-Long B., et al: A study on the use of 8-directional features for online handwritten chinese character recognition. In: *Proceedings eighth international conference on IEEE* (2005)
15. Kato Nei, et al.: A handwritten character recognition system using directional element feature and asymmetric mahalanobis distance. *Pattern Anal. Mach. Intell., IEEE Trans.* **21**(3), 258–262 (1999)
16. Impedovo, D., Giuseppe, P.: Zoning methods for handwritten character recognition: a survey. *Pattern Recogn.* **47**(3), 969–981 (2013)
17. Phokharatkul, P., et al.: Off-Line hand written thai character recognition using ant-miner algorithm. *Int. J. Comput. Control Quantum Inf. Eng.* **1**(8), (2007)
18. Hecht-Nielsen, R.: Theory of the Backpropagation Neural Network. In: *IJCNN, International Joint Conference on Neural Networks* (1989)
19. Hagan, M.T., Demuth, H.B., Beale, M.H.: *Neural Network Design*. Pws Pub, Boston (1996)
20. Eberhart, R.C. (ed.): *Neural Network PC Tools: A Practical Guide*. Academic Press (2014)

# Chapter 16

## Energy Decomposition Model Using Takagi-Sugeno Neuro Fuzzy

Yusak Tanoto and Felix Pasila

**Abstract** Decomposition analysis is useful method to determine significant factors contribute towards the development of energy consumption. This paper presents factors decomposition of electricity consumption in Indonesia's household sector using artificial intelligent method. The proposed artificial intelligent technique used in this study is the Neuro Fuzzy Takagi-Sugeno (NFTS) network, which is worked under multiple input multiple output condition. By tuning the appropriate Gaussian parameters, which are mean and variance, and two Takagi-Sugeno weight, the changes in electricity consumption that is decomposed into production effect, structural effect, and efficiency effect, has revealed. Compared to the common method, the performance of NFTS network for both constant and current price variables is quite satisfied, given the error generated in the network ranges between 0.003 and 2.09 %, which is quite low and acceptable.

**Keywords** Takagi-Sugeno Neuro Fuzzy · Factors decomposition · Household · Electricity consumption

### 16.1 Introduction

Energy factors decomposition is a useful method to determine significant factors contribute towards the development of energy consumption over the observed period. Several studies have reported the factors decomposition of the electricity energy using the well-known decomposition technique, Logarithmic Mean Divisia Index, or hereafter called LMDI. The technique is currently applied in many decomposition study. LMDI is used to reveal the electricity development of the Brazilian residential sector [1]. Decomposition of four term energy intensity of Hong Kong residential sector is studied using LMDI method [2]. Additive-LMDI

---

Y. Tanoto (✉) · F. Pasila  
Electrical Engineering Department, Petra Christian University, Surabaya, Indonesia  
e-mail: tanyusak@petra.ac.id



with emphasis on both current and constant price based is used to observe Indonesian household electricity decomposition [3].

In this paper, a novel approach in obtaining the energy factors decomposition is used. One of the objective is to decompose production, structure, and efficiency effect using alternative technique that are reliable, accurate and without having to understand mathematical model of the method. Therefore, artificial intelligent based method is used to obtain those decomposition factors of electricity utilization. The proposed Neuro Fuzzy Takagi-Sugeno network is applied to the Indonesia's electricity energy in the household sector. The data used in this study are the same with that applied in the previous study with LMDI method, in order to compare results obtained by the proposed method with that demonstrated by Additive-LMDI.

This paper is organized as follows; the methodology consists of NFTS network architecture and the data is presented in the following section. Subsequently, followed by results and discussion section. Finally, conclusion of the work is presented in the last section.

### 16.2 Methodology

The proposed NFTS network model in which applied in this study is shown in Fig. 16.1 below. The method is already proven as one of artificial intelligence approximator for modelling and control [4]. The proposed network consists of 5 set

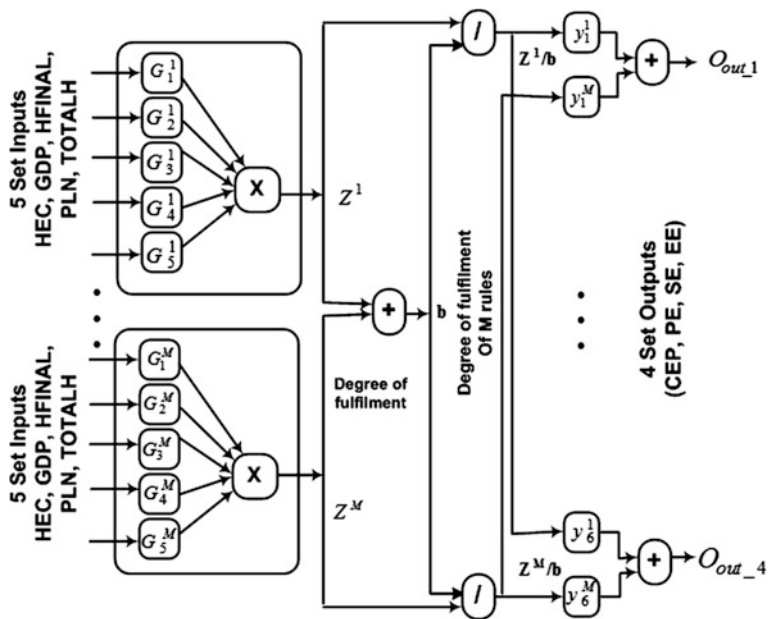


Fig. 16.1 NFTS network model for the case study with 5 set inputs and 4 set outputs

inputs, i.e. household electricity consumption (HEC), Gross Domestic Product (GDP), household final consumption expenditure (HFINAL), PLN's household customer (PLN), and total number of household (TOTALH), and 4 set outputs, i.e. changes in electricity consumption (CEC), production effect (PE), structure effect (SE), and efficiency effect (EE).

The proposed model of NFTS as shown in Fig. 16.1 is based on TS-fuzzy rule, product inference, and weighted average defuzzification. All nodes in the Gaussian layer calculate the degree of membership of the fundamental input values (HEC, GDP, HFINAL, PLN and TOTALH) in the antecedent fuzzy parts. The division and the summation nodes in the degree of fulfillment parts, join to make the normalized units of the corresponding rules, which after multiplication with the corresponding TS parts, is used as input to the last summation part at the four outputs.

The outputs of NTFS, which being crisp, are directly well-approximated with the related outputs (CEP, PE, SE and EE). If all the parameters for NFTS network are selected, then the NFTS can approximate any nonlinear model based on given related data between 5 inputs and 4 outputs. The parameters used in the NFTS network, such as Gaussian and TS parameters can be optimized through Levenberg-Marquardt Algorithm (LMA) learning procedure. In this study, we apply the same data in accordance to previous study made with the Additive-LMDI method. The five set inputs for the data are taken from year 2000 to 2010. Also, the GDP and household final consumption expenditure are expressed either in current price and constant price 2000. All data are shown in Tables 16.1 and 16.2, respectively.

**Table 16.1** Data required for conducting Indonesian household electricity decomposition (current price)

Year	Household electricity consumption (MWh) [5]	GDP (million Rupiah) [6]	Household final consumption expenditure (million Rupiah) [6]	PLN's household customer [5]	Total number of household [5]
2000	30,538,269	1,389,769,900	856,798,300	26,796,675	52,008,300
2001	33,318,312	1,646,322,000	1,039,655,000	27,905,482	53,560,200
2002	33,978,744	1,821,833,400	1,231,964,500	28,903,325	55,041,000
2003	35,697,122	2,013,674,600	1,372,078,000	29,997,554	55,623,000
2004	38,579,255	2,295,826,200	1,532,888,300	31,095,970	58,253,000
2005	41,181,839	2,774,281,100	1,785,596,400	32,174,924	59,927,000
2006	43,748,580	3,339,216,800	2,092,655,700	33,118,262	55,942,000
2007	47,321,668	3,950,893,200	2,510,503,800	34,684,540	57,006,400
2008	50,182,040	4,948,688,400	2,999,956,900	36,025,071	57,716,100
2009	54,944,089	5,606,203,400	3,290,995,900	37,099,830	58,421,900
2010	59,823,487	6,436,270,800	3,643,425,000	39,324,520	61,363,100

**Table 16.2** GDP and household final consumption expenditure (constant price 2000)

Year	GDP (million Rupiah) [6]	Household final consumption expenditure (million Rupiah) [6]
2000	1,389,769,900	856,798,300
2001	1,440,405,700	886,736,000
2002	1,505,216,400	920,749,600
2003	1,577,171,300	956,593,400
2004	1,656,516,800	1,004,109,000
2005	1,750,815,200	1,043,805,100
2006	1,847,126,700	1,076,928,100
2007	1,964,327,300	1,130,847,100
2008	2,082,456,100	1,191,190,800
2009	2,178,850,400	1,249,070,100
2010	2,313,838,000	1,308,272,800

### 16.3 Results and Discussion

The changes in Indonesia's household electricity consumption during year 2000–2010 according to the current price and constant price are shown in Fig. 16.2 and Table 16.3, respectively.

In the case of current price data, changes in electricity consumption is driven by 224.66 % production effect, 21.47 % structural effect, and -137.67 % efficiency effect. Meanwhile, in the case of constant price based data, the changes in electricity consumption is affected by percentage of production effect, percentage of structure effect, and percentage efficiency effect.

Table 16.4 gives the comparison between results obtained by NFTS network model and by Additive-LMDI. In this regards, the results achieved by the LMDI method are taken as the baseline. The performance of NFTS network is quite satisfied. The error generated in the network is in the range between 0.003 and 2.09 %, which is quite low and acceptable. For instance, the largest error with 2.09 % means according to the NFT network, the 2000–2010 changes in electricity consumption is affected by 5,593,004.21 MWh consumption contributed by structure effect. This value is only a difference of 119,592 MWh compared to LMDI. The least difference is obtained for the case of current price based data, particularly for structural effect, provided a difference of only 210 MWh between NFTS and LMDI.

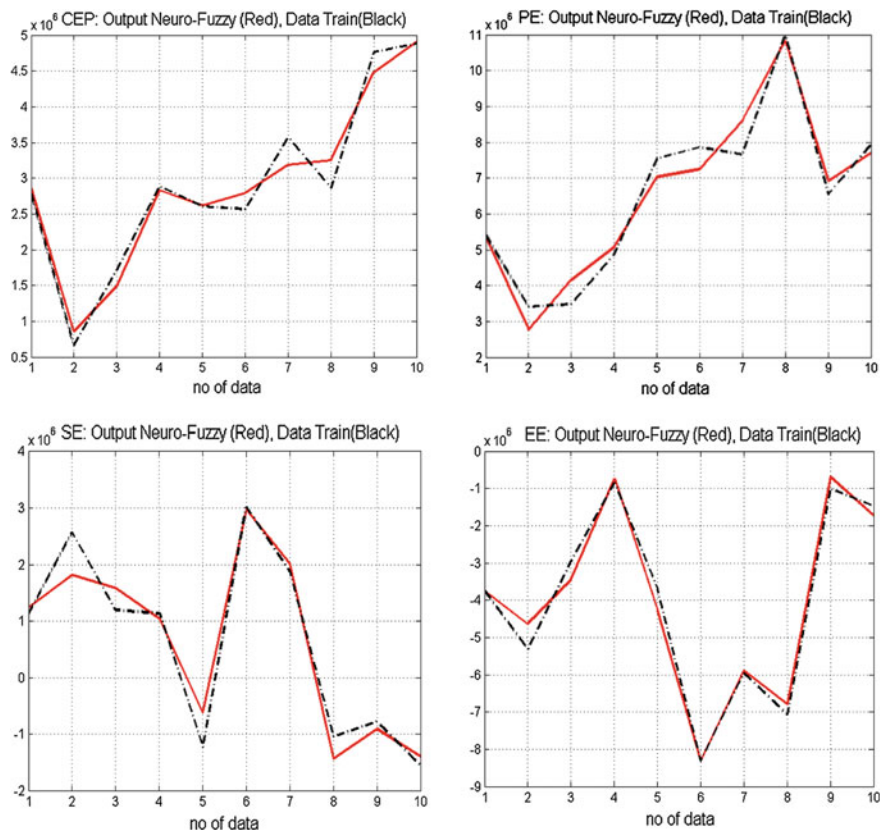


**Fig. 16.2** NFTS output versus data trained: CEC (first upper), PE (second upper), SE (lower), EE (lowest)

**Table 16.3** NFTS output: 2000–2010 (constant price 2000)

Year	Changes in electricity consumption ( $\Delta E_{tot}$ in MWh)	Production effect ( $\Delta E_{act}$ in MWh)	Structural effect ( $\Delta E_{str}$ in MWh)	Efficiency effect ( $\Delta E_{int}$ in MWh)
2000–2001	2,782,762.14	1,169,160.93	308,740.49	1,307,567.53
2001–2002	953,571.05	1,349,106.83	11,641.39	−968,277.02
2002–2003	1,669,749.11	1,647,257.37	616,649.55	−554,780.20
2003–2004	2,486,164.26	2,029,069.96	−26,214.54	973,591.61
2004–2005	2,622,593.22	2,160,692.25	−691,953.41	1,178,029.05
2005–2006	2,591,168.35	2,369,558.62	3,150,399.62	−2,775,936.45
2006–2007	3,299,091.29	2,637,449.12	787,838.87	36,358.10
2007–2008	3,273,223.22	2,711,828.61	357,713.70	−166,207.44
2008–2009	4,694,108.54	2,498,907.49	1,201,014.41	1,333,001.74
2009–2010	4,771,860.99	3,460,405.03	−122,825.88	1,168,861.27
2000–2010	29,144,292.18	22,033,436.22	5,593,004.21	1,532,208.20
		75.60 %	19.19 %	5.25 %

**Table 16.4** Result comparison between NFTS model and Additive-LMDI

Tools (Type of data)	CEC	PE	SE	EE
LMDI (current)	29,285,218.00	65,685,080.79	6,280,558.64	-40,413,112.57
NFTS (current)	29,244,768.02 (Error: 0.14 %)	65,701,890.94 (Error: 0.03 %)	6,280,768.654 (Error: 0.003 %)	-40,261,612.49 (Error: 0.375 %)
LMDI (constant)	29,285,218.00	22,021,829.43	5,712,597.09	1,550,791.46
NFTS (constant)	29,144,292.18 (Error: 0.48 %)	22,033,436.22 (Error: 0.05 %)	5,593,004.21 (Error: 2.09 %)	1,532,208.20 (Error: 1.19 %)

## 16.4 Conclusion

This paper presents the utilization of Artificial Intelligence tool based to model factors decomposition of Indonesia household electricity consumption. Based on the testing to the provided data, changes of household electricity consumption can be modelled satisfactory by the NFTS network along with three types of effect that affecting the changes in electricity consumption. Despite of the limited set of data, the multi input-multi output NFTS can performed well and results achieved in term of error are very low, especially for the case of current price based data.

## References

1. Achao, C., Schaeffer, R.: Decomposition analysis of the variations in residential electricity consumption in Brazil for the 1980–2007 period: Measuring the activity, intensity and structure effects. *Energy Policy* **37**(12), 5208–5220 (2009)
2. Chung, W., et al.: A study of residential energy use in Hong Kong by decomposition analysis 1990–2007. *Appl. Energy* **88**(12), 5180–5187 (2011)
3. Tanoto, Y., Praptiningsih, M.: Factors decomposition of Indonesia's household electricity consumption. *Eng. J.* **17**(2), 19–28 (2013)
4. Pasila, F., Alimin, R., Natalius, H.: Neuro-fuzzy architecture of the 3D model of massive parallel actuators. *ARNP J. Eng. Appl. Sci.* **9**(12), 2900–2905 (2014)
5. S. Corporate: PLN Statistics 2010. PT. PLN (Persero), Jakarta, Indonesia (2011)
6. Bank Indonesia: Special Data Dissemination Standard. [http://www.bi.go.id/sdds/series/NA/index\\_NA.asp](http://www.bi.go.id/sdds/series/NA/index_NA.asp) (2010)

# Chapter 17

## Odometry Algorithm with Obstacle Avoidance on Mobile Robot Navigation

Handry Khoswanto, Petrus Santoso and Resmana Lim

**Abstract** Many algorithms have been devised on mobile robot navigation system. Some of them use algorithm based on newer concept like fuzzy logic or genetic algorithm. Some are stick on older algorithm like odometry. A simple, less intensive calculation algorithm for a lightweight telepresence robot is required. To accommodate the requirement, odometry algorithm is chosen specifically. Obstacle avoidance feature is proposed to enhance the algorithm. A mobile robot prototype is implemented using Arduino UNO, two DC geared motors, single caster wheel, and an ultrasonic sensor. Two kind of experiments are performed. The first experiment is to verify that odometry algorithm is working. The second one is used to verify obstacle avoidance mechanism. The results are satisfying. Mobile robot can avoid the obstacle and reach the destination correctly. Further experiment is needed to decide about ultrasonic sensor placement in a real telepresence robot.

**Keywords** Odometry algorithm · Mobile robot · Telepresence robot · Arduino

### 17.1 Introduction

An autonomous robot is required to have navigation capability. Given a certain destination point in its environment, the robot is expected to reach the destination autonomously. Many algorithms with different degrees of complexities have been devised in the recent years. Some of them use fuzzy logic [1–3], genetic algorithms [4–6]. Some also stick on older algorithm like odometry. Odometry is a basic method of navigation, used by virtually all robots [7]. Odometry also proven successfully used on project like Mars Exploration Rovers [8].

---

H. Khoswanto (✉) · P. Santoso · R. Lim  
Department of Electrical Engineering, Petra Christian University, Surabaya, Indonesia  
e-mail: handry@petra.ac.id

There is a need to have a simple, less intensive calculation to support an ongoing project of telepresence robot with an open protocol framework [9]. In this case, a design decision has been made to do an exploration on the potential of odometry algorithm. An obstacle avoidance feature also proposed to enhance the algorithm when facing unexpected obstacle on the robot's navigation route.

The paper describes how the odometry algorithm can be used by a mobile robot to reach a certain goal location using single ultrasonic sensor and servo motor. Using knowledge of wheel's motion, an estimation of robot's motion can be derived. The mobile robot prototype uses Arduino controller, L298 DC Motor driver, and disk encoder using optocoupler sensor. The mobile robot is differentially driven, it has a motor on the left and right side and equipped with single caster wheel on the back side. To add the capability of obstacle avoidance, a single ultrasonic sensor and Tower Pro micro servo motor are added to the prototype.

## 17.2 Hardware and Mechanic Design

This paper designed mobile robot with the aim of reaching the destination point even though there are particular obstacles on its route. The system block diagram is given on Fig. 17.1.

The robot uses ultrasonic sensors to detect the distance of objects in front of it. Ultrasonic sensors placed on servo motors so that it can rotate  $180^\circ$ . The rotation of the servo starting from  $-90^\circ$  to  $90^\circ$  in increments of  $45^\circ$ . Using servo motors, the ultrasonic sensor is capable of facing on five different directions (left, oblique left, front, oblique right, and right). To calculate the rotation of the motor, a mobile robot uses an acrylic disc encoder with 12 holes that can be read by optocoupler. Installation of disc encoder is parallel with the wheels. The actuator uses two geared DC motor with two shafts. The first shaft installed on encoder disk and the other shaft is mounted on wheel. Figure 17.2 represent the mechanical design of mobile robot prototype.

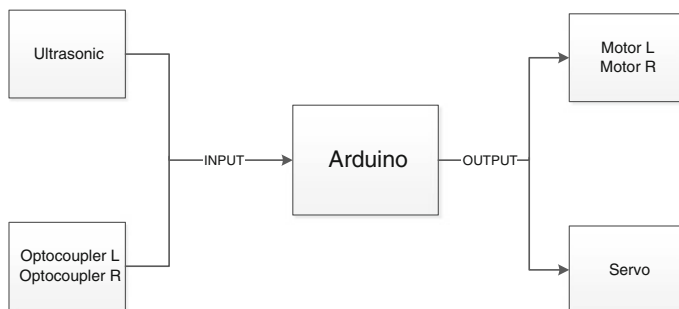


**Fig. 17.1** System block diagram

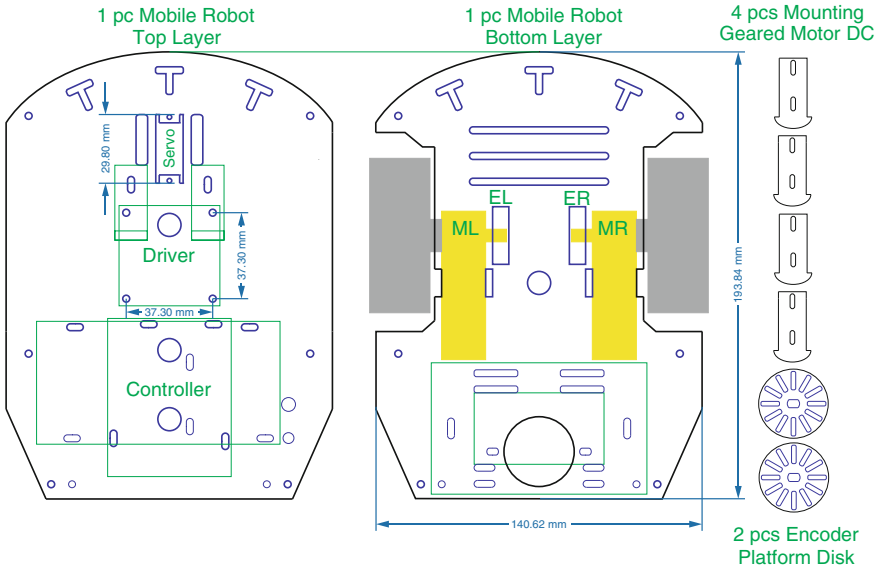
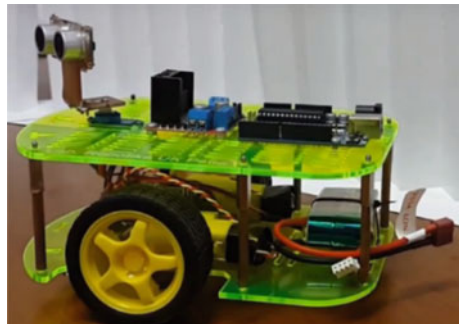


**Fig. 17.2** Acrylic mobile robot platforms and mounting parts

Figure 17.2 shown the top and bottom platform layer, and the mounting accessories for DC Geared Motor and disc encoder. On the top layer there is a square hole which is used to place a micro servo motors. Micro servo motor is used to enable the movement of ultrasonic sensor. The second devices on top layer are L298 DC motor driver and Arduino UNO controller. On bottom layer, there are two geared DC motors, namely motor left (ML) and motor right (MR). Two DC motors are installed using 4 mounting pieces in the right places. Each disc encoder has 12 holes for one rotation. So, one tick represents 30 degrees of rotation of the wheel. Each of these holes will generate a pulse that will be read by optocoupler sensor. An optocoupler, also known as an optoisolator or photocoupler, is an electronic component that interconnects two separate electrical circuits by means of a light sensitive optical interface. Figure 17.3 represents the implemented mobile robot prototype.

**Fig. 17.3** Mobile robot prototype





### 17.3 Odometry and Robot Model

Odometry is measurement method from motion sensor or rotation sensor to estimate change in position over time. Odometry is used by some robots, whether they be legged or wheeled, to estimate (not determine) their position relative to a starting location. This method is sensitive to errors due to the integration of velocity measurements over time to give position estimates. Rapid and accurate data collection, equipment calibration, and processing are required in most cases for odometry to be used effectively.

Figure 17.4 explain about detailed odometry geometry for our mobile robot. The vehicle starts from  $(x, y, \theta)$  and destination position at  $(x', y', \theta')$ . The center between two wheels of the robot travels along an arc trajectory. Remembering that arc length is equal to the radius times the inner angle, the length of this arc is:

$$d_{center} = \frac{d_{left} + d_{right}}{2} \tag{17.1}$$

On basic geometry, the equation is:

$$\varphi r_{left} = d_{left} \tag{17.2}$$

$$\varphi r_{right} = d_{right} \tag{17.3}$$

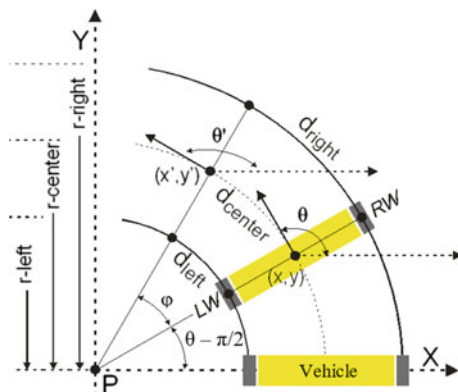
If  $d_{baseline}$  is distance between the left and right wheels:

$$r_{left} + d_{baseline} = r_{right} \tag{17.4}$$

Subtracting from Eqs. (17.2) and (17.3) above:

$$\varphi = \frac{d_{right} - d_{left}}{d_{baseline}} \tag{17.5}$$

**Fig. 17.4** Odometry geometry for mobile robot



Wheel encoders give the distance moved by each wheel, left and right wheel. Assume the wheels are following an arc trajectory for short time scale.

$$x' = x + d_{center} \cos \emptyset \tag{17.6}$$

$$y' = y + d_{center} \sin \emptyset \tag{17.7}$$

$$\emptyset' = \emptyset + \frac{d_{right} - d_{left}}{d_{baseline}} \tag{17.8}$$

Calculation of wheel circumference is needed to know how far motion of the robot. Mobile robot uses two wheels with 65 mm diameter. Each wheel is equipped with 12 holes disc encoder for one rotation. The equation is as follows.

$$\Delta tick = tick' - tick \tag{17.9}$$

$$d_{left} = 2.\pi.r.\frac{\Delta tick_{left}}{N} \tag{17.10}$$

$$d_{right} = 2.\pi.r.\frac{\Delta tick_{right}}{N} \tag{17.11}$$

### 17.4 Software Design

The flowchart of the system is depicted on Fig. 17.5. Position estimation is used to predict robot position by counting the pulse sent by optocoupler. The direction of the robot can be known from the result of pulse count from the left and right optocoupler. Robot reads the destination coordinate and always check the odometry pulses (dtick1 and dtick2). Controller updates the newest position of mobile robot (x\_new, y\_new, teta\_new). After the robot gets the newest coordinate, controller calculates the difference between destination coordinate and current coordinate.

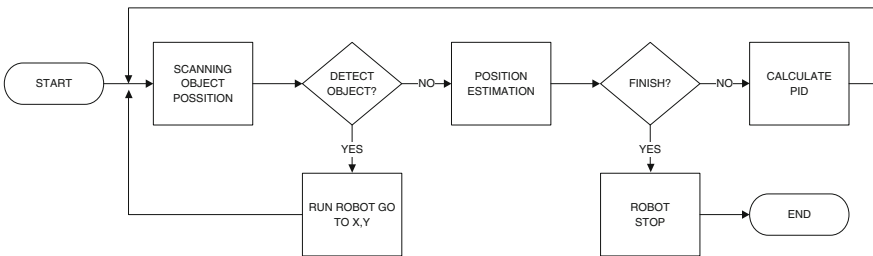


Fig. 17.5 System flowchart

Error is used to calculate PID parameters and determine the speed of left motor and right motor. This algorithm is repeated until destination point is reached.

Obstacle avoidance mechanism begins with the reading of obstacle position. Servo will rotate the ultrasonic sensor and get the data of distance between robot and obstacles from several different angles (0, 45°, 90°, 135°, and 180°). Each distance is saved and transformed using rotation and 2D translation depicted in Eqs. 17.12 and 17.13. Equation 17.12 is derivation of Eq. 17.13 where  $R(x, y, \theta)$  is a  $3 \times 3$  matrix. The transformation result gives the coordinate of world view depicted at Eq. 17.13.

$$R(x', y', \theta') = \begin{bmatrix} \cos(\theta') & -\sin(\theta') & x' \\ \sin(\theta') & \cos(\theta') & y' \\ 0 & 0 & 1 \end{bmatrix} \quad (17.12)$$

$$\begin{bmatrix} x_{di} \\ y_{di} \\ 1 \end{bmatrix} = R(x, y, \theta)R(x_{si}, y_{si}, \theta_{si}) \begin{bmatrix} d_i \\ 0 \\ 1 \end{bmatrix} \quad (17.13)$$

## 17.5 Result and Discussion

Mobile robot starts at the origin, pointed down the xy axis. Its starting state is  $(x, y, \theta)$  on  $(0, 0, 0)$  and the mobile robot will go to  $(x', y', \theta')$ . The experiment result will prove the usability of the navigation method.

The first experiment of mobile robot goes to goal without any obstacles with destinations coordinate  $(180, 50)$  cm. The second one goes to goal with obstacles with the same coordinate. Figure 17.6 shows how the mobile robot reach the destination on coordinates  $(180, 50)$  cm. The research experiment is completed with four obstacles. The obstacles are paper board sound damper with the height 25 cm and paper fold 1 cm. The obstacles are used to disturb ultrasonic wave transmission.

From 10 experiments with 4 obstacles and random position a success rate of 90 % is achieved. Without obstacles, 100 % success rate can be achieved.

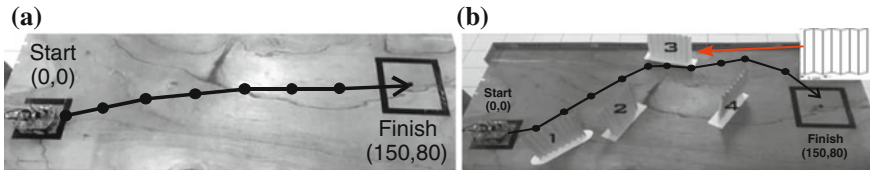


Fig. 17.6 Experiment: **a** without obstacles, **b** with obstacles

## 17.6 Conclusion

Odometry method is able to carry the mobile robot to reach its destination. One of the weaknesses of the system is drifting of the wheels. In the second experiment paper board sound damper as obstacles is added. In this schema, the mobile robot still can reach its goal. Considering the result of the experiment, there is still a need of further experiment to decide on ultrasonic sensor placement on a real telepresence robot.

**Acknowledgment** This Research is funded by Competitive Research Grants fund of Indonesian Higher Education Directorate under contract no. 30/SP2H/PDSTRL\_PEN/LPPM-UKP/IV/2015.

## References

1. Oriolo, G.: Real-time map building and navigation for autonomous robots in unknown environments. *IEEE Trans. Syst. Man Cybern. B Cybern. Soc.* **28**(3), 316–333 (1998)
2. Yang, X., et al.: A layered goal-oriented fuzzy motion planning strategy for mobile robot navigation. *IEEE Trans. Syst. Man Cybern. B Cybern.* **35**(6), 1214–1224 (2005)
3. Budiharto, W., et al.: Obstacles avoidance for intelligent telepresence robot using interval Type-2 FLC. *CIC Express Lett.* **8**(3), 821–827 (2014)
4. Sugihara, K., Smith J.: Genetic algorithms for adaptive motion planning of an autonomous mobile robot. In: *International Symposium on Computational Intelligence in Robotics and Automation* (1997)
5. Hu, Y., Yang, S.X.: A knowledge based genetic algorithm for path planning of a mobile robot. In: *International Conference on Robotics and Automation* (2004)
6. Sedighi, K.H., Ashenayi, K., Manikas, T.W., Wainwright, R.L., Tai, H.M.: Autonomous local path planning for a mobile robot using a genetic algorithm. In: *Congress on Evolutionary Computation* (2004)
7. Olson, E.: *A primer on odometry and motor control* (2004)
8. Maimone, M., et al.: Two years of visual odometry on the mars exploration rovers. *J. Field Robot.* **24**(3), 169–186 (2007)
9. Petrus, S., Handry, K.: Open protocol framework for telepresence robot. *ARNP J. Eng. Appl. Sci.* **9**(12), 2437–2440 (2014)

**Part III**  
**Technology Innovation in Electrical**  
**Engineering, Electric Vehicle**  
**and Energy Management**

# Chapter 18

## Vision-Based Human Position Estimation and Following Using an Unmanned Hexarotor Helicopter

Jung Hyun Lee and Taeseok Jin

**Abstract** We describe the design and performance of a prototype hexarotor unmanned aerial vehicle (UAV) platform featuring autonomous flying based on an inertial measurement unit (IMU) for use in bluetooth communication environments. A recent trend in studies on free-flying UAVs with hexarotors has been to outfit UAVs with gimbals to support various services. To realize this, it is necessary for UAVs to carry out human tracking's ability. We present preliminary results of human-following control with this UAV platform and implement a simple following flight strategy, based on a vision-based Kalman filter. The moving object (a walking human) is assumed to be a point object and is projected onto an image plane to form a geometrical constraint equation that provides the position data of the object based on kinematics in the local north-east-down (NED) coordinate system. Computer presents the simulation results of the predicting and following of a walking human using a UAV.

**Keywords** Hexarotor · UAV · Tracking · Recognition · CCD camera

### 18.1 Introduction

In accordance with the remarkable progress achieved recently in unmanned aerial vehicles (UAV) miniaturization and performance [1, 2], ongoing research and efforts toward commercialization of UAVs have been pursued in various fields of application such as logistics services, disaster relief, surveillance, and entertainment. In many applications, vision systems play an indispensable role in UAV

---

J.H. Lee · T. Jin (✉)

Electronics and Telecommunications Research Institute, Daejeon, Korea  
e-mail: hwigangkim@etri.re.kr

J.H. Lee

e-mail: twbae@etri.re.kr

systems in order to successfully complete tasks. A variety of vision systems using off-the-shelf components have been reported in the literature [3]. By integrating information from vision system and other adopted sensors, the functions of unmanned systems can be fully extended to perform missions such as surveillance, human following [4], vision-aided flight control [5], object tracking [6], terrain mapping [7], and navigation [7, 8]. These missions are derived from both military and civilian requirements, such as aiding soldiers in urban operations to effectively spot, identify, designate, and destroy targets, and assisting rescuers in missions after natural disasters. Compared to traditional navigation systems and sensors, vision systems offer the unique capability of providing rich information on objects of interest and their surrounding environments, including shape and appearance.

This paper presents a mathematical model for the construction of a system structure and control method in order to implement remote control technology for application to a hexarotor helicopter whose development is the ultimate objective of this study. The hexarotor UAV in development will be used in actual tasks such as gathering information during disasters or for security's purpose as a small autonomous flying robot. Two studies were conducted to identify a design solution for achieving this purpose [3, 9]. The first involved the design of a north-ease-down (NED) frame-based UAV where vehicle position is introduced in order to follow a walking human along the shortest-time trajectory. Here the UAV was controlled to follow a walking human using a vision sensor centered on an inertial measurement unit (IMU) and a microcontroller unit (MCU). The second study involved the design of a human-following algorithm and an operational program optimized for computed attitude in order to implement the two requirements of autonomous control and task completion (Fig. 18.1).

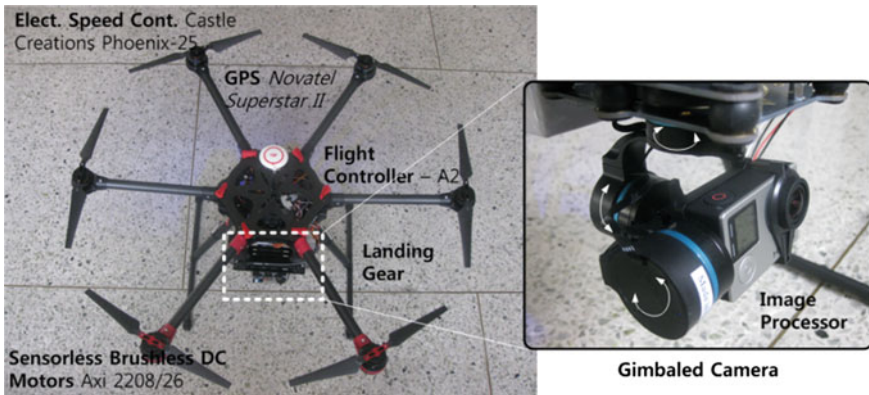


**Fig. 18.1** Flight-capable hexarotor prototype

## 18.2 System Configuration

### 18.2.1 Test Configuration

In this paper, we follow the results reported in [5, 6] to present the design and implementation of a comprehensive vision system for an unmanned hexarotor. More specific, we focus on issues related to vision-based human following on the ground. Interested readers are referred to Caballero [7] for more information on the development and applications of vision systems for unmanned helicopters.

The linear and angular velocities of a walking human were estimated to allow a hovering UAV to predict human's future trajectory, planning the shortest-time path to predict and follow the walking human's movement. A state estimator was designed to overcome the uncertainties from the image data caused by the point object assumption and physical noise, using Kalman filter. Based on the estimated velocities of the human, the position of the UAV was controlled to follow the walking human in the center of the image frame.

The camera system of the UAV has the ability to pan and tilt, as shown in Fig. 18.2. The position and posture of the camera are defined with respect to the base frame. According to NED coordinates, the position  $\mathbf{p}$  can be obtained after establishing the camera coordinate system and representing parameters, including the attitude vector in spherical coordinates represented by the Radius ( $r_{sp}$ ), azimuth

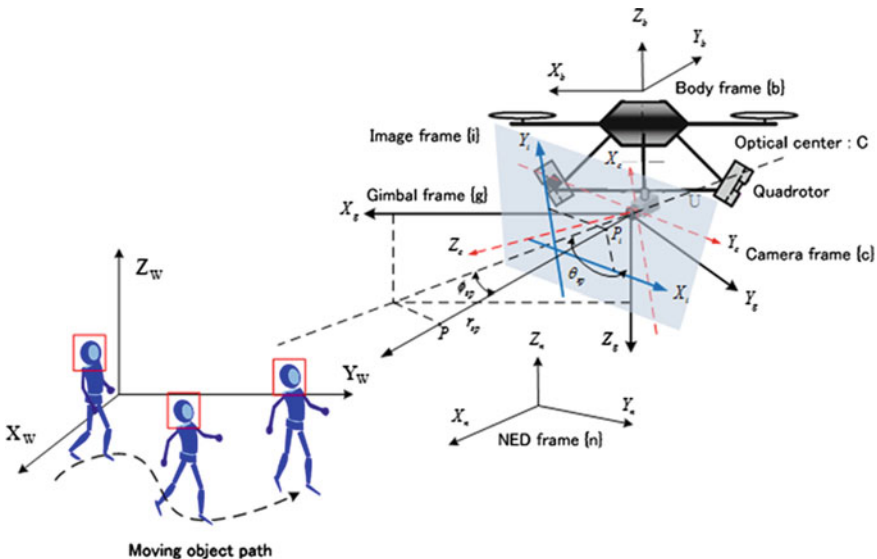


**Fig. 18.2** Estimation of position information, radius  $r_{sp}$ , azimuth angle  $\theta_{sp}$ , and elevation angle  $\phi_{sp}$



angle ( $\theta_{sp}$ ), and elevation angle ( $\phi_{sp}$ ), by tilting and panning angles of the camera as in Xiao [8].

## 18.2.2 Coordinate Frames Used in Vision Systems

Depicted in Fig. 18.2 are coordinate systems that are adopted in UAV vision systems. These are as follow:

The local north-east-down (NED) coordinate system (labeled with a subscript  $n$ ) is the same as that defined in Stevens [10]. We recall it here for ease of reference. It consists of an orthogonal frame on the surface of the earth whose origin is the launching point of the aircraft from the earth's surface. The  $X_n$ - $Y_n$  plane of the NED frame is tangent to the surface of the earth at the origin of the NED frame. The coordinate  $X_n$ ,  $Y_n$  and  $Z_n$ -axes of the NED frame are specified to point toward the north, east, and down (i.e., toward and into the earth, vertical to the earth's surface), respectively.

The spherical coordinate system (labeled with a subscript  $sp$ ) is attached to the base of the pan/tilt servo mechanism. It is used to define the orientation of the camera and the target with respect to the UAV. Given a generic point  $P_s$  in the servo-based coordinate system, we write

$$P_s = \begin{pmatrix} x_s \\ y_s \\ z_s \end{pmatrix} \quad (18.1)$$

This point's position can be defined in the spherical coordinate system by three numbers: radius  $r_{sp}$ , azimuth angle,  $\theta_{sp}$ , and elevation angle  $\phi_{sp}$ , which are given by

$$P_{sp} = \begin{pmatrix} r_{sp} \\ \theta_{sp} \\ \phi_{sp} \end{pmatrix} \quad (18.2)$$

where,  $r_{sp} = \sqrt{x_s^2 + y_s^2 + z_s^2}$ ,  $\theta_{sp} = \tan^{-1}\left(\frac{y_s}{x_s}\right)$ ,  $\phi_{sp} = \sin^{-1}\left(\frac{z_s}{r_{sp}}\right)$ ,

The camera coordinate system or camera frame (labeled with a subscript  $c$ ) describes the orientation of the camera which is attached to the end of the gimbal. Here, the pan/tilt rotation with respect to the servo-based frame are given as

$$X_{c,sp} = \begin{pmatrix} \theta_{c,sp} \\ \theta_{c,sp} \end{pmatrix} \quad (18.3)$$

The origin of the camera coordinate system is the optical center of the camera.

The  $Z_c$ -axis is aligned with the optical axis of the camera and points from the optical center C toward the image plane, when the camera frame coincides with the

servo-based frame,  $\mathbf{x}_{c,sp} = 0$ . Otherwise,  $\mathbf{x}_{c,sp}$  corresponds to the rotation of the camera frame first about the  $Y_s$ -axis by an angle of  $\theta_{c,sp}$ , and then about the  $X_s$ -axis by an angle of  $\phi_{c,sp}$ . This rotation sequence is defined in terms of the structure of the pan/tilt servo mechanism. The object coordinate system or object frame (labeled with a subscript o) is attached to a fixed ground landmark.

## 18.3 Trajectory Estimation of Walking Human

### 18.3.1 Walking Human Model

When the velocity and acceleration of a walking human and a mobile robot can be estimated, the future human position ( $\hat{T}_x, \hat{T}_y$ ) can be predicted as follows:

$$\hat{T}_{x+\delta t} = \hat{T}_x + \hat{V}_x \delta t + \frac{1}{2} \hat{A}_x \delta t^2 \quad (18.4)$$

$$\hat{T}_{y+\delta t} = \hat{T}_y + \hat{V}_y \delta t + \frac{1}{2} \hat{A}_y \delta t^2 \quad (18.5)$$

where  $\delta t$  is the sampling time and  $(\hat{T}_x, \hat{T}_y)$ ,  $(\hat{V}_x, \hat{V}_y)$  and  $(\hat{A}_x, \hat{A}_y)$  are the current Cartesian coordinate estimates of the human position, velocity, and acceleration, respectively.

In X-Y coordinates, movement of the human can be decomposed into linear velocity elements and angular velocity elements as follows:

$$\delta x_{k+\delta t,k} = v_k \delta t \cos(\theta_k + \frac{1}{2} \omega_k \delta t) \approx v_k \cos(\theta_k) \delta t - \frac{1}{2} \omega_k v_k \sin(\theta_k) \delta t^2 \quad (18.6)$$

$$\delta y_{k+\delta t,k} = v_k \delta t \sin(\theta_k + \frac{1}{2} \omega_k \delta t) \approx v_k \sin(\theta_k) \delta t + \frac{1}{2} \omega_k v_k \cos(\theta_k) \delta t^2 \quad (18.7)$$

$$\delta \theta_{k+\delta t,k} = \omega_k \delta t, \quad \delta v_{k+\delta t,k} = \xi_v, \quad \delta \omega_{k+\delta t,k} = \xi_\omega \quad (18.8)$$

where  $v_k$  and  $w_k$  are the linear and angular velocities of the objects, and  $\xi_v$  and  $\xi_\omega$  are the variations of linear and angular velocity, respectively.

From (18.6)–(18.8), we obtain the state transition matrix:

$$\begin{aligned} \mathbf{x}_k &= \Phi_{k,k-1} \mathbf{x}_{k-1} + \mathbf{w}_{k-1} \\ \mathbf{z}_k &= \mathbf{H}_k \mathbf{x}_k + \mathbf{v}_k \end{aligned} \quad (18.9)$$

Notice that  $\Phi_k$  is the state transition matrix,  $\mathbf{w}_k$  is the vector representing process noise,  $\mathbf{z}_k$  is the measurement vector,  $\mathbf{H}_k$  represents the relationship between the measurement and the state vector, and  $\gamma_x$  and  $\gamma_y$  are x and y directional measurement errors, respectively.

### 18.3.2 State Estimation

Input data such as image information include uncertainties and noise generated during data-capturing and processing steps. Furthermore, the state transition of a moving object also includes irregular components. Therefore, as a state estimator robust in the face of these irregularities, Kalman filter was adopted to form as state observer [10]. The Kalman filter minimizes estimation error by modifying the state transition model based on the error between the estimated and measured vectors with an appropriate filter gain. The state vector, which consists of position on the x-y plane, linear/angular velocities, and linear/angular accelerations, can be estimated using the measured vectors representing the position of a moving object on the image plane [11].

The covariance matrix of the estimated error must be calculated in order to determine the filter gain. The projected estimate of the covariance matrix of the estimated error is represented as

$$P'_k = \Phi_{k,k-1} P_{k-1} \Phi_{k,k-1}^T + Q_{k-1} \quad (18.10)$$

where  $P'_k$  is a zero-mean covariance matrix representing prediction error,  $\Phi_k$  represents system noise,  $P_{k-1}$  is an error covariance matrix for the previous step, and  $Q_{k-1}$  represents other measurement and computational errors.

The optimal filter gain  $K_k$  that minimizes the errors associated with the updated estimate is

$$K_k = P'_k H_k^T [H_k P'_k H_k^T + R_k]^{-1} \quad (18.11)$$

where  $H_k$  is the observation matrix and  $R_k$  is the zero-mean covariance matrix of the measurement noise.

The estimate of the state vector  $\hat{x}_k$  from the measurement  $Z_k$  is expressed as

$$\hat{x}_k = \Phi_{k,k-1} \hat{x}_{k-1} + K_k [Z_k - H_k \Phi_{k,k-1} \hat{x}_{k-1}]. \quad (18.12)$$

Therefore,  $\hat{x}_k$  is updated based on the new values provided by  $Z_k$ . The error covariance matrix used for the prediction  $P_k$  can be updated as follows:

$$P_k = P'_k - K_k H_k P'_k \quad (18.13)$$

After the current time is updated to  $k + 1$ , a new estimation can be provided using Eqs. (18.10)–(18.13). To incorporate measurement noise, which is empirically assumed to be zero-mean Gaussian random noise with a variance of 2, the linear and angular velocities of the object are set as follows:

$$\begin{aligned} v_k &= 15 * (\sin(0.02 * k) + 1) + \xi_v \text{ [cm/sec]} \\ \omega_k &= 0.7 * \cos(0.01 * k) + \xi_\omega \text{ [rad/sec]} \end{aligned} \quad (18.14)$$

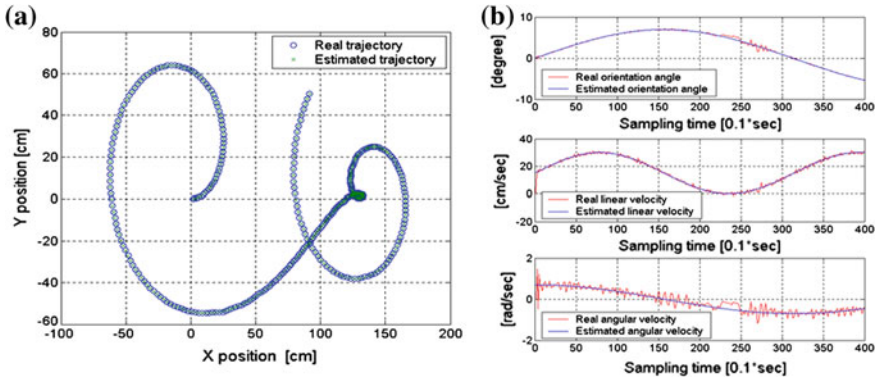


**Fig. 18.3** A real trajectory and state estimation results: **a** The trajectory of a walking human and **b** state estimations  $\theta_k$ ,  $v_k$ , and  $\omega_k$  using a Kalman filter

where the linear and angular velocities ( $\zeta_v$ ,  $\zeta_w$ ) are assumed to include Gaussian random noise with the variance of 3 and 0.1, respectively. Figure 18.3 shows the real trajectory of a walking human and Kalman filter estimation of the states in a noisy environment.

## 18.4 Conclusion

This study analyzed the system configuration of a hexarotor helicopter, advancing hexarotor design a step beyond what currently exists; it also analyzed flight motion based on the rotation of each rotor. In order to evaluate the hexarotor's wing control performance in roll and pitch, we presented simulation results for each response based on the heading reference value in the mathematical model using a local north-east-down (NED) coordinate system. Furthermore, we presented the result of an ongoing indoor human-tracking and following simulation. The proposed model is able to close the gap between the motion of the human and that of the UAV's. We showed that movement estimation using Kalman filter-based vision sensor can enable a UAV to hover and follow a walking human, based on their estimated trajectories along the shortest-time path.

In future research, we plan to study a sensor-based feedback control method in order to advance the intelligence part of the system with the goal of achieving autonomous decision making and flight features.

**Acknowledgements** This paper was supported by the Ministry of Education, (MOE) through the fostering project of the Innovation for Engineering Education, and the Basic Science Research Program through the National Research Foundation of Korea (NRF) funded by the Ministry of Education, Science and Technology (No. 2010-0021054).

## References

1. Abdolhosseini, M., Zhang, Y.M., Rabbath, C.A.: An efficient model predictive control scheme for an unmanned quadrotor helicopter. *J. Intell. Rob. Syst.* **70**, 27–38 (2013)
2. Nonami, K., et al.: *Autonomous Flying Robots: Unmanned Aerial Vehicles and Micro Aerial Vehicles*. Springer (2010)
3. Ritz, R., Muller, M.W., Hehn, M., D'Andrea, R.: Cooperative Quadcopter Ball Throwing and Catching. In: *IEEE/RSJ International Conference on Intelligent Robots and Systems*, pp. 4972–4978 (2012)
4. Achtelik, M., Bachrach, A., He, R., Prentice, S., Roy, N.: Autonomous navigation and exploration of a quadrotor helicopter in GPS-denied indoor environments. In: *Robotics: Science and Systems Conference* (2008)
5. Phillips, W.F.: *Mechanics of Flight*. Wiley (2004)
6. Stengel, R.F.: *Flight Dynamics*. Princeton University Press (2004)
7. Caballero, F., Merino, L., Ferruz, J., Ollero, A.: Vision-based odometry and slam for medium and high altitude flying UAVS. *J. Intell. Robot. Syst.* **54**, 137–161 (2009)
8. Xiao, J., Yang, C., Han, F., Cheng, H.: Vehicle and Person Tracking in Aerial Videos, *Multimodal Technologies for Perception of Humans*, pp. 203–214. Springer, Berlin (2008)
9. Alaimo, A., Artale, V., Milazzo, C., Ricciardello, A.: Pid controller applied to hexacopter flight. *J. Intell. Rob. Syst.* **73**, 261–270 (2014)
10. Stevens, B.L., Lewis, F.L.: *Aircraft control and simulation*, 2nd edn. Wiley, Hoboken (2003)
11. Miller, A., Babenko, P., Hu, M., Shah, M.: Person, Tracking in UAV Video, *Multimodal Technologies for Perception of Humans*, pp. 215–220. Springer, Berlin (2008)

# Chapter 19

## The Role of Renewable Energy: Sumba Iconic Island, an Implementation of 100 Percent Renewable Energy by 2020

Abraham Lomi

**Abstract** Sumba Iconic Island is a pilot project. This project is initiated for the development of the Sumba Island as the iconic island of renewable energy. The aim of this project is to improve the access to energy through the development and utilization of new renewable energy resources. By the year of 2020, the 100 % realization of this project should be achieved. The initiative of Sumba Iconic Island on Renewable Energy has been started since 2010 by the Ministry of Energy and Mineral Resources, together with Bappenas and Hivos, a non-Governmental International organization. In November 2012, ADB also joined to accelerate the realization of this initiative. In 2013, the Norwegian Embassy in Indonesia has also taken a role in supporting the implementation of initiatives of Sumba Iconic Island. The selection of Sumba as an iconic island is based on studies. Those studies showed that the potential of renewable energy in Sumba is very large. The potential can be used as one of the main tools to drive the economic community in Sumba Island. Since it was initiated in 2011, the project has installed renewable electricity with capacity of about 5.87 MW. They consist of Micro-hydro power plant, solar power plant, Solar Water Pumping, Wind turbine generator, Biomass, Biogas, and Energy efficient furnaces.

**Keywords** Hivos · Off-grid · Renewable energy · Rural areas · Sumba Iconic Island · Urban area

### 19.1 Introduction

Global warming and the depletion of fossil fuel reserves have raised a lot of concern for utilizing renewable energy sources. This energy creates green environment as well as preserve the earth for future generations. In addition to hydropower, the

---

A. Lomi (✉)

Department of Electrical Engineering, Institut Teknologi Nasional Malang,  
Jl. Raya Karanglo, Km. 2, Malang 65143, Indonesia  
e-mail: abraham@itn.ac.id

energy which is generated from wind, photovoltaic and biomass have great potential usage to meet the energy needs, especially in the remote areas. Those areas are far from the State Electricity Company (“Perusahaan Listrik Negara”–PLN) grid. The latest developments and trends in electrical power consumption indicates the use of renewable energy is increasing. The electrification of rural and remote areas is potentially a desirable investment. However, there has been considerable discussion about the social economic and other benefits as well as the costs of the electrification of these areas in developing countries. Apart from the benefits related to the improvement of the living conditions, the potential benefits include (1) socioeconomic, (2) sociopolitical, and (3) environmental benefits [1]. Solar energy and wind energy are two sources of renewable energy that are most commonly used. Wind energy has become the most expensive technology. Many scientists are interested in doing research in that field. Solar cells convert energy from sunlight into DC electricity. Photovoltaic (PV) offers many advantages over other renewable energy in the absence of noise and minimal maintenance.

The island of Sumba is located in eastern part of Indonesia archipelago. It is located between Sumbawa Island to the Northwest and West Timor to the East and Australia to the far South at a distance of about 700 km.

The island is part of East Nusa Tenggara province (Nusa Tenggara Timur), and one of the four largest islands in NTT. The total land area is approximately 11,052 km<sup>2</sup>, and has population of only 656,259 inhabitants and density of 58.62 inhabitants per km<sup>2</sup>. The island is mountainous with small pockets of flat land, and its highest point is Wanggameti Mountain (1,225 m), as shown on the base map of Sumba (Fig. 19.1).

Administratively the island is divided into four regencies (Kabupaten), East Sumba (7000.5 km<sup>2</sup>), Central Sumba (1,868.19 km<sup>2</sup>), West Sumba (737.42 km<sup>2</sup>), and Southwest Sumba (1,445.32 km<sup>2</sup>) [2]. The biggest city is Waingapu, which is the capital city of East Sumba district. Like many developing regions, not only are the effects of climate change felt more acutely, but also electricity is not widely available, and where it does exist, it is supplied with polluting, expensive, imported resources in Sumba’s case, diesel and kerosene [3]. The Sumbanese are among the



**Fig. 19.1** Map of Nusa Tenggara

billions of people on this planet who do not have access to clean energy. They are forced to cook over unhealthy wood fires and their source of light is only smoking oil lamps. In most of the villages on the island, life stops as soon as the sun goes down.

HIVOS [4], a non-Governmental International organization first visited the island of Sumba in 2009. This organization was looking for a location where they could show the access to renewable energy that can alleviate poverty even in remote and isolated areas. Sumba was an ideal candidate and located in one of the poorest areas of Indonesia. Its inhabitants are without prospects of economic advancement and the island has one of the lowest electrification ratios in Indonesia.

Sumba Iconic Island initiative was launched through the effort of HIVOS at the Indonesia-Netherlands Joint Energy Working Group in 2010. This program is aimed at developing a “model” island supplied entirely by renewable energy. With this initiative, Sumba Island has been selected as a pilot example of scaling up access to energy by renewable resources utilization due to its existing energy profile: (1) low level of access to modern energy (less than 30 %); (2) high dependence on fossil energy (Diesel); and various types of renewable energy resources exist: hydro, solar, wind, and biomass resources. Sumba Iconic Island initiative sets ambitious targets to reach 95 % electrification ratio and meet 100 % energy demand by 2020.

Sumba Iconic Island Road Map was formally released during a “National Seminar & Stakeholder Meeting on Sumba” on February 13–15, 2013 in Jakarta. This Road Map distinguishes 15 activities classified by renewable energy technologies of which each activity is divided into a uniform 5 sub-activities, namely, (a) Renewable energy technology Installation; (b) Supporting regulations and policies; (c) Institutional framework and stakeholder roles; (d) Investment and funding; and (e) Research and development [5].

Based on the SII roadmap, the total capacity to fulfil the need of energy 2025 of about 32.57 MW, while the total installed capacity of renewable energy in Sumba island from 2011 to 2014 is about 4.87 MW or about 15 % from target. The electrification ratio target on Sumba Iconic Island will be 100 % in 2020. The existing electrification ratio for Sumba Island is about 37.41 %, while the contribution of EBT is about 9.76 %. This shows that the construction of new EBT plant in the next 5 years is about 24 MW.

## 19.2 The Global Electrification Challenge

The World Energy Outlook 2013 of the International Energy Agency (IEA) states that access to electricity is still lacking for some 1.3 billion people—some 20 % of the world’s population. Those people are located mostly in Asia and sub-Saharan Africa. Most of these people live in rural and remote areas of the developing countries. In the past few decades, the donor community, development banks, the private sectors, nongovernmental organizations (NGOs), and other organizations



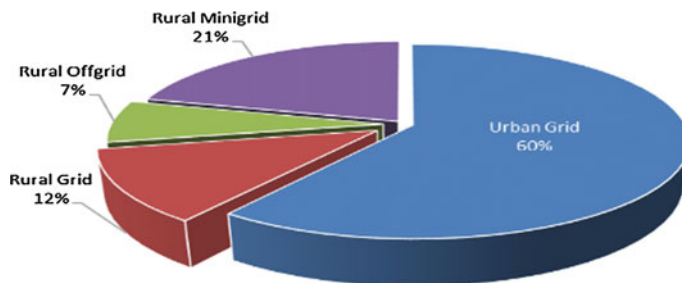


**Fig. 19.2** Universal electrification and expected share connections by type

have developed and implemented a number of initiatives to help improve modern energy supplies to deprived regions in the developing world.

The electrification of rural areas has often been based on the electricity supply from a central grid. But current renewable energy technologies offer enhanced opportunities for off-grid power systems and include photovoltaic (PV) systems, wind turbines, bio-mass fueled combined-heat-and-power units, hybrid systems, storage facilities, and fuel cells. Off-grid options include solar home systems (SHSs), portable battery kits, and similar solutions that can satisfy initial electricity needs. To achieve universal access by 2030, it is estimated that the period 2010–2030 some 550 million households need to be provided with electricity services; this figure takes into account expected population growth to 2030. Some 60 % (330 million) of the new connections will be needed in urban areas, and 40 % (220 million) must be installed in rural areas (see Fig. 19.2) [6].

### 19.3 Indonesia Renewable Energy Policy

A Strategy on Renewable Energy will be developed to achieve the goals, objectives and set out into a practical implementation plan. A number of important investigations will be undertaken during the strategy development. The strategy includes how the renewable energy target will be periodically reviewed with respect to the different primary energy carriers, the mechanism in the selection electricity's feed-in which is generated from the renewable resources, into the national electricity grid, and the modalities of the various financial, legal and regulatory instruments to be employed as part of the enabling framework of mechanisms to support the promotion of renewable energy (Fig. 19.3).

The main aim of the policy is to create the conditions for the development and commercial implementation of renewable technologies. Government will use a phased, managed and partnership approach to renewable energy projects that are well conceived and show the potential to provide acceptable social, environmental and financial returns for all investors and stakeholders. Renewable energy will

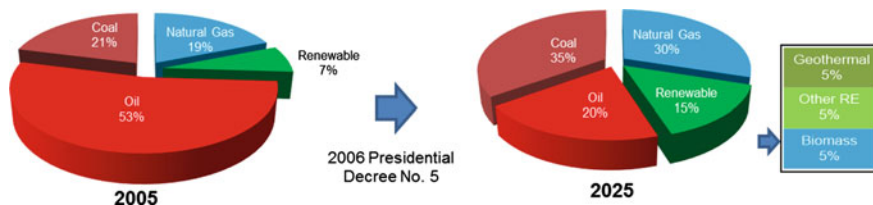


Fig. 19.3 Current energy mix versus future energy goals

contribute to the diversification of energy resources through the implementation of a properly managed programme of action that will provide sufficient incentive for the sustainable development of the renewable energy-based industries. Today, renewable energy accounts for a small but growing portion of Indonesia’s electricity portfolio. Most renewable energy comes from the hydropower and geothermal industries. Presidential Decree No. 5 mandates an increase in renewable energy production from 7 to 15 % of generating capacity by 2025 [7].

### 19.4 Indonesia Renewable Energy Potential

Indonesia is a country which is rich of natural resources. The Indonesia primary energy source can be managed and used to meet national energy needs, especially for the remote communities. However, the dependency to the energy derived from fossil attenuated the opportunity to develop environmentally friendly energy sources, i.e., sources of energy derived from new and renewable energy sources. Based on ESDM data (2013), Indonesian geothermal reserves amounted to 16,502 MW and geothermal potential of about 29 MW. The installed capacity of geothermal power plant (until May 2013) is 1,341 MW. Electricity potency from large scale hydro power amounted at 75 GW, while the potential of mini/micro hydro was about 769.69 MW. Meanwhile, the potential of electricity from biomass amounted to 13,662 MWe and the installed capacity of on grid power plant is 75.5 MWe.

Hydropower energy resource is grouped into large scale (can be developed for power plants above 10 MW per location) and small-scale/micro (potential electricity generation less than 10 MW). The potential for large-scale hydropower and small-scale/micro estimated respectively at about 75 GW and 450 MW. The potential is fairly spread in various parts of Indonesia. The use of hydropower resource is still relatively low at 4.2 GW of large-scale and small-scale of about 84 MW. Utilization of hydropower resources should be developed primarily with small-scale power spread schemes to meet local electricity needs.

Indonesia has a potential possibility for developing biomass power. Currently, only 443 MW have been commercially developed and the 49,810 MW biomass energy is undeveloped. By 2025, Indonesia has targeted to install about 810 MW of biomass power, an increase of 80 %. That amount is still far less than the potential contribution. Large-scale biomass projects would likely require new infrastructure to gather and deliver what is now considered as a waste item.

As a tropical country, the potential of solar power in Indonesia is quite high with an intensity of 4.8 kWh/m<sup>2</sup>/day and current installed capacity of solar power plant is 42.78 MW. Indonesia offers significant solar power resources (4.8 kilowatt-hours per square meter per day [kWh/m<sup>2</sup>/day]), but the country has yet to develop a strong market. In 2013, Indonesia has installed 12.1 MW of solar power, which is mostly from roof-mounted solar photovoltaic (PV) cells in urban areas. The use of solar energy in Indonesia is still very low at about 8 MW in the form of Solar Home System for the supply of electricity in rural areas. The low utilization of solar energy potential due to the cost of equipment (solar panels) is still expensive. With the growing market demand for solar panels in the world, estimated future prices of solar panels will tend to fall. Therefore, solar energy utilization in Indonesia should be developed including the possible use of the integrated scheme with grid. The total installed capacity of solar energy from 2005 to 2009 of 31.94 MWp and in 2009 is increased of 4.83 MWp (or 35.8 %) [8].

## 19.5 Renewable Energy Potential in Sumba Island

Even though the island of Sumba clearly has a significant renewable energy potential, the electrification ratio in 2009 has lagged behind other provinces and is amongst the lowest in Indonesia with i.e. 24.55 %.

Delivering power on an island with a unique topography and its people living scattered around this large island is costly and logistically challenging. In order to increase the number of households that enjoy some form of electrification, national and local governments have supplied a variety of small RE power systems to those area which not served by the PLN grid. Desk research and field validation uncovered that Sumba has a significant renewable energy resources potential. Hydro, solar, wind and biogas (from cattle) resources have been identified on the islands and compared to many other island in Indonesia, Sumba Island really stands out [9]. Although Renewable Energy sources were found abundantly, similarly to other islands the development of renewable energy in Sumba Island has stayed behind in terms of growth and capacity compared to diesel fueled power generation which is still the main source of electric power. Figure 19.4 shows the renewable energy resources locations in Sumba Island.

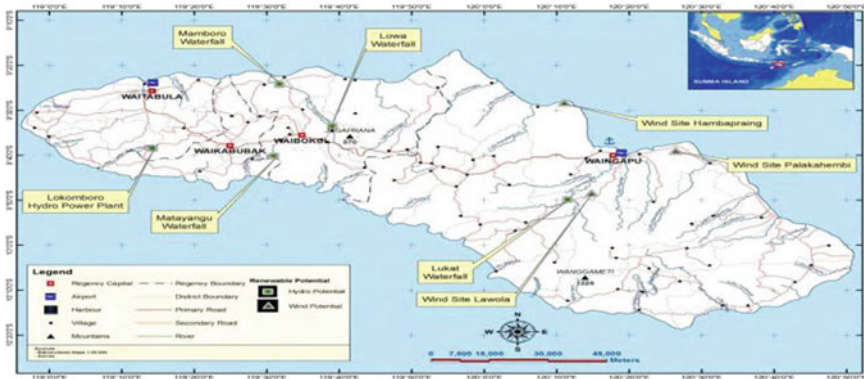


Fig. 19.4 Map of Sumba Island with renewable energy resources identification

### 19.6 Hydro Resource Potential Assessment

The hydro energy resource potential is concentrated mostly in the western part of Sumba Island and in addition some sites are located in the central and eastern part Sumba Island. Sites in West Sumba with the most significant potential are the Lapopu and Lokomboro waterfall, which have a measured net ‘head’ of 70 and 45 m respectively. Both this hydro potential has been operated since 1999 with the total capacity of 3.9 MW. Meanwhile, in the East Sumba, the site with the most significant hydro potential site is the Lukat/Maidang water, which has a measured head of 15 meters and is located about 30 km up river Kambaniru. Kambaniru Dam (see Fig. 19.5) located just outside the capital of Waingapu was planned to be utilized for a micro hydro installation with an electric capacity of a total of 2 MW. The potential of hydro power resources in Sumba Island as shown in Table 19.1.



Fig. 19.5 Kambaniru dam, Lokomboro waterfall, and Lapopu waterfall

**Table 19.1** Hydro energy potential

Site name	Debit (m <sup>3</sup> /s)	Head (m)	Predicted power (kW)
Luku Waiwuang/Wanokaka River Waterfall Lapopu	1.12–20.6	70	1,107
	Average 5.38		
Luku Mareha/Kalada River Waterfall Lokomoro	0.38–6.48	43.5	330
	Average 2.59		
Waterfall Lukat	3.83	25	282
Waterfall Lowa	1.82	10	54
Luku Panggulamba River Waterfall Memboro	12.84	25	944
Kambaniru Dam	13.6–85.7	5.4	618
	Average 38.9		

## 19.7 Wind Resource Potential Assessment

The large potential of wind energy has been found at Hambapraing, Tanjung Mondu, and Lawola. Lawola is expected to have even better wind resources although the local grid is relatively far from this site (see Fig. 19.6). This site is closed to Lukat waterfall which poses some interesting options to combine hydro and wind resources in one system [10]. These three sites have a potential of about 129 to 181 MW. It is fair to conclude that the wind energy could play a very significant role in electrification of Sumba. A prediction of theoretical wind energy power potential on the island of Sumba as shown in Table 19.2.

**Fig. 19.6** Wind energy farm at Kamanggi**Table 19.2** Prediction of wind energy potential

Wind Speed (m/s)	Power per square meter (W/m <sup>2</sup> )	Available Area (km <sup>2</sup> )	Power (GW)	Annual Energy (TW.h)
4.3–5.0	1.51–2.37	n/a	–	–
5.0–5.5	2.37–3.16	924	2,194–2,920	19,219–25,580
5.5–6.3	3.16–4.75	1.193	3,770–5,667	33,030–49,641
6.3–7.0	4.75–6.52	364	1,727–2,369	15,130–20,754
7.0–8.2	6.52–10.47	170	1,107–1,779	9,695–15,585
8.2–9.1	10.47–14.31	178	1,863–2,546	16,319–22,304

## 19.8 Solar PV Resource Potential Assessment

Being a tropical country, most of locations in Indonesia have a good solar radiation. The average daily solar insolation map above shows that Sumba has  $5 \text{ kWh/m}^2/\text{day}$ , which means that sun shines 5 h a day with a solar radiation  $1000 \text{ Watt/m}^2$ . If Sumba Island has an area of  $11,153 \text{ km}^2$ , therefore the solar energy potential on the island is about  $55,765 \text{ GW}$ . On practically all locations in Sumba it is technically feasible to install either a stand-alone PV systems, such as solar home systems or grid connected PV systems, as all locations have good solar insolation. According to data from ESDM, up to 25 thousands PV modules have been installed in Sumba altogether. Figure 19.7 shows the installed PV in different locations.

## 19.9 Biogas Resource Potential Assessment

Domesticated animals are an integral part of Sumba's society which becomes apparent to anyone that travels through the island; villages a diversity of pigs, horses, goats, cows and buffaloes roam around either freely, or are held in open stables and even under the traditional Sumbanese houses that are built on a raised platform; the animals stay here during the night. Herds of cows and horses roam freely in Savanna alike grasslands in which a large part of the island and is covered [11]. In order to estimate the biogas potential in the different regencies in Sumba 2014 data was obtained from the statistical agency BPS on live stock. As expected, it was found that cattle density per capita on the island of Sumba in 2014 is shown in Table 19.3 (Fig. 19.8).

## 19.10 Biofuels Resource Potential Assessment

Sumba was planned to be targeted for large scale development of particularly *Jatropha* in 2007. Although coconut was dismissed by the head of the Agriculture and Plantations agency, it seems to be the most likely candidate for biofuels production on the island of Sumba. Sumba produces about 7,491 tons of coconut on a



Fig. 19.7 Installed solar panel system

**Table 19.3** Large livestock population by kind and regency 2014

No	Regency	Cow	Buffalo	Horse	Pig	Goat/Sheep	Total	Inhabitants	Cattle/capita
1	West Sumba	2,585	16,611	5,526	81,003	4,173	109,898	103,481	1.06
2	Southwest Sumba	2,717	11,930	4,713	43,426	10,838	73,623	302,241	0.24
3	Central Sumba	7,788	7,920	7,341	47,225	4,674	74,921	65,606	1.14
4	East Sumba	50,435	34,469	29,336	97,933	52,815	264,985	241,416	1.09
	Total 2013	50,453	70,930	46,916	269,587	72,500	523,427	712,744	0.73



**Fig. 19.8** Livestock population

yearly base and as it is such a common commodity it would be relatively easy to expand. In addition excess shell and peat could, once dried, be used for biomass boilers to generate electricity. A total of 12,074 ha of coconut is already yielding and another 15,143 ha has been planted which if exclusively used for biofuel could yield 75 million liter of Crude Coconut Oil. The largest producer of coconut is now South West Sumba producing almost 3600 ton in 2013, a figure that is likely to triple as almost double of the current yielding area is classified as not yielding yet. Coconut oil is suitable for the production of biodiesel and therefore it would potentially serve the demand for fuel for (1) diesel generating sets for power generation (2) diesel trucks and (3) diesel engine power boats. Harvested area for Cassava, a main feedstock for Bioethanol, which could power small generator sets, motorcycles and cars, is currently about 10,736 ha equivalent a total of 113,458 ton of cassava [6, 11].

## 19.11 Conclusion

To achieve the goal of implementation 100 % of renewable energy resources in Sumba Island, these three actions should be as follows:

1. Implementation of Sumba Iconic Island with the multi actors (government, private, Banking Institutions, NGOs, and Community) and multi-funding (APBN, Private Sector, Foreign Grants, and Community), which encourages stakeholders in the renewable energy sector contribute to the development renewable energy in Sumba.
2. The multi actors and multi funding have to synchronize the detail program with the Sumba Iconic Island road-map, that by 2020, the implementation of renewable energy resources is fully implemented in Sumba Island.
3. Through a multi-party strategic cooperation, it is hoped the program can be implemented and can be replicated to other areas, especially in the eastern part of Indonesia.



## References

1. Lomi, A.: The role of renewable resources: an impact of distributed generation. In: Proceeding of the MICEEI, 29 Nov 2011
2. Badan Statistik Provinsi Nusa Tenggara Timur (2015)
3. <http://www.hivos.org>
4. Sumba, H.: An Iconic Island to demonstrate the potential of renewable energy, Poverty reduction, economic development and energy access combined (2012)
5. Road-map of Sumba Iconic Island 2025 (2011)
6. Zomers, A.: Context, challenges, and obstacles in rural electrification. *IEEE Power Energy Mag.* **12**(4) (2014)
7. Presidential Decree No. 5/2006, on the National Energy Policy
8. Indonesia Energy Outlook (2013)
9. Winrock International, Fuel Independent Renewable Energy Iconic Island, Preliminary Resource Assessment (2010)
10. Lomi, A., Soetedjo, A., Nakhoda, Y., The role of renewable resources: a hybrid system of wind and solar energy. In: Prosiding Seminar Nasional, SENATEK (2015)
11. Asian Development Bank, Monitoring and Evaluation Sumba Iconic Island, Final Report (2014)

# Chapter 20

## Electromechanical Characterization of Bucky Gel Actuator Based on Polymer Composite PCL-PU-CNT for Artificial Muscle

Yudan Whulanza, Andika Praditya Hadiputra, Felix Pasila and Sugeng Supriadi

**Abstract** Artificial Muscle is a common term for material that able to actuate because of external stimulus such as electric. The Artificial Muscle has promising future in application of medical and robotic disciplines. Bucky Gel Actuator is one example of Artificial Muscle which consists of electrolyte layers sandwiched with electrode layers. In this paper, we proposed an alternative material for electrode and electrolyte layers. The electrolyte layer was synthesized from Polycaprolactone-Polyurethane copolymer (PCL-PU). On the other hand, the electrode layer was composited between PCL-PU and carbon nanotube (CNT) in percentage of 0.5, 1.5, and 2.4 wt%. Furthermore, we measured electrode conductivity and elastic modulus as key physical properties for our artificial muscle. Our results have shown that the polymer electrode starts to be conducting at a mixture of 2.4 wt% CNT. At this concentration, the elastic modulus is 6.2 MPa and its conductivity is  $1.6 \text{ Sm}^{-1}$ .

**Keywords** Artificial muscle · Bucky gel actuator · Electrode layer · Electrolyte layer · CNT

### 20.1 Introduction

Research about artificial muscle as an actuator has already reached certain point where people realized all of its potentials. Artificial muscle held high potential due to its high flexibility and power-to-weight ratio. Artificial muscle commonly has contraction and relaxation movement as normal muscle does [1].

---

Y. Whulanza (✉) · A.P. Hadiputra · S. Supriadi  
Mechanical Engineering Department, Indonesia University, Depok, Indonesia  
e-mail: yudan@eng.ui.ac.id

F. Pasila  
Electrical Engineering Department, Petra Christian University, Surabaya, Indonesia

Bucky gel actuator is an example of artificial muscle which mainly consists of ionic liquid, polymer, and carbon nanotube. The actuator movement is produced by different electric potential of its electrolyte and electrode layers. Electrolyte layer is made by polymerizing ionic liquid and polymer [2, 3]. On the other hand, electrode layer is made by mixing electrolyte layer with carbon nanotube [4–7]. The high electrical conductivity of carbon nanotube creates certain amount of electric discharge that ultimately able to move this muscle [8, 9].

Nowadays, the application of artificial muscle includes robotics, biomedical, and electronics areas. In medical fields, artificial muscle is utilized as prosthetic limb which function as close as possible to actual muscle of human beings. Furthermore, artificial muscle is also engineered as a micro sensor and micro actuator in implanted device in human body. These applications bring hope to handicapped person to live normally. Robotic application is using artificial muscle for certain activity in production line. Moreover with the increasing popularity of rapid prototyping, artificial muscle will be likely to have a high potential to be mass production [10].

However, many obstacles are still eminent so that artificial muscle is not ready to be fully utilized. Characterization of such material is not plausible enough to be used in above corresponding areas. The required energy activation of artificial muscle is currently too high to be used safely. Additionally, there were no significant research about durability and lifetime of artificial muscle. Therefore, our research is aimed to investigate new material to be used as artificial muscle with relatively low voltage activation i.e. less than 10 VDC.

## 20.2 Experimental

### 20.2.1 Artificial Muscle Preparation

Basically, artificial muscle is composed of electrolyte layer and electrode layers. Firstly, ionic solution salt is being prepared by mixing two salts i.e. aluminum chloride ( $\text{AlCl}_3$ ) and Urea ( $\text{CO}(\text{NH}_2)_2$ ) with molar ratio of 1:2. This mixing salt was then dissolved into Dimethyl Sulfoxide (DMSO) with molar ratio of 1:3 to have the ionic solution.

Secondly, electrolyte layer was prepared by mixing the ionic solution with Polycaprolactone-Polyurethane copolymer (PCL-PU). The mixture was arranged to have 50 % w/w of salts to polymer. Later, the mixture was mixed in ultrasonic vibration for 2 min and dried by heating to 50 °C for about 10 min.

Thirdly, electrode layer was prepared by mixing carbon nanotube with ionic solution and PCL-PU polymer. The CNT content in electrolyte layer was arranged to have various concentration i.e. 0.5, 1.5 and 2.5 % w/w. The solution mixture was mixed thoroughly in ultrasonic vibration and heated with the same condition as above to realize electrode layer.

Lastly, artificial muscle is assembled by hot pressing electrolyte layer that sandwiched with two electrode layers. The temperature was kept at 70 °C for 2 min.

## ***20.2.2 Material Testing and Measurement***

### **20.2.2.1 Conductivity Measurement**

Artificial muscle specimen was prepared into a dimension of 2 cm x 1 cm in length and width. The thickness was also measured using micrometer. A two point probe is employed to measure sample's resistivity using digital multimeter.

### **20.2.2.2 Elastic Modulus Measurement**

Elastic modulus measurement is done by using ASTM D1708 micro tensile testing method. Four specimens with a dimension of 2 and 1 mm were prepared. The deformation rate was set to 0.5 mm/min.

## **20.3 Results and Discussion**

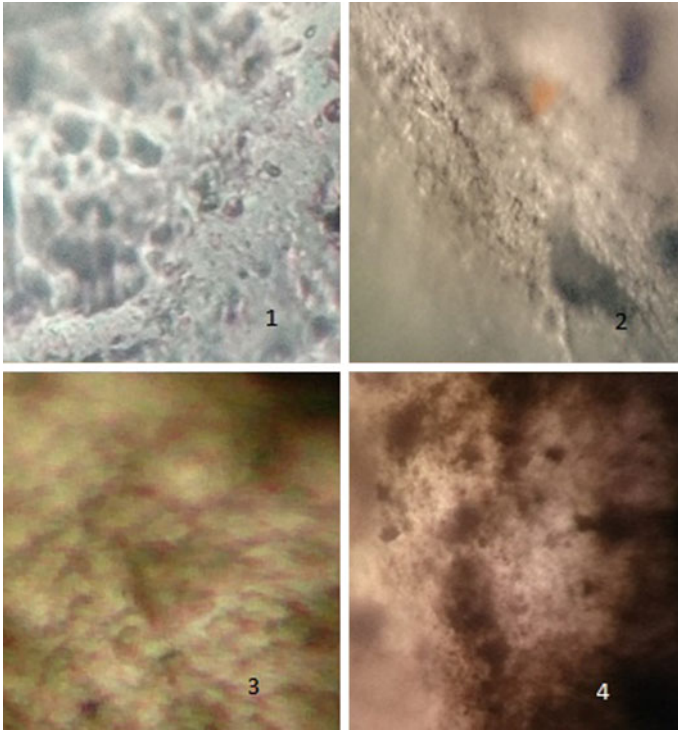
### ***20.3.1 Image Acquisition***

Figure 20.1 shows stereomicroscope images of electrode layer of artificial muscle from various concentration of CNT. Obviously, the more CNT concentration it has, the higher intensity of the image. Here, a higher intensity of an image represents a darker colour of image. However, at 2.4 wt%, it can be seen that the CNT agglomeration is evident. This agglomerate indicates a low dispersion quality of CNT throughout the polymer electrode. Intuitively, dispersion quality of CNT shall affect the mechanical and electrical properties of electrode layer.

### ***20.3.2 Mechanical Property Measurement***

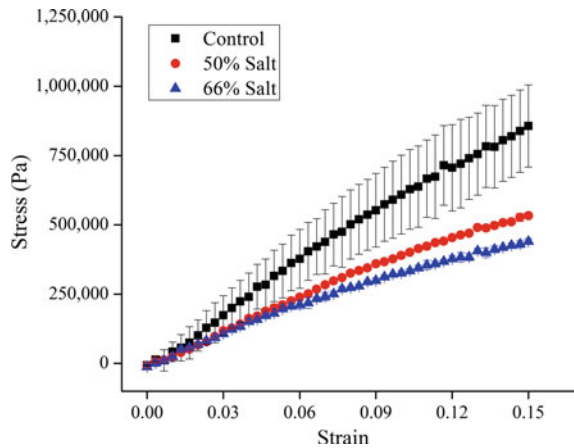
Stress-strain curve is acquired after the elastic modulus test as shown in Figs. 20.2 and 20.3. Figure 20.2 represents the result from electrolyte layer that mainly is a mixture of polymer and salts. Here, the control specimen is composed of polymer PCL-PU layer. The addition of 50 % w/w salts results in lower tensile strength and later also elastic modulus. It can be seen that at 15 % of elongation, the tensile is lowered by 50 %. It can be indicated that the salts left more micropores during the drying process to realize the electrolyte layer. A further addition of salt (66 %) brings a lower tensile strength as shown in Fig. 20.2. However, a statistical analysis shows that the difference is not significant.

Figure 20.3 shows the result of mechanical testing from electrode layer specimens. With respect to control specimen, the addition of CNT is not showing any significant difference of tensile strength property until the 2.4 % CNT



**Fig. 20.1** Stereomicroscope images from electrode layer at various CNT concentration: (1) 0%, (2) 0.5%, (3) 1.5% and (4) 2.4%

**Fig. 20.2** Stress-strain curve of electrolyte polymer layer at various salt concentrations



**Fig. 20.3** Stress-strain curve of electrode layer at various CNT concentrations

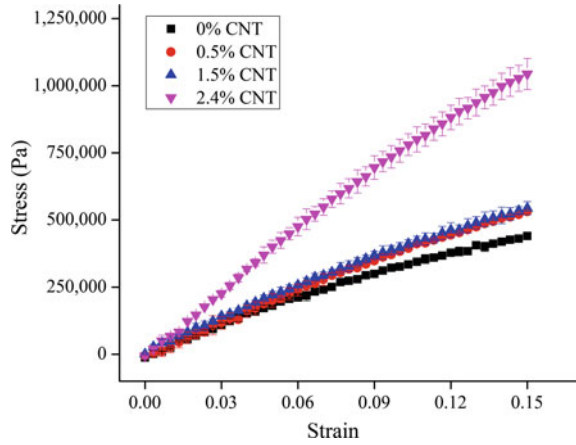


**Fig. 20.4** Result of elastic modulus measurement from electrolyte layer at various salt concentrations

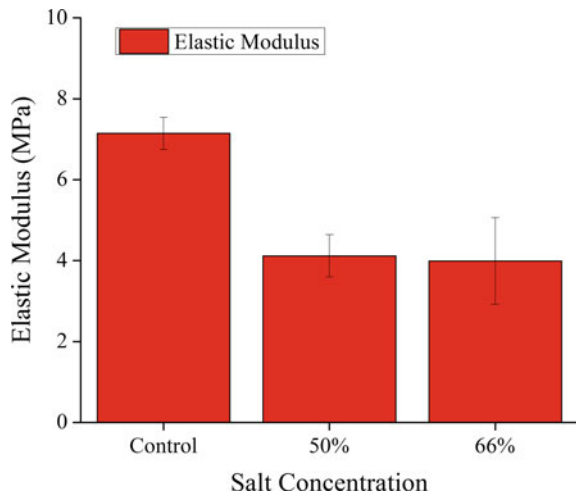
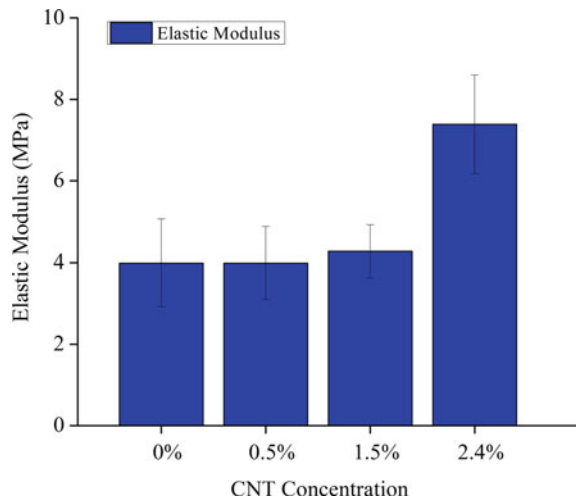


**Fig. 20.5** Result of elastic modulus measurement from electrode layer at various CNT concentrations



concentration. Intuitively, this increasing tensile strength is correspondingly with the amount of carbon nanotube in the electrode layer.

Furthermore, the measurement of elastic modulus is depicted in Figs. 20.4 and 20.5 for electrolyte and electrode layer respectively. Similarly to the strength property, the stiffness of electrolyte layer is decreasing as the salt was added in Fig. 20.4. In addition, Fig. 20.5 confirms that the addition of CNT bring a much higher elastic modulus of polymer membrane.

### 20.3.3 Conductivity Measurement

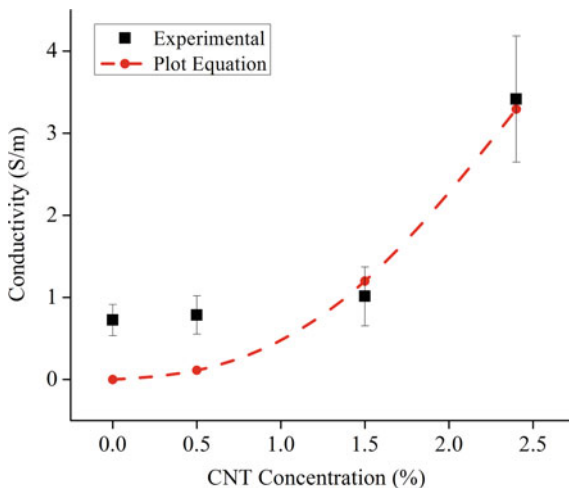
The conductivity result of electrolyte and electrode layer is reported in Fig. 20.6. Here, specimens with 50 % salt were taken into account as control for electrode layer. Note that the electrode layers are a mixing between electrolyte material and carbon nanotube as conductive filler. The conductivity results show that the electrical property corresponded positively with mechanical properties. It can be concluded that the micropores by salts and CNT affect the electrical property as much as mechanical properties.

Furthermore, Fig. 20.6 shows a small improvement of conductivity is shown at the 1.5 wt%. Later, an abrupt conductivity value at 2.4 wt% is evident. This can be explained that the percolation threshold of electrode is reached at near 1.5 % w/w CNT addition. The conductivity measurement at 2.4 wt% is comparable to those of germanium (2.17 s/m 20 °C). This substance is widely used as a semiconductor material. Thus, PCL-PU CNT might be used as a flexible electrode in electrical field.

A simple plot line as suggested by below equation was applied.

$$\sigma \propto (p - p_c)^t \quad (20.1)$$

**Fig. 20.6** Conductivity measurement result of electrolyte and electrode layers



The equation is employed to predict the value of conductivity ( $\rho$ ) at any concentration of conductive substance ( $p$ ) as the conductive threshold concentration ( $p_c$ ) is known from experimental. Our previous result gives the value of conductive threshold to be near 1.5 % w/w carbon nanotube. By inputting the power value ( $t$ ) of 2.15 at Eq. 20.1, we shall have a prediction line of conductive as plotted in Fig. 20.6. This result is interesting in that the power constant is similar to that theoretically predicted for a 3D percolation model. The percolation theory suggests that a substance has a power constant to be about 2 in order to behave as conducting material.

## 20.4 Conclusion

The main material for artificial muscle is realized and characterised completely. This paper shows the strong relation between mechanical property and electrical property that driven by the particle contents. The anion salt and carbon nanotube affect the microstructure of polymer which evident in the electromechanical properties. The experiment shows that the percolation threshold occurred between 1.9 and 2.4 wt% CNT concentrations for electrode layer. Modulus elastic value at percolation point has a value of 7 MPa. Conductivity value at percolation point is around 1.6 S/m.

**Acknowledgment** This research is funded by Ministry of Research Technology and Higher Education of Indonesia in year 2014–2015 under scheme of International Collaboration and Publication grant.

## References

1. Kruusamäe, K., Mukai, K., Sugino, T., Asaka, K.: Mechanical behaviour of bending bucky gel actuators and its representation. *Smart Mater. Struct.* **23**(2), 025–031 (2014)
2. Fukushima, T., Asaka, K., Kosaka, A., Aida, T.: Fully plastic actuator through layer-by-layer casting with ionic-liquid-based bucky gel. *Angew. Chem.* **44**(16), 2410–2413 (2005)
3. Kamamichi, N., Yamakita, M., Asaka, K., Zhi-Wei, L., Mukai, T.: Sensor property of a novel eap device with ionic-liquid-based bucky gel. *Sensors IEEE*, 221–224, 28–31 Oct 2007
4. Takeuchi, I., Asaka, K., Kiyohara, K., Sugino, T., Terasawa, N., Mukai, K., Shiraishi, S.: Electromechanical behavior of a fully plastic actuator based on dispersed nano-carbon/ionic-liquid-gel electrodes. *Carbon* **47**(5), 1373–1380 (2009)
5. Whulanza, Y., Battini, E., Vannozzi, L., Vomero, M., Ahluwalia, A., Vozzi, G.: Electrical and mechanical characterisation of single wall carbon nanotubes based composites for tissue engineering applications. *J. Nanosci. Nanotechnol.* **13**(1), 188–197 (2013)
6. Takeuchi, I., Asaka, K., Kiyohara, K., Sugino, T., Mukai, K.: Electrochemical impedance spectroscopy and electromechanical behavior of bucky gel actuators containing ionic liquids. *J. Phys. Chem. C* **114**(34), 14627–14634 (2010)
7. Naohiro, T., Takeuchi, I., Matsumoto, H.: Electrochemical properties and actuation mechanisms of actuators using carbon nanotube-ionic liquid gel. *Sens. Actuators, B* **139**(2), 624–630 (2009)



8. Bisio, M., Ansaldo, A., Futaba, D.N., Hata, K., Ricci, D.: Cross-linking supergrowth carbon nanotubes to boost the performance of bucky gel actuators. *Carbon* **49**(7), 2253–2257 (2011)
9. Terasawa, N., Takeuchi, I., Matsumoto, H., Mukai, K., Asaka, K.: High performance polymer actuator based on carbon nanotube-ionic liquid gel: Effect of ionic liquid. *Sens. Actuators, B* **156**(2), 539–545 (2011)
10. Kamamichi, N., Maeba, T., Yamakita, M., Mukai, T.: Fabrication of bucky gel actuator/sensor devices based on printing method, Intelligent Robots and Systems, IROS 2008. In: *IEEE/RSJ International Conference*, pp. 582–587, 22–26 Sept 2008

# Chapter 21

## A Single-Phase Twin-Buck Inverter

Hanny H. Tumbelaka

**Abstract** This paper proposes a simple single-phase twin-buck inverter to interface a DC source such as a renewable energy source to AC loads. It consisted of two identical buck converters with a sinusoidal duty ratio. The first converter produced a positive half cycle of a 50 Hz sinusoidal output voltage, and the second converter produced the negative one. Then, both of them are integrated using transistors Q3 and Q4. By shifting the phase angle of signals for triggering transistor Q3 and Q4 from a sinusoidal reference signal, the distortion around zero crossing was reduced. The computer simulation results show that the output voltage and current were sinusoidal with harmonic distortion of 1.12 and 0.49 % respectively.

**Keywords** Buck converter • Single-phase inverter

### 21.1 Introduction

An inverter converts a DC voltage source or a DC current source to an AC voltage/current. It takes power from a DC source and sends the power to AC loads using power electronic devices. An inverter can be used to interface a renewable energy source such as PV panels to AC loads or a grid [1, 2]. A solar home system is one of the single-phase inverter application. Lamps and home appliances are connected to PV panels as well as to batteries through a single-phase inverter.

There are many types of a single-phase inverter. The most common inverter, especially a voltage source inverter (VSI) is a single-stage bridge pulse-width-modulation (PWM) inverter [2–4]. It generally consists of four switches configured as a bridge with a filter. PWM signals trigger the switches to generate a sinusoidal AC waveform. Recently, a dual-buck full-bridge inverter [5, 6] as well as a two identical boost or buck-boost inverter [1] has been proposed. The main idea in

---

H.H. Tumbelaka (✉)

Electrical Engineering Department, Petra Christian University, Surabaya, Indonesia  
e-mail: tumbekh@petra.ac.id

developing this inverter was to mitigate a shoot-through problem in a bridge voltage source inverter, which was usually overcome by a dead time to block the upper and lower transistors of each leg.

A different configuration for a single-phase stand-alone inverter comprising of two identical but independent step-down DC-DC converters is presented in this paper to generate a sinusoidal voltage. Basically, a step-down (buck) DC-DC converter changes a high DC value from a DC source to a low DC value needed by a DC load. Therefore, this proposed inverter is very simple and easy to implement. The controller is uncomplicated as well. By varying the duty ratio, it is possible to create a sinusoidal inverter.

## 21.2 Circuit Configuration

### 21.2.1 A Basic Step-Down DC-DC Converter

A Single-phase Twin-Buck inverter basically consists of two step-down DC-DC converters. A schematic diagram of a single step-down (buck) DC-DC converter is shown in Fig. 21.1. The working principle of a buck converter has been elaborated in [3, 4]. The transistor is switched ON (during  $t_{ON}$ ) and OFF (during  $t_{OFF}$ ).  $t_{ON} + t_{OFF} = T_S = 1/f_S$ ,  $f_S$  is a fixed switching frequency. When the transistor is on (mode 1), the inductor current ( $i_L$ ) builds up. Energy is transferred to the capacitor and the load from the DC voltage source ( $V_S$ ). The inductor current for mode 1 ( $0 \leq t \leq t_{ON}$ ) is:

$$V_S = V_O + L \frac{di_L}{dt} \quad (21.1)$$

$$i_L(t) = \frac{V_S - V_O}{L} t + I_{L1(0)} \quad (21.2)$$

where  $I_{L1(0)}$  = initial value of  $i_L$  for mode 1, and  $V_O$  = output voltage

When the transistor is switched off (mode 2), the energy stored in the inductor ( $L$ ) is released to the capacitor and the load through the free-wheeling diode ( $D_F$ ). The inductor current decreases. The inductor current for mode 2 ( $t_{ON} \leq t \leq T_S$ ) is:

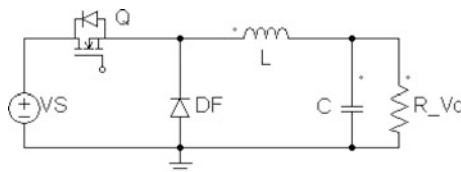


**Fig. 21.1** A Step-down (buck) DC-DC converter

$$0 = V_O + L \frac{di_L}{dt} \quad (21.3)$$

$$i_L(t) = \frac{-V_O}{L}t + I_{L2(0)} \quad (21.4)$$

where  $I_{L2(0)}$  = initial condition of  $i_L$  for mode 2.

In a stable operating cycle, the average inductor voltage is zero, then

$$(V_S - V_O)t_{ON} - V_O t_{OFF} = 0 \quad (21.5)$$

where  $t_{ON} = K T_S$  and  $t_{OFF} = (1-K) T_S$ .  $K$  = duty ratio, constant value in a range 0–1.

Solving the Eq. (21.5), the relationship of the input-output voltage of the step-down converter is

$$\frac{V_O}{V_S} = \frac{t_{ON}}{t_{ON} + t_{OFF}} = K \quad (21.6)$$

The Eq. (21.6) is valid when the inductor current stays in a continues conduction mode (CCM), which is  $i_L(t) > 0$ .  $I_{L1(0)}$  and  $I_{L2(0)}$  never go to zero.

### 21.2.2 A Single-Phase Twin-Buck Inverter

In order to generate a sinusoidal output voltage using a buck converter,  $t_{ON}$  and  $t_{OFF}$  can be varied in proportion to the amplitude of a sine wave. In this case, the duty ratio  $K$  is not a constant but has to be controlled according to a sinusoidal pulse-width-modulation (SPWM) rule [3]. The duty ratio becomes  $k(t) = m_a \sin t$ , where  $0 \leq m_a \leq 100\%$ . Then, from Eq. (21.6), the output voltage becomes

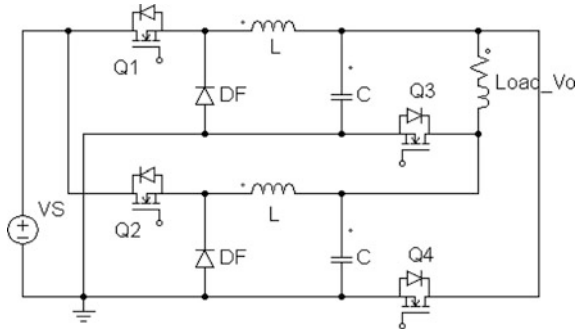
$$V_O = V_S m_a \sin t \quad (21.7)$$

However, the converter only produces a positive voltage. Therefore, to generate a complete 50 Hz sinusoidal output voltage, two identical step-down (buck) DC-DC converters are needed. The first converter produces a positive half cycle of a sine wave, while the second converter produces a negative half cycle of a sine wave by inverting the output voltage. Both of them are independent. Hence, each converter only operates in a half period (10 ms).

Figure 21.2 shows the two identical (twin) step-down (buck) DC-DC converter working as an inverter.

From Fig. 21.2, both the upper and the lower buck converter generate a positive half cycle of a 50 Hz sine wave. To produce a sinusoidal output voltage, transistors Q3 and Q4 are used to connect both converters to the load. When Q3 is switched on (Q4 is switched off), the load receives the voltage from the upper converter.

**Fig. 21.2** A twin-buck inverter circuit



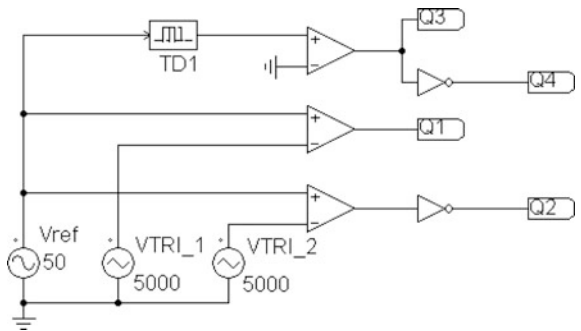
When Q4 is switched on (Q3 is switched off), the load receives the voltage (inverting) from the lower converter. The transition happens in zero crossing of a sine wave. Hence, for a full period (20 ms for 50 Hz), the load receives an AC sinusoidal voltage.

### 21.3 Inverter Controller

In order to generate a sinusoidal duty ratio ( $k(t)$ ), a SPWM controller is used. The circuit diagram of the controller is shown in Fig. 21.3.

$V_{REF}$  is a sinusoidal reference signal with frequency of 50 Hz and the amplitude of  $m_a$ . As carrier signals with a constant high switching frequency,  $V_{TRI} (1)$  is a triangular wave above the  $t$  axis, and  $V_{TRI} (2)$  is a triangular wave below the  $t$  axis. As a result, during a positive half cycle, the controller produces SPWM signals to trigger transistors Q1, while signals for Q2 are low. The controller also generates a 50 Hz signal for transistor Q3, which is high. During a negative half cycle, the controller produce SPWM signals to trigger Q2, while signals for Q1 are low. The controller also generates a 50 Hz signal for transistor Q4, which is high.

**Fig. 21.3** Control circuit diagram



Figures 21.4 and 21.5 demonstrate the sinusoidal reference signal  $V_{REF}$  and the carrier signals  $V_{TRI} (1)$  and  $V_{TRI} (2)$ . In this case, the  $V_{TRI}$  amplitude = 1 and the frequency is 5 kHz. The amplitude of  $V_{REF} (m_a) = 0.95$  and the frequency is 50 Hz. By using comparators, the controller generates SPWM signals for triggering transistor Q1 and Q2 as shown in Fig. 21.6.

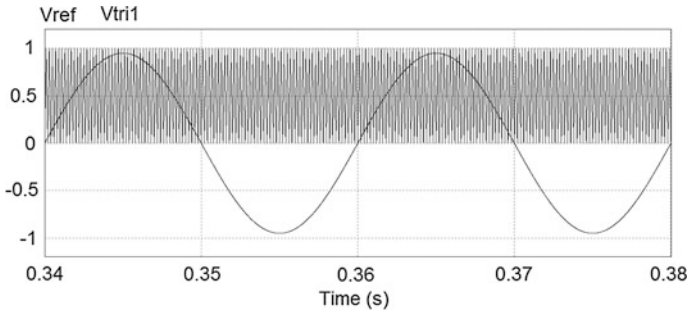


Fig. 21.4  $V_{REF}$  and  $V_{TRI} (1)$

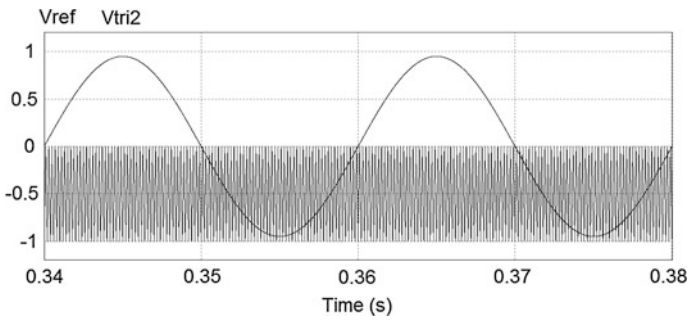


Fig. 21.5  $V_{REF}$  and  $V_{TRI} (2)$

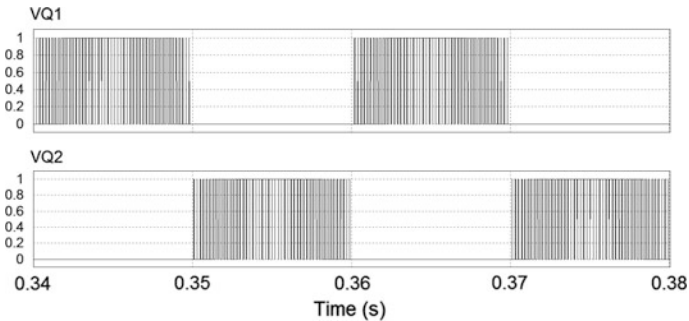
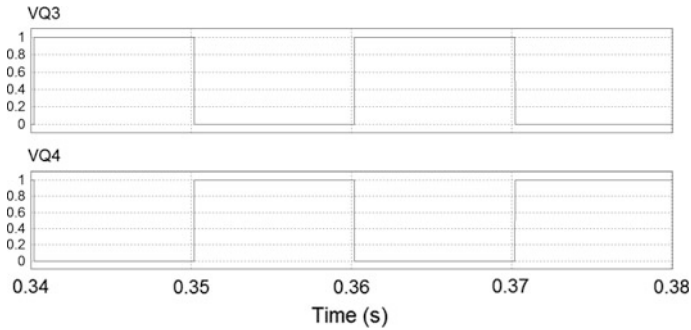


Fig. 21.6 SPWM signals for triggering transistors Q1 and Q2



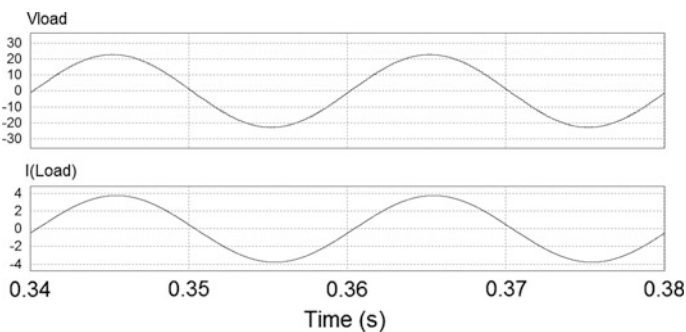
**Fig. 21.7** Square signals for triggering transistors Q3 and Q4

Figure 21.7 shows signals for triggering transistors Q3 and Q4.  $V_{REF}$  is compared to a zero voltage. During a positive half cycle, the comparator output voltage (Q3) becomes high, and Q4 becomes low. During a negative half cycle, the comparator output voltage (Q3) becomes low, and Q4 becomes high. TD1 is used to shift  $V_{REF}$  for several degrees. As a result, the phase of the comparator output voltage Q3 and Q4 will also be shifted compared to the phase of  $V_{REF}$ .

## 21.4 Simulation Results

The circuits in Figs. 21.2 and 21.3 are tested using PSIM simulator to verify the concepts described in previous sections. Circuit parameter values for simulation: source voltage  $V_S = 24$  V,  $L = 1.2$  mH,  $C = 47$   $\mu$ F,  $R_{load} = 6$   $\Omega$  and  $L_{load} = 1.4$  mH.

Figure 21.8 demonstrates that the output voltage of the twin-buck inverter is sinusoidal similar to the sinusoidal reference signal  $V_{REF}$ . The amplitude equals to a



**Fig. 21.8** Output voltage and current

DC input voltage ( $V_S$ ) multiplied by  $m_a$ . It is proven that the twin-buck inverter is able to generate an AC sinusoidal voltage. The transition between a positive half cycle and a negative half cycle is smooth. The total harmonic distortion (THD) of this output voltage is 1.12 %. Figure 21.8 also shows the load current, which is an AC sinusoidal current. There is a small phase difference between the output voltage and current due to an inductive component of the load. The total harmonic distortion (THD) of this output current is 0.49 %.

The process to create an AC sinusoidal voltage can be seen from inductor currents  $i_L$  (Fig. 21.9) and capacitor voltages  $V_C$  (Fig. 21.10). The inductor currents is going up and down in high frequency when the transistor is switched on and off. Because  $t_{ON}$  and  $t_{OFF}$  are varied according to a sinusoidal duty ratio, then the inductor currents look like a sinusoidal waveform with ripples according to Eqs. (21.2) and (21.4). Figure 21.9b shows the inductor current in detail. The inductor currents are in continuous conduction. Figure 21.10 shows the capacitor voltages. The value of a capacitor determines the ripple of the output voltage. It can be seen that each step-down DC-DC converter operates in a half period and generates a positive half cycle of a sinusoidal waveform.

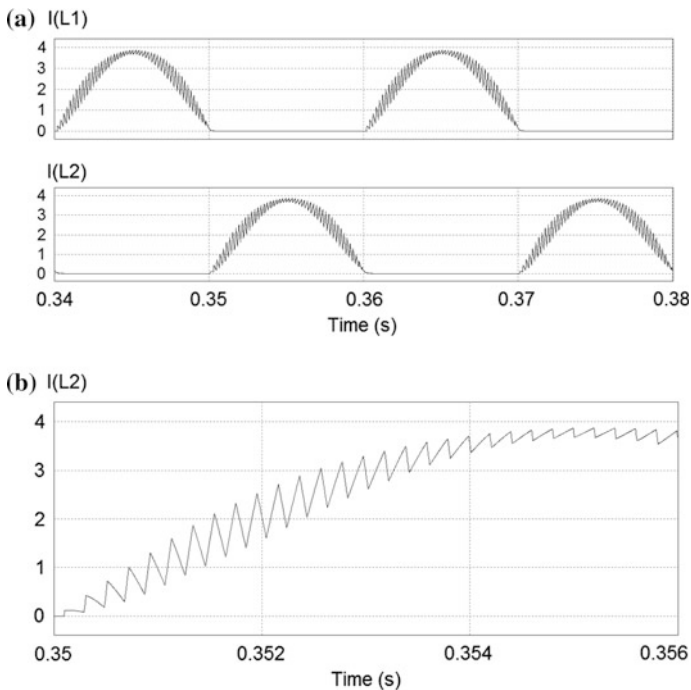


Fig. 21.9 a inductor current b inductor current in details for time period 0.35 s–0.356 s



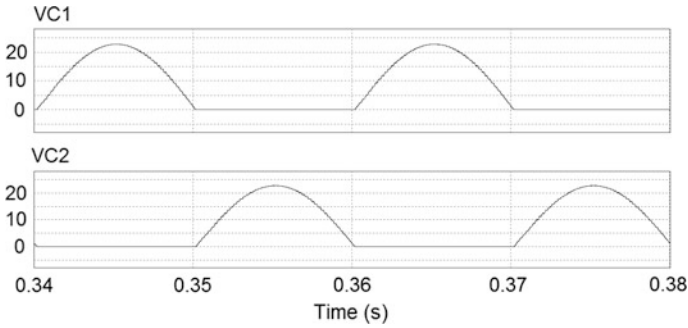


Fig. 21.10 Capacitor (output) voltages

### 21.4.1 $V_{REF}$ Phase Delay

As mention before in Fig. 21.3, there is a function block TD1 that shifts  $V_{REF}$  for several degree. As a result, there is a phase difference between  $V_{REF}$  and square signals to trigger transistors Q3 and Q4. The phase shift is needed to overcome the problem of zero-crossing distortion [6]. In the simulation results above, the phase delay is selected to be  $3.5^\circ$ .

Figure 21.11 shows the output voltage and current without phase shift. It can be seen that there is a distortion around zero crossing of the sinusoidal waveform. The total harmonic distortion (THD) of the output voltage and current are 2.42 % and 1.43 % respectively. Compare to inductor current in Fig. 21.9b, the inductor current without phase shift (Fig. 21.12) goes to discontinuous conduction around zero crossing. Consequently, the capacitor voltage is distorted (Fig. 21.13).

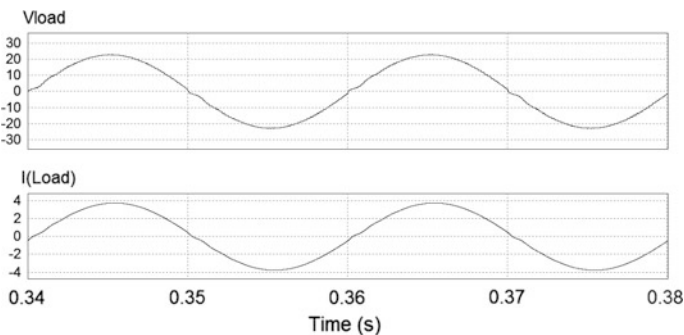


Fig. 21.11 Output voltage and current without phase shift

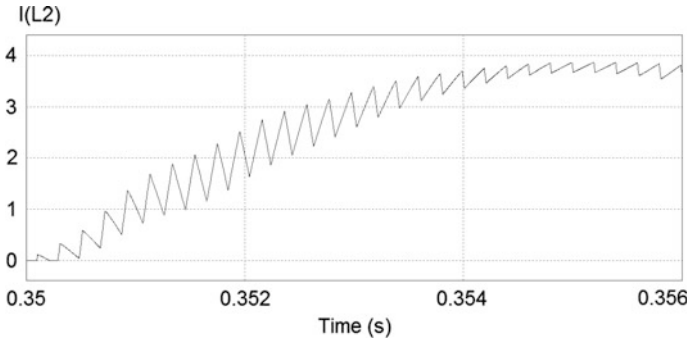


Fig. 21.12 Inductor current without phase shift

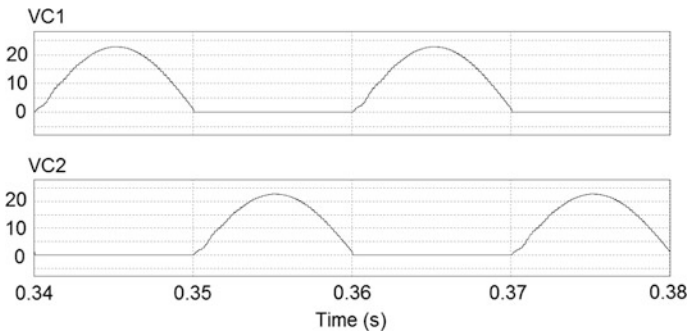


Fig. 21.13 Capacitor voltages without phase shift

### 21.5 Conclusion

This paper proposes a single-phase twin-buck inverter. The inverter interfaces a DC source to AC loads. It consists of two identical step-down (buck) DC-DC converters with a sinusoidal duty ratio. The first converter produces a positive half cycle of a 50 Hz sinusoidal output voltage, and the second converter produces the negative one. Each converter operates in a half period and generates a positive half cycle of a sinusoidal waveform. Then, both of them are integrated using 2 transistor that operate alternately every 10 ms. By shifting the phase angle of signals ( $3.5^\circ$ ) for triggering transistor Q3 and Q4 from  $V_{REF}$ , the distortion around zero crossing is reduced. Simulation using PSIM shows that the inverter generates a 50 Hz sine wave. The output voltage THD becomes 1.12 %.

## References

1. Xue, Y., Chang, L., Kjær, S.B., Bordonau, J., Shimizu, T.: Topologies of single-phase inverters for small distributed power generators: an overview. *IEEE Trans. Power Electron.* **19**(5), 1305–1314 (2004)
2. Kjaer, S., Pedersen, J.K., Blaabjerg, F.: A review of single-phase grid connected inverters for photovoltaic modules. *IEEE Trans. Ind. Appl.* **41**(5), 1292–1306 (2005)
3. Rashid, M.H.: *Power Electronics: Circuits, Devices, and Application*. Prentice Hall, Upper Saddle River (1988)
4. Mohan, N., et al.: *Power Electronics: Converter, Applications, and Design*. Wiley, New York (1995)
5. Yao, Z., Xiao, L., Yan, Y.H.L.: Dual-buck full-bridge inverter with hysteresis current control. *IEEE Trans. Ind. Electron.* **56**(8), 3153–3160 (2009)
6. Sun, P., et al.: Cascade dual buck inverter with phase-shift control. *IEEE Trans. Power Electron.* **27**(4), 2067–2077 (2012)

# Chapter 22

## Performance Comparison of Intelligent Control of Maximum Power Point Tracking in Photovoltaic System

Daniel Martomanggolo Wonohadidjojo

**Abstract** In this study, two models of power generation system are developed. They consist of the PV module, boost converter and the controller. The models utilize intelligent controllers, Perturb and Observe algorithm and Fuzzy Logic Controller. The objective of this study is to compare the performance of each controller in the system by using the same input which are the varying solar irradiance and the constant solar temperature. The simulations are undertaken to compare the PV power, the output power and the output voltage as the performance indicators. The results show that the FLC performs better in the developed system. It generates higher PV power, output power and output voltage than the P&O algorithm.

**Keywords** Performance comparison · Maximum power point tracking · Photovoltaic · Fuzzy logic controller · Perturb and observe

### 22.1 Introduction

Photovoltaics (PV) module generates electricity by converting irradiation of the sunlight without polluting the environment. The conversion is undertaken by electronics circuits. Nowadays this power generation system is known as one of the renewable energy systems. In order to use the electricity from PV modules, a PV generation system should be developed. In developing such a system, a model that is developed to simulate the behavior of the system is useful. As a result of the simulation of the solar PV system one can benefit from this model as a photovoltaic generator in the field of solar PV power conversion systems. The objective of this study is to develop a model of PV generation system with Maximum Power Point Tracking (MPPT) capability controlled by intelligent controller. Two intelligent

---

D.M. Wonohadidjojo (✉)  
Ciputra University, Surabaya, Indonesia  
e-mail: daniel.m.w.10@gmail.com

controllers utilized in this model are using Fuzzy Logic Controller and Perturb and Observe algorithm. The performance of these controllers are simulated, the evaluation is based on the power and voltage generated by the system. The model is developed within MATLAB—Simulink environment. Such model discussed in this study would provide a tool to predict the behavior of solar PV cell and module.

## 22.2 Photovoltaic Generation System

There have been a number of studies on MPPT algorithms over the years. The studies of algorithms were conducted for the MPPT including perturb and observe, incremental conductance, parasitic capacitance, constant voltage and fuzzy logic algorithms [1–4]. There are a number of algorithms reported utilized in the recent studies. They were using GA [5] and Fuzzy Logic [6, 7].

A photovoltaic system is built from several photovoltaic solar cells. A single PV cell is capable of generating a small amount of power that depends on the type of material used. PV cells can be connected together to generate higher power modules that answers the need of higher power output. It is usual in practice that a photovoltaic generation system consists of a solar PV and a boost converter. The solar PV generates electricity from the light dependent diode, the BC amplifies the current (and voltage) to obtain the desired level of power. The block diagram of the system is depicted in Fig. 22.1.

### 22.2.1 Solar Photovoltaic

The electrical circuit equivalent of solar photovoltaic cell is depicted in Fig. 22.1. It is usually referred to the one diode model of the PV cell. The model consists of a current source, a diode shunt and series resistor and a resistive load. The equation of this model is represented as Eq. (22.1) [8].

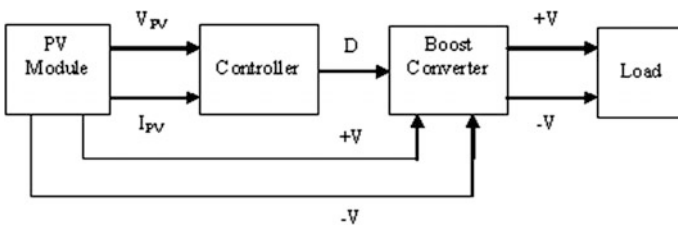


Fig. 22.1 Block diagram of the power generation system

$$I_{PV} = I_{ph} - I_r \left[ \exp \left( \frac{V_{PV} + I_{PV} R_{se}}{V_t} \right) - 1 \right] - \frac{(V_{PV} + I_{PV} R_{se})}{R_{sh}} \quad (22.1)$$

where  $I_{PV}$  and  $V_{PV}$  is the solar cell current and voltage,  $I_{ph}$  is the light generated current,  $R_{se}$  is the series resistance,  $R_{sh}$  is the shunt current and  $V_t$  is the thermal voltage.

Only a limited amount of current is produced by a single cell. In order to get the desired power, the cells are connected in parallel and series. Then the modules are connected in array to obtain the desired voltage and current.

The current that is generated by the PV cell depends linearly on the solar irradiation and is influenced by the temperature as well [9] as shown in Eq. (22.2).

$$I_{PV} = [I_{PV,n} + K_I \Delta T] \frac{G}{G_n} \quad (22.2)$$

where  $I_{PV}$  is the light generated current at nominal condition (25 °C and 1000 W/m<sup>2</sup>),  $\Delta T = T - T_n$ ,  $T$  is the actual temperature [K],  $T_n$  is the nominal temperature [K],  $K_I$  is the current coefficients,  $G$  is the irradiation on the device surface [W/m<sup>2</sup>] and  $G_n$  is the nominal irradiation.

### 22.2.2 Boost Converter

To enable the effective flow of desired current to feed the load in a PV generation system, a power electronics circuit such as DC to DC converter is utilized. The converter can be implemented in several topologies such as buck converter, boost converter, buck-boost converter and others converter topology as power conditioning circuitry. The DC–DC converters are electrical circuits that transfer the energy from a DC voltage source to a load and regulate the output voltage. The energy is transferred via electronic switches, made with transistors and diodes, to an output filter and then is transferred to the load. DC–DC converters are used to convert unregulated DC voltage to regulated or variable DC voltage at the output [10].

In this proposed system, a DC–DC converter is included to maintain the load voltage constant. The block diagram of the power generation system is depicted in Fig. 22.1. The converter is implemented as step up configuration and supplied by the PV module. In this converter, the input and output relationship is expressed as Eq. (22.3) [10].

$$\frac{V_{out}}{V_{in}} = \frac{1}{1 - D} \quad (22.3)$$

where  $V_{in}$  and  $V_{out}$  are the input and output voltage of the converter respectively and  $D$  is the duty cycle produced by the converter. Since the value of  $D$  must be

between 0 and 1, the magnitude of output voltage should be higher or the same as the input value. When the DC voltage supply from the PV module varies as a result of irradiation variation, then the amplitude and frequency of the DC voltage should be maintained.

### 22.2.3 *Perturb and Observe Algorithm*

The principle of this algorithm is to provoke perturbation by decreasing or increasing the Pulse Width Modulation (PWM) duty cycle, and observing the effect on the output of PV power. If the power  $P(k)$  is greater than the previous computed power  $P(k-1)$ , then the direction of perturbation is maintained otherwise it is reversed [6].

### 22.2.4 *Fuzzy Logic Controller*

The use of FLC in MPPT has several advantages. Fuzzy logic controllers are capable of working with imprecise inputs, handling nonlinearity and without an accurate mathematical model. Fuzzy logic control generally consists of three stages: fuzzification, inference system that is implemented in rule base, and defuzzification. During fuzzification, numerical input variables are converted into linguistic variables based on a membership function (MF). The MFs of FLC designed in this study is shown in Figs. 22.2 and 22.3. In this case, seven fuzzy levels are used: NB (Negative Big), NM (Negative Medium), NS (Negative Small), ZE (Zero), PS (Positive Small), PM (Positive Medium) and PB (Positive Big).

In those Figures, the range of MF is based on the range of values of the numerical variable. The inputs to a MPPT using FLC are the error  $E$  and change of error  $\Delta E$ . The error and change of error are calculated to generate the control signal

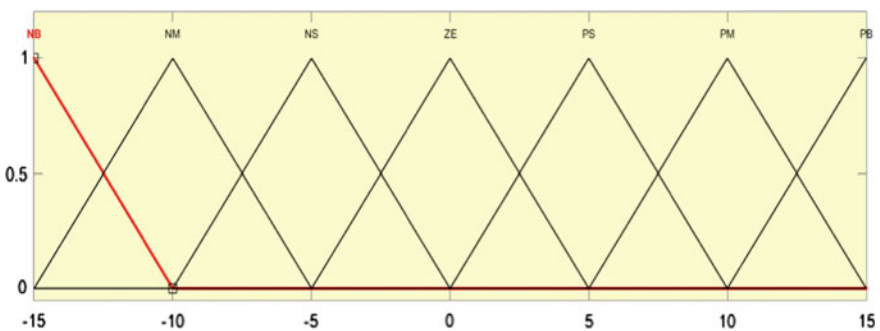


Fig. 22.2 Membership function of input ( $E$  and  $\Delta E$ )

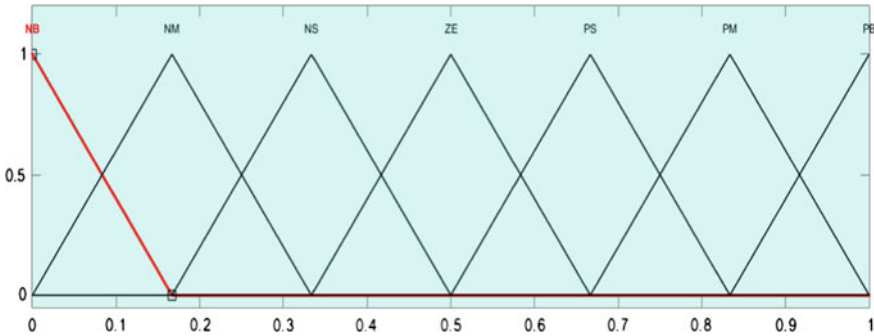


Fig. 22.3 Membership function of output

that maintains the output of the system to track the maximum power point. The  $E$  and  $\Delta E$  are expressed in Eqs. (22.4) and (22.5).

$$E_n = \frac{P(n) - P(n - 1)}{V(n) - V(n - 1)} \tag{22.4}$$

$$\Delta E(n) = E(n) - E(n - 1) \tag{22.5}$$

Once  $E$  and  $\Delta E$  are calculated and converted to the linguistic variables, the fuzzy logic controller outputs the change in duty ratio  $\Delta D$  of the power converter according to the rules that is composed in a rule base table [11]. The table is shown in Table 22.1. The rule base to control the  $\Delta D$  for different combinations of  $E$  and  $\Delta E$  are based on the power converter being used and also on the knowledge of the user. The rule base shown in Table 22.1 is designed to track the maximum power point by controlling the duty cycle that drives the boost converter. If for example, the operating point is far to the left of the MPP, that is  $E$  is PB, and  $\Delta E$  is NB, then we want to increase the duty ratio largely, that is  $\Delta D$  should be PB to reach the MPP.

In the defuzzification stage, the fuzzy logic controller output is converted from a linguistic variable to a numerical variable by using the same membership function

Table 22.1 Rule base of the fuzzy logic controller

	$\Delta E$						
	NB	NM	NS	ZE	PS	PM	PB
NB	ZE	ZE	ZE	NB	NB	NB	NM
NM	ZE	ZE	ZE	NS	NM	NM	NM
NS	NS	ZE	ZE	ZE	NS	NS	NS
E	NM	NS	ZE	ZE	ZE	PS	PM
PS	PS	PM	PM	PS	ZE	ZE	ZE
PM	PM	PM	PM	ZE	ZE	ZE	ZE
PB	PB	PB	PB	ZE	ZE	ZE	ZE



as shown in Figs. 22.2 and 22.3. This generates a signal that controls the power converter to the MPP. This means that the effectiveness of FLC depends on how the error and change of error were chosen, the design of membership functions and the knowledge to develop the rule base table.

## 22.3 Design and Model

### 22.3.1 PV Module

The module is designed as PV module based on the Kyocera KC50T specifications. It is based on electrical performance under standard test condition that is depicted in Table 22.2. Using the specifications in Table 22.2, the PV module characteristics is simulated and depicted in Figs. 22.4 and 22.5.

### 22.3.2 Simulink Model

The Simulink model of the power generation system is shown in Fig. 22.6. The model is developed with three subsystems: the PV module, controller and boost converter.

## 22.4 Simulations

Simulations were performed by using constant values of irradiation and temperature that are usually used in standard test condition: Irradiation of 1000 W/m<sup>2</sup> and Temperature of 25 °C. In the first simulation, the P&O algorithm is used in the MPPT block to track the maximum power point. Then in the second one, the FLC is utilized under the same STC.

**Table 22.2** PV module specifications [11] electrical performance under Standard Test Conditions (STC): irradiance 1000 W/m<sup>2</sup>, module temperature 25 °C

(STC)	
Maximum Power (Pmax)	54 W (10 %/- 5 %)
Maximum Power Voltage (Vmpp)	17.4 V
Maximum Power Current (Impp)	3.11 A
Open Circuit Voltage (Voc)	21.7 V
Short Circuit Current (Isc)	3.31 A
Max System Voltage	600 V
Temperature Coefficient of Voc	$-8.21 \times 10^{-2} \text{ V}^{\circ}\text{C}$
Temperature Coefficient of Isc	$1.33 \times 10^{-3} \text{ A}^{\circ}\text{C}$

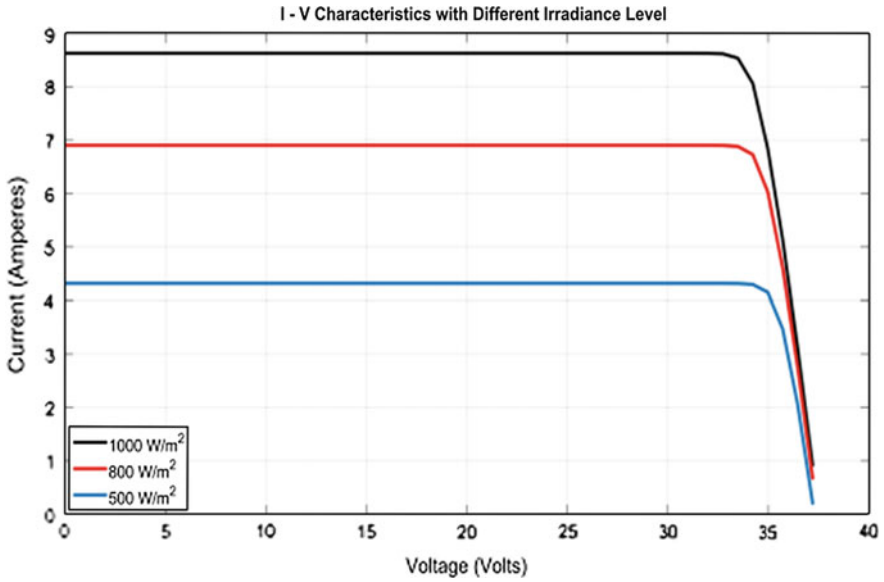


Fig. 22.4 Current–voltage characteristics under 3 different irradiance level

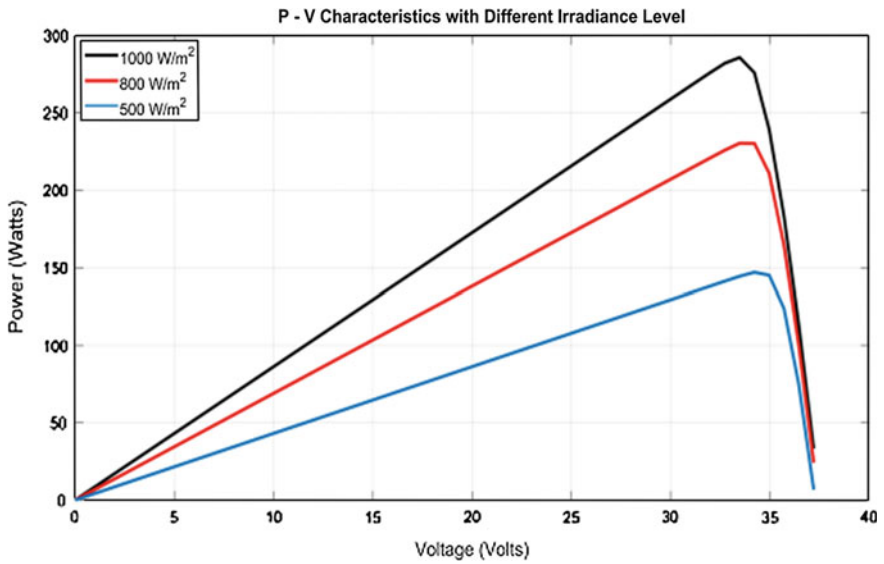


Fig. 22.5 Power–voltage characteristics under 3 different irradiance level

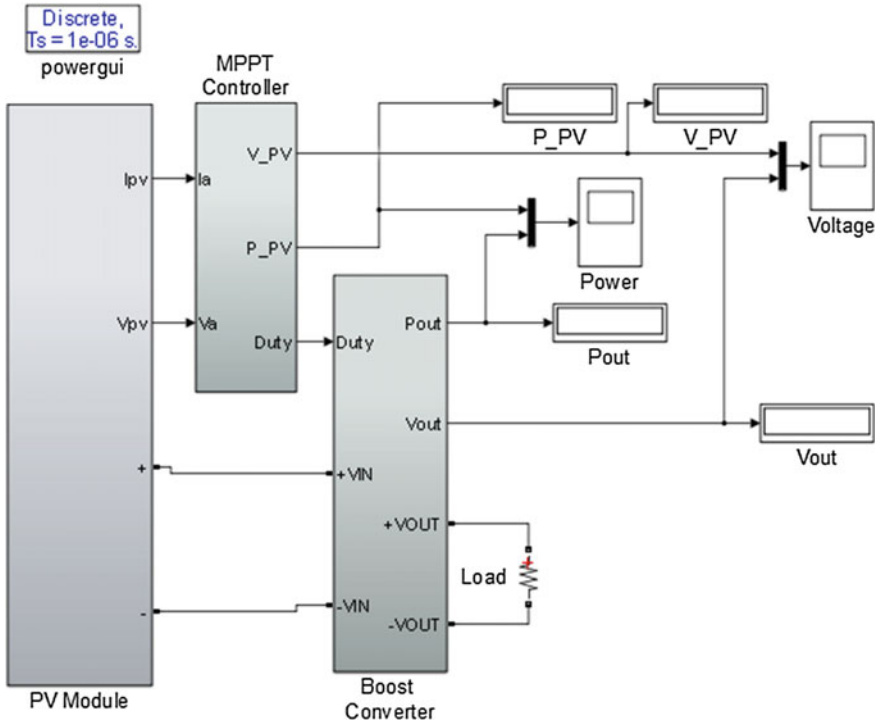


Fig. 22.6 Simulink model of the power generation system

## 22.5 Results and Discussion

The generated PV power is simulated under two conditions, first using the FLC and second using P&O algorithm. The irradiance used as the input of the solar PV is depicted in Fig. 22.7, and the PV power generated using P&O and FLC is depicted in Fig. 22.8. The figures show that both controllers are able to track the irradiance variation. However, the FLC is able to control the system so that it generates power higher than the P&O after 0.1 s.

The output power and voltage generated by the system is also simulated under two conditions, first using the FLC and second using P&O algorithm to track the maximum power point. The results are shown in Figs. 22.9 and 22.10 respectively. The figures indicate that the FLC performs better in terms of the amount of power and voltage generated. It generates higher power and voltage after 0.1 s than the P&O algorithm. The PV power and output power generated by utilizing the FLC

**Fig. 22.7** Irradiance of the solar PV

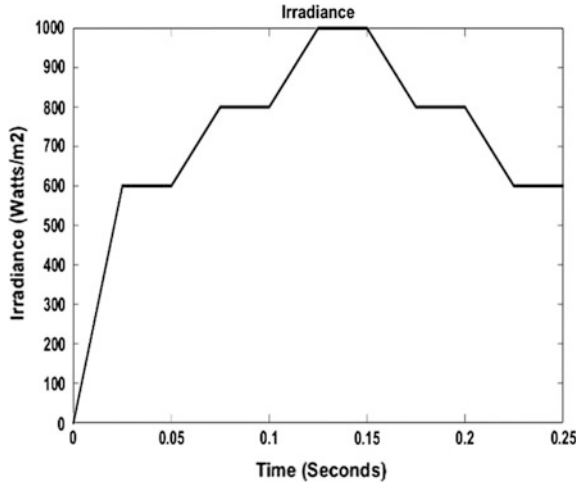
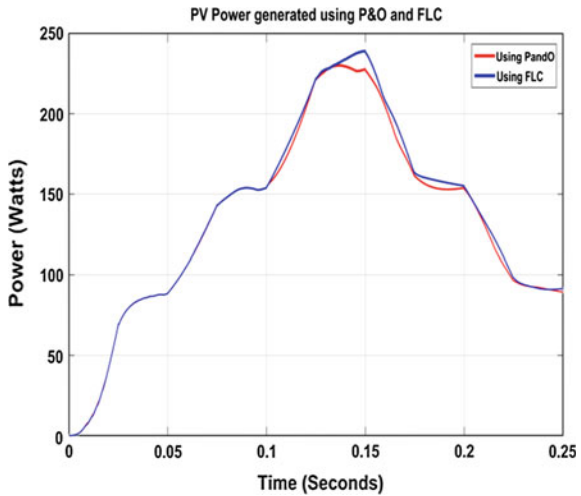


**Fig. 22.8** PV power generated using P&O and FLC



are 1.55 and 1.47 % higher than the ones generated using P and O algorithm. Using the FLC, the PV voltage and output voltage are 1.43 and 0.65 % higher than using the P and O algorithm.

Compared with the result in [6], the power and voltage generated with P&O in this study are smoother than the ones in that study. The power and voltage signal in that study that using P&O are generated with chattering. That degrades the quality of the electricity produced and the performance of the PV system.

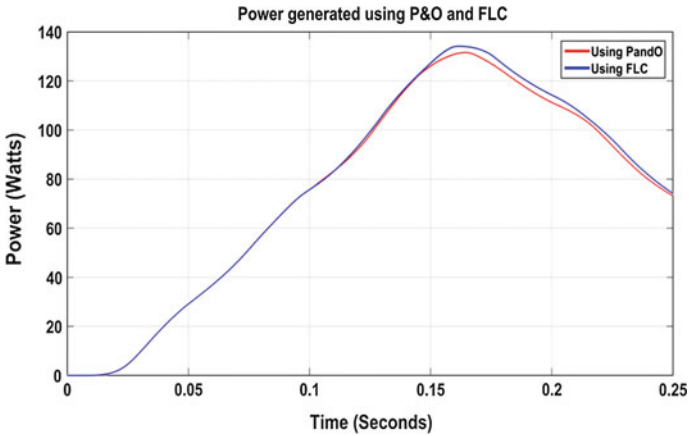


Fig. 22.9 Output power generated using P&O and FLC

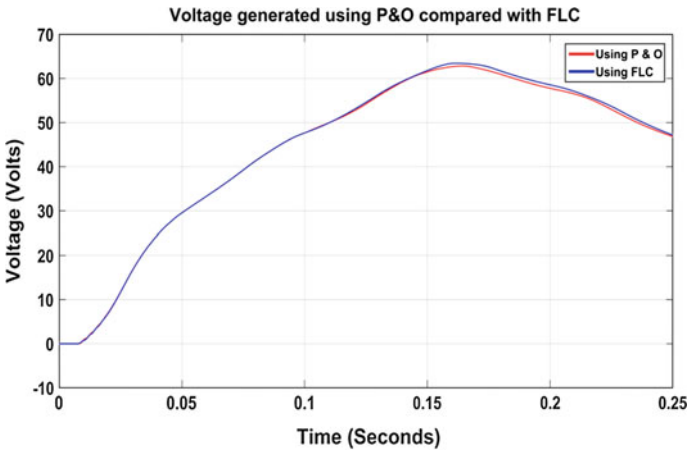


Fig. 22.10 Output voltage generated using P&O and FLC

## 22.6 Conclusion

A model of power generation system using photovoltaic has been developed and presented. It consists of a solar module, a boost converter and a controller. Two controllers have been utilized in the system, the P&O and FLC. The simulation results show that FLC outperforms P&O in terms of higher amount of PV power, generated output power and voltage.

The power amounts generated between the two controllers are not significantly different. Further studies need to be considered by utilizing different intelligent controller that generates significantly higher power while tracking the maximum power point.

## References

1. Hua, C., Shen, C.: Comparative study of peak power tracking techniques for solar storage system. In: IEEE Applied Power Electronics Conference and Exposition Proceedings, vol. 2, pp. 679–683 (1988)
2. Hussein, K.H., Muta, I., Hoshino, T., Osakada, M.: Maximum photovoltaic power tracking: an algorithm for rapidly changing atmospheric conditions. In: IEEE Proceedings on Generation, Transmission and Distribution, vol. 142, pp. 59–64 (1995)
3. Brambilla: Liew approach UI photovoltaic arrays maximum power point tracking. In: Proceedings of 35th IEEE Power Electronics Specialists Conference, vol. 2, pp. 632–637 (1998)
4. Huh, D.P., Ropp, M.E.: Comparative study of maximum power point tracking algorithm using an experimental, programmable, maximum power point tracking test bed. In: Proceedings of 28th IEEE Photovoltaic Specialists Conference, pp. 1699–1702 (2000)
5. Ramaprabha, R., Mathur, B.L.: Intelligent controller based maximum power point tracking for solar PV system. *Int. J. Comput. Appl.* **12**, 37–41 (2011)
6. Singh, S., Mathew, L., Shimi, S.L.: Design and simulation of intelligent control MPPT technique for PV module using MATLAB/SIMSCAPE. *Int. J. Adv. Res. Electr. Electron. Instrum. Eng.* **2**, 4554–4566 (2013)
7. Jose, P., Jose, P.R.: Grid connected photovoltaic system with fuzzy logic control based MPPT. *Int. J. Eng. Innovative Technol. (IJEIT)* **3**, 142–148 (2014)
8. Balasubramanian, G., Singaravelu, S.: Fuzzy logic controller for the maximum powerpoint tracking in photovoltaic system. *Int. J. Comput. Appl.* **41**, 22–28 (2012)
9. Patel, H., Agarwal, V.: MATLAB based modeling to study the effects of partial shading on PV array characteristics. *IEEE Trans. Energy Conv.* **23**(1), 302–310 (2008)
10. Pop, O.A., Lungu, S.: Intechopen. [http://cdn.intechopen.com/pdfs/11613/intech-modeling\\_of\\_dc\\_dc\\_converters.pdf](http://cdn.intechopen.com/pdfs/11613/intech-modeling_of_dc_dc_converters.pdf)
11. Singh, R., Rajpurohit, B.S.: Performance evaluation of grid-connected Solar Photovoltaic (SPV) system with different MPPT controllers. In: Hossain, J., Mahmud, A. (eds.) *Renewable Energy Integration: Challenges and Solutions*, pp. 97–124. Springer, Singapore (2014)

## Chapter 23

# Vehicle Security and Management System on GPS Assisted Vehicle Using Geofence and Google Map

Lanny Agustine, Egber Pangaliela and Hartono Pranjoto

**Abstract** Global Positioning System (GPS) receiver installed in motor vehicles have been used to track vehicles. The position of vehicle is transmitted via a wireless network using cellular telephone network known as GSM (Global System for Mobile communication). A vehicle that has GPS receiver installed onboard connected with GPRS modem and connected to a computer system in the Internet can be monitored and then provide alert when it travels outside the predefined area. This area is very important for many situations such as city car rental, trucking company to send goods from one city to another and logistic company with many fleets. The system designed here is a module with a GPS and a GPRS already integrated in one module. The output of the GPS receiver is connected to a microcontroller. The microcontroller dictates which data is collected via the GPS receiver and then sends the information to a computer system via GPRS modem. The microcontroller also receives command from the computer system via the GPRS connection and then can act accordingly, such as change the frequency of geo-coordinate or turn the vehicle engine off if necessary. This device will help the user to track its vehicle via Google Map with the GPS coordinate data sent to the database server every 10. This device will enable the operator to turn off the vehicle engine and one other device onboard the vehicle if necessary. With the feature of Geofence on the Web server using HTML5, a virtual fence has been built around the Google Map and when the vehicle moving outside the fence the user can be alerted either via email or color change on the web page. The device has been tested and shown to be working with all the conditioned mentioned above. The computer system that displays the web page together with the geofence has been developed and shown to be working properly as indicated.

**Keywords** Vehicle geofence · Google map · Fleet management · GPS assisted vehicle tracking

---

L. Agustine · E. Pangaliela · H. Pranjoto (✉)  
Electrical Engineering Department, Widya Mandala Catholic University, Surabaya, Indonesia  
e-mail: pranjoto@yahoo.com

## 23.1 Introduction

Vehicle tracking system using Global Positioning System (GPS) is a system that uses the GPS to locate the geographic coordinate of vehicle was developed previously [1]. The device itself is basically a radio receiver tuned into the frequency of the transmitting frequency of the GPS satellites in which it enables the receiver to compute its geographic coordinate. There are several data sets that can be obtained from the GPS satellites such as the accurate position of the receiver within certain radius, number of satellites received by the unit, speed of the GPS receiver moving, and accurate date/time based on the Universal Time Coordinated). Distance between the transmitting satellites and the GPS receiver is determined by using accurate time lapse between the satellites—which uses very accurate atomic clock—and the receiver using less accurate quartz crystal. Although the crystal clock is less accurate, but the result of the distance is still very accurate up to one meter resolution or less. The signal sent by the satellites includes the timestamp of the signal send and the receiver will determine the distance by measuring the time to travel to the receiver.

Using a triangulation method based on the distance from the GPS satellites, the position of the GPS receiver will be known precisely within a few meters as describe in [1–5]. This can be achieved because the precise position of the GPS satellites is excellent and reliable. Uncertainties of the distance can arise because of several physical phenomena such as temperature gradient on the atmosphere, signal bounce due to objects, and strength of satellites signals received by the GPS receiver. Other data is also obtained from the GPS receiver such as speed of the vehicle moving, heading of the movement of the GPS receiver, accuracy of position, number of satellite signal received, and strength of the signal received.

Data send from the GPS receiver is generally already in digital format and send to a computer or microcontroller using serial connection with signal amplitude of 0–5 V. Format of the data is already standardized using format of NMEA-0183 with the latest standard being version 4.10. Based on the NMEA-0183 standard, the serial data rate of the GPS receiver is 4800 bits per second with 8 bits of data and one stop bit (4800 bps 8N1). Other than sending data via this serial connection, setting of the GPS receiver can be performed via this serial connection. Setting includes the data format, unit of measurement, and time information.

The GPS data obtained from a moving vehicle is transmitted using wireless data network from part of the GSM (Global System for Mobile Communication) also known as cellular telephone. The data component part of the GSM is called General Packet Radio Service (GPRS) can connect to the host computer with speed up to 128 kbit/s which is fast enough for this application. In order to use the GPRS part of the GSM network, a GPRS modem is needed to connect the data portion of the wireless network. The GPRS modem connects to the microcontroller via a serial connection similar to the connection to the GPS mentioned previously.

Figure 23.1 illustrates the system used for Vehicle security and management system on GPS assisted vehicle using geofence and Google map system. There are



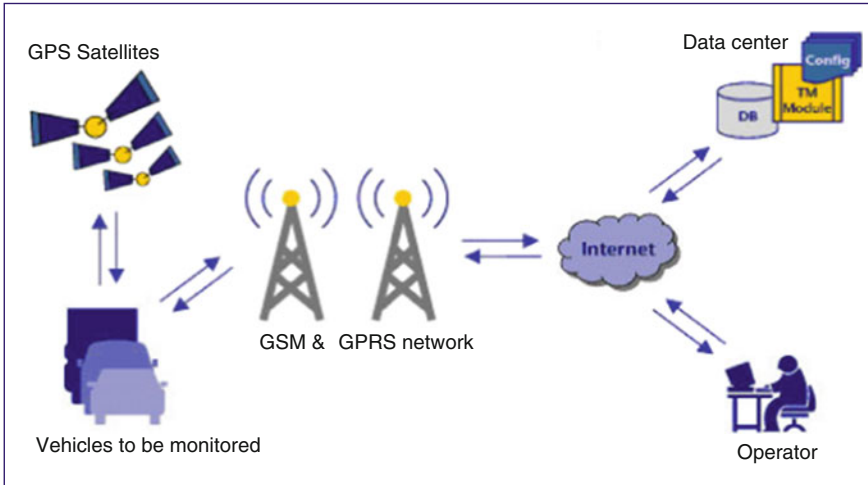


**Fig. 23.1** Vehicle monitoring/management system using GPS via GPRS network

GPS satellites to assist the GPS receiver mounted on vehicles to be monitored to find their geographical coordinates. The coordinates of the vehicles are send via GPRS modem using GSM network to the Internet to a computer system—usually in a data center—with database server and web server already installed on the system. An operator—also connected to the Internet—access the server via web browser to access the coordinate data of the vehicles to be monitored. The web server of the computer system with HTML5 capability can provide the geolocation of the vehicle to be monitored on the web page overlaid with the map of the location using Google Map.

The operator has several monitoring privileges and control of the vehicle. Operator can track the vehicle and place a geo-fence around the vehicle and some other features discussed later. With this feature, a vehicle that is going beyond the geo-fence or virtual fence can be displayed on the screen and operator can be visually alerted and then can take action accordingly.

## 23.2 System Design and Constructions

The system design of the vehicle security and management system in block diagram is shown in Fig. 23.2. There is a GPS module and a GPRS module integrated in one larger module in SIMCOM 908. This system also has a power management module to control the charging of a backup lithium battery which will be used to power the system in case there is a power failure of the main power system. Each of the modules (GPS and GPRS) has serial input/output UART (Universal Asynchronous

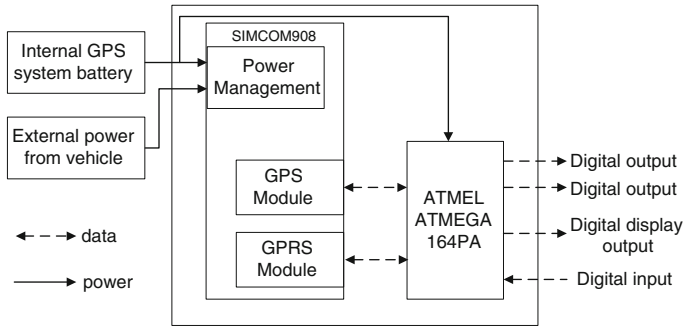


**Fig. 23.2** Block diagram of vehicle monitoring/management system using GPS via GPRS network

Receiver Transmitter) in which the devices will send or receive the data. The serial input/output is connected to a microcontroller ATMEGA 164PA which has two serial input/output. All of the modules are powered using the same power supply which is 3.3 V which can be obtained from the external power or from the internal lithium battery.

### 23.2.1 Global Positioning System (GPS)

Global Positioning System (GPS) is a satellite based positioning, in which there is a need for at least three visible satellites to determine the position—including altitude—of a GPS receiver. The basic method of position determination is trilateration which has been described elsewhere [6–8]. In reality with more than three visible satellites, the accuracy of the position will increase and accuracy can be within 2 m in many situations where there is not much obstruction to the satellite signals. In many situations the signal strength received from the satellites will also improve the accuracy the calculation of the position. On the average without any special antenna a GPS receiver can detect 7–11 satellites at the same time with signal strength between 11 and 25 dB with accuracy of less than 5 m.

Most GPS systems have serial output similar to RS-232 or UART (Universal Asynchronous Receiver Transmitter) and the output format usually comply with the NMEA-0183 output. Serial output of NMEA-0183 compliance device will have character '\$' as the first character followed by two characters talker identification such as 'GP' for GPS device. The next identifier after the \$GP are three letter-identifier related to the GPS data such as GGA (constant GPS data), GLL (Geographic Position Latitude/Longitude), GSA (GNSS/Global Navigation Satellite Systems Dilution of Accuracy), ZDA (GPS time and date Information), VTG (Course Over Ground and Ground Speed), RMB (Recommended Minimum Navigation Information), and RMC (Recommended Minimum Specific GNSS

Data). The data followed after the three-letter-identifier is data related to the identifier. For example, after ZDA identifier, the time and date data will follow, each data are separated by comma and then the last data is character ‘\*’ followed by the checksum data of two characters ended by < CR > < LF > [9, 10].

### **23.2.2 General Packet Radio Service (GPRS)**

General packet radio service (GPRS) is a packet oriented mobile data service available to users of the 2nd generation cellular communication systems global system for mobile communications (GSM). This system developed here uses the 2nd generation instead of the 3G system. In 2G systems, GPRS provides data rates of 56–114 kbit/s [1, 2, 11, 12]. The purpose of this system is to communicate data from the GPS to the computer which is attached to the Internet. Detail connection of a GPRS modem to the Internet is described in details in [1].

Connection establishment from the device to the GPRS network is conducted via a GPRS modem with connection which has a serial connection to computer/microprocessor. Command to connect to the GPRS network is via Hayes command which is also known as AT+ command (Attention Command) [13–15].

### **23.2.3 SIMCOM908 (GPS and GPRS Modules in One Unit)**

One of the most important modules used in this device is SIMCOM908. It is a module which comprise of a GPS module which is described above combined with a GPRS and GSM modules integrated into one larger module with its function blocks shown in Fig. 23.3a.

As shown in Fig. 23.3a, this module also has a power management module which is utilized to manage internal rechargeable battery. This battery is a backup power in case the external power from the car battery is unplugged and the backup in embedded inside the unit. Charge management unit include the full power recharge if the backup battery is low in power, trickle charge the backup battery for a period of time when it is full, and then stop the charging when the backup battery is completely full. Figure 23.3a also shows that the module has complete GPS receiver, complete GPRS packet data connection along with GSM telephone with external SIM card connection for the GSM with ‘Mini SIM (2FF)’ form factor. The GPS, GSM and GPRS unit are controlled by two different UART port, one UART for the GPS and the other UART for the GSM/GPRS unit. The GSM module is Quad-band with power to the SIM card (1.8–3 V) compatible with providers in Indonesia. Serial port connection support data rate from 4800 to 115,200 bit/second (bps). Figure 23.3b is the photograph of the top side of the

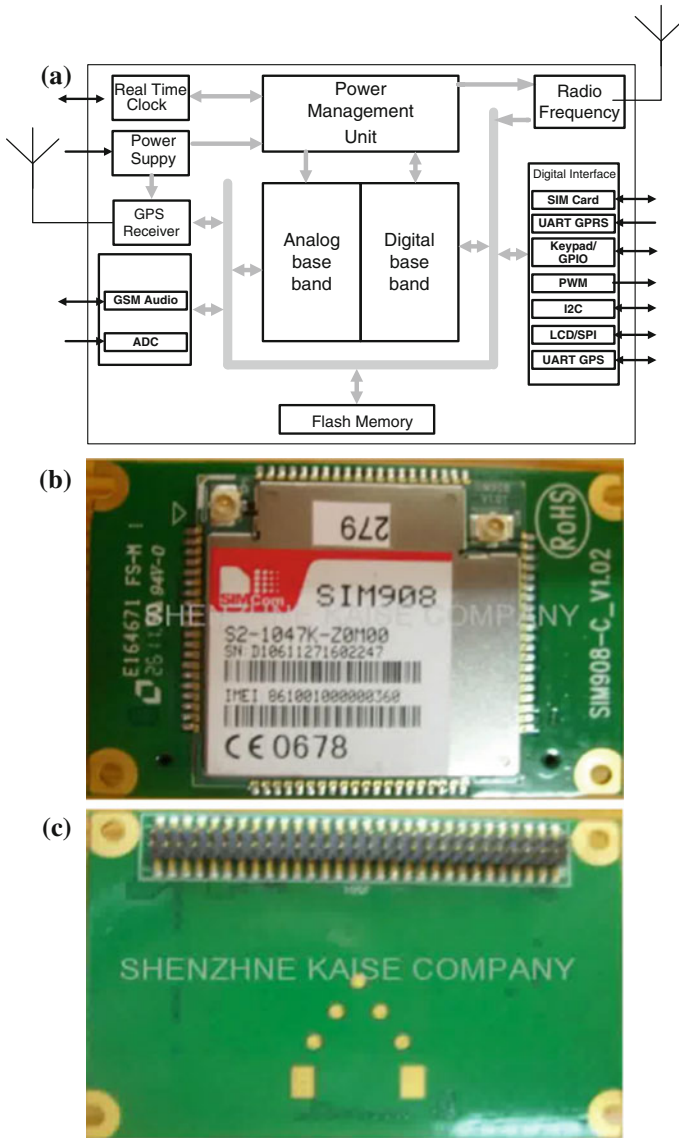


**Fig. 23.3** a SIMCOM908nfunction block with power management. b Top view of SIMCOM908 module with I-Pex antenna connector. c Bottom view of SIMCOM908 module with the pin connection to PCB

module and Fig. 23.3c is the bottom part. Antennas for the GSM and GPS module are connected via two different I-Pex connectors on the component side as shown in Fig. 23.3b. The same module is used in previous work [1].

### **23.2.4 *Microcontroller ATMEL ATMEGA164PA***

The SIMCOM908 module used for this device has two serial UART connections to control the GPS and GPRS modules. Controlling the sub-system requires two different UART connections that can be active at the same time, therefore a microprocessor with two serial ports will be used. The choice of this system is the ATMEGA164PA. This microcontroller has two independent serial ports that can be programmed for different types of data requirements.

### **23.2.5 *Data Connection to the Server in Internet***

Before sending the data, GPRS modem must establish data connection via APN (Access Point Name) which is the gateway to the public Internet. A user needs to know the APN the provider in order to connect, and the information is usually available in the Internet. Connection to the APN will involve sending the user name and the password. Usually the provider will inform the username and password, but it must be programmed first in the microcontroller.

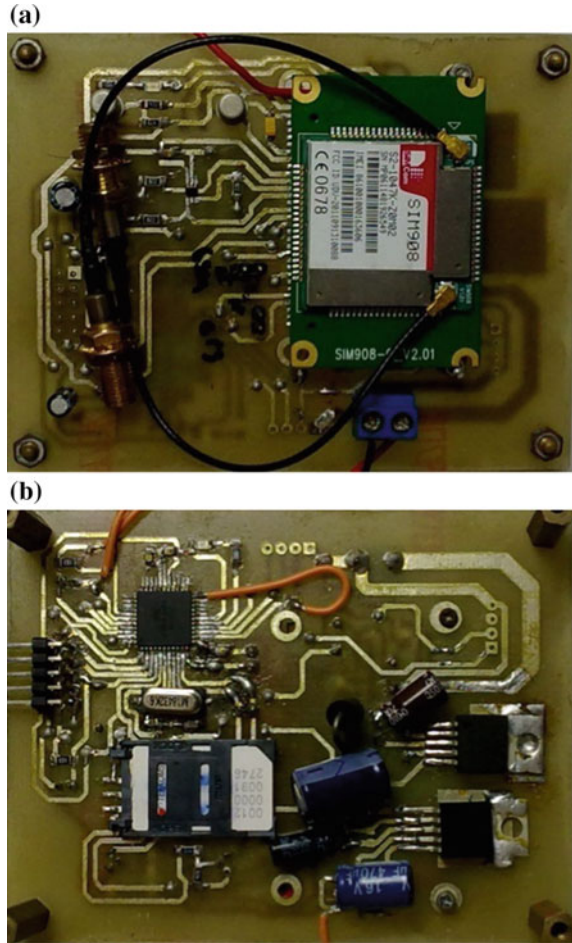
After the establishment of data connection, the system onboard the vehicle will start sending information of its location, speed, heading and other information to the computer system in the Internet which already has MySQL database application software installed. MySQL is a Relational Database Management System (REBMS) capable of handling large amount of data arranged as tables with rows and columns.

Google Maps is a web mapping service application and technology provided by Google free of charge—for non-commercial use—that provides information about geographical region such as road and places. Google Maps uses JavaScript very extensively together with the API key to display the map. Google user account is needed via '<https://developers.google.com/maps/licensing>' to obtain the key. After the connection to the Internet, this system has to connect to the proper website to display the location of the vehicle using Google Map. The website is coded into the system is '[www.gpsfence.web.id](http://www.gpsfence.web.id)'.

## **23.3 Implementation of the GPS/GPRS System and Geo-Fence Web Interface**

The vehicle tracking system using GPS and GPRS for data connection has been designed and constructed using all the subsystem mentioned above. The system uses double sided board to conserve space with the SIM908 on one side together

**Fig. 23.4** **a** Top side of the GPS vehicle tracking with the SIM908 module shown on top of it. **b** Bottom side of the GPS vehicle tracking with microprocessor and SIM card shown



with several external parts such as output driver and regulator. The top part of the system with the SIM908 module is shown in Fig. 23.4a. Shown also in this figure the pigtail for the antennas, the top part is the GPS antenna connector while the bottom connection is for the GPRS antenna. Figure 23.4b is the reverse side of the circuit board. On this side there is the microprocessor in the form of SMT quad pack together with the crystal and the SIM card holder, and two regulators and on the left-hand side of the board there is an 8-pin header for the programming of the microprocessor via the ISP port of the microcontroller.

The vehicle location information obtained from the GPS is stored in a database file (MySQL) with the data shown in Table 23.1. Other than geographic data, the time, battery condition and vehicle status are also stored in the database and can be

**Table 23.1** Parameters saved on the database for the information of the vehicle

Field	Parameter saved
UTC	Time data are taken based on the Universal Time Coordinated time zone
Longitude	Longitude coordinate of the vehicle in signed degree format (DDD.dddd) from -180 East to +180 West
Latitude	Latitude coordinate of the vehicle in signed degree (DD.dddd) from -90 North to +90 South
GPSU	Number of satellites visible to the GPS receiver and used to calculate the position
Speed	Speed of the vehicle in kilometer per hour
Internal battery	Internal battery capacity in percent
External power	Indicator of external battery connection
Relay 1	ON/OFF condition (usually for engine, normally open)
Relay 2	On/OFF condition usually for external alarm or others (normally closed)
Emergency	On/OFF condition of emergency button, normally off/open

recalled from the web by clicking on the marker of the vehicle. The database and also the web interface can be accessed via <http://www.gpsfence.web.id>.

Data transmission from the GPS to the database is done via GPRS wireless connection which has been discussed previously. Data connection has been tested with all the prepaid GSM network in Indonesia and it has been shown to work properly. For this work, the data connection uses Telkomsel GSM provider with the Access Point Name (APN) coded internally to the microcontroller. The code for the work has been discussed elsewhere [1].

The web page stated on the address above is HTML5 capable and therefore can accommodate geofence and the first page shown is similar to Fig. 23.5. When the location of the vehicle is within the geofence (made with gray color of a quad-angle) the marker is shown red and when the location is outside the fence, then the marker is shown as blue color. Clicking on the market will show that the location is inside or outside the geofence. In this figure the vehicle is monitored using the GPS and shown to be inside the geo fence (four locations) and two locations are outside the fence. The page will also show that the vehicle is outside the fence when the mouse is clicked. When the vehicle inside the fence is clicked, then a window will show that the vehicle is inside the fence as shown in Fig. 23.6.

A vehicle equipped with GPS receiver can obtain its geographical coordinate easily and accurately and the data can be sent to a server in the Internet via GPRS wireless network. The data can then be displayed/overlaid using map to indicate the location of the vehicle and then can be enhanced further by displaying a virtual fence called geofence. With this geofence, the vehicle can be enclosed to be at certain area of operation and when it moved outside the specified enclosed position

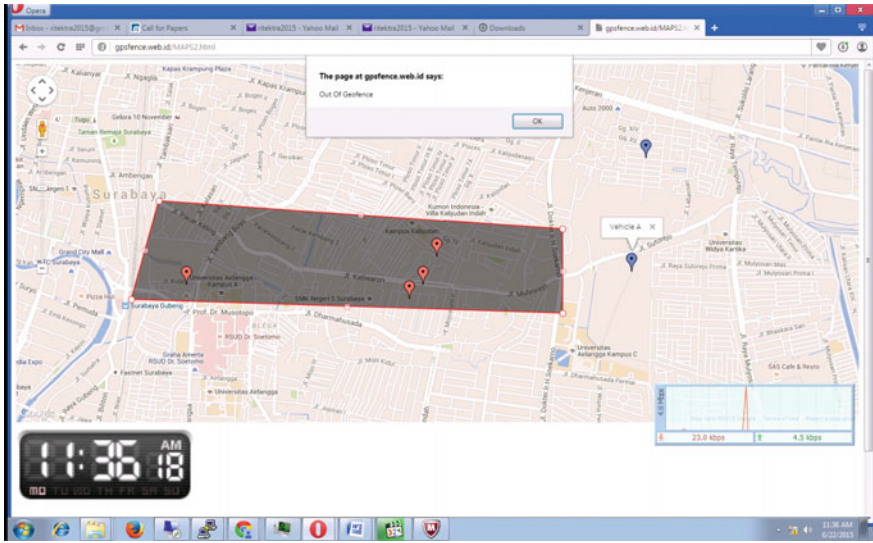


Fig. 23.5 First page of the vehicle tracked inside and outside the geo-fence

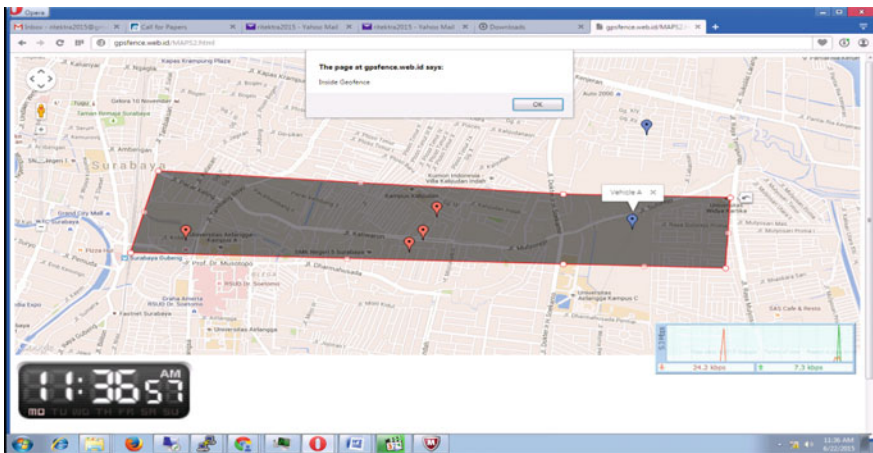


Fig. 23.6 First page of the vehicle tracked inside and inside the geo-fence

an operator can be alerted. With this alert system, the vehicle can be more secured against any wrong doing or any other bad intention and thus the security of the vehicle is enhanced even further (Fig. 23.7).



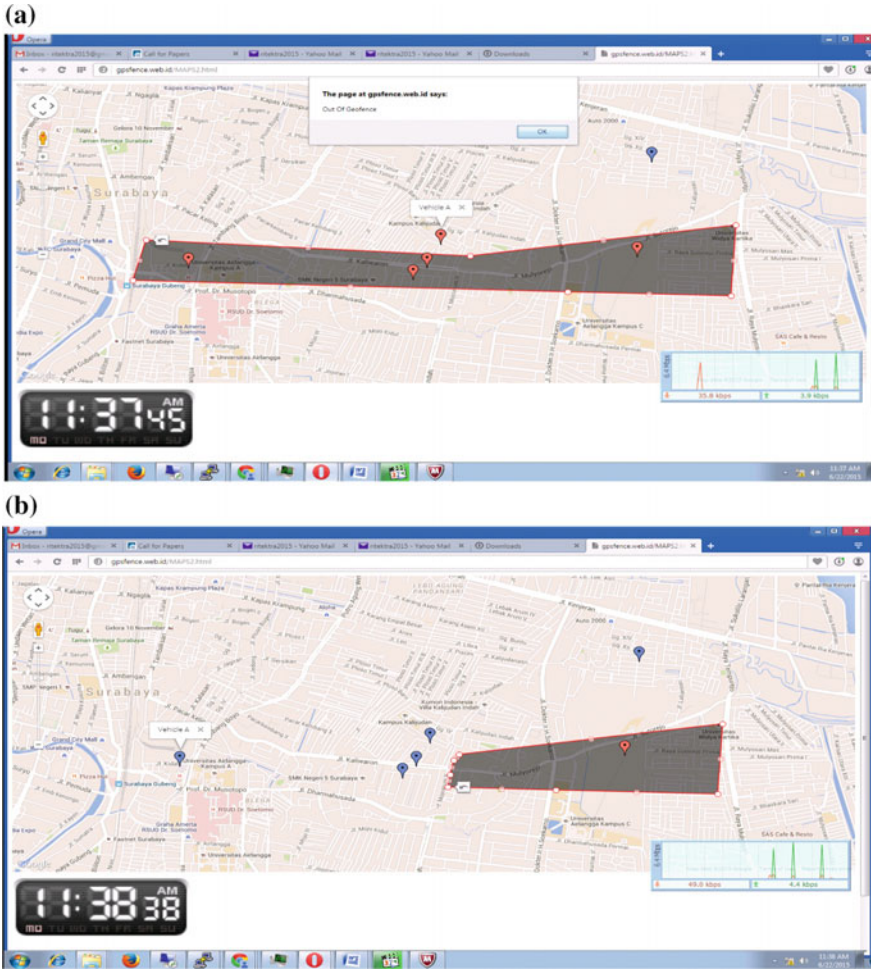


Fig. 23.7 a Vehicle is outside the fence after reshaping the geo-fence. b Vehicle is inside the fence after reshaping the geo-fence

### 23.4 Conclusion

This work has shown the work of tracking the vehicle using GPS and GPRS is successful. From the end result of data, they show that the vehicle can be tracked properly using GPS and GPRS. When the emergency button is pressed for more than 3 s the status will be displayed on the web page. Control of vehicle can be carried out by the operator in charge of the vehicle to turn on and turn of the vehicle or part of the vehicle when necessary.

**Acknowledgements** This work is supported by the Indonesian Directorate General of Higher Education under grant No: 003/SP2H/P/K7/KM/2015, dated 02 April 2015.

## References

1. Pranjoto, H., Agustine, L., Susilo, Y.S., Tehuayo, R.: GPS based vehicle tracking over GPRS for fleet management and passenger/payload/vehicle security. *ARPN J. Eng. Appl. Sci.* **9** (11) (2014)
2. Grewal, M.S., Weill, L.R., Andrews, A.P.: *Global Positioning System. Inertial Navigation and Integration*. Wiley, New York (2001)
3. Halonen, T., Romero, J., Melero, J. (eds.): *GSM, GPRS, and EDGE Performance: Evolution Towards 3G/UMTS*, 2nd edn. Wiley, New York (2003)
4. Kaplan, E., Hegarty, C.: *Understanding GPS: Principles and Applications*, 2nd edn. Artech House, Norwood (2006)
5. Kingsley-Hughes, K.: *Hacking GPS*. Wiley, New York (2005)
6. Maral, G., Bousquet, M.: *Satellite Communications Systems, Systems, Techniques and Technology*, 5th edn. Wiley, Chichester (2009)
7. Meyer, E., Ahmed, I.: Benefit-cost assessment of automatic vehicle location (AVL) in highway maintenance. In: *Proceedings of the 2003 Mid-Continent Transportation Research Symposium*, Ames, Iowa (2003)
8. Peng, Z.R., Beimborn, E.A., Octania, S., Zygowics, R.J.: *Evaluation of the Benefits of Automated Vehicle Location Systems in Small and Medium Sized Transit Agencies*. Center for Urban Transportation Studies, Milwaukee (1999)
9. Portillo, D.: *Automated Vehicle Location using Global Positioning Systems for First Responders*, Institute for Information Technology Applications. Technical report series, Colorado (2008)
10. National Marine Electronic Association: *NMEA 0183 Version 4.10 Electronic*, National Marine Electronic Association, Severna Park, Maryland (2012)
11. *SIRF Technology: NMEA Reference Manual*, San Jose (2007)
12. Seurre, E., Savelli, P., Pietri, J.P.: *GPRS for Mobile Internet*. Artech House, Norwood (2003)
13. Eberspächer, J., Vögel, H.J., Bettstetter, C., Hartmann, C.: *GSM—Architecture, Protocols and Services*, 3rd edn. Wiley, Stuttgart (2009)
14. European Telecommunications Standard Institute: *Technical Specification AT command set for User Equipment 3GPP TS27.007 version 11.5.0 Release 11* (2013-01), Januari (2013)
15. *SIM Tech: SIM 908 Hardware Design V. 2.00* (2012)

# Chapter 24

## Security and Stability Improvement of Power System Due to Interconnection of DG to the Grid

Ni Putu Agustini, Lauhil Mahfudz Hayusman, Taufik Hidayat and I. Made Wartana

**Abstract** This paper developed a novel method to improve the performance of power network based on system stability, namely voltage stability index and line stability factor, as well as system security that is a bus voltage violation factor and thermal limits of the transmission line. This method has been analyzed and evaluated in a standard test system due to the interconnection of a distributed generation (DG) into a grid as an anticipation to an increase in load demand. To ensure the stability and security of the system as a result of the interconnection of the DG, an optimal placement of one type of shunt Flexible AC Transmission Systems (FACTS) controller, namely Static Var Compensator (SVC), is conducted. The device which is proficient for injecting and absorbing reactive power is modeled and subsequently combined in Newton Raphson power flow analysis. The effectiveness of the methodology developed has been successfully tested on IEEE 14-bus standard test system with integration of the DG into the test system.

**Keywords** DG · FACTS · SVC · System stability · System security

### 24.1 Introduction

In recent decades, the electric power system faces new challenges as a result of the impact of deregulation and restructuring of the electricity market [1]. Along with the deregulation of the electrical load continues to increase so that the need for the addition of new power plants into the electric power system network (grid) in

---

N.P. Agustini (✉) · L.M. Hayusman · T. Hidayat · I.M. Wartana  
Electrical Department, National Institute of Technology (ITN) Malang,  
Jl. Bend. Sigura Gura no. 2, Malang, Indonesia  
e-mail: niputu.agustini@yahoo.co.id

anticipation of an increase in load demand of consumers. This condition has forced the transmission lines to distribute power loads approaching its thermal limits.

This condition would attract electric power system to find the right way that enables the distribution of electric power to consumers in a more efficient way to control the flow of electrical power [2]. A lot of the latest technology developed in the electric power system, which makes the utility is able to control the flow of power in anticipation of an increase in electric power loadability, thermal limit of the line, the stability of the transmission system, and improve the security of the transmission system [3]. In addition, a variety of modern control devices have been developed and used to maximize the power transfer capability while minimizing power loss transmission system, which leads to efficient utilization and improved performance of existing power systems [4].

When compared with the corrective control strategy, such as scheduling and termination load generation, the utilization of modern control systems such as FACTS devices in the future is a more economical alternative because it reduces the operating costs and the investment in developing a new network system, although the cost of the device is still relatively expensive and it is a quite complicated operation [5, 6].

To anticipate the increasing demand for electricity, and the gradually reduced dependence on electricity supplies from outside the island, the operation of a distributed generation (DG) are absolutely necessary. Operation of this plant can provide influence on grid's system performance which is represented in the reduction of the voltage profile and power losses of the grid system. In order to anticipate the increase in electrical load that occurs for several years into the future with continuity and reliability, the stability and security of the grid system needs to be analyzed and evaluated.

This research proposes a novel method based on evolutionary optimization techniques known as Particle Swarm Optimization (PSO) in analyzing and evaluating the stability and security of the power system at a maximum system loadability by operating a distributed generation (DG). This is done by optimal placement of a shunt FACTS controller i.e. SVC on a IEEE 14-bus standard test system [7]. With interconnecting DG into the grid, it still ensures the stability of the system at its margins, which are fast voltage stability index (FVSI) and line stability factor (LQP); and maintain the security of the system i.e. bus violation factor and thermal limit. Furthermore, to avoid an excessive increase in line losses due to increased system loadability, a technique is developed simultaneously to minimize active power losses as a result of DG interconnection to the grid with the aim to improve the performance of the system.

## 24.2 Problem Formulation

### 24.2.1 DG Modeling

A precise dynamic modeling of DG unit, to study the dynamic behavior, is the key issue in obtaining an idea of the impact on the network resulting from the presence of the generating units that follows a few distractions. Synchronous machines must be modeled through conventional state equation that describes the electrical machine, automatic voltage regulator, equations swing, speed regulator and the main engine [8]. However, this modeling depends on the type of plant. In some industrial plants which have cogeneration facilities, speed regulator became active only in an isolated mode of operation. Generator with the power electronic converter can be modeled as a controlled current source or sources of active and reactive power [9] since the fast transients in this converter, associated with the operation of electronic switches and controls, which are not the interest of analysis.

### 24.2.2 Shunt FACTS Modeling

Static Var Compensator (SVC) is one type of shunt FACTS controllers which are widely used in modern electrical systems in some parts of the world. The SVC is connected in parallel (shunt) with the load bus to compensate the inductive reactance on the bus. In this study SVC is modeled as an ideal reactive power injection at bus  $i$  [10].

$$\Delta Q_i = Q_{SVC} \quad (24.1)$$

The model is completed by the algebraic equation expressing the reactive power injected at the SVC node [11, 12]:

$$Q_{SVC} = b_{SVC} V^2 \quad (24.2)$$

where,  $V$  and  $b_{SVC}$  are the voltage magnitude of a bus at which the component are connected, and total reactance of the controller, respectively.

### 24.2.3 System Loadability

To ensure the security of the system due to DG interconnection to the grid, the system loadability is increased without exceeding their thermal and bus violation limit factor.

$$\text{Maximize } F_1(\mathbf{x}, \mathbf{u}) = \{\lambda_1\} \quad (24.3)$$

$$\text{Subject to } VL = \sum_{i=1}^{N_l} OLL_i x \sum_{j=1}^{N_b} BVV_j \quad (24.4)$$

where  $VL$  is the thermal and bus violation limit factor,  $OLL_i$  and  $BVV_j$  represent the overloaded line factor and branch the bus voltage violation factor, respectively;  $N_l$  and  $N_b$  are the total numbers of transmission lines and buses, respectively. In addition  $\lambda_1$  is a load parameter of the system, which intends to locate the maximum sum of power that the network is able to supply within the system security margin [4].

#### 24.2.4 Total Power Losses

An exact loss equation in (24.5) represents the total real power loss in a power system [13].

$$P_{loss}(\mathbf{x}, \mathbf{u}) = \sum_{i=1}^N \sum_{j=1}^N [\alpha_{ij}(P_i P_j + Q_i Q_j) + \beta_{ij}(Q_i P_j + P_i Q_j)] \quad (24.5)$$

where

$$\alpha_{ij} = \frac{r_{ij}}{V_i V_j} \cos(\delta_i - \delta_j); \beta_{ij} = \frac{r_{ij}}{V_i V_j} \sin(\delta_i - \delta_j)$$

- $V_i \angle \delta_i$  complex voltage at the bus  $i$ th;
- $r_{ij} + jx_{ij} = Z_{ij}$   $ij$ th element of  $[Zbus]$  impedance matrix;
- $P_i$  and  $P_j$  active power injections at the  $i$ th and  $j$ th buses, respectively;
- $Q_i$  and  $Q_j$  reactive power injections at the  $i$ th and  $j$ th buses, respectively;
- $N$  number of buses

#### 24.2.5 Stability Constraints

##### 24.2.5.1 Fast Voltage Stability Index

Fast Voltage Stability Index ( $FVSI$ ) proposed by Musirin [14] is utilized in this paper to assure the safe bus loading. The  $FVSI$  is the device used to indicate the voltage stability condition formulated based on a line or a bus as defined by

$$FVSI_{ij} = \frac{4Z^2 Q_j}{V_1^2 X} \quad (24.6)$$

where,  $Z$  is the line impedance,  $X$  is the line reactance,  $Q_j$  is the reactive power at the receiving end, and  $V_i$  is the sending end voltage.  $FVSI$  index incorporation in the controller assures that no bus will collapse due to overloading.

### 24.2.5.2 Line Stability Factor

System stability index is also assured by Line Stability Factor ( $LQP$ ) proposed by Mohamed et al. [15]. The formulation begins with the power equation in a power system and is expressed as

$$LQP = 4 \left( \frac{X}{V_i^2} \right) \left( \frac{X}{V_i^2} P_i^2 + Q_j \right) \quad (24.7)$$

where,  $X$  is the line reactance,  $V_i$  is the sending end voltage,  $P_i$  is the sending end real power, and  $Q_j$  is the receiving end reactive power. The  $LQP$  must be kept less than 1.00 to maintain a stable system.  $LQP$  assures the controller that no line is overloaded under any grid condition.

## 24.3 Methodology Development

### 24.3.1 Overview of PSO

In a PSO system [16], each particle in search space is defined by the following elements:  $x_i^k$  is the value of particle  $i$  at generation  $k$ . The update of particle  $i$  in the search space is defined by (24.11);  $p_{best}$  is the best value found by the particle  $i$  until generation  $k$ ;  $v_i^{k+1}$  is the velocity of particle  $i$  at generation  $k$ . The update of velocity during the search procedure is presented by (12);  $g_{best}$  is the best particle found in the group until generation  $k$ .

$$x_i^{k+1} = x_i^k + v_i^{k+1} \quad (24.8)$$

$$v_i^{k+1} = \omega \times v_i^k + c_1 \times rand_1 \times (p_{best_i} - x_i^k) + c_2 \times rand_2 \times (g_{best} - x_i^k) \quad (24.9)$$

where,  $\omega$  is weighting function,  $c_j$  is weighting factor,  $rand_i$  is random number between 0 and 1,  $p_{best}$  and  $g_{best}$  are “ $p_{best}$  of particle  $i$ ” and “ $g_{best}$  of the group”, respectively.

The following weighting function is usually utilized [17]:

$$\omega = \omega_{\max} - \frac{\omega_{\max} - \omega_{\min}}{iter_{\max}} \times iter \quad (24.10)$$

where:  $\omega_{\max}$ ,  $\omega_{\min}$ ,  $iter_{\max}$  are the initial weight, the final weight, and the maximum iteration number, respectively.

### 24.3.2 Calculation of Fitness Function

The optimization problem for the best promising placement of the SVC controller is changed into an unconstrained optimization problem using a penalty factor ( $PF$ ) as given in (14). This becomes the fitness function ( $FF$ ) in the PSO technique.

$$FF = \mu_1 F_1 - \mu_2 F_2 + PF \times |VL - 1| \quad (24.11)$$

Equation (14) is composed of three parts equation. The first term is a function of the goal to maximize the loading system as shown Eq. (24.3), the second term is a second objective function to minimize power loss transmission line as shown in Eq. (24.5). While the last term, a constraint violation of system security according to the Eq. (24.4) which is multiplied by the PF to calculate the fitness function given by (14) for each particle.  $\mu_i$  is the weighting coefficient used to adjust the tilt PSO. For each particle, the data bus line is updated according to the increase in the system load. NR power flow method run to get on any bus voltage and line power flow. With this result, the value VL for each particle obtained by using (4) and the fitness function of each particle is calculated by using (14). Particles that provide maximum value to the fitness function in a population regarded as  $g_{\text{best}}$  particles.

Speed and new position of each particle are calculated respectively using Eqs. (12) and (13). This procedure is repeated until the maximum number of iterations is reached so that the value of VL and all obstacles stability as shown in (9) and (10) for particles  $g_{\text{best}}$  are examined. If the value is equal to 1, then by using a particle  $g_{\text{best}}$ , the current value of the loading system can be met without a breach in the flow line power, bus voltage limit constraints and all the constraints of stability are within the allowable limits. The  $g_{\text{best}}$  particles are stored together with the loading system and lines power losses. Then the system load increases again when PSO algorithm is executed. If the value VL for  $g_{\text{best}}$  particles is not equal to 1 then the particle  $g_{\text{best}}$  cannot meet the current system loading and particle  $g_{\text{best}}$  with  $VL = 1$  obtained in the previous step. This is considered as the best optimal setting. Imposition of a particle system in accordance to  $g_{\text{best}}$  is regarded as maximum system loading.



### 24.4 Result and Discussion

To investigate and validate the method in solving the optimization problems developed in this study, the simulation have been implemented on IEEE 14-bus standard test system [7] using the PSO technique. The simulation has also been carried out to resolve the two objective functions simultaneously i.e. maximizing the system loadability (Max SL) whereas minimizing the active power losses (Min  $P_{loss}$ ) of transmission line by considering the security and stability margins. This is done on the three cases: base case, without DG interconnection to the grid, and by optimal placement of SVC device in both cases viz.: to the base case (Case-1) and after a specified amount DG of 10 MVA, 13.8 Volt is interconnected to the grid (Case-2). The SVC device used in this study, modeled using power system analysis toolbox (PSAT) [7]. PSO parameters are presented in Table 24.1.

The load is modeled as a constant PQ load with constant power and load factor increased by using the PSO technique according to the Eqs. (24.10) and (24.11). Each additional system load that occurs in this study is assumed to be borne by the slack generator.

The location and setting of SVC set as a decision variable, while all bus load of test systems IEEE 14-bus chosen as candidate locations for the placement of the SVC. Based on these data [7] the IEEE 14-bus is fed by two generators on the bus 1 and 2, three synchronous condensers are located on bus 3, 6 and 8, with 20 lines and 11 bus loads. From the simulation results carried out in both cases, we found that the optimal placement and setting of SVC equipment on the IEEE 14-bus network to maximize SL and minimize  $P_{loss}$  of the transmission line are presented in Table 24.2.

From Table 24.2 it can be observed that in Case-1, the SVC installation on 14-bus with a maximum setting of 0.98 pu resulted a maximum system loadability (Max SL) and the minimum active power losses line (Min  $P_{loss}$ ) are 166.46 % and 0.474 pu, respectively. Moreover in Case-2, after the DG interconnection to the grid on one bus load, where the chosen bus is the bus 14, the optimal placement and setting the SVC on the bus 4 have been able to increase of the loading system up to

**Table 24.1** PSO parameters

$c_1, c_2$	$\omega_{max}$	$\omega_{min}$	Iteration number	Population number
2.0	0.9	0.4	50	50

**Table 24.2** Optimal location of the SVC for bi-objective optimization

Cases	Location (bus)	Setting (pu.)	Max SL (%)	Min $P_{loss}$ (pu.)
Base case	–	–	100	0.761
Case-1	14	0.98	166.46	0.474
Case-2	4	0.97	183.47	0.482

183.47 %. The increase in load is spread proportionally almost in all of the load bus. In this condition, despite an increase in SL,  $P_{loss}$  is not much different from the Case-1 is 0.482 pu.

This result suggests that the optimal placement and setting SVC to the grid which is interconnected to the DG is not only improve the loading system (SL) but also at the same time it able to minimizing  $P_{loss}$  of the transmission line with all the security and stability system constraints are guaranteed at the limit of the allowable margin.

Figure 24.1 shows the voltage profile of the Case-2 which proves that the optimal placement of SVC at bus 4 ensure the security of the system which is at their limit allowable voltage. While Fig. 24.2 shows the stability of the system which is represented by FVSI and LQP factor are less than one.

The results obtained in the IEEE 14-bus system compared to those reported in [4] as shown in Table 24.3. In Case-1, Max SL obtained in this study compares favorably with results reported in [4], although with the number of controllers required is the same but different types of devices. In this study, Min  $P_{loss}$  are considered, but the reference concerned with the cost of the controller because the cost of UPFC is more expensive than the cost of SVC. In addition, stability constraints applied in both studies is different. Case-2 of the standard IEEE 14-bus test system has not been reported in the reference.

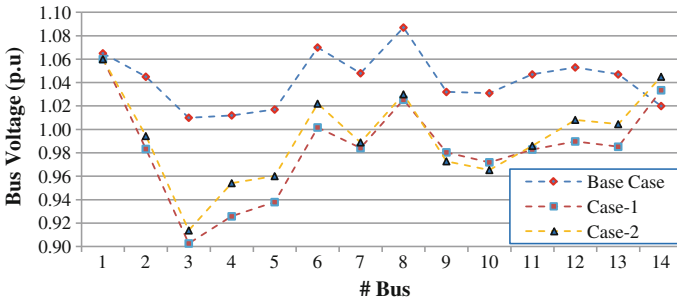


Fig. 24.1 Voltage profile for Case-1 and Case-2 on IEEE 14-bus standard test system

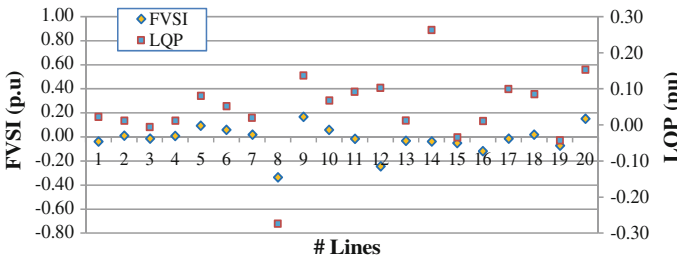


Fig. 24.2 FVSI dan LQP for Case-2 on IEEE 14-bus standard test system

**Table 24.3** Maximum system loadability (Max SL), Minimum  $P_{loss}$ , and Minimum cost of FACTS (Min cost) needed in IEEE 14-bus system

Cases	Type of FACTS	Result obtained in this study				Type of FACTS	Result reported in [4]			
		Max SL	Min $P_{loss}$	Min Cost ( $\times 10^6$ US\$)	Stability constraint		Max SL	Min $P_{loss}$	Min Cost ( $\times 10^6$ US\$)	Stability constraint
Case-1	SVC	166.46	0.474	–	FYSI & LQP	150.29	–	0.2878	Small signal	
Case-2		183.47	0.482	–		–	–	–		

## 24.5 Conclusion

This study has successfully implemented one type of the advanced evolutionary optimization techniques, namely PSO which is used to solve a bi-objective optimization problem, viz.: increasing the system loadability due to DG interconnection to the grid whereas reducing active power losses of transmission line. The optimization problem involving simultaneous bi-objective was solved with optimal placement of one type of shunt FACTS device namely SVC at the best location whereas ensuring the security and stability of the system, and they are expressed as FVSI and LQP. The simulation results performed on the IEEE 14-bus standard test system show that system loadability can be increased up to 83.4 % of the base case using the PSO technique with an index of performance in achieving accurate and fast convergence.

In addition, the algorithm developed in this study is not only able to solve the bi-objective optimization problem, but also has superior features that include high-quality solutions, stable convergence characteristics and good calculation efficiency. Thus the proposed optimization technique can be developed further to cover more than two objectives and applied on a practical power system for validation and supporting the superiority of the proposed technique.

**Acknowledgements** Authors are grateful to the Director General of Higher Education that have assisted in funding this research through the Institute for Research and Community Service ITN Malang.

## References

1. Cai, L.J., Erlich, I., Stamtis, G.: Optimal choice and allocation of FACTS devices in deregulated electricity market using genetic algorithms. In: Power Systems Conference and Exposition, vol. 1, pp. 201–207. IEEE PES (2004)
2. Lu, Z., Li, M.S., Jiang, L., Wu, Q.H.: Optimal allocation of FACTS devices with multiple objectives achieved by bacterial swarming algorithm. In: Power and Energy Society General Meeting—Conversion and Delivery of Electrical Energy in the 21st Century, pp. 1–7. IEEE (2008)
3. Hingorani, N.G.: Role of FACTS in a deregulated market. In: Power Engineering Society Summer Meeting, pp. 1463–1467. IEEE (2000)
4. Wartana, I.M., Agustini, N.P.: Optimal placement of UPFC for maximizing system loadability by Particle Swarm Optimization. Presented at the Proceedings of the 12th International Conference on Quality in Research (QiR 2011), Bali-Indonesia (2011)
5. Shaheen, H.I., Rashed, G.I., Cheng, S.J.: Optimal location and parameters setting of unified power flow controller based on evolutionary optimization techniques. In: IEEE Power Engineering Society General Meeting, pp. 1–8 (2007)
6. Saravanan, M., Slochanal, S.M.R., Venkatesh, P., Abraham, J.P.S.: Application of particle swarm optimization technique for optimal location of FACTS devices considering cost of installation and system loadability. *Electr. Power Syst. Res.* **77**, 276–283 (2007)
7. Milano, F.: An open source power system analysis toolbox. *IEEE Trans. Power Appar. Syst.* **20**, 1199–1206 (2005)

8. Gautam, D., Vittal, V., Harbour, T.: Impact of increased penetration of DFIG-based wind turbine generators on transient and small signal stability of power systems. *IEEE Trans. Power Syst.* **24**, 1426–1434 (2009)
9. Lopes, J.A.P., Hatziargyriou, N., Mutale, J., Djapic, P., Jenkins, N.: Integrating distributed generation into electric power systems: a review of drivers, challenges and opportunities. *Electr. Power Syst. Res.* **77**, 1189–1203 (2007)
10. Hingorani, N., Gyugyi, L.: *Concepts and Technology of Flexible AC Transmission Systems*. IEEE, New York (1999)
11. Povh, D.: Modeling of FACTS in power system studies. In: *Power Engineering Society Winter Meeting*, vol. 2, pp. 1435–1439. IEEE (2000)
12. Milano, F.: an open source power system analysis toolbox. *IEEE Trans. Power Syst.* **20**, 1199–1206 (2005)
13. Quoc, H.D., Mithulananthan, N.: Multiple distributed generator placement in primary distribution networks for loss reduction. *IEEE Trans. Ind. Electr.* **60**, 1700–1708 (2013)
14. Musirin, I., Rahman, T.K.A.: Novel fast voltage stability index (FVSI) for voltage stability analysis in power transmission system. In: *Student Conference on Research and Development, SCORed*, pp. 265–268 (2002)
15. Suganyadevia, M.V., Babulal, C.K.: Estimating of loadability margin of a power system by comparing voltage stability indices. In: *2009 International Conference on Control, Automation, Communication and Energy Conservation, INCACEC*, pp. 1–4 (2009)
16. Kennedy, J., Eberhart, R.: Particle swarm optimization. In: *IEEE Proceedings of International Conference on Neural Networks*, Perth, WA, Australia, vol. 4, pp. 1942–1948 (1995)
17. Birge, B.: PSO—a particle swarm optimization toolbox for use with Matlab. In: *Proceedings of the 2003 IEEE, Swarm Intelligence Symposium SIS 2003*, pp. 182–186 (2003)

# Chapter 25

## Solar Simulator Using Halogen Lamp for PV Research

Aryuanto Soetedjo, Yusuf Ismail Nakhoda, Abraham Lomi and Teguh Adi Suryanto

**Abstract** This paper presents the development of solar simulator using the halogen lamp for PV research. The proposed simulator simulates both the irradiation level and the movement of the sun. The sun irradiation was simulated by varying the brightness of halogen lamp using a lamp dimmer controlled by the microcontroller. While the sun's movement was simulated by rotating the lamp on a frame actuated by a DC motor. A computer was employed to control the simulator in the manual mode where the user could input the desired position and irradiation level of the sun, or in the automatic mode where the desired position and irradiation level were calculated automatically based on the predefined data. The experimental results show that the proposed simulator works appropriately in simulating the sun's movement while varying the irradiation level. The average error of irradiation measurement between the sun and the solar simulator was 7.196 %.

**Keywords** Halogen lamp · Irradiation level · Solar simulator · PV

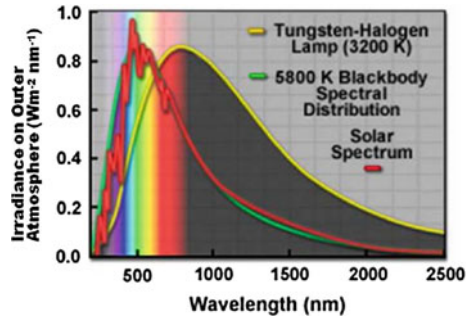
### 25.1 Introduction

Nowadays, the renewable energy resources, such as the PV system is widely used. The research and development of the PV system increase significantly. Naturally, the experiments on PV system require the sun light. Therefore, to provide the flexibility of testing and validating the PV system, the solar simulator was utilized [1–6]. The solar simulator uses the different kind of light sources such as carbon arc lamp, metal oxide arc lamp, quartz halogen lamp, xenon arc lamp, mercury xenon lamp, argon arc lamp, and LED (Light Emitting Diode) to simulate the solar lighting [6]. The halogen lamp is widely used due to inexpensive and the excellent

---

A. Soetedjo (✉) · Y.I. Nakhoda · A. Lomi · T.A. Suryanto  
Department of Electrical Engineering, ITN Malang, Malan, Indonesia  
e-mail: aryuanto@gmail.com

**Fig. 25.1** Halogen lamp spectrum distribution [4]



light output [4]. However it radiates the weak output in the blue and ultraviolet spectrum and strong output in infrared spectrum as illustrated in Fig. 25.1.

A simple solar simulator using the halogen lamp was developed in [5]. The developed solar simulator was used to measure the I-V characteristic of the PV module. In the experiments they changed the distance between the lamp and the PV module to vary the irradiation level. The irradiation level of 1 Sun ( $1000 \text{ Watt/m}^2$ ) was achieved when the distance is 80 cm with the 4000 W halogen lamp.

The LED based solar simulator was developed in [2]. The objective of their research is to match the spectrum of solar simulator according to the ASTM E927-05 Standard Specification for Solar Simulation for Terrestrial Photovoltaic Testing. They used five types of high power LEDs having the wavelengths of 470, 505, 530 and 655 nm, and white color. The spectral matching was carried out by controlling the intensity of LEDs using the PWM signal controlled by a microcontroller.

The combination of halogen lamp and LED for solar simulator was proposed in [1, 3]. The advantages of LED are the high efficiency and low cost. But for NIR (Near Infra Red) spectrum, the emission band is narrow and very expensive. Therefore, they used the halogen lamp to replace the LED in the NIR spectrum.

In this paper, we propose a simple solar simulator using the halogen lamp. Our proposed solar simulator has two main contributions, i.e.: (a) It provides the varying irradiation by changing the lamp intensity; (b) It simulates the movement angle of the sun from rising time in the morning until sunset time in the afternoon. The computer software is utilized to operate such system in the automatic mode and manual mode.

The rest of paper is organized as follows. Section 25.2 presents the proposed system. Section 25.3 presents the experimental results. Conclusion is covered in Sect. 25.4.

## 25.2 Proposed System

The block diagram of proposed system is illustrated in Fig. 25.2. It consists of a computer, a microcontroller unit, a servo motor, a dimmer unit, a DC motor, a halogen lamp, and the mechanical parts. The computer is used by the user to control

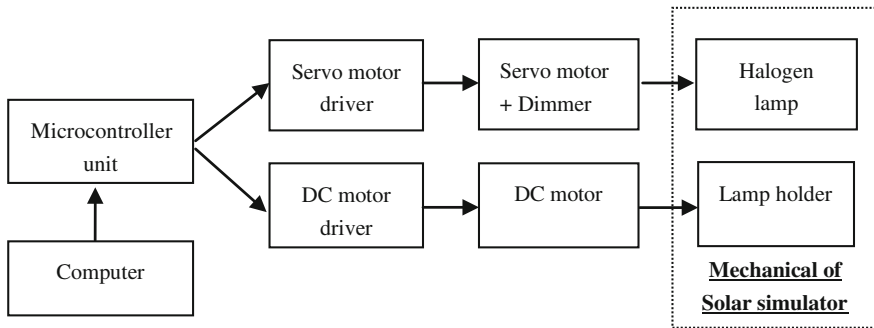


**Fig. 25.2** Block diagram of solar simulator

the solar simulator. The microcontroller unit is employed for interfacing between the computer and the motors. It receives the command for rotating the DC motor and servo motor from the computer. The DC motor is used to rotate the lamp frame for simulating the sun rotation. The motor is equipped with the gear reduction and is driven by the driver that provides the high current.

The dimmer unit is a device used to control the light intensity of the lamp. Commercially, the dimmer is equipped with a potentiometer for adjusting the lamp intensity. In the research, we adopt the existing dimmer by modifying it with a servo motor coupled with the potentiometer. Using this arrangement, the rotation of potentiometer could be controlled by the microcontroller.

The halogen lamp is installed on a rotating frame that moves  $180^{\circ}$  from the left to right, vice versa. The rotating frame is installed above the base where the PV module is placed. Using this construction, we could simulate the movement of sun rising and sunset by moving the rotating frame controlled with the DC motor.

In the research, the solar simulator is designed to simulate the sun rotation from 07:00 until 17:00. In this experiment, the start position of halogen lamp is set to  $15^{\circ}$ , and the final position is set to  $165^{\circ}$ . Therefore the position of  $90^{\circ}$  is achieved when the lamp is located in the above middle of the PV module. This position represents the position of the sun at noon (12:00).

The computer software is designed to control both the lamp position and brightness. Two modes are available, i.e. manual mode and automatic mode. In the manual mode, the user enters the lamp position and the required irradiation level. In the automatic mode, the system will run automatically by reading the predefined values of lamp position and the corresponding irradiation level.

### 25.3 Experimental Results

The hardware of proposed solar simulator is illustrated in Fig. 25.3. Several experiments are conducted to validate the proposed system. In the first experiment, the relationship between the potentiometer position (i.e. the servo position) and the



**Fig. 25.3** Hardware of solar simulator



brightness level represents the irradiation level is observed. To measure the irradiation level, the Solar Power Meter (Tenmars TM-206) is employed. The measurement result is given in Table 25.1 and Fig. 25.4. From the figure, it is clearly shown that the relationship is almost linear. Thus the irradiance level for a certain value could be determined easily based on the position of servo motor.

From the table, the relationship between servo position and irradiation level could be expressed using the following equation

$$y = 8.204x - 334.6 \tag{25.1}$$

where,  $y$  is the irradiation level in  $\text{Watt/m}^2$  and  $x$  is the servo position in degree.

In the second experiment, we compare the irradiation level of the sun and the solar simulator. At first, the sun irradiation level is measured from 07:00 until 17:00 with 15 min interval. This measurement is conducted during the sunny day. The measurement result is listed in Table 25.2. Then the solar simulator is run in the

**Table 25.1** Relationship between servo position and irradiation level

Servo position (degree)	Irradiation level ( $\text{Watt/m}^2$ )	Servo position (degree)	Irradiation level ( $\text{Watt/m}^2$ )	Servo position (degree)	Irradiation level ( $\text{Watt/m}^2$ )
45	60	90	340	135	812
50	92	95	442	140	804
55	120	100	490	145	885
60	155	105	502	150	875
65	200	110	563	155	940
70	245	115	625	160	973
75	282	120	646	165	1005
80	315	125	713	–	–
85	335	130	750	–	–

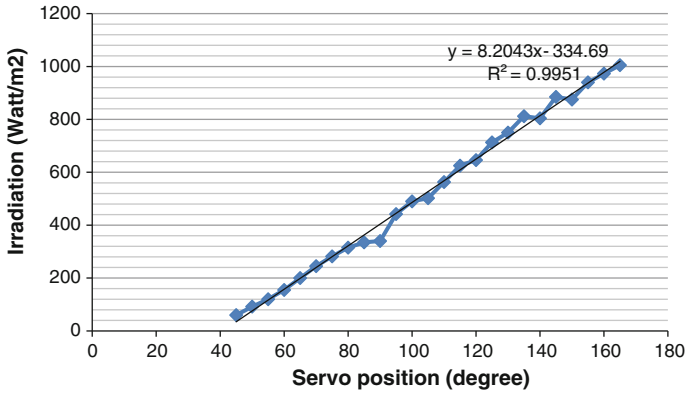
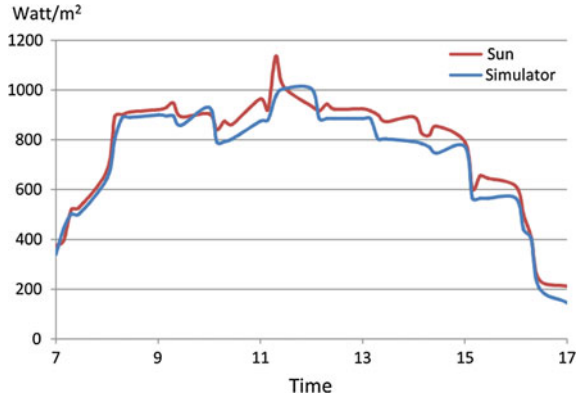


Fig. 25.4 Linearity between servo position and irradiation level

Table 25.2 Measurement of irradiation level of the sun and solar simulator

Time	Lamp position (degree)	Irradiation level (Watt/m2)		Time	Lamp position (degree)	Irradiation level (Watt/m2)	
		Sun	Solar simulator			Sun	Solar simulator
7:00	15	375	340	12:00	90	935	1005
7:15	18.75	395	442	12:15	93.75	917	885
7:30	22.5	519	502	12:30	97.5	943	885
7:45	26.25	527	502	12:45	101.25	922	885
8:00	30	678	646	13:00	105	924	885
8:15	33.75	893	804	13:15	108.75	917	885
8:30	37.5	901	890	13:30	112.5	899	804
8:45	41.25	911	890	13:45	116.25	873	804
9:00	45	921	900	14:00	120	892	792
9:15	48.75	929	896	14:15	123.75	827	785
9:30	52.5	947	896	14:30	127.5	818	771
9:45	56.25	893	858	14:45	131.25	854	746
10:00	60	904	930	15:00	135	790	772
10:15	63.75	841	791	15:15	138.75	603	565
10:30	67.5	874	793	15:30	142.5	655	565
10:45	71.25	862	804	15:45	146.25	645	565
11:00	75	964	875	16:00	150	613	565
11:15	78.75	923	880	16:15	153.75	498	440
11:30	82.5	1134	973	16:30	157.5	404	400
11:45	86.25	1016	1005	16:45	161.25	238	205
12:00	90	935	1005	17:00	165	212	145

**Fig. 25.5** Comparison of Sun irradiation versus solar simulator irradiation



automatic mode. Thus it will rotate and vary the brightness of halogen lamp automatically. During this movement, the irradiation level of the simulator is measured and listed in Table 25.2.

Figure 25.5 illustrates the measurement results of the irradiation level of the sun and the solar simulator. From the figure, it is obtained that the result of the solar simulator is almost the same with the sun. The error between the real measurement of the sun irradiation and the solar simulator is calculated as

$$\frac{|Lamp\ irradiation - Sun\ irradiation|}{Sun\ irradiation} \times 100\% \tag{25.2}$$

From the table, the average error for the data given in Table 25.2 is obtained as 7.196 %.

Two important results are achieved by our proposed system. The first is a method to change the lamp intensity by utilizing the the simple lamp dimmer coupled with the servo motor. This simple arrangement offers the linear relationship between the servo position and the irradiation level produced by the halogen lamp. The second is the capability of the proposed system to simulate the irradiation level generated by the sun during the sunny day. It is validated by the experiment that the proposed solar simulator is able to move while varying the lamp intensity closely to the real sun.

### 25.4 Conclusion

The simple and low cost solar simulator is developed. The main objective of the proposed simulator is to simulate the sun irradiation and the sun movement. The solar simulator could be used to examine and test the research on PV system. The irradiation of solar simulator could be controlled using the computer and almost the same as the real measurement of the real sun irradiation.

In future, the simulator will be extended in the size which is used by the larger PV module. Further the software simulation will be improved and integrated with the PV system.

## References

1. Grandi, G., Ienina, A., Bardhi, M.: Effective low-cost hybrid LED-halogen solar simulator. *IEEE Trans. Ind. Appl.* **50**(5), 3055–3064 (2014)
2. Mohan, A., Pavithran, J., Osten, K.L., Jinumon, A., Mrinalinim C.P.: LED based solar simulator. Student Application Papers Applying Industry Standards approved by IEEE Standards Education Committee (2014)
3. Namin, A., Jivacate, C., Chenvidhya, D., Kirtikara, K., Thongpron, J.: Construction of tungsten halogen, pulsed LED, and combined tungsten halogen-LED solar simulators for solar cell—characterization and electrical parameters determination. *Int. J. Photoenergy*, **2012**, 1–9 (2012)
4. Shatat, M., Riffat, S., Agyenim, F.: Experimental testing method for solar light simulator with an attached evacuated solar collector. *Int. J. Energy Environ.* **4**(2), 219–230 (2013)
5. Sidopekso, S., Nasbey, H., Wibowo, H.: I-V measurement using simple sun simulator. *Elite Elektro Sci. J.* **2**(2), 79–82 (2011). Indonesian language
6. Wang, W., Laumert, B.: Simulate a ‘Sun’ for Solar Research: A Literature Review of Solar Simulator Technology. Internal report, Royal Institute of Technology, Stockholm (2014)

# Chapter 26

## Artificial Bee Colony Algorithm for Optimal Power Flow on Transient Stability of Java-Bali 500 KV

Irrine Budi Sulistiawati and M. Ibrahim Ashari

**Abstract** Power flow optimization is a growing issue today. The system does not grow or develop, in contrast to the electricity power demand from consumers. Therefore, smart efforts have to be done to overcome this increasing electricity power demand. Power flow optimization is one of the efforts that can be done to optimize the current system. The use of Artificial Bee Colony algorithm can give an optimal result without being disturbed by mathematical problems that need much computation time. From the simulation result on Java-Bali 500 kV System, an optimal result has been achieved, in which this method can reduce system power losses from active power losses of 297.607 MVA and reactive power losses of 2926.825 MVAR to become 71.292 MVA and 530.241 MVAR, respectively.

**Keywords** Artificial bee colony · Optimal power flow · Transient stability

### 26.1 Introduction

Electricity power system cannot be separated from the effort to optimize its operation, which means that the control variable has to be arranged to produce a system operation that is safe and cheap. To gain this desired system operation process, Optimal Power Flow (OPF), a method that uses mathematical calculation to gain a cheap fuel cost result, is often used as the prescribed limit. According to [1–5], Non Linear Programming and Linear Programming are widely used to solve several problems in the optimal power flow.

Like another conventional method, this method is considered a classic method due to its limitation in solving mathematic equations that represent dynamic system characteristics; that is, an optimization problem in a transient condition.

---

I.B. Sulistiawati (✉) · M.I. Ashari  
Department of Electrical Engineering, National Institute of Technology (ITN) Malang,  
Raya Karanglo Km. 2, Malang, Indonesia  
e-mail: irrine\_budi@yahoo.com

If we observe the operation condition in field, system operations of electricity power all this time are operated at a condition far from their safety limit. Systems operate at a maximum operating condition, because the increasing electricity energy demand is not followed by the addition of new power plants for the reasons of cost efficiency; thus, the systems are always fully operational. This condition certainly makes the system operation prone to collapse if there is a small interference or change in the system. Based on this condition, a preventive action has to be done for planning and operating electricity power system. This is accomplished by performing system optimization while observing the system transient condition.

However, transient stability analysis cannot be separated from the use of mathematic equations with their non-linear patterns that need time and accuracy to get the results. This is the challenge because those are differential equations that describe dynamic behavior of the system [1–5].

Past research [6, 7] involved sensitivity in rescheduling to obtain solution in power plant cost, while other research with discretization scheme [8] converted differential equations to algebra equations as inequality constraints produce low accuracy solution.

In some advanced research [9, 10], since the system being used was increasingly big and the variables were increasingly complex, the calculation convergence would be a problem by itself. The use of a method with transformation technique [11] can change an infinite-dimensional problem of Transient Stability Control Optimal Power Flow (TSCOPF) to become a finite-dimensional programming problem. Yet, like the other classical optimization methods, this method has a weakness, that is, it experiences convergence at local optima, thus transient stability limit is not included in the constraints of optimization problem. A solution to address those problems is to use Artificial Intelligence to solve the transient stability calculation problem [1–3]. The use of AI eases the burden to solve the Transient Stability Control Optimal Power Flow (TSCOPF) problem and can find global optimum or good solution without being restricted by the model employed. Several applications that use AI like Genetic Algorithm (GA), Particle Swarm Optimization (PSO), and Differential Evolution (DE) can give satisfied results in TSCOPF problem.

Research in this paper tries to propose a solution for the Transient Stability Control Optimal Power Flow (TSCOPF) problem using a modern heuristic optimization technique—i.e., Artificial Bee Colony Algorithm (ABC), which is an algorithm that simulates the behavior of honey bee—for solving the problem of electricity power system optimization.

## 26.2 Methodology

### 26.2.1 Transient Stability Control Optimal Power Flow Formula

Transient Stability Control Optimal Power Flow (TSCOPF) problems basically are formulated from system fuel cost, that is expressed as a quadratic equation function:

$$f_i = a_i + b_i P_{Gi} + c_i P_{Gi}^2 \quad (26.1)$$

where  $a_i$ ,  $b_i$ , are  $c_i$  are the cost coefficients from each power plant unit.

By incorporating various constraints, like fuel losses due to valve opening process at turbine and generator effect due to valve point effect, the objective function becomes non linear, non convex with several minima. So, the equation becomes:

$$\begin{aligned} F = & \sum_{i=1}^N (a_i + b_i P_{Gi} + c_i P_{Gi}^2) + K_p (P_{G1} - P_{G1}^{\text{lim}})^2 \\ & + K_v \sum_{i=1}^{NL} (V_i - V_i^{\text{lim}})^2 + K_q \sum_{i=1}^N (Q_{Gi} - Q_{Gi}^{\text{lim}})^2 \\ & + K_s \sum_{i=1}^{nl} abs(S_i - S_i^{\text{lim}})^2 + K_l \sum_{j=1}^{NL} (L_j - L_j^{\text{lim}})^2 \end{aligned} \quad (26.2)$$

where  $K_p$ ,  $K_v$ ,  $K_q$ ,  $K_s$ , and  $K_l$  are penalty factors, NL is the number of load buses, nl is the number of transmissions and  $x^{\text{lim}}$  is the margin limit. Incorporating valve point loading effect to power plant cost curve, the equation becomes [1]

$$f_i = a_i + b_i P_{Gi} + c_i P_{Gi}^2 + |d_i \sin(e_i (P_{Gi}^{\text{lim}} - P_{Gi}))| \quad (26.3)$$

Combining the objective function and the constraints, the complete equation becomes:

$$\begin{aligned} F = & \sum_{i=1}^N (a_i + b_i P_{Gi} + c_i P_{Gi}^2 + |d_i \sin(e_i (P_{Gi}^{\text{lim}} - P_{Gi}))|) + K_p (P_{G1} - P_{G1}^{\text{lim}})^2 + K_v \sum_{i=1}^{NL} (V_i - V_i^{\text{lim}})^2 \\ & + K_q \sum_{i=1}^N (Q_{Gi} - Q_{Gi}^{\text{lim}})^2 + K_s \sum_{i=1}^{nl} abs(S_i - S_i^{\text{lim}})^2 + K_l \sum_{j=1}^{NL} (L_j - L_j^{\text{lim}})^2 \end{aligned} \quad (26.4)$$

where  $a_i$ ,  $b_i$ ,  $c_i$ , and  $e_i$  are cost coefficient from each power plant unit,  $K_p$ ,  $K_v$ ,  $K_q$ ,  $K_s$ , and  $K_l$  are penalty factors, NL represents the number of load buses, nl and  $x^{\text{lim}}$  are

respectively the number of transmissions and the margin limit. So, the non linear equations of power flow are:

$$\begin{aligned} P_{Gi} - P_{Di} - V_i \sum_{j=1}^N V_j (G_{ij} \cos \alpha_{ij} + B_{ij} \sin \alpha_{ij}) &= 0 \\ Q_{Gi} - Q_{Di} - V_i \sum_{j=1}^N V_j (G_{ij} \sin \alpha_{ij} - B_{ij} \cos \alpha_{ij}) &= 0 \end{aligned} \quad (26.5)$$

where N is the total number of buses,  $P_{Gi}$  and  $Q_{Gi}$  are active and reactive power of ith power plant bus,  $P_{Di}$  and  $Q_{Di}$  are active power for ith load bus,  $V_i$  is the magnitude of voltage bus,  $\alpha_{ij}$  is the voltage angle difference between ith bus and jth bus,  $G_{ij}$  and  $B_{ij}$  are the transfer conductance and susceptance between ith bus and jth bus.

### 26.2.2 Transient Stability

In transient condition, the power system generator is described with equation:

$$\begin{aligned} M_i \frac{d^2 \delta_i}{dt^2} &= P_{mi} - P_{ei} \\ \dot{\delta}_i &= \omega_i \end{aligned} \quad (26.6)$$

where  $\delta_i$  and  $\omega_i$  are rotor angle and velocity angle of ith generator,  $P_{mi}$  and  $P_{ei}$  are mechanic power input and electricity power output from ith generator, and  $M_i$  is inertia moment from ith generator.

*Center of inertia* (COI) of the electricity power system can be represented by linear combination of every generator's rotor angles such as follows:

$$\delta_{COI} = \frac{1}{M_T} \sum_{i=1}^{N_G} M_i \delta_i \quad (26.7)$$

where  $M_T = \sum_{i=1}^{N_G} M_i$  is the center of inertia. Rotor angle and velocity in COI frame are shown by Eqs. (26.8) and (26.9).

$$\theta_i = \delta_i - \delta_{COI} \quad (26.8)$$

$$\dot{\theta}_i = \tilde{\omega}_i \quad (26.9)$$



Therefore, the equations in COI frame become:

$$M_i \dot{\tilde{\omega}}_i = P_{mi} - P_{ei} - \frac{M_i}{M_T} P_{COI} \equiv PAC_i \quad (26.10)$$

$$P_{COI} = \sum_{i=1}^{N_G} (P_{mi} - P_{ei}) \quad (26.11)$$

where  $PAC_i$  is accelerating power from  $i$ th generator.

Transient Energy Function (TEF) from the model of electricity power system above is defined as follows:

$$TEF = KE + PE \quad (26.12)$$

$$KE = \frac{1}{2} \sum_{i=1}^{N_G} M_i \tilde{\omega}_i^2 \quad (26.13)$$

$$PE = - \sum_{i=1}^{N_G} \int_{\theta_i^{SEP}}^{\theta_i} PAC_i^P d\theta_i \quad (26.14)$$

where KE is kinetic energy, PE is potential energy,  $\theta_i^{SEP}$  is rotor angle of the post-fault system at the stable equilibrium point, and  $PAC_i^P$  is accelerating power of the post-fault system.

### 26.2.3 Artificial Bee Colony Algorithm (ABC)

Artificial Bee Colony is an algorithm that adopts the behavior of bee colony in search of food. When bees are searching for food, they divide their duty in three groups, which are labor, onlooker, and scout bees. The food searching process is started with bees gathering in a hall called dance area, where they make a decision to determine food sources that they have known before. The decision maker are bees group called onlooker bees. Meanwhile, labor bees are bees group that will visit those food sources. Bees that have to find food sources randomly are called scout bees.

Based on [12], to solve the problem, the control variable can be expressed as

$$u^T = [P_{g2}, \dots, P_{gN2}, V_{g1}, \dots, V_{gN2}] \quad (26.15)$$

This equation does not consider slack bus. To measure the quality of the artificial bee colony algorithm, the calculation of fitness  $F_i$  can be expressed as:

$$F_i = 1/(f_i + K_v F_{vi} + K_q F_{qi} + K_{ps} F_{ps}) \quad (26.16)$$

where  $f_i$  is the generating fuel cost, while  $F_{vi}$  and  $F_{qi}$  are the sums of normalized PQ bus voltage and reactive power from output generator  $i$ , respectively.

### 26.3 Implementation

To see the effectiveness of the proposed method, a test was performed at Java Bali 500 kV system, as shown in Fig. 26.1. The electricity system of Java Bali 500 kV consists of 8 generators and 25 buses that are interconnected together. Some power plants are water power plant, but most of them are steam power plant. Their specifications can be seen in Table 26.1.

The generators are Suralaya, Muaratawar, Cirata, Saguling, Tanjungjati, Gresik, Paiton, and Grati. Among these eight plants, power plants Saguling and Cirata are water power plants, while others are steam power plants. In this study, Suralaya power plant acted as a slack generator.

The load data were obtained from PT PLN (Persero). The kV base is 500 kV, MVA base is 1000 MVA, and the system frequency is 50 Hz. Generator data used are shown in Table 26.1.

Simulation was run on the system for as many as 50 cycles to achieve the best result. From the test that had been performed, that number of cycles could give us the desired result. The number of bees in the colony that was employed is 50.

### 26.4 Result and Analysis

From the performed simulation, the initial result was obtained, and it can be seen in Table 26.2. In the table, losses at every bus can be seen. The total losses of the system are 297.607 MVA for active power and 2926.825 MVAR for reactive power.

The next step is to perform load flow optimization using the method that had been proposed, which is the artificial bee colony algorithm. From the performed simulation, the obtained results are as follows (Table 26.3):

To further determine the effectivity of the proposed method, calculation simulation was performed as many as 125 times to validate its reliability and accuracy. Figure 26.2 depicts the results for as many as 125 iteration. Figure 26.2 shows the total losses of the system. It can be seen that the proposed method gives the same losses values at various iteration and this means that statistically the proposed method can prove its reliability.

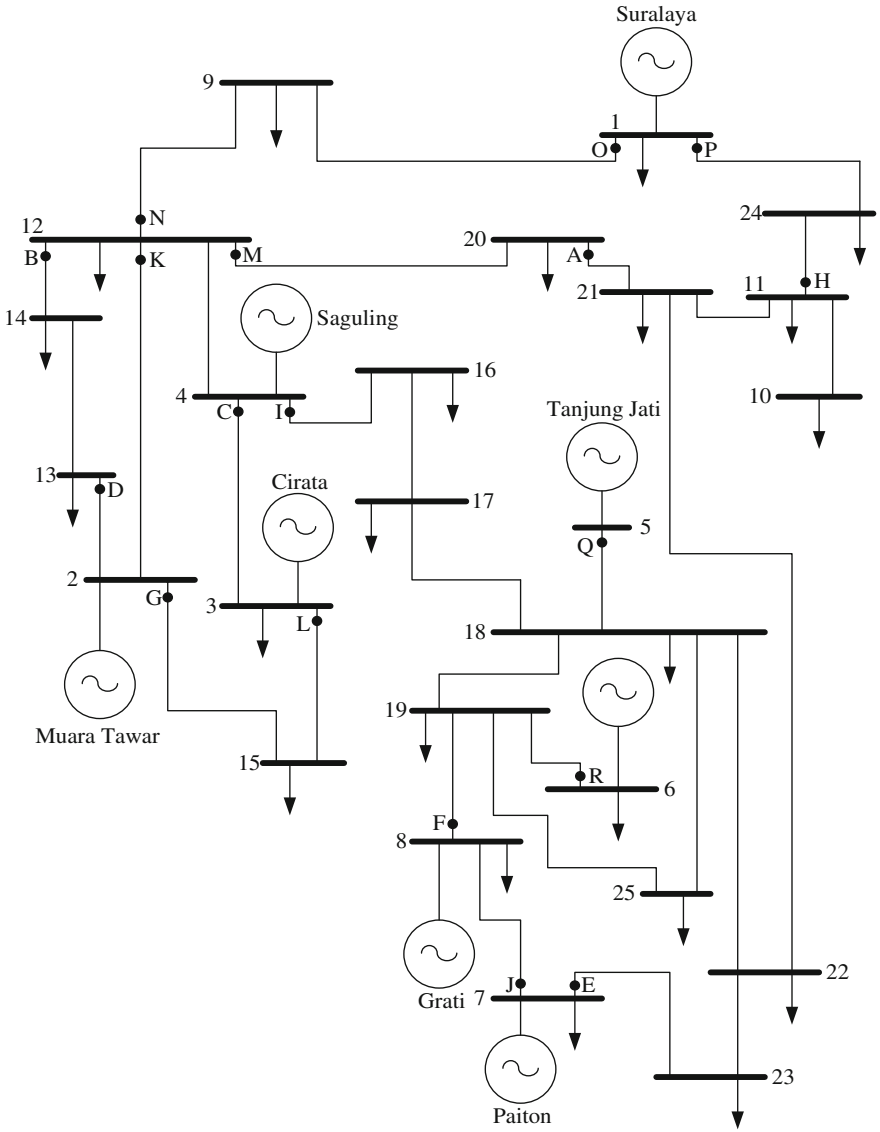


Fig. 26.1 Java Bali 500 kV system

**Table 26.1** Generator data

Generator Number	Generator Name	Xd' (pu)	H	Generator Number	Generator Name	Xd' (pu)	H
1	Suralaya	0.297	5.19	5	Tanjung Jati	0.258	3.2
2	Muaratawar	0.297	1.82	6	Gresik	0.297	2.54
3	Cirata	0.274	2.86	7	Paiton	0.297	4.42
4	Saguling	0.302	1.64	8	Grati	0.297	3.5

**Table 26.2** Initial condition

No bus	Voltage	Losses		No bus	Voltage	Losses	
		P	Q			P	Q
10	0.980	0.003	0.033	15	1.000	5.075	49.663
11	0.970	0.510	5.705	16	0.963	0.818	27.875
12	0.948	0.053	11.623	17	0.970	0.228	2.193
13	0.911	1.928	4.987	18	0.960	0.080	0.772
14	0.907	2.086	5.975	19	0.875	0.342	24.145

**Table 26.3** Final condition

No bus	Voltage	Losses		No bus	Voltage	Losses	
		P	Q			P	Q
10	0.980	0.003	0.033	15	1.000	5.075	49.663
11	0.980	0.51	5.705	16	0.971	3.223	27.875
12	0.973	1.928	4.987	17	0.970	0.228	2.193
13	0.970	1.928	4.987	18	0.974	0.08	0.772
14	0.977	2.086	5.975	19	0.950	0.343	24.145

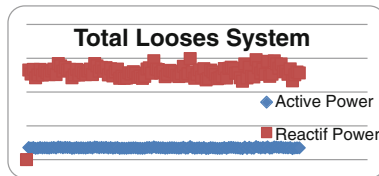


**Fig. 26.2** Total looses system

## 26.5 Conclusion

From evaluating the proposed method, it can be concluded that the proposed ant bee colony algorithm can give satisfied results for reducing losses, particularly for optimizing the system's power flow. The proposed method can statistically be proven to be capable, reliable, and accurate.

**Acknowledgements** The authors are very grateful to the Department of Electrical Engineering, National Institute of Technology (ITN) Malang Indonesia, to all facilities provided during this research. The authors would like to thank Indonesian Directorate of Higher Education for the research Grant No. DIPA-023.04.1.672453/2015, revision 01, dated March 03, 2015.

## References

1. Cai, H.R., Chung, D.Y., Wong, K.P: Application of differential evolution algorithm transient stability constrained optimal power flow. *IEEE Trans. Power Sys.* **23**, 719–728 (2008)
2. Vaisakh, K., Srinivas, L.R., Meah, K.: Genetic evolving ant direction particle swarm optimization algorithm for optimal power flow with non-smooth cost function and statistical analysis. *Appl. Soft Comput.* **13**(12), 4579–4593 (2013)
3. Xia, S.W., Zhou, B., Chan, K.W., Guo, Z.Z.: An improved GSO method for discontinuous non-convex transient stability constrained optimal power flow with complex system model. *Electr. Power Energy Syst.* **64**, 483–492 (2015)
4. Momoh, J.A., El-Hawary, M.E., Adapa, R.: A review of selected optimal powerflow literature to 1993. I. Nonlinear and quadratic programming approaches, *IEEE Trans. Power Syst.* **14**(1), 96–104 (1999)
5. Momoh, J.A., El-Hawary, M.E., Adapa, R.: A review of selected optimal powerflow literature to 1993. II. Newton, linear programming and interior point methods. *IEEE Trans. Power Syst.* **14**(1), 105–111 (1999)
6. Nguyen, T., Pai, M.A.: Dynamic security-constrained rescheduling of power systems using trajectory sensitivities. *IEEE Trans. Power Syst.* **18**(2), 848–854 (2003)
7. Shubhanga, K.N., Kulkarni, A.M.: Stability-constrained generation rescheduling using energy margin sensitivities. *IEEE Trans. Power Syst.* **19**(3), 1402–1413 (2004)
8. Gan, D., Thomas, R.J., Zimmerman, R.D.: Stability-constrained optimal power-flow. *IEEE Trans. Power Syst.* **15** (2), 535–540 (2000)
9. Yuan, Y., Kubkawa, J., Sasaki, H.: A solution of optimal power flow with multicontingency transient stability constraints. *IEEE Trans. Power Syst.* **18** (3), 1094–1102 (2003)
10. Layden, D., Jeyasurya, B.: Integrating security constraints in optimal power flow studies. In: *Proceedings of IEEE Power Engineering Society. General Meeting*, vol. 1 (2004)
11. Chen, L., Tada, Y., Okamoto, H., Tanabe, R., Ono, A.: Optimal operation solutions of power systems with transient stability constraints. *IEEE Trans. Circuits Syst. I* **48**(3), 327–339 (2001)
12. Sayah, S., Zehar, K.: Modified differential evolution algorithm for optimal power flow with non-smooth cost functions. *Energy Convers. Manage.* **49**, 3036–3042 (2008)

# Chapter 27

## Sizing and Costs Implications of Long-Term Electricity Planning: A Case of Kupang City, Indonesia

Daniel Rohi and Yusak Tanoto

**Abstract** This paper presents long-term electricity supply-demand scenarios for Kupang City, Indonesia. The objective of the analysis is to reveal the alternatives sizing of power plants along with the power generation costs that is potentially incurred during the study period. The study is conducted using bottom-up energy model. Electricity energy in terms of supply-demand variation is taking into account both fossil fueled and renewable energy potential in the supply side, and the scheme of high as well as average electricity growth rate in the demand side. Four variations of supply-demand conditions is presented as the study result. The results has shown total energy supplied which is required in order to satisfy the usual demand growth and the total saving potential under the demand scheme. The variation in terms of costs also shown depending upon the renewable energy penetration. The study is expected to contribute towards the utilization of more renewable energy potential, particularly the possible implementation of Photovoltaic plants and the campaign of energy efficiency and conservation within the observed area.

**Keywords** Kupang City · Renewable energy · Sizing · Generation costs

### 27.1 Introduction

Energy system model, particularly in the area of electricity supply-demand can be constructed using several approaches. As part of the energy system model, the long-term electricity planning is dealing with some scenarios of supply and demand which reflect potential utilization of supply as well as demand management in a certain economy boundary, such as in a nation wide or within smaller boundary. Commonly, two approaches are used to deal with the problem of constructing appropriate model, i.e. the top-down method and the bottom-up method. The first

---

D. Rohi (✉) · Y. Tanoto

Electrical Engineering Department, Petra Christian University, Surabaya, Indonesia  
e-mail: rohi@petra.ac.id

© Springer Science+Business Media Singapore 2016

F. Pasila et al. (eds.), *Proceedings of Second International Conference  
on Electrical Systems, Technology and Information 2015 (ICESTI 2015)*,

Lecture Notes in Electrical Engineering 365, DOI 10.1007/978-981-287-988-2\_27

257

method uses aggregated economic data and suffers many drawbacks when applied in the area of energy planning. In addition, it is not well suited for examining technology-specific policies. Types of top-down approaches include macroeconomic assessment, input-output method, and general equilibrium method [1]. The second approach comprises three broad methods to matching with the study objectives. The accounting frameworks based model is a type of method used in the bottom-up energy model. One advantage of the bottom-up model over the previous one is the ability to capture interactions among projects and policies, as the analysis is assessing costs, resources allocation, and benefits of the projects. One example of accounting framework based model is the long-term forecast of Taiwan's energy supply and demand [2]. Another bottom-up approach is the utilization of either linear programming model or goal programming model for solving decentralized energy planning [2].

This paper uses the accounting framework based model similar in [2], to construct long-term electricity supply-demand model for Kupang City, Indonesia. However, the analysis is focusing in the sizing and essential generation costs implications from the potential electric power mix and aggregated long-term electricity demand of the city. The methodology is described in the next section followed by the simulation results and discussion.

## 27.2 Methodology

Kupang City is the capital of East Nusa Tenggara. Geographically located between 10° 39' South Latitude and 123° 37' East Longitude, the city has 180.27 km<sup>2</sup> land area. Kupang City often been called the rock city due to its dry area and crisis of fresh water that is happened in the dry season. The condition in fact offering other benefit in terms of solar energy potential. The monthly percentage of sunshine in Kupang City is quite good. During April to November, the percentage of sunshine can achieve roughly 79–100 % [3].

Up to now, Kupang City is the only city or regency in East Nusa Tenggara which has 100 % electrification rate. It is reflected from the data of the percentage of fuel used for lighting. Kupang City uses 100 % electricity for household lighting. In 2013, the population of Kupang City was 378,425 people. Aggregately, total number of PLN (state electricity company) customer along with the number of consumption in 2009–2013 is shown in Table 27.1.

**Table 27.1** Number of PLN customer and electricity consumption in Kupang City during 2009–2013 [3]

Year	Number of customer	Electricity consumption (MWh)
2009	55,480	134,594
2010	59,311	156,097
2011	74,040	172,070
2012	79,354	203,471
2013	89,564	253,940

**Table 27.2** Current installed and available capacity of power plant in Kupang Area [4]

Power Plant	Type	Installed (kW)	Available (kW)
Kuanino	Diesel	5,000	2,300
Tenau	Diesel	46,122	11,550
Rental	Diesel	23,000	18,930
Bolok	Coal	33,000	33,000
Gudang	Diesel	1,220	372

The current power generation has been relied on diesel power plants as well as the relatively new coal fired power plant. The installed power capacity as well as the available capacity of both types of plant is presented in Table 27.2, including the rental based plant.

The simulation is conducted using LEAP (Long range Energy Alternatives Planning System), a tool developed by Stockholm Environment Institute (SEI) [5]. The tool is classified as bottom-up method and worked based on the accounting framework. The tool itself has been utilized in many studies, reports, and journal papers [6]. Focusing in the end-use driven scenario-based analysis, the advantages of the tool include flexibility in processing the amount of available data. Despite the data limitation, the tool can be used to evaluate impacts that is potentially occurred due to scenarios selection. The tool is equipped with several modules to enable analysis of energy flow from the supply side into demand side. In the context of the study, data of electricity consumption of Kupang City is aggregated from all customer sectors.

The objective of the study is to match the long-term demand of the city through appropriate generation mix up to 2025 by possibly reducing the role of diesel power plant and increasing the penetration of renewable energy, particularly solar energy, in parallel with the contribution of coal fired power plant as the backbone of the system. By conducting the simulation under several scenarios, the energy mix and the associated costs will be revealed. In this study, two scenarios are taken into account. The first scenario deals with fully non-renewable power plants whereas the second scenario includes Photovoltaic plants. Please be noted, the contribution of diesel power plants in terms of its capacity will be reduced in both scenarios. Meanwhile, the demand side considers high growth rate and average growth rate of electricity consumption over the simulation period. Some important key parameters imposed into the simulation are as follows: the high and average growth rate of electricity consumption are taken 20 and 15 %, respectively, the high and average growth rate of users are taken 15 and 10 %, respectively, the capital cost of coal fired power plant, Photovoltaic, and diesel power plant per MW are USD 1.26 million, USD 2 million, and USD 200 thousand, respectively, the variable operation and maintenance costs per MWh include the fuel cost are USD 8, USD 20, and USD 20, respectively, the plant efficiency are taken 35, 15 and 30 % for coal, Photovoltaic, and diesel, respectively, the starting year of operation is 2013 for coal and diesel plant, and in 2018 onwards for Photovoltaic, the transmission and distribution losses is set 8.6 % in 2013 and interpolated to 6 % in 2025, and the discount rate is taken 5 %.



### 27.3 Results and Discussion

The electricity demand projection up to 2025 is shown in Table 27.3. The projection is based on the high and average growth as indicated in earlier section.

As seen in Table 27.3, the anticipated electricity consumption growth would be in the range of 5–8 times higher compared to 2013. According to the LEAP simulation, existing available power plant capacity would only meet the demand within the Kupang City system up to 2018 and 2019, for the case of average growth and high growth, respectively. Additional supply would be needed up to 865.9 MWh in 2025 for the average growth scenario, and around 1,829 MWh in the same year for the high growth scenario.

To meet both demand scenarios, more capacity of coal fired power plants is required, considering no more additional capacity of diesel power plant. Figure 27.1 shows the graph of required energy supply in the case of high growth demand as well as average growth demand.

Initially in 2013, both power plant types’ share were roughly equal. Nevertheless, in 2025, the share of coal fired power plant would be around 88 % for scenario-1, and around 80.3 % for scenario-2. In this case, the required demand would potentially be meet by increasing the coal fired power plant capacity up to 120,000 MW in 2018 and 245,000 MW in 2025, for the case of high growth. Meanwhile, the capacity should be increased up to 70,000 Mw in 2018 and 135,000 MW in 2022, for the case of average growth.

Additional capacity of coal fired power plants that is required to meet both demand scenarios would slightly lower compared to scenario-1. Table 27.4 shows the required capacity in the case of high growth demand as well as average growth demand, under scenario-2, so that energy import from outside Kupang City system would be unnecessary.

**Table 27.3** Electricity consumption of Kupang City up to 2025 (in MWh)

Scenario	2017	2019	2021	2023	2025
High growth	526.5	758.3	1,091.9	1,572.3	2,264.2
Average growth	444.1	587.4	776.8	1,027.3	1,358.6

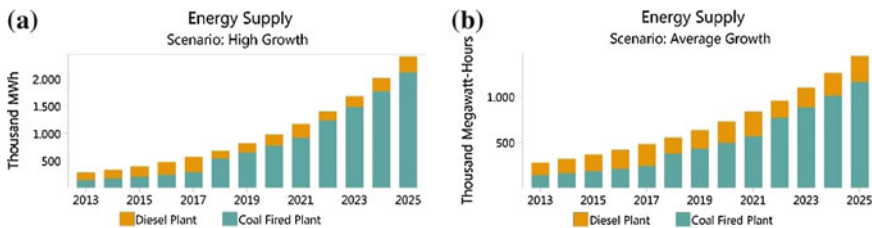


**Fig. 27.1** a Required energy supply for high growth, b required energy supply for average growth

**Table 27.4** Required additional power plant capacity for scenario-2

Demand scenario	Power plant	Sizing (MW)	Year
High growth	Coal fired	33	Existing
		60	2018
		158	2022
	Diesel	33.15	Existing—2025
	PV	10	2018
		15	2022
Average growth	Coal fired	33	Existing
		27	2018
		50	2022
	Diesel	33.15	Existing—2025
	PV	10	2018
		15	2022

The electricity generation costs for scenario-2 is shown in Fig. 27.2. The cost component are capital cost, fuel cost, and operation and maintenance cost over the simulation years. The cost comparison between scenario-1 and scenario-2 is given in Table 27.5.

From Table 27.5, we can see that the implementation of renewable energy resources while reducing the share of diesel power plant capacity would result the competitive generation cost compared to the condition without Photovoltaic. Moreover, the total sizing of coal fired power plant could be significantly reduced

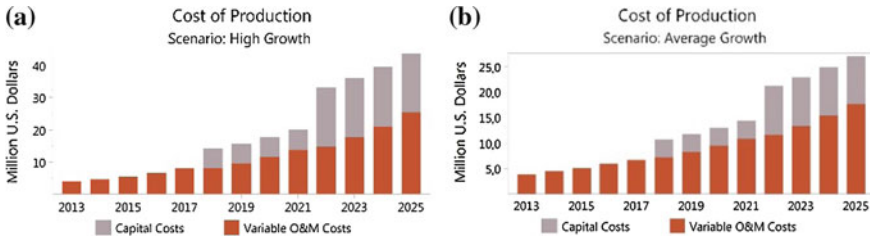


**Fig. 27.2** Electricity generation cost for scenario-2. **a** High demand growth, **b** average demand growth

**Table 27.5** Cost comparison between scenario-1 and scenario-2 (in USD million)

Year	Scenario-1		Scenario-2	
	High demand growth	Average demand growth	High demand growth	Average demand growth
2018	15.7	10.9	14.3	10.7
2021	20.9	14.2	20.1	14.4
2025	43.3	26.6	45.8	27.1

by introducing Photovoltaic plant. In this study, however, the sizing of Photovoltaic plant is used as indication to help find the possible contribution of the renewable energy resources.

## 27.4 Conclusion

This paper presents the study of three possible options. One of feasible option to meet the ever growing electricity demand in Kupang City is by having higher share of coal fired power plants, in addition to the possible implementation of centrally located Photovoltaic plants. To reduce the generation costs originating from non-renewables, no additional capacity of diesel power plants is considered. The study also captures the potential benefit of involving Photovoltaic plant so that the generation cost can be competitive with that achieved by the scenario without energy supplied from renewables.

**Acknowledgements** Authors are grateful for financial support given by the Institute of Research and Community Outreach, Petra Christian University, for conducting this research.

## References

1. Heaps, C.: UNCS2012 (2012). <http://www.uncsd2012.org/content/documents/Heaps-LEAP%20Slides.pdf>
2. Huang, Y., Bor, Y.J., Peng, C.Y.: The long-term forecast of Taiwan's energy supply and demand: LEAP model application. *Energy Policy* **39**(11), 6790–6803 (2011)
3. Hiremath, R.B., Kumar, B., Balachandra, P., Ravindranath, N.H.: Bottom-up approach for decentralised energy planning: case study of Tumkur district in India. *Energy Policy* **38**(2), 862–874 (2010)
4. BPS Kupang: Kupang in Figures. BPS, Kupang, Indonesia (2014)
5. Electricity Center for Kupang. PLN Kupang (2014)
6. Tanoto, Y., Handoyo, E.A.: Renewable energy potential for sustainable long-term electricity energy planning: A bottom-up model application. *Int. J. Renew. Energy Res.* **5**(3), 919–925 (2015)
7. LEAP: <http://www.energycommunity.org/default.asp?action=45>

# Chapter 28

## Dynamic Simulation of Wheel Drive and Suspension System in a Through-the-Road Parallel Hybrid Electric Vehicle

Mohamad Yamin, Cokorda P. Mahandari and Rasyid H. Sudono

**Abstract** In this paper the dynamics of a through-the-road parallel hybrid are presented in term of suspension selection and stability. Characteristics and dynamics of the suspension are investigated using Adams/Car software. Double Wishbone and MacPherson front suspension system and Torsion Bar Coil, Multi Link and Double Wishbone rear suspension are compared and selected based on camber, toe and caster parameter. The dynamic simulation of the front and rear wheel drive system is analyzed and compared. The results show that the Double Wishbone in the front and rear suspension met the criteria of selection. The dynamic of front and rear wheel drive system yields neutral steer and stable in cornering. It can be considered as guidance for converting an internal combustion engine vehicle into a parallel hybrid.

**Keywords** Suspension selection · Dynamic simulation · Parallel hybrid · Adams/car

### 28.1 Introduction

Hybrid Electric Vehicle (HEV) offers improvements over conventional vehicle in terms of fuel efficiency and environmental issue. This is the main reason why hybridization program takes placed. The development of HEV in this paper is based on the electrification from existing conventional vehicle powering by internal combustion engine (ICE). A parallel hybrid architecture, known as through-the-road hybrid is chosen for converting a sedan Toyota Soluna XLi 2003. This configuration enables an existing conventional vehicle driven by an ICE to be

---

M. Yamin (✉) · C.P. Mahandari · R.H. Sudono  
Mechanical Engineering Department, University Gunadarma, Jl. Margonda Raya 100,  
Depok, Jawa Barat, Indonesia 16424  
e-mail: mohay@staff.gunadarma.ac.id

converted into a hybrid electric vehicle within minimal modification, i.e. by replacing the rear axle with the in-wheel-motor (IWM) and powering with a battery bank located in the vehicle's trunk.

The dynamic characteristic of a through-the-road parallel hybrid and the original conventional vehicle must be the same or better. This is important, in order to make sure the behavior of the converted vehicle could be handled when facing any difference or irregularities, especially the two power trains are not directly connected to each other and coupled mainly through road-tire force interaction. Recent studies on this new powertrain configuration has focused on control strategies for torque vectoring [1], the dynamics and the drivability using linearized mathematical models, considering the effect of gear ratio [2], and energy management strategies via dynamic programming [3]. To determine the optimal operation, simulation tests are necessary to investigate the effect of certain parameters for examples the effect of delaying the motor start time, for different rates of vehicle acceleration [4, 5]. In this paper, dynamic simulation of front wheel drive (FWD) and rear wheel drive (RWD) were investigated after selecting the best suspension system. This was done using commercial Adams/Car software, in order to increase performance and driving stability.

## 28.2 Research Methods

This research was conducted following the step as in the flowchart that shown in Fig. 28.1.

Two different type of suspension, i.e. MacPherson and Double Wishbone, on the FWD and three type on RWD, i.e. Torsion Bar Coil, Multi Link and Double Wishbone, were compared and analyzed. Parallel wheel travel simulation for all type of suspension is done by using Adams/Car Test Rig. A drive ratio of 100 % and brake ratio of 70 % are assigned for analysis of bump travel of 100 mm and rebound travel of -100 mm.

The best suspension system is properly selected based on criteria neutral camber and toe at neutral wheel travel, toe in at positive camber with a maximum camber  $2,5^{\circ}$ , toe out at negative camber with a maximum negative camber  $-3,5^{\circ}$ , and have positive caster  $1,5^{\circ}$  up to  $13,5^{\circ}$ . Dynamics simulation of FWD and RWD systems are evaluated on the condition of ISO lane change, acceleration and cornering with the same speed i.e. 60 km/h.

## 28.3 Result and Discussion

Suspension characteristics, i.e. camber, toe and caster of existing MacPherson front suspension is compared to a Double Wishbone, as shown in Table 28.1.

**Fig. 28.1** Flowchart of research methods

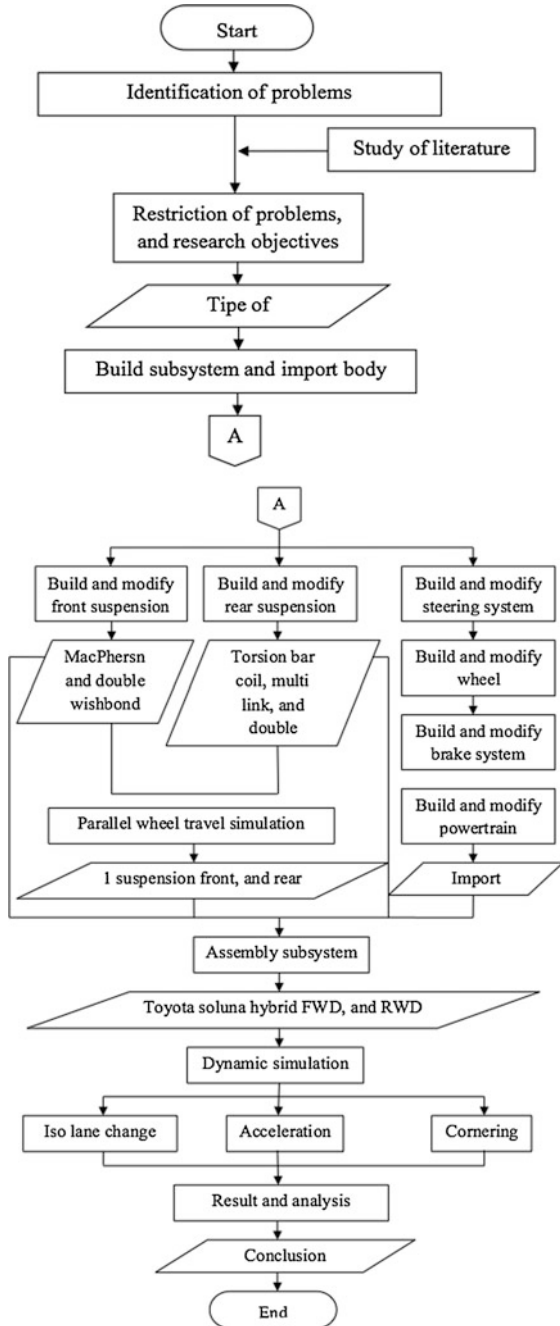


**Table 28.1** Comparison result of front suspension

Macpherson	Bump travel	Rebound travel
Camber angle	100 mm, 0.4861°	-43.6476 mm, 0.8064°
Toe angle	100 mm, -2.2968°	-43.6476 mm, 0.7164°
Caster angle	100 mm, 10.5935°	-43.6476 mm, 6.9387°
Double wishbond	Bump travel	Rebound travel
Camber angle	100 mm, -.6825°	-75.6323 mm, 1.0705°
Toe angle	100 mm, -1.8393°	-75.6323 mm, 3.8377°
Caster angle	100 mm, 5.8646°	-75.6323 mm, 5.5942°

For rear suspension, the existing Torsion Bar Coil is compared to Multi Link and Double Wishbone. The simulation results are presented in Table 28.2.

From above result, the best suspension system for both front and rear suspension system was the Double Wishbone. This type of suspension met the criteria of the analysis on parallel wheel travel simulation for both bump and rebound travel. With this suspension, the dynamic analysis is performed using ISO lane change, acceleration and cornering.

On ISO lane change, longitudinal velocity, roll, pitch, yaw rate and side slip angle were analyzed for both FWD and RWD. Figure 28.2 shows side slip angle response as one of sample of the simulation results. Results of all simulation are compared in Table 28.3.

Table 28.3 illustrated that longitudinal velocity on the FWD slightly higher than on the RWD. This shows that the FWD system is more stable when driving on velocity fluctuation in longitudinal direction compared to the RWD system. The value of roll rate, pitch rate, and yaw rate also showed the same characteristic. This mean that vehicle body oscillation reduced, as delivery of power and steering allows the driving force to act in the same direction as the wheel track. This made the car good in road holding [6]. The maximum side slip angle in this simulation

**Table 28.2** Comparison result of parallel wheel travel rear suspension

Torsion bar coil	Bump travel	Rebound travel
Camber angle	100 mm, -3.5898°	-55.0393 mm, 0.0829°
Toe angle	100 mm, 0.405°	-55.0393 mm, 0.0106°
Caster angle	100 mm, -1.4963°	-55.0393 mm, -4.0172°
Double wishbond	Bump travel	Rebound travel
Camber angle	100 mm, -2.689°	-75.078 mm, 1.0659°
Toe angle	100 mm, -1.8325°	-75.078 mm, 3.7995°
Caster angle	100 mm, 5.8622°	-75.078 mm, 5.5906°
Multi link	Bump travel	Rebound travel
Camber angle	100 mm, -7.4518°	-42.2894 mm, 0.9304°
Toe angle	100 mm, -0.1018°	-42.2894 mm, 0.0731°
Caster angle	100 mm, -11.695°	-42.2894 mm, -18.176°

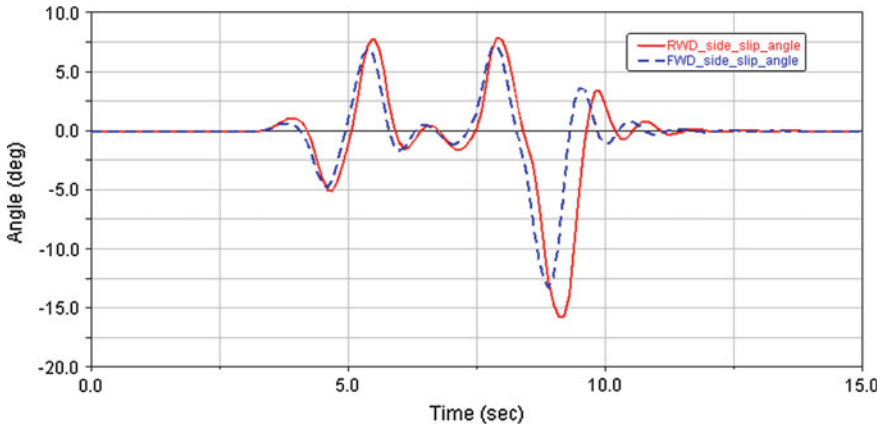


Fig. 28.2 Side slip angle response of FWD and RWD on ISO lane change

Table 28.3 Comparison result wheel drive system of ISO lane change simulation

Parameters	FWD	RWD
Longitudinal min	57.1329 km/h	56.8676 km/h
Longitudinal max	61.4576 km/h	61.5887 km/h
Longitudinal average	60.0008 km/h	59.9962 km/h
Roll min	-10.2403 deg/s	-12.1984 deg/s
Roll max	13.3031 deg/s	13.2267 deg/s
Roll average	-0.0003 deg/s	-0.0021 deg/s
Pitch min	-0.8666 deg/s	-1.4324 deg/s
Pitch max	1.4502 deg/s	1.434 deg/s
Pitch average	-0.0591 deg/s	-0.0663 deg/s
Yaw min	-37.6113 deg/s	-38.7894 deg/s
Yaw max	47.6996 deg/s	45.9841 deg/s
Yaw average	-0.0026 deg/s	-0.0099 deg/s
Side slip angle min	-13.2428°	-15.7552°
Side slip angle max	7.2009°	7.8491°
Side slip angle average	-0.1603°	-0.3172°

shows a lower value in case of FWD system. It is acceptable because side slip angles partially diminish steering angle accuracy [6].

Figure 28.3 shows an acceleration for both front and rear wheel drive as sample of simulation. Comparison of all acceleration simulation are presented in Table 28.4.

Table 28.4 reveals that FWD system has higher acceleration and velocity, lower longitudinal slip than RWD system because on FWD system the vehicle was pulled. There is equilibrium between the driving forces and the inertia force on FWD system so that the vehicle runs very stable in straight direction [6].



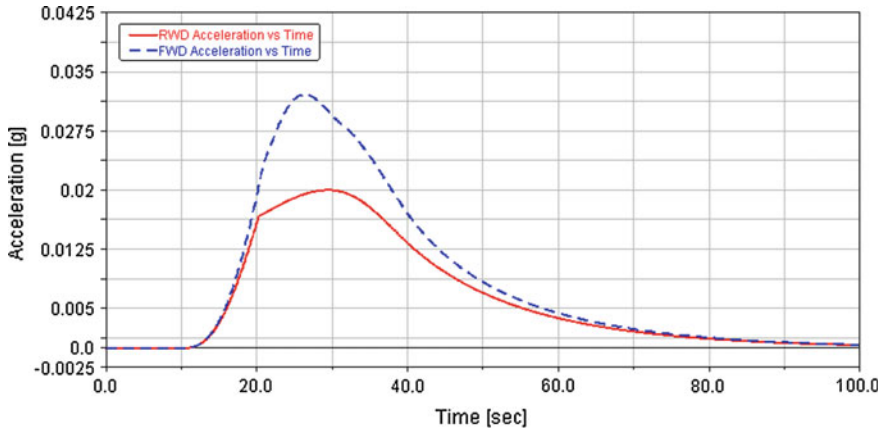


Fig. 28.3 Acceleration of FWD and RWD

Table 28.4 Comparison result of wheel drive system on acceleration simulation

Parameters	FWD	RWD
Acceleration max	0.0322 g	0.0201 g
Acceleration average	0.0083 g	0.0062 g
Velocity min	59.9994 km/h	59.9993 km/h
Velocity max	89.4601 km/h	81.8423 km/h
Velocity average	78.7886 km/h	73.6814 km/h
Longitudinal slip front min	0.5282 %	0.0913 %
Longitudinal slip front max	0.918 %	0.0962 %
Longitudinal slip front average	0.6987 %	0.0945 %
Longitudinal slip rear min	0.0847 %	0.6488 %
Longitudinal slip rear max	0.095 %	0.9695 %
Longitudinal slip rear average	0.0921 %	0.8052 %

Figure 28.4 shows chassis longitudinal velocity for FWD and RWD system as sample of cornering simulation. Comparison of all simulation are shown in Table 28.5.

In cornering simulation, longitudinal velocity and yaw rate for both front and rear wheel drive system had similar linear characteristics resulting in neutral steer that made the vehicle stable in cornering [7].

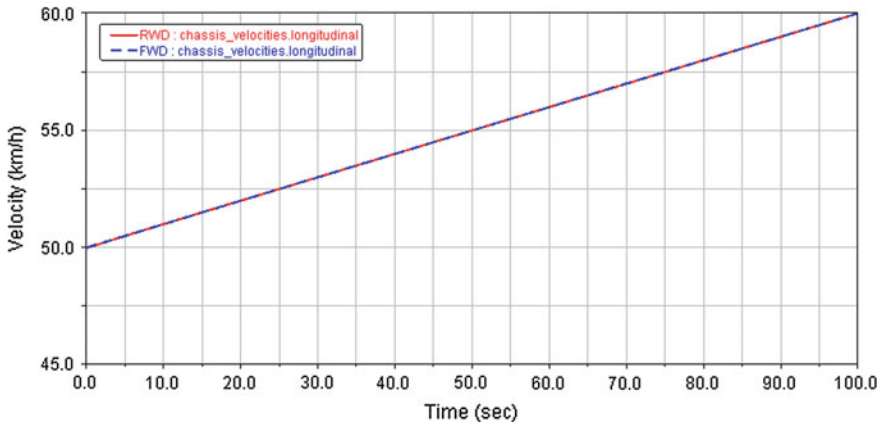


Fig. 28.4 Longitudinal velocity on FWD and RWD system in cornering simulation

Table 28.5 Comparison result of wheel drive system on cornering simulation

Parameters	FWD	RWD
Longitudinal min	49.9993 km/h	49.9969 km/h
Longitudinal max	59.994 km/h	59.9939 km/h
Longitudinal average	54.994 km/h	54.9932 km/h
Yaw min	7.8572 deg/s	7.8227 deg/s
Yaw max	9.5562 deg/s	9.5574 deg/s
Yaw average	8.7589 deg/s	8.7597 deg/s

## 28.4 Conclusion

Dynamic simulation of wheel drive and suspension system in a through the road parallel hybrid electric vehicle was done successfully. The methods presented in this paper could be used to select the best suspension system and to investigate the dynamic behavior of the car after converting from conventional vehicle either powered by petrol or diesel into a through the road parallel hybrid vehicles.

**Acknowledgments** This work was partly funded by the Ministry of Higher Education Indonesia under the scheme of Hibah Unggulan Penelitian contract No. 111/K3/KM/2015, 23 February 2015.

## References

1. Kaiser, G., Holzmann, F., Chretien, B., Korte, M., Werner, H.: Torque vectoring with a feedback and feed forward controller applied to a TTR HEV. In: Proceeding of IEEE Intelligent Vehicles Symposium, pp. 448–453 (2011)

2. Galvagno, E., Morina, D., Sarniotti, A., Velardocchia, M.: Drivability analysis of through the road parallel hybrid. *Meccanica* **48**(2), 351–366 (2013)
3. Pisanti, C., Rizzo, G., Marano, V.: Energy management of through the road parallel hybrid vehicles. In: *Proceeding of the 19th International Federation of Automatic Control World Congress*. Cape Town, South Africa (2014)
4. Zulkarnain, N., Zamzuri, H., Mazlan, S.A.: Ride and handling analysis for an active anti-roll bar: case study on composite nonlinear control strategy. *Int. J. Automot. Mech. Eng.* **10**, 2122–2242 (2014)
5. Nagarkar, M.P., Vikhe, G.J., Borole, K.R., Nandedkar, V.M.: Active control of quarter car suspension system using linear quadratic regulator. *Int. J. Automot. Mech. Eng.* **3**, 364–372 (2011)
6. Reimpell, J., et al.: *The Automotive Chassis*. Butterworth-Heinemann, London (2001)
7. Gillespie, T.D.: *Fundamentals of Vehicle Dynamics*. Society of Automotive Engineers, Warrendale (1992)

# Chapter 29

## A Reliable, Low-Cost, and Low-Power Base Platform for Energy Management System

Henry Hermawan, Edward Oesnawi and Albert Darmaliputra

**Abstract** In this project, a prototype of low-cost, low-power energy management system that can control lights and AC has been developed. This system has multi-master, multi-slave controller module that use wireless communication link for ease of installation on building. This system can be accessed remotely by user in intranet and/or internet network by implementing an embedded web server that letting users to control the devices and showing the status of the controlled devices. This system has been tested at home and office buildings. As results, the system can work well at home buildings less than 180 m<sup>2</sup> area and less than 350 m<sup>2</sup> area of three-floor office building. The best installation for office building of this system is the slave controllers should be installed at one upper and one lower floor relatively to master controller position. To extend the range of communication between controllers, multi-master wireless communication system can be implemented. This implementation has been tested as well and it works without problems.

**Keywords** Energy management system · Wireless communication · Multi-master · Multi-slave

### 29.1 Introduction

The background of this project is our observations in energy usage at home, office, and campus building. Energy is waste in daily life due to incorrect planning and implementation of electrical devices. This finding inspired us to develop a reliable, low-cost, and low-power base platform to monitor and control building resources, such as lights and ACs, in proper usage.

Our focus on this project is helping people to have awareness and manage the energy usage in their daily life at home and office. We designed the platform for

---

H. Hermawan (✉) · E. Oesnawi · A. Darmaliputra  
Department of Electrical Engineering, University of Surabaya, Surabaya, Indonesia  
e-mail: henryhermawan@staff.ubaya.ac.id

energy management system that can be operated easily by young people and elderly. We also consider the installation the platform without huge renovation to old buildings. At last, we also tried to put at low cost and low power in installation, operation, and maintenance, as well. This project will lead people to manage their energy usage without spending much additional cost. By this project, we make following contributions in technology innovation. We propose a base platform for a low-cost, low-power system for monitoring and controlling lights and ACs usage. Although this system is low cost and low power, it has a reliable, simple communication protocol.

## 29.2 Related Works

Today, there are some energy management systems that are commercially used in worldwide. To assist people in managing the energy usage, particularly in managing the use of electric energy, several consulting firms that engaged in the field of electric energy have developed some energy management systems that have been ready for commercial use. Those systems can be configured or designed according to user needs. Savant Systems LLC [1] has a system that allows users to control the use of lighting, audio-visual equipment, room temperature, security cameras, and security system for home and business remotely from mobile gadgets such as tablet PCs and smartphones. Encelium [2] offers energy management system for smart building that is claimed to be able to reduce energy usage for lighting by up to 50–75 %. As a well-known company in the field of light bulbs production, Koninklijke Philips [3] also provides a system that can manage the use of electric energy efficiently both indoors and outdoors for home and industrial-scale buildings. Those systems are inarguable that they are reliable, many-feature, great systems for energy management, however, they are very expensive, more suitable for new building, and sometimes need slightly more power for the system itself.

Some researchers have tried to reduce the cost in maintenance and operation by developing the low-cost energy management systems. Ramlee et al. [4] and Chindujaa et al. [5] have developed the bluetooth home automation systems. These systems have a limitation in user's connectivity since they used a short-range wireless technology. Baraka et al. [6] and Delgado et al. [7] use the IP client-server application, such as web-based application, for remote-controlling the energy management system. The use of IP-based technology can encounter the limitation of the use of short-range wireless technology.

Our project offers a reliable, low-cost, and low-power energy management system. This system has been designed so that it can be installed with minor modification on building structure. We propose simple communication protocol in order to simplify the system so that we can reduce production cost and daily operational cost, as well. We also use client-server application so that user can control this system remotely using web access.

### 29.3 Implementation and Testing

In this project, we developed a preliminary prototype of the system [8, 9]. For developing this prototype, we focused on:

- designing a reliable, two-way communication protocol between master-slave controllers and server (this is a closed-loop communication), and
- creating a base platform for a low cost, low power energy management system that is ease in installation for new and old building construction and ease in operation for most users.

The initial target for this system is managing lights and ACs usages in home and office building to saving energy and daily cost. This system, as shown in Fig. 29.1, relies on embedded systems platform that have low power consumption so that the system needs small energy to operate. The use of embedded systems will lead us to small footprint and inexpensive system. We also did not remove the capability to control and monitor lights and AC remotely. It uses web-based access system so that any gadgets and computers that have intranet or internet connection can access the system. In order to reduce complexity on installation, we decided to use less cabling systems by maximizing the usage of wireless network between multi-master, multi-slave controllers.

Master controller has two main tasks. The workflow of these tasks is shown in Fig. 29.2. First, it sends a request to the embedded web server for grabbing user’s command or response. This command or response has been inputted by clicking the menu that can be accessed through web browser on PC or mobile gadget. Every time user gives response to the system through web browser, the system will write the given response to stat.php file. The saved data in this file will be sent to master controller when it requests this data. The second task, after executing user’s

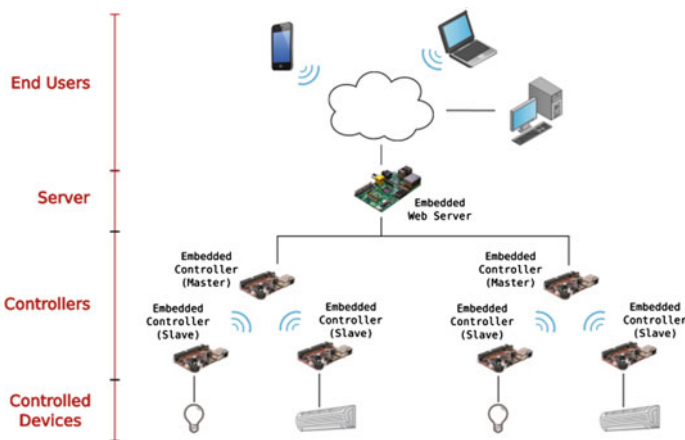


Fig. 29.1 Design concept of the energy management system project

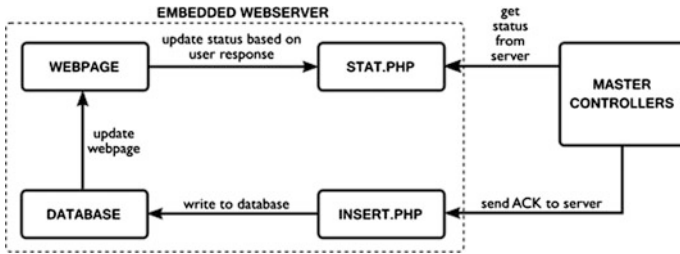
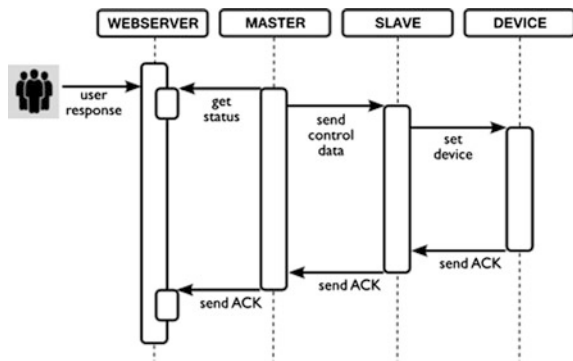


Fig. 29.2 Workflow of communication protocol between server and master controller

Fig. 29.3 Proposed communication sequence protocol that is simple and reliable



command or response (see the Fig. 29.3 for communication protocol of the system), master controller sends the acknowledge data to server. This data is grabbed by insert.php then stored it into database. The webpage routine will check the database then show the corresponding data on webpage to user. The communication protocol of this system is a closed-loop communication between web server and multi-master, multi-slave controllers (Fig. 29.3).

We have tested this prototype both in outdoor and indoor environment. For indoor environment, we tested at one-floor home building, two-floor home building, and seven-floor office building. The installation of this prototype can be shown at Fig. 29.4. We just put the slave controllers near controlled devices without or with some minor modification of building structure. The reliable wireless communication range in outdoor environment without barrier is a proximally of 60 meters and about 29 meters when tested in indoor environment with barrier (thickness = 20 cm, floor height = 4.25 m). These results are shown at Fig. 29.5. For building that have more than two floors, this prototype worked well at three-level floor building. For more than three floors, we have to use multi-master controllers to overcome the reliability issue. We also tested the user interface of web application (Fig. 29.6) for this prototype to some users. Mostly, they were satisfied with the user interface; however, it needs improvements on the legends of controlled devices (Table 29.1).

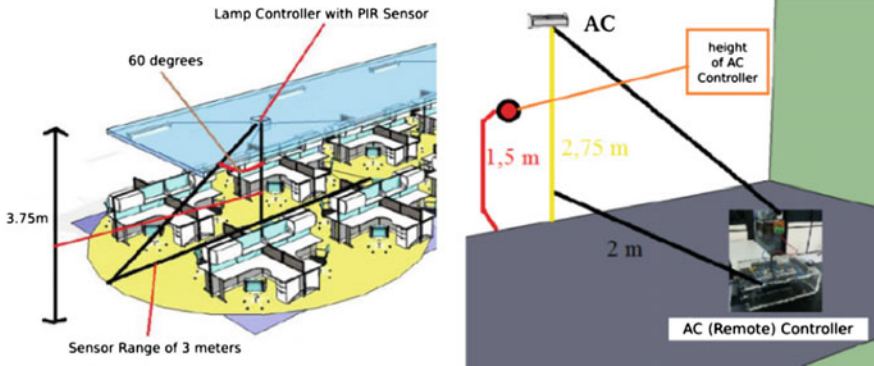


Fig. 29.4 Installation of slave controllers

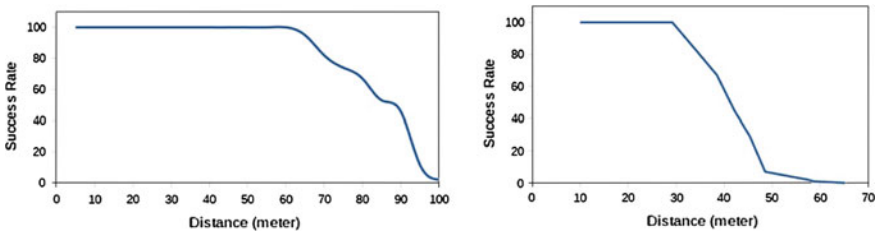


Fig. 29.5 Testing result in outdoor environment (left) and indoor environment (right)



Fig. 29.6 The user interface of web application

In prototype testing, we found that this system can work well at not more than 180 m<sup>2</sup> area of home building and less than 350 m<sup>2</sup> area of three-floor office building. The total cost of this prototype was not more than four million rupiah (less than USD 400), including the installation fees and labor cost. We have noted that for office buildings, which have more than three floors, the best option for installation of this system is the slave controllers should be installed at one upper and one lower floor relatively to master controller position.



**Table 29.1** Some user's comments related to the operation of this prototype

Gender	Age	Comment
Male	22	Good user interface, easy to operate. The interface should be more informative by adding the ID of controlled devices.
Male	19	Good website. If possible, user has right to add controlled devices.
Female	20	Good website. Adding the controlled device information would be better.
Female	53	Good user interface, easy to understand. If there are controlled devices ID, it would be very useful.

## 29.4 Conclusion

As summary of the implementation and testing result of this prototype, we can conclude:

- This system is low in cost and power by fostering the use of embedded systems. For greater impact in low-cost and low-power, we should select the right components and single board computer (SBC).
- Our proposal of the use of wireless connection between controllers and sensors can reduce the complexity of installation for new and old building construction.
- By implementing simple user interface and leveraging web-based system, this system has led us to ease in operation.
- At last, the closed system and simple communication protocol can help us to build a reliable system although it only uses low resources for its daily operation.

## References

1. Savant System. [http://www.savantsystems.com/intelligent\\_lighting.aspx](http://www.savantsystems.com/intelligent_lighting.aspx) (2014). Accessed 22 Mar 2014
2. Encelium. <http://www.encelium.com> (2014). Accessed 22 Mar 2014
3. Koninklijke Philips N.V.: <http://www.lighting.philips.com/main/products/controls> (2014). Accessed 22 Mar 2014
4. Ramlee, R.A., Leong, M.H., Singh, R.S.S., Ismail, M.M., Othman, M.A., Sulaiman, H.A., Misran, M.H., Said, M.A.M.: Bluetooth remote home automation system using android application. *Int. J. Eng. Sci. (IJES)* **2**(01), 149–153 (2013)
5. Chindujaa, C., Mary, J.L., Ragavee, B., Sakthi, S.: Development of in-home display and smart home system. *Int. J. Res. Dev. Eng. (IJRDE)*, 532–537 (2014). *Methods Enriching Power and Energy Developments (MEPED 2014) Special Issue*
6. Baraka, K., Ghobril, M., Malek, S., Kanj, R., Kayssi, A.: Low cost Arduino/Android-based energy-efficient home automation system with smart task scheduling. In: *Proceedings of the 2013 Fifth International Conference on Computational Intelligence, Communication Systems and Networks (CICSyN)*, pp. 296–301, 5–7 June 2013

7. Delgado, A.R., Picking, R., Grout, V.: Remote-controlled home automation systems with different network technologies. In: Proceedings of the 6th International Network Conference (INC 2006), pp. 357–366, 11–14 July 2006
8. Oesnawi, E., Hermawan, H.: Perancangan Sistem Pengontrolan Lampu Dan AC Yang Terintegrasi Secara Nirkabel Berbasis Low Cost Dan Low Power Radio Frequency. CALYPTRA: J. Ilmiah Mahasiswa Universitas Surabaya. **3**(1) (2014)
9. Darmaliputra, A., Hermawan, H., Pembuatan Web Server Berbasis Raspberry Pi untuk Kontrol Lampu dan AC. CALYPTRA: Jurnal Ilmiah Mahasiswa **3**(1) (2014)

# Chapter 30

## Android Application for Distribution Switchboard Design

Julius Sentosa Setiadji, Kevin Budihargono and Petrus Santoso

**Abstract** Mobile applications for distribution switchboard design are very rare. Currently, existing program is a program on a PC that can be used to perform complex electrical switchboard design but is not considered practical. An Android application is proposed to be used design a distribution switchboard in a practical way. The application is designed for 10.1” tablet platform with API 16 android operating system. This application was developed by using “Eclipse” software. Distribution switchboard designed follows the standard PUIL, SPLN, IEC, and IEEE. Distribution switchboard that has been designed by this application can be compared to the result of “MyEcodial L 3.4” software.

**Keywords** Distribution switchboard · Electrical switchboard design · Mobile application

### 30.1 Introduction

Mobile Application has the potential to grow very rapidly. This is because mobile phones (smart phones) have a crucial role, namely in the fields of communication, information, mobility, and entertainment. On the other hand, the use of mobile applications to support hobby and engineering application are still very underdeveloped [1]. It is very possible to use mobile applications to support the work in the field of engineering.

The development of mobile applications in the electrical power engineering sector is still very minimal. In the other hand, there is PC version program that can be used to perform complex electrical switchboard design but it is considered as not practical.

---

J.S. Setiadji (✉) · K. Budihargono · P. Santoso  
Electrical Engineering Department, Petra Christian University,  
121-131 Siwalankerto Street, Surabaya, Indonesia  
e-mail: julius@petra.ac.id

P. Santoso  
e-mail: petrus@petra.ac.id

With the need to design electrical switchboards rapidly and mobile in the workplace, it is become necessary to develop mobile applications in the field of electricity, especially in the electrical switchboard design that is simple yet compact so that the electrical switchboard design can be done easily and flexibly.

This application is designed the tablet platform size of 10.1” with android operating system API 16. This application is developed by using “Eclipse” software. Electrical switchboard that can be designed Distribution Switchboards follows the standard PUIL, SPLN, IEC, and IEEE. Electrical switchboard that has been designed by this application will be compared or “MyEcodial L 3.4” software.

## 30.2 Electrical Switchboard

Electrical switchboard is an arrangement of electrical components arranged in a control board so those components interrelated and form functions as needed [2].

Distribution switchboard is an electrical switchboard which serves to maintain the availability of electrical power by performing the function of insulating electrical faults [2]. Distribution switchboard design covers the placement of the following components: circuit breaker, busbar and cable. Nominal current rating of circuit breaker can be determined by using formula [3]:

$$P_{3\phi} = \sqrt{3} \times V_{\phi-\phi} \times I \times \cos \varphi \quad (30.1)$$

where, I is current (A),  $P_{3\phi}$  is 3-phase active power (W),  $V_{\phi-\phi}$  is line to line voltage (V),  $\cos \varphi$  is load power factor.

Breaking capacity of circuit breaker can be determined by using formula [4]:

$$I_{sc} = \frac{V_{\phi-\phi}/\sqrt{3}}{Z_{sc}} \quad (30.2)$$

where,  $I_{sc}$  is short circuit current (A),  $V_{\phi-\phi}$  is line to line voltage (V),  $Z_{sc}$  is  $\sqrt{(\sum R)^2 + (\sum X)^2}$  (m $\Omega$ ),  $\sum R$  is sum of resistance (series) (m $\Omega$ ),  $\sum X$  is sum of reactance (series) (m $\Omega$ ).

## 30.3 System Design and Implementation

The developed application has a function to perform calculation to design a distribution switchboard. Distribution switchboard that has been designed by this application can be saved. That has been done so that data can be loaded and used as guidelines for the manufacturing of electrical switchboard as well as bidding references.

### ***30.3.1 Database Design***

In this application, the usage of database has two functions, namely to call component availability and to save the electrical switchboard design process. Component availability database include the availability of the following components: transformers, circuit breakers, cables, and busbars.

### ***30.3.2 Interface Design***

This application interface design consists multiple pages as follows:

- **Electrical switchboard selection page**  
This page accommodate user to select which electrical switchboard will be designed. This page contains ImageViews to inform the user which distribution switchboard they will design and buttons to accommodate the user to choose an electrical switchboard to design (Fig. 30.1).
- **Distribution switchboard section**  
This section will be split into 3 input pages (see Fig. 30.2a, b and c) to accommodate the user to enter the data and 1 result page (see Fig. 30.2d).

The input pages contain ImageViews and TextViews to inform the user what data they should enter, EditTexts and Spinners to accommodate the user to enter the data, and buttons to accommodate user to go to the next page.

The result page contains ImageViews to display single line diagram of the designed distribution switchboard and TextViews to display the specification of the components that construct the distribution switchboard.

### ***30.3.3 System Implementation***

Implementation of the system can be summarized in a few process as follows:

- **Electrical Switchboard Selection:** when application is opened, user will be asked to choose which electrical switchboard to design.
- **Distribution switchboard design:** if user choose to design a distribution switchboard, user will be asked to input data as follow:
  - (a) Transformer data that includes transformer apparent power, transformer impedance, load losses and transformer secondary voltage.
  - (b) Cable between transformer and LV-MDP (Low Voltage—Main Distribution Panel) data that includes cable length, cable safety factor and cable placing.

**Fig. 30.1** The design of the electrical switchboard selection page interface



- (c) LV-MDP data that includes LV-MDP busbar safety factor, LV-MDP busbar type, system power factor and number of SDP.
- (d) SDP data that include cable length between LV-MDP and SDP, SDP busbar safety factor, SDP busbar type and number of grouping each SDP.
- (e) Grouping data that include load phase and load active power.

Based on formula, application will calculate the specification of the following components: cable between transformer and LV-MDP, LV-MDP circuit breaker, LV-MDP busbar, circuit breaker outgoing LV-MDP to SDP, cable between LV-MDP and SDP, SDP circuit breaker, SDP busbar, grouping circuit breaker. Standards used in this application are:

- (a) Short circuit current calculation using IEC 60909
- (b) Transformer database using SPLN 50/82
- (c) Cable database using SNI 04-0225-2000—Persyaratan Umum Instalasi listrik 2000 (PUIL 2000, in Bahasa Indonesia)

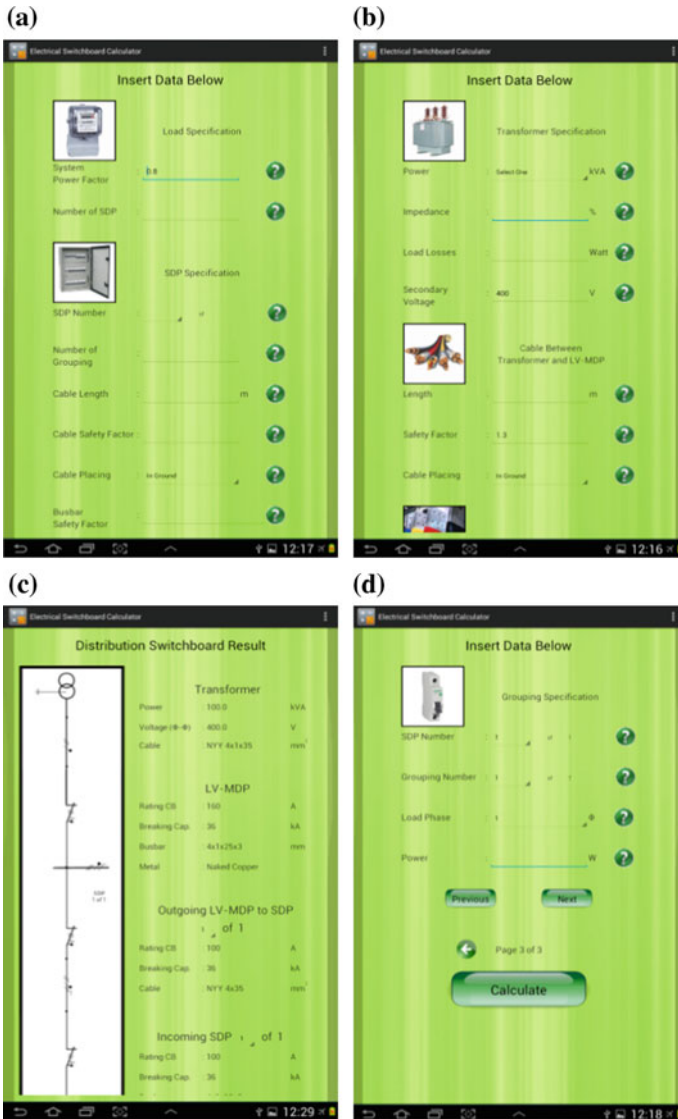


**Fig. 30.2** The design of the distribution switchboard, **a** to input transformer, cable and busbar data, **b** to input SDP (Sub Distribution Panel) and load data, **c** to input grouping data, **d** to display result page

- (d) Calculation of circuit breaker with breaking capacity 4.5 kA using IEC 60898-1
- (e) Calculation of circuit breaker with breaking capacity over 4.5 kA using IEC 60947-2


- (f) Capacitor database using IEC 60831-1/-2
- (g) Capacitor bank’s per step circuit breaker calculation using IEC 60831-1 and IEC 60931-1

### 30.4 System Testing

#### 30.4.1 Database Testing

Database testing is performed by pulling the database from android and open the database using “SQLiteBrowser” application. Database testing is performed to ensure all component availability table has been successfully created entirely. The test result can be seen in the following figure (Figs. 30.3 and 30.4).

**Fig. 30.3** Database transformer availability (in Bahasa Indonesia)

Table:  tabeltrafo

	daya	impedansi	rugitembaga
	Filter	Filter	Filter
1	Select One		
2	25	4	680
3	50	4	1100
4	100	4	1750
5	160	4	2350
6	200	4	2850
7	250	4	3250
8	315	4	3900
9	400	4	4000
10	500	4	5500
11	630	4	6500
12	800	4.5	10200
13	1000	5	12100
14	1250	5.5	15000
15	1600	6	18100



**Fig. 30.4** Electrical switchboard selection page



### 30.4.2 Interface Testing

Interface testing is performed by displaying the interface that has been created using Samsung Galaxy Table 30.1 (10.1”). Interface testing is performed to determine whether the interface runs well on Android or not.

**Table 30.1** Examples of calculation results table

Discription	Calculated with this application	Calculated with “MyEcodial L 3.4”
<i>Rating circuit breaker LV-MDP</i>	160 A	160 A
<i>Breaking capacity circuit breaker LV-MDP</i>	36 kA	25 kA
<i>Arus short circuit LV-MDP</i>	3, 286 kA	3, 31 kA
<i>Main Busbar LV-MDP</i>	4 × 1 × 25 × 3 mm	4 × 1 × 15 × 5 mm
<i>Rating circuit breaker outgoing SDP</i>	100 A	125 A
<i>Breaking capacity circuit breaker outgoing SDP</i>	36 kA	36 kA

### **30.4.3 Design Result Testing**

Design result testing is performed by comparing the design result by application with “MyEcodial L 3.4” software. Design result testing is performed to verify distribution switchboard designed by this application.

The difference in form of circuit breaker specification occurred because of differences in the usage of circuit breaker database between this application and “MyEcodial L 3.4” software, different ways of calculating the requisite of circuit breaker nominal current rating and the application does not perform design with cascading system. These differences can be tolerated because they both meet the applicable standards.

## **30.5 Conclusion**

The conclusion that can be drawn is as follows:

- The user is able to perform computerized process of designing distribution switchboards with this application.
- There were some differences in the design result using this application with the design result by “MyEcodial L 3.4” software. The differences are in the form of the short circuit current calculation and circuit breaker specifications.

## **References**

1. Plaza, I., Martin, L., Martin, S., Medrano, C.: Mobile applications in an aging society: status and trends. *J. Syst. Softw* **84**(11), 1977–1988 (2011)
2. Schneider Electric Indonesia: Panduan Aplikasi Teknis, (in Bahasa Indonesia) (2010)
3. ABB: Technical Application Papers No. 8: Power Factor Correction and Harmonic. ABB SACE, Bergamo (2010)
4. De Mets-Nobalt, B., Dumas, F., Poulain, C.: Cahier technique no. 158—Calculation of short-circuit currents. Schneider Electric, Grenoble (2005)

**Part IV**  
**Technology Innovation in Electronic,  
Manufacturing, Instrumentation  
and Material Engineering**

# Chapter 31

## Adaptive Bilateral Filter for Infrared Small Target Enhancement

Tae Wuk Bae and Hwi Gang Kim

**Abstract** When applying a basic bilateral filter for an infrared small-target detection, its traditional structure and implementation should be changed in order to recover the background that is covered by small target. This paper presents an adaptive bilateral filter incorporating a surrounding block-variance analysis and an adaptive standard deviation based on this variance, which is able to obtain and analyze more information from the vicinity of both the target and the background. This concept enables a bilateral filter to predict a background image excluding a small target because the surrounding block variance is adaptively mapped to the standard deviations of bilateral filter according to the target and background. Finally, a small target can be detected by subtracting the predicted background from the original image. In order to compare existing target detection methods against the proposed adaptive bilateral filter, the signal-to-clutter ratio gain and background suppression factor are employed. Experimental results show that the proposed adaptive bilateral filter method has a superior target enhancement performance compared to existing methods.

**Keywords** Bilateral filter · Clutters · Infrared · Sensor · Small target

### 31.1 Introduction

Among IR imaging systems, an infrared search and tracking system is an important IR defense technique against attacks by cruise missiles or infiltration by low-flying objects [1]. The targets can be observed, detected, and recognized based on their radiant features, which differ from the background. However, in general, an IR

---

T.W. Bae (✉) · H.G. Kim

Electronics and Telecommunications Research Institute, Daejeon, Republic of Korea  
e-mail: twbae@etri.re.kr

H.G. Kim

e-mail: hwigangkim@etri.re.kr

© Springer Science+Business Media Singapore 2016

F. Pasila et al. (eds.), *Proceedings of Second International Conference on Electrical Systems, Technology and Information 2015 (ICESTI 2015)*,

Lecture Notes in Electrical Engineering 365, DOI 10.1007/978-981-287-988-2\_31

image has a very low signal-to-noise ratio from various optical factors such as target sources, background radiation, transmission properties in the atmosphere, and limitations of the IR sensor. Since these factors bring significant amount of clutter and false targets in an IR image, it is a difficult task to detect dim, small, and moving targets. Moreover, small targets appear as a dim point embedded in a heavily cluttered background owing to the long distances between the IR sensor and the targets. Because these factors bring about a large amount of clutter and false target detections, it is very challenging to detect and track dim, small, and moving targets. Nevertheless, a target-detection algorithm is an essential technique for IR countermeasures (IRCM) and directed IRCM, which protect friendly aircraft or ground vehicles from enemy missiles or aircraft [2]. For the development of these IRCM or DIRCM systems, small target detection techniques must come first. Over the past few decades, many spatial target detection techniques have been presented.

Many researchers have developed several spatial-based small-target detection methods for detecting moving targets in IR images [3–5]. Deshpande et al. suggested the use of max-mean and max-median filters for preserving structural backgrounds, such as clouds in an IR image [3]. Zhang et al. presented a target detection method using top-hat for tracking dim moving-point targets in IR sequences [4]. Cao et al. proposed a target detection method using a 2D least mean square based on a neighborhood analysis for a local filter [5]. The mentioned methods assumed that a small target has a brighter intensity from higher temperatures compared to the background region. However, it is difficult to identify the real target region precisely when many non-target objects have bright gray levels in the IR images. In these spatial-based methods, background prediction when covered by targets is the key of small target detection, since small targets can be detected by subtracting the predicted image from the original [6]. To efficiently perform this procedure, this paper presents an adaptive bilateral filter (ABF) incorporating a surrounding block variance analysis and an adaptive nonlinear standard deviation based on this variance.

## 31.2 Bilateral Filter and Its Application

Bilateral filter (BF) was proposed as a nonlinear filter that smoothest the noise while preserving the edges [6]. A predicted pixel from the BF is given by

$$Y(m, n) = \sum_{l=-p}^p \sum_{k=-p}^p H(m, n; l, k) X(l, k) \quad (31.1)$$

where  $Y(m, n)$  is the output image,  $H(m, n; l, k)$  is the nonlinear combination between pixels  $(l, k)$  and the center pixel  $(m, n)$  in the filter window with

$(2p + 1) \times (2p + 1)$ , and  $X(l, k)$  is a degraded image (the original image). The nonlinear combination in the filter window is given by

$$H(m, n; l, k) = \begin{cases} w_{m,n}^{-1} \exp\left(-\frac{(l-m)^2 + (k-n)^2}{2\sigma_d^2}\right) \exp\left(-\frac{(X(l,k) - X(m,n))^2}{2\sigma_r^2}\right), & (l, k) \in \Delta_{m,n} \\ 0, & \text{otherwise} \end{cases} \quad (31.2)$$

where  $\Delta_{m,n} = \{(l, k) : (l, k) \in (m-p, m+p) \times (n-p, n+p)\}$  represents pixels in the filter window,  $\sigma_d$  and  $\sigma_r$  are standard deviations of the domain and range filters, and  $w_{m,n}$  is a normalization factor given by,

$$w_{m,n} = \sum_{l=m-p}^{m+p} \sum_{k=n-p}^{n+p} \exp\left(-\frac{(l-m)^2 + (k-n)^2}{2\sigma_d^2}\right) \exp\left(-\frac{(X(l,k) - X(m,n))^2}{2\sigma_r^2}\right) \quad (31.3)$$

To apply a basic BF to the small target detection, the most important consideration is the image variation by  $\sigma_d$  and  $\sigma_r$ . First,  $\sigma_d$  controls the Gaussian weighting rate based on distance for all pixels in filter window. Generally, the more  $\sigma_d$  increases for a fixed  $\sigma_r$ , the greater the smoothing-effect is for filter window. Meanwhile,  $\sigma_r$  controls the Gaussian weighting rate based on the pixel range for all pixels in filter window. If  $\sigma_r$  is larger than the pixel range in filter window, it means that the range low-pass Gaussian filter assigns a similar weight and causes a smoothing effect for every pixel in the filter window. We can induce that a smaller  $\sigma_d$  and  $\sigma_r$  keeps the original shape of the small target owing to the edge-preserving feature; on the other hand, larger values make the small target blur owing to the smoothing feature.

To predict the background covered by small targets, the BF should have a relatively smaller  $\sigma_d$  and  $\sigma_r$  for the background or object regions (such as a cloud) for its preservation, but on the other hand, should have a larger  $\sigma_d$  and  $\sigma_r$  for the small target region for smoothing or blurring.

### 31.3 Proposed Adaptive Bilateral Filter Based on Surrounding Block Variance

The proposed ABF is a novel BF with an adaptive standard deviation mapping function based on a surrounding block variance analysis by means of the basic BF features explained in section II. The procedure of the proposed ABF is as follows. First, we analyze the surrounding block variances for small targets, various objects, and background regions. The block variance is mapped to the two standard-deviations of the BF. The background region covered by the small targets is then predicted. By subtracting the predicted image from the original, small targets can be detected.

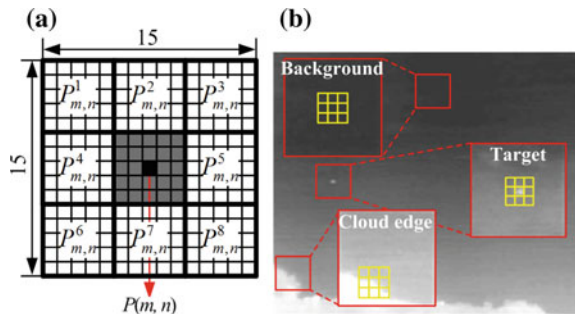
### 31.3.1 Surrounding Block Variance Analysis

To apply the BF features to IR small target detection, we need a mechanism that can tell the filter how likely it is that the image covered by the filter window is going to be a small target or a background, allowing the filter to adjust its two standard deviations accordingly. Figure 31.1a shows a novel input structure for the proposed ABF, which is capable of acquiring and analyzing more information from the vicinity of the target and from the background region. For input IR image  $X$  with a size of  $M \times N$ , the proposed ABF uses surrounding blocks with  $5 \times 5$  sizes centered at  $P_{m,n} = \{1 \leq m \leq M, 1 \leq n \leq N | P_{m,n}^1, P_{m,n}^2, \dots, P_{m,n}^8\}$ , as the input blocks. The input block variance, the variance of mean values of the respective input blocks at  $(m, n)$  is given by  $V(m, n) = \text{var}(P_{m,n})$ .

Figure 31.1b shows the position of the input blocks on a small target, a cloud edge, and the background of an original IR image. Since input blocks surrounding the small target and background have very similar statistical properties, the respective mean values corresponding to input blocks will be very similar. In other words, variances in these two regions will be similar. However, around the cloud edge, respective mean values corresponding to the input blocks can vary, as shown in the cloud edge region, since the cloud (or object) neighborhood is complicated. Thus, when the mean values of the input blocks cluster tightly, it means that the filter window is moving on a flat background or a small target, and the BF needs to increase the standard deviations to smooth these regions.

Even if larger standard deviations cause a smoothing effect, it does not affect the background region, but smooths a small target region; on the other hand, if the mean values of input blocks are widely separated, it means that the filter window is moving over a chaotic region, like the edge of a background object, and the standard-deviations need to be reduced for an edge-preserving effect on the region. Therefore, a mapping function of the input-block variance and two standard deviations are needed for this purpose.

**Fig. 31.1** a Input structure and b its position for various objects and background



### 31.3.2 Mapping Function of Standard Deviations Based on Surrounding Block Variance

We should consider a mapping function for the surrounding variance of input blocks to the standard-deviations of the BF. Based on the relation between the input block variance and standard deviations, we can easily use a linear mapping of inverse proportion to predict a background that does not include a small target. However, to map this efficiently, this paper employs a nonlinear mapping function. The nonlinear mapping functions for  $\sigma_d$  and  $\sigma_r$  are

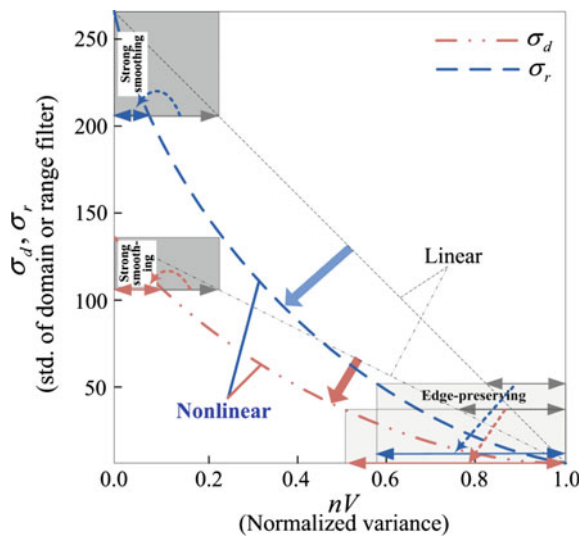
$$\sigma_d = (\sigma_{d\_max} - \sigma_{d\_min})(1 - \sqrt{nV}) \tag{31.4}$$

$$\sigma_r = (\sigma_{r\_max} - \sigma_{r\_min})(1 - \sqrt{nV}) \tag{31.5}$$

where  $nV$  is the normalization of input block variance at any coordinate, in the range of  $nV_{min} = 0$  to  $nV_{max} = 1$ . And  $\sigma_{d\_min}(= 0)$ , and  $\sigma_{d\_max}(= 127)$ ,  $\sigma_{r\_min}(= 0)$ , and  $\sigma_{r\_max}(= 255)$  are the min and max of the standard deviations for the domain and range filters in the BF. The normalized input block variance at any coordinate is calculated by max and min input block variances at all the coordinates in entire input image.

Figure 31.2 represents two kinds of mapping functions (straight line [Linear] and curve [Nonlinear]) for surrounding variances to standard deviations of the BF. It shows smoothing and edge-preserving regions determined from standard-deviations of the domain or range filters in the BF. Compared to a linear straight line, the nonlinear curve has a narrow surrounding variance range for a smoothing region (a smaller smoothing effect) and a wide surrounding variance range for an

**Fig. 31.2** Non-linear mapping function for surrounding variance and standard deviations





edge-preserving region (a bigger edge-preserving effect). This means that this mapping function can smooth only small targets while making other objects (such as clouds) visible on the predicted background since it tends to make an IR image edge-preserved. As a result, small targets can be more efficiently detected by differences between the original image and a predicted image. Now, the proposed ABF can predict a background that does not include a small target from the adaptive  $\sigma_d$  and  $\sigma_r$  mapping mechanism based on the surrounding variances, which distinguishes small targets, the back-ground region, and object regions such as cloud edges in an IR image.

### 31.3.3 Post-Processing Using Min and Max Filter

After subtracting a predicted background  $Y(m, n)$  by the proposed ABF from an original image  $X(m, n)$ , a min-max filter is applied for the subtracted image  $S(m, n)$ . Among the subtracted image, pixels with a negative sign are mapped to zero. We regard pixels larger than threshold  $Th = 0.8 \times S_{max}$  as the candidate target region, where  $S_{max}$  is the maximum gray scale in the subtracted image  $S(m, n)$ , as follows:

$$\begin{cases} \text{Candidate target region,} & \text{if } S(m, n) \geq Th \\ \text{Non - target region,} & \text{otherwise} \end{cases} \quad (31.6)$$

To detect the target well and reduce the clutter, the candidate target region is processed using a  $3 \times 3$  mean filter, and the residual region is processed using a  $3 \times 3$  min filter. The detection results are then acquired. This post-processing is useful to the background suppression with the target enhancement.

## 31.4 Experimental Results

Three IR images (A, B, and C) were used for an objective performance assessment. Image A includes a flying target with low contrast and a size of  $320 \times 240$ .

Image B and C include a flying target against a cloudy background and a uniform background, respectively, each sized  $360 \times 240$ . Figure 31.3 shows the detection results from the proposed ABF. Figure 31.3a shows the original images containing a small target in various backgrounds, and Fig. 31.3b shows the predicted background images from the proposed ABF. We can see that background images of the original images are predicted on the whole, while the targets are largely ignored, or almost disappear in the predicted background images. Figure 31.3c represents the surrounding block variance over the image. Red corresponds to larger values, and blue corresponds to smaller values. We can see that the dim cloud and cloud edge are high, while variance in the target and uniform

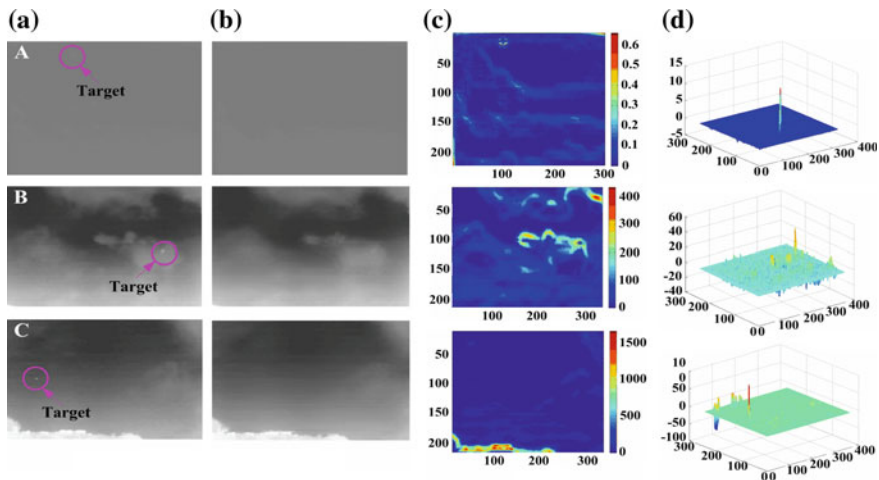


**Fig. 31.3** Detection results on three IR images with small targets: **a** original IR images, **b** predicted background images, **c** surrounding block variance over the image, where *red* corresponds to larger values and *blue* corresponds to smaller values, and **d** the detection results

background is low. Figure 31.3d shows a subtracted image, obtained by subtracting the predicted background image from the original image.

Figure 31.4 shows the target detection results between the existing methods and the proposed ABF. The proposed ABF suppresses the cloud edges and background clutter better than the existing methods. We confirmed that the proposed BF is more effective on IR images with various backgrounds, compared to the other existing methods. To evaluate the performance of the existing methods and the proposed ABF quantitatively and objectively, two metrics, that is, the signal-to-clutter ratio

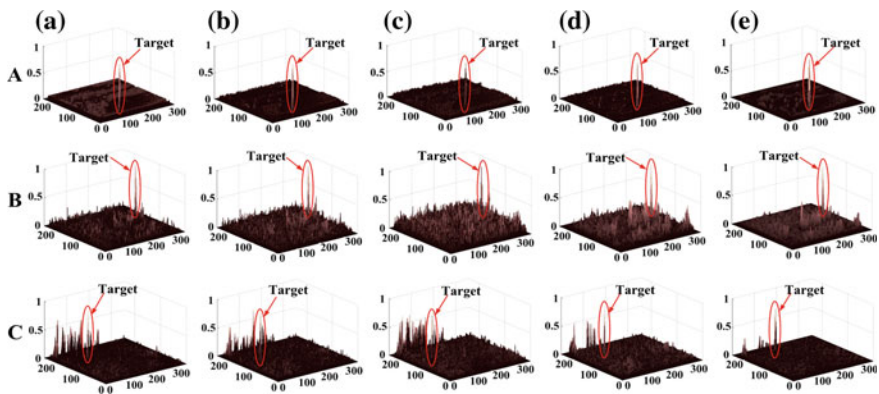


**Fig. 31.4** Comparison of the results between the conventional methods and proposed BF: **a** max-mean, **b** max-median, **c** Zhang's method, **d** Cao's method, and **e** proposed ABF

**Table 31.1** Spatial result comparison for several methods

	A		B		C	
	SCRG	BSF	SCRG	BSF	SCRG	BSF
Max-mean method	4.45	6.59	1.85	2.28	5.65	8.78
Max-median method	4.56	6.61	1.83	2.21	6.65	8.83
Zhang's method	6.72	7.65	1.41	2.19	4.55	7.21
Cao's method	7.29	8.03	2.11	2.86	6.73	8.07
Proposed ABF	9.14	11.54	2.73	4.06	14.27	10.07

gain (SCRG) and background suppression factor (BSF) [7], are employed and defined as follows:

$$SCRG = (S/C)_{out}/(S/C)_{in} \quad (31.7)$$

$$BSF = C_{in}/C_{out} \quad (31.8)$$

where  $S$  is the signal amplitude and  $C$  is the clutter standard deviation in a normalized subtraction image. The subscripts in and out indicate the input and output images. We confirmed that the proposed ABF offers a superior performance, that is, 1.85–4.69, 0.62–1.32, and 7.54–9.72 in SCRG and 3.51–4.95, 1.20–1.87, and 1.24–2.86 in BSF for A, B, and C image, compared to the existing methods, as shown in Table 31.1.

## 31.5 Conclusions

This paper presents a novel image based IR small target detection method as applying basic BF. With development of camera technology, image based target detection is becoming very important requisite for IRCM or DIRCM. In the small target detection, rapid and precise detection is an essential problem for coping with upcoming enemy aircrafts or missiles. Therefore, computation time reduction should be accompanied with precision enhancement in target detection, as the future work.

## References

1. Wolfe, S.L.: Introduction to infrared system design. SPIE Optical Engineering Press, Bellingham, WA (1996)
2. Bae, T.W., Kim, B.K., Kim, Y.C., Ahn, S.H.: Jamming effect analysis of infrared reticle seeker for directed infrared countermeasures. *Infrared Phys. Technol.* **55**, 431–441 (2012). doi:[10.1016/j.infrared.2012.05.001](https://doi.org/10.1016/j.infrared.2012.05.001)
3. Deshpande, S.D., Er, M.H., Venkateswarlu, R., Chan, P.: Max-mean and max-median filters for detection of small targets. *Proc. SPIE* **3809**, 74–83 (1999). doi:[10.1117/12.364049](https://doi.org/10.1117/12.364049)

4. Zhang, F., Li, C., Shi, L.: Detecting and tracking dim moving point target in IR image sequence. *Infrared Phys. Technol.* **46**, 323–328 (2005). doi:[10.1016/j.infrared.2004.06.001](https://doi.org/10.1016/j.infrared.2004.06.001)
5. Cao, Y., Liu, R., Yang, J.: Small target detection using two-dimensional least mean square (TDLMS) filter based on neighborhood analysis. *J. Infrared Millimeter Waves* **29**, 188–200 (2008). doi:[10.1007/s10762-007-9313-x](https://doi.org/10.1007/s10762-007-9313-x)
6. Tomasi, C., Manduchi, R.: Bilateral filtering for gray and color images. In: *Proceedings of International Conference Computer Vision*, pp. 839–846 (1998). doi:[10.1109/ICCV.1998.710815](https://doi.org/10.1109/ICCV.1998.710815)
7. Hilliard, C.I.: Selection of a clutter rejection algorithm for real-time target detection from an airborne platform. *Proc of SPIE* **4048**, 74–84 (2000). doi:[10.1117/12.392022](https://doi.org/10.1117/12.392022)

# Chapter 32

## Innovative Tester for Underwater Locator Beacon Used in Flight/Voyage Recorder (Black Box)

Hartono Pranjoto and Sutoyo

**Abstract** All commercial airplanes that carry more than 20 passengers and all sea merchant vessels with sizes above 3000 gross tonnage must be equipped with flight/voyage data recorders or more popularly known as black box. All black boxes aboard those vessels must be equipped with a completely independent ultrasonic sonar finder device called Underwater Locator Beacon (ULB). In case the device is immersed in water due to an accident, this device will emit ultrasonic signal at 37.5 kHz of a certain pattern for 30 days. The chance of finding the vessel (an airplane or a ship) sinking in the ocean is almost solely depend on the working order of this device. The work presented here is about testing the ULB for its performance using simple system by the use of a microprocessor. The tester will check the voltage of the battery inside the ULB, the expected length of usage of the battery, the generation of the ultrasonic signal at 37.5 kHz, and also about the pattern of the signal. The device designed and built will be small and easy to use with good visual and audio feedback to indicate the result of the UTB test. At the termination of this work, a working system to test a ULB on the voltage and also detection of the ultrasonic signal has been built which is small and intelligent. The usage of the system is very simple, just by inserting the ULB into the system and pressing the unit for 5 s, a thorough result of the ULB test is presented on an LCD screen together with a blinking color light emitting diode (LED) and audible sound via buzzer to prove that the ULB under test is in good working order.

**Keywords** Flight recorder tester · Under water locator beacon · Flight black-box

---

H. Pranjoto (✉) · Sutoyo  
Electrical Engineering Department, Widya Mandala Catholic University, Surabaya, Indonesia  
e-mail: pranjoto@yahoo.com

## 32.1 Introduction

All commercial airplanes that carry more than 20 passengers and all sea merchant vessels with sizes above 3000 gross tonnage must be equipped with flight/voyage data recorders or more popularly known as black box. The actual color of the recording unit is actually bright orange color with marking that the device is a flight or voyage data recorder. For an airplane there are two different and independent unit of data recorder, one data recorder is for the cockpit voice data recorder which record all conversation taking place inside the cockpit and a flight data recorder which record all the parameters of the flight such as heading, altitude, position of rudder, position of elevator and many other parameters All black boxes aboard those vessels must be equipped with a completely independent ultrasonic sonar finder device called Underwater Locator Beacon (ULB). In case the device is immersed in water due to accident, this device will emit ultrasonic signal of a certain pattern for 30 days [1–3].

Figure 32.1 shows the recording unit for an airplane. Figure 32.1a is a typical photograph of a cockpit audio voice data recorder (CAVR) while Fig. 32.1b is a photograph of a flight data recorder. There no significant difference between those two devices. Figure 32.1c is a typical photograph of voyage data recorder usually found above the bridge of a sea vessel.

In all figures above (Fig. 32.1a, b, c) although they are built by different manufacturers there is one common unit—the ULB—shown as white cylinder on the right hand side of the recorder (Fig. 32.1a) on the left hand side of the recording unit (Fig. 32.1b) and above the recording unit (Fig. 32.1c). The length of a ULB is 10 cm and the diameter is 3.3 cm. A detailed view of the beacon and example of mounting on FDR is shown in Fig. 32.2a, b.

A ULB by itself when stored anywhere—such as mounted next to a data recorder—will not transmit any ultrasonic signals because the positive pole and the body of the ULB is not connected or it is an open circuit. Upon completion of the circuit such as shorting the positive pole to the body or by immersing the ULB underwater—thus create a short circuit, then the ULB will emit ultrasonic signal. The ultrasonic signal will have a frequency of  $37.5 \text{ kHz} \pm 1 \text{ kHz}$ . The frequency will be transmitted for a period of 10 ms (0.01 s) with a silent period of 99 ms (0.99 s) to provide a period of 1 s modulation. Figure 32.3 shows the timing and the ultrasonic pulses emitted by the ULB. Figure 32.3a shows in illustration of how to short the positive pole to the body of the ULB using simple wire and Fig. 32.3b shows the ultrasonic output of the ULB. From Fig. 32.3b, it shows clearly that the frequency output of the ultrasonic is 37.5 kHz and the active period of 10 ms. During the remaining 990 ms, the ULB does not transmit any ultrasonic signal thus giving a period of 1 s of modulation period [1–6].

**Fig. 32.1** **a** Cockpit audio voice recorder unit of an airplane. **b** Flight data recorder of an airplane. **c** Voyage data recorder for sea vessel



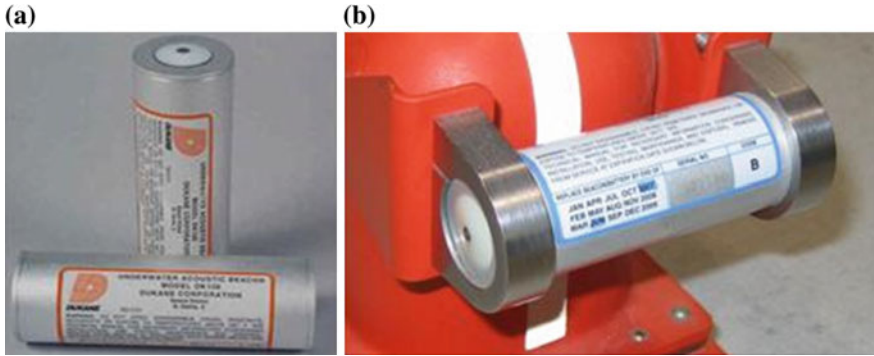


**Fig. 32.2** a Detailed view of a ULB on with the positive node shown on the vertical unit. b ULB mounted on the side of an FDR shown together with the expiration date (June, 2007)

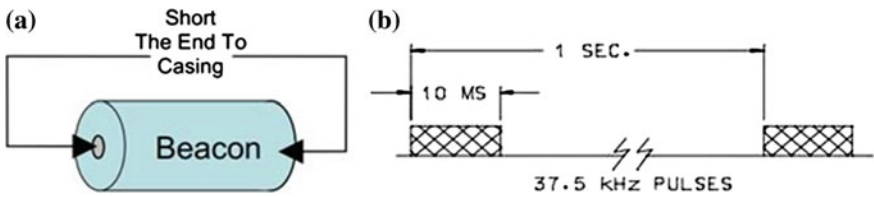


**Fig. 32.3** a Activation of ULB by shorting the positive pole to the body of the beacon. b Timing of the ultrasonic pulses emitted by the ULB

### 32.2 Annual Performance Test of ULB

By regulation, the CAVDR, FDR, or VDR must be tested at least once a year by a qualified personnel endorsed by the maker of the corresponding maker. After the test is performed, temporary certificate is given by the personnel when he/she thinks the unit is working in satisfactory condition. Later on, the data must be sent to the maker and the maker will review the result, and if the maker is satisfied, then a 1-year certificate for the unit is issued.

During the test, most of the work is on the recording unit, the ULB is only checked for the battery expiration and the voltage of the battery. No test is usually performed to check for the performance of the ultrasonic transmitter, although this is the only chance of finding the data of the recording unit if the vehicle is immersed underwater.

There are manufacturer that provide ultrasonic test, but the test is cumbersome. It involves taking the battery out of the mounting unit, short the pole and the body similar to Fig. 32.3a, and then place an ultrasonic transducer near the ULB to listen to the signal. This task is not easy because the location of the unit is not easy to reach and also to work with and therefore performing the task of testing the ULB becomes more demanding.



### ***32.2.1 Testing the Underwater Locator Beacon (ULB)***

The most important parameter of testing the Underwater Locator Beacon (ULB) is (1) to check the expiry date of the lithium battery of the beacon, (2) testing the voltage of the lithium battery to be within certain value (above 2.97 V) and (3) test if the ULB transmit ultrasonic signal with the predetermined pattern. The first two tasks have been performed traditionally by the surveyor, but to test the actual transmission is not performed because the device currently used is cumbersome. In this tester, the last two tasks will be performed very easily just by pushing the ULB into the socket inside the tester. The tester will perform a self test itself, then check the battery voltage of the ULB and then test the presence of ultrasonic signal from the ULB.

Testing the ULB can be performed by using one simple task b inserting the ULB inside the opening of the testing unit. Upon pressing the ULB into the test unit, there is a small switch that turns on the entire system and start the sequence of ULB testing will be as follows:

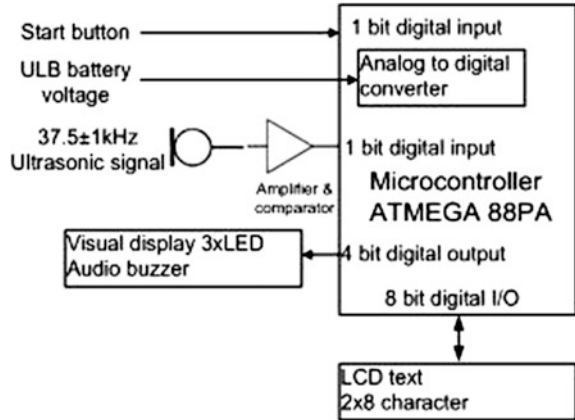
- (1) Do a power on self test on the ULB tester to ensure that the tester is in good working order such as the battery voltage supply, the buzzer, LCD and LED indicator
- (2) Do a voltage measurement of the lithium battery of the ULB and predict based on the voltage the length of time the battery will last for storage. If the prediction of the lifespan of the battery is less than 1 year, the system will show a warning.
- (3) Short the positive probe and the body of the ULB and then the ultrasound microphone will listen for the ultrasonic tone of the ULB at certain voltage level. The microprocessor will count the number of pulses to ensure that there are between 365 and 385 pulses within the 10 ms of the transmission windows

After all sequence described above is passed, then the unit will show a satisfactory condition which is shown on the LCD, blink of the green LED and also single beep of the buzzer.

## **32.3 Description of the ULB Tester**

The main unit of the ULB tester is a microcontroller ATMEGA88PA SMD—to make the entire device small in size—and a ultrasonic transducer as shown in Fig. 32.4. When the ULB is inserted and then pressed, the start button will turn on the microprocessor, do a self test within 300 ms, and then measures the voltage of the lithium battery to a specific voltage (3 V) several times. The unit will then shorted the body of the ULB with the positive probe to start the transmission of the ultrasonic signal at 37.5 kHz. The signal is then picked up by an ultrasonic

**Fig. 32.4** Block diagram of the innovative ULB tester



transducer and then amplified/compared with an op-amp. The output is fed to the microcontroller that measures the number of pulses to be between 375 pulses  $\pm 10\%$ —a 37.5 kHz signal will generate 375 pulses within 10 ms. This detection is performed three times. After all measurements are finished, a single audible beep is generated together with the lighting of the green LED (light emitting diode) and the word “PASSED” and Volt = 2.98 to indicate the voltage of the lithium battery on a  $2 \times 8$  character text LCD.

The first ULB tester is quite compact measuring only 13 cm in length as shown in Fig. 32.5 along with a measuring ruler on the bottom side. The casing is made of acrylic to show all the components. On the left side is the opening to insert the ULB under test and then push the ULB to start the entire sequence of testing from measuring the battery voltage and then check the presence of ultrasonic signal when the ULB is shorted. Shown on top of the tester is the  $2 \times 8$  character text LCD. Underneath the LCD is the microcontroller with all the connection to the other peripherals. On the bottom part of the microcontroller board is the power supply board and the ultrasonic transducer circuitry.

**Fig. 32.5** a ULB tester unit from the top view



**Fig. 32.6** **a** Top circuit board with microcontroller.  
**b** Bottom circuit board with transducer

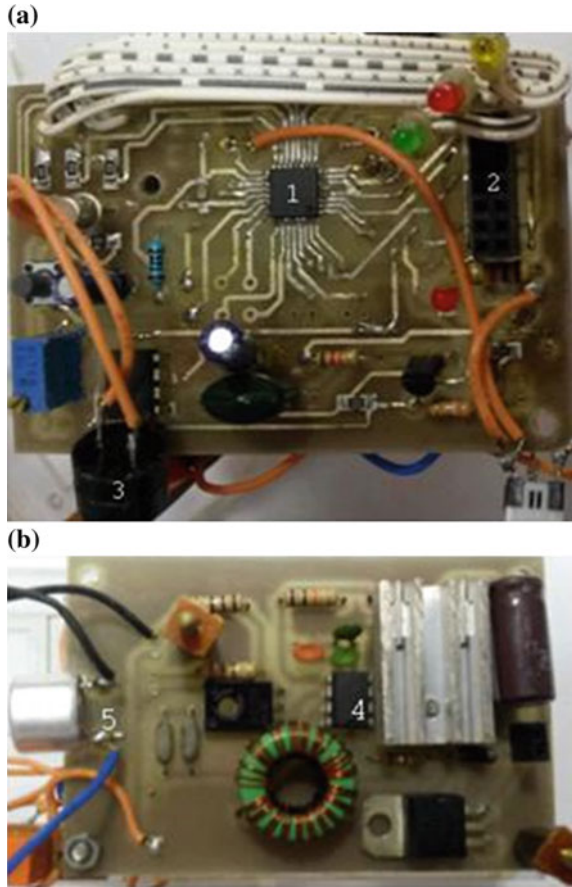


Figure 32.6a shows the top circuit board of the tester with marking (1, 2, 3) of the microcontroller, connector to the LCD module, and buzzer. Figure 32.6b shows marking (4, 5) the ultrasonic amplifier and the ultrasonic transducer itself.

### 32.4 ULB Tester Performance Test

Performance of the tester is conducted in two different prerequisite. The first is the performance of the voltage of the tester as compared to the voltage of the ULB itself. Measurement of the ULB battery voltage uses the internal Analog to Digital Converter of the microcontroller. The resolution of the ADC is 10 bit resulting in voltage differentiation of 0.005 V for a span of 5 V reference which is good enough.

Testing is conducted using different supply voltage with different values and then compared with calibrated voltmeters. Performance of the analog to digital converter of the microcontroller is very similar to that of calibrated voltmeters and therefore simple in comparison. Comparison of voltage between ADC and calibrated voltmeter is very negligible and still within the 0.005 V resolution and the result of the test is displayed on the LCD display to indicate the voltage measured.

Testing the ultrasonic signal is a time domain process instead of frequency domain. First the signal must be captured by the ultrasonic transducer and the result of ultrasonic signal emission by the ULB is shown in Fig. 32.7 which illustrates that the signal will emit for 10 ms every 1 s. Testing of the ULB tester involves changing/sweeping the frequency of the ultrasonic signal from 32.5 kHz up to 42.5 kHz. The result of the ULB tester can indicate that it can detect the signal from 36.5 kHz up to 38.5 kHz and provide message that the signal is good. When the signal is outside the range, then the ULB tester must indicate that the ULB is not in good condition because emitted ultrasonic signal is outside the range. During the ULB test period, the number of pulses within 10 ms is counted and the number must be between 365 and 385 counts.

After the conclusion of the test (battery voltage test and ultrasonic generation test), a test result will be displayed on the LCD, color LED indicator and audio beep as indicated in Table 32.1.

Before the ULB test is conducted by the tester, the tester will perform a rigorous self-test (internal battery test, ultrasonic detection and visual/audio test. When one of the test fails, then the tester will lit a red LED and sound three beeps.



Fig. 32.7 Ultrasonic signal emitted by the ULB captured by the ultrasonic transducer

**Table 32.1** Audio and visual feedback of the ULB test

Battery voltage	Ultrasonic signal count	LCD row 1	LCD row 2	LED	Audio beep
2.80–2.97	365–385	Voltage	GOOD	Green LED	1 beep
2.80–2.97	<365, > 385	Voltage	Bad	Yellow LED	2 beeps
<2.80	X	Voltage	Bad	Yellow LED	2 beeps

## 32.5 Conclusion

A ULB tester with more comprehensive result has been designed and built. The tester will test the voltage of the lithium battery and also the emission of the ultrasonic signal with frequency ranging between 36.5 and 38.5 kHz. More important the device designed and built is very compact and also the very easy to use—by pressing the ULB into the slot of the tester—and the result will be displayed on the LCD, LED indicator and also audio beep.

## References

1. US Department of Transportation, Flight Recorder and Cockpit Recorder Underwater Locating Devices. Advisory Circular, AC-21–10A (1983)
2. United Kingdom Civil Aviation Authority, Underwater Sonar Location Device Approval Installation and Maintenance. Specification 12 no. 1 (1974)
3. United Kingdom Civil Aviation Authority, Flight Data Recorder systems Specification 10 no. 2 (1974)
4. Piccinelli, M., Gubian, P.: Modern ships Voyage Data Recorders: A forensics perspective on the Costa Concordia shipwreck. *Digital Investigations* **10**, S41–S49 (2013)
5. Dukane Corporation Seacom Division, Technical Manual Underwater Acoustic Beacon Models DK100/DK120/DK130/DK140 Rev. 13 (2004)
6. SeacomDukane, Technical Manual Underwater Acoustic Beacon Models DK100/DK120/DK130/DK140 Rev. 16 (2009)

# Chapter 33

## 2D CFD Model of Blunt NACA 0018 at High Reynolds Number for Improving Vertical Axis Turbine Performance

Nu Rhahida Arini, Stephen R. Turnock and Mingyi Tan

**Abstract** A 2D CFD model of a modified turbine blade was investigated numerically in this work. The turbine utilized NACA 0018 which had airfoil chord length of 0.75 m and operated at Reynolds number (Re) of  $1.07 \times 10^6$ . The model was simulated using OpenFoam with steady solver named simpleFoam. The aim of airfoil modification was to gain more power by increasing turbine lift force. The increase of lift force was obtained by truncating the trailing edge at 15 % chord length. The investigation of single normal and blunt were conducted prior to evaluation of turbine power. Some CFD simulation parameters were evaluated in the normal single NACA 0018 model and the best parameter combination were decided to resolve the physical turbulence phenomena and the fluid airfoil interaction. The best parameters was chosen by validating the simulation result to some reference data and then assigned to a CFD model of blunt NACA 0018. From the simulation result, it was found that the blunt NACA 0018 had 15.83 % higher lift coefficient than the normal and the turbine power was increase significantly when use blunt airfoil.

**Keywords** 2D CFD model · Blunt airfoil · NACA 0018 · Truncated turbine blade · Renewable energy

### 33.1 Introduction

A preliminary 2D CFD model of single NACA 0018 was investigated in this research. Some CFD parameters were utilized and combined in the simulations to perform turbulence condition in the steady fluid flow. The goal of the research was to provide 2D CFD simulation set-up to model blunt NACA 0018 and compare

---

N.R. Arini (✉) · S.R. Turnock · M. Tan  
Fluid Structure Interactions Group, University of Southampton, Boldrewood Campus,  
Southampton, UK  
e-mail: nra1c12@soton.ac.uk

normal and blunt airfoil simulation result when both were applied in vertical axis turbine design in terms of the power generation. The normal NACA 0018 model had airfoil chord length of 0.75 m, in the fluid flow of 1.4 m/s and associated Re of  $1.07 \times 10^6$ . The investigation was performed by constructing a 2D model in OpenFOAM and simulated using steady state solver, simpleFoam, at  $6^\circ$  angle of attack.

Single airfoil evaluation reveals the interaction between the fluid and structure and establishes the pressure and velocity field in the entire domain. The evaluation can also estimate other fluid dynamic parameter such as force and drag coefficient for predicting airfoil performance. It is hardly possible to evaluate fluid flow analytically because the complex physical fluid flow. However with the helping of major advance in computer technology currently, the fluid flow is possibly resolved, yielding accurate output using CFD method approach. The investigation of NACA 0018 began few decades ago when Sheldahl and Klimas [1] had their experiment. Srivastav [2] used CFD to describe the aerodynamics characteristic of NACA 0018 by applying surface modification using  $k - \omega$  turbulence model. The strong capability of CFD to calculate the physical turbulence phenomena was also implemented in unsteady condition for predicting stall and acoustic area of an airfoil [3, 4].

CFD solves the fluid dynamic formula which was derived from Newton's second law for Newtonian fluids. This formula is one of the basic equations for fluid flow alongside the conservation of mass equation and the energy equation. By calculating the equation in the airfoil vicinity and whole domain, CFD solves pressure and velocity field and force coefficients. Sahin [5] used CFD for observing force coefficient in NACA airfoil and the numerical result gave a good agreement with his experiment. Razak [6] carried out numerical calculations which were in agreement with his experimental data for studying the behavior of airfoil NACA0018 stall flutter which occurred in the condition of separated and reattached flow. The fluid speed and angle of attack were the variables of his study and investigated with the respect to its influence on airfoil cycle oscillation, amplitude and force coefficients.

### 33.2 Computational Fluid Dynamics

In this present work, the CFD model was simulated using openFoam [7] which was based on the finite volume method. Finite volume method discretises a domain into numerous cells and for each cell the Navier-stokes and the mass integral equation are applied. An integral equation calculates flux of a variable in the control volume with an approximation of two levels [8]. The first level approximation calculates variable value from one or more points from the cell face in the boundary surface. Cell values can be approximated in terms of value of the nodal centre thus it needs interpolation to get the values at the cell face.

The interpolation for finding the value on the cell face can be determined using an interpolation scheme such as upwind, linear or other higher order schemes such as QUICK and cubic. Numerical methods for solving the problem of fluid dynamics are complex and consume lots of time because of the number of equations and iterations. The requirement for a high specification and advanced computer becomes a must to acquire accurate and time efficient calculations. The success of a numerical method depends on discretized (meshing), choosing the scheme of interpolation and how the iteration solves the equation. The mesh which had been generated was then simulated using simpleFoam for turbulent, steady state and incompressible cases which was based on the SIMPLE (Semi-Implicit Method for Pressure-Linked Equations) algorithm.

SIMPLE algorithm procedure begins with setting the boundary condition of the problem such as initial condition in the domain including velocity, turbulent kinetic energy and inlet pressure. Other parameter such as density and dynamic viscosity remain constant during the calculation. Next step the solver solves velocity field from the momentum equation for all cell and calculate the mass flux. The result is inputted to find the pressure in the equation. The resulted pressure then is fed back to the mass equation and used to find the velocity value. All parameters from the first calculation are applied in the boundary condition and start the second equation and goes on the iteration until the result become converged. The converged criteria depends on the difference value of the initial value of all the parameter and the value from the previous result (residual factor). All residual factors need to meet convergence criteria simultaneously to provide converged simulation.

In the fluid flow point of view, above certain  $Re$ , fluid flow appears to be unsteady and irregular which is caused by fluctuating and mixing of all three velocity components. However the fluid dynamics equations have to be able to capture the physical phenomena of all cases of which it represents including the turbulence condition. Some turbulence models had been developed based on Reynolds Averaged Navier Stokes (RANS) theory and classified according to additional number of equations being solved in the numerical process. The turbulence models without any additional equation are zero equation model. Spalart-Almaras is the example of one equation turbulence model as it takes one more equation into account. For two equations models,  $k - \epsilon$  and  $k - \omega$  are in the common use. Advance models have been developed following the invention of the super computer such as Large Eddy Simulation (LES) and Direct Numerical Simulation (DNS). LES calculates time dependent flux energy of small eddies and allow the model to capture more detailed phenomena in turbulent flow. DNS provides an exact solution of Navier stokes equation without developing a model for the turbulent fluid flow. In this work, two equations turbulence models were applied ( $k - \omega$  and  $k - \epsilon$ ).



### 33.2.1 2D CFD Model of NACA 0018

In this work, symmetric NACA airfoil was drawn in a 2D model approach using openFoam. 2D airfoil model approach arises as knowing the fact that spanwise velocity is much lower than the streamwise velocity component, hence the  $z$  component could be negligible. From 2D CFD analysis, force components in terms of their coefficients can be calculated. The two force components work on an airfoil are illustrated in Fig. 33.1. The resultant force ( $F$ ) of lift ( $L$ ) and drag ( $D$ ) force is essential parameter as it predominantly affect turbine performance.

### 33.2.2 Airfoil Force and Turbine Power

From the illustration of flow in Fig. 33.1, the flow passes leading edge of an airfoil is brought into rest at the stagnation point and breaks up towards the upper and lower airfoil surface path. Different distance paths at non-zero angle of attacks generates different velocity magnitude for upper and lower surfaces thus producing different total pressures along those surfaces. The upper surface experiences higher velocity therefore the total pressure is smaller (negative pressure) than the lower one. Combining the total pressure force for upper and lower surface creates a lift force of an airfoil. The lift force is accompanied by drag force to build up the force resultant which is adopted for harnessing renewable energy in a turbine operation.

A turbine fundamentally is a device which extracts energy from renewable resources by converting its kinetic energy to electricity. A tidal turbine works with the same mechanism as a wind turbine except to operate in about nine hundreds denser fluid. It needs a large amount of driven force to start rotating and maintain the rotation stable. The tides motion rotates the turbine blade which is coupled to an electricity generator. The rotation of tidal turbine mainly is driven by lift force therefore the more lift force can be generated on the blade the more power is obtained by the turbine. The amount of power generated by the turbine is proportional to lift force times the tangential turbine velocity.

**Fig. 33.1** Force components work on an airfoil [9]

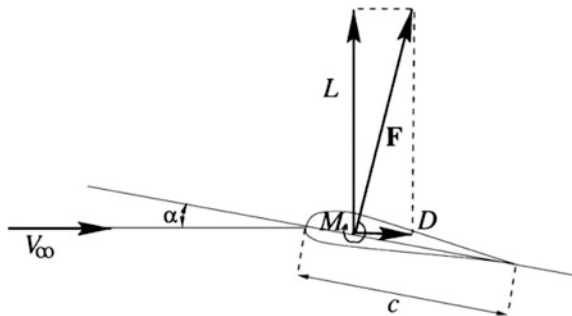
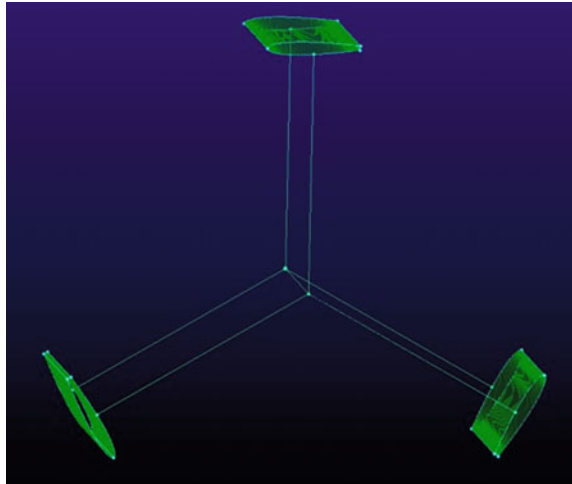


**Fig. 33.2** Vertical axis tidal turbine design



Darrieus vertical axis tidal turbine was designed based on previous research [10] and its power associated with normal and blunt trailing edge was evaluated. The turbine utilized three NACA 0018 blades which were arranged symmetrically as illustrated in Fig. 33.2. The blades were geometrically attached at centre of turbine hub, normal to the chord length at which tangential velocity vector exerts. All blades were assumed to produce the same amount of power thus the evaluation was conducted only in one airfoil at the same single airfoil simulation angle of attack. Turbine power was induced by turbine rotation which was driven by lift force. It is an indicator of how much renewable energy could be harnessed from a tidal turbine and mathematically expressed by a dot product of resultant force vector and turbine velocity vector. The tip speed ratio and solidity of turbine were 6 and 0.19 respectively [11] which gave turbine radius and angular velocity of 2 m and 4.2 rad/s. The span of a turbine blade was 1 m long.

### 33.2.3 Numerical Parameters

Twelve different models were developed and simulated from the combination of two different mesh topologies, two turbulence models, and two types of interpolation scheme and eventually validated using Weller [12] data.

The parameter used in seven different cases were C-grid structured and snappyHexMesh for mesh topology,  $k - \omega$  and  $k - \epsilon$  for turbulence model, and upwind, QUICK, and cubic for interpolation schemes. The topology of C-grid and snappyHexMesh on the airfoil vicinity and whole domain are drawn in Figs. 33.3 and 33.4 respectively.

Eleni et al. [13] simulated models of an airfoil with C-structured grid which showed that independent mesh simulation was performed when number of cell

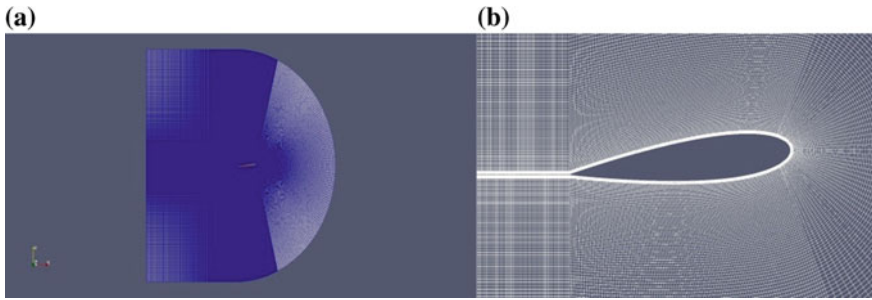


**Fig. 33.3** Mesh topology of C structured grid, **a** whole domain, **b** around airfoil

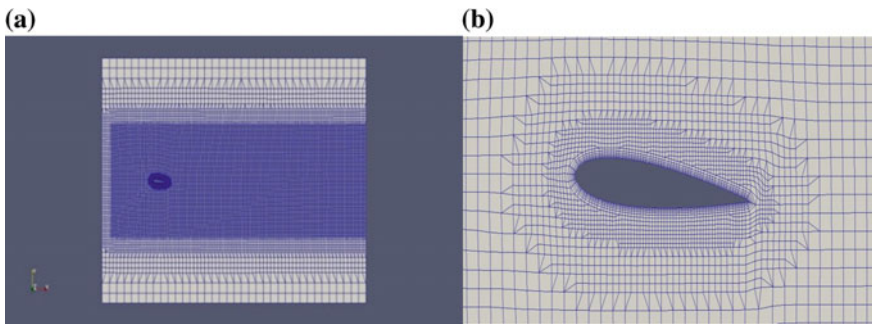


**Fig. 33.4** Mesh topology of snappyhexmesh, **a** whole domain, **b** around airfoil

reached 80,000. In C structured grid topology, airfoil mesh was generated with 10 boundary layers in 0.01 m height. The inlet radius curvature of the domain where the flow came in was  $17c$  which was also the same length as the outlet height. There were 100 points in the lower and upper part of the airfoil with equal distribution. For far region from boundary layer and downstream direction behind the trailing edge region, 200 and 800 nodes were developed with the growth rate of 0.01 for vertical direction (far region) and 0.25 for horizontal direction (downstream behind the trailing edge). The front angle was  $65^\circ$  with the equal distribution along the curvature line. In the snappyHexMesh topology, number of boundary layers was 6 with the expansion ratio of 1.3.

### 33.3 Result and Discussion

The investigation of simulation parameters for normal NACA 0018 model is discussed first followed by the simulation of blunt NACA 0018 using the chosen parameter from normal airfoil simulation and eventually the model of vertical axis will be observed.

### 33.3.1 Normal NACA 0018

Simulation result of lift coefficient (Cl) is presented in the Table 33.1. Each grid was simulated with two different turbulence models which were  $k - \omega$  and  $k - \epsilon$  and for the each variation the model took three different interpolation schemes (upwind, QUICK and cubic). The lift coefficient then was validated with experimental data [12] and the best combination parameters which had least error were chosen to model blunt airfoil.

The lift coefficients for all simulations are listed in Table 33.1 except for simulations using QUICK interpolation schemes as those were crashed with the chosen generated mesh. The failure was likely because of QUICK sensitivity to interpolate the diffusion term although it was accurate for convective term of the fluid momentum equation. In general lift coefficient which was simulated from C structured grid topology showed less error than snappyHexMesh because the better ability of cell arrangement in structured than unstructured grid (snappyHexMesh). In structured grid cells which were generated from hexahedral shape, were well organized thus suitable for regular object. Total number of cells in the model was 781,121 which exceeded the required number for independent mesh [13].

From Table 33.1, it can be found that all simulations which run with  $k - \epsilon$  turbulence model showed less error as  $k - \epsilon$  gave better prediction in far region while  $k - \omega$  resolved accurately in boundary layer field. For large boundary layer thickness ( $y^+ > 30$ ) the simulation took wall function into account, and for that condition  $k - \omega$  was less accurate to predict the turbulence condition near the wall. Cubic interpolation schemes gave more precise result than upwind but had less residual value which made all the simulation not converged after 5000 iterations. On the other hand, upwind interpolation brought the simulation to converged condition which was specified by  $10^{-5}$  residual of  $p, v, k, \omega$ .

On the airfoil surface the highest pressure took place in the stagnation point which laid in the lower surface at leading edge. The upper pressure profile appeared to have negative pressure while on the other hand it occurred to be positive in the lower part of an airfoil. The total pressure distribution of the lower and upper part of

**Table 33.1** Lift coefficient from simulation

Grid	Turbulence model	Interpolation scheme	Cl	Error (%)
C-structured	$k - \epsilon$	upwind	0.585	3
		cubic	0.593	1
	$k - \omega$	upwind	0.561	6
		cubic	0.569	5
snappyHexMesh	$k - \epsilon$	upwind	0.574	4
		cubic	0.548	9
	$k - \omega$	upwind	0.570	5
		cubic	0.561	6
Weller			0.600	

the airfoil developed a lift force. If more negative pressure occurred in the upper part or more positive pressure occurred in the lower part, higher lift was created. In the stagnation point of the velocity, the velocity magnitude reached zero because the fluid hit the airfoil surface. As it went along further downstream, the velocity magnitude increased both in the upper and the lower surface however the upper had a higher velocity than the lower surface.

### 33.3.2 CFD Model for Blunt Airfoil

The blunt NACA 0018 model was designed with 15 % of chord length truncation [14] and operated in Re of  $1.07 \times 10^6$ . The truncated airfoil were simulated using best combination from the preliminary investigation which took C-structured grid,  $k - \epsilon$  turbulence model and upwind interpolation scheme. The mesh around blunt airfoil is shown in Fig. 33.5a.

Total number of cells in the model was 827,579 which exceeded the required number for independent mesh [13]. The diameter of the front side where the incoming fluid passed, was  $17c$  to avoid blockage effect during simulation. The mesh was occupied by ten subdomains composed from hexahedral cells. The mesh adjustment can be set up from the number of points in the leading edge angle, upper and lower surface of the airfoil, streamwise connector behind the trailing edge and vertical direction for all over the domain. Behind the trailing edge, mesh was refined to resolve the turbulence fluid flow condition which was apparently crucial region as the effect of truncation. That mesh was arranged from 30 layers with the same distribution in vertical direction and growth ratio of 0.01 at streamwise points which was denser toward the trailing edge.

Pressure coefficient for both airfoil are depicted in Fig. 33.5b. From that picture, it can be seen that blunt airfoil had higher pressure coefficient magnitude than normal one which created higher lift. From the pressure coefficient, the velocity profile can also be deduced which are proportional to the  $C_p$  magnitude. The  $C_p$

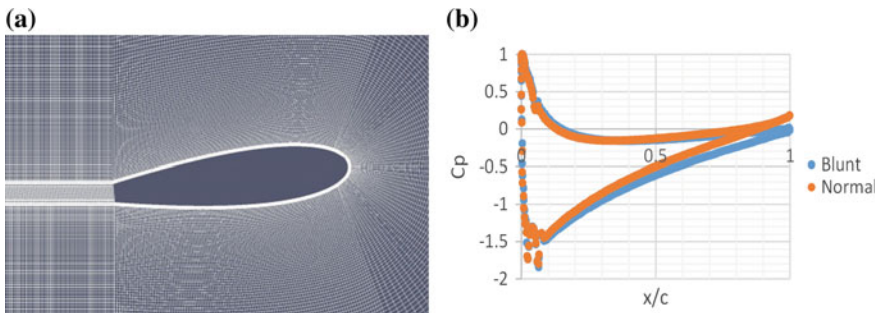


Fig. 33.5 a Blunt airfoilmesh, b Pressure coefficient of blunt and normal airfoil

magnitude of blunt airfoil in general along the upper and lower surface was higher than normal which indicate the velocity profile on the blunt airfoil surface increase. The velocity increase was the influence of the sudden profile change in the trailing edge as the effect of truncation. The flow was accelerated and affected to all surface velocity. The lower minimum pressure in upper surface of blunt airfoil contributed to higher lift force comparing to normal NACA 0018 thus resulting higher lift coefficient. From the simulation the Cl value reached 0.678 which was 15.83 % increase from the normal NACA0018. The fluid behind the trailing edge was regular, smooth and no vorticity was found as the airfoil was immersed at very low angle of attack.

### 33.3.3 Turbine Power

From normal and blunt simulation, drag force was also calculated which gave 0.045 for normal and 0.044 for blunt NACA 0018. The power extracted from the normal and blunt airfoil which was designed as explained above, were 234.23 W and 320.89 W. From the calculation it can be found that blunt airfoil produce higher lift and drag force than normal NACA 0018. However the use of blunt airfoil was still advantageously as the power extracted was increase to 37 %.

## 33.4 Conclusion

From the simulation result, it can be concluded that the best combination for modelling the normal NACA 0018 in steady flow was using C-structured grid mesh,  $k - \omega$  turbulence model and cubic interpolation scheme. The best combination gave least error as the mesh was more organized in space and the turbulence model was better to resolve the turbulence phenomena particularly in the trailing edge region where generally the vorticity appears. The result was implemented to predict blunt airfoil performance and found 15.83 % of Cl increase than the normal airfoil.

## References

1. Sheldahl, R.E., Klimas, P.C.: Aerodynamics characteristics of seven symmetrical airfoil sections through 180-degree angle of attack for use in aerodynamic analysis of vertical axis wind turbines. Sandia National Laboratories Energy Report, National Technical Information Service. U.S Department of Commerce (1981)
2. Srivastav, D.: Flow control over air foils using different shaped dimples. In: International conference on fluid and thermodynamics technologies (FDTT 2012). IPCSIT, 33, IACSIT (2012)

3. Gharali, K., Johnson, D.A.: Dynamic stall simulation of a pitching air foil under unsteady freestream velocity. *J. Fluids Struct.* **42**, 228–244 (2013)
4. Gloerfelt, X., Le Garrec, T.: Trailing edge noise from an isolated airfoil at a high Reynolds number. In: 15th AIAA/CEAS Aeroacoustics conference (2009)
5. Sahin, I., Acir, A., Numerical and experimental investigation of lift and drag performances of NACA 0015 wind turbine air foil. *Int. J. Mater. Mech. Manuf.* **3**(1) (2015)
6. Razak, N.A., Andrienne, T., Dimitriadis, G.: Bifurcation analysis of a wing undergoing stall flutter oscillating in a wind tunnel. In: ISMA—International Conference on Noise and Vibration (2010)
7. OpenFoam Foundation: The Open source CFD Toolbox, user guide, openFoam. <http://www.openfoam.org/docs/user/tutorials.php> (2015). Accessed March 2015
8. Ferziger, J.H., Peric, M.: *Computational Methods for Fluid Dynamics*, 3rd edn. Springer, Berlin (2002)
9. Hansen, M.O.L.: *Aerodynamics of Wind Turbine*, 2nd edn. Earth-scan, London (2008)
10. Arini, N.R., Ariwibowo, T.H., Nugroho, S.: Fluid dynamic analysis on vertical axis tidal turbine design for predicting its performance for Indonesian ocean. *Int. J. Appl. Eng. Res.* **9**(2), 15159–15166 (2014)
11. Gosselin, R., Dumas, G., Boudreau, M.: Parametric study of H-Darrieus vertical axis turbines using uRANS simulations. In: 21st annual conference of the CFD society of Canada (2013)
12. Weller, T.: Two dimensional low Reynolds number wind tunnel results for airfoil NACA 0018. *Wind Eng.* **32**(6), 525–537 (2008)
13. Eleni, D.C., Athanasios, T.I., Dionissios, M.P.: Evaluation of the turbulence models for the simulation of the flow over a NACA 0012 airfoil. *J. Mech. Eng. Res.* **4**(3), 100–111 (2012)
14. Ramjee, V., Tulapurkara, E.G., Balabaskaran, V.: Experimental and theoretical study of wings with blunt trailing Dede. *J. Aircr.* **23**(4), 349–352 (1986) (Aerospace Research Central)

## Chapter 34

# Recycling of the Ash Waste by Electric Plasma Treatment to Produce Fibrous Materials

S.L. Buyantuev, A.S. Kondratenko, E.T. Bazarsadaev  
and A.B. Khmelev

**Abstract** The article presents the results of processing of technogenic waste ash and slag in arc plasma. It performs calculations of the reactor core power generation capacity of the current density and voltage gradient. When calculating the diameter of the reactor chamber is adopted for determining the size and all the basic laws of the electric band are expressed through it. Research performed by methods of X-ray energy dispersive spectral analysis and electron microscopy. Experiments without additional charging melting ash show high refractoriness (above 2000 °C) and viscosity during processing, so to reduce the melting temperature and reducing energy required additional charging dolomite ( $\text{CaCO}_3$ ) to obtain homogenous melts for subsequent production of the melt and fiber materials its basis. Melting additional charging wastes conducted with 10–30 %  $\text{CaCO}_3$  were investigated, thereby reducing melting time and thereby reduce energy costs in the future to receive fibers from the melt. When additional charging melting ash with 10 %  $\text{CaCO}_3$  was observed a small gassing, approximate energy consumption for production of 1 kg of the melt was 4 kWh/kg. Melting additional charging with 20 %  $\text{CaCO}_3$  further reduce the melting time by 25 % and reduce energy consumption to 2.8 kWh/kg, the process was easy to moderate gassing. Additional charging 30 %  $\text{CaCO}_3$  and increased melting time respectively (compared with 20 % additional charging) energy to 3.4 kWh/kg, the melting took place violently with strong gas formation. Thus, the experimentally found optimum concentration additional charging make 20 %  $\text{CaCO}_3$ . There is present the principle possibility of melting the wastes with additional charging dolomite ( $\text{CaCO}_3$ ) to produce a melt thereof and generation of thin mineral wool as a component of composite materials, and insulating materials for the fibrous structure.

---

S.L. Buyantuev (✉) · A.B. Khmelev  
East Siberian State University of Technology and Management, Ulan-Ude,  
Buryat Republic, Russia  
e-mail: buyantuevsl@mail.ru

A.S. Kondratenko · E.T. Bazarsadaev  
Buryat State University, Ulan-Ude, Buryat Republic, Russia



**Keywords** Arc plasma · Plasma reactor · Slag waste with additional charging · Dolomite · Mineral melt · Fiber melt · X-ray spectral analysis · Surface microscopy

## 34.1 Introduction

The need for a variety of industries in mineral fiber materials is constantly increasing. For the production of mineral fibers is appropriate to use technological wastes resulting from the combustion of solid fuel, in connection with the fact that the formation of technogenic waste has been increasing significantly in the future, which contributes to a steady accumulation of [1, 2]. Recycling of solid waste in technogenic fiber materials is an important scientific and technical challenge, as these types of wastes have high melting point, so it can not be used for the production of mineral wool by known melting units (cupola furnaces, tank furnaces, etc.) [3].

Throughout the world, researchers are working to obtain mineral fiber materials with high physical-chemical and mechanical properties. In addition to the requirements of GOST to produce the quality of fibrous materials, it has always been a problem of reducing the energy consumption and the cost of production of these materials. The solution to these complex and sometimes controversial issues requires a preliminary experimental and theoretical studies of raw materials in order to develop practical recommendations for the production of fibrous materials using modern achievements of science and new technical solutions [4].

One promising direction in this area is the use of a plasma arc to melt the raw material to produce heat-insulating fiber materials. When it is used as a thermal energy source of the electric arc due to the high temperature, it sharply decreases during melt preparation due to the elimination of the induction period melting point [5].

## 34.2 The Experimental Setup and Methods of Research

Our research on the production of the melt and fibers from industrial waste used an experimental setup as shown schematically in Fig. 34.1 [1, 5]. The advantage of this reactor is that the combination of zones of allocation of thermal energy and its absorption during the flow of the process, provides an intensification of heat and mass transfer arc plasma heated material in the reaction chamber through the creation of a solid in the reactor chamber area—plasma volume, filling her cross section. All this is accompanied by the presence of a reaction volume in a sufficiently high concentration level of power and temperature, which reduces the time of melting the treated material [6].

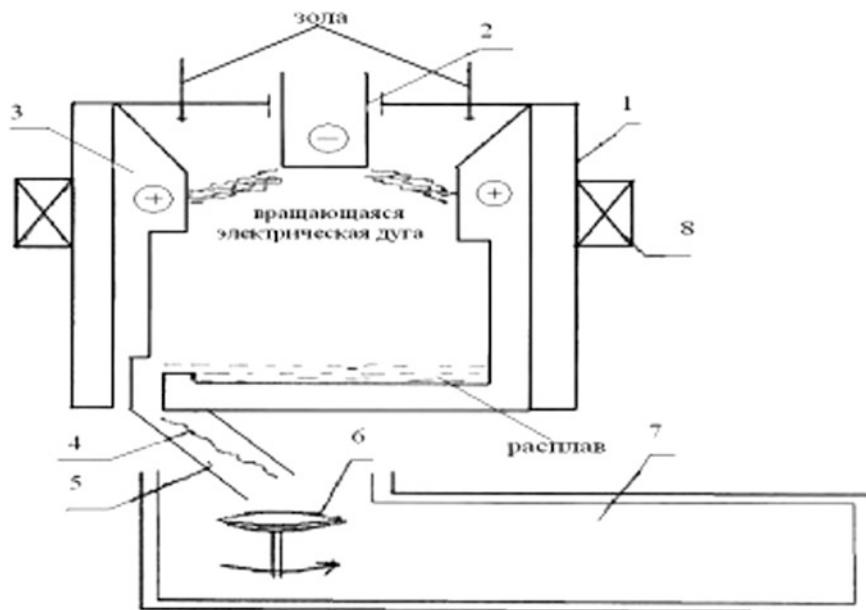


**Fig. 34.1** Experimental setup for melting raw materials. 1—plasma reactor; 2—core graphite cathode; 3—graphite anode; 4—melt; 5—a tray for transporting the melt; 6—rotating disk; 7—fiber deposition chamber; 8—electromagnetic coil

In the chamber of the plasma reactor core 1 between the cathode 2 and the housing 3 is burning electric arc. Electromagnetic coil 8 creates a magnetic field. Under the action of the arc Lorentz force moves in the electrode gap, overlapping section of the chamber high temperature region. When moving arc column due to the difference in aerodynamic drag and the wall of the arc electrodes extend and in which there are high-speed plasma flows toward the wall of the chamber 3.

The arc of the reactor type described in the camera administered electric arc power is converted into heat. Thus, the arc zone is a zone for generating thermal energy, its absorption, it covers the entire section of the chamber, allows adjustment of the melting time of the processed material, the concentration of power, and hence temperature. This area is limited in height planes perpendicular to the chamber axis and passing through the electrode end (top), and through the middle of an electromagnetic-solenoid coil (lower) [7, 8]. Thermal energy generated in the vicinity of the rotating arc while stirring the melt and thereby distributed throughout its volume.

The power generation area is calculated based on the terms of its distribution uniform. When calculating the diameter of the reactor chamber accepted for determining the size and all the basic laws of the electric band are expressed through it. This makes it possible to extend the experiment results obtained in small

reactors, geometrically similar to the reactors of high power and hence a large diameter chamber [9, 10].

Reactor current  $I_p$  is expressed by current density, referred to the cross-sectional area chamber. The calculated values were as follows: diameter of the chamber  $D_k = 15$  cm; arc current  $I_p = 200$  A, respectively:

$$I_p = \Delta i_p \pi D_k^2 / 4 \quad (34.1)$$

Accordingly, the current density  $\Delta i_p = 4 I_p / \pi D_k^2 = 1,132$  A/sm<sup>2</sup>. Power of reactor  $U_p = 200$  Vis a voltage gradient across the electrode gap:

$$U_p = E_p D_k / 2 \quad (34.2)$$

Here  $D_k/2$ —interelectrode gap, which include arc voltage, to determine the voltage gradient (in the reactor core at the cathode). Accordingly, the voltage gradient  $E_p = 2 U_p / D_k = 26,7$  V/sm.

As a result, taking into account the expressions for  $I_p$  and  $U_p$  derive the formula for the power reactor:

$$P_p = U_p * I_p = \pi / 4 * 1/2 E_p \Delta i_p D_k^3 \approx 0,39 E_p \Delta i_p D_k^3 \quad (34.3)$$

Which is equal to:  $P_p \approx 0,39 E_p \Delta i_p D_k^3 = 0,39 * 26,7$  V/sm \*  $1,132$  A/sm<sup>2</sup> \*  $(15)^3$  cm<sup>3</sup> = 40 kw.

As a result of reforms concluded that the amount allocated in the area of generating thermal power equal to input electrical power is proportional to the cube of the diameter of the chamber, it is also proportional to the current density of  $\Delta i_p$  and a voltage gradient of  $E_p$  or different volume capacity  $P_p$ , allocated in the area. The value of  $P_p$  determines the temperature level is, obviously, a constant for the production of geometrically similar to the reactors:

$$P_p = \text{const} \quad (34.4)$$

Consequently, it is possible to adopt constants  $\Delta i_p$  и  $E_p$ :

$$\Delta i_p \approx \text{const} \quad (34.5)$$

$$E_p \approx \text{const} \quad (34.6)$$

A value of  $\Delta i_p \equiv I_p / D_k^2$  is determined using models [11]. The conditions of process parameters at a high plant capacity. Then, for a given diameter of the reactor provides a selection of its current value.

### 34.3 Results and Discussion

The work was carried out to study the material composition of the resulting ash waste melt and mineral fibers using electric arc plasma reactor of the combined type. The study was conducted by the method of energy dispersive X-ray spectral analysis followed by identification of the spectra.

For the processing to obtain the melt and fibers, we used technological slag waste following elemental composition (Table 34.1) derived from the combustion of coal.

The experiments of melting ash showed its high refractoriness (above 2000 °C) which is measured by a high-temperature optical pyrometer neighbor (>1 micron) IR and viscosity. To reduce the melting temperature and energy, it demands additional charging ( $\text{CaCO}_3$ ) to obtaining homogenous melt for subsequent generation of the melt and the fibrous materials based on it.

The purpose of the task is to solve for the maximum use of technogenic slag waste. Originally studied showed that the possibility of melts with a mass content of ash components: additional charging 50:50 Principal possibility of melting these compositions. Table 34.2 shows the material composition of the resulting melt. Elevated levels of calcium, indicating a low acidity module, as well as the presence of the crystalline compound—calcium metasilicate  $\text{CaSiO}_3$ , the carbon content of the melt in the melting explained arc gap graphite reactor followed by diffusion electrode erosion products.

Get the fiber at these concentrations the composition failed to haunt the high content of calcium in the melt leads to the formation metasilicate  $\text{CaSiO}_3$ . Therefore, guided by tasks and obtained preliminary data, the melting of waste carried out in the range of mass concentrations of 10–30 %, thereby reducing the melting time and energy costs will avoid the formation of metasilicate, due to it continue to receive the fibers from the melt.

The melting ash with additional charging 10 % of dolomite melt was obtained with the following material composition (Table 34.3). Figure 34.2 shows the

**Table 34.1** Elemental composition of ash waste

O	Na	Mg	Al	Si	K	Ca	Ti	Fe	Result
52.1	0.37	0.44	7.3	34	0.87	1.63	0.31	3.07	100.00

**Table 34.2** Elemental composition of ash composition: dolomite 50:50

C	O	Na	Mg	Al	Si	K	Ca	Ti	Fe	Result
5.83	44.57	0.39	0.68	9.23	17.61	0.74	17.62	0.65	2.70	100.00

**Table 34.3** The elemental composition of ash composition: dolomite 90:10

O	Na	Mg	Al	Si	K	Ca	Ti	Fe	Result
50.39	3.36	0.96	12.96	23.73	1.11	2.65	0.93	3.91	100.00

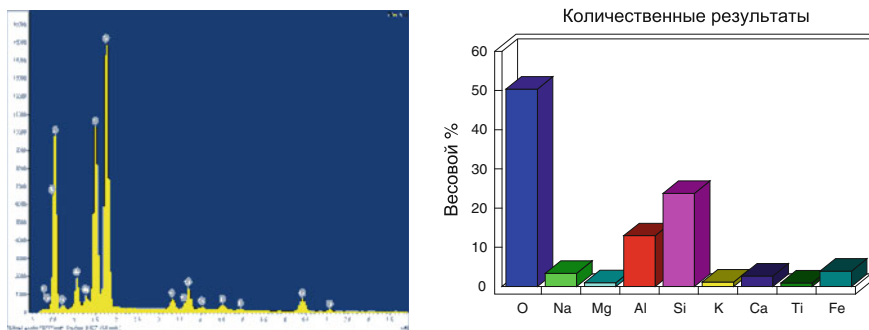


**Fig. 34.2** Spectral distribution line elements in the melt and mass concentration

spectral lines of the elements and their content by weight. Melting passed quietly with a small gassing, approximate energy consumption for production of 1 kg. Melt was 4 kWh/kg. When pumping the melt was held stretch fibers, the fine fibers obtained having compositions shown in Table 34.4.

Subsequently additional charging was increased by 10 % (to 20 %). This will further reduce the melting time by 25 % and reduce power consumption up to 2.8 kWh/kg. Melting also carried out calmly with moderate gassing. Figure 34.3 shows the spectral lines of the elements and their weight content, and Table 34.5 the material composition of the melt. When pumping the melt extrusion was carried out fibers and their characteristics are given in Table 34.6.

**Table 34.4** The elemental composition of fibers with a mass concentration of ash dolomite 90:10

O	Na	Mg	Al	Si	K	Ca	Ti	Fe	Result
61.01	0.72	0.99	11.25	19.84	0.56	3.14	0.53	1.95	100.00

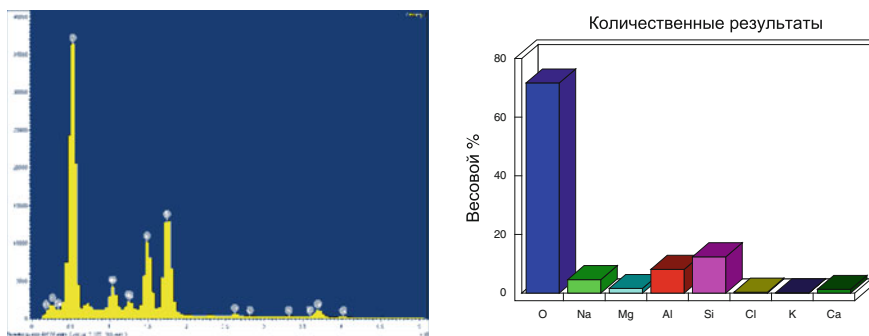


**Fig. 34.3** The spectral distribution line elements in the melt and mass concentration

**Table 34.5** The elemental composition of ash composition: dolomite 80:20

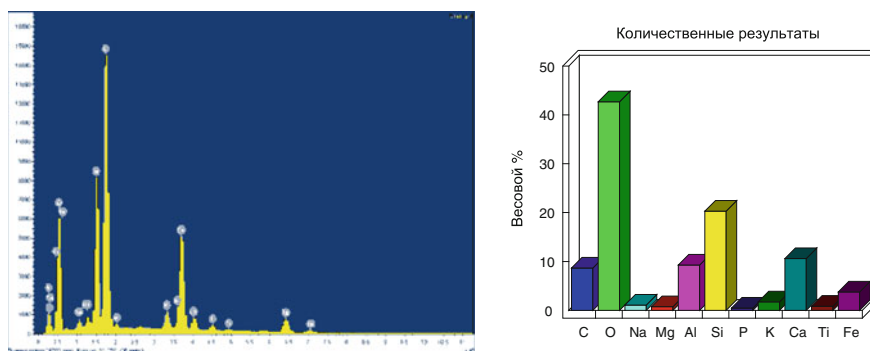
O	Na	Mg	Al	Si	K	Ca	Ti	Fe	Result
52.03	2.46	0.98	9.96	20.7	1.34	7.65	0.67	4.21	100.00

**Table 34.6** The elemental composition of fibers with a mass concentration of ash dolomite 80:20

O	Na	Mg	Al	Si	K	Ca	Ti	Fe	Result
57.62	0.71	0.78	10.60	19.32	0.82	7.74	0.50	1.92	100.00

At the final stage additional charging concentration was 30 %. Here, however, the melting time and increase, respectively (compared to 20 % additional charging) energy to 3.4 kWh/kg. Melting held violently with strong outgassing. Figure 34.4 shows the spectral lines of the elements and their weight content, and Table 34.7 material composition of the melt. When pumping the melt extrusion of fibers are also carried out, their characteristics are shown in Table 34.8.

As can be seen from the tables, the change in the concentration of additional charging melts will yield significant impact on the process of melting and energy indicators.

**Fig. 34.4** Spectral distribution line elements in the melt and mass concentration**Table 34.7** The elemental composition of ash composition: dolomite 70:30

C	O	Na	Mg	Al	Si	K	Ca	Ti	Fe	Result
8.66	43.12	1.06	0.74	9.28	20.28	1.72	10.58	0.83	3.75	100.00

**Table 34.8** The elemental composition of fibers with a mass concentration of ash dolomite 70:30

C	O	Na	Mg	Al	Si	K	Ca	Ti	Fe	Result
6.32	50.92	0.35	0.71	9.41	19.10	0.58	9.69	0.58	2.36	100.00

## 34.4 Conclusion

We have presented arc melting reactor, which is a type of plasma reactors allowed to smoothly adjust the temperature of the melt and maintain the output stream from the tap hole, which made it possible to reduce the viscosity and increase the melt flow rate. It can be recommended that ash waste process electric arc plasma method in the melt with mass content of the waste components/dolomite is 90:10 or 80:20. It will provide the mineral casting and fine fiber as a component of composite materials, as well as for thermal insulation materials fibrillation [12–15].

## References

1. Buyantuev, S.L., Sultimova, V.D.: Production of thermal insulating materials from ash waste tpp using low-temperature plasma. *Constr. Mater.* **10**, 51–53 (2004)
2. Popov, V.V.: *Materials for Thermal Insulation Works*. M., pp. 20–37 (1978)
3. Chaus, K.V., Tchistov, U.D., Labzina, U.V.: Technology of production of building materials, products and designs. In: M. Stroyizdat (ed.) p. 478 (1988)
4. Spirin, Y.P., Ustenko, A.A., Volodin, M.N.: Some of the performance of the insulation wool. *Constr. Mater.* **6**, 24–25 (1968)
5. Buyantuev, S.L., Sultimova, V.D.: The Use of Low-Temperature Plasma for Fibrous Insulation Materials from Slag Waste of Thermal Power Plants, p. 132. ESSTU, Ulan-Ude (2010)
6. Buyantuev, S.L.: Insulation Materials Fibrous Structure of Melts Rocks and Ash And Slag Waste of Technogenic: a Monograph. In: Buyantuev, S.L., Kondratenko, A.S. (eds.) p. 180. ESSTU, Ulan-Ude (2014)
7. Buyantuev, S.L., Sultimova, V.D., Dondokov, A.T., Volokitin, G.G., Zyachanov, M.E., Tsyrenov, S.A.: Production Of Heat-Insulating Building Materials Using Electric Plazma Processing, Building Complex of Russia: Science, Education, Practice: International scientific and practical conference, pp. 90–93. Ulan-Ude (2006)
8. Jukov, M.F.: *Electric Arc Gas Heaters (Plasma Torches)*, Jukov
9. Smolyakov, M.F., Uryukov, V.Y., Nauka, B.A.: p. 232 (1973)
10. Bron, O.B.: The movement of the electric arc in the magnetic field. *Electricity* **7**, 76–81 (1966)
11. Buyantuev, S.L., Kondratenko, A.S.: The physical model of the electric zone in a plasma reactor of the combined type. *Vestn. BSU* **3**, 114–119 (2013)
12. Sergeev, P.V.: *The Electric Arc In Electric Reactors*, p. 140. Alma-Ata, Nauka (1978)
13. Kondratenko, A.S.: The Insulation Material of the Fibrous Structure of the Basalt and Ash Waste Produced Using Electromagnetic Reactor, Abstract of diss, for the degree of candidate of technical sciences, p. 22. Ulan-Ude (2013)
14. Zyablitsky, A.V., *Theoretical Basis Spinning*, M.: Chemistry, p. 503 (1979)
15. Bobrov, Y.L., Ovcharenko, E.G., Shoikhet, B.M., Petukhova, E.Y., *Thermal Insulation Materials and Construction*, p. 268. M.: INFRA-M (2003)

# Chapter 35

## Performance Evaluation of Welded Knitted E-Fabrics for Electrical Resistance Heating

Senem Kursun Bahadir, Ozgur Atalay, Fatma Kalaoglu,  
Savvas Vassiliadis and Stelios Potirakis

**Abstract** This paper presents a study conducted on electrical resistance heating of knitted e-fabric structures including silver plated conductive yarns. The study further investigates the application of ultrasonic welding technology on these knitted e-fabrics in order to see their effect on heating performance. Thermal analysis was carried out under different voltage values to observe temperature variations over the knitted e-fabrics. It was found that the linear resistance of conductive yarns and its interaction with voltage values considerably affect the temperature as well as heating performance of the e-fabrics. In addition, ultrasonic welding parameters also need to be carefully controlled in order to obtain sufficient heating performance.

**Keywords** Conductive yarns · Electrical resistance heating · E-textiles · Knitted fabrics · Ultrasonic welding

### 35.1 Introduction

Electrical resistance heating is any process in which electrical energy is transferred to heat. When electric current passed through a conductive material, the resistance it encounters leads the material to heat up. The current depending on the resistance of material flows from one electrode to another causing conversion of electrical energy into heat and directs that heat into the space to be warmed. If the current is passing through the fabric structure, in that case fabric becomes heated. Depending on

---

S.K. Bahadir · O. Atalay (✉) · F. Kalaoglu  
Department of Textile Engineering, Istanbul Technical University,  
Beyoglu, 34437 Istanbul, Turkey  
e-mail: atalayoz@itu.edu.tr

S. Vassiliadis · S. Potirakis  
Department of Electronics Engineering, T.E.I. Piraeus, Egaleo, 12244 Athens, Greece



the fabric structure and the used materials as well as power source and system configuration, the heating capacity of the fabric changes. Uniform distribution and dissipation of heat are unique characteristics for performance of the heating structures that should be well controlled by the location of heating elements in a close proximity to the heated area. As a fabric heating element, one possible option is to use conductive yarns inside the fabric structure in order to develop electrical circuit in the fabric.

Electrical circuits in the textile structures for different applications have been obtained through several methods such as direct insertion of conductive yarns, while weaving or knitting processes; depositions of electro-conductive thin layers on flat textile surfaces; overprinting or coating of conductive materials/polymers like polypyrrole, polyaniline, polythiophene, etc., as well as metal particles, carbon nanotubes and carbon black particles on flat textile surfaces, and direct insertions of conductive yarns through sewing or embroidery methods [1–5]. The conductive materials inside the fabric structure have electrical resistance. Thus, they can be used as electrical resistance for heating applications. However, the selection of the appropriate conductive yarn with a base yarn is a crucial issue since the voltage applied on the conductive yarn causes fabric to be heated and in case of excessive current, heat may lead to damage or burning of the fabric. In order to increase the durability of the structure as well as prevention of probable short circuits inside the fabric, welding techniques can be used.

Fabric welding is a kind of process to join the fabric pieces using heat, pressure and/or ultrasound. Thermoplastic fabrics with a higher synthetic composition ratio are generally used to obtain welded fabrics. In general, polyvinylchloride (PVC), polyurethane (PU), polyethylene fabric (PE) and polypropylene (PP) are used for heat sealing. Welding of fabrics can present highly functional effects such as water resistant, abrasion resistant at the seam, resistant to thread decay and fine appearance which are the most challenging issues in the area of e-textiles. The conductive yarns placed in the fabric structure should be protected from the environmental effects in order to increase their durability and reliability. In addition, in case of water contact they should not cause short circuit since in the presence of water or even moisture in electrical applications, leakage current may appear. In fact, water conducts electricity and when there is a wet area, a current will flow between the contacts. Therefore, this is extremely important to protect the e-textile circuit from water contact. This problem can be avoided using welding tapes over the e-textile circuits.

The literature review concerning weld-line formation on textiles mainly focus on the quality of the welded seams. For instance; in their study, Kakubcionien et al. examined the quality of hot welded seams using the thermoplastic tape and reported that the quality of fabric bonding depends on the proper selection of the welding parameters [6, 7]. There are also some studies focusing on ultrasonic welded seams [8]. One of the studies indicated that due to the thicknesses of the layers, some of the ultrasonic welded seams are of insufficient quality in terms of bonding strength [9]. Further, the effects of vibration welding parameters have also been studied regarding the qualities of those joins made of polyamide 6.6 [10]. In the literature, a handful of

attempts can be observed regarding the issue of using welding technologies within the textile area and their effective parameters on textile joining. However, less attention has been paid to use of welding techniques in e-textile researches. Moreover, with regard to fabric based electrical resistance heating, a few studies showed the implementation of conductive yarns inside the fabric structures for heating applications. Hamdani et al. [11] studied the thermo-mechanical properties of knitted structures designed by using silver-coated Nylon 6.6 filaments. Similarly, Sezgin et al. investigated the heating behavior of silver conductive threads through woven structures [12]. Apart from these studies, Kayacan et al. used stainless steel yarns in a knitting structure in order to obtain heating panels [13].

In this study, electrical resistance heating performances of knitted fabrics containing silver plated conductive yarns have been studied. As a contribution to the literature, this research work offers the application of ultrasonic welding technology on these knitted fabric structures for the formation of heating panels. In the study, the silver plated yarns were connected to power supply and the resulting temperature rise of the fabric heating panels was measured with a temperature sensing device. Moreover, the welded samples are compared and discussed for heating performance with the knitted samples regarding the various aspects of conductive yarns.

## 35.2 Experimental Work

### 35.2.1 Materials

In this study, to test the electrical resistance heating of e-fabrics, two silver conductive yarns with different electrical linear resistances were used to form electrical circuits in knitted fabric samples. The linear resistance of the conductive yarns was measured in ohm per meter (ohm/m) using a TTi 1906 computing multimeter. Meta-aramid/lycra and polyamide covered lycra yarns were used to form an insulating area in the structure. The samples were produced by Shima Seiki SES124-S 12GG flat knitting machine. Details of these materials are listed in Table 35.1.

**Table 35.1** Materials used in the study

Role of yarn in the fabric	Material type	Yarn count	Linear resistance (ohm/m)
Conductive	Silver coated PA	235 dtex	235
Conductive	Silver coated PA	235 dtex × 4	50
Non conductive	PA covered lycra	576 dtex	–
Non conductive	PA covered lycra	800 dtex	–
Non conductive	Meta-aramid (100 %)+lycra	166 dtex + 70 denier	–

**Fig. 35.1** Model image of knitted e-fabric structure

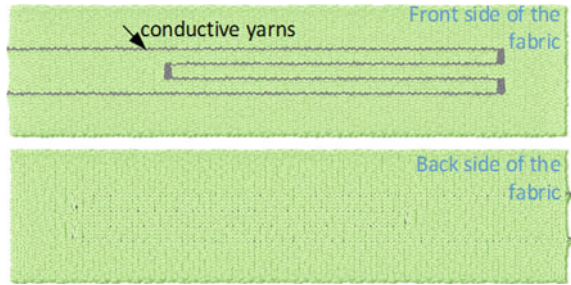
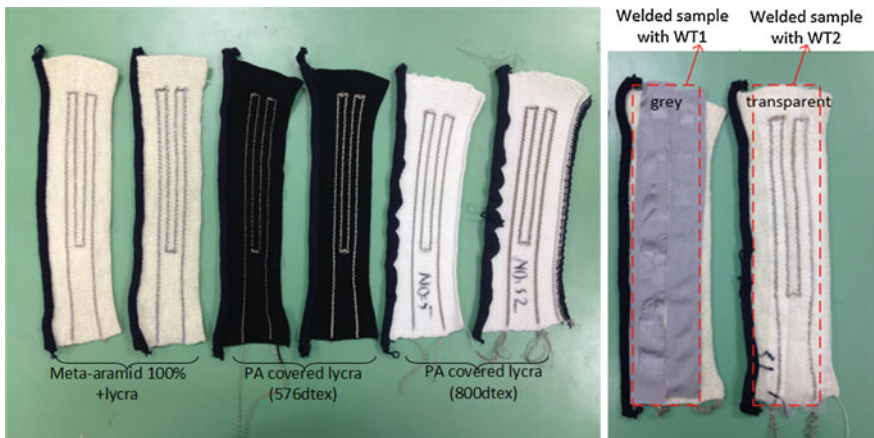


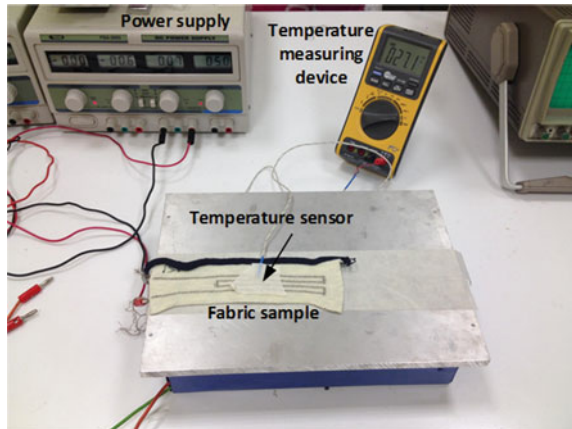
Figure 35.1 shows the model image of the knitted e-fabric structure. As seen from the figure that conductive yarns are seen over the fabric surface, however they are positioned as they are not visible from the backside of the fabric. In Fig. 35.2, the whole samples used in the study are presented. Application of ultrasonic welding has also been investigated for these samples in order to investigate their heating performance.

Two different welding tapes were used. The welding tape WT1 is made from three layers (P/PU/Nylon tricot), grey in color, with thickness 0.014 in. and width of 22 mm, while tape WT2 is made from two layers (PU/PU), transparent with thickness 0.004 in. and width 22 mm. Both tapes are breathable, waterproof and windproof. The tapes were chosen in order to prevent probable short circuits during electric operation as well as for obtaining a water-resistant fabric structure when considering the usage issues of e-textiles. The welded samples are shown in Fig. 35.2.



**Fig. 35.2** Knitted e-fabric samples and welded samples using welding tapes

**Fig. 35.3** Temperature measuring over the sample



### 35.2.2 Method for Electrical Resistance Heating Measurement

In order to test the thermal properties of samples, all the fabrics first were placed on a flat surface for at least 24 h prior to testing under standard atmospheric conditions ( $65 \% \pm 2 \% \text{ RH}$ ,  $20 \text{ }^\circ\text{C} \pm 2 \text{ }^\circ\text{C}$ ). To carry out thermal analysis, temperature measuring device with temperature sensor and DC power supply were used. The required energy to e-fabric samples was provided from DC power supply.

At the beginning of the experiments, e-fabric samples were placed on a plate to satisfy stable measurement. After that, positive and negative poles of DC power supply were clamped to the ends of two parallel conductive yarns as shown in Fig. 35.3.

Voltage supplied from DC power supply was increased starting from 5 to 10 V and 15 V. The amount of current passing through the conductive yarns was recorded via DC power supply. To let the temperature stabilized, a delay of 30 s after setting the voltage value has been introduced. After stabilization, instant temperature values over the fabric sample at each voltage value were recorded for 10 min. The average temperature value was calculated to prevent the diversity that can be comprised due to experimental conditions.

## 35.3 Results

Constant voltage values of 5, 10, 15 V were applied to the conductive lines of the e-fabric structures for 10 min. The obtained temperature over the fabric structures due to the voltage change are shown in the Figs. 35.4, 35.5, 35.6 and 35.7. The increased length due to the conductive yarn insertion resulted in an increase in the electrical resistance of the fabric samples. This increased resistance produced a

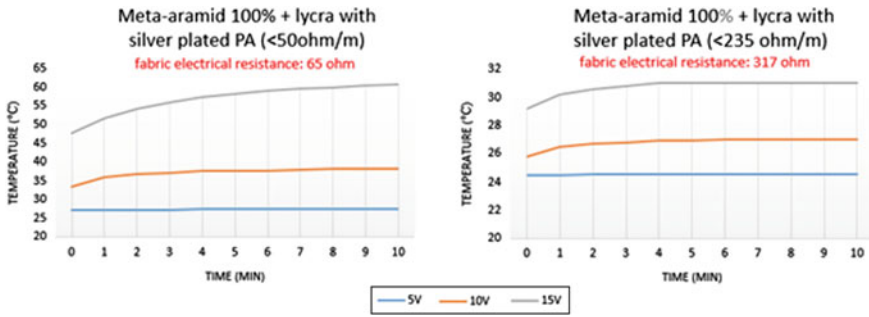


Fig. 35.4 Temperature change due to applied voltages: fabric composed of meta-aramid 100 % +lycra with silver plated PA (<50 ohm/m) and (<235 ohm/m)

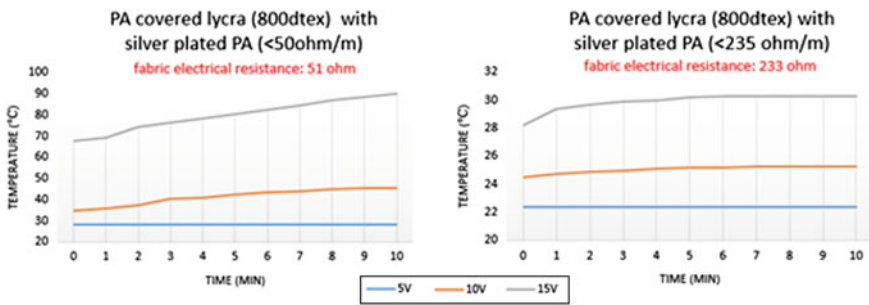


Fig. 35.5 Temperature change due to applied voltages: fabric composed of PA covered lycra (800 dtex) with silver plated PA (<50 ohm/m) and (<235 ohm/m)

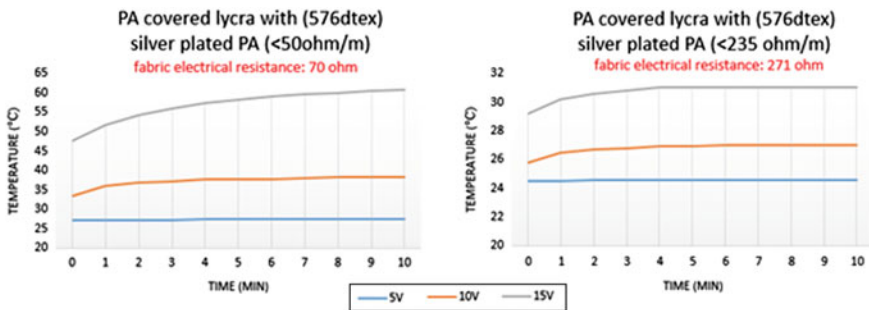
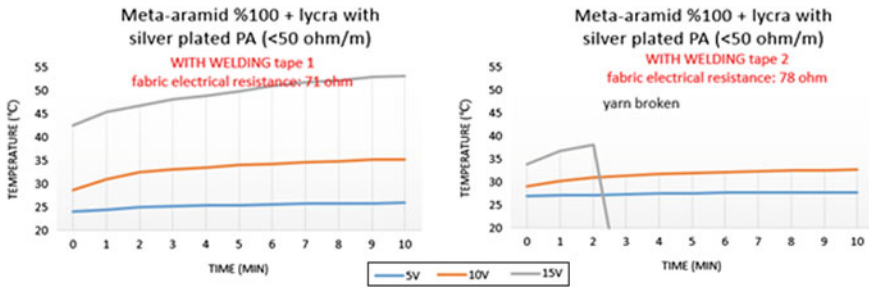


Fig. 35.6 Temperature change due to applied voltages: fabric composed of PA covered lycra (576 dtex) with silver plated PA (<50 ohm/m) and (<235 ohm/m)

lower current due to the Ohm's law and thus at the same voltage values due to the change in electrical resistance, the observed temperatures have also showed differences.



**Fig. 35.7** Temperature change due to applied voltages: welded fabric with welding tape 1 and tape 2 composed of meta-aramid 100 %+lycra and silver plated PA (<50 ohm/m)

For instance, although the same yarn is used in the fabric structure at the same rate of feeding, the contacts in the knitted fabric structure depend on the ratio of the tightness and lycra cause a difference in the fabric’s electrical resistance. As it is seen in Figs. 35.4, 35.5, fabrics’ resistances are 65 and 51 ohm with silver plated PA (<50 ohm/m) and 317 and 233 ohm with silver plated PA (<235 ohm/m) in fabrics produced using meta-aramid 100 %+lycra and PA covered lycra, respectively. Therefore, depending on the fabric material type as well as the fabric resistance values, the temperature observed over the fabrics is varying.

At 10 V, the temperature reaches 40 °C with meta-aramid 100 %+lycra while it reaches 50 °C with PA covered lycra (800 dtex) when silver plated PA with a linear resistance of 50 ohm/m is used. However, at the same voltage value, the temperature observed over the fabric containing meta-aramid fibers is 27 °C, whereas it is 25 °C with fabric containing PA covered lycra (800 dtex) when silver plated PA with a linear resistance of 235 ohm/m is used.

Thus, it can be said that since the sample resistances are higher, the currents passing through the structures are lower. For this reason in all cases the obtained temperature does not change so much and it stayed almost the same such that 24 °C at 5 V, 26 °C at 10 V and 30 °C at 15 V.

In fact, Joule energy available in the electrical conductor material is based on the passing current flow, which is expressed by  $I^2R$ . In this manner, it can be said that at lower voltages the heat generated is dominated by the yarn electrical resistance, however at higher voltages the phenomena is mainly based on the current passing through the conductive yarn itself.

Indeed, this is confirmed with all cases such that when the applied voltage is increased from 5 to 15 V, the observed temperatures over the fabrics increased (Figs. 35.4, 35.5 and 35.6).

Fabric composed of meta-aramid 100 %+lycra and silver plated PA (<50 ohm/m) was chosen as reference structure for ultrasonic welding application. The observed temperatures in welded samples also showed similar results compared to reference values. With an increase in applied voltage, the temperature observed over the welded samples has also increased.

Thus, it could be concluded that applied voltage with respect to linear resistance of conductive yarns have high effect on the temperature obtained over the e-fabric samples whether they are welded or not. However, a small decrease was observed in obtained temperatures. For instance, at 15 V the welded sample including welding tape 2 reaches up to 55 °C (Fig. 35.7), whereas the sample without welding reaches up to 60 °C in 10 min (Fig. 35.4). This is probably attributed to heat dissipation of the welding tape. On the other hand, welded sample including welding tape 2 damaged after 2 min at 15 V because of excessive heat (Fig. 35.7b). Therefore, ultrasonic welding parameters need to be carefully controlled to avoid excessive melting and polymer degradation.

## 35.4 Conclusion

In this study, knitted fabric samples including silver plated yarns with different linear resistance values have been studied for electrical resistance heating. In addition, the application of ultrasonic welding technique on these knitted fabric structures has also been investigated for heating purposes. To carry out electrical resistance heating, various voltages (5 V–10 V–15 V) were applied on the knitted e-fabric samples for a defined time interval and then, the temperatures observed over the e-fabrics were recorded.

It is found that the electrical resistance heating can be successfully obtained using fabrics knitted with silver plated PA yarns. These fabrics can be useful to design personal textile heating products since they are capable of generating sufficient heat to warm up the human body. However, depending on the desired heating level, a high input battery with adjustable control unit can be used.

Moreover, it is also found that the use of ultrasonic welding technology can be a convenient technique for constructing durable heating textile patches if the welding parameters with respect to functioning performance are well controlled.

**Acknowledgments** This project has received funding from the European Union's Horizon 2020 research and innovation programme under the Marie Skłodowska-Curie grant agreement No 644268. The article describes the part of the project which was realized by the Department of Textile Engineering of ITU, Technological Education Institute of Pireus and Theta Metrisis SA.

## References

1. Negru, D., Buda, C.T., Avram, D.: Electrical conductivity of woven fabrics coated with carbon black particles. *Fibres Text. East. Europe* 20 1(90), 53–56 (2012)
2. Kim, B., Koncar, V., Dufour, C.: Polyaniline-coated PET conductive yarns: study of electrical, mechanical, and electro-mechanical pro-perties. *J. Appl. Polym. Sci.* **101**(3), 1252–1256 (2006)
3. Gasana, E., Westbroek, P., Hakuzimana, J., De Clerck, K., Priniotakis, G., Kiekens, P., Tseles, D.: Electroconductive textile structures through electroless deposition of polypyrrole and copper at polyaramide surfaces. *Surf. Coat. Technol.* **201**(6), 3547–3551 (2006)

4. Atalay, O., Kennon, W.K., Demirok, E.: Weft-knitted strain sensor for monitoring respiratory rate and its electro-mechanical modeling. *IEEE Sens. J.* **15**(1), 110–122 (2015)
5. Vassiliadis, S.: *Electronics and Computing in Textiles*. [www.bookboon.com](http://www.bookboon.com) (2012)
6. Jakubčionienė, Ž., Masteikaitė, V.: Investigation of textile bonded seams. *Mater. Sci. (Medžiagotyra)* **16**(1), 76–79 (2010)
7. Ghosh, S., Reddy, R.: Ultrasonic sealing of polyester and spectra fabrics using thermo plastic properties. *J. Appl. Polym. Sci.* **113**, 1082–1089 (2009)
8. Shi, W., Little, T.: Mechanisms of ultrasonic joining of textile materials. *Int. J. Cloth. Sci. Technol.* **12**(5), 331–350 (2000)
9. Seram, N., Cabon, D.: Investigating the possibility of constructing different seam types for clothing using ultrasonic. *Int. J. Cloth. Sci. Technol.* **25**(2), 90–98 (2013)
10. Węglowska, A.: Effect of vibration welding parameters on the quality of joints made of polyamide 66. *Polymery* **59**(3), 239–245 (2014)
11. Hamdani, S.T.A., Potluri, P., Fernando, A.: Thermo-mechanical behavior of textile heating fabric based on silver coated polymeric yarn. *Materials* **6**, 1072–1089 (2013)
12. Sezgin, H., KursunBahadır, S., Boke, E., Kalaoglu, F.: Thermal analysis of e-textile structures using full factorial experimental design method. *J. Industrials Text.* (2014) doi:[10.1177/1528083714540699](https://doi.org/10.1177/1528083714540699)
13. Kayacan, O., Bulgun, E.Y.: Heating behaviors of metallic textile structures. *Int. J. Cloth. Sci. Technol.* **21**(2/3), 127–136 (2009)



# Chapter 36

## IP Based Module for Building Automation System

J.D. Irawan, S. Prasetyo and S.A. Wibowo

**Abstract** Embedded systems technology has a lot of applications in the various fields of life to bring ease and comfort for humans. One kind of applications is in the development of modern buildings, where embedded systems are applied to the control system. Building Automation Systems (BAS) are often encountered in modern buildings today. They are responsible to automatically control the building appliances such as electrical equipments, fire alarms, security systems, and others. Conventionally, a smart home that can be controlled by an embedded system is connected to a central monitoring unit such as a computer. The system commonly employs RS232 or RS485 serial communication, so that the control activities cannot be carried out from a long distance. With the rapid technology development in the field of communication, many recent communication devices are practical and have a good performance. One of them is a device with the Android operating system that can access the internet, thus it has a significant role in simplifying the management of smart homes. This research proposes the design of a smart home that can conserve energy by turning off unneeded electrical appliances, detect disorders such as flood, fire, and theft, and also serve as an early warning system through SMS Gateway. It can be monitored and controlled remotely over the Internet by an Android device.

**Keywords** Building automation system · IP based module · Smart house

### 36.1 Introduction

A lot of embedded systems technologies are applied in various fields of life to fulfill the human desire to live easily and comfortably. One example is the building of a house. Currently, building a house or modern building requires electronic control

---

J.D. Irawan (✉) · S. Prasetyo · S.A. Wibowo  
Informatics Engineering, National Institute of Technology, Malang, Indonesia  
e-mail: joseph\_dedy@yahoo.co.id

tools. The Building Automation System (BAS) is often encountered in the construction of modern buildings [1].

BAS provides automatic control of the environmental conditions in buildings. BAS was begun from process automation to the heating, ventilation and air conditioning systems (HVAC) in large functional buildings. The ultimate goal is to save energy and reduce costs. However, this system can be developed and applied to a house to build a smart home that can monitor all conditions and manage all electrical appliances. Hence, even if the occupants are not in the house, they can still monitor and control it, and need not feel anxious.

This gave us the idea to design a smart home that can control the entire electrical loads inside the house; each point of loads can be monitored and even its activity scheduled. The system was designed based on TCP/IP and the main component is an embedded web server. The house is also equipped with an early warning system that will inform the occupants via SMS in case of fire or flood, as well as a theft detection system with cameras that can be monitored remotely over the internet using an Android device that can monitor and control all electrical appliances at home.

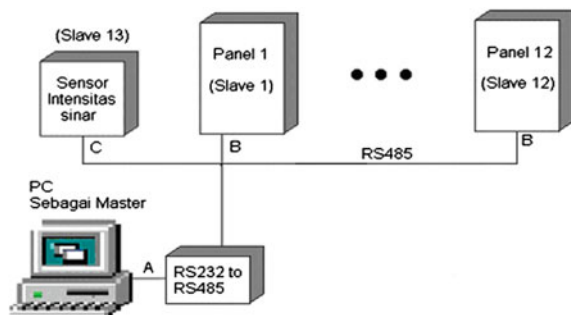
## 36.2 Related Works

### 36.2.1 Serial Communication

Serial data communication has the impression of being more complicated than parallel data communication, but serial data communication has a lot of advantages compared with parallel data communication, such as it requires only three wires (i.e., Tx, Rx, and Ground) to transmit information. In addition, the communication distance can also be increased further.

In the serial data communication, we can perform data communication using RS232 with a maximum distance of 10 meters, but data communication using RS486 can be carried out up to approximately 100 meters. Besides the advantage of a longer distance, communication using RS485 can be done with more than two terminals, in full duplex, and with high data accuracy [2]. Figure 36.1 below is an

**Fig. 36.1** Block diagram of building automation system using serial communication [2]



example of serial data communication using RS485 for monitoring and controlling a Building Automation System [3].

### 36.2.2 Monitoring and Controlling via Internet

With the advancement of Internet technology, which is considered a reliable communication, it is obvious that the Internet can be used as a medium for long-distance monitoring and controlling. Internet is expected to be a good medium because there are many available communication protocols on it with the ability to reduce errors during transmission.

Communication over the Internet can be used to monitor as well as control equipment located far away from the user easily and quickly, as can be seen in Figs. 36.2 and 36.3 below.

**Fig. 36.2** Block diagram of temperature monitoring via web [4]

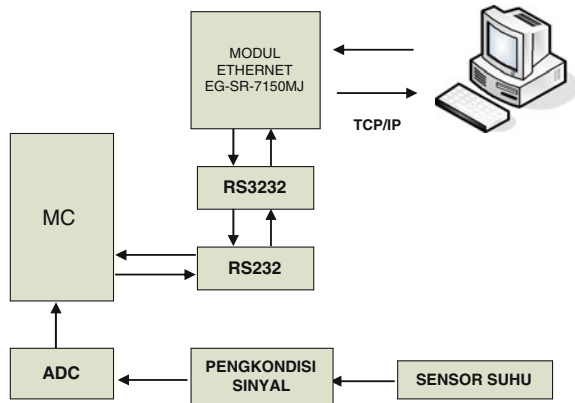
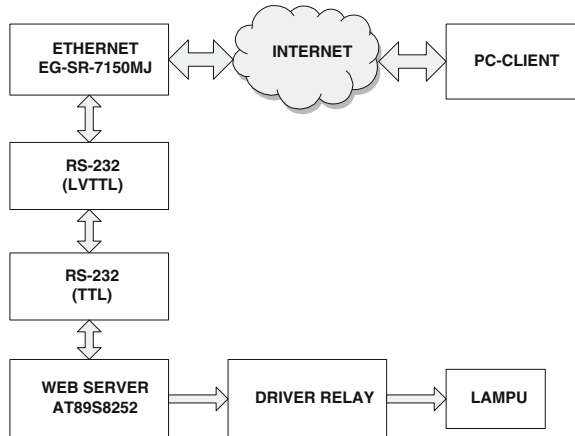


**Fig. 36.3** Block diagram of controlling lights via web [5]



However, when a Personal Computer (PC) is used as a Web Server connected to the appliance so that it can be controlled over the Internet, the solution becomes non portable and requires a lot of power because the PC must be running continuously and should never be turned off. Therefore, for the purpose of portability and power efficiency, a small device can be created to replace the PC as a Web Server; the device can be used to, in this case, monitor and control lights remotely. Microcontrollers are used as a Web Server and equipped with Ethernet Module for connection to the Internet. The advantage of this system, compared to Web servers on the market, is the TCP/IP (Ganesh, 2008) embedded in the microcontroller as software, so that it becomes much more efficient, more compact, and cheaper since it does not require a PC to work as the Web Server. The use of microcontroller can be replaced with other control equipment such as PLC.

### 36.3 System Model

The system discussed in the related works has some shortcomings, mainly to meet the demanding need of online access over computer networks and the Internet.

To improve the performance of the system, this study proposed the design of building automation system, which is implemented as a Smart House, with embedded web server application as the main component. The proposed system can be accessed over the Internet by means of a device with Android operating system.

The system block diagram, as shown in Fig. 36.4, consists of several parts: embedded web server and switching panel, monitor unit, LAN, and internet proxy server [6].

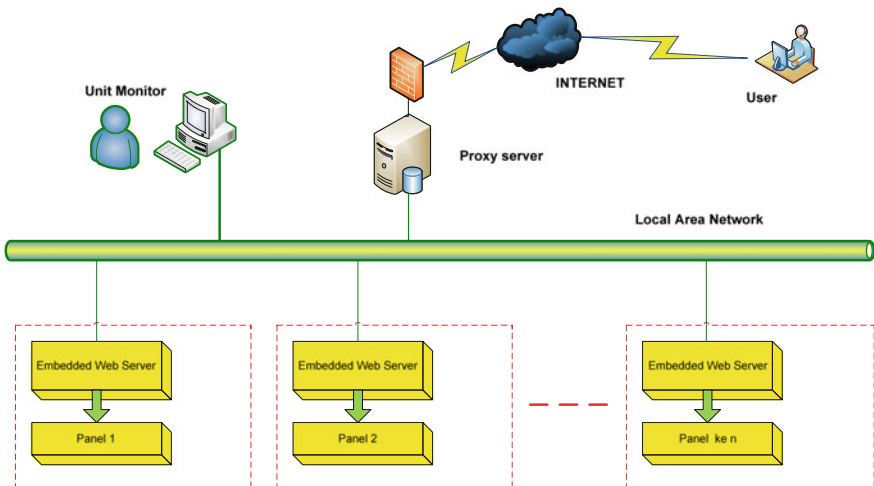
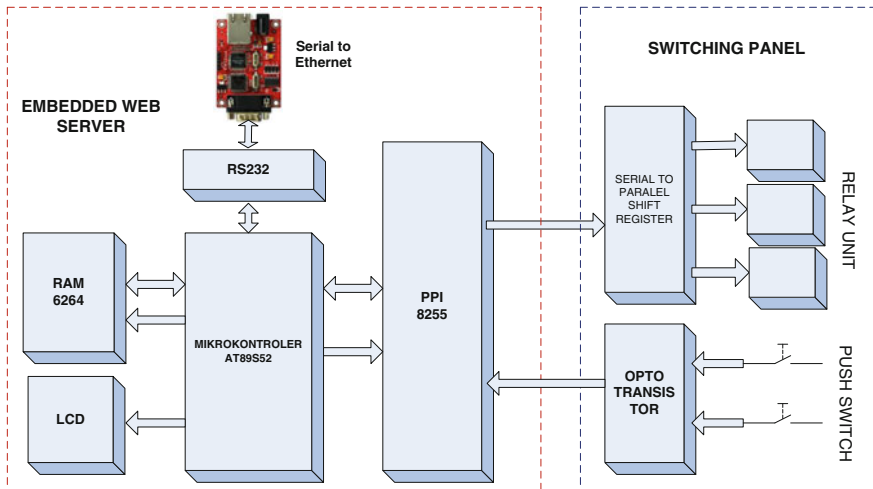


Fig. 36.4 System block diagram of the IP based module for smart houses



**Fig. 36.5** IP based module and switching panel

The embedded Web Server module and the switching panel are shown in Fig. 36.5. The embedded web server is built using the microcontroller as the main component and is equipped with supporting components such as RAM, I/O, and serial to Ethernet converter unit.

The switching panel is a functional unit for termination between power load and BAS module. The main components are the optocoupler as a signal isolator and switching components in the form of push buttons and sensors as input/output relays.

Figure 36.6 indicates that initially the system reads the temperature, light intensity of the sensor, and relay status; the data are published on the Web so that the user can monitor the status of electronic equipment in the house. After that, the user can switch the light of the house by pressing the ON or OFF so that the condition of the relay will change according to the user's wish.

## 36.4 Results

As shown in Fig. 36.7, the temperatures of bedroom 1 and bedroom 2 can be monitored. The user can turn on or turn off the air conditioners by pressing the ON or OFF buttons on the application.

Other buttons can be used to turn on or turn off the lights in the house. When the button is pressed, the application will send the data to change the state of the lamp according to the user's demand.

Fig. 36.6 System flowchart

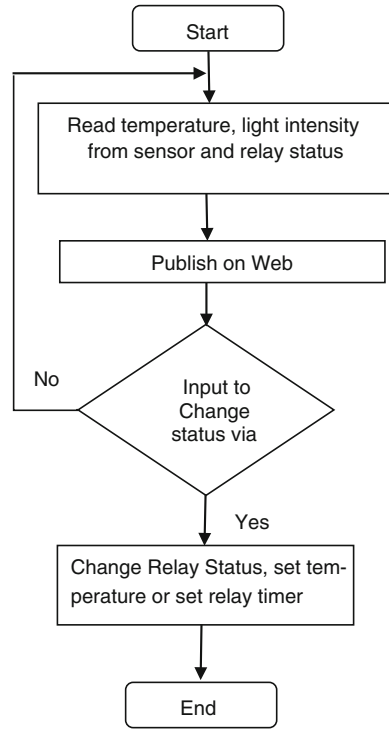
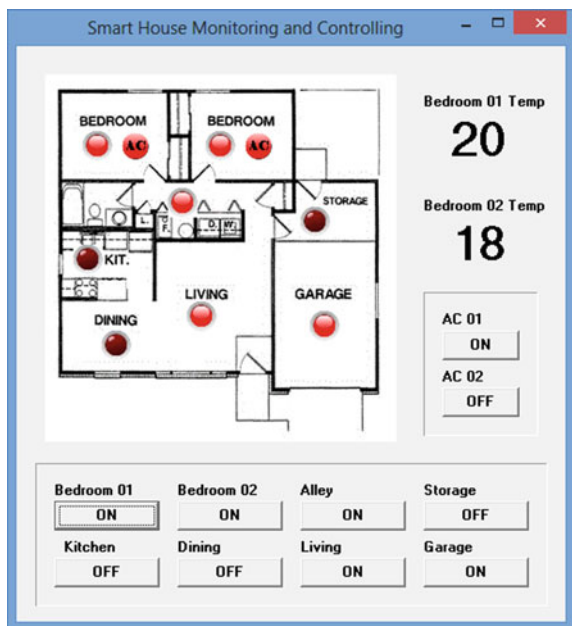


Fig. 36.7 Smart house monitoring and controlling



## 36.5 Conclusion

The IP Based Module for Building Automation System is very easy to implement because, by using the IP based module controlling unit, installation can be done quickly. Also, with the IP based program module, data communication becomes easier to do.

## References

1. Ganesh, S.: TCP/IP Implementation Using Embedded Controller, Mobile and Pervasive Computing (2008)
2. Irawan, J.D.: Building Automation System untuk Konservasi Energi Listrik. Universitas Trisakti Jakarta, Seminar nasional SNTI (2008)
3. Kastner, W.: Communication systems for building automation and control. In: Proceedings of the IEEE **93**(6) (2005)
4. Irawan, J.D.: Embeded Web Server Berbasiskan Mikrokontroler AT89S8252 dengan Modul Ethernet EG-SR-7150 MJ untuk Mengendalikan Lampu secara Remote. Seminar Nasional SITIA, ITS Surabaya (2008)
5. Irawan, J.D.: Pembuatan Embeded Web Server untuk Monitoring Suhu Lewat Internet Berbasiskan Mikrokontroler AT89S8252. Universitas Brawijaya Malang, Seminar nasional EECCIS (2008)
6. Limpraptono, F.Y., Ratna, A.A.P., Sudiby, H.: New architecture of remote laboratories multiuser based on embedded web server. *Int. J. Online Eng. IJOE* **9**(6), 4–11 (2013)

# Chapter 37

## Influence of CTAB and Sonication on Nickel Hydroxide Nanoparticles Synthesis by Electrolysis at High Voltage

Yanatra Budipramana, Suprpto, Taslim Ersam  
and Fredy Kurniawan

**Abstract** CTAB and Sonication has been used for preparing Ni(OH)<sub>2</sub> nanoparticles by electrolysis at high voltage. The effect of CTAB and sonication on the morphology and size of Ni(OH)<sub>2</sub> nanoparticles was observed. The results obtained were characterized with UV-Vis spectroscopy, X-ray Diffraction (XRD), Fourier Transform Infrared Spectrometer (FTIR), and Transmission Electron Microscopy (TEM). The TEM image shows that Ni(OH)<sub>2</sub> nanoparticles obtained with and without CTAB under sonication were nearly spherical. UV-Vis Spectrums show that with CTAB has higher concentration in comparison with without CTAB. But no significant different was found for FTIR spectrum. Thermogram shows Ni(OH)<sub>2</sub> nanoparticles obtained with and without CTAB have different properties at 60–140 °C due to association of water and CTAB. The most stable Ni(OH)<sub>2</sub> nanoparticles were obtained by addition CTAB under sonication.

**Keywords** Sonochemistry · Ni(OH)<sub>2</sub> · CTAB · Nickel

### 37.1 Introduction

In earlier work we reported synthesis nickel hydroxide using electrochemical by high voltage [1]. In this study, we would like to improved synthesis method by addition of CTAB as surfactant and sonication process. Ni(OH)<sub>2</sub> nanoparticles also have been synthesized through different methods such as hydrothermal [2–4], precipitation [5], and oxidation with microwave [6], ethanol solvent method [7] and immersion [8]. Cetyltrimethyl ammonium bromide (CTAB) was added during synthesis as a cationic surfactant that can form ((C<sub>16</sub>H<sub>33</sub>)N(CH<sub>3</sub>)<sub>3</sub>Br structure which induced the sphere–rod transition of micelles in aqueous solution [9].

---

Y. Budipramana · Suprpto · T. Ersam · F. Kurniawan (✉)  
Chemistry Department, Institut Teknologi Sepuluh Nopember, Surabaya,  
Indonesia 60111  
e-mail: fredy@chem.its.ac.id



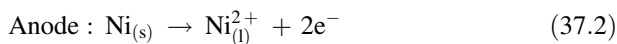
Nickel hydroxide has been potentially applied in such material as catalyst, capacitors and batteries. Sonochemistry is the application of ultrasound to chemical reactions and processes. In this present work we reported synthesis nickel hydroxide using sonochemistry method with and without CTAB and their characterization. The advantages of this method are simplicity, reliability, accuracy, versatility, and low cost. The power density from ultrasound gives mechanical energy to produce cavitation bubble and make electrochemical reactions [9]. Moreover this method was easy to be performed in laboratory or scale up in industry [10].

## 37.2 Experimental

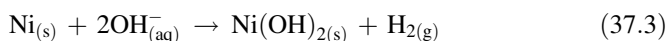
Synthesis of nickel hydroxide by electrolysis at high voltage on this experiment was performed according to Budipramana et al. [1]. Briefly pure nickel metal sheet was cut into dimension of 1 mm × 1 cm × 7.5 cm. 400 ml of H<sub>2</sub>O and 10 ml of Na-citrate 0.3 M were placed in 500 ml beaker glass. Electrolysis was conducted by using nickel metal sheet as the cathode and the anode and the solution which were prepared. The beaker glass was put in ultrasonic cleaner model PS—120. Initially, the Na citrate solution was heated at 80 °C with the frequency of 40 kHz and then the power supply unit was operated at constant potential (i.e. 15; 25; 35; 45; or 55 V). Ultrasonic radiation was continually applied during the electrolysis process. The reaction was performed for 30 min. The product obtained was cooled in ambient temperature and characterized using Genesys 10S UV-Vis spectrophotometer, Philips X' Pert MPD (Multi-Purpose Diffractometer) XRD, and JEOL JM140 m HR-TEM test (High Resolution Transmission Electron Microscope).

## 37.3 Results and Discussion

Electrolysis using nickel sheet at anode and cathode at high voltage produces Ni(OH)<sub>2</sub> nanoparticles as Eqs. (37.1) and (37.2):



The Ni<sup>2+</sup> obtained at the anode diffused in the solution and then mixed together to form Ni(OH)<sub>2</sub> nanoparticles as Eq. (37.3).



Formation of Ni(OH)<sub>2</sub> nanoparticles can be observed from colorless solution change to green [1].

### 37.3.1 UV-Vis Characterization

UV-Vis spectrum of Ni(OH)<sub>2</sub> nanoparticles obtained at varied electrolysis potential under sonication in the absent and present of CTAB can be seen at Fig. 37.1.

Figure 37.1 shows that Ni(OH)<sub>2</sub> nanoparticles intensity with CTAB (b) has higher absorbance compare to without CTAB. It indicates more Ni(OH)<sub>2</sub> nanoparticles are produced in the solution during electrolysis. Both experiment show that the peak of plasmon band reached at 387 nm, but CTAB increase the intensity all the wavelength regions. It indicates that size of Ni(OH)<sub>2</sub> nanoparticles obtained in the present of CTAB is more heterogen in comparison with in the absent of CTAB.

### 37.3.2 TEM Characterization

TEM images of the Ni(OH)<sub>2</sub> nanoparticles obtained that was prepared at voltage 55 V without CTAB are shown in Fig. 37.2a (Potential applied was selected based on optimal condition according to Budipramana et al. [1]). The morphology of Ni(OH)<sub>2</sub> nanoparticles is nearly spherical. Figure 37.2b is TEM image of Ni(OH)<sub>2</sub> nanoparticles obtained with CTAB under the same electrolysis synthesis condition in without CTAB (a). The result shows that with CTAB has less tendency for agglomeration in comparison without CTAB. It can be seen from the gap between particles. The gap between particle in Fig. 37.2a is closer than Fig. 37.2b, so that the tendency for agglomeration for Ni(OH)<sub>2</sub> nanoparticles in the absent of CTAB is higher.

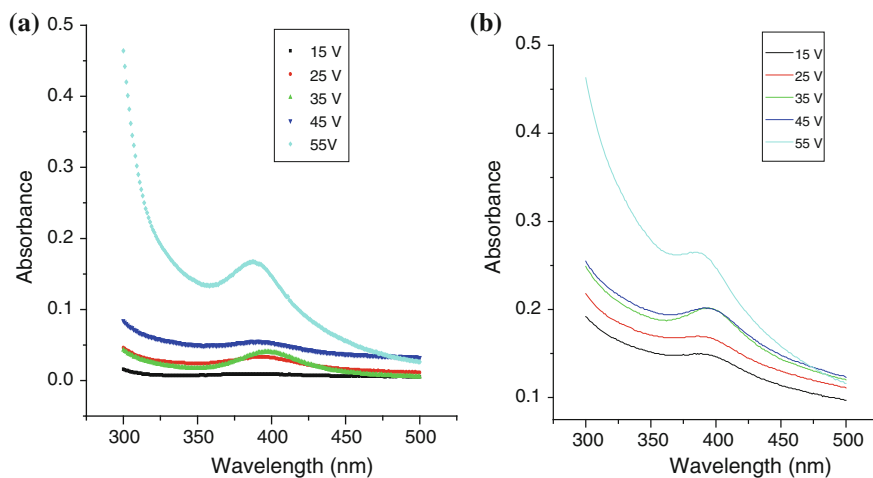


**Fig. 37.1** UV-Vis spectrum of Ni(OH)<sub>2</sub> nanoparticles obtained at varied potential by electrolysis at high voltage with sonication **a** in the absent and, **b** in the present of CTAB

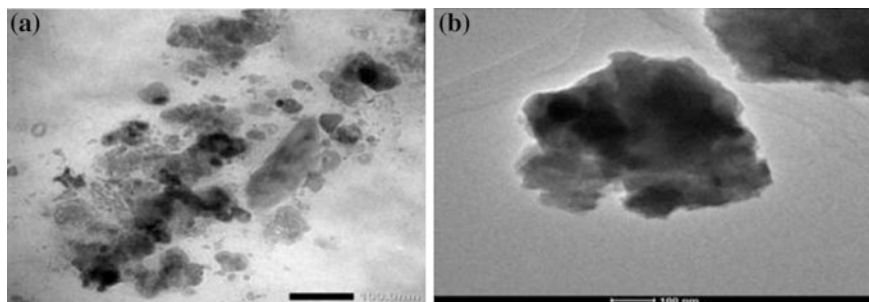


**Fig. 37.2** TEM image of  $\text{Ni}(\text{OH})_2$  nanoparticles which was obtained by electrolysis at high voltage with sonication **a** in absent and, **b** in the present of CTAB

CTAB provide not only favorable sites for particulate growth, but also influence the formation process including nucleation, growth, coagulation and aggregation. In the presence of CTAB and sonication, a layer of CTAB surrounds the  $\text{Ni}(\text{OH})_2$  with electrostatic interactions. After nucleation, the surfactant could influence particles growth, coagulation and aggregation [9].

### 37.3.3 DTA/TGA Characterization

Thermograms of  $\text{Ni}(\text{OH})_2$  nanoparticles which were obtained by electrolysis at high voltage with sonication and (a) in the absent of CTAB, (b) in the present of CTAB are shown at Fig. 37.3. Figure 37.3a shows three steps loss of weight. First,  $\text{H}_2\text{O}$  is released, it is started at  $60.81^\circ\text{C}$  until  $140^\circ\text{C}$ . Then lost of weight is continued till  $330^\circ\text{C}$  due to evaporation of crystalized water (second step). The final step of weight lost is formation of  $\text{NiO}$  from  $\text{Ni}(\text{OH})_2$  [1]. In general, Fig. 37.3b shows no

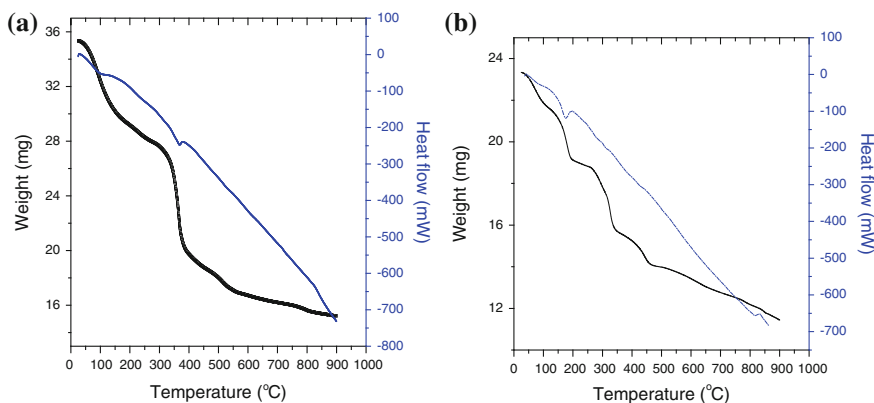


**Fig. 37.3** Thermograms of  $\text{Ni}(\text{OH})_2$  nanoparticles which was obtained by electrolysis at high voltage with sonication and **a** in the absent and, **b** in the present of CTAB

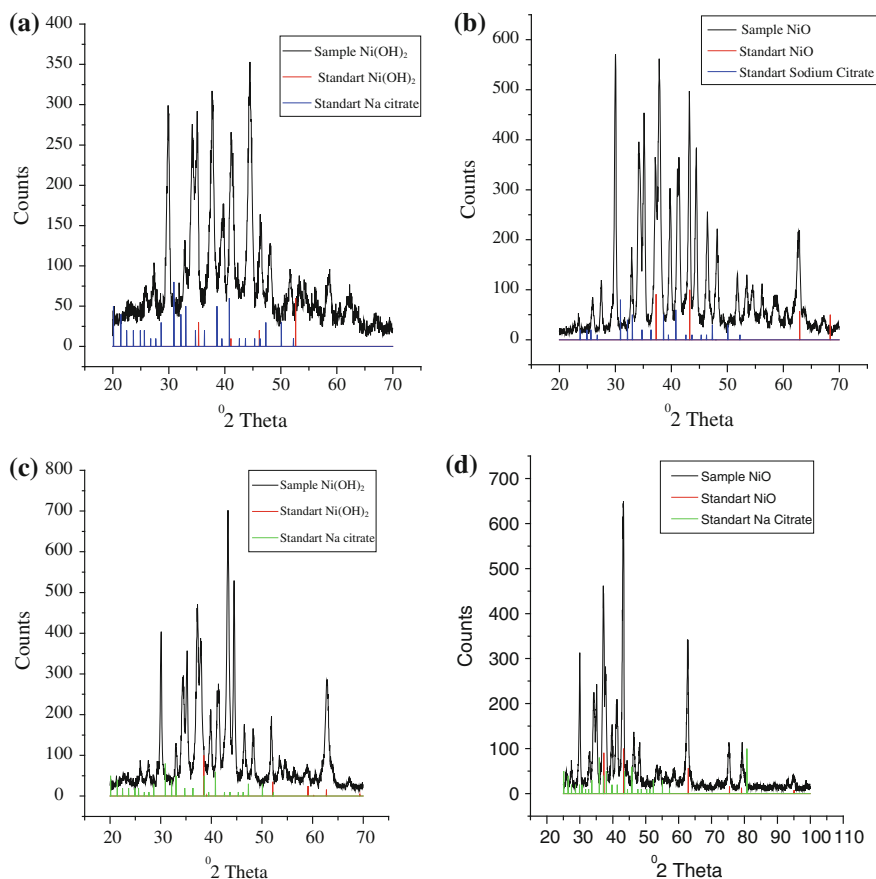


**Fig. 37.4** Diffractograms of Ni(OH)<sub>2</sub> which were obtained by electrolysis at 55 V under sonication **a** in the absent of CTAB **c** in the present of CTAB. Diffractograms of NiO nanoparticles which was obtained after calcination of Ni(OH)<sub>2</sub> which were synthesized, **b** in the absent and, **d** in the present of CTAB

significant different thermogram in comparison with Fig. 37.3a. There is only one additional step of weight lost between 60.81–140 °C. Most probably it is related to the release of water which associates with the surfactant added. Apart from that the thermogram is similar. So we can conclude that Ni(OH)<sub>2</sub> nanoparticles obtained with and without CTAB have the same thermal properties.

### 37.3.4 XRD Characterization

Diffractogram of Ni(OH)<sub>2</sub> nanoparticles obtained at voltage 55 V (a) in the absent of CTAB and (c) in the present of CTAB are shown in Fig. 37.4. The XRD

diffraction obtained represent  $\text{Ni(OH)}_2$  nanoparticles has crystal formed. All characteristic diffraction peaks are well consisted with the hexagonal  $\text{Ni(OH)}_2$  (ICCD file no.117). All of the peaks could be indexed as tetragonal. The difference in diffraction relative intensity between the samples indicates their difference in microstructure and morphology [5]. Additional diffractogram of NiO which obtained after calcination of  $\text{Ni(OH)}_2$  which was synthesis (b) in the absent and (d) in the present of CTAB at 400 °C are also shown at Fig. 37.4.

### 37.3.5 FTIR Characterization

FTIR spectrum of the  $\text{Ni(OH)}_2$  nanoparticles obtained at voltage 55 V (a) in the absent of CTAB and (b) in the present of CTAB are shown in Fig. 37.5

The wide band at range 2750–3750  $\text{cm}^{-1}$  indicates O–H group which is characteristic of  $\beta\text{-Ni(OH)}_2$  and also water which is adsorbed in the surface of  $\text{Ni(OH)}_2$  nanoparticles. The band at 1740  $\text{cm}^{-1}$  is due to bending vibration of the adsorbed water molecules. The weak absorption band at 591  $\text{cm}^{-1}$  is assigned to Ni–O–H bending vibration [2].

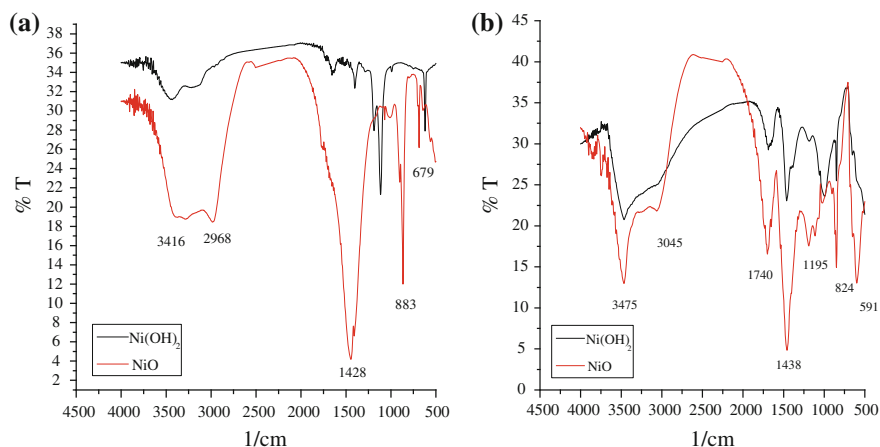


**Fig. 37.5** FTIR spectrum  $\text{Ni(OH)}_2$  nanoparticles and NiO obtained **a** in the absent and, **b** in the present of CTAB.  $\text{Ni(OH)}_2$  nanoparticles was synthesized by electrolysis at high voltage under sonication. NiO was obtained by calcination process of  $\text{Ni(OH)}_2$  nanoparticles at 400 °C

## 37.4 Conclusion

In this experiment Ni(OH)<sub>2</sub> nanoparticles was successfully synthesized in the absent and in the present of CTAB. Employing ultrasonic waves prevents particles from aggregation that it is shows from the results of TEM. UV-Vis Spectrum, FTIR spectrum, and thermogram show the Ni(OH)<sub>2</sub> nanoparticles obtained has different properties. TEM image show well morphologies corresponding to nano size about ±50 nm.

## References

1. Hua, C., Shen, C.: Comparative study of peak power tracking techniques for solar storage system. *IEEE Appl. Power Electron. Conf. Exposition Proc.* **2**, 679–683 (1988)
2. Hussein, K.H., Muta, I., Hoshino, T., Osakada, M.: Maximum photovoltaic power tracking: an algorithm for rapidly changing atmospheric conditions. *IEE Proc. Gener. Transm. Distrib.* **142**, 59–64 (1995)
3. Brambilla, L.: Approach UI photovoltaic arrays maximum power point tracking. In: *Proceedings of 35th IEEE Power Electronics Specialists Conference*, vol. 2, pp. 632–637 (1998)
4. Huh, D.P., Ropp, M.E.: Comparative study of maximum power point tacking algorithm using an experimental, programmable, maximum power point tracking test bed. In: *Proceedings of 28th IEEE Photovoltaic Specialists Conference*, pp. 1699–1702 (2000)
5. Ramaprabha, R., Mathur, B.L.: Intelligent controller based maximum power point tracking for solar PV system. *Int. J. Comput. Appl.* **12**, 37–41 (2011)
6. Singh, S., Mathew, L., Shimi, S.L.: Design and simulation of intelligent control MPPT technique for PV module using MATLAB/SIMSCAPE. *Int. J. Adv. Res. Electr. Electron. Instrum. Eng.* **2**, 4554–4566 (2013)
7. Jose, P., Jose, P.R.: Grid connected photovoltaic system with fuzzy logic control based MPPT. *Int. J. Eng. Innovative Technol.* **3** (2014)
8. Balasubramanian, G., Singaravelu, S.: Fuzzy logic controller for the maximum powerpoint tracking in photovoltaic system. *Int. J. Comput. Appl.* **41**, 22–28 (2012)
9. Patel, H., Agarwal, V.: MATLAB based modeling to study the effects of partial shading on PV array characteristics. *IEEE Trans. on Energy Conv.* **23**(1), 302–310 (2008)
10. Pop, O.A., Lungu, S.: Intechopen Homepage. [http://cdn.intechopen.com/pdfs/11613/intech-modeling\\_of\\_dc\\_dc\\_converters.pdf](http://cdn.intechopen.com/pdfs/11613/intech-modeling_of_dc_dc_converters.pdf)

# Chapter 38

## Waste Industrial Processing of Boron-Treated by Plasma Arc to Produce the Melt and Fiber Materials

S.L. Buyantuev, Ning Guiling, A.S. Kondratenko, Junwei Ye,  
E.T. Bazarsadaev, A.B. Khmelev and Shuhong Guo

**Abstract** The article presents the results of the melting of waste industrial processing of boron in the arc plasma to obtain melts and fibrous materials. It performs calculations power generation capacity of the reactor core of the current density and voltage gradient. When calculating the diameter of the reactor chamber accepted for determining the size and all the basic laws of the electric band are expressed through it. Research performed by methods of X-ray spectral analysis and electron microscopy. We studied the material composition of the melt and the mineral fiber obtained his blow from the man-made boron-containing waste using plasma arc reactor of the combined type. Experiments showed high refractoriness waste without additional charging (above 2800 °C) and the intensive evolution of gas during processing. To reduce the melting point, reduction of gas and evaporation substance as additional charging waste cullet used to produce uniform composition melts. Melting waste was investigated by mass concentration of 50 % (by waste) with finishing, eventually up to 60 %. At higher concentrations of mass (65 % or more) to obtain fiber failed to haunt the high content of magnesium in the waste, leading to the formation  $MgSiO_3$ . Melting of the components with mass concentration (waste—glass) 50:50 passed quietly with low gas emission, energy consumption for the melt was 3.4 kWh/kg, with melt draining conducted stretch fibers. Melting of the components with mass concentration (waste—glass) 60:40 also carried out calmly with a low gas emission, energy consumption for the melt has reached 4.5 kWh/kg. When pumping the melt was also carried stretch fibers, but fibers obtained differed inhomogeneity thickness (diameter). Thus, the content of magnesium in the melt increases with the concentration of waste, which increases the refractoriness and

---

S.L. Buyantuev (✉) · A.B. Khmelev  
East Siberian State University of Technology and Management,  
Ulan-Ude, Buryat Republic, Russia  
e-mail: buyantuevsl@mail.ru

N. Guiling · J. Ye · S. Guo  
Buryat State University, Ulan-Ude, Buryat Republic, Russia

A.S. Kondratenko · E.T. Bazarsadaev  
Dalian University of Technology, Dalian, China

hence the duration of melting with increasing energy costs. When increased (to 60 %) in the concentration of waste melt is a sharp decrease of the silicon content in the fiber, which in turn explains the change in the surface structure.

**Keywords** Arc plasma · Plasma reactor · Waste of boron extraction · Glass · X-ray spectral analysis · Surface microscopy · Stone melt · Mineral fiber

## 38.1 Introduction

The requirement for variety of industries in mineral fiber materials is continually increasing. The production of mineral fibers, mainly used rocks such as basalt, gabbro, diabase, porphyry and others [1]. However, with all the abundance of rocks needed in the production of technogenic mineral fibers used waste arising as a side (end) product during various kinds of processes, due to the fact that the formation of technogenic waste tends to considerable growth in the future, contributing to their steady accumulation [2]. Recycling of solid waste in technogenic fiber materials is an important scientific and technical challenge.

One promising direction in this area is the use of a plasma arc to melt the raw material to produce heat-insulating fiber materials. When used as a thermal energy source of the electric arc due to the high temperature sharply decreases during melt preparation due to elimination of the induction period melting [3–5].

## 38.2 The Experimental Setup and Methods of Research

We produce melt and fibers from industrial waste. We used an experimental setup as shown on Fig. 38.1 [2, 6]. The advantage of this reactor is that the combination of zones of allocation of thermal energy and its absorption during the flow of the process, provides an intensification of heat and mass transfer arc plasma heated material in the reaction chamber through the creation of a solid in the reactor chamber area—plasma volume, filling her cross section. All this is accompanied by the presence of a reaction volume in a sufficiently high concentration level of power and temperature, which reduces the time of melting the treated material [7].

In the chamber of the plasma reactor core 1 between the cathode 2 and the housing 3 is burning electric arc. Electromagnetic coil 8 creates a magnetic field. Under the action of the arc Lorentsa move in the electrode gap, overlapping section of the chamber high temperature region. When moving arc column due to the difference in aerodynamic drag and the wall of the arc electrodes extend and in which there are high-speed plasma flows toward the wall of the chamber 3.

The arc of the reactor type described in the camera administered electric arc power is converted into heat. Thus, the arc zone is a zone for generating thermal energy, its absorption, it covers the entire section of the chamber, allows adjustment of the melting time of the processed material, the concentration of power, and hence



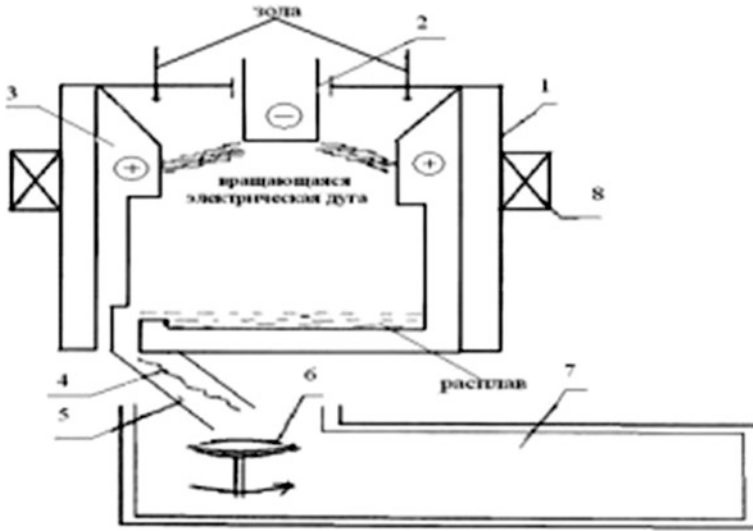


**Fig. 38.1** Experimental setup for melting raw materials. 1—plasma reactor; 2—core graphite cathode; 3—graphite anode; 4—melt; 5—a tray for transporting the melt; 6—rotating disk; 7—fiber deposition chamber; 8—electromagnetic coil

temperature. This area is limited in height planes perpendicular to the chamber axis and passing through the electrode end (top), and through the middle of an electromagnetic-solenoid coil (lower) [8]. Thermal energy generated in the vicinity of the rotating arc while stirring the melt and thereby distributed throughout its volume.

The power generation area is calculated based on the terms of its distribution uniform. When calculating the diameter of the reactor chamber accepted for determining the size and all the basic laws of the electric band are expressed through it. This makes it possible to extend the experiment results obtained in small reactors, geometrically similar to the reactors of high power and hence a large diameter chamber [9].

Reactor current  $I_p$  is expressed by current density, referred to the cross-sectional area chamber, the calculated values were as follows: diameter of the chamber  $D_k = 15$  cm; arc current  $I_p = 200$  A, respectively:

$$I_p = \Delta i_p \pi D_k^2 / 4 \tag{38.1}$$

Accordingly, the current density  $\Delta i_p = 4 I_p / \pi D_k^2 = 1,132$  A/sm<sup>2</sup>.

Power of reactor  $U_p = 200$  Vis a voltage gradient across the electrode gap:

$$U_p = E_p D_k / 2 \tag{38.2}$$

Here  $\Delta_k/2$ —inter electrode gap, which include arc voltage, to determine the voltage gradient (in the reactor core at the cathode). Accordingly, the voltage gradient  $E_p = 2 U_p/\Delta_k = 26.7$  V/sm.

As a result, taking into account the expressions for  $I_p$  and  $U_p$  derive the formula for the power reactor:

$$P_p = U_p * I_p = \pi/4 * 1/2 E_p \Delta_i \Delta_k^3 \approx 0,39 E_p \Delta_i \Delta_k^3 \quad (38.3)$$

Which is equal to:  $P_p \approx 0,39 E_p \Delta_i \Delta_k^3 = 0,39 * 26.7$  V/sm \*  $1.132$  A/sm<sup>2</sup> \*  $(15)^3$  cm<sup>3</sup> = 40 kW.

As a result of reforms concluded that the amount allocated in the area of generating thermal power equal to input electrical power is proportional to the cube of the diameter of the chamber, it is also proportional to the current density of  $\Delta_i$ , and a voltage gradient of  $E_p$  or different volume capacity  $P_p$ , allocated in the area. The value of  $P_p$  determines the temperature level is, obviously, a constant for the production of geometrically similar to the reactors:

$$P_p = \text{const} \quad (38.4)$$

Consequently, it is possible to adopt constants  $\Delta_i$  and  $E_p$ :

$$\Delta_i \approx \text{const} \quad (38.5)$$

$$E_p \approx \text{const} \quad (38.6)$$

A value of  $\Delta_i \equiv I_p/\Delta_k^2$  is determined using models [10]. The conditions of process parameters at a high plant capacity. Then, for a given diameter of the reactor provides a selection of its current value.

### 38.3 Results and Discussion

An experiment was carried out to study the material composition of the melt and the mineral fiber obtained its blow from industrial waste using plasma arc reactor of the combined type.

For the treatment to obtain a melt and the fibers, we used manmade waste industrial processing of boron constituting a powdery substance (Fig. 38.2) of the following elemental composition (Table 38.1).

The experiments on the melting of the waste showed its high refractoriness (above 28000 °C) with the help of some high-temperature short-range optical pyrometer (>1 micron) infrared radiation and intense release of gas during processing. To reduce the melting point, reduction of gas and evaporation of substance has been to use as additional charging waste cullet to obtain homogenous melts with subsequent generation of mineral fiber materials and stone casting. It should be

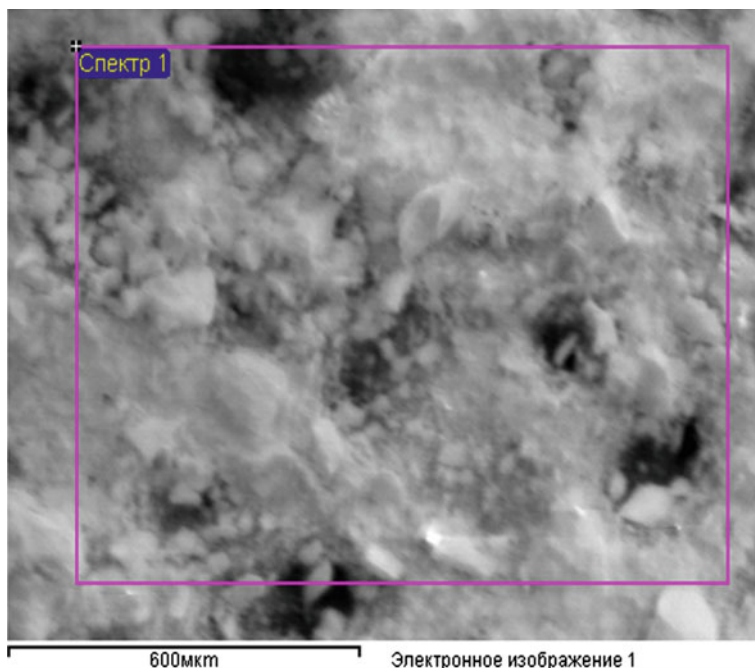


**Fig. 38.2** Micrograph of *technogenic* waste

**Table 38.1** Elemental composition of technogenic waste

B	C	O	Na	Mg	Al	Si	Result
3.44	12.26	52.89	0.91	23.22	0.94	6.34	100.00

noted that the processing of this waste can't be performed in the "classical" melting aggregates (cupola, bathroom and tunnel glass furnaces) because they generate low temperature (up to 2000 °C) so the industrial processing of this waste can be realized only electric arc (plasma) or induction (UHF) method, however, induction furnaces because of the very high energy, strong electromagnetic radiation and radio interference caused by them, as well as the risk of explosion of the inductor in the event of a short circuit in the industry used is limited. Arc plasma devices are preferred in melting refractory materials thanks to the special properties of the plasma, such as: high temperature (up to 50000 K), the specific power per unit volume of the reactor and thus the speed of the process, the presence of large amounts of electrons, ions and free radicals in the bulk of the reactor causing rapid melting the particles of the processed material. The process is intensified due to the rotating plasma arc uniformly mixing and homogenizing the entire volume of the melt, thereby eliminating the zone of fusion lack.

If this waste composed without an additional charging (i.e. due to high magnesium content and a very low content of silicon, it is impossible to obtain a satisfactory melt viscosity to develop a fine fiber.

Therefore, the solution of the problem was to maximize the use of the waste with additional charging of the other waste industry—cullet.

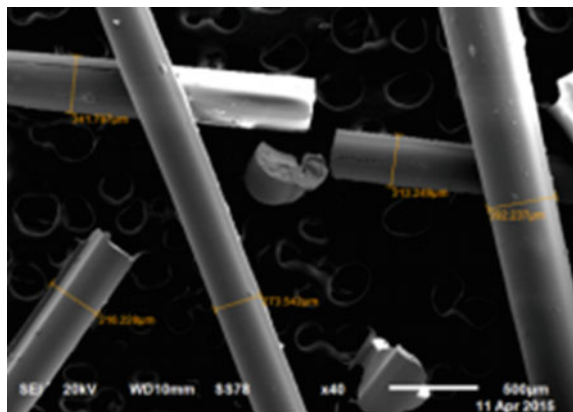
It was studied that the possibility of obtaining the contents of the melts at intervals of waste was within 5–30 % and 95–70 % cullet. Principal possibility of melting these compositions. Therefore, guided by tasks and preliminary findings, the melting of waste began with a mass concentration of 50 % (for waste) with bringing in a subsequent 60 %. At higher concentrations of mass (65 % or more) to obtain fiber failed to haunt the high content of magnesium in the waste, leading to the formation of crystalline magnesium metasilicate  $MgSiO_3$ .

Figure 38.3 shows the appearance of the melt with mass concentrations of the components (waste—glass) 50:50. Figure 38.4 and Table 38.2 show the spectral

**Fig. 38.3** Appearance of the melt from technogenic waste and broken glass with a mass content of components 50:50 (waste: cullet)



**Fig. 38.4** The spectral lines of the distribution of elements and their mass concentrations



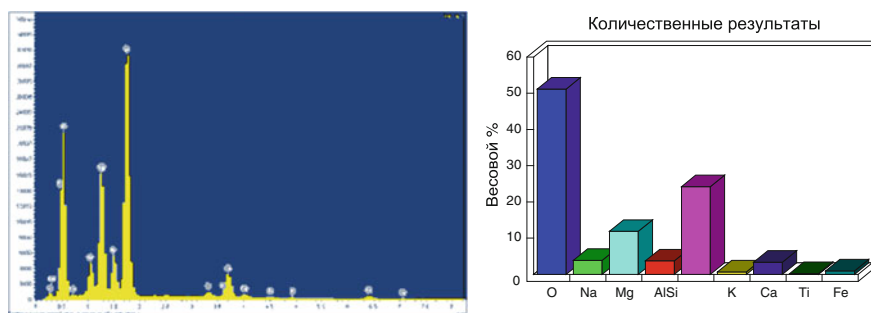
**Table 38.2** Elemental composition of the melt with mass concentration 50:50

C	O	Na	Mg	Al	Si	K	Ca	Ti	Fe	Result
10.55	51.63	3.63	8.01	3.54	19.30	0.44	2.56	0.12	0.22	100.00

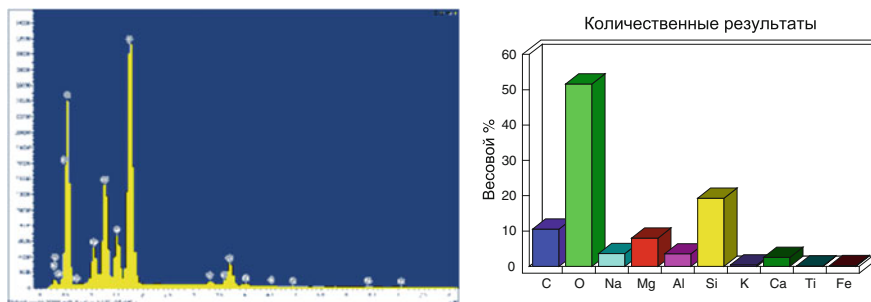
lines of the elements and their content by weight. Melting passed quietly with a small gassing, the approximate energy consumption for the melt was 3.4 kWh/kg.

When pumping the melt was conducted stretch fibers obtained long thin fibers, whose characteristics are shown in Fig. 38.5 and Table 38.3.

Subsequently waste concentration was increased by 10 %. Figure 38.6 shows the appearance of the melt with mass concentrations of the components (waste—glass) 60:40. Figure 38.7 and Table 38.4 shows the spectral lines of the elements and their content by weight. Melting also passed quietly with a small gassing, the

**Fig. 38.5** A micrograph of the fibers with a concentration of waste—glass 50:50**Table 38.3** The elemental composition of fibers with mass concentration 50-50

O	Na	Mg	Al	Si	K	Ca	Cr	Fe	Cu	Zn	Result
43.7	4.69	5.00	1.77	35.28	0.73	7.11	0.28	0.74	0.35	0.34	100.00

**Fig. 38.6** Appearance melt technogenic waste and broken glass with a mass content of components 60:40 (waste: cullet)

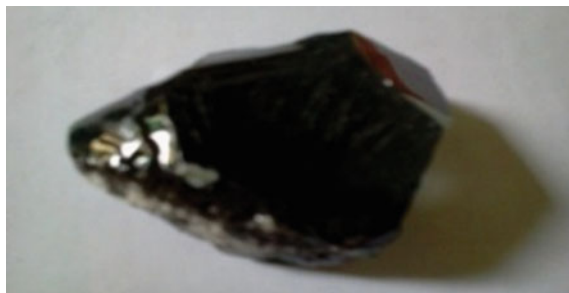


**Fig. 38.7** The spectral lines of the distribution of elements and their mass concentrations

**Table 38.4** Elemental composition of the melt with mass concentrations 60:40

O	Na	Mg	Al	Si	K	Ca	Ti	Fe	Result
51.14	3.87	11.88	3.73	24.22	0.67	3.33	0.20	0.97	100.00

approximate energy consumption for the melt has reached 4.5 kWh/kg. When pumping the melt was also carried stretch fibers, but fibers obtained differed inhomogeneity thickness (diameter), characteristics of the obtained fibers are shown in Fig. 38.8 and Table 38.5.

**Fig. 38.8** A micrograph of the fibers with a concentration of waste—glass 60:40

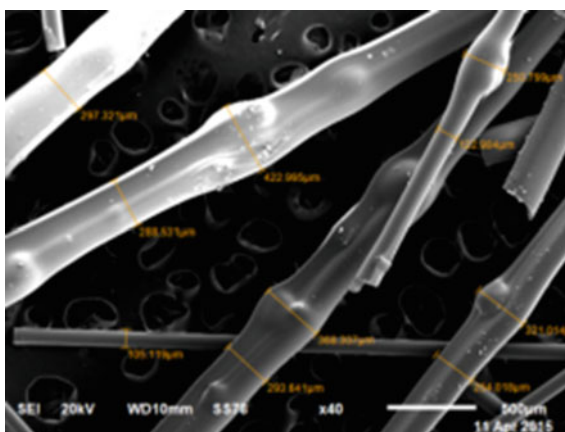


**Table 38.5** Elemental composition of fibers with a mass concentration 60:40

O	Na	Mg	Al	Si	K	Ca	Ti	Fe	Cu	Result
47.68	3.78	11.84	3.83	26.29	0.79	3.86	0.20	1.43	0.29	100.00

As can be seen from Tables 38.2 and 38.4 in molten magnesium content increases with increasing concentration of waste, which leads to an increase in refractoriness and hence the duration of melting with increasing energy costs. Tables 38.3 and 38.5 show a dramatic reduction in the content of silicon (as silica) fiber, which in turn it explains the change in the surface structure.

## 38.4 Conclusion

We have presented the arc melting reactor, which is a type of plasma reactors allowed to smoothly adjust the temperature of the melt and maintain the output stream from the tap hole, which made it possible to reduce the viscosity and increase the melt flow rate. We recommend that waste can be treated as plasma arc process in the melt with mass content of the waste components/cullet 50:50 or 60:40 to get stone looking casting and thin mineral fiber as a component of composite materials, as well as for thermal insulation materials fibrillation.

## References

1. Myasnikov, A.A., Aslanova, M.S.: Election of mountain basalt fibers for various purposes. *Glass Ceram.* **3**, 12–15 (1965)
2. Buyantuev, S.L., Sultimova, V.D.: Production of thermal insulating materials from ash waste TPP using low-temperature plasma. *Constr. Mater.* **10**, 51–53 (2004)
3. Buyantuev, S.L., Sultimova, V.D.: The Use of Low-Temperature Plasma for Fibrous Insulation Materials from Slag Waste of Thermal Power Plants, p. 132. ESSTU, Ulan-Ude (2010)
4. Buyantuev, S.L., Kondratenko, A.S.: Study of physico-chemical properties of the mineral fibers obtained by the electromagnetic process reactor. *Vestnik* **5**(44), 123–129 (2013)
5. Buyantuev, S.L.: Insulation Materials Fibrous Structure of Melts Rocks and Ash And Slag Waste of Man-Made: A Monograph. In: Buyantuev, S.L., Kondratenko, A.S. (eds.) p. 180. ESSTU, Ulan-Ude (2014)
6. Buyantuev, S.L., Sultimova, V.D., Dondokov, A.T., Volokitin, G.G., Zyachanov, M.E., Tsyrenov, S.A.: Production of Heat-Insulating Building Materials Using Electric Plazma Processing, Building Complex of Russia: science, education, practice. In: International scientific and practical conference, pp. 90–93. Ulan-Ude (2006)
7. Jukov, M.F.: Electric Arc Gas Heaters (Plasma Torches). In: Jukov, M.F., Smolyakov, V.Y., Uryukov, B.A. (eds.) p. 232. M, Nauka (1973)
8. Bron, O.B.: The movement of the electric arc in the magnetic field. *Electricity* **7**, 76–81 (1966)
9. Buyantuev, S.L., Kondratenko, A.S.: The physical model of the electric zone in a plasma reactor of the combined type. *Vestnik BSU* **3**, 114–119 (2013)
10. Sergeev, P.V.: The Electric Arc in Electric Reactors, p. 140. Nauka, Alma-Ata (1978)

# Chapter 39

## Design of Arrhythmia Detection Device Based on Fingertip Pulse Sensor

R. Wahyu Kusuma, R. Al Aziz Abbie and Purnawarman Musa

**Abstract** Much research has been done to detect heart disease arrhythmias. Arrhythmia was usually diagnosed by a doctor based on a paper ECG (Electrocardiogram) or system that can classify arrhythmias based on ECG signals obtained from the doctor. The author aims to ensure that everyone can easily identify arrhythmias in case of abnormalities in the heart without having to see a doctor. In the present study the authors purpose to make the arrhythmia detector uses an optical sensor input. The method in this research is to process the input signal from the optical sensor, which then amplified by the signal conditioner, Arduino detect the inter-pulse period and save the eight periods for analysis using Arrhythmia Algorithm to define type arrhythmia. The hardware used consists of a photodiode and an infrared LED as heart rate detection, and signal conditioning board Arduino Uno as a processing of data. Design software in the system using the Arduino IDE based programming language C. The results of this study are success to calculate arrhythmia algorithm with percentage error to get period R-to-R are 0.25 % and precision get 99.947 %. Based on overall system testing for ten respondents result value of average precision was 77.25 %.

**Keywords** Arrhythmia detection • Fingertip pulse sensor • Arduino uno • LCD display

---

R. Wahyu Kusuma (✉) · R. Al Aziz Abbie  
Electrical Engineering, Gunadarma University, Jakarta, Indonesia  
e-mail: wahyukr@staff.gunadarma.ac.id

P. Musa  
Computer System, Gunadarma University, Jakarta, Indonesia



## 39.1 Introduction

Heart arrhythmias occurs when the electrical impulses in heart that coordinate your heartbeats don't work properly, causing heartbeats too fast, too slow or irregularly [1]. Arrhythmias can take place in a healthy heart and be of minimal consequence but they may also indicate a serious problem that may lead to stroke or sudden cardiac death [2, 3]. Heart arrhythmia treatment can often control or eliminate irregular heartbeats.

The heart is a vital organ in the human body that functions to pump blood throughout the body. Therefore, heart monitoring is very important because our bodies continue doing circulation of blood throughout the body organs, from the heart rate people will be known types of illnesses suffered. Arrhythmias or heart rhythm disorder is a natural human heartbeat rhythm in abnormal condition. Heart rhythm abnormalities can be used as an early sign of a serious heart attack.

Usually arrhythmia is diagnosed by doctor or paramedic by using graphic of ECG (Electrocardiograph) paper. In 2008, research has been conducted by Agus Sukoco Heru from Politeknik Negeri Malang that entitled *Desain Alat Deteksi Dini dan Mandiri Aritmia* (in Bahasa Indonesia), the research build device made with EKG as input, MCU as process unit and LED as output [4].

Electrocardiogram (ECG) is a diagnosis tool that reported the electrical activity of heart recorded by skin electrode. The morphology and heart rate meditates the cardiac health of human heart beat [5]. It is a noninvasive technique [6]. The ECG signal provides important information of a human heart for detection of diseases [7]. To acquire the signal, ECG devices with varying number of electrodes (3–12) can be used. Multi lead systems exceeding 12 and up to 120 electrodes are also available [8].

Based on previously research, this research will change input device with infrared LED and photodiode, use Arduino Uno as microcontroller and output display on LCD display. Cardiac monitoring sensors utilize infrared as the heart pulse sensor, the use of infrared is expected to minimize the cost for utilizing infrared and IC op-amp as well as more easy because with these sensors monitoring heart pulse enough just to put a finger on the sensor and then with programmed system will be determine type of arrhythmia disease.

## 39.2 Arrhythmia Premonitory

This type of arrhythmia indicates a condition that harmful to the health of the patient [9], including Premature Ventricular Contraction (PVC), Interpolated PVC, Bigeminy, Trigeminy, R-on-T Beat, Atrial Premature Beats (APB), and Skipped Beat.

There are several methods to determine the presence of cardiac rhythm disorders, there are:

1. Doctor or paramedic who is an expert in analyzing using direct observation of paper cardiogram

**Table 39.1** Arrhythmia algorithm

Type of aritmia	Algorithm
PVC	$RR_{t-1} > 0.9 (AR_{t-2}), RR_{t-1} + RR_t = 2(AR_{t-2})$
R-on-T	$RR_{t-1} < 0.33 (AR_{t-2}), RR_{t-1} + RR_t = 2(AR_{t-2})$
Bigeminy	$RR_{t-3} < 0.9 (AR_{t-4}), RR_{t-1} < 0.9 (AR_{t-4})$ $RR_{t-3} + RR_{t-2} = 2(AR_{t-4}), RR_{t-1} + RR_t = 2(AR_{t-4})$
Trigeminy	$RR_{t-2} < 0.9 (AR_{t-3}), RR_{t-1} < 0.9 (AR_{t-3})$ $RR_{t-1} + RR_{t-1} + RR_t = 2(AR_{t-3})$
Interpolated PVC	$RR_{t-1} < 0.9 (AR_{t-2}), RR_{t-1} + RR_t = 2(AR_{t-2})$
APB	$RR_{t-1} < RR_{t-1} + RR_t < (AR_{t-2})$

2. Arrhythmias can be diagnosed by the method of comparing the output signal with a variety of ECG arrhythmia signal images were then analyzed by using ANN (Artificial Neural Network). de Chazal [7] using a mathematical model analysis of ECG signal output by the algorithm as shown in the Table 39.1.

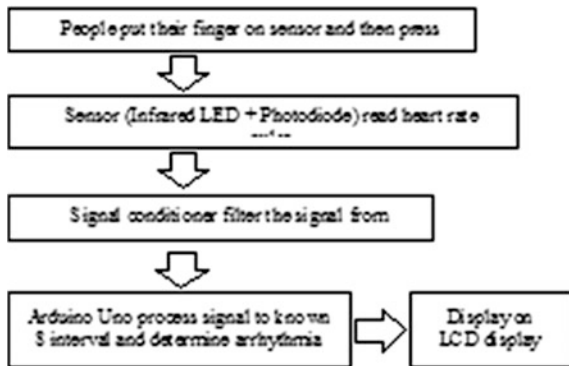
### 39.3 Architecture and Its Implementation

In general, the system will be built at the end of this project can be seen in the block diagram below (Fig. 39.1):

#### 39.3.1 Hardware Design

Hardware design of the device can be seen in Fig. 39.2. Construction sensor block is shown in Fig. 39.3. The use of optical sensors for process monitoring heart rate with fingertip illustrated as a Fig. 39.4.

**Fig. 39.1** Block diagram of system



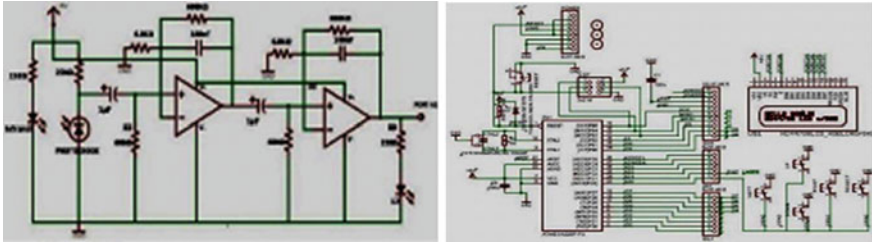


Fig. 39.2 Arrhythmia detection device schematic

Fig. 39.3 Optical sensor circuit

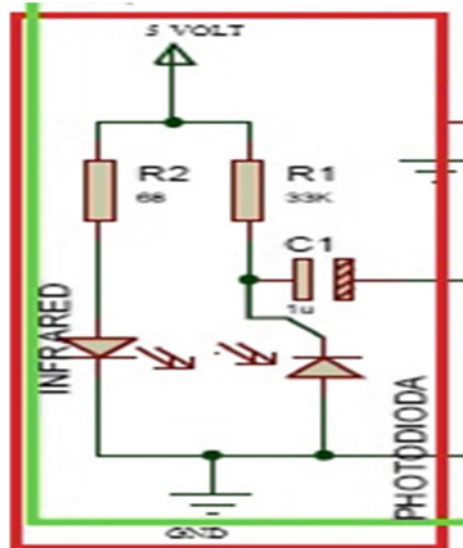
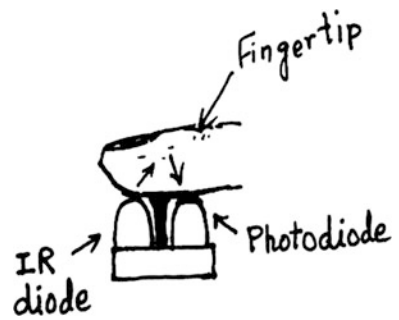


Fig. 39.4 Illustration fingertip to optical sensor



When the sensor reading fingertip up of sensor, the photodiode gave HIGH when a lot of infrared light reflected off the blood vessels when blood vessels were full, and gave LOW when little reflected infrared light because the blood vessels are not full of blood vessels.

Since the output value of the sensor is too low around 100 mV, need signal conditional that will erase high frequency noise and amplify signal to around 0–5 V. Microcontroller will receive input values from signal conditional. The results of the reading sensor system is processed by the microcontroller to get eight interval and determine arrhythmia. Output will be displayed on LCD display  $16 \times 2$ .

### 39.3.2 Software Design

In the program, there are two variables RR and AR. RR is the interval R-to-R and AR is the average range of the period specified intervals. Subscript is used as a sign associated with time.  $RR_t$  means the last interval.  $RR_{t-1}$  means the interval R-to-R interval of seven of the eight sampled period.  $AR_t$  is the average time the R-to-R of the eight intervals sampled.  $AR_{t-1}$  means that the average time-to-R R seven intervals of eight intervals were sampled (Fig. 39.5).

When peak signal of heartbeat is detected, peak signal will be marked as R plus subscript as a sign of the numbering of the order of detected heartbeat. To process formula of Arrhythmia Algorithm, it needs to know interval between R-to-R and period of each heartbeat. T1 value from  $R_1$  to  $R_2$ , T2 value from  $R_3$  to  $R_2$  and so on until the period to eight.

The period shown before on the program labeled to RR. Subscript after RR was labeled the order of the period,  $RR_t$  was the period of the last period of the nine signals captured.  $RR_{t-1}$  was the period of one before the last of eight intervals that captured, continued to the first period  $RR_{t-7}$ .

Definition of AR was the average of each period based labeled on the subscript. ART was the average of eight intervals that captured, ART value was  $RR_t + RR_{t-1} + RR_{t-2} + RR_{t-3} + RR_{t-4} + RR_{t-5} + RR_{t-6} + RR_{t-7}$  divided by eight.  $AR_{t-1}$  value was  $RR_{t-1} + RR_{t-2} + RR_{t-3} + RR_{t-4} + RR_{t-5} + RR_{t-6} + RR_{t-7}$  divided by seven, continued to get  $RR_{t-7}$ .

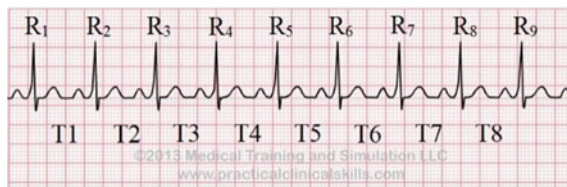


Fig. 39.5 Heartbeat signal shown R as peak and T as period

## 39.4 Device Testing and Analysis

### 39.4.1 Conditional Circuit Testing

The first analysis used the sensor output signal from the combined process of the infrared LED with a photodiode. The purpose of device testing is to know the signals generated by sensor and signal conditioner circuit. In this testing, the authors have measured the amount of voltage, and noise signal are visible from oscilloscope. Sensor was connected to voltage source, output of sensor connected to oscilloscope to measure signal of detected heartbeat taken from the oscilloscope as Fig. 39.6.

In this capture, the value of the voltage coming out of the photodiode at 84 mV and the lowest value  $-28$  mV. For a human heartbeat can be seen when there is a change in amplitude between the amplitude value of the other, but the electronic system value as a rate to be determined at a certain value, from the existing signal system will be difficult to distinguish which one is ticking. The heart rate is around 84 mV value, while the value of the noise is around 20 mV. The distance is very small compared to the value of the analog inputs on Arduino A1, range from 0 to 5 V. Because of this, it takes the one amplifier and filter that really valid value. After that output from first amplifier to measure the amount of voltage, and noise signal from pin 1 LM 358 are visible oscilloscope. Following figure shows the sign of sensor testing by connecting output of sensor to oscilloscope. Pin 1 was connected to oscilloscope to measure signal of detected heartbeat taken from the oscilloscope as Fig. 39.7.

Signals from the sensors are still very weak that need to be strengthened, the sensors detect the heartbeat signal has a voltage ( $-30$  to  $60$  mV), not much different from before output from photodiode at 84 mV and the lowest value  $-28$  mV, but DC component has gone. To make it easier to measure the heartbeat signal must to amplified and filtered again.

The last analysis used the sensor output signal from the pin 7 output from LM358. The purpose of device testing is to know the signals generated by sensor

**Fig. 39.6** Testing output signal from photodiode

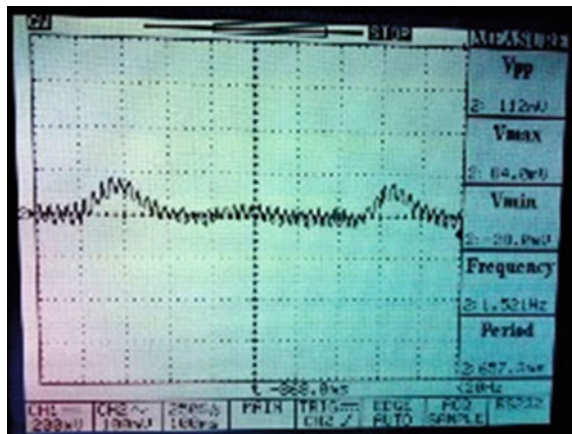
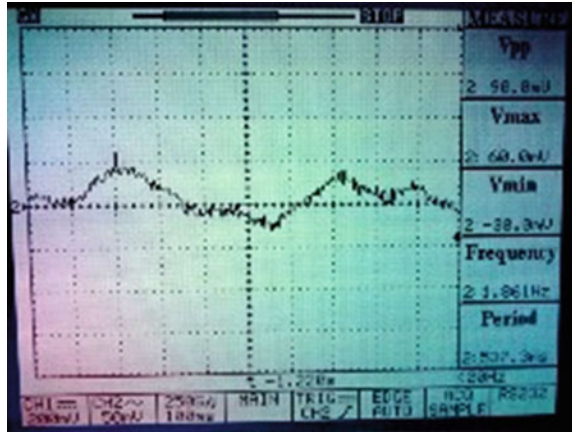


**Fig. 39.7** Testing oscilloscope on output Pin 1 LM358



and signal conditioner circuit. In this testing, the authors have measured the amount of voltage, and noise signal are visible from oscilloscope. Following Fig. 39.8 shows the sign of sensor testing by connecting output of sensor to oscilloscope.

Output signal of sensor then processed by signal conditioner. The signal filtered and amplified using two stage active low pass filter. The cut-off frequency indicate from oscilloscope at frequency 2.731 Hz.

### 39.4.2 R-to-R Testing

The test is done by compared R-to-R period collected from the device with showed by oscilloscope. The test was to know how accurate.

From Table 39.2, data comparison above, can get total percentage error of detecting period of heartbeat is 0.25 %, Std. deviation data is 0.053 %, so precision is 99.947 %.

**Fig. 39.8** Testing output signal pin 7 LM358

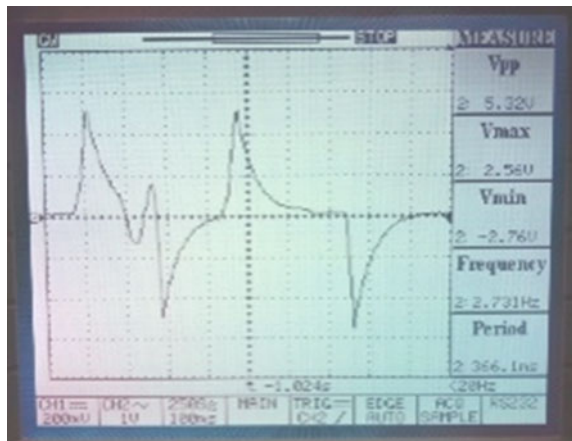


**Table 39.2** Result R-to-R testing

Attempt		Period (ms)								Avg error (%)
		T1	T2	T3	T4	T5	T6	T7	T8	
1st	Device	892	907	915	923	931	905	830	796	0.2
	Oscilloscope	890	905	917	922	930	906	831	800	
	% error	0.22	0.22	0.22	0.11	0.11	0.11	0.12	0.50	
2nd	Device	915	880	920	890	892	896	850	821	0.18
	Oscilloscope	914	881	921	891	895	899	852	820	
	% error	0.11	0.11	0.11	0.11	0.34	0.33	0.23	0.12	
3rd	Device	871	889	923	901	906	898	841	786	0.27
	Oscilloscope	873	890	920	900	905	890	840	788	
	% error	0.23	0.11	0.33	0.11	0.11	0.90	0.12	0.25	
4th	Device	892	903	924	895	911	903	869	807	0.29
	Oscilloscope	890	900	920	900	910	900	870	805	
	% error	0.22	0.33	0.43	0.56	0.11	0.33	0.11	0.25	
5th	Device	920	887	904	924	913	907	873	792	0.30
	Oscilloscope	921	890	900	921	910	905	870	790	
	% error	0.11	0.34	0.44	0.33	0.33	0.22	0.34	0.25	

### 39.4.3 Overall System Testing

The test is done by put the respondent’s finger on the sensor, get eight interval R-to-R and the type of disease and then displayed on LCD Display. Test repeat five time to get percentage error of the system.

1st Respondent, Name: Al Aziz Abbie R., Gender: Male, Age: 22, Height/Weight: 177 cm/65 kg (Table 39.3).

Based on overall system testing to 10 (ten) respondent results value of average precision was 77.25 %.

**Table 39.3** Testing device from 1st respondent

Period	Attempt	Standard deviation				
		1st	2nd	3rd	4th	5th
T1 (ms)	892	915	871	892	920	19.84
T2 (ms)	907	880	889	903	887	11.37
T3 (ms)	915	920	923	924	904	8.17
T4 (ms)	923	890	901	895	924	15.92
T5 (ms)	931	892	906	911	913	14.05
T6 (ms)	905	896	898	903	907	4.66
T7 (ms)	830	850	841	869	873	18.28
T8 (ms)	796	821	786	807	792	13.83
Result	ND	ND	ND	ND	ND	

**Table 39.4** Calculation data *1st Respondent* result on arrhythmia algorithm

Type arrhythmia	Calculation on arrhythmia algorithm	Detect condition
PVC	<ul style="list-style-type: none"> <li>• <math>830 &gt; 0.9 (912.17), 830 + 796 = 2(912.17)</math></li> <li>⇒ <b>830 &gt; 820.95, 1626 = 1824.34</b></li> </ul>	Unconditional → not detect
R-on-T	<ul style="list-style-type: none"> <li>• <math>830 &lt; 0.33 (912.17), 830 + 796 = 2(912.17)</math></li> <li>⇒ <b>830 &lt; 301.016, 1626 = 1824.34</b></li> </ul>	Unconditional → not detect
Bigeminy	<ul style="list-style-type: none"> <li>• <math>931 &lt; 0.9 (909.25), 830 &lt; 0.9 (909.25)905 = 2(909.25), 830 + 796 = 2(909.25)</math></li> <li>⇒ <b>931 &lt; 818.325, 830 &lt; 818.325, 1836 = 1818.5, 1626 = 1818.5</b></li> </ul>	Unconditional → not detect
Trigeminy	<ul style="list-style-type: none"> <li>• <math>905 &lt; 0.9 (913.6), 830 &lt; 0.9 (913.6), 830 + 830 + 796 = 2 (913.6)</math></li> <li>⇒ <b>905 &lt; 822.24, 830 &lt; 822.24, 2456 = 1827.2</b></li> </ul>	Unconditional → not detect
Interpolated PVC	<ul style="list-style-type: none"> <li>• <math>830 &lt; 0.9 (912.17), 830 + 796 = 2(912.17)</math></li> <li>⇒ <b>830 &lt; 820.95, 1626 = 1824.34</b></li> </ul>	Unconditional → not detect
APB	<ul style="list-style-type: none"> <li>• <math>830 &lt; (830 + 796) &lt; 912.17</math></li> <li>⇒ <b>830 &lt; 1626 &lt; 912.17</b></li> </ul>	Unconditional → not detect

This test is needed to know whether the overall design determine algorithm is work properly or not. These tests done by calculated manually then compare the result of calculation to the result of the device. Data used in this calculation from respondent 1st. The test is done by put eight periods to variable in algorithm, after get all variable value algorithms will decide what type of arrhythmia. The result is match (Table 39.4).

$$\begin{aligned}
 \text{ARt}_2 &= (892 + 907 + 915 + 923 + 931 + 905)/6 = 912.17; \\
 \text{ARt}_3 &= (892 + 907 + 915 + 923 + 931)/5 = 913.6; \\
 \text{ARt}_4 &= (892 + 907 + 915 + 923)/4 = 909.25; \\
 \text{RR}_t &= 796; \text{RR}_{t-1} = 830; \text{RR}_{t-2} = 905; \text{RR}_{t-3} = 931.
 \end{aligned}$$

### 39.5 Conclusion

Based on the testing of hardware and application programs also the analysis has been done in the making of this final task can be concluded that Design Arrhythmia Detection Device with Optical Sensor Based Arduino Uno has been successfully detects, calculates and determines the type of Arrhythmia with Arrhythmia Algorithm, by using Arduino Uno Board, Infrared LED, Photodiode and LCD display.

Testing in ten respondents get result average precision of overall system process was 77.25 %. Percentage error from detecting eight periods was 0.25 % and



precision value was 99.947 %. Manual calculated from data has been conducted and it showed correctly same result. The testing of the device has not been done in different disease type of arrhythmia.

## References

1. Sandoe, E., Sigurd, B.: Arrhythmia, a Guide to Clinical Electrocardiology. Publishing Partners Verlags GmbH, Bingen (1991)
2. Goldberger, L., Goldberger, E.: Clinical Electro Cardiography. The Mosby Company, Saint Louis (1997)
3. Sideris, D.A.: Primary Cardiology. Scientific Editions Grigorios K Parisianos (in Greek), Athens (1991)
4. Sukoco, H.: Desain Alat Deteksi Dini dan Mandiri Aritmia 6 no. 3. Politeknik Negeri Malang, Malang (2008)
5. Pan, J., Tompkins, W.J.: A real time QRS detection algorithm. *IEEE Trans. Biomed. Eng.* **32**, 230–236 (1985)
6. Yeha, Y.C., Wang, W.J.: QRS complexes detection for ECG signal: the difference operation method (DOM). *Comput. Methods Programs Biomed.* **9**, 245–254 (2008)
7. de Chazal, P., Duyer, M.O., Reilly, R.B.: Automatic classification of heartbeat using ECG morphology and heart beat interval features. *IEEE Trans. Biomed. Eng.* **51**, 1196–1206 (2004)
8. Zarychta, P., Smith, F.E., King, S.T., Haigh, A.J., Klinge, A., Zheng, D., Stevens, S., Allen, J., Okelarin, A., Langley, P., Murray, A.: Body surface potential mapping for detection of myocardial infarct site. In: *Proceedings of IEEE Computer Cardiology*, pp. 181–184 (2007)
9. Webster, EDS.: *Design of Microcomputer-Based Medical Instrumentation*. Prentice Hall International, New Jersey (1981)

# Chapter 40

## Analysis of Fundamental Frequency and Formant Frequency for Speaker ‘Makhraj’ Pronunciation with DTW Method

Muhammad Subali, Miftah Andriansyah and Christanto Sinambela

**Abstract** This article aims to look at the similarities and differences in the fundamental frequency and formant frequencies using the autocorrelation function and LPC function in GUI MATLAB 2012b on sound hijaiyah letters for adult male speaker beginner and expert based on makhraj pronunciation and both of speaker will be analyzed on the matching distance of the sound use DTW method on cepstrum. Subject of speech beginner for makhraj pronunciation are taken from college students of Universitas Gunadarma aged 22 years old. Data of the speech beginner for makhraj pronunciation is recorded using MATLAB algorithm on GUI. Subject of speech expert for makhraj pronunciation are taken from previous research. They are 20–30 years old from the time of taking data. The sound will be extracted to get the value of the fundamental frequency and formant frequency. After getting both frequencies, analysis will be obtained of the similarities and differences in the fundamental frequency and formant frequencies of speech beginner and expert and it will show the matching distance of both speech. The result is, all of speech beginner’s and expert’s based on makhraj pronunciation have different values of fundamental frequency and formant frequency. Then the results of the matching distance analysis using DTW method showed that there is no identical similarity between speech beginner’s and expert’s based on makhraj pronunciation.

**Keywords** Fundamental frequency · Formant frequency · Hijaiyah letters · Makhraj pronunciation

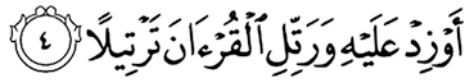
---

M. Subali (✉) · M. Andriansyah  
Jurusan Teknik Informatika, Sekolah Tinggi Teknik Multimedia Cendikia Abditama,  
Pamulang, Indonesia  
e-mail: muhammadsubali@yahoo.com

C. Sinambela  
Jurusan Teknik Elektro, Universitas Gunadarma, Jakarta, Indonesia

## 40.1 Introduction

Al-Qur'an is religious text of Islam given by Allah SWT to Prophet Muhammad SAW. Every Muslim are required to read Al-Qur'an with good vowel according to one of text of Al-Qur'an Al-Muzamill: 4 which says:



It means, “*Or add to it, and recite the Al-Qur'an with measured recitation.*”

To be able to read Al-Qur'an with measured recitation needs to learn knowledge of tajwid and makhraj pronunciation so it is not just reading like reading a book. In reading a book, we don't have to distinguish the voice pronunciation because for every each Latin letter, it doesn't have any meaning. It is different with hijaiyah letters that requires distinguishing of voice pronunciation for each hijaiyah letter [1]. Usually there is a teacher to help the people to pronounce Al-Qur'an well. If there is mispronunciation of hijaiyah letters, it will change the meaning of Al-Qur'an. So it needs an algorithm to make a decision to know the similarity of a random speech makhraj pronunciation from the real makhraj pronunciation. Usually, the beginner speaker on makhraj pronunciation cannot read or say the sound of makhraj pronunciation with measured recitation. Although he knows how to pronounce the sound of makhraj but it still has different result or matching distance from the expert makhraj pronunciation.

The human has diversity voice according to human physic perception to sound of the human's voice such as pitch and formant [2–4]. With the rapid development technology in communication and information, it will help the identification process between experts and beginners on makhraj pronunciation [5].

This research focus on analysis of the fundamental frequency and formant frequency for speaker makhraj pronunciation with DTW method. There are two type of speakers in this research, that will be taken their voice. First is the beginner, he is a Muslim who can speak Arabic but he does not know about makhraj pronunciation. Second is an expert, he is a Muslim who can speak Arabic and know about makhraj pronunciation. It needs two speakers to obtain the similarities and differentiations based on the mean value of F0, F1, F2, F3, and matching distance with DTW method [6–9]. Each speech's speaker are recorded and taken their fundamental frequency and formant frequency for analysis. Therefore, it needs a system like GUI for solving that problem in the real time.

## 40.2 Theoretical Framework

Makhorijul is a sound area of Hijaiyah letters that comes out when it is read by human. There are specific sound areas for each Hijaiyah letters. Usually someone makes a mistake when pronounces an Hijaiyah letter, it could be because of the similarity of a sound of one letter with the others and it is hard to pronounce correctly without some practice. For example when it says ذ(Dzal) and ظ(Zho). Therefore, Makhorijul is an area of letter out from the reader. All of Hijaiyah letters have different area for the readers to say so that it would form a certain sound. It would be haziness for the reader and the listener to listen to it and cannot be divided from one letter to the other if it cannot be pronounced from the correct source area (Fig. 40.1).

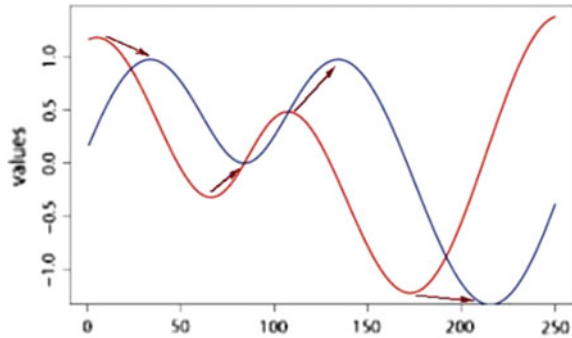
### 40.2.1 Analysis of Linear Predictive Coding (LPC)

LPC is one of method for voice recognition based on the human voice. Its purpose is to separate formants frequency with fundamental frequency from the human voice. Analysis of Linear Predictive Coding (LPC) is one of the methods to get an approach of sound spectrum [2, 9].

**Fig. 40.1** Sound area Makhraj from each Hijaiyah letters



**Fig. 40.2** Graphic of comparison values between X and Y



### 40.2.2 Dynamic Time Warping (DTW)

Dynamic time warping is one of method to calculate matching process of similarity between the different of two time series of signals on it's velocity and time. Matching is done using the approach to find the smallest distance [9]. Example there are two data. Someone is walking slowly, and the second data is someone who walk quickly, there are two time series  $X = (x_1, x_2, \dots, x_n)$  dan  $Y = (y_1, y_2, \dots, y_n)$ . It will be graphed on Fig. 40.2.

On Fig. 40.2, there are two graphs in time series. They have same pattern but not on the same position. It can be because of the interval different between X and Y. Now the main problem is, how to identify those two time series and can be told as a same graph although their intervals are different.

## 40.3 Research Methodology

Our research could be depicted on a block diagram as shown on Fig. 40.3.

Block of input:

1. Research's subject for speech's beginner of makhray pronunciation are taken from college student of Universitas Gunadarma aged 22 years old. Data of the speech's beginner makhray pronunciation is recorded using MATLAB algorithm on GUI. Speech samples are taken by recording sound with arrangement specification of 44100 Hz sampling frequency and the amount of bit that is adjusted, and then changed them into digital data that is saved in the form of wav file.
2. Research's subject for speech's expert of makhray pronunciation are taken from previous research "Frekuensi Forman Sebagai Model Akustik Tabung Sederhana Dari Vocal Tract". This data has already in the form of average value of 5 times pronunciation on 84 kinds of letters. They are 20–30 years old from

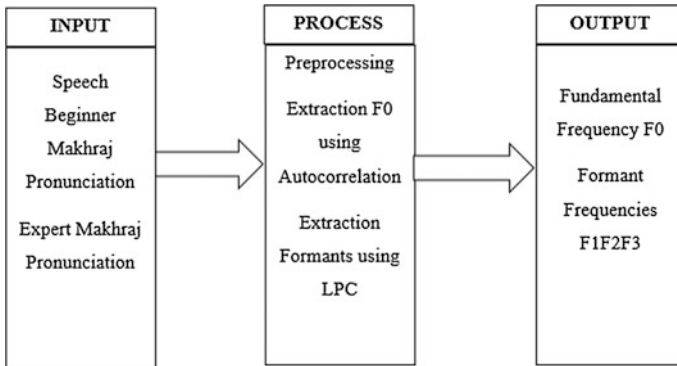


**Fig. 40.3** Block diagram of the research

the time of the data taken. Speech samples are taken by recording sound with arrangement specification of 44100 Hz sampling frequency and the amount of bit that is adjusted

Block of Proses:

1. Preprocessing has been done to enhance the accuracy and efficiency of the extraction processes, speech signals are normally pre-processed before their features are extracted. There are two steps in Pre-processing that is, pre-emphasis and Voice Activation Detection (VAD).
2. To get F0 value from a sound file, autocorrelation algorithm is used on MATLAB GUI. The autocorrelation approach is used for extracting F0 from speech file.
3. To get F1, F2 and F3 value from a sound file, LPC algorithm is used on MATLAB GUI. The LPC approach is used for extracting F1, F2 and F3 from the speech file.

### 40.4 Matching Distance Using DTW Algorithm

The program is started by reading the speech signal in wav format to get the vector value and sampling frequency from the recording and then extracting the cepstral component of the speech signal to get cepstral coefficient value from the signal [10, 11]. Last stage, the process of the matching distance using DTW algorithm to get pattern and value of the matching distance of beginner’s and expert’s makhraj pronunciation.

## 40.5 Results and Discussion

### 40.5.1 Analysis of Speech Beginner of Makhraj Pronunciation

In this section, an analysis has been obtained on the fundamental frequency F0 and formant frequencies F1, F2, and F3 based on the speech beginner, that has been recorded from GUI programming. After that, it will be statically analyzed to get the mean value of fundamental and formant frequencies of the speech beginner of makhraj pronunciation.

Figure 40.4 is the pattern signal of a phoneme hijaiyah letter fat-hah/ba/that produce by beginner speaker based on makhraj pronunciation and it also showing the pattern signal after preprocessing process. We can see that Fig. 40.4a has silent and unvoiced parts. This parts can be avoided from voice signal by preprocessing. So on Fig. 40.4b, it shows only the pattern of voiced signal, from which it can be obtained the fundamental frequency and formant frequencies. Figure 40.5 is the pattern of autocorrelation of voiced frame phoneme hijaiyah letter fat-hah/ba/that produced by beginner speaker based on makhraj pronunciation. Following the F0 estimation algorithm in the previous chapter and it can be obtained the value of F0 is 165.045 Hz (Fig. 40.6).

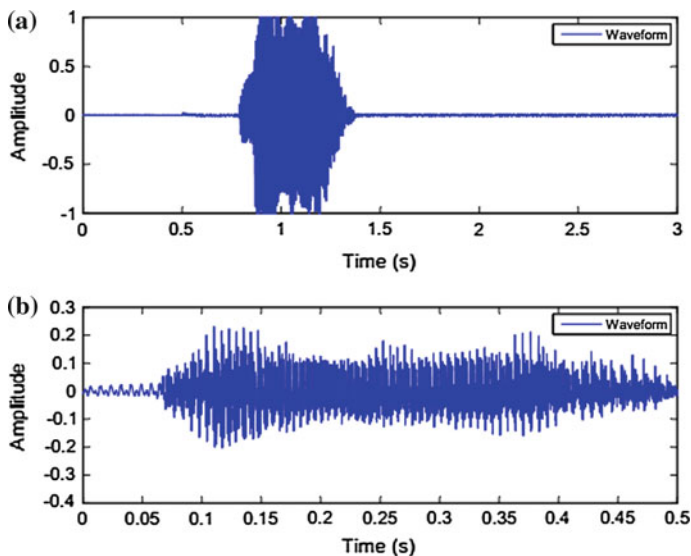


**Fig. 40.4** Phoneme Hijaiyah letter Fat-hah/ba/produce by beginner speaker, **a** Original speech and **b** speech after preprocessing

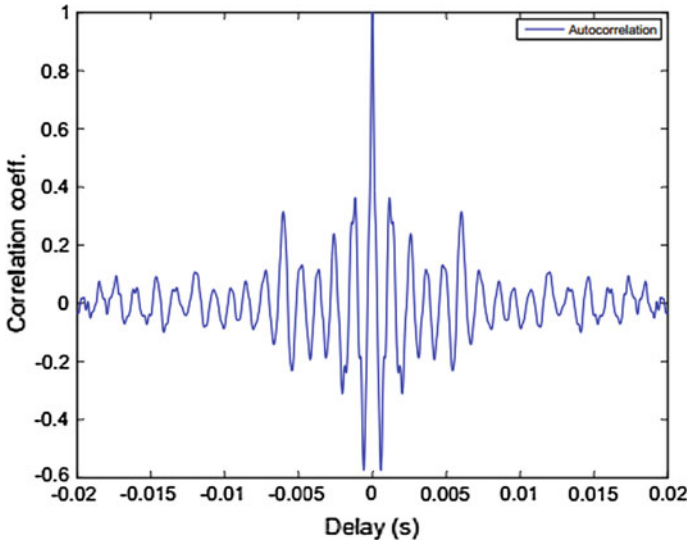


Fig. 40.5 Autocorrelation of phoneme Hijaiyah letter Fat-hah/ba/

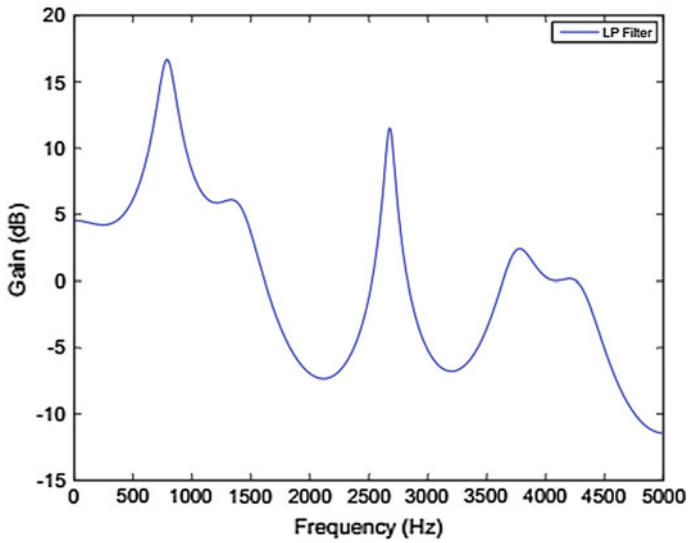
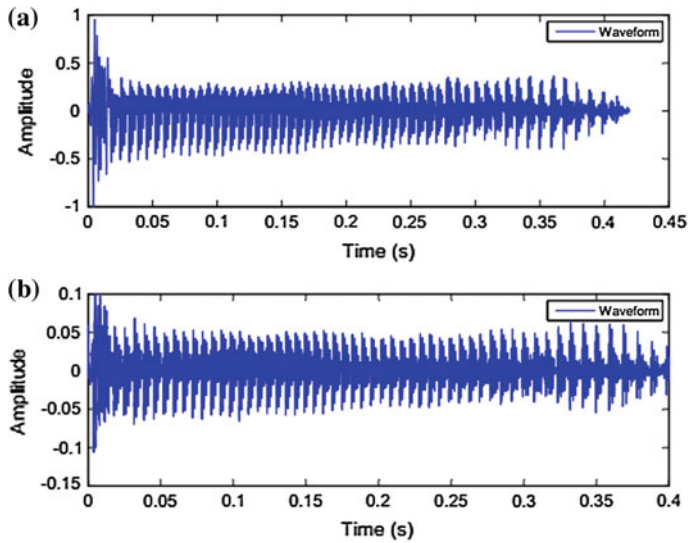


Fig. 40.6 Filter response of Hijaiyah letter Fat-hah/ba/of speech beginner





**Fig. 40.7** Phoneme Hijaiyah letter Fat-hah/ba/produce by expert speaker; **a** Original speech, and **b** speech after preprocessing

The formant frequencies value can be found by LPC algorithm followed from the previous chapter. LPC function has been there in MATLAB function and the formant frequencies are obtained by finding the roots of the prediction polynomial and F1 is 788.3 Hz, F2 is 1410.3 Hz, and F3 is 2678.6 Hz.

Figure 40.7 is the pattern signal of phoneme hijaiyah letter fat-hah/ba/that produce by expert speaker based on makhraj pronunciation and the pattern signal after preprocessing process. We can see that Fig. 40.7a doesn't have silent and unvoiced parts, as well as Fig. 40.7b, that makes the signal tight on preprocessing process and it will be obtained the fundamental frequency and formant frequencies.

### **40.5.2 The Result of Matching Distance Analysis Using DTW Method**

This section displays the results of using DTW matching distance analysis between speech beginner and expert speakers in the form of graphs and the smallest distance value.

Figure 40.8 shows the distance identical for the hijaiyah letter dham-mah/su/between sound of speech expert and expert makhraj pronunciation, and the matching distance value is 0. The best distance in distortion matrix is diagonal because the matching distance value between speech beginner and expert makhraj pronunciation is equal to zero.

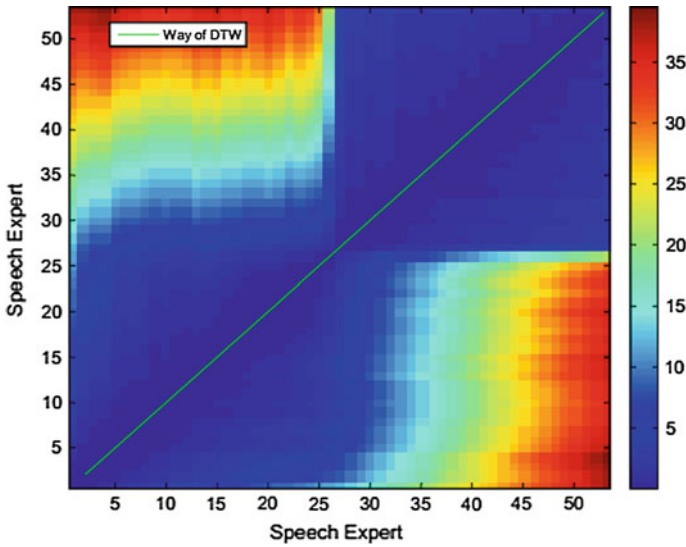


Fig. 40.8 Matching distance for identical the Hijaiyah letter/su/

## 40.6 Conclusion

The designed application for recognition of makhraj pronunciation and analysis of fundamental frequency and formant frequency has been accomplished. Some analysis data has been identified during designing and analysis process as follows:

1. Autocorrelation function can be used to obtain fundamental frequency from the speaker with makhraj pronunciation and LPC function can be used to obtain formant frequency from the speaker with makhraj pronunciation.
2. DTW method can be used to obtain matching distance between speech of beginner and expert makhraj pronunciation. All of hijaiyah letters with fat-hah, kas-rah, and dham-mah have matching distance's range of 28.9746–136.4. On the other hand, in an identical pattern the matching distance values is 0. Therefore, if an hijaiyah letter has higher matching distance than 0, it is incompatible the speech signal from source signal.

**Acknowledgments** We would like to thanks for the support of Ministry of Research Technology and Higher Education (Kemenristek-Dikti) for gave the grant of this research. Research grant scheme of *Program Hibah Bersaing* year 2014–2015.

## References

1. Mustari: Aplikasi Makharijul Huruf Hijaiyah Berbasis Multimedia. Universitas Islam Negeri Syarif Hidayatullah, Jakarta (2009)
2. Rabiner, L., Hwang-Juang, B.: Fundamentals of Speech Recognition. PTR Pentice-Hall Inc., (1993)
3. Rose, E.G.H.: Fundamental Frequency Estimation and Modelling for Speaker Recognition. University of Joensuu (2005)
4. Agus, H., Suyanto, H.: Pola Frekuensi Dasar Suara Penyiar Radio Indonesia. In: Digital Information & System Conference. Yogyakarta (2009)
5. Altedzar, R.W.D., Susetyo, B.B.: Aplikasi Pengenalan Gender Melalui Suara. Yogyakarta, Seminar Nasional Aplikasi Teknologi Informasi (2010)
6. Camell, T.: Spectrogram reading: what are formants? <http://www.cslu.ogi.edu/tutordemos/SpectrogramReading/ipa/formants.html> (1997). Accessed 12 Jan 2015
7. Fitch, J.L.: Voice and articulation. In: Lahey, B.B. (ed.) The modification of language behavior, pp. 130–177. Charles C. Thomas Publisher, Springfield, IL (1973)
8. Fitch, W.T.: Vocal Tract Length Perception and The Evolution of Language. Department of Cognitive and Linguistic Sciences at Brown University, Thesis (1986)
9. Kurnianto. N.A.: Penentuan Jenis Kelamin Itik Dengan Metode Dynamic Time Warping (DTW). Diponegoro University, Semarang (2005)
10. E. group: Cepstrum method. <http://www.clear.rice.edu/elec532/PROJECTS98/speech/cepstrum/cepstrum.html> (1998). Accessed 12 Jan 2015
11. Heeger, D.: Perception lecture notes: cochlear implants and speech perception. <http://www.cns.nyu.edu/david/courses/perception/lecturenotes/speech/speech.html> (2006). Accessed 12 Jan 2015

# Chapter 41

## Design and Fabrication of “Ha ( $\mu\text{m}$ )” Shape-Slot Microstrip Antenna for WLAN 2.4 GHz

Srisanto Sotyohadi, Sholeh Hadi Pramono and Moehammad Sarosa

**Abstract** This paper, a  $\mu\text{m}$  (is read “Ha”) shaped slotted microstrip antenna is designed, fabricated and analyzed. The proposed antenna used  $\mu\text{m}$ -shape slot is to improve return loss and operate for wireless LAN 2.4 GHz frequency band. The proposed antenna utilize transmission line model for analysis and simulation for return loss as well as VSWR with the support CST studio software. After doing some optimization on simulation, finally the dimension of microstrip patch antenna (MSPA) which operated on WLAN frequency 2.4 GHz is obtained. The best simulation results are then used as reference for MSPA fabrication on FR4 substrate with dielectric constant ( $\epsilon_r$ ) = 4.3 and thickness ( $h$ ) = 1.5 mm. The measurement result shows that the  $\mu\text{m}$ -slot microstrip antenna can achieve return loss (S11) -29.81 dB and VSWR 1.068 at 2.4640770 GHz. The proposed design shows that  $\mu\text{m}$  shape technically can be used as slot within patch to improve microstrip antenna performance.

**Keywords** CST studio software ·  $\mu\text{m}$ -shape slot · Microstrip antenna · Transmission line · Return loss

---

S. Sotyohadi (✉)

Department of Electrical Engineering, National Institute of Technology,  
Jalan Raya Karanglo, Km 2, Malang 65145, East Java, Indonesia  
e-mail: sotyoahadi@yahoo.com; sotyoahadi@fti.itn.ac.id

S.H. Pramono

Department of Electrical Engineering, University of Brawijaya,  
Jalan Veteran, Malang 65145, East Java, Indonesia

M. Sarosa

Department of Telecommunication Engineering, Polytechnic,  
Jalan Soekarno Hatta no. 9, Malang 65141, East Java, Indonesia

## 41.1 Introduction

Microstrip antenna becomes popular and it is widely used for wireless communication devices. This is due to its advantages compared to conventional antennas, such as Yagi-Uda, Horn, etc. [1]. The main advantages of microstrip antenna are light weight, low profile, small in size, ease to integrate with Microwave Integrated Circuit (MIC) and Monolithic Microwave Integrated Circuit (MMIC) [2]. However besides its advantages, microstrip antenna has some drawbacks like low efficiency, narrow bandwidth, and low gain [3].

There are several methods and techniques that have been introduced in order to enhance the bandwidth and gain of microstrip antenna, including enlargement of the substrate thickness, low permittivity dielectric substrate utilization, and implementation of slot in microstrip patch antenna, etc. [4]. One of techniques that has been implemented is the usage of slot in patch to improve the microstrip antenna parameter. There are several shapes of slot, most of them are in the form of alphabetical, as well as C and S-slot [5], combination between I and E-slot [4], double C-slot [6] and many others.

This paper presents a new  $\text{Ha}$ -shaped slot in microstrip patch antenna.  $\text{Ha}$  (“Ha”) is ancient Javanese letter, in which the form is similar to a combination of inverted S and M letter. The reason of using  $\text{Ha}$ -slot is to improve the return loss ( $S_{11}$ ) in comparison to the previous research which reaches maximum in the range of  $-26$  dB for C and S-Slot, while others as describe previously is less than  $-26$  dB. Besides technical aspect, the use of  $\text{Ha}$ -slot is to maintain the cultural heritage of Indonesian by using Javanese ancient letter as an alternative form of slots besides the alphabetic letters and other shape of patch slot.

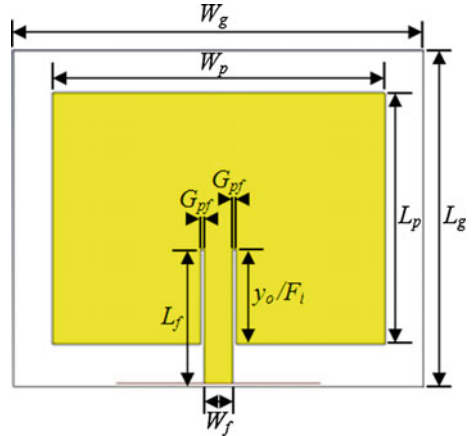
## 41.2 Antenna Design

### 41.2.1 Reference Antenna

Rectangular microstrip patch antenna shows in Fig. 41.1 is the reference antenna for the proposed  $\text{Ha}$ -shaped slot in microstrip patch antenna. This antenna has implemented an inset feed line technique for matching impedance [3].

The dimension of the rectangular microstrip patch antenna has substantial parameter such as resonant frequency ( $f_r$ ), dielectric permittivity constant of the substrate ( $\epsilon_r$ ), and height or thickness of the substrate ( $h$ ). Those substantial parameters are considered for calculating the length and width of the patch, as well as calculating the length and the width of the ground plane.

**Fig. 41.1** Profil of rectangular microstrip antenna with inset feed



### 41.2.2 Design Procedure

**Step 1:** Determination of the MSPA Width ( $W_p$ ) [2]:

$$W = \frac{1}{2f_r \sqrt{\frac{\epsilon_r + 1}{2}}} \tag{41.1}$$

where  $c = 3 \times 10^8$  m/s,  $\epsilon_r = 4.3$ ,  $f_r = 2.4$  GHz. By substituting the above equation with the given value, it can be determined that  $W_p = 38.3934$  mm.

**Step 2:** Determination the effective dielectric constant  $\epsilon_{reff}$  [3]:

$$\epsilon_{reff} = \frac{\epsilon_r + 1}{2} + \frac{\epsilon_r - 1}{2} \left( 1 + 12 \frac{h}{W} \right)^{-1/2} \tag{41.2}$$

From step 1 known parameter and thickness of the substrate  $h = 1.5$  mm,  $W = W_p$ , it can be determined that  $\epsilon_{reff} = 4.0114$ .

**Step 3:** Determination of the effective length ( $L_{eff}$ ) [7]:

$$L_{eff} = \frac{c}{2f_r \sqrt{\epsilon_{reff}}} \tag{41.3}$$

By replacing  $c$ ,  $f_r$  and  $\epsilon_{reff}$  it can be determined that  $L_{eff} = 31.2$  mm.

**Step 4:** For the length extension ( $\Delta L$ ) of the patch can be determined [8]:

$$\Delta L = 0.412h \frac{(\epsilon_{reff} + 0.3) \left(\frac{W}{h} + 0.268\right)}{(\epsilon_{reff} - 0.258) \left(\frac{W}{h} + 0.8\right)} \quad (41.4)$$

By substituting the result that have been obtained from step 1 until 3, it can be determined that  $\Delta L = 0.69546$  mm.

**Step 5:** For the actual length ( $L_p$ ) of the MSPA can be calculated using following equation [9]:

$$L = L_{eff} - 2\Delta L \quad (41.5)$$

After substituting the above equation with the obtained result, the actual patch length can be determined as  $L = L_p = 29.8145$  mm.

According to Punit S. Nakar, the size of ground plane is larger than the patch dimensions by approximately six times the height or thickness of the substrate all around the periphery. Hence for the dimension design of the ground plane is determined by [10],

$$L_g = 6h + L \quad (41.6)$$

$$W_g = 6h + W \quad (41.7)$$

Finally it can be determined the value for  $L_g = 38.8145$  mm and  $W_g = 47.3934$  mm.

### 41.2.3 Transmission Line Model

Inset feed microstrip line is a technique in transmission line to match the impedance between patch antenna which typically has the value between 150–300  $\Omega$  and the desired impedance for transmission line typically 50  $\Omega$  [3].

The dimension of the transmission line has important value in order to match condition between antenna and the transmission line, as does the length of feed line in which can be determined from following equation [3],

$$L_f = \frac{\lambda}{4\sqrt{\epsilon_{reff}}} \quad (41.8)$$

By replacing  $\lambda = 125$  mm and the  $\epsilon_{\text{reff}} = 4.0114$  then the result for  $L_f = 15.6027$  mm.

The following calculation is determined the width of the feed line, which can be calculated by equation [11],

$$W_f = \left(2 \frac{h}{\pi}\right) \frac{(B - 1 - x(\epsilon_r - 1))}{2 \cdot \epsilon_r} \left(n + \left(\frac{0.39 \times 0.61}{\epsilon_r}\right)\right) \quad (41.9)$$

From above equation if  $B = 5.7115$ ,  $n = 1.5500$  and  $x = 1.9299$ , it can be determined for width of the feed line  $W_f = 3.3639$  mm.

The gap ( $G_{pf}$ ) between microstrip feed line and the patch of microstrip antenna can be determined [12],

$$G_{pf} = \frac{v_o}{\sqrt{2 \times \epsilon_{\text{reff}}}} \frac{4.65 \times 10^{-12}}{f} \quad (41.10)$$

By substituting  $v_o = 3.10^8$  m/s,  $f = 2.4$  GHz and  $\epsilon_{\text{reff}} = 4.0114$  it will have for  $G_{pf} = 0.20521$  mm.

For the inset feed line length  $y_o$  or  $F_i$  is determined by [12],

$$y_o = \left(\frac{L_p}{\pi}\right) \cdot \left(\text{acos} \sqrt{\frac{z}{R_{in}}}\right) \quad (41.11)$$

After substituting  $L_p = 29.8145$  mm,  $z = 50 \Omega$  and for  $R_{in} = 317.6670 \Omega$ , it can be determined for  $y_o = 11.0356$  mm.

### 41.3 Proposed Antenna

The proposed antenna dimension and the shape of  $\Pi$ -slot in the MSPA is shown in Fig. 41.2. From the Fig. 41.2 shows that the slots are placed above the inset feed transmission line. The dimension value of the proposed  $\Pi$ -slot MSPA is obtained after optimizing and tuning the length of patch ( $L_p$ ), the gap of inset feed ( $G_{pf}$ ), the length of transmission line ( $L_f$ ), and slot width  $S_1$ - $S_9$  using CST studio. Finally the dimension of proposed antenna and the slots are given in the Tables 41.1 and 41.2 respectively.



**Fig. 41.2** Profil of  $\Omega$ -slot placed in patch of microstrip antenna

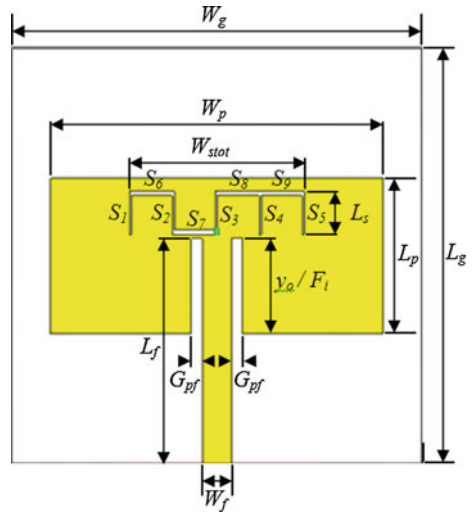


**Table 41.1** Proposed antenna dimension

No.	Antenna dimension	Value (mm)
1	$L_p$	18
2	$W_p$	38.3934
3	$L_g$	48
4	$W_g$	47.3934
5	$h$	1.5
6	$L_f$	26
7	$W_f$	3.3639
8	$F_i$	11.0356
9	$G_{pf}$	0.9

**Table 41.2**  $\Omega$ -slot dimension

No.	Slot width dimension	Value (mm)
1	$S_1$	0.25
2	$S_2$	0.25
3	$S_3$	0.25
4	$S_4$	0.25
5	$S_5$	0.25
6	$S_6$	0.5
7	$S_7$	0.5
8	$S_8$	0.5
9	$S_9$	0.5
10	$L_s$	5
11	$W_{stot}$	10.25

## 41.4 Simulation Result

### 41.4.1 Return Loss

For simulating the design of  $\Omega\Omega$ -slot MSPA, CST studio software is used. After simulation the design, the result for return loss (S11) is shown in Fig. 41.3. The equation for return loss is calculated from the reflection coefficient [13],

$$\text{Return Loss (in dB)} = 20 \log_{10}(\text{VSWR}/\text{VSWR} - 1) \tag{41.12}$$

For good result, the return loss should be less than  $-10$  dB. Which equivalent to  $\text{VSWR} < 2$ . From the Fig. 41.3. It is clear that the simulation result for S11 is  $-24.282264$  dB at resonance frequency  $2.412$  GHz.

### 41.4.2 VSWR

Voltage Standing Wave Ratio (VSWR) can be calculated using the following equation [14],

$$\text{VSWR} = \frac{1 + |\Gamma|}{1 - |\Gamma|} = \frac{1 + |S_{11}|}{1 - |S_{11}|} \tag{41.13}$$

where  $\text{VSWR}$  = reflection coefficient,  $\Gamma$  = voltage sent/voltage reflected. If  $\Gamma = 0$ , there is no reflection, it represents that perfect matching. Figure 41.4 shows the simulated result for  $\text{VSWR} = 1.130$ , which is less than 2.

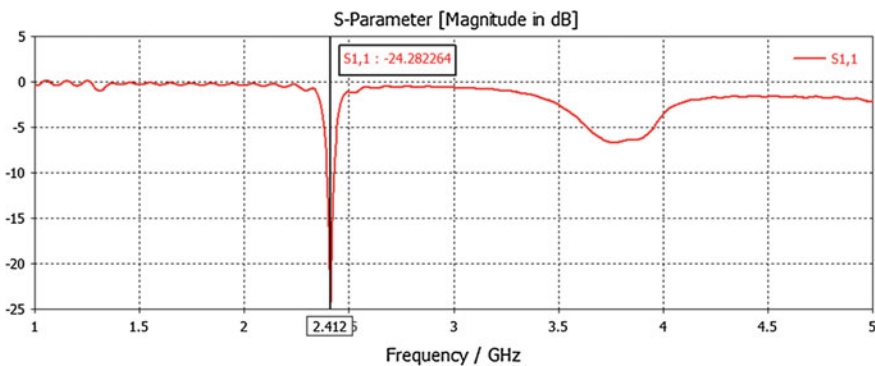


Fig. 41.3 Return loss (S11) of the proposed  $\Omega\Omega$ -slot microstrip patch antenna

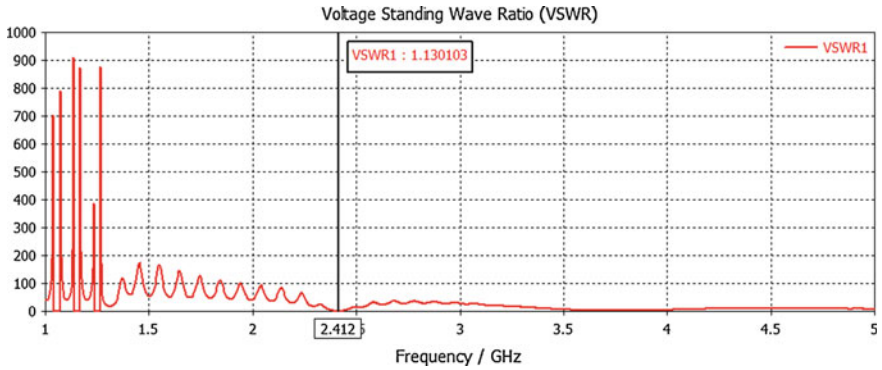


Fig. 41.4 Simulated VSWR of the proposed antenna

### 41.5 Measurement Result

The measurement result for return loss (S11) is shown in Fig. 41.5a. While the measurement result for VSWR is shown in Fig. 41.5b. Both measurements were performed using vector network analyzer (VNA).

The obtained return loss for measurement is  $-29.81$  dB and VSWR is 1,068 at resonant frequency of 2.460770 GHz.

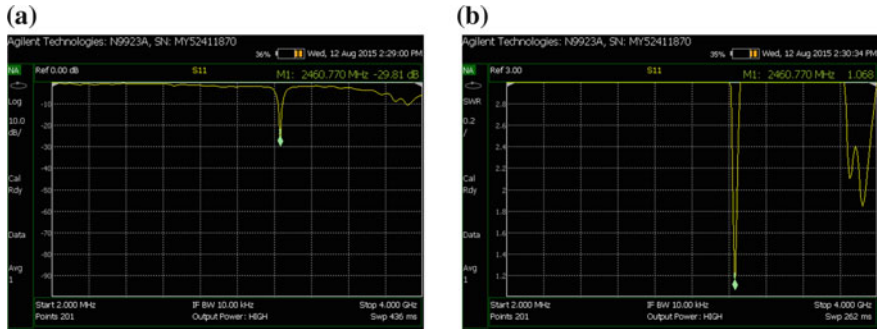


Fig. 41.5 a Return loss  $\Gamma$ -slot MSPA, b VSWR  $\Gamma$ -slot MSPA

## 41.6 Conclusion

A  $\Omega$ -slot microstrip patch antenna for 2.4 GHz is fabricated and presented. The proposed antenna is suitable and effectively operated for WLAN applications. The fabricated antenna has good performance and almost perfectly impedance matching. It can be concluded from the measurement result that the antenna has satisfactory performance for operating indoor WLAN applications.

## References

1. Singh, D., Gupta, K.A., Prasad, R.K.: Design and analysis of C-shaped microstrip patch antenna for wideband application. *VSRD Int. J. Electr. Electron. Commun. Eng.* **3**(1) (2013)
2. Girish, K., Ray, K.P.: *Broadband Microstrip Antennas*, pp. 3–4. Artech House, London (2005)
3. Balanis A: *Constantine, Antenna Theory Analysis and Design*, 3rd edn. John Wiley and Sons (2005)
4. Kushwaha, R.S., Srivastava, D.K., Saini, J.P.: A multi-slotted wide microstrip patch antenna for dual frequency. *Int. J. Comput. Sci. Inf. Technol.* **3**(2), 3523–3525 (2012)
5. Li, F., Ren, L.S., Zhao, G., Jiao, Y.C.: Compact triple-band monopole antenna with C-shaped and S-shaped meander strips for Wlan/Wimax applications. *Prog. Electromagnet. Res. Lett.* **15**, 107–116 (2010)
6. Boutheina, T.: Design of Double C-Slot Microstrip Patch Antenna for WiMax Application. 978-1-4244-4968-2/10, IEEE (2010)
7. Divya, R., Priya, M.: Design and characterization of E-shape microstrip patch antenna for wireless communication. *ICTACT J. Commun. Technol.* **4**(1) (2013)
8. Pauria, B.I., Kumar, S., Sharma, S.: Design and simulation of E-shape microstrip patch antenna for wideband applications. *Int. J. Soft Comput. Eng.* **2**(3) (2012)
9. Singh, J., Tiwari, M., Neha, P.: Design and simulation of microstrip E-shaped patch antenna for improved bandwidth and directive gain. *Int. J. Eng. Trends Technol.* **9**(9) (2014)
10. Punit, N.S.: Design of a compact microstrip patch antenna for use in wireless cellular devices. Master thesis, Florida State University (2004)
11. Liang, J., Antenna study and design for ultra-wideband communication applications. Doctor of Philosophy thesis, Queen Mary University of London, UK (2006)
12. Matin, A.M., Sayeed, I.A.: A design rule for inset-fed rectangular microstrip patch antenna. *WSEAS Trans. Commun.* (2010)
13. Atser, R.A., Joseph, M.M., Gabriel, I.A.: Enhancing the bandwidth of a microstrip patch antenna using slots shaped patch. *Am. J. Eng. Res.* **2**(9), 23–30 (2013)
14. Pozar, D.M.: *Microwave Engineering*, 3rd edn. John Wiley & Sons, Inc. New Jersey (2005)

# Chapter 42

## Investigation of the Electric Discharge Machining on the Stability of Coal-Water Slurries

S.L. Buyantuev, A.B. Khmelev, A.S. Kondratenko  
and F.P. Baldynova

**Abstract** The paper presents the characteristics of coal-water slurries (CWS) prepared by electric discharge methods. The radius of the minimum size, most probable size and maximum size particles of CWS was found. The sedimentation speed of the particles of each size was defined. The sedimentation curve, integral distribution curve, differential distribution curve after and without electric discharge machining were structured. The process of sedimentation by the analytical method, integral sedimentation distribution law and the differential form of this equation were described. As a result of investigations it was found that coal-water slurry after discharge treatment has lower sedimentation speed than before treatment. Differential distribution curves show that the treated coal-water slurry is dominated by the particle size of substantially  $0.1537 \cdot 10^{-4}$  m, whereas in the untreated slurry predominate particle size is  $0.413 \cdot 10^{-4}$  m, that indicates an increase in aggregate stability of the treated system.

**Keywords** Coal-water slurry · Electric discharge methods · Sedimentation analysis · Particle radius

### 42.1 Introduction

Currently, the deficit increases the liquid and gaseous fuels on the market, which is reflected in the growth of their value. Analysis of the world's resources of non-renewable fuels leads to the conclusion that the most promising for use in energy is coal, because its reserves on Earth many times the total oil and gas

---

S.L. Buyantuev (✉) · A.B. Khmelev · F.P. Baldynova  
East Siberian State University of Technology and Management, Ulan-Ude,  
Buryat Republic, Russia  
e-mail: buyantuevsl@mail.ru

A.S. Kondratenko  
Buryat State University, Ulan-Ude, Buryat Republic, Russia

reserves. However, environmental problems arising from the use of coal fuel, require the development and introduction of new effective economic and environmental points of view coal technologies. This requires improved consumer properties of coal and master to obtain coal-based alternative fuels by replacing scarce natural resources: gas and liquid petroleum fuels.

In connection with this is the actual use of coal as a coal-water slurry fuel or coal-water slurry (CWS) [1]. CWS has technological properties of liquid fuels (transportation to road and rail tanks through pipelines, tankers and bulk vessels, storage in closed containers) and must retain their properties during prolonged storage and transportation, meanwhile it has to be sedimented in stability [2].

## 42.2 Experiment Setup and Methods

The solution is based on the use of plasma and electrolytic methods for the preparation of the CWS without the use of plasticizers. The methodology of the experiment and previously obtained micrographs and elemental analysis of coal before and after treatment was considered in detail in [3].

Today, there are many industrial methods of obtaining the CWS, but almost all of them require the use of reagent-plasticizer for special characteristics: low viscosity, good fluidity, long-term stability of suspended particles of coal.

Experimental setup described in this article will allow to get the CWS with a maximum energy efficiency and minimum cost by using of electric discharge methods. Key parameters and technical condition related to experimental setup of electric discharge: amperage 10–30 A, voltage 200 V, time of machining 10–30 min, the concentration of coal 40–60 %, the concentration of water 60–40 %, the size of coal fraction 0–200  $\mu$  [4]. The electric discharge machining can form nano carbon materials [5].

This article shows the results of the study particle radius of CWS before and after discharge machining method and the sedimentation rate of subsidence.

Sedimentation method of analysis is the definition of particle size distribution based on the difference in the speed of sedimentation of particles in a viscous medium, depending on their size. By measuring the sedimentation speed, you can determine the radius of the settling particles by the Stokes' law [6]:

$$r = \sqrt{\frac{9 * \eta * U}{2 * (\rho_y * \rho_B) * g}}, \quad (42.1)$$

where  $r$ —particle radius,  $U$ —settling speed of a particle in a liquid medium,  $\rho_y$ —density of the coal powder,  $\rho_B$ —density of the liquid medium,  $g$ —acceleration of gravity,  $\eta_B$ —the viscosity of the liquid medium.

Sedimentation speed of the particles measured by a special instrument designed to sedimentation analysis. The liquid medium is water with a known value of

viscosity, in which coal powder is dispersed to yield 0.5 % solution (by volume) of the suspension. After mixing, the suspension left to flake, periodically weighing precipitated by the load on the cup. As a result of continuous determination of the mass of sedimentation precipitate sedimentation curve was build (Fig. 42.1).

Then sedimentation curve is treated graphically (by constructing tangents at the points of the curve, corresponding to different values of  $\tau$ ) and receive data to build integral and differential distribution curves (Figs. 42.2 and 42.3).

The shape of the differential distribution curve shows the uniformity of coal powder size. However, when using a graphical method of calculating the distribution curves there are possible errors related to insufficient accuracy of the tangent to the curve. These disadvantages can be avoided by the analytical method of the construction of the distribution curves which is proposed by Tsyurupa N. (Fig. 42.4).

The following calculation shows the numeric values and the CWS after electric discharge treatment. In the analytical method, the process of sedimentation is described by:

$$Q = Q_m = \frac{\tau}{\tau + \tau_0} \tag{42.2}$$

Fig. 42.1 The sedimentation curve

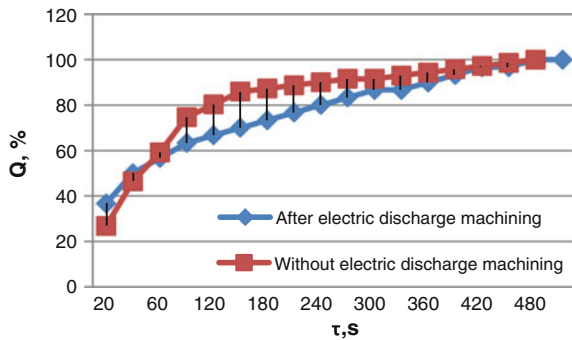
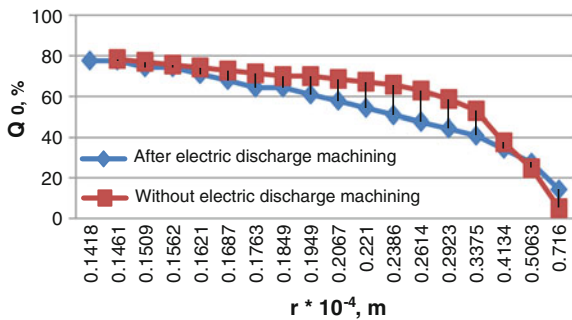
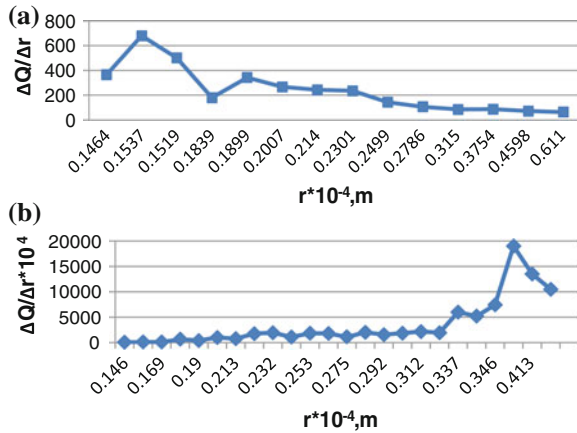


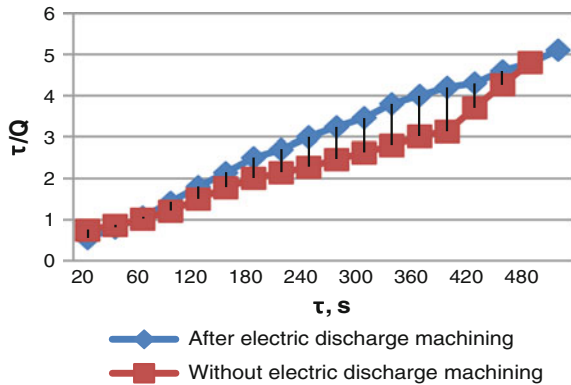
Fig. 42.2 The integral distribution curve



**Fig. 42.3** The differential distribution curve. **a** After electric discharge machining, **b** without electric discharge machining



**Fig. 42.4** The sedimentation curve



where  $Q$ —fraction weight,  $\tau$ —time,  $Q_m$  and  $\tau_0$ —constants, wherein  $Q_m$ —It depends on the polydispersity and is called the coefficient of polydispersity. This equation is better to use in the linear form (Fig. 42.4):

$$\frac{\tau}{Q} = \frac{\tau_0}{Q_m} + \frac{\tau}{Q_m}, \tag{42.3}$$

After getting straight  $\frac{\tau}{Q} = f(\tau)$ ,  $Q_m$  is calculated according to the values cotangent angle it to the x-axis:

$$Q_m = ctg\alpha = \frac{1}{tg\alpha} = \frac{1}{0.2671} = 4.6(\%), \tag{42.4}$$

$$\frac{\tau_0}{Q_m} - \text{over the interval on the ordinate and } \tau_0 = \frac{\tau}{Q} Q_m$$



$$\frac{\tau_0}{Q_m} = 0.4322, \tau_0 = 0.4322 * 4.6 = 1.9881(\text{s})$$

Using the equation

$$r_0 = \sqrt{\frac{K * h}{\tau_0}}, K \text{ is calculated:}$$

$$r_0 = \sqrt{\frac{10.2521 * 10^{-8} * 16.5 * 10^{-2}}{1.9881}} = 9.22 * 10^{-5}(\text{m}), \quad (42.5)$$

$$K = \frac{9 * \eta * h}{2 * (\rho_y * \rho_B) * g} = \frac{9 * 0.897 * 10^{-3} * 16.5 * 10^{-2}}{2(1.66 - 0.9971) * 10^3 * 9.8} = 10.2521 * 10^{-8} \quad (42.6)$$

From the kinetic equation obtained the following integral sedimentation distribution law [4]:

$$Q_0 = Q_m \left( \frac{r_0^2}{r^2 + r_0^2} \right)^2, \quad (42.7)$$

where  $Q_0$ —the proportion of fractions having a radius  $\leq r$ ;  $r_0$ —coefficient depending on the dispersion. The differential form of this equation has the form:

$$F = \frac{dQ_0}{dr} = 4Q_m \cdot r_0^4 \frac{r}{(r^2 + r_0^2)^3}. \quad (42.8)$$

Next, define three major radius characterizing the particle distribution curve.

### 42.3 Results and Discussions

The minimum size of the particles:

$$\begin{aligned} r_{min} &= r_0 * \sqrt{0.1 * (\sqrt{Q_m} - 1)} = 9.22 * 10^{-5} * \sqrt{0.1 * (\sqrt{4.6} - 1)} \\ &= 3.11 * 10^{-5}(\text{m}) \end{aligned} \quad (42.9)$$

The most probable particle size:

$$r_{H.B.} = \frac{r_0}{2.24} = \frac{9.22 * 10^{-5}}{2.24} = 4.12 * 10^{-5}(\text{m}) \quad (42.10)$$

The maximum size of the particles:

$$r_{\max} = 3 * r_0 = 3 * 9.22 * 10^{-5} = 27.66 * 10^{-5}(\text{m}). \quad (42.11)$$

The system is polydisperse, the sedimentation speed of the particles is as follows:

$$U_{ce\partial} = \frac{2gr^2(\rho - \rho_0)}{9\eta}. \quad (42.12)$$

where  $U$ —sedimentation speed,  $r$ —the radius of the particles of coal,  $g$ —acceleration of gravity.

CWS without electric discharge treatment has the following characteristics:

The minimum size of the particles:  $r_{\min} = 4.3726 * 10^{-5}(\text{m})$ ,

The speed of sedimentation of the minimum size particles:  
 $U_{ce\partial} = 30.77 * 10^{-4} \text{ m/s}$

The most probable particle size:  $r_{\text{H.B.}} = 4.6083 * 10^{-5}(\text{M})$

The speed of sedimentation of the most probable size particle:  
 $U_{ce\partial} = 34.1783 * 10^{-4} \text{ m/s}$ ,

The maximum size of the particles:  $r_{\max} = 30.9681 * 10^{-5}(\text{M})$ ,

The speed of sedimentation of the maximum size particles:  
 $U_{ce\partial} = 1543.47 * 10^{-4} \text{ m/s}$ .

CWS after electric discharge treatment has the following characteristics:

The minimum size of the particles:  $r_{\min} = 3.11 * 10^{-5}(\text{m})$ ,

The speed of sedimentation of the minimum size particles:  
 $U_{set.} = 15.58 * 10^{-4} \text{ m/s}$ ,

The most probable particle size:  $r_{m.p.} = 4.12 * 10^{-5}(\text{m})$ ,

The speed of sedimentation of the most probable size particle:  
 $U_{set.} = 27.35 * 10^{-4} \text{ m/s}$ ,

The maximum size of the particles:  $r_{\max} = 27.66 * 10^{-5}(\text{m})$ ,

The speed of sedimentation of the maximum size particles:  
 $U_{set.} = 1232.59 * 10^{-4} \text{ m/s}$ .

## 42.4 Conclusions

Our experiments have shown that the electric discharge machining coal-water slurry makes the system stable. Using an analytical method for constructing the distribution curves proposed by NN Tsyurupa, determined the rate of sedimentation of particles in suspensions treated by electric discharge and not treated. Analysis showed that the sedimentation velocity of the particles is reduced in the treated coal-water slurry from  $U_{ce\partial} = 30.77 * 10^{-4} \text{ m/s}$  to  $U_{ce\partial} = 15.58 * 10^{-4} \text{ m/s}$ , with a minimum particle size. Particles with size  $r_{\text{H.B.}} = 4.12 * 10^{-5}(\text{m})$  the suspension

treated and  $r_{H.B.} = 4.6083 \cdot 10^{-5}(\text{m})$  in the untreated slurry have sedimentation speed  $U_{ce\partial} = 27.35 \cdot 10^{-4} \text{ m/s}$  and  $U_{ce\partial} = 34.1783 \cdot 10^{-4} \text{ m/s}$ , respectively. The particles having a maximum particle  $r_{max} = 27.66 \cdot 10^{-5}(\text{m})$  of the treated slurry and  $r_{max} = 30.9681 \cdot 10^{-5}(\text{M})$  in untreated slurry have different speed:  $U_{ce\partial} = 1232.59 \cdot 10^{-4} \text{ m/s}$ —the speed of sedimentation of treated suspension,  $U_{ce\partial} = 1543,47 \cdot 10^{-4} \text{ m/s}$ —*the speed of sedimentation of untreated suspension*.

Differential distribution curves show that the treated coal-water slurry is dominated substantially by the particle size of  $0.1537 \cdot 10^{-4} \text{ m}$  (Fig. 42.3a), whereas in the untreated slurry predominate particle size  $0.413 \cdot 10^{-4} \text{ m}$  (Fig. 42.3b), that indicates an increase in aggregate stability of the treated system.

Thus, electric discharge machining improves the stability of coal-water suspension of dispersed systems.

## References

1. Senchurova, J., Murko, V., Fedyayev, V., Dziuba, D., Pusirev, E.: The Tomsk Polytechnic University news, pp. 37–40 (2008)
2. Zhuravlev, N., Murko, V., Fedyayev, V., Dziuba, D., Senchurova, Y., Zaostrovsky, A.: Ecology and Industry of Russia, pp. 6–9 (2009)
3. Buyantuev, S., Kondratenko, A., Khmelev, A.: ARPN J. Eng. Appl. Sci. **9**(11), 2102–2105 (2014)
4. Buyantuev, S., Kondratenko, A., Khmelev, A.: Vestnik ESSTU **5**, 72–75 (2014)
5. Buyantuev, S., Kondratenko, A., Khmelev, A.: Vestnik ESSTU **3**, 21–25 (2013)
6. Baldynova, F.: Surface phenomena and disperse systems, Eds. ESSTU, 160 (2010)

# Chapter 43

## A River Water Level Monitoring System Using Android-Based Wireless Sensor Networks for a Flood Early Warning System

Riny Sulistyowati, Hari Agus Sujono and Ahmad Khamdi Musthofa

**Abstract** The water level of a river needs to be monitored to anticipate the occurrence of flooding. People who live in flood prone areas should know the height of the river water level early enough before flooding occurs. This study had designed and developed a river water level monitoring systems using ultrasonic sensors and a microcontroller-based Android smartphone. The sensor system sends information about the river water level continuously to the microcontroller. The microcontroller analyzes the information and the analysis results are disseminated to the public by means of the Android smartphone equipped with the flood detection application. The test results on the performance of ultrasonic sensors show an average error rate of 1.121 % and an error rate on the speed of change in the water level of 1 cm. Sending SMS on smartphones gets the average delivery time of 5.414 s. For further research, we will design a system monitoring the water level of the river using wireless ultrasonic sensor network as a flood early warning system based on microcontroller and Android smartphone.

**Keywords** Monitoring system · Water level · Ultrasonic sensor · Wireless · Android-based flood detection

### 43.1 Introduction

Flood disasters still occur frequently in Indonesia. There are many impacts of the flood on the economic, social and environmental sectors. Flooding occurs because the water volume in the river exceeds its containing capacity. The damages caused by flood are not only in material losses, but also in deaths. The impacts of flood can be mitigated if people are better prepared for the coming flood. One of the ways is

---

R. Sulistyowati (✉) · H.A. Sujono · A.K. Musthofa  
Department of Electrical Engineering, Faculty of Industrial Technology, Institute of  
Technology Adhi Tama Surabaya, Surabaya, Indonesia  
e-mail: riny.itats@yahoo.com

to disseminate information to the people quickly in the form of a flood early warning system [1]. One of the media that can be used to disseminate the information is a communication network using wireless Android-based flood detection devices.

### 43.2 Literature Review

#### 43.2.1 Past Research

Studies on the systems monitoring the water level of a river for early warning of flooding had been conducted in the past. Detecting the water level can be done using Doppler radar, but it requires a complex hardware design [2, 3]; besides, it requires considerable cost. A cheaper alternative to detect the water level is to use a microcontroller based ultrasonic sensor [4]. Another study built the water surface level monitoring system with a display on the social networking site Twitter as an early warning against floods; results were obtained in the form of a flood warning system that was connected with social networking site Twitter [5]. However, the social networking site is not accessible to all levels of society.

#### 43.2.2 PING Ultrasonic Sensor

A PING ultrasonic transmitter and receiver are used as a sensor measuring the distance of an object, which is—in this case—water. Usage of this sensor is very simple and it can be easily linked to a microcontroller through an input/output pin as shown in Fig. 43.1a.

Figure 43.1b shows the ultrasonic sensor consisting of two circuits: transmitter (Tx) and receiver (Rx). The sensor circuit that functions as a transmitter will emit an

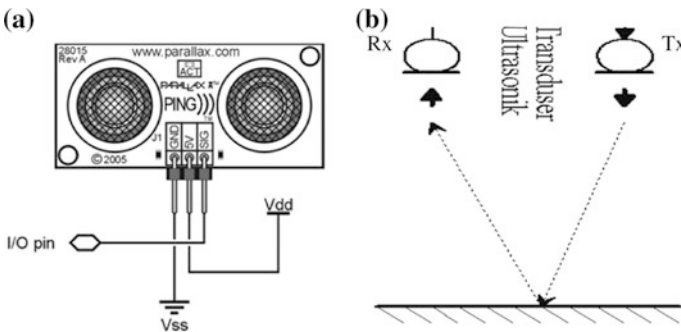


Fig. 43.1 a PING ultrasonic sensor [8]. b Working system of ultrasonic sensor

ultrasonic wave with a certain frequency. When it collides with an object, the ultrasonic wave will be reflected and received by the sensor circuit that functions as a receiver [6]. The maximum distance that can be read by the ultrasonic sensor is 2–3 m. The sensor distance toward the reflecting object can be calculated with the following formula (43.1):

$$S = \frac{(t_{IN} \times V)}{2} \quad (43.1)$$

Where,  $S$ : sensor distance toward the object,  $t_{IN}$ : time difference between transmitting and receiving the reflected wave,  $V$ : velocity of ultrasonic wave in the air (344 m/s).

### 43.2.3 Data Communication Based on Wireless Sensor Network Zigbee

One basic component of a wireless sensor is a wireless communication device. The wireless communication device is used as the communication medium for the water level sensor mounted on the monitoring area on the server to provide an early warning in case of a possible flood. Wireless communication device used in this research is based on Zigbee.

ZigBee is an IEEE 802.15.4 based standard for data communication on personal and business devices. ZigBee is designed with low power consumption and is working on a low level of personal network. A ZigBee device is commonly used to control another device or used as a wireless sensor. ZigBee has features to manage its own network as well as data exchange on the network. The advantage over other ZigBee devices is low power consumption so that it can be used as a wireless device controller whose installation only needs to be done once; that is, only with one battery ZigBee can last up to a year [7].

## 43.3 Research Methodology

### 43.3.1 Design of System Block Diagram

Figure 43.2 shows the block diagram of hardware design of controller system and early flood warning system using ultrasonic sensors, microcontroller 32 minimum system, zigbee wireless communication module, power supply, LCD display and Android smartphone. Figure 43.3 shows the flowchart of the system.

The set value of the water level in the laboratory testing: 1. Normal Level, (distance  $\geq 60$  cm), 2. Alert Level 1 (60 cm  $>$  distance  $\geq 40$  cm), 3. Alert Level 2 (40 cm  $>$  distance  $\geq 25$  cm) and 4. Warning Level (distance  $< 25$  cm)

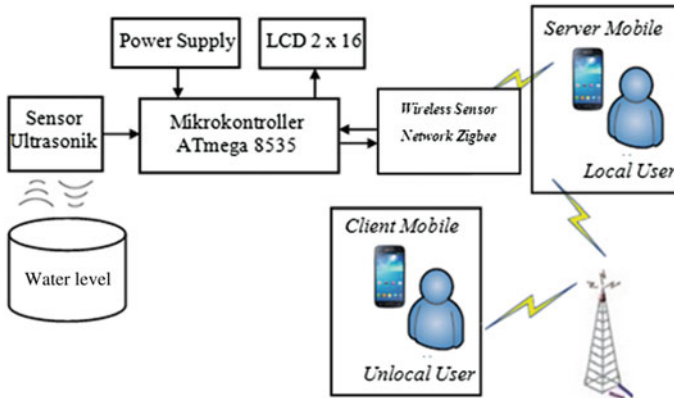


**Fig. 43.2** System block diagram

### ***43.3.2 Mechanical Design and Building***

Mechanical design of this control system application is very crucial in achieving optimal results, as shown in Fig. 43.4. In general, the mechanics and software or hardware of this control system application must be balanced or complementary. According to the block diagram in Fig. 43.2, the PING Ultrasonic Sensor is installed on this tool to measure the water surface level against the land, while the liquid crystal display (LCD) and ZigBee Wireless Sensor Network (Android) provide output; the sensor and the output are connected directly to the port on the microcontroller.

### ***43.3.3 Android Smart Phone Application Development***

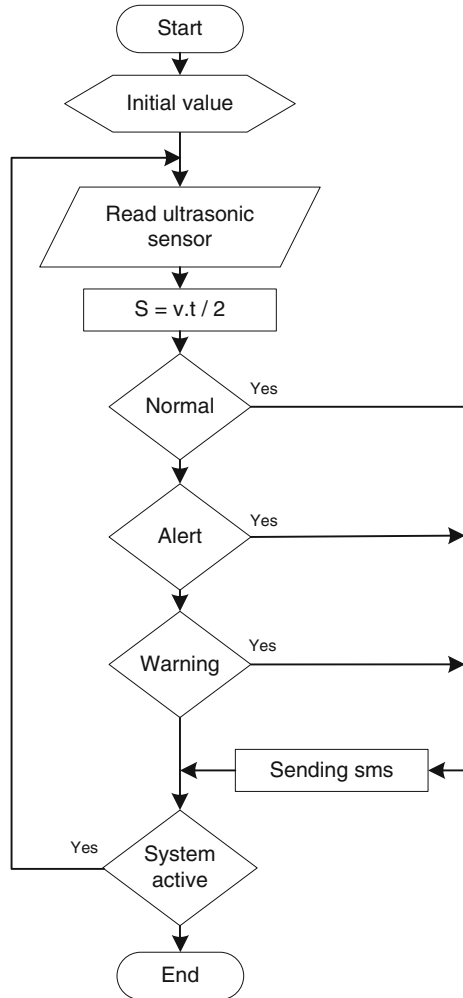
When developing the Android Smart Phone application, the authors opted to use the IDE APP MIT Inventor 2 software, with Kawa programming language, which is easy to develop. The coding method is like playing a puzzle, just drag and drop the required components in the software working window, without having to type the program code manually.

## **43.4 Results and Discussion**

### ***43.4.1 Hardware Testing***

Hardware testing was carried out to determine whether the designed hardware works or functions properly as expected. The tests performed on the hardware

Fig. 43.3 System flowchart



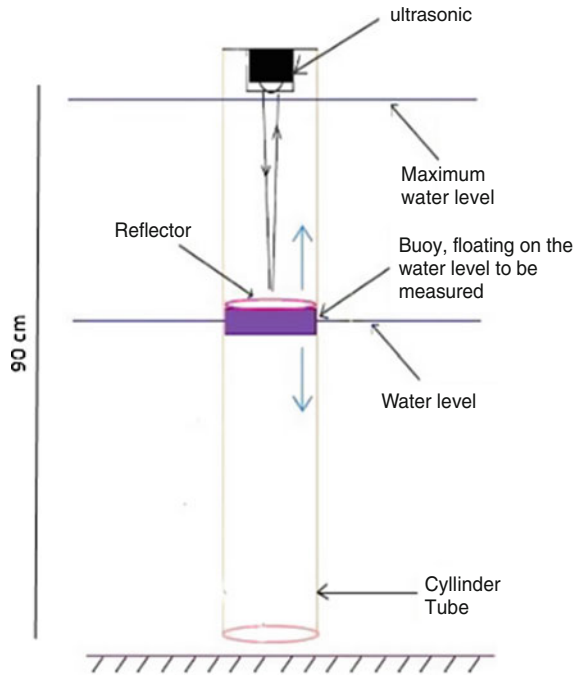
included several circuit blocks and the combination of several circuit blocks. The tests on the whole blocks were conducted to find out whether the entire hardware performs well and to discover undesirable errors.

### 43.4.2 Ultrasonic Sensor Testing

The tests carried out in this project were to measure the distance change that occurred on the sensor when a reference for measurement was given. Results of several experiments were noted and compared between the distance displayed by



**Fig. 43.4** The mechanical design of the ultrasonic sensor



the ultrasonic sensor and the one given by a measurement ruler with different temperature conditions. From the experiment result at a temperature of 27 °C with the ultrasonic sensor reflected wave distance 2–170 cm, an average error rate 1.728 % was obtained. The result at a temperature of 30 °C with the ultrasonic sensor reflected wave distance 2–170 cm produced an average error rate of 1.236 %. In the experiment result at a temperature of 32 °C with the ultrasonic sensor reflected wave distance 2–170 cm, an average error rate 0.4 % was obtained.

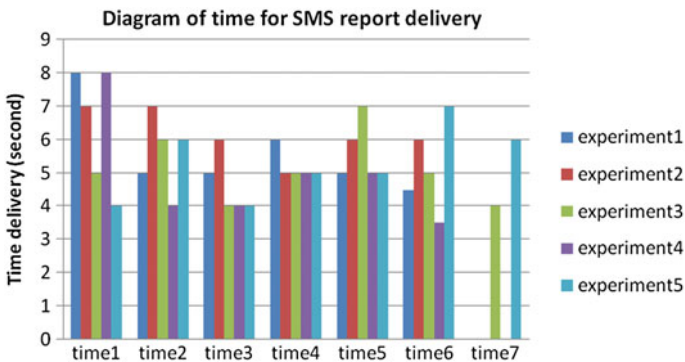
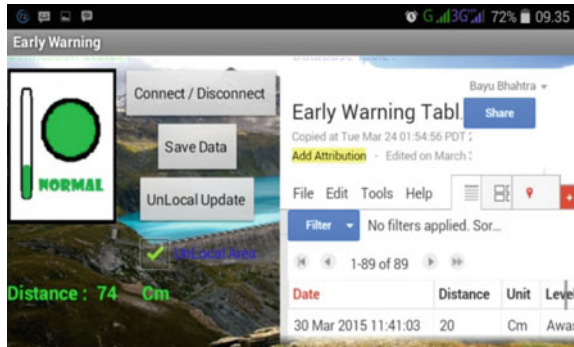


**Fig. 43.5** The result of laboratory testing on SMS delivery time

**Fig. 43.6** The result of laboratory experiments on SMS delivery



After testing the accuracy of ultrasonic sensor in measuring distance, compared to the distance measured by a measurement ruler, a further test was carried out to evaluate the accuracy of the sensor on the speed change of the moving reflected distance of the ultrasonic wave. For this test, we simulated it by adjusting the water level at a different speed. The ultrasonic sensor accuracy on different speed of water level changes—i.e., 3 L/30 s, 3 L/20 s, and 3 L/10 s—had the highest error rate of 1 cm, and it yielded the highest error rate of 0.47 % occurred at the speed of decreasing water of 3 L/10 s.

### 43.4.3 Data Transmission Testing on Android

This testing was conducted to send measurement data to an Android devices as an information receiver. Based on the results of five experiments, the comparison between the initial water level and the change after the water level increases or decreases, as well as the time of data transmission from the microcontroller to Android device was shown in Fig. 43.5. It can be concluded that SMS delivery time from the micro-controller to the Android device ranges from 3.5 to 8 s, and the average delivery time is 5.414 s for one time SMS delivery.

Figure 43.6 is present the results of data delivery to the Android device showing the water level and the stored data sent to the early warning table.

## 43.5 Conclusion

Based on the results of the design and testing at the end of the project, it can be concluded:

1. PING ultrasonic sensor can work well with objects that have water level of 10–40 cm, with the highest error rate of 0.47 %.

2. The Android device works according to the received data from the sensor with predetermined parameters such as follows: a distance of 60 cm and up from the sensor (normal), 59–40 cm (alert 1), 39–26 cm (alert 2), 25 cm to approaching the sensor (warning).
3. The testing on SMS delivery time for the water level monitoring device shows the average delivery time of 5.414 s

## References

1. Basha, E., Rus, D.: Design of early warning flood detection systems for developing countries. *IEEE Trans.* 612–6175 (2007)
2. Raj, B., Kalgaonkar, K., Harrison, C., Dietz, P.: Ultrasonic doppler sensing in HCI. *IEEE* (2012). doi:[10.1109/MPRV.2012.17](https://doi.org/10.1109/MPRV.2012.17)
3. Guochao, W., Changzan, G., Jennifer, R., Takao, I., Changzhi, L.: Highly accurate noncontact water level monitoring using continuous-wave doppler radar. *IEEE* (2013). doi:[10.1109/WiSNet.2013.6488620](https://doi.org/10.1109/WiSNet.2013.6488620)
4. Taufiqurrahman, B.A., Albana, Y.: Perancangan Sistem Telemetri Untuk Pengukuran Level Air Berbasis Ultrasonic. In: *Proceeding Conference on Smart-Green Technology in Electrical and Information Systems*, Bali, Indonesia, 125–130 (2013)
5. Jati, E.W., Arrofiq, M.: Sistem Pemantau Ketinggian Air Sungai Dengan Tampilan Pada Situs Jejaring Sosial Twitter Sebagai Peringatan Dini Terhadap Banjir. Universitas Gadjah Mada, Yogyakarta (2013)
6. Martani, M.: Endarko, Perancangan dan Pembuatan Sensor Level Untuk Sistem Kontrol Pada Proses Pengendapan  $\text{CaCO}_3$  Dalam Air Dengan Metode Medan Magnet (in Bahasa Indonesia). *Jurnal Sains dan Seni Pomits* 2(2), 1–5 (2014)
7. Widiarini, T.R.F.: Zigbee: Komunikasi Wireless Berdaya Rendah (in Bahasa Indonesia), *Seminar Nasional Aplikasi Teknologi Informasi 2005 (SNATI 2005)*, Yogyakarta, Indonesia (2005). ISBN: 979-756-061-6
8. Parallax: PING™ Ultrasonic Distance Sensor (#28015) 1 no. 3 1-13, Parallax, California (2006)

# Chapter 44

## The Influence of Depth of Cut, Feed Rate and Step-Over on Surface Roughness of Polycarbonate Material in Subtractive Rapid Prototyping

The Jaya Suteja

**Abstract** Rapid prototyping is fast and automatic three dimensions physical modeling that uses computer aided design model as the input. One of the important requirements in various products is the surface quality. Therefore, the aim of this research is to study and then develop a model that shows the influence of depth of cut, feed rate, and step-over on the vertical and horizontal surface roughness of polycarbonate material in subtractive rapid prototyping. The subtractive rapid prototyping process is performed by using Roland MDX 40 machine assisted by CAM Modela Player 4.0 software. This research implements response surface methodology to develop the model and then followed by the residual tests. The result shows that the increase of the depth of cut and the interaction between the step-over and the depth of cut will increase the horizontal surface roughness. Meanwhile, the vertical surface roughness will be affected mostly by the step-over. This research provides an insight on how to rapid prototype the polycarbonate material in order to achieve the surface requirement. The result of this research is the basis for achieving the main purpose of subtractive rapid prototyping which are maximum material rate removal and the minimum surface roughness.

**Keywords** Polycarbonate · Subtractive rapid prototyping · Surface roughness · Process parameters

### 44.1 Introduction

Polycarbonate is a strong, tough, and transparent thermoplastic material that is most commonly used and most widely tested in the medical device. As most of the prosthetic products are customized for each patient, the feasible process to fabricate

---

T.J. Suteja (✉)

Manufacturing Engineering Department, University of Surabaya, Surabaya, Indonesia  
e-mail: jayasuteja@staff.ubaya.ac.id

it is by using rapid prototyping. Rapid prototyping is fast and automatic three dimensions physical modeling that uses computer aided design model as the input. Two methods in rapid prototyping are additive and subtractive rapid prototyping. Subtractive Rapid Prototyping implements milling process to cut material with tool that rotates in very high speed (high speed milling). According to Toh, C.K., high speed milling refers to milling process with 10 mm tool diameter that is rotated in 10,000 rpm [1].

Nieminem, I., et al., have investigated the possibility to use high speed milling to fabricate a thin fin of polycarbonate material by changing the depth of cut and step-over [2]. However, Nieminem, I., et al. did not investigate the influence of the depth of cut and the step-over on the important factors such as surface roughness of the polycarbonate material.

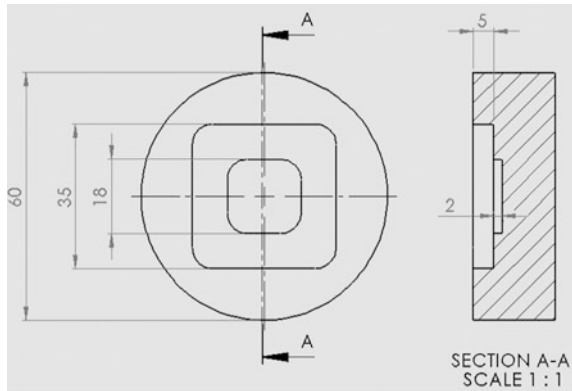
As no other research investigate the influence of high speed milling process parameters on the polymer materials, this research conduct a literature review on its influence on metal materials. In this research, studies by Albertí et al. [3], Vivancos [4], and Urbanski [5], are reviewed. In addition, the influence of non-high speed milling process parameters is also reviewed. The studies conducted by Oktem et al. [6], Ardiansyah [7], Suteja [8] are studied. Based on the reviews, it is shown that material removal rate, surface roughness, and dimension accuracy of a material are affected by interpolation type, tool holder type, controller of the machine, computer aided manufacturing software, physical and mechanical characteristics of the material, physical and mechanical characteristics of the tool, vibration, depth of cut, step-over, feed rate, cutting speed, and cut type.

One of the important requirements in various products especially medical device is the surface quality. Therefore, the aim of this research is to study and then develop a model that shows the influence of depth of cut, feed rate, and step-over on the vertical and horizontal surface roughness of polycarbonate material in subtractive rapid prototyping. These three process parameters are selected because these parameters are the dominant factors that influence the main purpose of subtractive rapid prototyping, which are to achieve the maximum material rate removal and the minimum surface roughness.

## 44.2 Research Design

This research implements response surface methodology to develop a surface roughness model. Then it is followed by conducting three residual tests, which are independence test, constant variance test, and normality test. By applying subtractive rapid prototyping process on the polycarbonate material, this research expects to achieve the final shape shown in Fig. 44.1. The subtractive rapid prototyping process is performed by using Roland MDX 40 machine assisted by CAM Modeler Player 4.0 software. The software is used to generate the tool path of Roland MDX 40 machine. The input in order to generate the tool path is a three dimension model in STL format. The cutting tool used in this research is carbide

**Fig. 44.1** The final shape



solid square end mill with 5 mm diameter. The tool is moved by the software based on the zigzag cut type.

In order to fabricate the shape, roughing and finishing processes are required. Each of the processes requires different parameter values. Roughing process is performed by implementing the parameters value shown in Table 44.1. This parameter value is determined based on the machine specification, literature study, and the preliminary experiment. The range of subtractive rapid prototyping parameters value for finishing process used in this research is shown in Table 44.2. The spindle and the entry speed for finishing process are 10,000 rpm and 4 mm/s consecutively. In this research, no coolant is used in performing the subtractive rapid prototyping.

This research takes some assumptions, which are: the polycarbonate material is always homogeneous, the cutting temperature is always constant, and the tool wears after performing three roughing and finishing processes.

**Table 44.1** Parameters value for proses roughing

Parameters	Value
Feed rate	12 mm/s
Entry speed	4 mm/s
Spindle speed	8500 rpm
Depth of cut	0.37 mm
Step-over	1 mm

**Table 44.2** Range parameters value for finishing process

Parameters	Low value	Middle value	High value
Depth of cut (mm)	0.1	0.235	0.37
Feed rate (mm/s)	12	14.5	17
Step-over (mm)	0.3	0.65	1

In this research, the surface roughness measurement is conducted at Industrial Metrology Laboratory of University of Surabaya. The surface roughness measurement device used in this research is Mitutoyo SJ 210 with 0.01  $\mu\text{m}$  of accuracy. After the measurement process, the measured data is analyzed by using MINITAB release 14 software.

### 44.3 Results and Discussion

The first order experiment is conducted in implementing response surface methodology. The experiment design and the result of the first order experiment are shown in Table 44.3. By using the experiment result, the first order models of horizontal and vertical surface roughness are developed. However, based on the data analysis, the first order model of horizontal surface roughness is not fit to the horizontal surface roughness values. As a result, the second order experiment must be conducted to develop a better horizontal surface roughness model. Meanwhile, the first order model of vertical surface roughness is fit and can be used to predict the vertical surface roughness values. For that reason, the mathematical model to predict the vertical surface roughness values is shown in Eq. 44.1.

$$Ra_{\text{ver}} = 0.250056 + 0.022.F + 11.1214.S + 1.42593.D \quad (44.1)$$

where  $Ra_{\text{ver}}$  is vertical surface roughness ( $\mu\text{m}$ ),  $F$  is feed rate (mm/s),  $S$  is step-over (mm), and  $D$  is depth of cut (mm).

**Table 44.3** Results of first order experiment

Std order	Run order	Feed rate (mm/s)	Step-over (mm)	Depth of cut (mm)	$Ra_{\text{Hor}}$ ( $\mu\text{m}$ )	$Ra_{\text{Ver}}$ ( $\mu\text{m}$ )
11	1	14.50	0.65	0.235	3.13	7.25
13	2	14.50	0.65	0.235	3.22	7.83
2	3	17.00	0.30	0.100	2.53	4.46
12	4	14.50	0.65	0.235	3.18	8.65
7	5	12.00	1.00	0.370	4.88	12.39
9	6	14.50	0.65	0.235	2.89	7.83
3	7	12.00	1.00	0.100	3.64	12.01
5	8	12.00	0.30	0.370	3.00	4.70
10	9	14.50	0.65	0.235	3.55	8.33
6	10	17.00	0.30	0.370	4.18	4.59
1	11	12.00	0.30	0.100	2.81	3.60
4	12	17.00	1.00	0.100	4.30	12.08
8	13	17.00	1.00	0.370	4.49	12.01

The first order model of vertical surface roughness can be used as the best prediction model for vertical surface roughness because analysis of the model shows that its lack-of-fit is not significant. This model shows that the increase of the feed rate, the step-over, and the depth of cut will increase the vertical surface roughness. However, the parameter that has the most influence to the vertical surface roughness is the step-over.

As the first order model of horizontal surface roughness is not fit to the horizontal surface roughness values, the second order experiment must be conducted to develop the prediction horizontal surface roughness model. The experiment design and the result of the second order experiment are shown in Table 44.4. By using the experiment result, the second order models of horizontal surface roughness are developed. The mathematical model to predict the horizontal surface roughness values is shown in Eq. 44.2.

$$Ra_{hor} = 2.44029 + 0.0736795.F - 1.36142.S + 1.36761.D + 1.43091.S^2 + 12.3338.D^2 - 0.485185.F.D + 3.73016.S.D \tag{44.2}$$

where  $Ra_{hor}$  is horizontal surface roughness ( $\mu m$ ), F is feed rate (mm/s), S is step-over (mm), and D is depth of cut (mm).

**Table 44.4** Results of second order experiment

Std order	Run order	Feed rate (mm/s)	Step-over (mm)	Depth of cut (mm)	Ra Hor ( $\mu m$ )
18	1	14.5000	0.65000	0.235000	3.64
19	2	14.5000	0.65000	0.235000	3.36
10	3	18.7045	0.65000	0.235000	2.80
15	4	14.5000	0.65000	0.235000	2.74
20	5	14.5000	0.65000	0.235000	2.72
13	6	14.5000	0.65000	0.007958	3.33
14	7	14.5000	0.65000	0.462042	3.90
5	8	12.0000	0.30000	0.370000	3.71
11	9	14.5000	0.06137	0.235000	2.35
8	10	17.0000	1.00000	0.370000	4.29
6	11	17.0000	0.30000	0.370000	3.51
2	12	17.0000	0.30000	0.100000	3.10
9	13	10.2955	0.65000	0.235000	3.28
7	14	12.0000	1.00000	0.370000	5.03
12	15	14.5000	1.23863	0.235000	4.60
4	16	17.0000	1.00000	0.100000	3.48
3	17	12.0000	1.00000	0.100000	3.26
16	18	14.5000	0.65000	0.235000	2.94
1	19	12.0000	0.30000	0.100000	2.95
17	20	14.5000	0.65000	0.235000	3.42



The analysis and the residual plots of the second order model of horizontal surface roughness show that the model is fit and satisfy all the assumptions. As a result, it can be used as the best prediction horizontal surface roughness model. This model shows that the horizontal surface roughness is mostly affected by the depth of cut and the interaction between the step-over and the depth of cut. The increase of the depth of cut and the interaction between the step-over and the depth of cut will increase the horizontal surface roughness.

#### 44.4 Conclusion

This result of this research shows that the increase of the feed rate, the step-over, and the depth of cut will increase the vertical surface roughness with the step-over as the most influenced parameter. In addition, the increase of the depth of cut and the interaction between the step-over and the depth of cut will increase the horizontal surface roughness. The models developed in this research give an insight on how the important parameters of rapid prototyping will influence the surface requirement of a polycarbonate material. The result of this research is the basis for achieving the main purpose of subtractive rapid prototyping which are maximum material rate removal and the minimum surface roughness.

#### References

1. Toh, C.K.: Surface topography analysis in high speed finish milling inclined hardened steel. *Precis. Eng.* **28**(4), 386–398 (2004)
2. Nieminen, I., Paro, J., Kauppinen, V.: High-speed milling of advanced materials. *J. Mater. Process. Technol.* **56**(1–4), 24–36 (1996)
3. Albertí, M., Ciurana, J., Rodriguez, C.A.: Experimental analysis of dimensional error versus cycle time in high-speed milling of aluminium alloy. *Int. J. Mach. Tools Manuf* **47**(2), 236–246 (2007)
4. Vivancos, J., Luis, C.J., Costa, L., Ortiz, J.A.: Optimal machining parameters selection in high speed milling of hardened steels for injection moulds. *J. Mater. Process. Technol.* **155**, 1505–1512 (2004)
5. Urbanski, J.P., Koshy, P., Dewes, R.C., Aspinwall, D.K.: High speed machining of moulds and dies for net shape manufacture. *Mater. Des.* **21**(4), 395–402 (2000)
6. Oktem, H., Erzurumlu, T., Kurtaran, H.: Application of response surface methodology in the optimization of cutting conditions for surface roughness. *J. Mater. Process. Technol.* **170**(1–2), 11–16 (2005)
7. Ardiansyah, S.D.: Pengaruh Parameter Proses Milling terhadap MRR dan Kekasaran Permukaan (Ra) pada Pemotongan Material Polyacetal menggunakan Pahat HSS. B.Eng. thesis, University of Surabaya, Surabaya, Indonesia (2010)
8. Suteja, T.J., et al.: Optimasi Proses Pemesinan Milling Fitur Pocket Material Baja KarbonRendahMenggunakan Response Surface Methodology. *Jurnal Teknik Mesin Universitas Kristen Petra* **10**(1), 1–7 (2008)

# Chapter 45

## Adaptive Cars Headlamps System with Image Processing and Lighting Angle Control

William Tandy Prasetyo, Petrus Santoso and Resmana Lim

**Abstract** The project proposed a prototype of an adaptive car headlamps control using image processing. The adaptive headlamps system focuses on the lighting angle control of low beam in the headlamps which its light tracks moved horizontally. The controller in headlamps is based on image processing from a camera mounted on the car. Adaptive headlamps system consists of portable tiny computer of Raspberry Pi, Arduino microcontroller, and two stepper motors for the left and the right headlamps. The system was implemented on the headlamps of a Toyota Avanza car. The adaptive headlamps system could detect most types of cars ahead. It could decrease a 'glare' effect and increase the driver sight based on survey taken from the driver and the driver of opposite car. The system still couldn't detect the opposite car with high intensity of light from braking lamps, as well as the light from the opposite front lamps.

**Keywords** Adaptive cars headlamps · Arduino · Image processing · Raspberry pi

### 45.1 Introduction

Night is the time when vehicle accidents often occurred [1]. The causes can be various such as the headlamps light in the car aren't focused or the lights intensity are too low or the lights make glared (dazzled) effect for other car drivers [2]. On the other side, technology for controlling headlamps light were rarely found these years. Nowadays, most of researches often focus on car speed controller research (cruise control), and automatic car parking system. The need of headlamps technology is important based on the facts above.

Several companies have produced and sold their headlamps technology products to the market. Hella, one of the automotive company sold their headlamps

---

W.T. Prasetyo (✉) · P. Santoso · R. Lim  
Electrical Engineering Department, Petra Christian University, Surabaya, Indonesia  
e-mail: wtp\_93@hotmail.com

technology product called “Adaptive Front-light System (AFS)” that can control the headlamps light based on car steering [3]. The AFS technology also proposed in [4]. Valeo company also provided their product “Light/on&off” that can switch the headlamps light on and off automatically based on light intensity around the car [5]. The headlamp technology that used by Valeo, also similar with Stein’s project [6]. Those two above still can’t reduce the dazzled (glared) effect for other cars.

This paper offers headlamps technology that can overcome the problems above. Headlamps technology in this paper can control headlamps light’s track adaptively based on object detection (car’s back side) data. The headlamps light’s track can move horizontally based on position of the object.

### 45.2 Adaptive Headlamps System Set-up

This section provides the outline of the adaptive headlamps controller system. The block diagram of the system displayed on Fig. 45.1.

There are two primary processes in the Fig. 45.1 such as object detection process on raspberry pi and stepper motor controller on arduino. Raspberry pi communicates with webcam through USB (Universal Serial Bus) interface. It also does I2C communication through GPIO pins (GPIO 03, GPIO 05) which SDA, and SCL port located on raspberry pi. Arduino as stepper motor controller also do I2C communication through I/O pins (digital pins 20, 21) which SDA, and SCL port located on Arduino. Arduino controls two stepper motors through L298N motor drivers which can drive them with higher current.

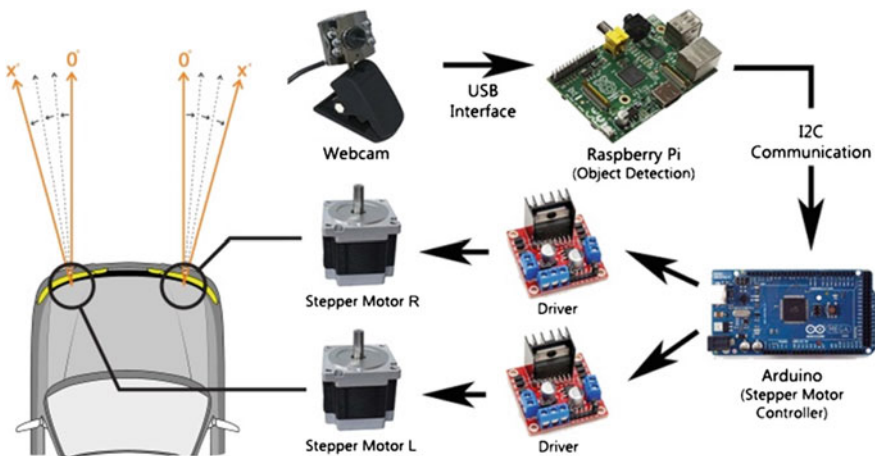


Fig. 45.1 Block diagram of adaptive headlamps controller system

### 45.3 Design of Adaptive Headlamps

Design of adaptive headlamps is divided into two parts, which are hardware and software. Hardware part consists of the design of headlamp itself, and installation of the controller, including installation of the webcam. The software design consists of Raspberry Pi's software design and Arduino's software design.

#### 45.3.1 Hardware Design

Headlamps that used in this paper are Toyota Avanza 2009 car's headlamps with projector lens. The headlamps were modified by adding limit switch behind the high beam lamp. It is used to limit the movement of the lamp and set the position of the stepper motor into zero position (Fig. 45.2).

Adaptive headlamps controller consists of one Raspberry Pi B tiny portable computer, one driverless webcam, one arduino mega R3 2560 microcontroller, two pieces of L298N motor driver, 12 V regulator to stabilize the voltage from car battery, and toggle switch for auto-manual control. There are also keyboard and mouse attached on Raspberry Pi for user interface. All of the components mounted on a board, then placed below left-front dashboard of the car. The webcam is installed inside of the car, and the position is on the middle of the car, and the height about half of car height, so its position in line with the detected object. The position of the adaptive headlamps controller board and webcam displayed in Fig. 45.3.

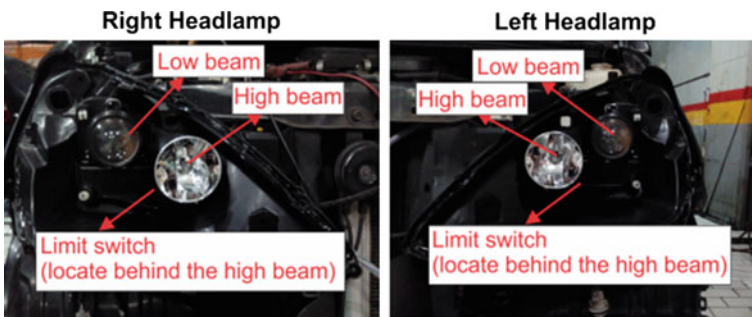


Fig. 45.2 Headlamp design

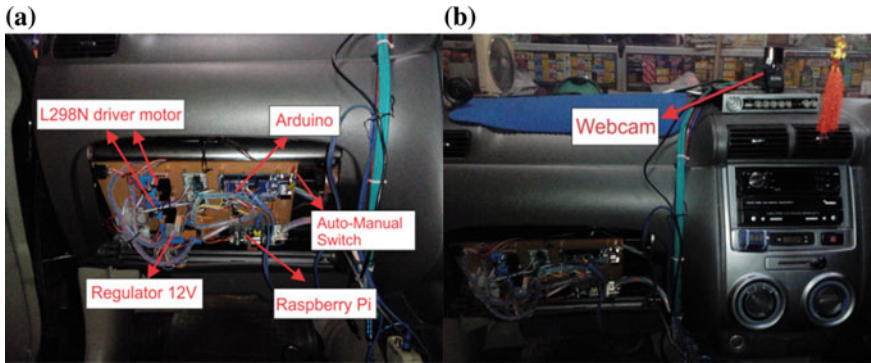


Fig. 45.3 a Location of adaptive headlamps controller board. b Location of webcam

### 45.3.2 Raspberry Pi's Software Design

Raspberry Pi's software design is divided into four points which are object detection, headlamps light track movement calculation, I2C communication, and manual control program. Raspberry Pi uses Raspbian operating system based on Linux kernel. Python is used to create the program and OpenCV library is used as compiler for image processing in the Raspberry Pi.

The program code starts with object detection by the webcam. Webcam captured the object by creating a ROI (Region of Interest) in window screen marked by blue rectangle when the object is correct and in range of detection. Webcam used  $320 \times 240$  pixel resolution due to low specification of the Raspberry Pi. Low resolution of webcam makes the Raspberry Pi works faster but as the compensation the image quality become lower. Object detection in Raspberry Pi used OpenCV library by importing "cv2" library in the program and used "cascade.xml" file that contain the trained data. Trained data were obtained by doing *haar* training on hundred images of cars. *Haar* training that used in this paper based on Viola-Jones paper which provides faster face detection using *haar* trained data [7].

Headlamps light track movement calculation starts from the distance calculation then calculate the position where the stepper motors will stop. Triangle similarity is used to calculate the distance from webcam to the object [8]. Triangle similarity equation shown as below:

$$F = (Px D) / W \quad (45.1)$$

where F is focal length of webcam, P is object length in webcam (pixel), D is the distance (cm), and W is object length in real (cm). This equation used to find the focal length of the camera, so all of the parameters except F should be known first

**Table 45.1** List of positions based on distance between webcam and detected object

Distance (cm)	Object position	Stepper position L	L degree	Stepper position R	R degree
–	No object	15	4.29°	15	4.29°
0–400	Left	0	0.00°	0	0.00°
400–800	Left	7	2.00°	15	4.29°
>800	Left	15	4.29°	15	4.29°
0–400	Right	0	0.00°	0	0.00°
400–800	Right	15	4.29°	7	2.00°
>800	Right	15	4.29°	15	4.29°

by manual measuring. Then triangle similarity equation used again in different way in program. The equation shown as below:

$$D' = WxF/P' \tag{45.2}$$

where *W* is object length in real (cm) same as before, *F* is focal length obtained from Eq. (45.1), *P'* is object length in webcam (pixel) and *D'* is the distance (cm). *P'* obtained by measuring the length of ROI rectangle that represents the object length in webcam and *D'* is the distance that used to determine the position where the stepper motor stopped. List of positions based on distance between webcam and detected object are shown at Table 45.1.

Numbers in stepper position L/R columns mean the position of rotation of stepper motor at that time, for example, number 7 means the stepper motor rotates 360° 7 times and stops at that position. Position number of stepper motors that determined from the list are sent to the Arduino through I2C port.

The manual control program designed for users so the users can move the headlamps light track movement manually. Users can give input “1, 2, 3 and 4” to the Raspberry Pi using keyboard to rotate stepper motors 180° clockwise or counter-clockwise. Left stepper motor is controlled by “1 and 2” input and the right side is controlled by “3 and 4” input, then the input sent to Arduino.

### 45.3.3 Arduino’s Software Design

Arduino’s software design is divided into three points such as automatic control (adaptive) of headlamps light track movement, manual control and I2C communication. Arduino IDE is used to design the program.

Automatic and manual control of headlamps light track movement program receive stepper motors position data from Raspberry Pi through I2C port. Automatic control’s program in Arduino converts the position data so it can rotate

the stepper motors precisely. Before automatic control program executed, the calibration program is run and rotates the stepper motors to move at zero position.

Manual control of headlamps light track movement program also converts the position data from Raspberry Pi to rotate the stepper motors based on users input. Program for automatic and manual control switch also configured in this software design.

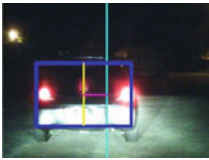


### 45.4 Results and Discussions

The system test has been done at night on the road which has been ‘conditioned’ for avoiding undesired incidents and safety. This system test consists of pictures which show webcam pictures results, and driver sights whether from the car with adaptive headlamps attached or the opposite car. Conditions on this system test was divided into three conditions based on the object condition. The first condition was the driver in opposite car didn’t push the brake pad, the second condition was the driver in opposite car pushed the brake pad, and the third, the position of opposite car was face to face with the car. Distance between car and the opposite car was approximately 4–8 m and the position of opposite car was at the left side of the car. The opposite car that used in this system test was Honda Brio 2014.





Table 45.2 shows the pictures results of webcam detection that can only detect object when the condition of the opposite car’s driver didn’t push the brake pad. It happened because the light intensity was too high for the webcam so webcam couldn’t detect the object properly.

System test on the driver sight has been done by taking pictures using DSLR camera with the same settings. The pictures consist of four pictures with different angles. The first and second took from the car driver sight with normal headlamps and adaptive headlamps. The third and fourth took from the opposite car driver

**Table 45.2** Pictures results of webcam detection based on object conditions

Object conditions	The driver in opposite car didn’t push the brake pad	The driver in opposite car pushed the brake pad	The position of opposite car was face to face with the car
Detection results in webcam	 <p>(object detected)</p>	 <p>(no object detected)</p>	 <p>(no object detected)</p>

**Table 45.3** Pictures results from car’s driver sight and opposite car’s driver sight

Picture angle	Normal headlamps	Adaptive headlamps
Driver sight		
Opposite driver sight		

sight with normal headlamps and adaptive headlamps. The condition of the opposite car was the same condition as the first condition in the system test before.

The light track of normal and adaptive headlamps on driver sight look different on Table 45.3. The light track on adaptive headlamps seems wider than the normal. The dazzled (glared) effect from opposite car also reduced at the adaptive headlamps pictures (the light intensity was lower than the normal).

### 45.5 Conclusion

The system test result shown that adaptive headlamps can increase the driver sight and decrease the dazzled (glared) effect on the opposite car side. The object detection also could run properly on the condition when the light intensity from the opposite lamps weren't too high for the webcam. In the future, there will be several improvements that can be applied with this paper for example improvement on webcam which can detect lights with higher intensity.



## References

1. Apriliananda, D.: Ini Waktu Rawan Kecelakaan Lalu Lintas! 11 September 2014. <http://otomotif.kompas.com/read/2013/12/24/1935538/Ini.Waktu.Rawan.Kecelakaan.Lalu.Lintas>
2. Kompasiana, 85% Kecelakaan Lalu-lintas Karena Human Error. 28 December 2011 (10 November 2014). <http://lifestyle.kompasiana.com/catatan/2011/12/28/85-kecelakaan-lalu-lintas-karena-human-error-422758.html>
3. Hella, Adaptive Frontlight System (AFS). 14 June 2012. 10 September 2014. [http://www.youtube.com/watch?v=Cu\\_0G9QtAMo](http://www.youtube.com/watch?v=Cu_0G9QtAMo)
4. light/on&off™, Automatic Car Headlight, Lights, Automatic Car Lighting System. t.thn. 11 September 2014. [http://www.smileyouaredriving.com/uk\\_en-products.driving-assistance.video-7.html](http://www.smileyouaredriving.com/uk_en-products.driving-assistance.video-7.html)
5. Antony, B., Manoj, M.: Control algorithm for adaptive front light systems. *Int. J. Comput. Trends Technol.* **9**(7), 339–343 (2014)
6. Stein, G.P., et al: Headlight, Taillight and Streetlight Detection. United States Patent (2009)
7. Open CV-Python Tutorials. Face Detection using Haar Cascades (2015)
8. Rosebrock, A.: Find Distance from Camera to Object/Marker using Python and Open CV. (2015)

# Chapter 46

## Changes in the Rheological Properties and the Selection of a Mathematical Model of the Behavior of Coal-Water Slurry During Transport and Storage

S.L. Buyantuev, A.B. Khmelev and A.S. Kondratenko

**Abstract** The aim of experimental research was to study the changes in the rheological properties of coal-water slurries (CWS) treated by the electric discharge methods and selection of a mathematical model of the rheological behavior of CWS that describes the experimental data. The objects of research were samples of CWS from brown coal. It is shown that the developed technology of CWS preparation provides a suspension with a dynamic viscosity of the corresponding standard GB/T18856.4. We define the type of liquid, structural and mechanical properties, the behavior of the system under the influence of mechanical action. On the basis of rheological model the current of CWS was described and determined that the CWS applies to plastic materials that capable of under the influence of external forces permanently deformed without breaking the integrity.

**Keywords** Coal-water slurry · Electric discharge methods · Viscosity · Rheological model

### 46.1 Introduction

Analysis of the world's resources of non-renewable fuels leads to the conclusion that the most promising for use in energy is coal, because its reserves on Earth many times the total oil and gas reserves. However, environmental problems arising from the use of coal fuel, require the development and introduction of new effective

---

S.L. Buyantuev (✉) · A.B. Khmelev  
East Siberian State University of Technology and Management,  
Ulan-Ude, Buryat Republic, Russia  
e-mail: buyantuevsl@mail.ru

A.S. Kondratenko  
Buryat State University, Ulan-Ude, Buryat Republic, Russia

economic and environmental points of view coal technologies. This requires improved consumer properties of coal and master to obtain coal-based alternative fuels by replacing scarce natural resources: gas and liquid petroleum fuels. In connection with this is the actual use of coal as a coal-water slurry fuel or coal-water slurry (CWS) [1]. CWS has technological properties of liquid fuels (transportation to road and rail tanks through pipelines, tankers and bulk vessels, storage in closed containers) and must retain their properties during prolonged storage and transportation, so the value of the viscosity and rheological model of behavior are important technical characteristics of CWS [2].

## 46.2 Experiment Setup and Methods

The solution is based on the use of plasma and electrolytic methods for the preparation of the CWS without the use of plasticizers. The methodology of the experiment and previously obtained micrographs and elemental analysis of coal before and after treatment was considered in detail in [3]. The article shows the data of the dynamic viscosity of CWS, the liquid type of and its rheological model.

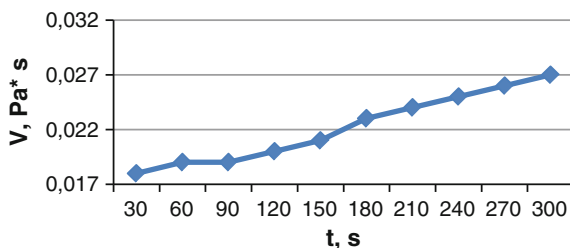
Our research used a rotational viscometer Brookfield RVDV-II + Pro (CCU Progress). Measurement of the sample of dynamic viscosity was performed at room temperature.

We measured the dynamic viscosity of samples in the range of from 0.003 to 2 Pa\*s at room temperature, using a spindle ULA with the speed of 50 rpm. In order to establish the type of fluid carried out in the study, we change the dynamic viscosity of the CWS in time.

The study refers to the CWS rheopex non-Newtonian fluids, as their viscosity increases with time at a constant rotational speed and to maintain a constant flow rate must be a gradual increase of shear rate (Table 46.1).

**Table 46.1** The dependence of viscosity on time

Viscosity (Pa*s)	Speed (rpm)	Torque (%)	Shear stress (N/m <sup>2</sup> )	Shear rate (1/s)	Temperature (°C)	Time interval (s)	Spindle
0.018	50	14.4	11.27	61.15	30.32	30	ULA
0.019	50	14.9	11.66	61.15	29.42	30	ULA
0.019	50	15.5	12.13	61.15	29.80	30	ULA
0.020	50	16.2	12.68	61.15	29.95	30	ULA
0.021	50	17.0	13.30	61.15	28.92	30	ULA
0.023	50	18.0	14.08	61.15	30.55	30	ULA
0.024	50	19.0	14.87	61.15	30.50	30	ULA
0.025	50	19.8	15.49	61.15	31.12	30	ULA
0.026	50	21.0	16.43	61.15	31.05	30	ULA
0.027	50	21.7	16.98	61.15	30.77	30	ULA

**Fig. 46.1** Dynamic viscosity of the studied system in time

It has been found that CWS has rheopex properties exhibit non-Newtonian systems, as evidenced by an increase in viscosity of from 0.018 to 0.027 Pa\*s. The developed technology of CWS preparation provides a suspension with a dynamic viscosity of 0.018–0.027 Pa\*s, corresponding to the standard GB/T18856.4: 0.0–1.2 Pa\*s [4].

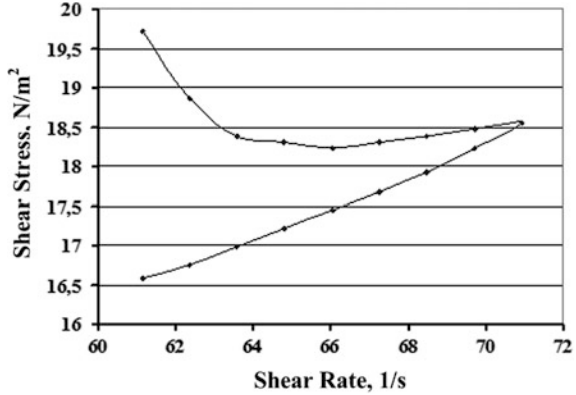
It is known [5] that rheopex system structured to form contacts between the particles resulting from the orientation by mechanical action with small velocity gradients. The resulting physical properties explained dependence coal units to structure formation and porosity and the ability to absorb water, resulting in an increase in the dynamic viscosity of the system when the load is applied (Fig. 46.1).

To study the behavior of the system under the action of mechanical impact study was carried out changing the dynamic viscosity of the CWS on the speed of rotation of the spindle (Table 46.2).

**Table 46.2** Dependence of viscosity on the spindle speed

Viscosity (Pa*s)	Speed (rpm)	Torque (%)	Shear stress (N/m <sup>2</sup> )	Shear rate (1/s)	Temperature (°C)	Time interval (s)	Spindle	Model
0.0271	50	21.2	16.59	61.15	30.57	60	ULA	RV
0.0268	51	21.4	16.75	62.37	30.62	30	ULA	RV
0.0267	52	21.7	16.98	63.59	30.57	50	ULA	RV
0.0265	53	22.0	17.21	64.81	30.30	15	ULA	RV
0.0264	54	22.3	17.45	66.04	30.25	10	ULA	RV
0.0262	55	22.6	17.68	67.26	30.40	10	ULA	RV
0.0261	56	22.9	17.92	68.48	30.42	10	ULA	RV
0.0261	57	23.3	18.23	69.71	30.45	10	ULA	RV
0.0261	58	23.7	18.55	70.93	30.60	10	ULA	RV
0.0264	57	23.6	18.47	69.71	30.35	10	ULA	RV
0.0268	56	23.5	18.39	68.48	30.65	10	ULA	RV
0.0272	55	23.4	18.31	67.26	30.32	10	ULA	RV
0.0276	54	23.3	18.23	66.04	30.30	10	ULA	RV
0.0282	53	23.4	18.31	64.81	30.42	15	ULA	RV
0.0289	52	23.5	18.39	63.59	30.25	20	ULA	RV
0.0302	51	24.1	18.86	62.37	30.32	30	ULA	RV
0.0322	50	25.2	19.72	61.15	30.32	60	ULA	RV

**Fig. 46.2** The dependence of the shear stress—shear rate CWS



The sample viscosity increased cases, as evidenced by the values of dynamic viscosity: 0.0271 Pa\*s at 50 rpm, at an intermediate point at 58 rpm viscosity was 0.0261 Pa\*s, and in the end at 50 rpm—0.032 Pa\*s.

Dependence “viscosity-speed” reflects on how much the system is destroyed, and whether it can recover its properties after exposure to mechanical spindle. Figure 46.2 shows that the system is not only destroyed by the rotation of the spindle, but on the contrary—with an increase in speed trials thicken.

### 46.3 Result and Discussions

In the formation of loops “hysteresis”, as in Fig. 46.2, according to describe using theoretical models for the systems, rheological properties are changed in the process of mechanical action—Bingham model, Caisson, a power law, the rheological behavior of pastes, Herschel-Bulkley. Model selection is at the rate of convergence, which should as much as possible close to 100 % (CoF = 100) [6].

Using the experimental data (Table 46.2) curve of the rheological behavior of CWS was structured according to Casson model (Fig. 46.3), the mathematical expression is represented by the Eq. (46.1):

$$\tau^{1/2} = \tau_0^{1/2} + (\eta D)^{1/2} \tag{46.1}$$

here  $\tau$ —shear stress N/m<sup>2</sup>;

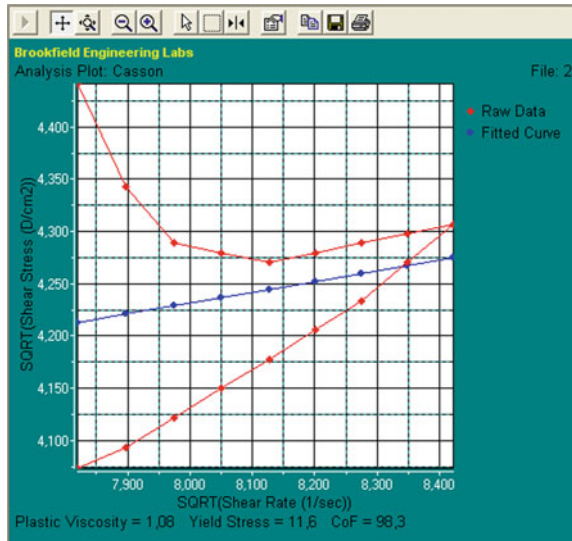
$\tau_0$ —shear strength (shear stress), N/m<sup>2</sup>;

$\eta$ —plastic viscosity, mPa\*s;

$D$ —shear rate, s<sup>-1</sup>.

Figure 46.3 shows two curves: 1 (red)—the dependence of the square root of shear stress (SQRT Shear Stress) by the square root of the shear rate (SQTR Shear Rate) in its gradual increase and decrease; 2 (blue)—powered program viscometer

Fig. 46.3 Model Casson



Reocalc straightforward relationship Casson model, built on the basis of the curve (1). For this model, the ultimate stress (Yield Stress) is defined as the length of the intercept on the axis of the direct shear stress squared ( $11.6 \text{ N/m}^2$ ).

Studies have shown that the Casson model peculiar to pseudoplastic bodies and provides good convergence of experimental and calculated data, as evidenced by a high coefficient of convergence (98.3 %). CWS is a plastic body with a coefficient of plasticity (Plastic Viscosity) of 1.08.

### 46.4 Conclusions

CWS is a complex rheological object, since they consist of a dispersion medium (water) and the dispersed phase—carbon particles having the same amount of units distributed in the water and related natural forces. Chemical interaction with water does not occur because the carbon aggregates are inert. Therefore, the nature of flow systems will depend on the ratio of the dispersion medium and the dispersed phase particle size, the interaction forces between the particles.

The developed technology of CWS preparation provides a suspension with a dynamic viscosity of  $0.018\text{--}0.027 \text{ Pa}\cdot\text{s}$ , corresponding to the standard GB/T18856.4:  $0.0\text{--}1.2 \text{ Pa}\cdot\text{s}$ .

Structural and mechanical properties of the systems investigated under shear stress (Yield Stress), equal to  $11.06 \text{ N/m}^2$  characterized by ductility, as evidenced by the ductility factor (Plastic Viscosity), the corresponding 1.08. This suggests that under load the CWS can be deformed by moderate effort, and save the form, i.e. exhibit permanent deformation at short action moderate in magnitude impulse

power. In the system there is a loss of energy due to the motion of the individual particles and aggregates.

Some authors [7] consider that by Casson plastic coefficient associated with the passage of individual particles in the complete destruction of aggregates. In this case, the plasticity will be determined by the ratio of the dispersion medium and the solid phase and the particle size. It is likely that the increase in the radius of the particle number density and lead to increased plasticity systems.

In accordance with the P.A. Rebinder and N.V. Mikhailov studied CWS are possessing static and dynamic critical shear stress. Thus, the described objects are plastic materials, i.e. capable of under the influence of external forces permanently deformed without breaking the continuity. Modeling of deformation behavior of CWS allows to justify theoretically and to adjust process conditions processing.

## References

1. Senchurova, J., Murko, V., Fedyaev, V., Dziuba, D., Pusirev, E.: The Tomsk Polytechnic University news, pp. 37–40 (2008)
2. Zhuravlev, N., Murko, V., Fedyaev, V., Dziuba, D., Senchurova, Y., Zaostrovsky, A.: Ecology and Industry of Russia, pp. 6–9 (2009)
3. Buyantuev, S., Kondratenko, A., Khmelev, A.: ARPN J. Eng. Appl. Sci. **9**(11), 2102–2105 (2014)
4. <http://www.sinowatt.ru/ser-211.aspx>
5. Pirogov, A.N., Donya, D.V.: Engineering rheology, Kemerovo Technological Institute of Food Industry, Kemerovo, p. 110 (2014)
6. Krupennikova, V.E., Radnaeva, V.D., Tanganov, B.B.: Determination of the dynamic viscosity by a rotary viscometer Brookfield RVDV-II + Pro
7. Kirsanov, E.A., Remisov, S.V., Novoselova, N.V., Vatveenkov, V.N.: The physical meaning of the coefficients in the generalized rheological models Casson, Bulletin of Moscow University. Ser.2 Chemistry, pp. 22–26 (2007)

# Chapter 47

## Design of a Fetal Heartbeat Detector

Nur Sultan Salahuddin, Sri Poernomo Sari, Paulus A. Jambormias  
and Johan Harlan

**Abstract** Fetal Doppler is an electronic tool that serves as a standard instrument to assess the health of pregnant mother and her fetus. This tool particularly detects the fetal heartbeat in the womb using ultrasound waves. In this paper, we proposed a prototype of fetal heartbeat detector which can detect fetal heartbeat directly without using ultrasonic waves. This detector uses Chebyshev bandpass filter circuit for passing a frequency of 2–3 Hz.

**Keywords** Band pass filter · Detector · Fetal heartbeat · Frequency

### 47.1 Introduction

Fetal Doppler is a tool that utilized ultrasonic waves particularly for detecting fetal heartbeats [1]. Ultrasonic waves are sound waves which have frequencies more than 20 kHz. For detecting the heartbeats the fetal Doppler is attached to lower abdominal skin, which lies near the fetal heart, using a transducer probe. The crystals in the transducer will capture reflections of the waves sent out by the transducer. Reflective waves to be captured are still in the form of ultrasonic waves, hence the crystals will convert the waves into electronic ones. The sound waves can penetrate the body and the boundaries between human tissues, e.g. those among body fluid, blood, muscles, and bones. Normal fetal heart rate ranges from 120 to 140 beats per minute. Fetal Doppler is often used in maternity clinics or for pregnant mothers who want to hear the heartbeat of their babies in the uterus [2].

Fetal heartbeats can be heard by amplifying signals from the fetal heart, using a microphone. Inside the womb, beside the fetal heart, there is also a maternal heart that produces heartbeats although with different frequencies. Fetal hearts' rate have

---

N.S. Salahuddin (✉) · S.P. Sari · P.A. Jambormias · J. Harlan  
Gunadarma University, Jl. Margonda Raya 100, Pondok Cina Depok 1642,  
West Java, Indonesia  
e-mail: sultan@staff.gunadarma.ac.id



a range from 120 to 140 beats per minute (about 2–2.33 Hz), while maternal heart rate have a range around 80–90 beats per minute (approximately 1.3–1.5 Hz) [3]. Those two types of waves are simultaneously captured by that tool. Therefore for hearing the pure fetal heartbeat, the maternal heartbeat should be separated from the fetal one. This can be done by applying several filtering techniques.

In this study we proposed a fetal heartbeat detector that functions exactly the same as the fetal Doppler in general, nevertheless by using the simple principles of analog electronics. Detection of fetal heartbeat is performed directly without using ultrasonic sensors as that in the fetal Doppler. The purpose of this study is to design and create a prototype of fetal heartbeat detector that can detect fetal heartbeat with the frequency of 2–3 Hz, without using ultrasonic waves.

### 47.2 The Design of Heartbeat Detector

The design of the fetal heartbeat detectors can be seen in Fig. 47.1 [3].

The working principle of the detector is based upon the electrical signals produced by the mic. The signals are further processed in pre-amplifier circuit, consisting of a parallel voltage feedback amplifier circuit and common emitter amplifier. Pre-amplifier circuit can increase the sensitivity of the sensor. Moreover, the produced sound is free from noise, and can easily set the sensitivity [3]. In the next procedure, we filtered the captured signals using Chebyshev bandpass filter

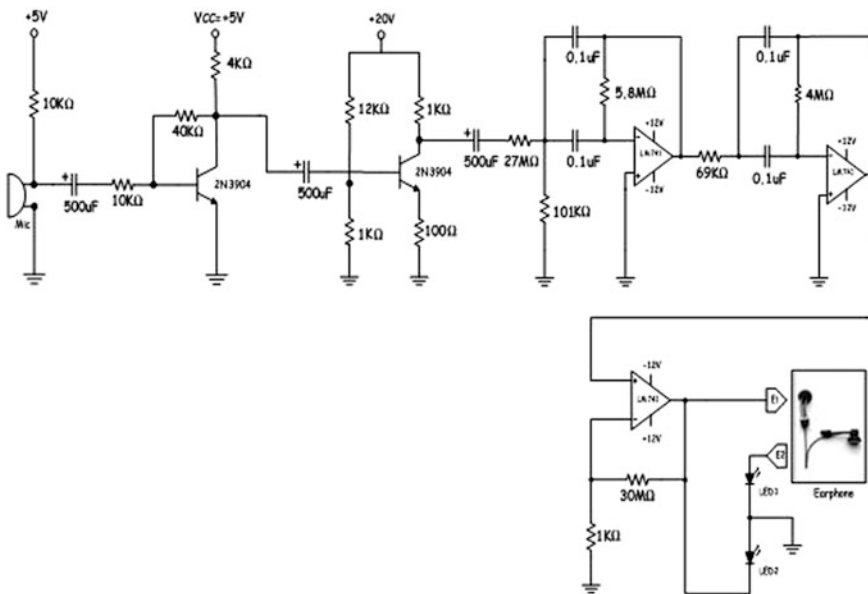


Fig. 47.1 Detector circuits

circuit for filtering the maternal heartbeat to the fetal one. Additionally, a non-inverting amplifier circuit is used to amplify the signals so the captured fetal heart beats can be heard by human ears using the Earphone. In this proposed device, the detector is also equipped with two LEDs. There two LED will flare alternately, that flare correspond to the detected the frequencies of the captured fetal heartbeat.

### 47.2.1 Chebyshev Band Pass Filter

The design of a Chebyshev Bandpass, which is used in this study, is Delyiannis & Friends circuit [4, 5]. This design is able for filtering frequencies 2–3 Hz using a 0.1  $\mu\text{F}$ , wherein the circuit component values were obtained from the calculation of previous studies in Ref. [6] (Fig. 47.2).

## 47.3 Testing and Results

Figure 47.3 shows the proposed prototype of fetal heartbeat detector.

We performed two types of tests, for testing the performance of the proposed detector. The first one is the laboratory test using a gauge and the second one is the direct test on the pregnant mothers. The results are explained in the following subsections.

### 47.3.1 Testing with a Gauge

The tests were carried out at the Laboratory of Electrical Engineering, Gunadarma University. They are aimed to determine whether the equipment functions properly

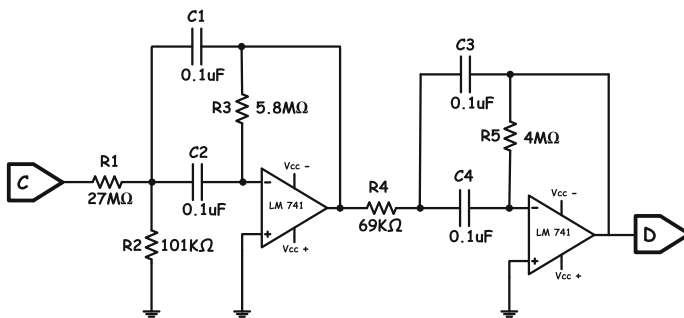


Fig. 47.2 Chebyshev band pass filter

**Fig. 47.3** Fetal heartbeat detector prototype



or not. The devices for performing the tests are function generator and oscilloscope. The output measurement was further processed using Eq. (47.1):

$$V_{out} = \text{number of peak - to - peak} \times \frac{\text{Volt}}{\text{Div}} \text{scala (in Oscilloscope)} \quad (47.1)$$

Equation (47.2) was used to calculate the frequency:

$$f = \frac{1}{T} \left( \text{number of peak - to - peak} \times \frac{\text{Volt}}{\text{Div}} \text{scala (in Oscilloscope)} \right) \quad (47.2)$$

To calculate the gain, we used Eq. (47.3):

$$A_{dB} = 20 \log \frac{V_{out}}{V_{in}} \quad (47.3)$$

The percentage error (% error) of the test was obtained using Eq. (47.4):

$$\text{Error percentage} = \left| \frac{\text{Calculated data} - \text{Test data}}{\text{Calculated data}} \right| \times 100\% \quad (47.4)$$

From the results shown in Table 47.1, it is concluded that the parallel voltage feedback amplifier circuit works as expectedly.

From the results shown in Table 47.2, it is concluded that the common emitter amplifier circuit works as expectedly, indicated by its small values of error percentages.

In Table 47.3, it is seen that the highest output voltage is generated at the input frequency of 2 Hz, i.e. 0.8 V<sub>pp</sub>, while at the input frequency of 3 Hz, the output is 0.4 V<sub>pp</sub>. It is concluded that the value of frequency response of the test results is close to the desired frequency response.

**Table 47.1** Test results of amplifier circuit of parallel feedback

Input frequency (Hz)	Calculation of gain		Gain testing		Error (%)	
	$A_v$	$A_{dB}$	$A_v$	$A_{dB}$	$A_v$	$A_{dB}$
1	3.58	11.07	2	6.02	39.66	45.65
2	3.58	11.07	3.75	11.48	4.74	3.63
3	3.58	11.07	3.43	10.72	3.98	3.18
4	3.58	11.07	2.75	8.78	23.18	20.68
5	3.58	11.07	2	6.02	44.13	45.65
6	3.58	11.07	2.33	7.35	34.82	30.56
7	3.58	11.07	2	6.02	44.13	45.65
8	3.58	11.07	2.5	7.95	30.16	28.15
9	3.58	11.07	2.25	7.04	37.15	36.41
10	3.58	11.07	3.09	9.81	13.54	11.4

**Table 47.2** Test results of common emitter amplifier circuit

Input frequency (Hz)	Calculation of gain		Gain testing		Error (%)	
	$A_v$	$A_{dB}$	$A_v$	$A_{dB}$	$A_v$	$A_{dB}$
1	7.5	17.5	10	20	25	12.49
2	8.33	18.41	10	20	16.66	7.91
3	9.09	19.17	10	20	9.09	4.13
4	8.72	18.81	10	20	12.72	5.91
5	10	20	10	20	0	0
6	8.57	18.66	10	20	14.28	6.69
7	9.37	19.43	10	20	6.25	2.8
8	8.88	18.97	10	20	11.11	5.11
9	10	20	10	20	0	0
10	9.23	19.3	10	20	7.69	3.47

**Table 47.3** Test results of chebyshev band pass circuit

Input frequency (Hz)	Output Voltage (Vpp)
1	0.06
2	0.8
3	0.4
4	0.16
5	0.08
6	0.06
7	0.04
8	0.04
9	0.04
10	0.04



**Fig. 47.4** Detector testing by doctor, accompanied by midwifery lectures and students

#### **47.4 Testing on Pregnant Women**

After laboratory tests with a gauge gave good results, i.e. the detector can detect the frequency of 2–3 Hz, the second test is then performed directly on pregnant women. The tests were conducted at the clinic of Gunadarma University which is located in the area Salemba Raya, Jakarta Indonesia by medical doctors, accompanied by midwifery lecturers and students (Fig. 47.4).

As the results, we found that the detector can detect the fetal heartbeat at the frequency of 2–3 Hz. However, there is still instability of the prototype performance in detecting fetal heartbeat. The instability happened especially because the electret condenser microphone is very sensitive to movement. During the test, the pregnant mother should be assured for not moving the body very much, because it will affect the test results.

#### **47.5 Conclusion**

In general the prototype working good. However, it has a drawback due to instability that occurred when the tested mothers are moved during the tests. In further research, a circuit detector is designed in a single integrated circuit using mentor graphics tools. Additionally, a screen is added to show which frequencies are detected in the range of 2–3 Hz.

## References

1. Nuryati, V.: Design build tool detector and counters fetal heart rate with doppler principle (in Bahasa Indonesia). Thesis, Faculty of Engineering, University of Indonesia (2010)
2. Kristyawati, D., Siswono, H.: Analysis, Simulation, and Design of Bandpass Filters Using PSPICE for Fetal Doppler, Thesis (2009)
3. Salahuddin, N.S., Triawati, E., Jambormias, P.: Mini Doppler detector circuit design (in Indonesia). Proceedings KOMMIT 7, 311–316 (2012)
4. Tomlison, G.H: Electrical Networks and Filters Theory and Design. Prentice Hall Europe, New York (1991)
5. Coughlin, R.F., Driscoll, F.F.: Operational Amplifiers and Linear Integrated Circuits. Prentice-Hall, New Jersey (2001)
6. Kristyawati, D., Nur'ainingsih, D.: Analysis and simulation Chebyshev bandpass filter for fetal doppler use tools mentor (in Bahasa Indonesia), Konferensi Nasional Sistem Informasi 2012, STMIK-STIKOM Bali 23–25 February 2012. [http:// repository.gunadarma.ac.id/bitstream/123456789/2481/1/095.pdf](http://repository.gunadarma.ac.id/bitstream/123456789/2481/1/095.pdf)

**Part V**  
**Technology Innovation in Internet  
of Things and Its Applications**

# Chapter 48

## Network Traffic and Security Event Collecting System

Hee-Seung Son, Jin-Heung Lee, Tae-Yong Kim and Sang-Gon Lee

**Abstract** In the beginning stage of the security functions, defending and monitoring was treated as a single solution. Today's security management system has reached at the state of integration of risk management systems and security management system. However, the existing system can have negatively leak of internal information and be inefficient for prevention and post event tracing of security instance. Therefore if we formalize the event information from a variety of security systems and do correlation analysis, we can establish a more active defense. In this paper we built up a developmental environment for network management system using a customized Linux System and several network devices. Using SNMP and SYSLOG, network information are collected from the network equipment and recorded on Maria DB in Linux Server. We also developed a database system and a monitoring system for the collected data.

**Keywords** Security management system · SNMP · Syslog · MIB · Linux OS

### 48.1 Introduction

In today's Internet environments, there are many varieties of security threats. Recently there have been some attacks using DDOS that paralyze computer networks. Network of the Republic of Korea and the United States government agencies, portal sites and financial institutions server were paralyzed by the DDOS attack in July 7, 2009 [1]. And in March 3, 2011 a more advanced method has been used to paralyze the computer network [2]. More recently in June 26, 2015, group of hackers in Europe attacked the three Korean bank's computer network including

---

H.-S. Son · T.-Y. Kim · S.-G. Lee (✉)  
Dongseo University, Busan, South Korea  
e-mail: nok6@dongseo.ac.kr

J.-H. Lee  
Mobilizone, Busan, Korea



Daegu Bank, which increased a lot of threats [3]. In addition to these DDOS attack, there are other attacks such as IP spoofing, MAC address spoofing, ARP spoofing and session hijacking. It is quite sure that a variety of attacks will be found in the future. Although many security control system has been built as responds to these attacks, most of them offer only single solution for a specific attack. Security devices such as IDS and firewall provide only partial protection [4].

While security control systems that are currently used can simply detect intrusions or block the packets [5], we are planning to build an integrated security control system which can actively cope with those attacks. If we use simple network management protocol (SNMP) and syslog, it is possible to collect various information from the network. And if we develop an algorithm to analyze this information, we can effectively respond to variety of threats.

In this paper, as the first phase of the study for the integrated security control system construction, we build an environment for collecting network traffic and security event (here after we call NTSE) based on SNMP and syslog. We also developed database system and monitoring system for the collected data.

## 48.2 Background Knowledge

### 48.2.1 SNMP

SNMP is an Internet-standard protocol for managing devices over IP networks. Typical devices that support SNMP include routers, switches, servers, workstations, printers, modem racks and more. SNMP is widely used in network management systems to monitor network-attached devices for conditions that warrant administrative attention. Version 3 is the most updated version with security enhancement.

As shown in Fig. 48.2, manager, the agent and management information base (MIB) is the major entities of SNMP. Manager will request the necessary information to the agent, then the agent responses by sending back the collected information from network device [6]. Finally, MIB is a database that actually stores the information in a structured format. Even though the devices in companies will have their own MIB, there is a standardized MIB. An object is a unit of information managed by the DB management target device. Objects in the SNMP are organized in a hierarchical structure or a tree structure (Fig. 48.1).

Fig. 48.1 SNMP information gathering process

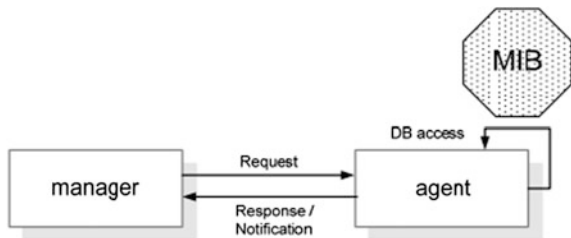


**Table 48.1** Syslog type

Log name	Log file name	Related daemon	Described
Kernel log	/dev/console		Log scattered on the console
System log	/var/log/messages	syslogd	Linux kernel log and main log
Security log	/var/log/secure	inetd	Log by inetd
Mail log	/var/log/maillog	sendmail popper	Mail log (Log by sendmail)
Cron log	/var/log/cron	crond	Log by crond
Booting log	/var/log/boot.log		Log on at system boot
FTP log	/var/log/xferlog	Ftpd	FTP log
Web log	/usr/local/apache/logs/access_log	httpd	Apache (web server) log
Name server log	/var/log/named.log	named	Name server (DNS) log

## 48.2.2 Syslog

In the computing system, syslog is a widely used standard for message logging. It permits separation of the software that generates messages which is then stored in the system, and the software that reports and analyzes them. Computer system designers may use syslog for system management and security auditing as well as general information, analysis, and debugging messages. A wide variety of devices, such as printers, routers, and message receivers across many platforms are using the syslog standard. This permits the consolidation of logging data from different types of systems in a central repository [7]. As shown in Table 48.1 the basic log files provided in the current Linux system are classified into 9 types.

In order to continuously operate a syslog server, system log management daemon is required. Daemon is a computer program that runs as a background process in a multitasking computer operating system rather than operates as direct control of an interactive use. It starts when the computer system is started and stops when the system is being shutdown.

## 48.3 Network Traffic and Security Event Collecting System

### 48.3.1 Log Collecting System Requirement

For the system design, we selected five requirements among several requirements [8].

**Correctness** As the most important requirement, in order to efficiently manage networks, it is necessary to collect correctly all of the logs that occur in the internal network. However, in the most business networks today, traffic capacity is extremely high because of the rapid increase of the network based business process. Even though the log-collecting-system receives, processes and compresses these

massive amounts of data, it should not offer a defective or erroneous information associated with that.

**Integrity** Because the collected log messages are used to monitor and detect future attacks, these messages are very important. Thus the reliability of the information source has a very close relationship with the system performance. Digital signature to the log data can provide reliability of the data, however it is impractical to apply the digital signature to the log data in the current network environment. If the log data is used as the evidence in criminal investigations, it may require a certain level of system integrity for legislation.

**Storage and processing** While storing the collected logs, they should not be tampered. The collecting system must be secure from the deletion and modification of log data by the insider or illegal intruder. Because the original log data is ill-formed, it should be processed before being provided to the administrator so that he/she can intuitively identify attacks.

**Normalization** Normalization is the task of normalizing the type of collected log data for the use of processing and reporting by network analyst or security analyst. That is a step of generating well-known log event formats. For this step, the various elements are mapped into the data to illustrate the log data into a common format. The original log data are converted into more meaningful information by classification and normalization.

**Log data mining** Data mining technology can be utilized to obtain better information from the raw log data for a better attack prediction and detection. Thus, by introducing this technology in the log collecting system, we can decrease the reliance on network exporter and make the general administrator to verify the log and to monitor the traces of penetration easily.

### ***48.3.2 System Design and Implementation***

In this paper we implemented a system that collects and analyzes all network traffic from a number of the network devices in an internal network. This system can provide basic data for detecting of attacks and provide a fast attack event extracting function by analyzing vast network traffic. If our system is utilized for detection and defense technology of attack events, based on the information that has been collected, it allows the detection and response to attacks through secure management and attack event analysis of the large capacity of the log data and network application systems.

Figure 48.2 is a schematic structure of the implemented system. Agent is a program that plays a role of Syslog and SNMP where such functions are not supported in an operating server. It is a TCP application program and sends NTSE from network device to our collecting system. Because most of the network devices provide Syslog and SNMP services, they can send NTSE directly using the Syslog and SNMP trap. However most of general servers do not provide these two

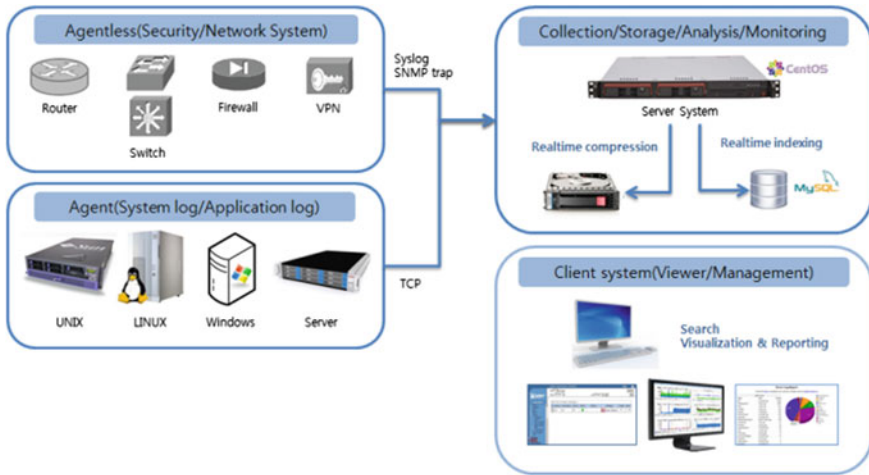


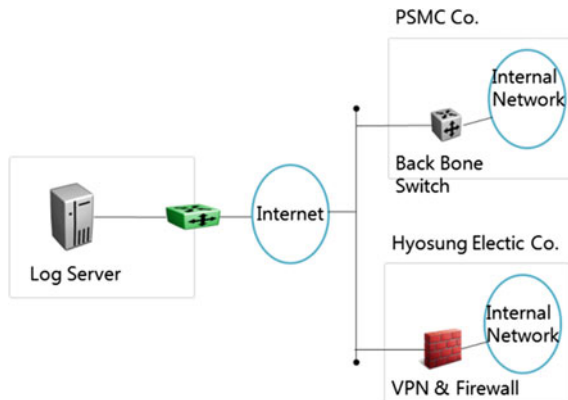
Fig. 48.2 The concept diagram for a network traffic and security event collecting system

services, therefore the agent creates packets for NTSE and sends them to the NTSE collecting system.

For the development environment, a log server was prepared by installing Centos 6.5 Linux system on a custom hardware platform and mounting the SNMP and syslog on the Linux system as shown in Fig. 48.3. Log server program has been implemented in the environment of C#, .NET 4.5 and a WPF (Windows Presentation Foundation). We used Maria DB for the archive of the collected data. Server program was coded in C++ utilizing the POCO Libraries [9]. We developed four data viewer for SNMP information, syslog event, syslog analysis, and network device status monitoring.

Our log server was deployed in the real time network to check the possibility of real time application. As shown in Fig. 48.3, the log collecting server, backbone

Fig. 48.3 Real implementation network diagram



Hostname	Timestamp	Level	Message
DongJu_nsisg1000	2015-07-17 10:30:54	Information	SNMP request from an unknown SNMP community dongju at 210.125.204.51:43252 has been received.
DongJu_nsisg1000	2015-07-17 10:30:54	Information	SNMP request from an unknown SNMP community dongju at 210.125.204.51:34166 has been received.
DongJu_nsisg1000	2015-07-17 10:30:54	Information	SNMP request from an unknown SNMP community dongju at 210.125.204.51:34166 has been received.
DongJu_nsisg1000	2015-07-17 10:30:53	Information	SNMP request from an unknown SNMP community dongju at 210.125.204.51:34166 has been received.
ISG-1000_HQ	2015-07-17 10:32:43	Alert	Port scan! From 192.168.60.6:56251 to 221.161.30.22:60827, proto TCP (zone Trust int. ethernet1/3). Occurred 1 times.
ISG-1000_HQ	2015-07-17 10:32:40	Information	IKE121.124.60.2.175.199.63.226 Phase 1: Initiated negotiations in aggressive mode.
YWCC_SSG140	2015-07-17 10:35:41	Information	IKE221.152.17.211.112.216.41.130 Phase 1: Initiated negotiations in main mode.
ISG-1000_HQ	2015-07-17 10:32:28	Information	IKE 175.199.63.226 Phase 1: Retransmission limit has been reached.
DongJu_nsisg1000	2015-07-17 10:30:25	Information	SNMP request from an unknown SNMP community dongju at 210.125.204.51:45605 has been received.

Fig. 48.4 SNMP information collection

switch and VPN firewall are located in separate networks. In the log server, SNMP/Syslog server has been installed so that it receives and processes NTSE from PSMC and Hyosung Electric network.

To collect NTSE for each network devices, Juniper’s backbone switches from PSMC network and VPN firewall from Hyosung Electric network were selected. Figure 48.4 shows a screen view of SNMP information collection. Figure 48.5 shows real time syslog event collection from PSMC backbone switch. Figure 48.6 shows syslog analyses view of data from Hyosung Electric VPN device. Figure 48.7 shows network device status monitoring of CPU load, memory usage, and session collected from Hyosung Electric VPN device.

### 48.3.3 The Result of System Implementation

To test our log system in the real network, the proposed system was link with the back bone switch, firewall and VPN equipment in the real network and carried out traffic analysis. As corporate networks become more complex and larger in size, the amount of logs will increase explosively. Furthermore, dealing with the big data and security issues, the need of integrated log management is increasing. If we

The screenshot shows a web-based interface for Syslog event collection. At the top, there is a dropdown menu for '장비 선택' (Device Selection) set to 'PSMC\_HQ'. Below it, a date range selector shows '기간 선택' (Date Selection) from '2015년 7월 16일' to '2015년 7월 17일'. A search bar with '검색' (Search) and '취소' (Cancel) buttons is on the right. Below the search bar, there are radio buttons for log levels: Debugging, Information, Notice, Warning, Error, Critical, Alert, and Emergency. The main area is a table with the following columns: '소속 그룹' (Source Group), '장비명' (Device Name), '날짜' (Date), 'Device ID', and 'Message'. The table contains 15 rows of log entries, all from '유지보수사이트' (Maintenance Site) with severity 'PSMC'. The messages include IKE negotiations, SPI responses, and an SNMP request.

소속 그룹	장비명	날짜	Device ID	Message
유지보수사이트	PSMC	2015-07-16 오전 11:23:16	PSMC_HQ	IKE 119.93.67.191 Phase 2: Initiated negotiations.
유지보수사이트	PSMC	2015-07-16 오전 11:23:16	PSMC_HQ	IKE 119.93.67.191 Phase 2 msg ID 6ffc58bd: Responded to the peer's first message
유지보수사이트	PSMC	2015-07-16 오전 11:23:16	PSMC_HQ	Rejected an IKE packet on ethernet0/0 from 210.124.139.60:4500 to 119.93.67.191
유지보수사이트	PSMC	2015-07-16 오전 11:23:16	PSMC_HQ	IKE 119.93.67.191: Received a notification message for DOI 1 40001 NOTIFY_NS_N
유지보수사이트	PSMC	2015-07-16 오전 11:23:16	PSMC_HQ	IKE 119.93.67.191 phase 2:The symmetric crypto key has been generated successfully
유지보수사이트	PSMC	2015-07-16 오전 11:23:16	PSMC_HQ	IKE 119.93.67.191 Phase 2 msg ID 79eb06da: Completed negotiations with SPI 871
유지보수사이트	PSMC	2015-07-16 오후 12:23:06	PSMC_HQ	IKE 119.93.67.191 Phase 2 msg ID 45307ec5: Responded to the peer's first message
유지보수사이트	PSMC	2015-07-16 오후 12:23:06	PSMC_HQ	IKE 119.93.67.191: Received a notification message for DOI 1 40001 NOTIFY_NS_N
유지보수사이트	PSMC	2015-07-16 오후 12:23:07	PSMC_HQ	IKE 119.93.67.191 phase 2:The symmetric crypto key has been generated successfully
유지보수사이트	PSMC	2015-07-16 오후 12:23:07	PSMC_HQ	IKE 119.93.67.191 Phase 2 msg ID 45307ec5: Completed negotiations with SPI 871
유지보수사이트	PSMC	2015-07-16 오후 12:22:57	PSMC_HQ	IKE 119.93.67.191 Phase 2 msg ID 163d3b11: Responded to the peer's first message
유지보수사이트	PSMC	2015-07-16 오후 12:22:57	PSMC_HQ	IKE 119.93.67.191: Received a notification message for DOI 1 40001 NOTIFY_NS_N
유지보수사이트	PSMC	2015-07-16 오후 12:22:57	PSMC_HQ	IKE 119.93.67.191 phase 2:The symmetric crypto key has been generated successfully
유지보수사이트	PSMC	2015-07-16 오후 12:22:57	PSMC_HQ	IKE 119.93.67.191 Phase 2 msg ID 163d3b11: Completed negotiations with SPI 871
유지보수사이트	PSMC	2015-07-16 오후 14:5:11	PSMC_HQ	SNMP request from an unknown SNMP community public at 184.105.139.67:5006

Fig. 48.5 Syslog event collection

장비 선택 HS\_JangAn\_HQ-FW

기간 선택 24시간 2015-07-16 부터 2015-07-17 까지

송신지 IP 숫자만 입력하세요. Port 수신지 IP 숫자만 입력하세요. Port

프로토콜 선택안함 전송률 선택안함 수신량 선택안함

검색 취소

날자	장비명	Source IP	Source Port	Destination IP	Destination Port	Protocol	Duration	수신	송신
2015-07-16 오전 10:45:45	표성전기	152.149.21.32	1466	168.126.63.1	53	UDP	1	88	160
2015-07-16 오전 10:45:45	표성전기	172.100.20.202	49654	168.126.63.1	53	UDP	1	95	377
2015-07-16 오전 10:45:45	표성전기	152.149.2.193	55992	168.126.63.1	53	UDP	1	86	252
2015-07-16 오전 10:45:45	표성전기	172.100.20.202	50222	168.126.63.1	53	UDP	1	95	239
2015-07-16 오전 10:45:45	표성전기	152.149.21.37	52924	199.59.148.21	443	TCP	311	2554	2322
2015-07-16 오전 10:45:45	표성전기	152.149.21.25	50900	211.106.65.158	80	TCP	132	13435	458672
2015-07-16 오전 10:45:45	표성전기	172.100.20.99	38924	202.131.28.33	80	TCP	2	754	728
2015-07-16 오전 10:45:45	표성전기	172.100.20.69	54540	211.53.214.11	80	TCP	2	1433	1230
2015-07-16 오전 10:45:45	표성전기	152.149.21.101	53580	114.111.46.229	80	TCP	10	2986	1446
2015-07-16 오전 10:45:45	표성전기	172.100.20.38	56473	168.126.63.1	53	UDP	1	95	239
2015-07-16 오전 10:45:45	표성전기	172.100.20.90	52064	61.111.62.149	80	TCP	2	831	523
2015-07-16 오전 10:45:45	표성전기	172.100.20.90	52050	216.59.220.234	443	TCP	242	1769	1399
2015-07-16 오전 10:45:45	표성전기	152.149.31.20	57090	168.126.63.1	53	UDP	2	76	172
2015-07-16 오전 10:45:45	표성전기	172.100.20.74	31782	125.209.214.36	80	TCP	1	1322	554
2015-07-16 오전 10:45:45	표성전기	172.100.20.74	31708	31.13.82.1	443	TCP	119	12012	6796
2015-07-16 오전 10:45:45	표성전기	152.149.21.37	52926	199.59.148.21	443	TCP	311	2602	2370
2015-07-16 오전 10:45:45	표성전기	152.149.21.25	50936	211.106.65.158	80	TCP	126	756	2317

Fig. 48.6 Syslog analysis view

장비 선택 표성전기

장비를 선택하세요.

기간 선택 24시간 2015년 7월 16일 목요일 부터 2015년 7월 17일 금요일 까지

CPU 사용량 선택안함 Memory 사용량 선택안함 Session 사용량 선택안함 상태 선택안함

검색 취소

날자	CPU 사용량	Memory 사용량	Session 사용량	상태정보	조위사항
2015-07-16 오전 10:42:00	2	21.92098	0.8697	정상	RealISMClient.StateLog + StateList
2015-07-16 오전 10:42:20	2	21.92098	0.86736	정상	RealISMClient.StateLog + StateList
2015-07-16 오전 10:42:40	2	21.92098	0.85643	정상	RealISMClient.StateLog + StateList
2015-07-16 오전 10:43:00	2	21.92396	0.78105	정상	RealISMClient.StateLog + StateList
2015-07-16 오전 10:43:20	2	21.92405	0.76543	정상	RealISMClient.StateLog + StateList
2015-07-16 오전 10:43:40	2	21.92405	0.78184	정상	RealISMClient.StateLog + StateList
2015-07-16 오전 10:44:00	2	21.921	0.78535	정상	RealISMClient.StateLog + StateList
2015-07-16 오전 10:44:20	2	21.92403	0.78652	정상	RealISMClient.StateLog + StateList
2015-07-16 오전 10:44:40	2	21.92108	0.81581	정상	RealISMClient.StateLog + StateList
2015-07-16 오전 10:45:00	2	21.92099	0.8205	정상	RealISMClient.StateLog + StateList
2015-07-16 오전 10:45:20	2	21.92108	0.86502	정상	RealISMClient.StateLog + StateList
2015-07-16 오전 10:45:40	2	21.92396	0.88259	정상	RealISMClient.StateLog + StateList
2015-07-16 오전 10:46:00	2	21.92099	0.86775	정상	RealISMClient.StateLog + StateList
2015-07-16 오전 10:46:20	2	21.92108	0.82128	정상	RealISMClient.StateLog + StateList
2015-07-16 오전 10:46:40	2	21.92108	0.85057	정상	RealISMClient.StateLog + StateList
2015-07-16 오전 10:47:00	2	21.92405	0.84783	정상	RealISMClient.StateLog + StateList

Fig. 48.7 Network device status monitoring

apply our system to the complex company networks for collecting logs of all networks and analyzing them in real time, it is possible to provide appropriate information as a response. Most network devices do not collect and save logs, but because we can collect and analyze the logs using our system,, the proposed system is very useful to solve this problem. Thus our system can be easily installed and managed in the existing network so that it is not necessary to build a new system to collect the logs.

## 48.4 Conclusion

In this paper, we designed and implemented a system for collecting and analyzing network traffics to analyze and monitor the security problem of the internal network of an organization in real-time. The proposed system saves all of the traffics generated from storage-less network devices and analyzes the security problem in real time. It enables the organization to monitor the state of the internal network. Also, when security incidents occur, our system can acquire the log data for the traffic information and rapidly analyzes it. The expected benefit of deploying our system is that the network security features can be enhanced by managing the network-based security issues while using the existing network systems.

**Acknowledgments** This paper was supported by the Ministry of Trade, Industry and Energy (MOTIE) through the fostering project of the Innovation for Engineering Education and by Ministry of Education (MOE) through the project of the Leaders in the Industry-university cooperation.

## References

1. Wikipedia Website on 7.7 DDoS Attack. [https://ko.wikipedia.org/wiki/7%C2%B77\\_DDoS\\_%EA%B3%B5%EA%B2%A9](https://ko.wikipedia.org/wiki/7%C2%B77_DDoS_%EA%B3%B5%EA%B2%A9)
2. Wikipedia Website on 3.3 DDoS Attack. [https://ko.wikipedia.org/wiki/3%C2%B73\\_DDoS\\_%EA%B3%B5%EA%B2%A9](https://ko.wikipedia.org/wiki/3%C2%B73_DDoS_%EA%B3%B5%EA%B2%A9)
3. Financial news website. <http://www.fnnews.com/news/201506261801326408>
4. Yu, Y.J.: DDoS Attack Detection Method Using Average Rate of Change of Traffic. MS thesis, Graduate school of Chungbuk National University (2011)
5. Tabona, A.: The Top 20 Free Network Monitoring and Analysis Tools for Sys Admins, GFI Blog, 15th, 4, 2015. <http://www.gfi.com/blog/the-top-20-free-network-monitoring-and-analysis-tools-for-sys-admins/>
6. Kim, Y.S.: Understanding of SNMP concept, Novo networks (2010)
7. Wikipedia Website on Syslog. <https://en.wikipedia.org/wiki/Syslog>
8. Chuvakin, A.A., Schmid, K.J., Phillips, C.: Logging and Log Management: The Authoritative Guide to Understanding the Concepts Surrounding Logging and Log Management, 1st edn. Syngress, California (2012)
9. POCO C++ Libraries. <http://pocoproject.org/>

# Chapter 49

## Paper Prototyping for BatiKids: A Technique to Examine Children's Interaction and Feedback in Designing a Game-Based Learning

Hestiasari Rante, Heidi Schelhowe and Michael Lund

**Abstract** Among all critical discussion about the usability of a low-fidelity paper prototyping with in design process, this paper will present the experience of authors when conducting paper prototype usability tests for children. The paper prototyping was applied as a technique in designing BatiKids, a game-based learning environment that is developed to support children in understanding the process of making batik, one of the cultural heritages from Indonesia. The test revealed that children generally enjoyed the game and that the proposed approach has promising potential in empowering the game designers for children. The game is offering supports for children's understanding of the aesthetics part of a traditional form of art. This paper also discusses how to conduct the usability test with paper prototype, how to evaluate it by using the usability quality metric called as Success Rate, and what to do with the test results.

**Keywords** Batik · BatiKids · Children · Design · Game-based learning · Interaction · Paper prototype

### 49.1 Introduction

Digital games as one part of creative technologies have been accepted as a motivating tool for children to learn new thing through engaging interactions. Games have the capacity to promote learning that goes beyond the traditional standard-based, declarative knowledge taught in schools that is offered by

---

H. Rante (✉) · H. Schelhowe · M. Lund  
Department of Computer Science, University of Bremen, Bremen, Germany  
e-mail: rante@informatik.uni-bremen.de

H. Rante  
Department of Creative Multimedia, Electronics Engineering Polytechnic  
Institute of Surabaya, Surabaya, Indonesia



traditional curricula. Developing games then become one of the most considered phase within the whole designing process [1, 2].

To ensure games are successfully developed it is extremely important to playtest them as early, and as often as possible during the development process. This is necessary to get feedback to improve the usability and address game balancing and motivation issues [3, 4]. Without the feedback, the user experience may not be optimal and the aims of the game will not be achieved. Usually user experience is evaluated after there is an early working prototype implemented which it is ready for testing [4, 5]. In the early stages of development prototypes can take the form of game sketches and thus, for some testing, a fully functional prototype may not be necessary. Time constraints and skill limitations often influence the fidelity of the prototype being developed.

Paper prototyping is a technique for usability testing where the representative users perform realistic tasks by interacting with a paper version of the interface that is manipulated by a person “playing computer”, who does not explain how the interface is intended to work. Paper prototyping highlights cost-effective usability testing techniques that produce fast results for improving an interface design. Anyone who is involved in the design, implementation, or support of user interfaces can benefit from paper prototyping because it fosters development of products that are more useful, intuitive, efficient, and pleasing [6].

Critics about the use of paper prototyping are coming from both researchers and professional practitioners [7, 8], while Gibson gives a comparison of the best uses and the poor uses of paper prototype [9]. Some of these arguments will be referred to the Sect. 48.2.

Paper prototyping is not a difficult technique. The real challenge often lies is convincing others to try it. It is not too hard for most people to grasp the benefits of testing a design without having to code it first. But even so, some people are still questioning the validation of test result. Does paper prototyping help to find real problems? Does it find the same problems as testing the real interface?

This paper discusses our experiences when conducting usability testing through paper prototyping with children as users. The benefits of this low-fidelity test are explored. Paper prototyping was applied as one method in designing the BatiKids, a game-based learning developed to support children in understanding the process of making batik, one of the cultural heritages from Indonesia. The game covers some tasks including drawing and coloring, and to know if children can accomplish the tasks we thought that paper prototyping test might be suitable.

In the second section the method will be described and enriched with some practical information on how to create the paper prototype. The third section lays out how the paper prototyping method is implemented for the design of BatiKids. The fourth section will describe results we got from the implementation of the method and the fifth section is conclusion.

## 49.2 Methodology

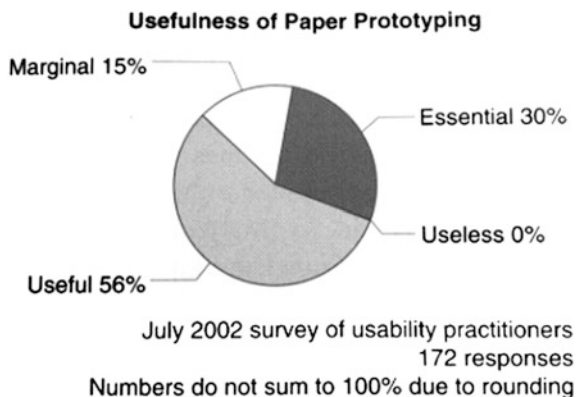
Paper prototyping is a technique widely used for the early stages of user interface design. Its goal is to present a more or less realistic design to the user, while minimizing the costs of creating, so that the designer is still willing to reject or modify the design if necessary. We consider paper prototypes as a suitable medium for iterative design.

In 2002, Snyder conducted an online survey for some usability professionals about the use of paper prototyping and the attitude toward it. Question delivered on the survey was: What is the importance of paper prototyping to your work? Responding users were 172 people and most of them are the usability specialists. 86 % of the respondents answered either “essential” or “useful”. “Useless” was one of the options but no one chose it [6]. This survey result is an indication that paper prototyping is no longer a fringe method and that it should be considered as part of the design process. Figure 49.1 shows the result of the survey.

Paper prototyping allows a designer to acquire early user feedbacks about a design. The designer can create an interface mockup of the application using paper artifacts such as hand drawings. The ideas can be evaluated and commented at a very early stage with a group of users in a visual and tangible way [10, 11]. Before the test starts, the designer has to give a brief introduction to the users about the product idea and the basic principles for using a paper prototype. After that, the designer can ask the users to process concrete tasks with the prototype possibly developed out of existing used scenarios.

During the test, the designer can play the role of the computer and presents an interface screen on pieces of paper, to a user according to the user’s actions. The user interacts with the interface by pointing at elements he would use as if it were a real system, then the designer reacts by changing the paper screens that reflect the interface. By asking the user to think aloud about their actions and the interface design as the test proceeds, a designer can get qualitative feedback.

**Fig. 49.1** Snyder’s online survey result



Although paper prototyping allows fluid and rapid iteration on a design, its spontaneous and physical nature makes it difficult to analyze and communicate a design and test findings to a wider audience. Designers are strongly suggested to video-record the test sessions to capture interaction scenarios and the conversation with the users [12]. In practice, seeing the users get confused and voice their concerns has more impact than simply hearing someone else describe what happened [9]. It is also important to write down as much as possible. One can write all observations, design suggestions and problems, also the steps the user takes, as completely as possible. It is important to note all of the user's remarks, and the own ideas in the margins. During the observations, it is advisable not trying to filter or compile the information, as time will be lost as well as information that could prove valuable at a later time [13].

Once the paper prototyping test is completed, it is essential to make an evaluation. In order to evaluate a paper prototype, there are two main evaluation methods. At first is users evaluation, that means users from the target group interact with the prototype or product and during this interaction their behavior and experiences are collected using a variety of techniques including observations [14] and think aloud [15]. The second evaluation method is to interview the users after test. Designers may ask the users how well they feel the tasks can be processed with the paper prototype. Designers may also ask every problem faced during the test and how they feel working with the prototype. Additionally designers should constantly try to interpret the non-verbal reactions of the users and question the accuracy of their own interpretation [13].

When evaluating prototypes, the results can be influenced by the fidelity effect associated with the form of the prototype. In a study examining usability, many of the problems were not reported in the low-fidelity version [16] as they were associated with the functionality of the device. In another study it was concluded that users appeared to over compensate for deficiencies in aesthetics in low-fidelity prototypes [17]. When evaluating prototypes of games designed for children, understanding the effect fidelity has on the results, has to be considered.

### **49.3 Paper Prototyping for BatiKids**

The interface designers and developers should be responsible to seek for a good quality products design which will positively contribute towards the children's development and health. It is very common to find in practice that children are being considered in user interface design guidelines. The involvement of children in the design process is very useful. This section reports our experience when doing paper prototypes test with children as the main user target.

BatiKids is a game-based learning we developed to support children understanding the process of making batik in traditional way. The game has two levels. In the Level 1, children have to do some tasks including selecting a batik pattern, drawing the pattern following dots, then coloring the pattern by choosing one color

or they can also mix two or three different colors, and the last is multiplying the pattern. Level 2 has the same structure as Level 1 with additional features such as resizing, rotating, and flipping the pattern.

### 49.3.1 Process

We divided the paper prototyping test for BatiKids into three parts. The first part was including preparing the materials, determining the aim of the test, defining scenario and tasks for the user, preparing the paper prototype and the properties, and handling narrative guidelines for the interview. As second part we conducted the test where one author/researcher played the role of the computer, another one noted all the important findings during the test, and with help of the internship students we video-recorded the test. The third part was interviewing the user based on questions guideline.

With qualitative user testing, it is enough to test three to five users [18]. We did the paper prototype test with four children in Germany and Indonesia: Nathan (7), Amadeo (7), Vanda (6), and Meme (6). As the first step, we delivered a short introduction about the history of batik and the traditional process of making it. Then we described the tasks and materials needed to work with. Figure 49.2 shows the materials used for the test and a child who was doing the test.

Nathan looked confident when he started the test. He firstly chose Level 1 and chose Dewa (boy figure) as his character companion for the game. He listened carefully to what we as designers told (playing the role of computer) and did the tasks straightforwardly. He knew well when he should point the “Back” and “Next” buttons. He seemed to be very glad when it came to the part of selecting one batik pattern that he could color. He colored the pattern and seemed to enjoy the activity. He finished Level 1 in 7 min. When it came to the end, he refused to finish the game and preferred to select the “Home” button rather than the “Finish” button. This selection brought him back to the main page. Then he began Level 2 which has

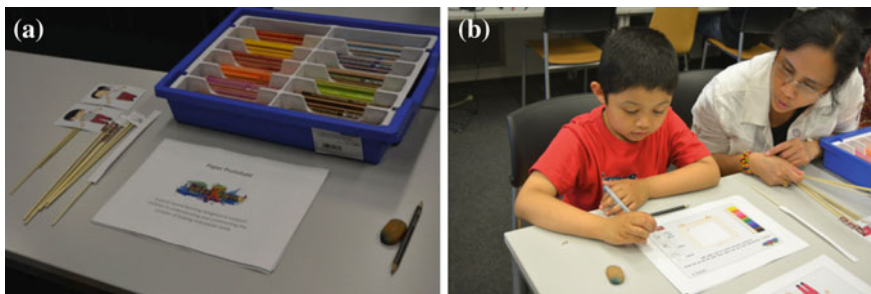


**Fig. 49.2** a Materials for BatiKids paper prototyping test; b a child was doing the test Snyder's online survey result

some additional interactions and more challenging than Level 1. He finished it within 9 min. He once mentioned that he wanted to change the flow of the game in Level 2. He would rather like to rotate the pattern first, then colored it. We encouraged him to do that. In the end, he said that it was a joyful game and that he was surprised that it should be ended.

A similar matter happened with Amadeo. He also chose Dewa as his character companion, played Level 1 and 2, and refused to finish the game. He needed 8 min to finish Level 1 and 9 min for the Level 2. The female testers, Vanda and Meme, both of them chose Dewi (girl figure) as their character companion for the game. Vanda played Level 1 only and shortly chose to finish the game. She said that she only liked the coloring part of the game, even though she did not finish the part. But Meme played Level 1 and 2, and also looked happy during the whole process of the game.

After the children tested, we took 5 min break for each then continued by interviewing them. Interviewing was based on the question lists we have prepared. All children said that they comprehended the aim of the game, they enjoyed it, and they would like to play the real game. However, we noticed that the main usability problems occurred during the tests is related to the tool used for drawing the selected pattern. When children had chosen one pattern, they should draw following dots that shaped the pattern. We gave pencil as tool for drawing. Since the pattern is an art batik form, we observed that children hardly moved the pencil in order to draw the pattern in a proper shape.

### 49.3.2 Evaluation

To collect metrics, Nielsen recommended using a very simple usability measure for user: Success Rate. This Success Rate is defined as the percentage of tasks that users complete correctly. This is an admittedly coarse metric; it says nothing about why users fail or how well they perform the tasks they did complete, but nevertheless the Success Rate is easy to collect and a very telling statistic [18].

According to Nielsen, if a user can perform tasks as specified completely, it is considered success and marked with S. If a user does not complete the tasks, it is considered failure and marked with F. If a user can complete tasks partially, then it is considered as partially success and marked with P.

$$Success\ Rate = \frac{\sum S + 0.5 \times \sum P}{\sum User \times \sum Task}$$

Test is considered success and can support users to achieve the goal of the game if Success Rate > 50 %. In this paper prototyping test we gave four main tasks to the children:

**Table 49.1** Result of all attempts on the test

	Task 1	Task 2	Task 3	Task 4
Nathan	P	S	S	S
Amadeo	P	S	S	S
Vanda	P	S	P	P
Meme	P	S	S	S

1. Understand the process of making batik and be able to tell it after finishing the game
2. Select and draw one pattern by following the dots
3. Color the pattern
4. Understand all the instruction and be able to select an appropriate buttons

In total, we observed 16 attempts from four children to perform the tasks. Of those attempts, 10 were successful, 6 were partially successful, and none was failed. Result is shown on Table 49.1.

Using Nielsen’s user usability measurement, we got Success Rate = 81.25 %. Result was >50 % and we considered the paper prototyping test was succeed. We also evaluated problems occurred during the test. But since only very few usability problems occurred in a specific part of the prototype, we conclude that using low-fidelity prototypes with children can give some experience about the suitability of general ideas and usability [4].

## 49.4 Results

We did the paper prototyping test to children from Germany and Indonesia. Regardless their cultural background we see the benefits of the test results as the following:

- Low cost, both for time and materials required to create the prototype.
- Provides practical user feedback early in the development process before investing effort in development.
- Facilitates communication between the development team, and the children as users.
- Does not require any technical skills, therefore a multidisciplinary team can work together.
- Encourages creativity in the product development process.
- Improves usability of the application.

With adaptation of narration usage, the test can help children to use the paper prototyping test as a simulation inspiring their imagination. The narration also can motivate children to express their feeling and feedback.

## 49.5 Conclusion

Even though some components of BatiKids were drastically simplified with the paper prototype, the introduction in the beginning and the narration told by the researcher during test helped children to understand the complexity of batik production in the real process. This complex combination of stories, actions, and feedbacks led authors to improve their concept for the application. Paper prototypes should be considered when the designer is in the following situation:

- The designer wants to make a sincere effort to allow all members of a team, including those with limited software skills, to take part in the design process.
- The designer needs a quick test result.
- Tests of a design that covers tasks such as drawing and coloring.

It is important to consider that the decision to choose the appropriate prototyping method should also depend on the subjects' characteristics. If paper prototypes are faster and cheaper to develop, still the problem of how to minimize the paper prototypes' disadvantages to give kids the feeling of being observed and of causing unnecessary effort for the designer will have to be solved.

We conclude that through a paper prototype test designers can get at a very early stage feedback by users at extremely low costs. Designers can fix usability problems at a very early time before wasting money implementing something that does not work. Paper prototyping test fits well for application such as game-based learning for children.

**Acknowledgments** We thank to children who participated in the study. We would also like to thank to the three internship students; Kanjana Jettammakun, Kanokporn Rattanacharoenporn and Napassawan Tangamporn from King Mongkut's University of Technology Thonburi, Thailand for their contribution in this study.

## References

1. Rante, H., Lund, M., Schelhowe, H.: A digital batik tool—supporting children in understanding and constructing traditional batik patterns within a museum context. *Int. J. Multi. Educ. Res. (IJMER)* **1**(2) (2014)
2. Shaffer, D.: *How Computer Games Help Children Learn*, 1st edn. Palgrave Macmillan, New York (2006)
3. Shell, J.: *The Art of Game Design*. Morgan Kaufmann, Burlington (2008)
4. Sim, G., Cassidy, B., Read, J.: Understanding the fidelity effect when evaluating games with children. In: *the Proceedings of the 12th International Conference on Interaction Design and Children*, pp. 193–200. ACM New York, NY, USA (2013)
5. Korhonen, H., Paavilainen, J., Saarenpaa, H.: Expert review method in game evaluations—comparison of two playability heuristics. In: *Proceedings of the MindTrek 2009*. ACM, Tampere (2009)
6. Snyder, C.: *Paper Prototyping: The Fast and Easy Way to Design and Refine User Interfaces*. Morgan Kaufmann, Burlington (2003)

7. Knapp, J.: Paper prototyping is a waste of time. <https://medium.com/@jakek/paper-prototyping-is-a-waste-of-time-353076395187>. Visit on 18 May 2015
8. Dubroy, P., Why I'm Not Doing a Paper Prototype. <http://dubroy.com/blog/why-im-not-doing-a-paper-prototype/>. Visit on 20 May 2015
9. Gibson, J.: Introduction to Game Design, Prototyping, and Development: From Concept to Playable Game with Unity and C# (Game Design and Development). Addison Wesley, Boston (2014)
10. Rettig, M.: Prototyping for tiny fingers. *Commun. ACM* **37**(4), 21–27 (1994)
11. Li, Y., Cai, X., Everitt, K., Dixon, M., Landay, J.A.: Frame wire: a tool for automatically extracting interaction logic from paper prototyping tests. In: the Proceedings of the SIGCHI Conference on Human Factors in Computing Systems, pp. 503–512. ACM, New York, NY, USA (2010)
12. Mackay, W.E., Fayard, A.L.: Video brainstorming and prototyping: techniques for participatory design. In: CHI '99 Extended Abstracts. CHI '99, pp. 118–119 (1999)
13. User Day Toolkit. [http://www.sapdesignguild.org/resources/user\\_day\\_toolkit/index.htm](http://www.sapdesignguild.org/resources/user_day_toolkit/index.htm). Visit on 18 May 2015
14. Sim, G., MacFarlane, S., Horton, M.: Evaluating usability, fun and learning in educational software for children. In: Proceedings of EDMEDIA. AACE, Montreal (2005)
15. Olsen, A., Smolentzov, L., Strandvall, T.: Comparing different eye tracking cues when using the retrospective think aloud method in usability testing. In: Proceedings of the 24th British HCI Conference—Play is serious business. ACM, Abertay (2010)
16. Liu, L., Khooshabeh, P.: Paper or interactive?—A study of prototyping techniques for ubiquitous computing environments. In: Proceedings of the CHI '03 Extended Abstracts on Human Factors in Computing Systems. ACM, Ft. Lauderdale, Florida, USA (2003)
17. Sauer, J., Sonderegger, A.: The influence of prototype fidelity and aesthetics of design in usability tests: Effects on user behaviour, subjective evaluation and emotion. *Appl. Ergon.* **40**, 670–677 (2009)
18. Nielsen, J.: Success Rate: The Simplest Usability Metrics. <http://www.nngroup.com/articles/success-rate-the-simplest-usability-metric/>. Visit on 16 July 2015



# Chapter 50

## Tracing Related Scientific Papers by a Given Seed Paper Using Parscit

Resmana Lim, Indra Ruslan, Hansin Susatya, Adi Wibowo,  
Andreas Handojo and Raymond Sutjiadi

**Abstract** The project developed a web site learning support for tracing scientific articles relating to a given input seed paper/article. The system will finds related articles that are listed on the references of the seed article. First, the reference list of an input seed article is extracted by utilizing Parscit citation extraction. Furthermore, the system searches the reference articles using Google Scholar and Mendeley API. Thus articles which are related to the seed article can be found. The system was built using PHP programming, it is utilizing Parscit modules, Google Scholar search and <https://www.mendeley.com/> API. Testing has been done by giving an input seed article. User will obtain the results of several articles related to the seed article.

**Keywords** Paper tracing · Citation extraction · Parscit · Google scholar · Mendeley.com

### 50.1 Introduction

To support literature review on a research, further reference search from an article/paper that we read is an important thing. When we read a scientific article, very often we are keen to discover more about the articles contained in the list of references. We can manually perform a search using Google scholar. But this will

---

R. Lim (✉) · H. Susatya  
Electrical Engineering Department, Petra Christian University,  
Surabaya, Indonesia  
e-mail: resmana@petra.ac.id

I. Ruslan · A. Wibowo · A. Handojo  
Informatics Engineering Department, Petra Christian University,  
Surabaya, Indonesia

R. Sutjiadi  
Computer Engineering Department, Institut Informatika Indonesia,  
Surabaya, Indonesia

take substantial efforts when there are many references that we will find. Therefore we need a tool to find or download the references we find automatically given an input seed article.

An automated extraction of paper's bibliography metadata is a challenging task given the variety of different paper's layouts and formatting (citation style) of its reference strings. Several automated extraction approaches have been proposed which are using unsupervised methods and template matching. It finds that the most promising approach is utilizing supervised sequence classification such as Hidden Markov Models (HMMs) [1] or Conditional Random Fields (CRFs) [2]. ParsCit [3] is a popular reference extraction system that uses heuristics approach to detect and segment references within a scientific paper. ParsCit uses CRF to assign labels to the tokens within each reference string. ParsCit is an open-source CRF-based citation parser that has been successfully used by CiteSeerx [4] and scientific papers harvester system [5].

Our project contributes to the purpose of enriching a scientific article (we call the seed paper) by identifying its bibliography (list of references) and connecting them to the original resources (full text if available) by utilizing google scholar and Mendeley API. The project uses Parscit, to process the bibliography in scientific articles. Parscit generate reference's meta-data such as author name, article title, year, etc. The meta-data is then used to perform queries to Google Scholar and Mendeley. The system seeks to connect the bibliography with its source full text using Google Scholar or Mendeley.

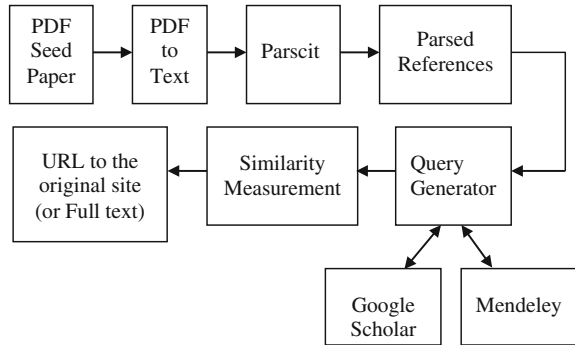
## 50.2 System Description

This web application is built by using PHP and HTML programming language and MySQL as database management system. The system uses Parscit as service provider to extract paper information data. All this components are run in a Linux based server. To accommodate function of parsing data to other data sources, PHP must be set to enable the cURL function.

In general, this system can be decomposed into parts of process as shown on Fig. 50.1. The first part is preprocessing. In this part, paper is prepared to be processed by Parscit by formatting PDF paper into TXT format. The second part is paper extraction process. This process is handled by Parscit to extract the paper meta-data such as: title, author(s), abstract, keywords. Parscit also do extract the list of references, which are used to make Google Scholar/Mendeley queries on the next phase. The third part is related paper searching process, where in this part, server makes query to other data sources (i.e. Google Scholar and <https://www.mendeley.com/>) to search related paper from references data. The last part is composing and presenting the information as the web output to the user.

As an input seed paper, user uploads a PDF paper into the system. Because Parscit can only process text based file, then before moving to the next part, unicode text must be extracted from PDF file. To do that, Apache PDFBox or similar

**Fig. 50.1** System block diagram



application is used to extract unicode text from the input PDF file. The result from this process is a TXT file format.

This TXT file format is processed further by Parscit to grab paper meta-data (i.e. title, author, affiliation, abstract, etc.) and parsed its references/bibliography data. Before the meta-data extraction, Parscit must be trained first with some sample data using similar paper format and language to detect the sections of paper. Make sure that there are enough sample paper data to increase the accuracy of data extraction. The output from the Parscit extraction is an XML file format that already accommodate extracted information which is grouped by different XML tags as shown in Fig. 50.2.

In the next step, each parsed reference data is forwarded to query generator. In this part, query generator searches related paper data from 2 data sources, Google Scholar and Mendeley. The system initiates HTTP query using Document Object

```

<citation valid="true">
<authors>
<author>Adi Kusrianto</author>
</authors>
<title>Pengantar Desain Komunikasi Visual.</title>
<date>2007</date>
<publisher>Penerbit ANDI.</publisher>
<location>Yogyakarta:</location>
<marker>Kusrianto, 2007</marker>
<rawString>Kusrianto, Adi. (2007). Pengantar Desain Komunikasi Visual.
Yogyakarta: Penerbit ANDI.</rawString>
</citation>
  
```

**Fig. 50.2** Part of XML citation data

Model (DOM) parsing method to Google Scholar to search related paper using title and author data that already classified by Parscit XML result above. This parsing method is used because Google Scholar does not provide Application Programming Interface (API). If similar data are found in Google Scholar, than system saves the result into database to be processed further in the next step.

For Mendeley, system makes the same query to search related paper information, but in easier way because Mendeley provides PHP API to query the searching result. If similar data are found in Mendeley, than system saves the result into database to be processed further in the next step.

After getting the result, in the next part, system runs similarity checking to compare Google Scholar and Mendeley results with parsed references data from Parscit. Similarity checking is done by comparing the author name and title data between each reference data and then calculating the similarity value using formula 50.1 and 50.2 respectively as used in [6, 7].

$$AS = \sum_n \frac{LS}{LN} \quad (50.1)$$

where:

AS final similarity score of author name between paper and reference data.

LS number of matched characters between author name in paper and reference data.

LN number of total author name characters.

$$Sr = 1 - \frac{\|r1 - r2\|}{\|r1 + r2\|} \quad (50.2)$$

where:

Sr efficiency metric as similarity indicator of title between paper and reference data.

r1 vector of word sequence in paper data.

r2 vector of word sequence in reference data.

After similarity value has been known, system arranges the descending order of related paper data for each reference. This similarity checking process is to make sure that top listed is the most appropriate related paper.



Fig. 50.3 Result of related paper query

As the output as shown in Fig. 50.3, system shows the result in form of web page format. Each reference data of a paper is added with an URL link to download the full text paper from the result of data query above.

## 50.3 Result and Discussion

For testing, we have already trained the Parscit to recognize the English paper optimally using the same writing format with paper that used as a sample for this testing. As the input, we use seed English paper in PDF format and gives the output as shown in Fig. 50.4.

From extraction result above, system can parse the reference data optimally. This reference data than processed further to Mendeley and Google Scholar to search related papers. As the result, system can list the related paper successfully as shown in Fig. 50.5.

**Application of a CC-VSI for Active Filtering and Photovoltaic Energy Conversion with a 1-to-1 MPPT controller**

**AUTHORS**  
Hanny H Tumbelaka, Masafumi Miyatake

**ABSTRACT**  
This paper focuses on the implementation of a three-phase four wire current-controlled Voltage Source Inverter (CC-VSI) as both PV energy extraction and power quality improvement. For power quality improvement, the CC-VSI works as a grid current-controller shunt active power filter. Then, the PV array supported by a Look-up Table type of a MPPT controller is coupled to the DC bus of the CC-VSI. The output of MPPT controller is a DC voltage that determines the DC-bus voltage according to the PV maximum power. The computer simulation results show that the system works properly in steady state and dynamic condition.

**EMAILS**  
tumbelh@petra.ac.id

**AFFILIATION**  
1Department of Electrical Engineering Petra Christian University, Surabaya, Indonesia 2Department of Engineering and Applied Sciences Sophia University, Tokyo, Japan

**KEYWORD**  
active power filter, MPPT, PV energy conversion

**RELATED CONFERENCES**  
[Show Related Conferences](#)

---

**RAW STRING**

- # Borle, L., Zero Average Current Error Control Methods for Bidirectional AC-DC Converters, PhD Thesis, Electrical and Computer Engineering, Curtin University of Technology, Western Australia, 1999.
- # Cheri, Y., and Smedley, K.M., "A Cost-Effective Single-State Inverter with Maximum Power Point Tracking", IEEE Transactions on Power Electronics, 2004, 19(5): p. 1289-1294.
- # Castaner, L., and Silvestre, S., Modelling Photovoltaic System using Pspice, John Wiley & Sons, 2002.
- # Wanzeller, M.G. et.al., "Current Control Loop for Tracking of Maximum Power Point Supplied for Photovoltaic Array", IEEE Transactions on Instrumentation and Measurement, 2004, 53(4): p. 1304-1310.
- # El-Habrouk, M., M.K. Darwish, and P. Mehta, "Active power filters: a review", Electric Power Applications, IEEE Proceedings, 2000. 147(5): p. 403-413.
- # Tumbelaka, H.H., L.J. Borle, and C.V. Nayar. "Analysis of a Series Inductance Implementation on a Three-phase Shunt Active Power Filter for Various Types of Non-linear Loads", Australian Journal of Electrical and Electronics Engineering, Engineers Australia, 2005. 2(3): p. 223-232.
- # Tumbelaka, H.H., L.J. Borle, C.V. Nayar, and S.R.Lee, "A Grid Current-controlling Shunt Active Power Filter", Proceedings of ICPE'07, 2007. Daegu, Korea.
- # Grandi, G., Casadei, D., and Rossi, C., "Direct Coupling of Power Active Filters with Photovoltaic Generation System with Improved MPPT Capability", in IEEE Power Tech Conference, 2003. Bologna, Italy. Application of a CC-VSI for Active Filtering and Photovoltaic Energy Conversion

Fig. 50.4 Result of parsit extraction process

HOME PAPERS AUTHORS CONFERENCES BATCH DOWNLOAD

Sign up Login

**CITATION 1**

TITLE : Zero Average Current Error Control Methods for Bidirectional AC-DC Converters,  
 ABSTRACT : Array  
 AUTHOR : L  
 DATE : 1999  
 PUBLISHER :

[Hide Scholar Result](#)

Zero average current error control methods for bidirectional AC-DC converters  
 Boris, Lawrence Joseph  
 No File Available

Zero average current error controlled power flow for AC-DC power converters  
 Boris, Lawrence J and Nayar, Chemmangot V  
[Click here to download file](#)

A review of three-phase improved power quality AC-DC converters  
 Singh, Bhim and Singh, Brij N and Chandra, Ambrish and Al-Haddad, Kamal and Pandey, Ashish and Kothari, Dwarka P  
[Click here to download file](#)

Unified constant-frequency integration control of active power filters-steady-state and dynamics  
 Smedley, Keyue M and Zhou, Luowei and Qiao, Chongming  
[Click here to download file](#)

Fig. 50.5 List of reference related paper

## 50.4 Conclusion

We have developed a web site learning support for tracing scientific articles relating to a given input seed article. The system finds related articles that are listed on the references of the seed article so that user could track and download the paper easily.

**Acknowledgments** The authors would like to thank the Indonesian Directorate General of Higher Education, which provided the funds for the research project.

## References

1. Hetzner, E.: A simple method for citation metadata extraction using hidden markov models. In: Proceedings of the 8th ACM/IEEE Joint Conference on Digital Libraries JCDL 08, vol. 18, no. 3, pp. 280–284 (2008)
2. Peng, F., McCallum, A.: Information extraction from research papers using conditional random fields. *Inf. Process. Manage.* **42**(4), 963–979 (2006)
3. Councill, I.G., Giles, C.L., Kan, M.: ParsCit: an open-source CRF reference string parsing package. In: Proceedings of LREC '08, pp. 661–667 (2008)
4. Teregowda, P.B., Uргаonkar, B., Giles, C.L.: Citeseerx: a cloud perspective. In: Proceedings of Second USENIX Work, Hot Topic in Cloud Computing (2010)
5. Sutjiadi, R., Lim, R., Wibowo, A., Handojo, A.: Mobile application for accessing paper citation with social network feature. *Adv. Sci. Lett.* **21**(7), 2179–2182 (2015)

6. Li, Y., Bandar, Z., McLean, D., O'Shea, J.: A method for measuring sentence similarity and its application to conversational agents. In: proceedings of FLAIRS Conference (2004)
7. Liliana, L., Lim, R., Kwan, E.: Voice conversion application (VOCAL). In: 2011 International Conference on Uncertainty Reasoning and Knowledge Engineering (URKE), vol. 1, pp. 259–262, IEEE August (2011)



# Chapter 51

## Factors Affecting Edmodo Adoption as Online Learning Medium

Iwa Sungkono Herlambangkoro and Trianggoro Wiradinata

**Abstract** The rapid advancement of internet based social network application has triggered many innovations, one of the most distinguished internet facilitated application in teaching learning is Edmodo. Ciputra University has started the use of Edmodo as the Online Learning Medium where lecturers and students may interact and exchange information regarding class materials. The use of Edmodo has helped increasing effectiveness in lecturers-students interaction, however the adoption remains varied. This study utilizes Technology Acceptance Model (TAM) with several antecedents including Personal Innovativeness, Cognitive Absorption, Perceived Playfulness and Computer Self-Efficacy. The population of this study are second and third year students of Ciputra University, which consisted of 1466 active students, hence the sample size (Confidence Level = 95 %, Margin of Error = 5 %) was determined as 306 students. The result suggests all lecturers who want to use Edmodo to pay more attention to Perceived Playfulness as significant determinant to the adoption of Edmodo for better lecturers-students online interaction.

**Keywords** Edmodo · Online learning · Technology Acceptance Model · Tam

### 51.1 Introduction

The development of Information and Communication Technology (ICT) sector in Indonesia is rapidly increasing, hence the need to improve mechanism of teaching learning utilizing ICT platform becomes inevitable. The advancement of ICT for teaching learning expands classroom beyond the boundaries of space and time. The increasing popularity of internet with web 2.0 features also affects almost every

---

I.S. Herlambangkoro (✉) · T. Wiradinata  
Department of Informatics Engineering, Ciputra University, Surabaya, Indonesia  
e-mail: iwaherlambang@gmail.com

school's teaching learning activities. The main characteristic of Web 2.0 tools is users' active participation in the content of creation process. Advantages of using Web 2.0 in education are creating new interaction styles between instructors and students whilst promoting students interaction outside classrooms [1].

E-learning is an educational system or the concept of using information technology in teaching and learning. E-learning allows students to learn through computers at their favorable places without necessarily having to physically go to follow lessons/lectures in class. Edmodo is a social networking and micro blogging service that is designed specifically for education, which can be operated like any other popular social networking application.

Past studies in e-learning adoption tried to analyze the factors influencing adoption Edmodo as a learning method by using the Technology Acceptance Model (TAM) framework. In this study TAM was chosen as the framework in developing models for Edmodo adoption.

## **51.2 Literature Review**

### ***51.2.1 Edmodo***

Edmodo is a private social platform that provides an online medium for teachers and students to connect and collaborate [1]. It's easy to apply to the class because its appearance is similar to Facebook, subsequently many students are familiar with it. Using Edmodo, Teachers and students may exchange notes, links, files, announcements, tasks, collecting pool, creating quizzes and exchange information in a secure environment [2].

### ***51.2.2 Technology Acceptance Model (TAM)***

Technology Acceptance Model (TAM) was first developed by Davis [3, 4] and then redeveloped in many later studies [5, 6]. More subsequent studies still prefer the use of TAM compared to other frameworks because of its simplicity.

TAM has the goal to explain and predict the user acceptance of the technology. TAM is the development Theory of Reasoned Action [7]. TAM predicts user acceptance of a particular technology based on the influence of two factors, namely the perceived usefulness and perceived ease of use [4].

### ***51.2.3 Variables Operationalization***

Kumar et al. [8] defines cognitive absorption as "someone deeply involved with the software". Cognitive Absorption were translated into five latent variables consist of

Temporal Dissociation, Focused Immersion, Heightened Enjoyment, Control, and Curiosity.

Agarwal and Prasad [9] defines Personal Innovativeness as the degree of willingness of an individual to try out new Information Technology application. Someone willingness to experiment with new technologies, possibility of someone to get something more than they knew before. The general term Personal Innovativeness also refers to how a person chooses and tries out new technologies.

Computer Playfulness shows the level of cognitive spontaneity in its interaction with the computer [10, 11]. The basic concept of computer playfulness is heading to the users propensity to explore and act spontaneously by the computer.

Self-efficacy is a person’s belief in his ability to organize and select the ways that can be taken to achieve goals [12]. A person with high self-efficacy will have the confidence that he is able to face the challenge and see a difficulty as a challenge that needs to be addressed, not as a threat to be avoided [12]. Self-efficacy affects a person’s thinking, feeling, motivate themselves and behave.

Davis [4] defines perceived ease of use as a level in which a person believes that a particular technology can easily be used as a mean to solve particular problem. Perceived Usefulness as the degree someone believes a particular technology is useful to help completing particular tasks. Intention to Use is the behavioral tendency to use a particular technology. The level of use of a computer technology on a person can be predicted from both perceived usefulness and perceived ease of use.

From the defined variables operationalization above, a research model was constructed and modified with the addition of external variables as shown in Fig. 51.1 below.

Figure 51.1 above shows the proposed theoretical model that can be used to analyze factors influencing the Intention to Use Edmodo as online learning medium. Relationships shown as arrows among variables in Fig. 51.1 will become hypotheses. Table 51.1 below lists the relationships among variables.

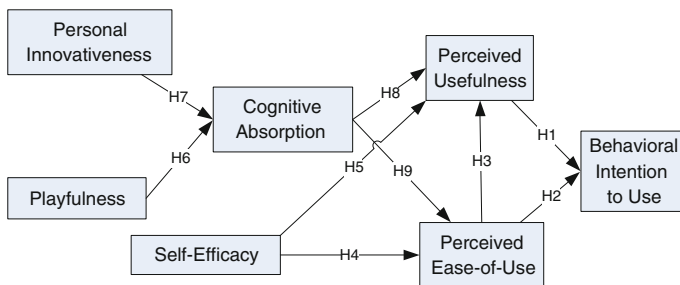


Fig. 51.1 Proposed theoretical model

**Table 51.1** Research hypotheses

Research hypotheses
H <sub>1</sub> : Perceived usefulness has a significant positive direct effect on behavioral intention to use
H <sub>2</sub> : Perceived ease of use has a significant positive direct effect on behavioral intention to use
H <sub>3</sub> : Perceived ease of use has a significant positive direct effect on perceived usefulness
H <sub>4</sub> : Self-efficacy has a significant positive direct effect on perceived ease of use
H <sub>5</sub> : Self-efficacy has a significant positive direct effect on perceived usefulness
H <sub>6</sub> : Playfulness has a significant positive direct effect on cognitive absorption
H <sub>7</sub> : Personal innovativeness has a significant positive direct effect on cognitive absorption
H <sub>8</sub> : Cognitive absorption has a significant positive direct effect on perceived usefulness
H <sub>9</sub> : Cognitive absorption has a significant positive direct effect on perceived ease of use

## 51.3 Research Method

### 51.3.1 Population and Sample

The population in this study were second and third year students of the Ciputra University. The number of total students are 1466 active students. The sampling technique for this studies will be using stratified random sampling which is a sampling technique applied to a population that has strata or levels and each level has its own characteristics. With the above known population hence the sample size in this study is determined to be 306 respondents [13].

### 51.3.2 Measurement Instrument

This study's data collection method uses online questionnaire as well as printed form with the same survey questions. Measurement data from the results of the questionnaire using five scaled Likert scale. Likert Scale used to measure attitudes, opinions, and perceptions of a person or a group of social phenomenon. In this scale, the respondents expressed approval and disapproval of a number of statements related to the variables being measured.

### ***51.3.3 Testing of Measurement Instrument***

Validity is demonstrating the extent to which a measuring instrument capable of measuring what you want to measure. Validity test is a step tests performed on the contents of an instrument, with the aim to measure the accuracy of the instruments used in a study. Validity test is done by calculating the correlation between the score of the response variable response with a total score of a variable called Pearson tolerance test. Value tolerance significance Pearson correlation coefficient is  $\alpha = 5\%$  or 0.05.

Reliability is to determine the consistency of the measurement results. In determining the reliability of the study, researchers used Cronbach alpha coefficient. This test is done to measure whether the proposed questionnaire is reliable or not. A variable is said to be reliable, if it gives the value of Cronbach alpha coefficient  $\geq 0.70$  [14].

Path analysis will be measured using AMOS statistical software, wherein the path diagram test performed after validity, reliability, and test assumptions. After the path diagram test fulfilled, the last test conducted was a model fit test [15]. This test assesses the fitness of a model in this study. There are nine criteria tested including Chi-Square, normed Chi-Square, RMR, GFI, AGFI, NFI, IFI, CFI and RMSEA.

## **51.4 Result**

### ***51.4.1 Demography of Respondents***

Profile of respondents were analyzed using descriptive statistics: frequency and percentage. Total survey form collected were 340, among the survey responds 39 were found incomplete or invalid, hence the total respondents with complete data were now 301 respondents, 145 respondents were male (48%), and 156 respondents were female (51%). Number of second and third year students is equal.

### ***51.4.2 Path Analysis and Fit Test***

Path analysis were conducted using AMOS software. This diagram as shown in Fig. 51.2 is used to help conceptualization problems and to determine the direct and indirect effect of independent and intermediary variables to the dependent variable (ITU).

Regression weights in Table 51.2 shows the effect PEOU to ITU as insignificant at the 0.63 can be considered the relationship of these pathways discarded.

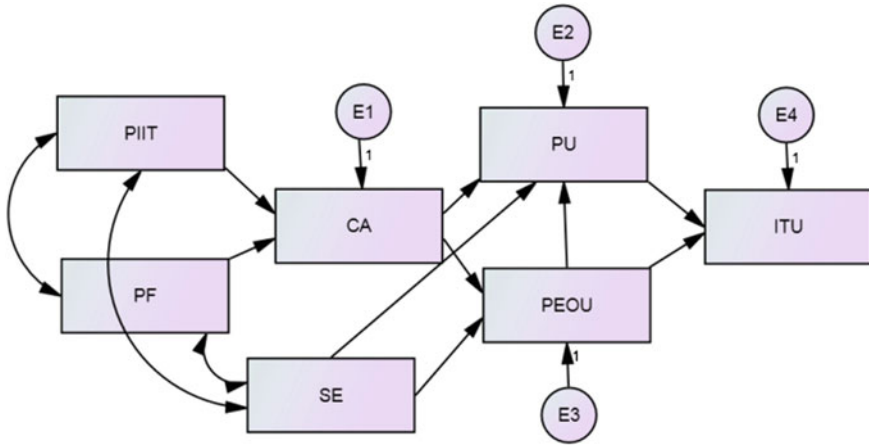


Fig. 51.2 Path diagram model

Table 51.2 Regression weight

Regression weights: (Group number 1—Default model)					
	Estimate	S.E.	C.R.	P	Label
CA ← PIIT	0.161	0.036	4.462	***	
CA ← PF	0.254	0.035	7.274	***	
PEOU ← SE	0.447	0.039	11.405	***	
PEOU ← CA	0.123	0.058	2.121	0.034	
PU ← PEOU	0.419	0.049	8.516	***	
PU ← CA	0.292	0.05	5.884	***	
PU ← SE	0.324	0.04	8.107	***	
ITU ← PU	0.494	0.075	6.56	***	
ITU ← PEOU	-0.039	0.08	-0.481	<b>0.63</b>	

Figure 51.3 above shows additional 4 direct relationship, namely PIIT towards PEOU, PF towards ITU, SE towards CA, and CA towards ITU. There is also a second reduction, namely a direct relationship PEOU toward CA and PIIT towards CA from the proposed theoretical model. After the modification, the modified model fulfills the fitness criteria as seen in the Table 51.3 below.

### 51.4.3 Final Model Analysis

The total effect of other factors consist of the direct effects and indirect effects. Tables 51.4 and 51.5 below contain summary of the total effect and the number of standardized total effects.

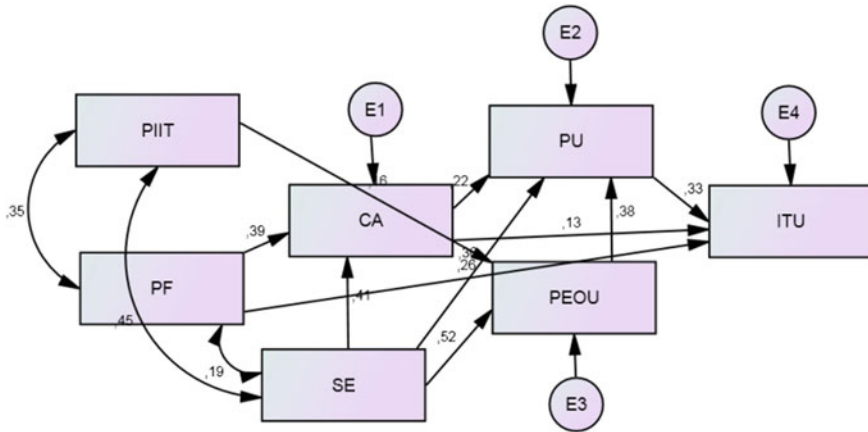


Fig. 51.3 Path diagram model after modification

Table 51.3 Goodness-of-Fit result

Model fit	Fit criteria	Result
Chi Square	$p > 0.05$	0.187
Normed Chi Square	$< 3$	1.409
RMR (Root Mean Square Residual)	Close to 0	0.012
GFI (Goodness of Fit index)	$> 0.90$	0.989
AGFI (Adjusted GFI)		0.963
NFI (Normal Fit Index)	$> 0.90$	0.986
IFI (Incremental Fit Index)		0.996
CFI (Comparative Fit Index)		0.996
RMSEA (Root Mean Square Error of Approximation)	$< 0.05$	0.037

Table 51.4 Total effects

Total effects (Group number 1—Default model)						
	PF	PIIT	SE	CA	PEOU	PU
CA	0.259	0	0.276	0	0	0
PEOU	0	0.131	0.428	0	0	0
PU	0.075	0.055	0.584	0.292	0.419	0
ITU	0.318	0.019	0.257	0.292	0.147	0.351

From the results of the above table shows the effect of data contained in each variable. From these results concluded that the variables that have the greatest influence on the variable ITU is variable Playfulness. Playfulness shown greatest significant positive effect at 0.318 (with medium magnitude) towards the Behavioral Intention to Use.

**Table 51.5** Standardized total effects

Standardized total effects (Group number 1—Default model)						
	PF	PIIT	SE	CA	PEOU	PU
CA	0.391	0	0.406	0	0	0
PEOU	0	0.157	0.516	0	0	0
PU	0.085	0.06	0.643	0.218	0.383	0
ITU	0.336	0.02	0.265	0.205	0.126	0.328

### 51.4.4 Practical Implications

The study results can be used as policy guidance when formulating strategies in the adoption of Edmodo which is paying bigger attention to improving the Perceived Playfulness by the users. Some efforts may include implementing gamification which influences the perception of users from learning to playing.

## 51.5 Conclusion

In this study, exogenous variables which has the greatest effect on Intention to Use Edmodo is Playfulness, however this study assumes the general use of Edmodo as common online learning medium without paying close attention to which features of Edmodo attracts its users the most. Subsequent study may explore more on those areas. Perceived Playfulness generates biggest effect to students intention to use Edmodo application. The influence was 0.318 with medium magnitude, hence the strategy to increase the adoption is to create more playful online interaction (e.g.: creating missions, milestones, etc.)

## References

1. Thongmak, M.: Adopting Edmodo to enhance classroom collaboration: Thailand Case. In: The 21st international business information management association conference, pp. 17–29. (2013)
2. Wankel, C.: Teaching Arts and Science with the New Social Media. Emerald, Bingley (2011)
3. Davis, F.D.: A technology acceptance model for empirically testing new end-user information systems theory and result, Massachusetts Institute of Technology (1986)
4. Davis, F.D.: Perceived usefulness, perceived ease of use, and user acceptance of information technology. *MIS Q.*, 319–340 (1989)
5. Igbaria, M., Iivari, J.: The effects of self-efficacy on computer usage. *Int. J. Manag. Sci.* **23**(6), 587–605 (1995)
6. Venkatesh, V., Davis, F.D.: A theoretical extension of the technology acceptance model: four longitudinal field studies. *Manage. Sci.* **46**(2), 186–204 (2000)



7. Fishbein, M., Ajzen, I.: Understanding attitudes and predicting social behavior. Prentice-Hall, Englewood Cliffs (1980)
8. Kumar, V.K., Pekala, R.J., Cummings, J.: Trait factors, state effects, and hypnotizability. *Int. J. Clin. Exp. Hypn.* **44**(3), 232–249 (1996)
9. Agarwal, R., Prasad, J.: A Conceptual and Operational Definition of Personal Innovativeness in the Domain of Information Technology. *Inf. Syst. Res.* **9**(2), 204–215 (1998)
10. Agarwal, R., Karahanna, E.: Time flies when you're having fun: cognitive absorption and beliefs about information technology usage. *MIS Q.* **24**(4), 665–694 (2000)
11. Webster, J., Martocchio, J.J.: The differential effects of software training previews on training outcomes. *J. Manag.* **21**(4), 757–787 (1995)
12. Bandura, A.: Self-efficacy: toward a unifying theory of behavioral change. *Psychol. Rev.* **84**(2), 191–215 (1977)
13. Krejcie, R.V., Morgan, D.W.: Determining sample size for research activities. *Educ. Psychol. Meas.* **30**, 607–610 (1970)
14. George, D., Mallery, P.: *Spss for Windows Step by Step: A Simple Guide and Reference*. Allyn and Bacon, Boston (2003)
15. Kline, R.B.: *Principles and Practice of Structural Equation Modeling*, 2nd edn. The Guilford Press, New York (2005)

# Chapter 52

## Principal Feature Selection Impact for Internet Traffic Classification Using Naïve Bayes

Adi Suryaputra Paramita

**Abstract** One of the important roles for internet traffic classification is feature selection method. This method will present more accurate data and more accurate internet traffic classification which will provide precise information for bandwidth optimization. One of the important considerations in the feature selection method that should be looked into is how to choose the right features which can deliver better and more precise results for the classification process. This research will investigate how to select the principal and discriminant feature. We plan to use Principal Component Analysis (PCA) technique in order to find discriminant and principal feature for internet traffic classification. This research will try to combine PCA with another feature selection algorithm. The feature selection algorithm is Correlation Feature Selection (CFS). The Correlation Feature Selection (CFS) is used in the feature selection to find a collection of the best sub-sets data from the existing data where the Internet traffic has the same correlation that could fit into the same class. Internet traffic dataset will be collected, formatted, classified and analyzed using Naïve Bayesian. Moreover, this paper also studied the process to fit the features. The result also shows that the internet traffic classification using Naïve Bayesian and PCA has improvement for the classification accuracy. The most significant result of this result is the combination between PCA and CFS for feature selection improved internet traffic classification accuracy more than 10 %.

**Keywords** Principal · Feature · Internet · Classification · Accuracy

---

A.S. Paramita (✉)  
University of Ciputra, UC Town Citraland Surabaya, Indonesia  
e-mail: adi.suryaputra@ciputra.ac.id

© Springer Science+Business Media Singapore 2016  
F. Pasila et al. (eds.), *Proceedings of Second International Conference  
on Electrical Systems, Technology and Information 2015 (ICESTI 2015)*,  
Lecture Notes in Electrical Engineering 365, DOI 10.1007/978-981-287-988-2\_52

## 52.1 Introduction

The objectives of internet traffic classification researches is to improve the internet traffic classification accuracy and execution time. In the past, internet traffic classification research method can be classified into port-based method, payload-based or heuristic protocol, behavior analysis-based and statistical data based methods. Due to the development of the application of flexible port, the research method has left the port-based and payload-based to focus on more intelligent methods in order to utilize the available bandwidth. Several researches can be mentioned such as Machine Learning (ML) Algorithms [1], Classification using The Self Organizing Map Algorithm (SOM) developed by Monash University which introduces clustering mechanism based on the volume of internet bandwidth usage [2].

The feature selection is applied to classify the generated data. Part of the data members may have the same features. Although the feature selection method could give better performance for the detection of the use of the Internet but the traffic still has modest complexity. The use of the Internet traffic for database and games (which are vulnerable to worms and viruses) are not taken into account [3].

Significant research in feature selection for Machine Learning is done by Zhao Jing-jing, Huang Xiao-hong in 2008. The result clearly explains that feature selection is the most important step in ML. Good feature does not only improve the accuracy of algorithms but also improve the computational performance [4]. Gu reported that there still need more work to find the features that are suitable and appropriate to improve the accuracy of classification internet traffic [5].

This paper will investigate how principal feature selection impact for internet traffic classification and try to combine principal feature selection with another feature selection algorithms. This research used Principal Component Analysis technique in order to find discriminant and principal feature for internet traffic classification. Moreover, this paper also studied the process to fit the features and combine it with PCA for improving accuracy from internet traffic classification. Formerly, the Correlation Feature Selection (CFS) is used in the feature selection to find a collection of the best sub-sets data from the existing data but failed to find the discriminant and principal of a body dataset. In previous research this model already implemented with 1 dataset, and now this model will implement with other 4 Moore set internet traffic datasets [6].

## 52.2 Research Methodology

The objective of this research is to investigate the discriminant feature selection technique and the combination between discriminant feature selection and traditional feature selection impact for Naïve Bayesian internet traffic classification. The block diagram of the research methodology is shown in Fig. 52.1. The third and fourth block (blue ones) indicate the main contribution of the work.

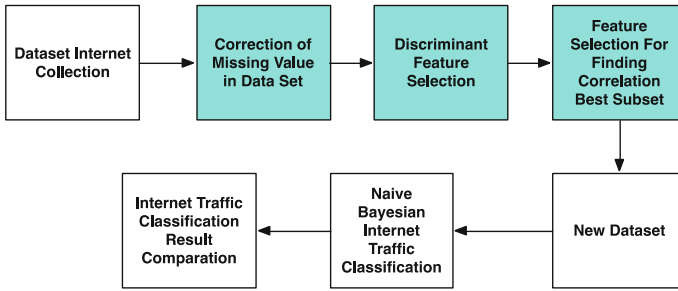


Fig. 52.1 Research methodology

## 52.3 Principal Component Analysis

Esbensen, in explained that the main component analysis (PCA) is a multivariate data analysis method mostly used for exploratory analysis of data, outlier detection, rank (dimension) reduction, graphical clustering, classification, and regression. The proper understanding of PCA is a prerequisite for the controlling other latent variable methods, including Principal Component Analysis regression, multivariate calibration and classification, it will lead to a deeper understanding which one of individual variables is possible [7]. PCA mostly used as the first data analysis conducted on multivariate data sets, although further data analysis with other methods even more advanced one may be required.

## 52.4 Correlation Feature Selection

Correlation-based Feature Selection (CFS) is a heuristic evaluation that takes into account the benefit of individual features for predicting the class along with the level of inter-correlation between them. CFS puts a high score as a subset of data that contains features that highly correlated with the inter-class but have a low correlation with each other [8]. CFS evaluates a subset of attribute values by considering the individual predictive ability of each feature data and the level of redundancy.

## 52.5 Experimental

The first phase in this research is collecting internet traffic dataset. The Moore set internet traffic dataset which has been used in previous research, is collected from <http://www.cl.cam.ac.uk/research/srg/netos/nprobe/data/papers/sigmetrics/>. In previous research only dataset 10 used for experiment [9], but in this research will use

**Table 52.1** Number of instance in dataset

	Dataset 9	Dataset 8	Dataset 5	Dataset 3	Dataset 10
Number of instance	66248	55494	21648	22392	65036

dataset 9, dataset 8, dataset 5, dataset 4. The next phase after collecting data is to find the discriminant features in the Internet traffic dataset. The Principal Component Analysis (PCA) are applied to find discriminant feature. Correlation Feature Selection (CFS) are applied to find the feature which have strong correlation with another feature. After the good features in the dataset has been obtained, the next process is to classify the Internet traffic dataset using Naïve Bayesian.

The number of instance in the dataset used in this research quite varied, Table 52.1 show summary of number of instance in each dataset used.

## 52.6 Result and Discussion

The experimental result of this research is shown in Tables 52.2, 52.3 and 52.4. These results show that the selection of the discriminant features using Principal Component Analysis (PCA) will significantly increase the accuracy of classification. The Combination between Principal Component Analysis (PCA) and Correlation Feature Selection (CFS) have contribution to increasing the percentage of true positive rate, but unfortunately this combination decrease the class precision in some data.

**Table 52.2** Internet traffic classification accuracy result

Dataset	No feature selection (%)	PCA (%)	PCA + CFS (%)
Dataset 10	56.1074	75.6212	83.5629
Dataset 9	67.4451	78.9669	85.7249
Dataset 8	58.3505	83.4811	89.9593
Dataset 5	78.2868	90.5072	91.2047
Dataset 3	84.454	89.9093	92.2466

**Table 52.3** True positive rate summary

Dataset	No feature selection (%)	PCA (%)	PCA + CFS (%)
Dataset 10	56.1	75.6	83.6
Dataset 9	67.4	79	85.7
Dataset 8	58.4	83.5	90
Dataset 5	79.3	90.5	91.2
Dataset 3	84.5	89.9	92.2

**Table 52.4** Average class precision summary

Dataset	No feature selection (%)	PCA (%)	PCA + CFS (%)
Dataset 10	97.1	92.8	92.1
Dataset 9	96.1	90.2	89.4
Dataset 8	98.1	93.9	93.3
Dataset 5	96.7	92.9	92.4
Dataset 3	98.2	93.2	93.1

Table 52.2 shown that Discriminant Feature Selection has significantly improving the internet traffic classification accuracy, the accuracy is improved more than 10 %. Correlation Feature Selection (CFS) has main contribution for improving True Positive (TP) rate in internet traffic classification result as shown in Table 52.3. Table 52.4 shown that discriminant feature selection and feature selection decreasing the class precision, it's probably because of PCA reduce feature which have significant contribution for dataset or CFS only select feature which have strongly correlation with another feature.

## 52.7 Conclusion

Discriminant Feature selection using Principal Component Analysis (PCA) and feature selection using Correlation Feature Selection (CFS) in this research has shown significant impact for improving internet traffic classification using Naïve Bayesian. The most significant result from discriminant feature selection is shown in the classification accuracy. PCA improves the classification accuracy more than 10 %. Meanwhile CFS improves True Positive (TP) rate in classification result. This research conclude that PCA is the best solution for discriminant feature selection. CFS can be one of the best alternatives for figuring out the subset in dataset. Future work suggested is to investigate how to improving class precision using discriminant feature selection and another feature selection.

## References

1. Mohd, A.B.: Towards a flow-based internet traffic classification for bandwidth optimization. *Int. J. Comput. Sci. Secur.* **3**(2), 146–153 (2009)
2. Wang, X., Abraham, A., Smith, K.: Intelligent web traffic mining and analysis. *J. Netw. Comput. Appl.* **28**(2), 147–165 (2005). doi:[10.1016/j.jnca.2004.01.006](https://doi.org/10.1016/j.jnca.2004.01.006)
3. Nguyen, T., Armitage, G.: A survey of techniques for internet traffic classification using machine learning. *IEEE Commun. Surv. Tutor.* **10**(4), 56–76 (2008)
4. Zhao, J., Huang, X., Sun, Q., Ma, Y.: Real-time feature selection in traffic classification. *J. China Univ. Posts Telecom-mun.* **15**, 68–72 (2008). doi:[10.1016/S1005-8885\(08\)60158-2](https://doi.org/10.1016/S1005-8885(08)60158-2)

5. Gu, C., Zhang, S., Xue, X.: Internet traffic classification based on fuzzy kernel K-means clustering. *Int. J. Adv. Comput. Technol.* **3**(3), 199–209 (2011). doi:[10.4156/ijact.vol3](https://doi.org/10.4156/ijact.vol3)
6. Moore, A., Zuev, D., Crogan, M.: Discriminators for use in flow based classification, (2005)
7. Esbensen, K.H.: *Principal Component Analysis: Concept, Geometrical Interpretation, Mathematical Background, Algorithms, History, Practice*. Elsevier (2009)
8. Zhao, J., Huang, X., Sun, Q., Ma, Y.: Real-time feature selection in traffic classification. *J. China Univ. Posts Telecom-mun.* **15**, 68–72 (2008). doi:[10.1016/S1005-8885\(08\)60158-2](https://doi.org/10.1016/S1005-8885(08)60158-2)
9. Antonio, T., Paramita, A.S.: Feature selection technique impact for internet traffic classification using naïve bayesian. *Jurnal Teknologi* **20**, 85–88 (2014)

# Chapter 53

## Study on the Public Sector Information (PSI) Service Model for Science and Technology Domain in South Korea

Yong Ho Lee

**Abstract** National level policies for information sharing have been suggested many times and it is the time to set up the system for public data sharing. Especially, Ministry of Science, ICT and Future Planning (MSIP) in South Korea has accumulated a big data collection from R&D results and it is necessary to find a way out to make use of it in a profitable way. Governments in every country take notice of the value created by using public data and deploy various policies to make them more accessible and easy, finally, to upgrade them as an information service industry. This study is focused on the analysis of public data status and suggests a roadmap to open 800 databases which count for the main contribution of the study.

**Keywords** Information service · Information sharing · Open data · Public sector information · Re-use of public sector information

### 53.1 Introduction

Open data movement is a great deal of excitement around the world for its potential to empower citizens, and businesses, to change government's performance, and to improve the delivery of public services [1, 2]. Recently, attention of major stakeholders in the open data community, including governments and businesses has shifted to the economic value of open data assets. Public sector information(PSI) is considered an important asset that has social and economic value. Hence, developed countries are competitively promoting various policies to actively promote access to public sector information and the use of such information for private purposes [3]. The Korean government is also boosting the Government 3.0 policy as a new governmental management paradigm that supports the creative economy. To do

---

Y.H. Lee (✉)

Department of Policy Research, Korea Institute of Science and Technology Information, 335 Gwahangno, Yuseong, Daejeon 305-806, Republic of Korea  
e-mail: stylee@kisti.re.kr



that, public bodies are by far the largest producers of information in Korea. In other words, the role of public agencies in creating, elaborating and releasing information would be very important for open data movement. In spite of increasing interest in open data, there is little agreement on how it should be opened properly and timely on behalf of users.

PSI is public sector information. It means the information is generated, created, collected, processed, preserved, maintained, disseminated, or funded by or for the government or public institution [4].

In this study, the concept of data from the user's perspective for the activation of private applications was defined by focusing on public sector information obtained by affiliated organizations of the Ministry of Science, ICT and Future Planning (MSIP). The new classification scheme and strategic approach on how data are opened has been suggested, and then we will focus our effort on the particular service model according to users' need.

## **53.2 Research Framework**

### ***53.2.1 Data Status***

See (Table 53.1)

### ***53.2.2 Classification Scheme***

We sort by these DB using suggesting classification scheme. The scheme is comprised of information management and exploitation perspectives (Table 53.2).

## **53.3 PSI Service Roadmap**

### ***53.3.1 Information Service Model for PSI***

There are 3 ways of information service. First, general information centers provide data all over the category in national level. In history, general information centers were founded and then specialized service centers were founded over time. Nowadays, clearing house concept is generally accepted when an agency provides information service. It guides proper information sources about know-where and know-who in addition to information itself.

**Table 53.1** DB status of public agencies in Korea (2013)

	Information characteristics					Sum
	Management	ICT/S&T related Info.	R&D Operational Info.	R&D Info.	Misc.	
Government ministry	9	5	74	1	0	89
Quasi-governmental institutions	2	3	0	0	0	5
Fund mgt. based	45	74	0	0	0	119
Commissioned-service-based	9	10	25	5	0	49
Mission—ICT facilitating	9	10	25	5	0	49
Mission—science culture facilitating	9	0	0	0	0	9
Misc.	185	2	12	57	0	256
Non-classified public institution	41	9	31	57	0	138
R&D mgt. agency	63	1	0	9	62	135
Misc.	363	104	142	129	62	800
Sum	45.4	13.0	17.8	16.1	7.8	100
Proportion						

**Table 53.2** Suggesting PSI classification scheme

7 Areas	21 Detailed fields	Concept
Health/Medical Services	Medicine	Information related to health, medical services, medicine, medical devices, cosmetics, Korea medicine, disease diagnosis, treatment and prevention
	Food	Information related to agro-fishery products, livestock products and to distribution, classification, securement of safe food products
Safety/Welfare	Addiction prevention	Information related to games, medias, mobile environment, violence, drugs and matters related to well-being of national mental health
	Public security/National security	Information related to public order and national security from crimes, war and any exterior threats (also includes the information regarding inter-Korean relations)
	Disaster response	Educational information to prevent disaster, fire and disaster preventive information to deal with any disasters
	Social welfare/Resolution of social class differences	Information related to welfare improvements for disabled persons, regional libraries, women, children, elderly and multi-cultural families
Environment/Energy	Environment protection/Preservation	Information related air, water, land pollutions, environmental protection and preservation
	Energy	Information related to the maintenance and securement of existing energy sources as well as next generation energy sources such as solar energy, hydrogen energy and etc.
	Ecosystem/Resource	Information on forests, marine environment, ecosystems and various life resources
	Earth observation	Information related to global detection and observatory activities for the sun, wind, rotation/revolution of the earth
Living Convenience/Culture	Household living information	Information closely connected to people's life such as public law, politics, tax, weather and etc.
	Culture/Travel/Sports	Information related to cultural life and those that make people's living more rich such as travels, history, cultural art, sports, religion and etc.
	Residential environment/Transportation and Traffic	Information related to national residential and traffic (distributional) environments

(continued)

**Table 53.2** (continued)

7 Areas	21 Detailed fields	Concept
Science Business/Job	Education/Finding Jobs	Information related to education and job opportunities (young adults, elderly job market) for all ages
	Business management/Establishment	Information related to intellectual properties, industries, finance and labor which are crucial elements of business establishment/management
	Support for science technology/Information on industrialization	Information related to technology transfer, industrialization, equipment research and development, external financing of the resources necessary for businesses
R&D/ICT	Science technology general information	Information on basic sciences, bio, nuclear energy, space engineering, nanoscience, information technology and various science technologies
	Information and communications infrastructures	Information related to broadcasting communications infrastructures
Public Administration	International cooperation/Global relations	Information related to international exchanges and cooperative activities between public/private entities
	National statistics/Index	Statistical information for figuring out national issues
	Public corporation information	Information related to policies, internal information of the institutions and records

### 53.3.2 Analysis Results

We developed service roadmap in consideration with open readiness and users' demand of the respective DB. A survey to identify demand of database was made on 800 DB according to suggesting classification scheme. Open readiness of DB was identified by public agencies respectively.

Judgmental criteria of DB open readiness as shown on Table 53.3.

We identified the willing to exploit database by two steps. During survey, users select categories first belong to DBs, then select specific DB. As results, we seized 168 databases belong to high exploiting expectation categories and high exploiting expectation DB at the same time(as shown in Table 53.4).

**Table 53.3** Judgmental criteria of DB open readiness

Open data level	Open	Open partially	Not allowed to open
Readiness level	High		Low

**Table 53.4** Evaluation results of DB open readiness and demand survey

Willing to exploit DB	High	Medium		Low
Number of DB	HH	HL	LH	LL
	168	108	287	237

*Notes* HH: DB belongs to category and DB ranks above median response value, HL: DB belongs to category above median response value and to DB below median response value

## 53.4 Conclusions

In spite of increasing interest in open data [5, 6], There is little agreement on how it should open properly and timely on behalf of users in the national level. In this study, we suggested a classification scheme to facilitate data exploitation and identification of users' demand by survey. The results, we identified 800 DBs in the public sector under the control of MSIP and match making DBs to the open readiness and demand. From this analysis, we explored the role of public agencies in their open data movement, and also identified the barriers to the movement. This research supports the concept of open service roadmap in the national level. Nevertheless, future research is still needed to improve our current understanding of PSI service roadmap. We identified several possibilities of facilitating open data business by matching information service model and open data roadmap but not verified it quantitatively.

## References

1. Conradie, P., Choenni, S.: On the barriers for local government releasing open data. *Gov. Inf. Q.* **31**, S10–S17 June (2014)
2. Janssen, K.: The influence of the PSI directive on open government data: An overview of recent developments. *Gov. Inf. Q.* **28**(4), 446–456 (2011)
3. Huijboom, N., Van Den Broek, T.: Open data: an international comparison of strategies. *Eur. J. ePractice* **12**(1), 4–16 (2011)
4. Davies, T.: Open data, democracy and public sector reform. A look at open government data use, data.gov.uk (2010)
5. Zuiderwijk, A., et al.: Open data disclosure and use: Critical factors from a case study. In: *CeDEM15: Conference for E-Democracy and Open Government*, p. 197, MV-Verlag (2015)
6. Zuiderwijk, A., et al.: Open data policies, their implementation and impact: A framework for comparison. *Gov. Inf. Q.* **31**(1), 17–29, Januari (2014)

# Chapter 54

## Digital Natives: Its Characteristics and Challenge to the Library Service Quality

Siana Halim, Felecia, Ingrid, Dian Wulandari and Demmy Kasih

**Abstract** Digital natives which always connect to the world through their gadgets have special needs for gathering information. Do libraries which in the past can be said as the sources of information can satisfy their needs? What should libraries do, so that they can answer those needs? Those queries are the prominent questions to be answered in this paper. In this paper we describe the digital natives' characteristics when they use their PC and gadgets. The data were collected from 460 university students in Surabaya. We also measure the library service quality (LibQual) for five university libraries in Surabaya. Moreover, using K-means, we also clustered the respondents into two groups, i.e., the first group is the ones who attach to their gadgets, and the second group is the ones who do not attach to their gadgets. For the first group the library online information and for the second group, the operational service are the most important factors for measuring the LibQual.

**Keywords** Digital native · LibQual · Clustering · K-means · Structural equation modeling

### 54.1 Introduction

Digital native or net generation is a generation which was born after 1994. Marc Prensky [1] defines the digital native as the young generation that “native” in the language of computers, videos, videos games, social media and other sites on the

---

S. Halim (✉) · Felecia · D. Kasih  
Industrial Engineering Department, Petra Christian University, Surabaya, Indonesia  
e-mail: halim@petra.ac.id

Ingrid  
Business Management Department, Petra Christian University, Surabaya, Indonesia

D. Wulandari  
Petra Christian University Library, Surabaya, Indonesia

internet. The digital natives have their own ways to gain the information. They connected to the world through their gadgets. Oblinger and Oblinger [2] states that the digital natives are digital literate, connected, immediate, experiential, prolific communicators (social), work in a team, their preference is for structure rather than ambiguity, oriented toward making observations, visual and kinesthetic, take part in the community activities. Digital natives are nontraditional learners [2].

Library as a collection of sources of information, archives and databases faces a new challenging to be existed in the digital era. The Digital natives recognize that library is very important, but internet promises ease and fast access. Search engine overcomes library in term of reliability, cost effectiveness, easiness to use, comfort and speed (de Rosa et al. [3]).

Lippincot [4] reported that by the end of the year 2005, the University of Southern California's Library has been visited for more than 1.4 million visitors. From 2009 to 2012, the physical visitors of the Petra Christian University (PCU) library were decreasing. In 2009 the rate of the visitor is 431 persons per day but in 2012 it becomes 384 persons per day [5]. In this recent year, the physical visitors of PCU library is increasing but the number of borrowed books is decreasing. Widjaja and Halim [6] reported that the easiness to access the web gives positive effects to the PCU students to visit the library, but the PCU library collections do not give positive effect for the students to visit the library. However, the digital PCU library is accessed for more than 6.7 million visitors per year [7]. This fact shows that library is still important for students, but it has to be developed to satisfy the digital natives' needs.

## 54.2 Methods

Answering the query which is explained in the introduction, we adapt the Library Service Quality (LibsQual [8]) for the digital natives' nature. There are six factors that measure the LibsQual, i.e., personal control, information access, library as place, affect of service (personal), affect of service (organizational) and interest to visit library (see Fig. 54.1). For each factors, there are several indicators for measuring them. To simplify the indicators for each factors, we applied the factor analysis technique (Sharma [9]) before measuring the LibQual models using structural equation modeling (Hair et al. [10]).

This model is applied to two groups of respondents, i.e., digital natives who attach to their gadgets and who do not attach to their gadgets. Those two groups were obtained via clustering analysis method, i.e., k-means [9]. We then applied the results of those groups to get the characteristics of each group.

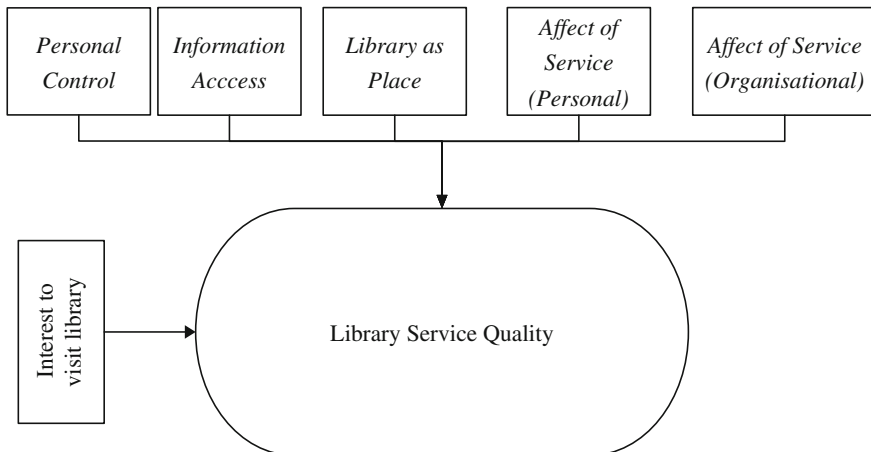


Fig. 54.1 Library service quality model

### 54.2.1 Data

The data were collected from 460 university students which studies in five universities in Surabaya. Those five universities are InstitutTeknologi Sepuluh Nopember Surabaya (ITS), Universitas Pembangunan Nasional-Veteran (UPN), Universitas Kristen Petra (UKP), Universitas Surabaya (UBAYA), Universitas Widya Mandala (UWM).

The respondents for each universities are 92 (20 %) from ITS, 48 (10.4 %) from UPN, 186 (40.4 %) from UKP, 87 (18.9 %) from UBAYA, 47 (10.3 %) from UWM. The proportion of respondents from each university is depend on the size of the library. ITS and UPN are state universities, while UKP, UBAYA and UWM are private universities.

## 54.3 Results and Discussion

### 54.3.1 The Digital Native Characteristics

Most of the respondents are listening to music (24 %), searching information using web (23 %), playing games (13 %) and writing documents (13 %) as their most frequent activities when the use their PC (see Fig. 54.2). Similarly, they use their gadgets frequently are for instant messaging or chatting (13 %), emailing (11 %), phone (10 %), searching information using internet (10 %), sending photos or videos (10 %) see Fig. 54.3 for the detail.

Applying the k-means with 2 classes, i.e., digital natives who attach to their gadgets (Cluster 1) and who do not attach to their gadgets (Cluster 2), the



**Fig. 54.2** The frequency of using computer

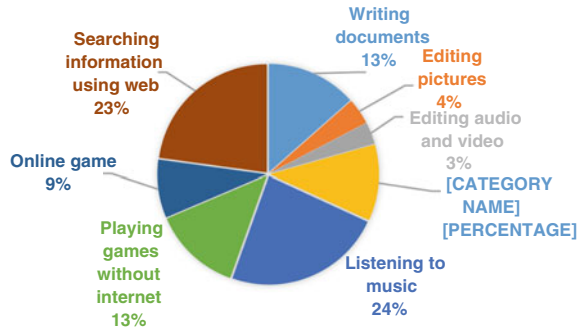


**Fig. 54.3** The frequency of using gadget

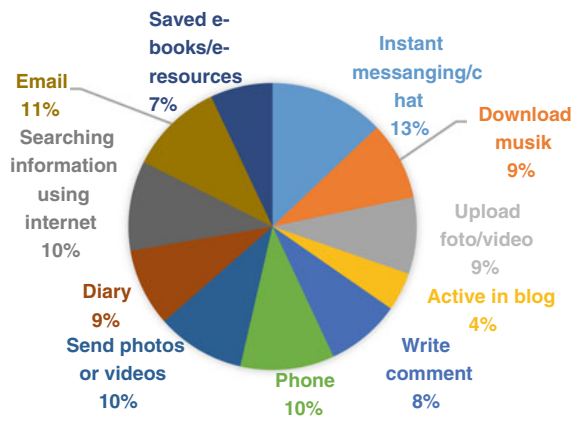


Table 54.1 shows the average of their several activities using their gadgets. It can be clearly seen that those two clusters is very distinct in the ability to use some apps. Digital natives which attach to their gadgets are the one who are powerful in using the apps in their gadgets. The apps here are including instant messaging/chatting (e.g. BBM, WhatsApp, Line, etc.), downloading music, uploading photos/videos (Instagram, path), Blogging, Social Media, Phone, Writing diary, searching information through internet access, emailing, saving ebooks/e-resources.

There are several variables used in this research for measuring the library service quality. There are eight variables for measuring the personal control, eleven for information access, and twelve for library as place, fourteen for personal affect of service, twelve for organizational affect of service and four for the external factors. Those original variables are then simplified using factor analysis to form a new ones. The new and the original variables are summarized in Table 54.2. Using the new variables, we then constructed the model.

Figures 54.4 and 54.5 show the result of SEM model for the digital native who attach and who do not attach to their gadgets consecutively. For both clusters the external factor do not contribute to the LibQuality. The external factors measures four factors, i.e., the willingness to visit the library deliberately, library has special

**Table 54.1** The average of several activities using gadgets for Cluster 1 and Cluster 2

Cluster	Readingebooks	Buying books	Downloading ebooks	Amount of gadgets on hand	Frequency of using gadgets	Ability to use gadgets	Number of social media	Frequency of using some apps	Ability to use some apps
1	1.81	0.78	1.36	5.20	2.55	3.60	1.95	6.20	8.82
2	1.48	0.57	0.87	4.86	2.03	1.52	1.64	5.60	1.55

**Table 54.2** The new and the original variables used for the model

Factor	New variabel	The original variables
Personal control	PCNEW1: Website and online catalog	PC1, PC2, PC3, PC4, PC5
	PCNEW2: Library online information	PC6, PC7, PC8
Information access	IANEW1: Online and non-online collection	IA1, IA2, IA3, IA4, IA5, IA6, IA9, IA10, IA11
Library as place affect of service (Personal)	IANEW2: Variabel of library info.	IA7, IA8
	LPNEW: Library as place	LP1–LP12
	ASPNEW1: The library’s staff skill	ASP4, ASP5, ASP6, ASP7, ASP8, ASP9, ASP10, ASP11, ASP12, ASP13
Affect of service (Organisational)	ASPNEW2: Hospitality	ASP1, ASP2, ASP3, ASP14
	ASONEW1: Operational service	ASO1, ASO2, ASO3, ASO5, ASO6, ASO8, ASO9, ASO10
External factors	ASONEW2: Library programs	ASO4, ASO7, ASO11, ASO12
	MBNEW1	MB1, MB2, MB3, MB4

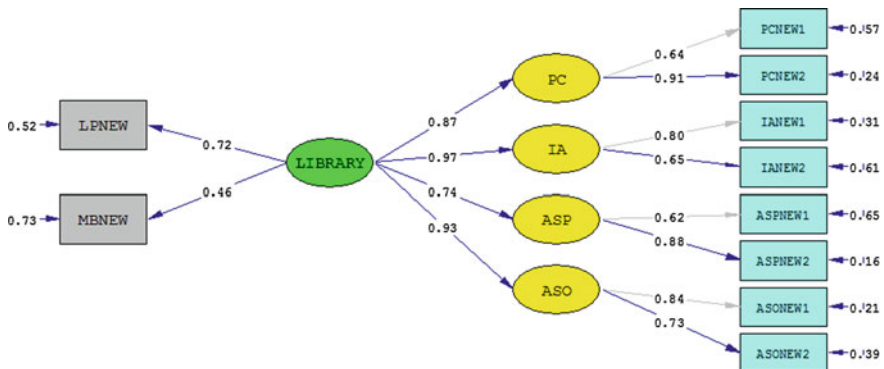


**Fig. 54.4** The SEM for the digital native who attach to their gadgets (Cluster 1)

interest to be visited, library escalates the academics competency, I go to the library without planning in advanced. This means that even the library itself has good quality in term of others measurement (personal control, information access, aspect of personal, aspect of organizational and library as a place) but without the external factors of the visitors, i.e., the library customer, the library will be empty.

For the digital native who attach to their gadgets (Cluster 1), the information access is the most important factors in the library quality. Additionally the library

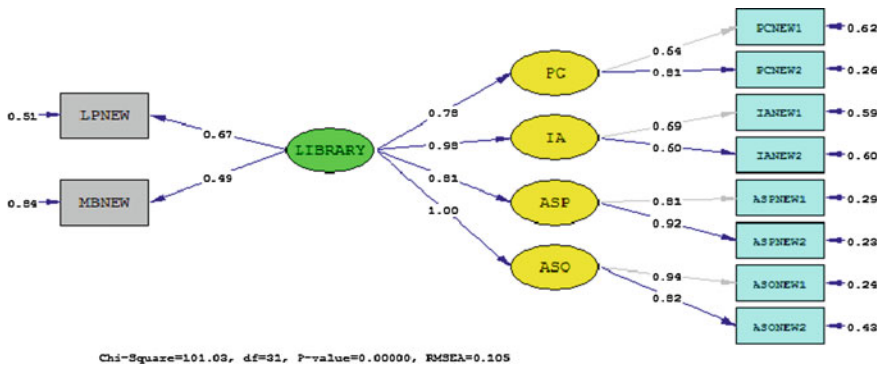


Fig. 54.5 The SEM for the digital native who do not attach to their gadgets (Cluster 2)

Table 54.3 The goodness of fit test

Model	Goodness of fit	Result	Cut off	Explanation
Digital native who attach to their gadgets	GFI	0.89	≥0.9	Acceptable
	AGFI	0.80	≥0.9	Acceptable
Digital native who do not attach to their gadgets	GFI	0.91	≥0.9	Acceptable
	AGFI	0.84	≥0.9	Acceptable

online information (PCNEW2) are the most influencing indicator for personal control. The PCNEW2 includes the easiness to access the library collection, the library collections suitable with my needs, the availability of online resources that can meet my needs. For the digital native who do not attach to their gadget (Cluster 2), operational service are the most important factors and the ASONEW1 is the most influencing indicator for them. The ASONEW1 includes the appropriateness and the punctuality in giving service. For both model the goodness of fit of the model is acceptable (see Table 54.3).

### 54.4 Conclusion

In this research the characteristics of the digital natives especially in their habit in using pc and gadgets has been explored. There are two types of digital natives, the ones who attach to their gadgets (Cluster 1) and who do not attach to their gadgets (Cluster 2). For the Group1 the library online information and for the Group2, the operational service is the most important factors for measuring the LibQuality. The library has to be innovated such that the external factors that affect the willingness the customers to visit the library will be increased.

**Acknowledgements** The authors are very grateful to the Indonesian Directorate of Higher Education (DIKTI) which give the financial support for this research.

## References

1. Prensky, M.: Digital natives, digital immigrants. *Horizon* **9**(5), 1–6 (2001)
2. Oblinger, D.G., Oblinger, J.L.: Is it age or IT: first steps toward understanding the net generation in educating the net generation. <http://www.educause.edu/educatingthenetgen/>
3. de Rosa: College Students' Perception of Libraries and Information Resources: A report to the OCLC membership. Retrieved from: <http://www.oclc.org/content/dam/oclc/reports/pdfs/studentperceptions.pdf>
4. Lippincot, J.K.: Net generation and libraries, in educating the net generation. <http://www.educause.edu/educatingthenetgen/>
5. Wulandari, D., Halim, S., Nugraha, A.: Analisa Faktor-faktor yang Mempengaruhi Minat Berkunjung Mahasiswa ke Perpustakaan UK. Petra Surabaya, Research Report, LPPM-UK, Petra (2012)
6. Widjaja, J., Halim, S.: Faktor—faktor yang mempengaruhi minat berkunjung mahasiswa ke perpustakaan universitas Kristen Petra. *Jurnal Titra* **2**(1), 1–5 (2014)
7. Wulandari, D.: Mengembangkan Perpustakaan Sejalan dengan Kebutuhan Net Generation: Surabaya, Research Report. Petra Christian University Library (2011)
8. LibQual: Society of college, national and university libraries (Sconul). <http://vamp.diglib.shrivenham.cranfield.ac.uk/quality/libqual> (2012)
9. Sharma, S.: *Applied Multivariate Techniques*. Wiley, New York (1996)
10. Hair, J.F., Thomas, G., Hult, M., Ringle, C., Sarstedt, M.: *A Primer on Partial Least Squares Structural Equation Modeling*. Sage Publication, California (2014)

# Chapter 55

## Web-Based Design of the Regional Health Service System in Bogor Regency

B. Sundari, Revida Iriana and Bertilia Lina Kusrina

**Abstract** The health service process for the middle and lower classes of people is organized by the local regional government. The health service process in Bogor has been implemented by utilizing the electric media. However, in the area of Bogor Regency it has not been fully integrated in terms of the data processing of patients and medicines, medical records and the report making. It can be seen when the patients are still requested to bring the administrative requirements in a different form. Based on this fact, it is necessary to design an Online-based Regional Health Service Information. This research objective is to provide a design of the health service information system. The method used is a field study (observation) by interviewing and SDLC (*System Development Life Cycle*) approaching. The pattern of SDLC approaching consists of several stages: planning, data analysis, designing data base by using the language of UML (Unified Modeling Language), and coding. The final stage is the implementation of a test. The final stage of this research is a prototype of the web-based health service information system, so that it will help the administrative staff when processing the health service in terms of preparing referral letters and even up to a recapitulation.

**Keywords** Design · Information systems · Health services · On-line

### 55.1 Introduction

The advance of the information technology is currently developed rapidly and it can be seen from the use of the computer technology in the various fields of life; one of them is in the field of health. The development has opened a big opportunity for the

---

B. Sundari · B.L. Kusrina (✉)  
Accounting Department Faculty of Economics, University Gunadarma, Depok, Indonesia  
e-mail: lkusrina@staff.gunadarma.ac.id

R. Iriana  
Information Systems, Faculty of Computer Science, University Gunadarma,  
Depok, Indonesia

processing, accessing, and using the information on a large scale by utilizing the electronic media. The use of the electronic media is a very important factor in every field, especially in the field of health, so that it is necessary to have a good arrangement and guidance in the implementation of the electronic media. The documenting and guiding are currently being conducted by the Bogor City Health Department, through the use of the electronic media is very helpful and encouraging for Bogor City towards the information society.

Based on the above description, it is necessary to design an integrated health service that helps the work process to be more effectively, and efficiently, and to provide the service of data and information to all related parties. There are two important things that resulted from the development of information systems [1]. The first one is the increasing in respondents' perceptions of the information system before it was developed, and the second one is to improve the quality of information produced. Both can be used to overcome the problems of the patient monitoring health financing for poor families.

Related to health care information systems, research [2] tried to design a system of outpatient registration information at health centers with a case study on the current health centers and procurement. The designed system can handle multiple processes so that patient registration, changes of the medical records and reports generation can be made automatically. System designed to help the process of service to the visitor of the community health center is a concern.

Health care information system is also used to reduce or minimize the loss of patient data. This information system, the health center will be facilitated in the processing of medical records of patients so as to minimize the error if medical records are needed or sought [3].

In a small scope, [4] tried to make the design of the school health care information system. With case studies Vocational School of Putra Telkom Sandhy Jakarta, design of the system put emphasis on record keeping, medical examination and drug use. Design of the system can generate information systems that can help the process of recording, medical examination and drug use on school health services.

The information system has been created, focused on web-based medical record that is devoted to the general hospital in Pacitan. This system is simply integrated with related units in general hospitals in Pacitan [5, 6].

This article outlines the analysis and development of the health care system design Bogor regency Online. Health care information systems in the area of web-based Bogor regency. Method for making system in this study using the approach pattern SDLC (System Development Life Cycle), which consists of several stages [7], namely data analysis, planning/designing databases using language UML (Unified Modeling Language), and coding as well as the implementation phase to do trial [8, 9].

Integrated data processing of the start of registration, health care, payment and reporting both financial and medical record became the focus of research. Ease of how the system works by the user is also a major consideration the development of

this system. The designed system is expected to help facilitate the process of health care for both patients and health care workers.

## 55.2 The Research Methods

Research was done with field observations and interviews. Data are collected and analyzed by qualitative descriptive method, by comparing the field data with database programming concepts and theories. The design of the system is done by using some patterns approaches [10]:

- a. Technical Approach, an approach which was conducted in the structured and patterned ways to conduct the activities starting from the levels of preparation, data collection, data processing, data designing, analyses, up to the level of development. The approach was conducted to generate the complete data that could be accessed rapidly, precisely and accurately when constructing the Application of Regional Health Service System in Bogor Regency.
- b. Client-Server Approach, a model of computerization where a client's application was run on a desktop computer or a private computer to access the information available in the server or in the host somewhere else, while the server provided the centralized process working in a multi-user way.
- c. Server-Side Programming Approach, a scripting technology or a web programming where the script (Program) was compiled or translated in the server.

All the above activities could be optimally implemented which referred to the SDLC (*System Development Life Cycle*) approach [10, 11]. The approach was conducted to synchronize the setting-up activity of the Application of the Regional Health Service (Fig. 55.1).

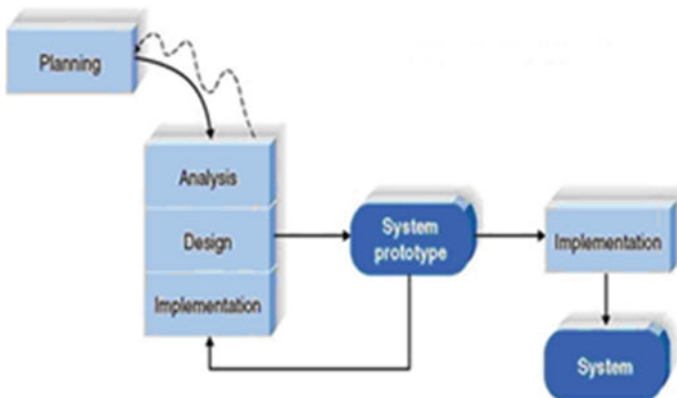


**Fig. 55.1** Flow of a prototype model of health service system application



### 55.3 Results and Discussion

The result is a prototype of Jamkesda Information System Web-Based Health Care. This application uses two functions:

- a. Functions for Admin (backend) to change the master data into the data support for Front End assigned to the administrator who then change affects the data can be displayed again by the frontend. The application starts with the appearance of the main page in the form of welcome, and a subsequent display the login page. On this page admin and user/attendant required to enter a username and password with a user or admin staff. Admin first page contains information that this page can only be accessed by administrators who receive priority access rights. This page contains a menu veranda, staff, setup, history and logout. On the menu there is a menu Staff added that is used to add the following new staff as the priority level of user access. While the Setup menu there is a menu of options Participants, Regional, Insurance, Rates, Claims, disease.  
In the setup menu the participants are localized pages for entering data Jamkesda participants. Also provided menu to upload Jamkesda participants if the number of participants Jamkesda too much or built a database that is possible only import data from an existing database (prepare data in Excel format, and can be directly uploaded). Page setup menu Regional, Insurance, consists of two columns that is the first column (left) to add and edit the region, while the second column (right) to filter or search areas that have been registered in the system which is equipped with a menu edit and delete data.
- b. Functionality for Users/user/attendant (Front End) to display all transaction data can be inputted by the user and displays all the information needs of the user. Front End Application is an application made for the recording of transaction data per operating day. Application allows users to make additions, changes and deletion of data and reporting. Form view UPT Jamkesda Bogor Regency frontend together with backend applications such as the following. Users can access the Cheque Guarantee (Member), with images like the one above. For column above (Cheque Guarantee) data will be filled in automatically.  
Consolidation menu is used to enter the file list of the claims of the KDP, using the *xls*. file as a data raw. This application is also a menu consisting of a Verification Report Claims per PPK, claims by hospitals and health centers.

These study has some result in common with [3, 4, 6], namely the application of health care information system-based desktop and web [12] (Figs. 55.2 and 55.3).

Information Systems Applications in previous studies applied to certain hospitals or health centers, but not yet integrated inter-related parts. In this study, a prototype Regional Health Service Information System has been connected with the related units include Public Health Centers, General Hospital, and the Regional Health Department.



Fig. 55.2 The display of claims



Fig. 55.3 Claims by hospitals and health centers

In addition, this prototype providing health services ranging from patient registration to make the required report. Reports generated in the form of a referral, the report claims, as well as check guarantee limit every patient.

## 55.4 Conclusions and Suggestions

Implementation of Information Systems Jamkesda used to process the registration of patients, old and new, to reduce and eliminate duplication of patient data, and reporting and the making of the relevant document or in accordance with the needs of the part that requires online.

The urgency of further research are modules for printing electronic patient card, the reservation and the choice of the patient and the room rates, menus schedule doctor and smart phone applications. So the anticipation time, ease of patient access and service performance management Hospital Bogor regency would be optimal.

## References

1. Jogiyanto, H.M.: Analisis dan Desain (Sistem Informasi: Pendekatan Terstruktur Teori dan Praktek Aplikasi Bisnis). Penerbit Andi, Yogyakarta (2005)
2. Solikhin, R.E., Rachmatullah, R.: Rancang Bangun Sistem Informasi Registrasi Pasien Rawat Jalan Pada Puskesmas (Studi Kasus Puskesmas Sekaran dan Pegandan). HIMSYATECH **9**(1), (2013)
3. Puspitasari, Y., Purnama, B.E.: Sukadi, Sistem Informasi Rekam Medis Pasien Rawat Jalan dan Observasi Pada Puskesmas Pringkuku Kabupaten Pacitan. Indonesian Journal of Network Security (IJNS) (2012)
4. Ferdiansyah, F., Subhan, A.A., Nurmaida, D.: Rancang Bangun Sistem Informasi Pelayanan Kesehatan Dengan Metodologi Berorientasi Obyek: Studi Kasus Smk Telkom Sandhy Putra Jakarta. In: Seminar Nasional Teknologi dan Komunikasi Terapan (SEMANTIK), Semarang 23 Juni (2012)
5. Susilowati, S., Kusuma, B., Riasti, R.: Pembuatan Sistem Informasi Klinik Rawat Inap Prima Husada Widoro Pacitan Berbasis Website. Indonesian, Jurnal on Computer Science-Speed (IJCSS), **9**(2), Agustus (2012)
6. Susanto Gunawan, Sukadi: Sistem Informasi Rekam Medis Pada Rumah Sakit Umum Daerah (RSUD) Pacitan Berbasis Web-Base. Indonesian Jurnal on Computer Science Speed (IJCSS), **9**(3), Desember (2012)
7. Pressman, Roger, S.: Rekayasa Perangkat Lunak (Pendekatan Praktis). Andi, Yogyakarta (2002)
8. Martin, F.: UML Distilled: A Brief Guide to the Standard Object Modeling Language, 3rd edn. Addison-Wesley (2003)
9. Munawar, Pemodelan: Visual dengan UML. Yogyakarta, Graha Ilmu (2005)
10. Rudyanto, A.M.: Pemrograman Web Dinamis Menggunakan PHP dan MySQL. Andi, Yogyakarta (2011)
11. Kay, R.: Das GIMP 2.8, Buch Orelly (2013)
12. Smith, P.: Professional Website Performance: Optimizing the Front-End and Back-End. Wiley, Indianapolis (2012)

# Chapter 56

## Security Handwritten Documents Using Inner Product

Syaifudin and Dian Pratiwi

**Abstract** Recently, it is common to find document forgery both in the private and government agencies. This research was conducted with the aim of designing a software system that can recognize hand writing by using computer technology from the digitization process of a written form. The method applied in this study consisted of several stages, namely the writing stage analog to digital conversion, pre-processing, segmentation, feature extraction writing and calculating the percentage of similarity algorithms written by Inner product. From the results of this study, it is expected that the system is able to recognize any handwriting owners of various writing forms, as well as to take into account the percentage of similarity to one another. This system can also be used to protect the owner against counterfeiting handwriting, as an authenticity tool for any form of writing in important documents.

**Keywords** The process of digitization • Segmentation • Feature extraction • Pattern recognition • The inner product

### 56.1 Introduction

Information technology is currently growing very rapidly, it is answering the demands of human needs both direct and indirect use. Computer technology is part of the information technology are no longer strangers and almost every individual is able to use it in everyday life, such as the use of a notebook or laptop. These advances also have an impact on developments in device software, such as the handwriting recognition device.

Handwriting recognition tool has been applied in a handheld device or mobile phone-based touch-screen. In term of functionality, the device is generally used

---

Syaifudin (✉) · D. Pratiwi  
Trisakti University, Jakarta, Indonesia  
e-mail: fudin178@gmail.com

only as a reader or readers from the user's handwriting on the screen to recognize the meaning of the sentence. Handwriting recognition function can then be developed further to identify the owner of the handwriting as a results of analyzing shapes or patterns in it. Handwriting patterns can be known through a series of image processing and feature extraction of texts that will produce features or special characteristics that can be used to identify each owner's handwriting. Pattern recognition using the Euclidean distance formula is sometimes less accurate [1].

In this study, we would use Methods Results In time because this method is more rigorous [2]. With the software's handwriting recognition, we are not only able to identify the owner of the handwritten pattern, but also using it as a protection system, such as in securing important documents from counterfeiting writings. The system is maintained through the input of writing patterns. The benefits of this research is providing assistance in differentiating forensic handwriting of each owner of an important document that requires authentication process, so that the crime of falsification of documents can be prevented.

## 56.2 Literature

Several theories are used to carry out this research, namely Pre-processing, Establishment of ROI (Region of Interest), feature extraction, pattern recognition, pattern recognition and success calculations, inner product.

### 56.2.1 *Pre-processing*

Experience in research on face recognition system, with great training for personal identification, usually achieves good accuracy. Ramesha et al. [3] proposes Facial Feature Extraction based on gender and age classification, with only a little training, the resulting algorithm can produce good results even with one image per person. This process involves three stages: Pre-processing, feature extraction and classification. Facial image geometric features such as eyes, nose, mouth etc. are located by using the operator Canny edge and face recognition is performed. Based on the texture and shape information, gender and age classification is done by using the Class Posteriori Probability and each of Artificial Neural Network. It is observed that facial recognition is 100 %, the classification of the sex and age of approximately 98 and 94 % respectively.

Here are the results of research experience gradations of an apple based single features such as size, shape or color. Research from Xianfeng and Weixing [4] proposed a multi-information fusion method based feature BP (back propagation) neural network and DS theory to improve the accuracy of grading apples. The first is the size, shape and color features extracted from images of apples. Secondly, apples are classified by each type of feature by BP network classification and

independent evidence. The output of the classifiers are combined to establish a basic probability assignment. Finally, using the DS fusion rules of evidence to make decisions and achieve the final gradation. The experimental results show that the decision information fusion method based on size, shape or color features have performed well in comparison with methods based on a single feature in the grading of apples.

Pre-processing is an early stage that needs to be done to get the post data in digital form with the size of the pixel and gray level values or the same gray level of a set of handwritten analog that has been digitized by means of a digitizer or scanner. This stage consists of conversion of RGB color to greyscale and thresholding.

### 56.2.1.1 Conversion RGB Color to Grayscale

RGB color conversion to greyscale is the stage for 24-bit color values to 8 bits, so the size of the resulting color will be smaller with the interval between 0 and 255 [5].

$$RGB = \frac{R + G + B}{3}$$

Where R is a red color pixel values, the pixel values of the color green is G, and B is a blue color pixel values (Fig. 56.1).

### 56.2.1.2 Thresholding

Thresholding is a process to separate the object region (foreground) to the background area (background) through a certain threshold value [6]. In this study, threshold or threshold value is also determined by trial and error.

## 56.2.2 Establishment of ROI or Gridding

Formation of ROI (Region of Interest) is a technique that is commonly performed to assist the analysis of the object to be observed, such as the fMRI image analysis

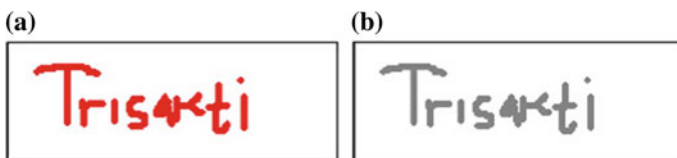


**Fig. 56.1** Digital image handwriting **a** The image is 24 bits. **b** The image size of 8 bits

conducted by researchers from the UCLA-Los Angeles, Poldrack [7]. This technique can improve the success on stage introduction, since the formation of ROI, feature extraction process to be performed is limited to a specific region or area that has been restricted [7].

### 56.2.3 Extraction Feature

Extraction characteristics is an important stage of the application of pattern recognition. This stage will give results in the form of values of the features to be measured or recognized as a pattern. With the extraction of features or traits, important information of the data (which in this study is in the form of image data) will be taken and stored in the feature vector or vector characteristics [6]. Features that can be extracted in the form of image data including color features, shapes, and textures, can be seen in Fig. 56.2. And in this study, which will be extracted feature is based on the representation of handwritten form. The values of the feature extraction forms-based handwriting will be binary values (value '0' or '1') to each grid for each image, where the value of '0' will be given if the representation of the grid is a background object, and value '1' if the foreground object representation of the grid is at least 15 % of the total pixels of each grid is a foreground object [8] (Fig. 56.3).

The picture above is an example image with a division-sized  $4 \times 8$  grid, where the results of the representation of the extracted shape 11100000 11111000 01111110 01111111 [8].

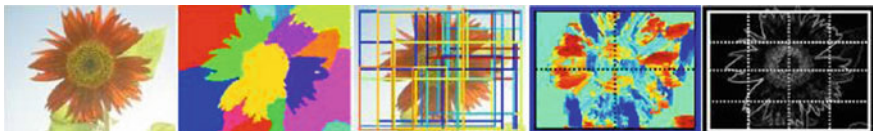
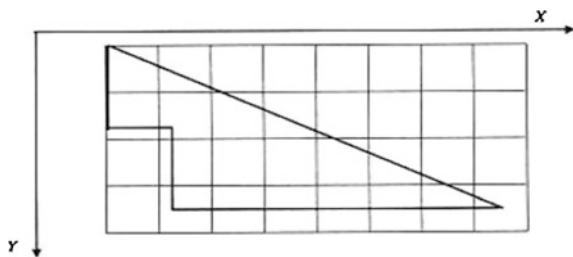


Fig. 56.2 Example of extraction through ROI [5]

Fig. 56.3 Example of images with a  $4 \times 8$  Grid Size [9]



### 56.2.4 *Pattern Recognition*

Pattern recognition is one of the techniques of the science of artificial intelligence or artificial intelligence (AI), which aims to recognize the features or specific characteristics of a set of data (both text and image documents) and classify them [9]. Pattern recognition can be done in several ways, one of which is by using the method of Similarity Measures.

Similarity measures is a method that can be used to look for similarities from one object to another, by calculating the distance among them [1]. As in the research conducted by Huang [1], this study also used the technique similarity measures in recognizing handwriting patterns by calculating the distance between the patterns by using the formula of the Euclidean distance formula [1].

$$d(u, v) = \left[ (u_1 - v_1)^2 + (u_2 - v_2)^2 + \dots + (u_n - v_n)^2 \right]^{1/2}$$

By using the Euclidean distance where  $d$  is the distance between the total value of the image pixel handwriting with each other,  $u$  and  $v$  are pixels image.

### 56.2.5 *Calculation of Percentage of Success of Pattern Recognition*

This stage is the final stage, where each image handwriting tested will be the level of success of its introduction. The formula used is:

$[(\text{total image that is recognizable handwriting}) / (\text{Total overall image of handwritten tested})] \times 100 \%$

### 56.2.6 *Inner Product*

If  $V$  is an inner product space, then the norm (length) vector  $u$  expressed by  $|u|$  defined by  $|u| = \langle u, u \rangle^{1/2} = (a_1u_1^2 + a_2u_2^2 + \dots + a_nu_n^2)^{1/2}$  and the distance between two vectors  $u$  and  $v$  is expressed by  $d(u, v)$  is defined by  $d(u, v) = |u - v| = \left[ a_1(u_1 - v_1)^2 + a_2(u_2 - v_2)^2 + \dots + a_n(u_n - v_n)^2 \right]^{1/2}$  where  $a_1, a_2, a_3, \dots, a_n$  is its weight.

There are several implementations of inner product including:

- a. Results of times a method used in the encryption. This method was introduced by Agrawal [10]. At first the traditional encryption result is very rough. By using the results once the encryption is very smooth results



- b. Inner product method used in color appearance models. Shape appearance model can be applied to solve several different problems. Successful program to this day is a medical image analysis and facial images. Early work only on the model form. This work was later expanded so that the model appearance (i.e. color image). By using the results of times in the model of appearance (color) which make the independent calculation of the size of the image, so the image looks good [2].
- c. Inner product used on Bayesian Network. Bayesian networks have become one of the main models used for statistical inference. Bayesian networks can be represented in an inner product space dimension. Focus on the classification label Boolean domain. As a main result we establish upper and lower bounds on the dimensions of the inner product for Bayesian networks with a collection of parameters. Bayesian networks and shows that each product space expressive dimension must have at least enough  $\Omega(n^2)$ , where  $n$  is the number of network nodes. As a major contribution, and this work reveals a combination of algebraic structures in the Bayesian network that known method for the derivation of lower limit on the dimensions of the inner product space can be brought into the role [11].

From previous research experience of the inner product can be used for encryption, the model appearance (color) and the use of the Bayesian network. With a wide range of interests, the inner product can produce better research.

## 56.3 Methods

In this study, the research methods to be implemented consist of several stages:

### 56.3.1 Data Collection Techniques

Collecting data in this study will be done through direct searches of a set of handwriting from a number of sources. Handwriting will be passed through the instrument digitizer or scanner, which will then generate digital data in the form of handwriting shaped JPEG image.

### 56.3.2 Location of Research

Handwriting data is captured in offices and Universities in the School of Jakarta. This study is planned to be held at the University of Trisakti namely in building E3 and 8th floor space lecturer/researcher, Faculty of Industrial Technology Department of Informatics.

### 56.3.3 Research Design

In this study, the research design can be described as follows: In the early stage, every handwriting that has been collected digitized by digitizer or scanner. Digitization results are then resized so that each image digitized handwriting result will have the same size, that is  $400 \times 1000$  pixels, as in Fig. 56.4.

The whole image of the digital handwriting and performed pre-processing, the phase change of the RGB color image into greyscale, and phase separation of the object from the background of his writing through thresholding method. The original color values in the image interval will be changed to 0–255 with a size of 8 bits. While the thresholding stage, the background pixels will be grouped with a value of 255 (white), and the object of writing pixels will be grouped with interval values between 128 and 255.

After the pre-processing phase is complete, each region of the image goes into gridding process or forming grids. Each image with  $400 \times 1000$  pixels will be divided into grids with each grid's size of  $100 \times 100$  pixels. The results of the gridding process is shown in Fig. 56.5. This would give a total of  $4 \times 10$  grids for each image of handwriting.

Each grid of each image will then go into handwriting feature based form extraction process, where each pixel of the grid will be analyzed by the rules:



Fig. 56.4 Example of handwriting digital image size  $400 \times 1000$  pixels

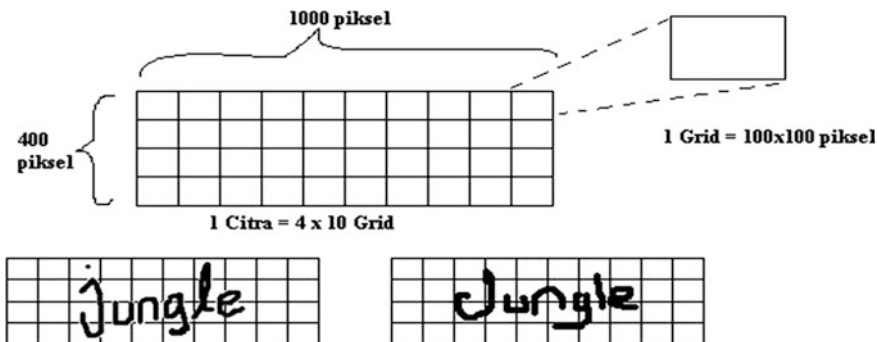
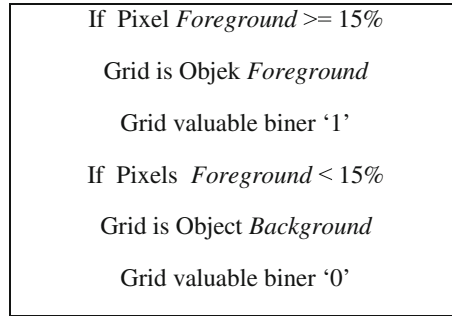


Fig. 56.5 Formation of grid or ROI (*Region of Interest*)



## 56.4 Proposed Model of Handwriting Recognition

After the feature extraction phase is complete, the pattern recognition process is carried out through the method of similarity measures, by calculating the distance of each pixel's binary difference on the image you wish to identify in the handwriting.

According to Netzell and Solem [2] who studied that using the product will produce better result. Besides, the picture is more convergent and calculation of time depends on the model image. Inner product formula can be written with weights  $a_1, a_2, \dots, a_n$  as follows:

$$\langle u, v \rangle = a_1 \cdot u_1 \cdot v_1 + a_2 \cdot u_2 \cdot v_2 + \dots + a_n \cdot u_n \cdot v_n$$

And the distance  $u$  to  $v$  is  $d(u, v) = |u - v| = \left[ a_1(u_1 - v_1)^2 + a_2(u_2 - v_2)^2 + \dots + a_n(u_n - v_n)^2 \right]^{1/2}$

From previous experience of various researches, it is important to examine security in the form of a handwritten document by using the results of times. If the distance is obtained from the smaller handwriting, the handwriting is increasingly matching or similar. The percentage of success rate of recognition results in this study can then be calculated by comparing the total number of images that successfully recognized the handwriting on the total image of handwritten tested.

## 56.5 Conclusion

We conclude that the method of inner product will give more accurate and clearer results. With the presence of weight, the distances become larger but if the distance is very low, nothing change. It is suggested that to get a more accurate result, it is better to use a lot of data, at least 100, such that the system can create zoom feature.

## References

1. Huang, A.: Similarity measures for text document clustering. In: New Zealand Computer Science Research Student Conference, Christchurch, New Zealand (2008)
2. Netzell, K., Solem, J.E.: Efficient image inner products applied to active appearance models, pp. 4244–2175. IEEE (2008)
3. Ramesha, K., Raja, K.B., Venugopal, K.R., Patnaik, L.M.: Feature extraction based face recognition, gender and age classification. *Int. J. Comput. Sci. Eng.* **02**(1S), 14–23 (2010)
4. Xianfeng, L., Weixing, Z.: Apple grading method based on features fusion of size, shape and color. *Procedia Eng.* **15**, 2885–2891 (2011)
5. Pratiwi, D.: The use of self organizing map method and feature selection in image database classification system. *Int. J. Comput. Sci. Issues (IJCSI)* **9**(3), 2 (2012)
6. Pratiwi, D., Santika, D.D., Pardamean, B.: An application of backpropagation artificial neural network method for measuring the severity of Osteoarthritis. *Int. J. Eng. Technol. (IJET-IJENS)* **11**, 3 (2011)
7. Poldrack, R.A.: Region of interest analysis for fMRI. *Oxford J.* **2**(1), 67–70 (2007). Los Angeles, USA
8. Lu, G.: *Multimedia Database Management Systems*. Artech House Inc., Norwood (1999)
9. Absultanny, Y.A.: Pattern recognition using multilayer neural genetic algorithm. *Neurocomputing* **51**, 237–247 (2003)
10. Agrawal, S., Freeman, D.M., Vaikuntanathan, V.: Functional encryption for inner product predicates from learning with errors. In: Lee, D.H., Wang, X. (eds.) *Advances in Cryptology—ASIACRYPT 2011*. LNCS, vol. 7073. Springer, Heidelberg (2011). Cryptology ePrint Report
11. Nakamura, A.: Inner product spaces for bayesian networks. *J. Mach. Learn. Res.* **6**, 1383–1403 (2005)

# Chapter 57

## Augmented Reality Technique for Climate Change Mitigation

Ruswandi Tahrir

**Abstract** The increasing number of people will relate with the amount of gas emissions into the air which concentrated in the green house and increases earth temperature, later known as *global warming*, which resulted the anomalous of weather and precipitation called as *climate change*. Drought and flood which happened has led to a huge losses treasures and soul and Indonesia as one of a gas emissions contributor called global warming due to deforestation and forest fires often happened. One of the best research related with the early warning system for fire management, used satellite data NOAA and MODIS has produced a series of climates, fires, indicators biophysic, precipitation, *IRI Climate and Fire Resources Room* and predicting fires activity. Based on rapid assessment, the problem of this early warning system for fire management was intended only for certain community likes college course. To make this research more useful for the community it must be easily understood, and *Augmented Reality* technology is expected to deal with this problem. This technology excellences can visualize the analysis of the early warning system easier to be understood, such as to utilize the *on line Data Library*. With a sound understanding about climate change and appropriate technology, the *mitigation* will be done well.

**Keywords** Climate change • Resources room • Data library • Augmented reality • Mitigation

---

R. Tahrir (✉)  
Gunadarma University, Depok 16591, Indonesia  
e-mail: ruswandi@staff.gunadarma.ac.id

## 57.1 Introduction

Indonesia as a state of wet tropical country was judged to be a contributor of global warming due to over the land function or deforestation in three biggest island of the country [1]. It is necessary to know comprehensively the relationship between the rainfall and features such as forest fire in Kalimantan as one of the biggest island.

Economic problem besides causing forest fire, health, the increase in local poverty, and the loss of biodiversity, also gave significant contribution to global carbon emission and impairment of smoke had damage the image of the nation and country. Hence various significant efforts have been done at national, province and regent level in order to reduce the risk caused by forest fire.

One of the best ever done is Early Warning System of Fire Management as the cooperation research between Columbia University and Bogor Agriculture Institute in 2007–2009 [1]. This Early Warning System (EWS) of Forest Fire Management (FFM) in Kalimantan originally was devoted to educate people how to reduced risk of disaster, but later apparently it only be utilized by a certain community with a good IT (information technology) understanding about environment. For instance, climate and fire resources system room or online data library which can only be accessed by those who have IT ability or technique to scrutinize fire management, so called very exclusive. Meanwhile, forest fire problem in Kalimantan should be understood by all relevant parties, including the layman who contact directly to the problems. Based on rapid assessment to make research successfully, the existence of an appropriate technology is necessary to support easy and better understanding of the people and hence the effort of climate change mitigation will be done better.

## 57.2 Constrains of EWS for FFM

To improve public understanding on the EWS of FFM and find its technology, firstly it is necessary to know the whole things associated with the EWS of FFM. It is expected that new technology will facilitate better understanding, so the effort to reduce the risk of disaster caused by Global Warming and Climate Change can be accomplished. This technology should be able to visualize the events of deforestation, forest fire, EWS and others related with Climate Change known as mitigation.

That important point is that there is a strong linkage between climate, fire and biophysic [2, 3]; the link of rainfall analysis tool in IRI *Climate and Fire Resources Room* (CFR Room); the link of forecast fire incident in Central Kalimantan, the concept of climate, the use of sea surface temperatures of (SSTs) to forecast of fire and nature as a possibility to be used; theory and implementation of augmented realty technology to the EWS of FFM as solution to make easier understanding about forest fire.

### 57.2.1 The Linkages of Climate, Fire and the Biophysic Indicators

#### 57.2.1.1 The Main Factors that Affect the Activity of Fire

- (1) Rainfall (Fig. 57.1)
- (2) Vegetation (Fig. 57.2)
- (3) Temperature and relative humidity

The temperature in Kalimantan was very stable with small variability. With respect to the relative humidity, its variants associated with a variation of

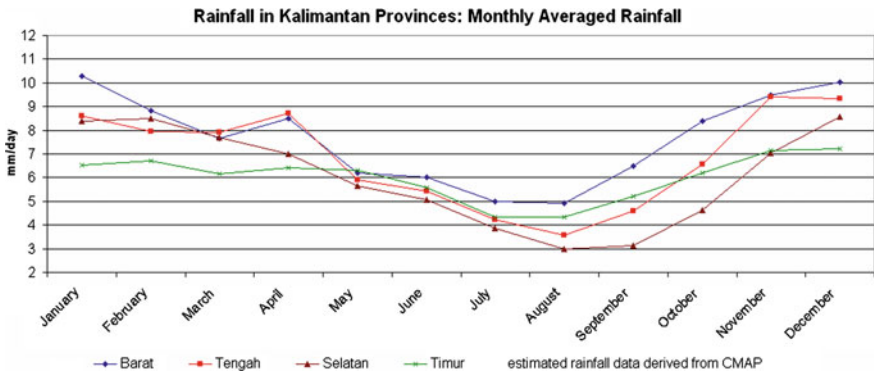


Fig. 57.1 Seasonal rainfall in four provinces in Borneo 1989–2006: “dry season is start June–October”

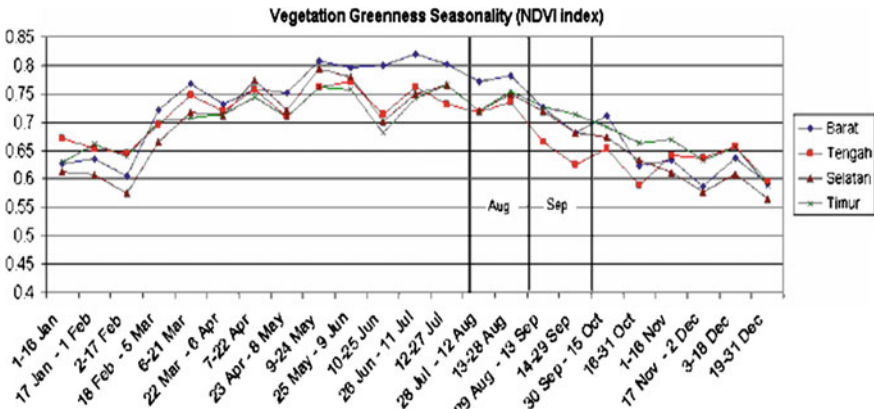


Fig. 57.2 Seasonal green plant in August and September is still high when the activity of fire reach its peak

rainfall. This shows that main environmental factors responsible for the variability inter years from the fire is anomalous rainfall during (June–October) the validation of *Fire Danger Rating System* (FDRS) of *Fire Danger System Assessment* (FDSA) in Central Kalimantan

(4) Fire Activities

The activity of fire data in the field available for several years and only for regions elected. Thus, satellite data used to determine number of active fire called hot spots. Data for hot spots was collected and consolidated from 2 satellites: National Oceanographic and Atmosphere Administration (NOAA) Advanced Very High Resolution Radiometer (AVHRR), and TERRA–Moderate Resolution Imaging Spectro radiometer (MODIS) [3].

### 57.2.1.2 Rainfall Estimation

An estimation of rainfall data from the station in Kalimantan was limited and does not provide complete for the entire year. Thus an estimation of rainfall of the two satellites are used to make a database rainfall. Estimation of rainfall was collected and consolidated from 2 source: NOAA—*Climate Prediction Center* (CPC) *Merged Analysis* (CMAP) available for the whole period fire data but resolution of its spatial were low (2.5 degrees) to analysis for the provincial level, and NOAA—CPC *Morphing Technique* (CMORPH) have high spatial resolution (0.25 degrees) but only available since 2003 to analysis of the district level.

## 57.2.2 The Linkages of Rainfall and Fire

Since 2007, IRI Columbia University has been working with Bogor Agriculture University and other partners to develop seasonal EWS. Research showed important relation between fire and anomalous rainfall. While the incident happened every year, the number grows when rainfall is lower than normal along the year.

The effort produce a better understanding on the relationship between the point of the fire and seasonal rainfall at the time scale, and demos with SSTs seasonal forecasts in the pacific ocean. IRI develop an instrument available online in the library, the stakeholders can access the high intensity of rain in Central Kalimantan obtained from satellite, and they can use of the forecasts of the risk to forecast 1–2 months ahead (Fig. 57.3).



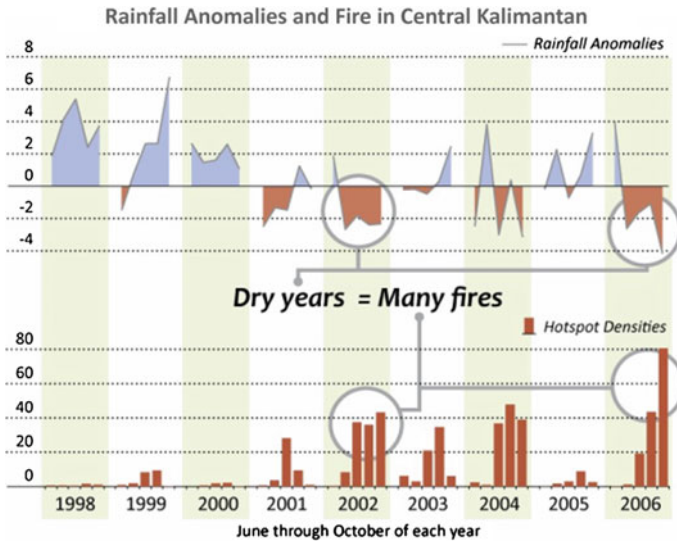


Fig. 57.3 Rainfall and fire

### 57.2.3 Estimation of Fire Events in Central Kalimantan

To understand some concept of climate related with forecasting of fire in Central Kalimantan by using of sea surface temperature (SSTs), and compiling tool for “Predicting Fire Activity” presented in IRI Map room to assess seasonal fire risk.

### 57.2.4 Hot Spot Detection with Remote Sensing System

There are several satellite and remote sensing system that can be used to monitor fire from the air. Sensors that used to monitor fire especially in Indonesia is Sensor of National Oceanographic and Atmosphere Administration (NOAA)—Advanced Very High Resolution Radiometer (AVHRR) and Terra—Moderate Resolution Imaging Spectro radiometer (MODIS). Both sensors have been used to take a number of hotspots which essentially measures the energy produced by the fire points. The variability of the number of hotspots is obtained from the AVHRR and MODIS data compared with a few years of hotspot ATSR [3] and smoke emission at the same time. The study shows the variability of temporary observation obtained from AVHRR and fashionable hotspot with its peak occurred in 2002, 2004 and 2006, and the activity of hot spot is happened in 1998–2001, 2003 and 2005.

### 57.3 AR Technology to Support Climate Change Mitigation

Augmented Reality (AR) technology aims to develop technology that would allow the merger in real-time against digital content that is made by a computer to the real world. AR allows users see an apparent object with two or three dimensions which are projected against the real world [4, 5].

Technology of AR make easier understanding of IRI CFR Room and on line DATA library in such a way that the purpose of establishing an EWS for Fire Management research project cooperation between Columbia University and partners in USA with Bogor Agriculture Institute and partners in Indonesia success. A graph technology computer is used to make visualize a graph data on climate and weather good to predict as well as the delineation of a certain point. Technology charts this computer produces an image fixed or animation either two or three dimensions to give the understanding of the condition of data is visual, so it expected to accelerate understanding and increase people awareness about the existing condition. The process of the transformation of climate data nor Fire Resources Room can use fluid dynamic calculation that simulates/to scatter fire hot climate on certain areas in accordance with environmental conditions existing so that data image real conditions of an area combine with visual digital chart (Fig. 57.4).

For example, in the following Fig. 57.5 there is a fire simulation which synchronized with the existing conditions of the forest environment.

The animation of its fire spreading was calculated based on simulation that can be customized with existing environmental data such as number of trees, its species and the average of wind direction. A Simulation is able to use fluid dynamic calculation so that it could be approximated as closely as possible with the real conditions.



**Fig. 57.4** Fires forest in Sumatra (*left*) 2012 and in Kalimantan (*right*) 2013



**Fig. 57.5** Fires forest simulation “UCF/IST researcher”, University of Central Florida 2007. <http://www.ist.ucf.edu/nlarchive/summer07/summer07.html>

### ***57.3.1 The Proposed Simulation Using AR Technology***

The desired of interactive features on an AR system is the ability to animate virtual existing object in the scene. The movement of virtual object on the scene caused by changes in the position of device nor based on the interaction of users or to the other objects. Displacement position will be done through a matrix of affine homogeneous transformation of the coordinates of an object to the world coordinate. Interaction in this AR technology could in the form of interactions among the object of both real and virtual or user interaction with a system of AR. Interaction among the object causing change towards an object virtual according to a simulation model executed as for interaction with users can be expressed in the form of haptic system in response to the user input.

Figure 57.6 describe the proposed AR architecture system. Users with devices display capture real environment via camera and interact with the device. In accordance with the scenario simulation, then virtual objects scene graph is taken from database of the graph in the form of animated and synchronized with the real visual objects that are retrieved from the camera capture including prediction of relative position of the real world scene.

The relative position is then synchronized with the position of real objects. The merger between scene real objects with scene virtual a graph then produce visual simulation sent to graphic engine. In graphic the engine will be render a computer graph then integrated with the real object and sent to a person to see the synchronization result in the form of AR model.

Instead of using AR technology, the statistical data of climate and fire at a particular period will be analyzed and simulated. To visualize the result of the simulation, it is expected to be described the conditions as well as the forecasting of fire. It will be used for better understanding to take action which must to be done to

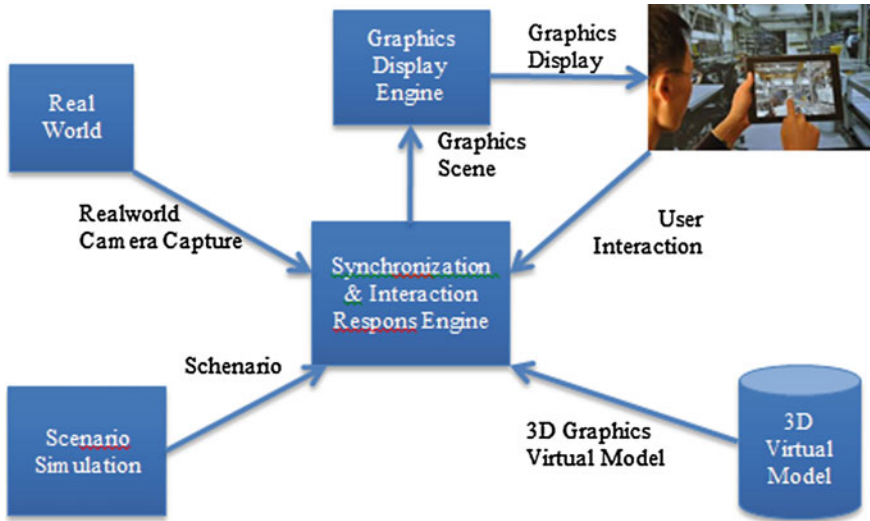


Fig. 57.6 Augmented reality system architecture

reduce the risk of wild fires, floods or other natural disasters. Climate change mitigation with AR technology is expected to reduce the threat of catastrophic impacts.

## 57.4 Conclusion

Computer graphic and Augmented Reality technology has been able to produce fix image or animation in two or three dimension, thereby it would give understanding to the condition of data visually, so that it is expected to accelerate and improve a better understanding of the observed condition. Fluid dynamic calculation has been used to stimulate the scatter of fire or heat the climate in certain areas in accordance with the visual condition combine with the digital charts.

## References

1. Early Warning System of Forest Fires Management, May 2009. International Research Institute for Climate and Society—Earth Institute, Columbia University in cooperation with Bogor Agriculture Institute. [http://crk.iri.columbia.edu/fire/exercises/fire\\_BAHASA.pdf](http://crk.iri.columbia.edu/fire/exercises/fire_BAHASA.pdf)
2. Weitzman, M.L.: On modeling and interpreting the economics of catastrophic climate change. *Rev. Econ. Stat.* **91**(1), 1–19 (2009)

3. Global Greenhouse Gas Emissions Data, Global Emissions by Source and Emissions by Country—US Environmental Protection Agency. Accessed 22 July 2015. <http://www.epa.gov/climatechange/ghgemissions/>
4. Haller, M. (ed.): *Emerging Technologies of Augmented Reality: Interfaces and Design: Interfaces and Design*. IGI Global, Hershey (2006)
5. Dangelmaier, W., Fischer, M., Gausemeier, J., Grafe, M., Matysczok, C., Mueck, B.: Virtual and augmented reality support for discrete manufacturing system simulation. *Comput. Ind.* **56** (4), 371–383 (2005)

# Chapter 58

## Cyber Security for Website of Technology Policy Laboratory

Jarot S. Suroso

**Abstract** Website is a collection of related web pages address with certain IP address in an Internet Protocol-based network. Website contains information to be shared and exchanged with others. Using an application called browser, users can browse any kind of website and connect with other users in network. Web pages are accessed and transported with Hypertext Transfer Protocol (HTTP), which can use encryption (HTTP Secure) as a security mechanism. Website is holding important role in the Internet world. Therefore, security is required in digital world to prevent crimes. Criminals targeted any situations where people unaware with. In this case, website as the front client application is a strategic place. It is important to aware about security, especially for the important websites that affect many people, such as banking, government, trading, and others. This research talks about design of cyber security for Website of Technology Policy Laboratory (TPL), aims to support the government's technology policy-making and to address social needs for globalization and the coming era of knowledge economy. One of the function is as the main government think-tank for technology policy and the major platform for incorporating Indonesian's research communities.

**Keywords** Cyber security · Website · Technology policy laboratory · Internet

### 58.1 Introduction

Cyber security has become a very big issue in recent years. Companies who went through corporate life thinking, "it will never happen to me" suddenly found themselves the victim of some sort of attack on their network. High profile

---

J.S. Suroso (✉)

Graduate Program, Binus University, Jl. Kebon Jeruk Raya no. 27,  
Jakarta 11530, Indonesia  
e-mail: jsembodo@binus.edu

companies are most certainly a bigger target for several reasons, including the notoriety the hacker receives for damaging their network or Web site, and the amount of financial damage that can be done by bringing down a successful e-commerce site. Recent attacks easily racked up 100 million dollars in damage. The “2010 CSI/FBI Computer Crime and Security Survey,” conducted in early 2010 by the Computer Security Institute (CSI) with participation by the San Francisco office of the Federal Bureau of Investigation (FBI), showed that 90 % of survey participants from large U.S. corporations, financial institutions, medical institutions, universities, and government agencies detected security breaches. About 70 % of the participants experienced breaches more serious than viruses or employee Web abuse [1]. Forty-two percent of survey participants (273 organizations) claimed financial losses totaling over 265 million dollars from cyber-attacks. These security threats were composed of an assortment of attacks and abuses that originated both internally and externally to their network borders. An effective security program includes awareness, prevention, detection, measurement, management, and response to minimize risk. There is no such thing as perfect security. The determined and persistent attacker can find a way to defeat or bypass almost any security measure. Network security is a means of reducing vulnerabilities and managing risks [2, 3]. Awareness should be tailored to the job requirements of employees. Employees must understand why they need to take information security seriously. End-users choosing weak passwords or falling for social engineering attacks can easily neutralize the best technical security solutions [2]. Upper management must provide for training, motivation, and codes of conduct to employees to comply with security measures.

The Internet is a worldwide system of computer network that use Internet Protocol Suite (TCP/IP) as standard. It is a large network that consists of millions of public and private computer in which users get any information from any other computers with or without permission. Chatting and video webcam have become more popular today as they are very easy to use for doing simple and fast communication. People can do their job from home as they work at workplace using Internet. Security goal was measured from confidentiality, integrity, and availability. That measurements must be fulfilled in the virtual world also, in this case is website security. This work designed a protection for the website which achieve the security standard.

## 58.2 Theory and Methods

Web applications are insecure by nature because it allows unknown users to have direct access to the server. Even used firewall, it must be an opening ports that allowed users connect to the server. Creating a website will combine some computers layers, which are hardware, connection, and application. All parts must be protected, however, this work is focusing on the PHP codes that included in an application layer. Though there is no 100 % security guarantee instead for the

offline product. Much better make a defense by writing a safe enough code. Attackers always search the weakest part to attack, but they will leave the Website if it is secure enough and pick other weak website. The first thing to learn about security is that never rely on just one method of protection. Since if it is failed, there will be no backup. Similarly like in a war strategy, when the plan A failed there is still plan B as backup.

In this research we used Microsoft Proxy server 2012 to aid in securing our network. Web Proxy Service is a core component of MS Proxy Server 2012 that will suit the needs of multiple network types because of its many features and its compatibility with various operating systems. Internet Service Manager administers this service, and the Web Proxy service can be used with almost any browser, and on almost any operating system platform Cunningham [4] (Fig. 58.1).

Web Proxy Service is the only service of the three offered that supports caching and routing of data. Caching can be passive or active, the administrator can set cache size, and cache filters can be defined. Routing can be used to define primary and secondary routes, and resolving them within an array before routing upstream can also be enabled. The Web Proxy service also offers Web publishing, reverse proxying, and reverse hosting, to assist in securing the internal servers from unwanted attacks from hackers or unwanted guests from outside the local network. These services are described later in the chapter. Clients can logged and monitored by checking protocols used, date and time of requests, domain names of the computer responding to requests, as well as the contents of the URL request.

For the method showed in Fig. 58.2, the circle is never ending, it means the security is never-ending job that need to be updated every time. This is the simple diagram about how this project works: The Software Development Kit (SDK) used to create this project are: (1) XAMPP as the offline web server, (2) MySQL as the database and (3) Hackertarget.com as the penetration tester.

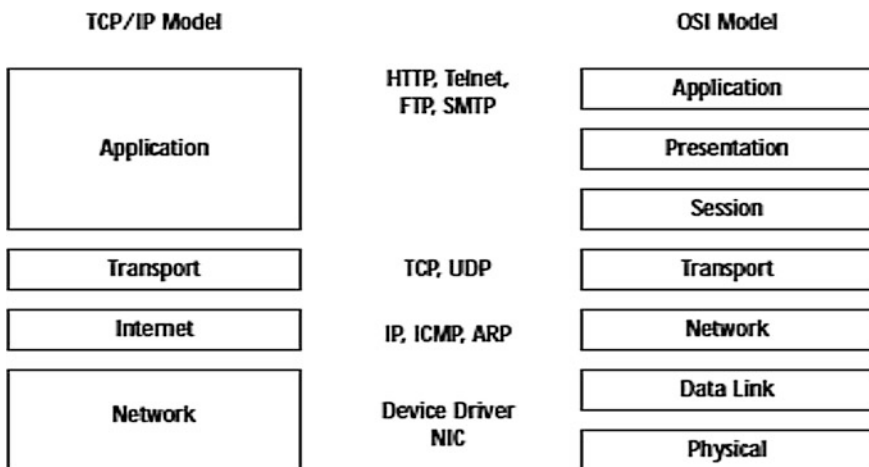


Fig. 58.1 Proxy server protect network



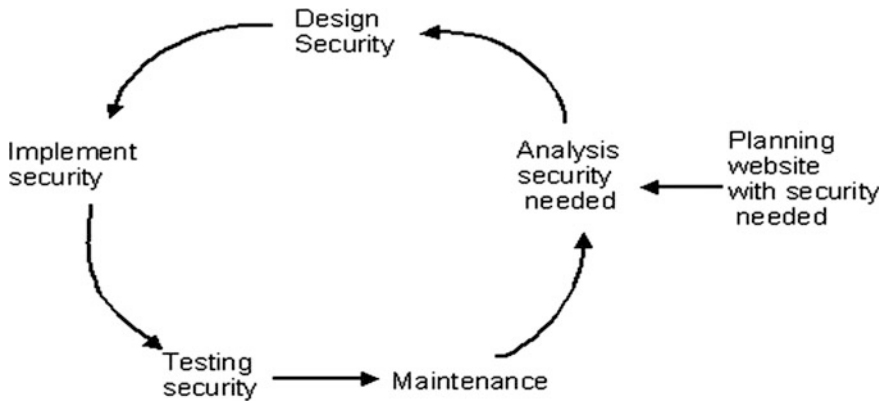
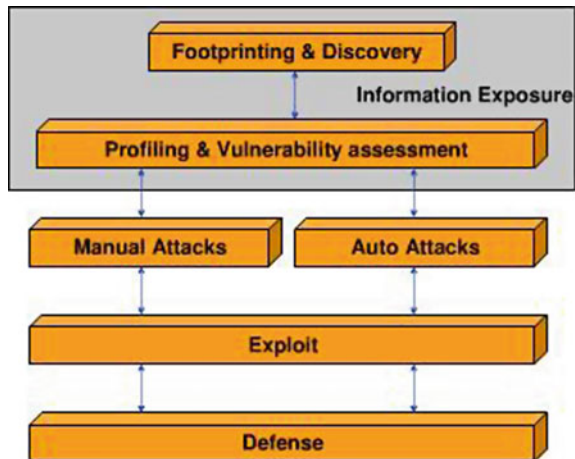


Fig. 58.2 Secure software development method

The hacking history is instead of diminishing, cyber crime becomes a greater threat today [5, 6]. The reason is because of the computer’s price today that quite cheap, then everyone is able to own it and learns it easily. But not all people have a good deed for learning computer. The Cracker is a computer expert that so something malicious whether the purpose is just for fun or pure crime. Website as the Internet user interface holds an important role in the Internet world, because website makes a direct connection with the user. Website is like a frontier soldier who is the first one that got attacked [7].

As shown in Fig. 58.3, attack methodology has many layers. Web designers who wish to implement security must be aware that those attack methods. The attacker can bypass each layer-level when there was the weak part though just a little. Therefore, security function must secure all layer levels. Foot printing is public data

Fig. 58.3 Attack methodology layers



information, like PHP version or server's operating system information. Attackers can get some hint from this public information. They will search for the bugs and weaknesses of this system. After found bugs, the cracker will start to assail either using manual or automatic approach (use bot computer). After that, the cracker created a defense mode to protect their identity, usually by hiding their IP address and using a zombie computer [1].

### 58.3 System Implementation

Agency for the Assessment and Application of Technology (BPPT) is a non-departmental government agency under the coordination of the Ministry of Research, Technology, and Higher Education, which has the tasks of carrying out government duties in the field of assessment and application of technology. BPPT created Technology Policy Laboratory (TPL), in 2004, aimed to support the government's technology policy-making and addressing social needs for globalization and the coming era of knowledge economy. Functioning as the main government think-tank for technology policy and the major platform for incorporating Indonesian's research communities, it has utilized over 10 year-experience in collecting, collating and disseminating technology information for the purposes of innovation, competitiveness, sustainable development and social well-being and has integrated and provided with several nationwide technology related information services in improving the efficiency of scientific research. With sound academic foundation and empirical research capabilities, TPL is advancing toward its major goal as a world-class policy research laboratory.

Now we will discuss how to embed the security function on the website. The prevention code put in the "security.php" file located under folder "function". This is the process flow that centralized in "controller". Controller is the one that controls "request" then forwards it to the "processing" function (Figs. 58.4 and 58.5).

Controller file located under folder "controller" the file already include "security.php" within. Included syntax is like this: `include("../function/security.php")`; The prevention code consists of many filtering and checking functions. Function named "filter(\$text)" uses to filter text for MySQL injection and XSS attack. This is the sample of filtering code: `filter($_POST['username'])` which filter username input from the `$_POST['username']` string. Sample filtering method in "login" feature (Fig. 58.6):

"DOScheck()" task utilizes for DoS attack protection, it works by identifying the user IP request and block it if the request exceeded the limit. "CSRF(\$function)" task operates for preventing CSRF attack which is skipping the legal form by means of create a direct request from the URL. And two methods again which are session

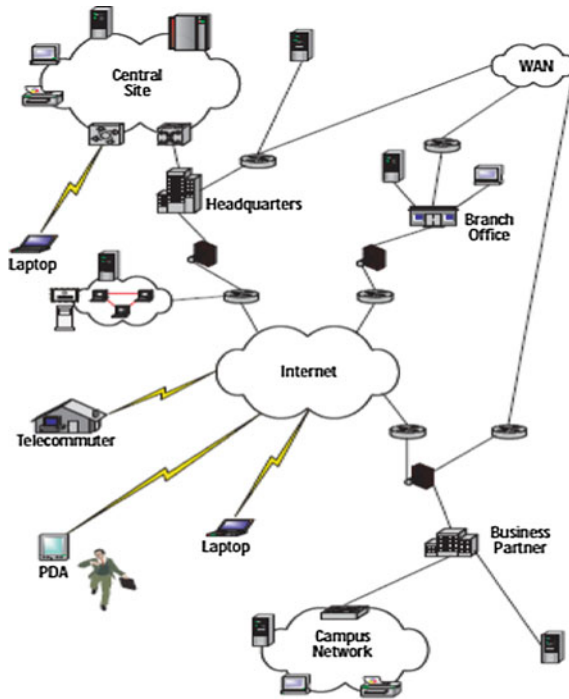


Fig. 58.4 Typical site scenarios

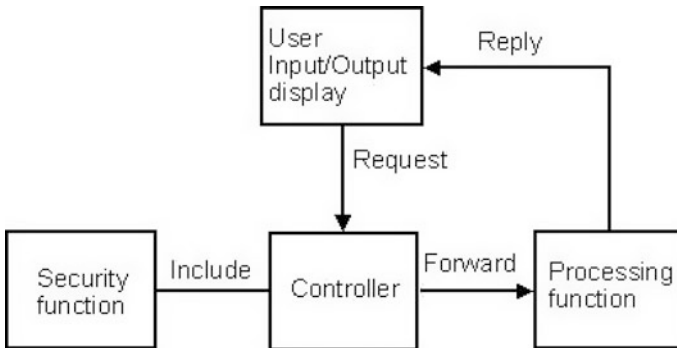


Fig. 58.5 Embedding security diagram

fixation and error display prevention that use `session_regenerate_id()` and `errorreport()`. “`Session_regenerate_id`” is PHP basic utility to regenerates “`session id`”. Regenerate “`session id`” for each request uses to prevent session fixation.

The website created and utilized as an information system website as follow (Fig. 58.7);

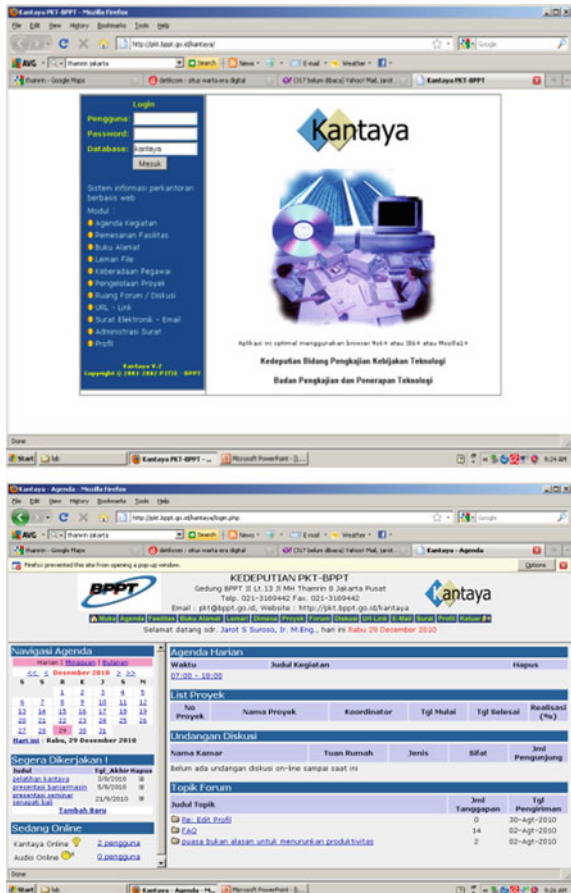
```

case "login":
$username = filter($_POST['username']);
$password = sha1($_POST['password']); DOScheck();
$function = login($username, $password);
csrf($function);

```

Fig. 58.6 Login filtering code

Fig. 58.7 Implementation of Kantaya



### 58.4 Conclusion

The website created and utilized by all researcher. The most stressed part in this research is to understand the way how the attack works and also how is the prevention method. In addition, it then should be combined it all and make it simple

to be implemented in website and it must be completed by the short time provided. It will be better to use hosting with unlimited privilege. Furthermore, the defense code implemented here is just the well-known attacks protection. As there are still so many threats, this code needs a lot of improvements. Since the security is a never-ending job, so maintenance needs every time. It will be very helpful for the new web developer to implement this security functionality in their website. Website of Technology Policy Laboratory (TPL), proved to be able to support the government's technology policy-making and to address social needs for globalization and the coming era of knowledge economy.

## References

1. Schweitzer, D.: Internet Security Made Easy: A Plain-English Guide to Protecting Yourself and Your Company Online. Amacom, New York (2012)
2. Cooper, F.J.: Implementing Internet Security. New Riders Publishing, Indianapolis (2013)
3. Cheswick, W.R., Bellovin, S.M.: Firewalls and Internet Security: Repelling the Wily Hacker. Addison-Wesley, Boston (2013)
4. Cunningham, S.: Internet Security. Syngress, Massachusetts (2010)
5. Watson Hall Ltd.: Web Security Issues. [www.watsonhall.com/resources/top10-website-security-issues.pdf](http://www.watsonhall.com/resources/top10-website-security-issues.pdf)
6. Robert, T.A.: History of Hacking. St Petersburg Times Online. <http://www.sptimes.com/Hackers/history.hacking.html>
7. Sheeraj S.: Advanced Web Hacking. <http://www.slideshare.net/shreeraj/advanced-web-hacking>

## Chapter 59

# TAM-MOA Hybrid Model to Analyze the Acceptance of Smartphone for Pediatricians in Teaching Hospital in Indonesia

Oktri Mohammad Firdaus, Nanan Sekarwana, T.M.A. Ari Samadhi and Kah Hin Chai

**Abstract** This research tries to explore the impact of smartphone usage among doctors, especially in the Department of Child Health at five teaching hospitals in Indonesia. Step taken to answer this research question is the development of a hybrid model which is a combination and modification of the Technology Acceptance Model (TAM) with Motivation, Opportunity, and Ability (MOA) framework. This research consists a survey disseminated to 197 pediatricians (residents, staff, consultant and professor) infive teaching hospitals in Indonesia and was conducted in 2014. The results of this research showed that the variables that significantly affect the intention of a doctor to use smartphone exactly are the motivation and the community. While most small variables influence are brand image and perceived ease of use. The conclusions of this research are a doctor at a Department of Child Health prefer the existence of a community in deciding to use a smartphone to support day-to-day activities, as well as most doctors do not feel disturbed if necessary to make investments independently to procure smartphones for obtaining value-added.

**Keywords** TAM · MOA · Smartphone · Pediatricians · Teaching hospital

---

O.M. Firdaus (✉)

Department of Industrial Engineering, Widyatama University, Bandung, Indonesia  
e-mail: oktri.firdaus@gmail.com

N. Sekarwana

Department of Child Health, Faculty of Medicine, Padjadjaran University,  
Bandung, Indonesia

T.M.A. Ari Samadhi

Department of Industrial Engineering, Bandung Institute of Technology,  
Bandung, Indonesia

K.H. Chai

Department of Industrial and Systems Engineering,  
National University of Singapore, Singapore, Singapore

© Springer Science+Business Media Singapore 2016

F. Pasila et al. (eds.), *Proceedings of Second International Conference*

*on Electrical Systems, Technology and Information 2015 (ICESTI 2015)*,

Lecture Notes in Electrical Engineering 365, DOI 10.1007/978-981-287-988-2\_59

## 59.1 Introduction

Indonesia since 2014 began to implement the National Social Security System or we called “Sistem Jaminan Sosial Nasional (SJSN)” with the aim towards Healthy Indonesia in 2019. Implementation of the Social Security for more than 1 (one) year cannot be separated from the various problems both minor and major. Constraints face by the organizers is “BPJS Kesehatan” and personal doctors in the implementation of the SJSN are still not integrated multiple sources of data and information which is indispensable in medical treatment. The role technology can actually minimize technical obstacles, such as integrate demographic data on the “e-KTP” card is managed by the Ministry of Internal Affairs and medical record data managed by each hospital under the auspices and coordination of the Ministry of Health. However, while the absolute requirements in this integration process is the change in paper-based medical records into electronic medical records. This means that if medical records are already in electronic-based form can directly improve the quality of medical treatment, so it can also support the implementation of the Social Security System.

This research will not fully discuss the process of migration of the medical record, but rather the impact of the technology used by doctors to support the smooth implementation of the Social Security System. Smartphone as a form of information technology is no longer a luxury item, but it has turned into one of the basic needs of a human being in everyday life. Doctors as one of the important actors in the implementation of the Social Security can also be said cannot be separated from the use of smartphones for daily needs, although with a different purpose. The features found on smartphones could help doctors both for communication with peers, share knowledge with colleagues and update information and knowledge related to medical treatment. The most significant impact of the use of smartphones is accelerating the transfer of information and knowledge itself.

Development of smartphones in the medical field actually began in the 2000s, when the development of PDA technology and the increasing ease with which people get Internet access [1]. PDA technology can be regarded as a forerunner to the development of today’s smartphones. Especially in the field of medicine PDAs and smartphones early generation are merely used as a storage area when the medical records of patients who were being treated by a doctor [1]. Medical records are stored in the PDA will simplify and accelerate the decision-making process of a doctor [1]. Other researchers specifically discuss the use of smartphones in the medical field explaining that the acceptance and adoption of smartphones is inseparable from its motivation [2]. Smartphones can be a bridge between doctor and nurses in decision-making related to medical treatment [2]. Another study that discussed the adoption of smartphones explained that conformity with the features of a person’s job would be the main reason for using these technologies [3]. The another thing is that the smartphone is considered to reduce costs of unnecessary routine, so it can be transferred to another development in the company [3].

Another benefit of the smartphone in the medical field is the development of a tool to monitor the patient's heart rate, so that a doctor can easily and in real time monitor the condition of these patients [4]. Other researchers have revealed that the main reason for someone to use a smartphone is the presence of a significant level of benefit to their work [5]. Smartphones are also considered to improve the ability of a nurse to innovate, especially with regard to the handling of cases that are difficult or unique [6]. Response smartphone users among students in Korea both for medicine and other fields also showed that the use of these technologies is strongly influenced by the social environment influences the students concerned [7]. Other studies are still discussing about the adoption of smartphones in Korea showed that the main factor of the high number of users of this technology due to the motivation of individuals and not because of the encouragement of the organization or institution [8]. In the end there is a detailed study discusses the role of smartphones in the process of birth control in order to achieve the human development index of a country that is optimal [9]. Based on the explanation of some previous studies it can be concluded that the smartphone has affected joints of life, especially in the medical field, so it is quite reasonable to continue a study to see how much the level of acceptance and adoption of these technologies in Indonesia, especially concerning interpersonal relationships of the doctors in a teaching hospitals. Reason selected teaching hospitals, among others, that the routine activities of the doctors in this place not only related to the medical treatment, but also for practical learning process. Department selected in this study is of Pediatrics, with the consideration that one of the goals is to reduce mortality SJSN infants and toddlers.

## 59.2 Model Development

The research model was developed from two (2) reference model that is developed enough that the Technology Acceptance Model (TAM) and Motivation, Opportunity, Ability (MOA) framework. The main constructs in TAM model are perceived usefulness and perceive ease of use [10]. Both of these constructs are expected to affect the intention to use that ultimately affects the actual use [10]. While the framework MOA describes the effect of the three constructs on performance [11]. Based on previous research, explained that the intention to use can also be influenced by the community, brand image, and trust [12, 13]. The biggest impact of the three additional constructs will vary depending on the results of the analysis of what kind of technology adoption and when [13]. Based on previous studies, then the process of merging both the reference models in a unified model of the named is TAM-MOA Hybrid models. This hybrid models are expected to answer the phenomenon of what factors are actually dominant on the intention to use, especially in the study of smartphone technology use among pediatricians in a teaching hospital in Indonesia in order to support the implementation of the Social Security. Detailed descriptions of this hybrid model can be seen in Fig. 59.1.



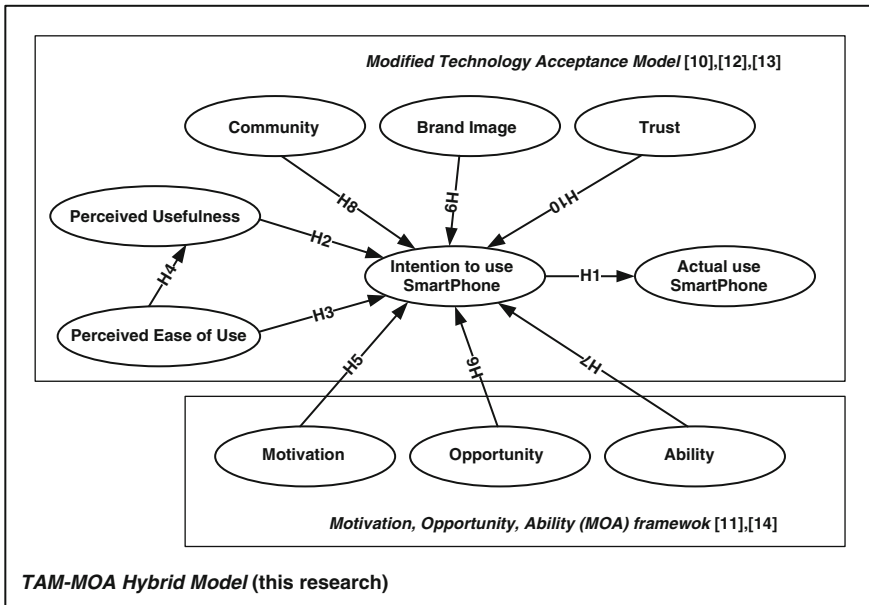


Fig. 59.1 TAM-MOA hybrid model

### 59.3 Method

The process of collecting the data used in this research is the method of computer-based survey using survey monkey.com assistance. Research questionnaires distributed by email of potential respondents. Information of email addresses of potential respondents was obtained from various sources, both professional associations and hospital education website in question. The number of questionnaires distributed as many as 455 pieces, and the back and deserves to be treated as many as 197 pieces or in other words the response rate of 43.29 %. These results are very encouraging, because for this type of electronic-based survey average response rate below than 20 % [14]. Data Processing used covariance-based structural equation model (CB-SEM) with the help of software LISREL 8.70. Considering the number of observed variables and also the number of respondents who exist, it was decided to use Maximum Likelihood estimation method [14].

### 59.4 Result and Discussion

Based on the results of the collection and processing of data obtained that the respondent is still dominated by women amounted to 59.89 %, and also in the age range between 31–40 years that is equal to 42.13 %. Focus on the age profile of the

respondents, it can be deduced that the survey using computer-based methods are still siding with young people, but it also respondents in the age range 31–40 years is at a prolific phase. Depth doctors most respondents in this study is resident (47.72 %). This is not too surprising, because at the level of resident doctor actually required to be able to communicate well, to share knowledge with colleagues on an ongoing basis and also must constantly update the information and knowledge related to medical treatment. While the type most widely used smartphone is Android (49.24 %). This relates to the price which is quite affordable android smartphone and its features are also considered quite fit the needs of physicians. Detailed descriptions can be seen in Table 59.1.

Data processing using CB-SEM with the help of LISREL 8.70 software indicates at least of 10 tested the hypothesis that there are three (3) hypotheses that have a high enough level of significance, namely H1, H5 and H8. The focus of the

**Table 59.1** Respondent's profile

Item	Amount	Percentage (%)
<i>Sex</i>		
Male	79	40.11
Female	118	59.89
<i>Age</i>		
Below 30 years old	31	15.74
31–40 years old	83	42.13
41–50 years old	59	29.95
Above 50 years old	24	12.18
<i>Level of pediatricians</i>		
Resident	94	47.72
Fellow	3	1.52
Staff	51	25.88
Consultant	38	19.29
Professor	11	5.58
<i>Type of smartphone</i>		
iPhone	65	32.99
Blackberry	28	14.21
Android	97	49.24
Windows Phone	6	3.05
Others	1	0.51
<i>The purposes using a smartphone</i>		
Communication with colleague	197	–
Sharing Knowledge	155	–
Update Information and Knowledge	183	–
E-Mail	138	–
Chat and Social Media	125	–
Others	59	–

discussion of the H5 and H8, indicates that motivation comes from individual doctors and also support a community that houses doctors will strongly influence the decision in the use of smartphones in everyday activities. Both of these indicate that the level of awareness of a doctor to use a smartphone in terms of supporting the performance of medical treatment is supported by the existence in question in a community. In another sense that they are would be willing to make an investment and the adoption of a new technology to maintain good relations within a community. This is quite reasonable because the role of the community is very big influence on the continuity of the career of a doctor in the future, and also the role of the community can influence the access is not easy to build a network with other doctors in other hospitals either a different city or a different country. This is because the reference is derived from a community can influence the decision of a doctor who later became its website.

Indicators are no less important in the covariance-based structural equation modeling (CB-SEM) is the value of the results of testing goodness of fit as shown in Table 59.3. One important indicator that can indicate whether the research

**Table 59.2** Hypothesis testing

Hypothesis	Result		
	Unstandardized coefficient	t-Value	Conclusion
<b>H1: Intention to use Smartphone direct effect to Actual use Smartphone</b>	<b>0.86</b>	<b>10.31****</b>	<b>Accepted</b>
H2: Perceived Usefulness direct effect to Intention to use Smartphone	0.51	3.11***	Accepted
H3: Perceived Ease of Use direct effect to Intention to use Smartphone	0.19	1.62*	Accepted
H4: Perceived Ease of Use direct effect to Perceived Usefulness	0.49	2.03**	Accepted
<b>H5: Motivation direct effect to Intention to use Smartphone</b>	<b>0.67</b>	<b>5.67****</b>	<b>Accepted</b>
H6: Opportunity direct effect to Intention to use Smartphone	0.38	2.35***	Accepted
H7: Ability direct effect to Intention to use Smartphone	0.25	1.99**	Accepted
<b>H8: Community direct effect to Intention to use Smartphone</b>	<b>0.55</b>	<b>4.99****</b>	<b>Accepted</b>
H9: Brand Image direct effect to Intention to use Smartphone	0.11	1.44*	Accepted
H10: Trust direct effect to Intention to use Smartphone	0.49	2.42***	Accepted

Note \*: significant at  $p < 0.1$ ; \*\*: significant at  $p < 0.05$ ; \*\*\*: significant at  $p < 0.01$ ; \*\*\*\*: significant at  $p < 0.001$  (one-tailed)

**Table 59.3** Goodness of fit measurements

GoF measures	Values	Result
Root Mean Square Error of Approximation (RMSEA)	0.057	Good Fit
<b>Goodness of Fit Index (GFI)</b>	<b>0.93</b>	<b>Satisfactory Fit</b>
Root Mean Square Residuan (RMR)	0.044	Good Fit
Critical Number CN)	127.4	Data was enough
Normed Fit Indez (NFI)	0.91	Good Fit
Adjusted Goodness of Fit Index (AGFI)	0.92	Good Fit
Comparative Fit Index (CFI)	0.92	Good Fit
Parsimony Normed Fit Index (PNFI)	0.95	Good Fit
Incremental Fit Index (IFI)	0.91	Good Fit
Relative Fit Index (RFI)	0.92	Good Fit

model has been completely goodness of fit is the value fit index (GFI). GFI value in the study was 0.93; meaning that this research model has been said to befit and worthy to serve as reference for future research model. The size of the other goodness of fittest is no less important is the root mean square error of approximation (RMSEA). RMSEA values in this study amounted to 0.057; meaning that the research model has the possibility of a small enough error rate [14]. Further explanation of the data processing results can be seen in Tables 59.2 and 59.3.

## 59.5 Conclusion

The simple conclusion can be drawn from this research is the need for education and the provision of a comprehensive understanding of the entire human medicine, especially in the Department of Pediatrics at a teaching hospital in Indonesia of the importance of maintaining good relations with a community will always overshadow the doctor in the future will come. This is important, because most doctors will be willing to invest and the adoption of a new technology that is actually quite ordinary before as well as smartphones, because of the community's role in it. Therefore, the input to the study should be done next is a more in-depth study of the design of the user interface of the features present in a smartphone that really fit the needs of a doctor and do not require a long time for the process of adaptation before using it.

**Acknowledgements** The authors would like to thank the Medical Ethics Committee of the Faculty of Medicine, University of Indonesia, CEEBM RSCM Jakarta, as well as the head of the Department of Child Health at five (5) Teaching Hospitals in Indonesia with the permission and support given during the research period.

## References

1. Paton, C., Al-Ubaydli, M.: The doctor's PDA and Smartphone handbook: medical records. *J. R. Soc. Med.* **99**, 183–184 (2006)
2. Park, Y., Chen, J.V.: Acceptance and adoption of the innovative use of smartphone. *Ind. Manag. Data Syst.* **107**(9), 1349–1365 (2007)
3. Kim, S.H.: Moderating effects of job relevance and experience on mobile wireless technology acceptances: adoption of a smartphone by individuals. *Inf. Manag.* **45**(6), 387–393 (2008)
4. Shim, H., Lee, J.H., Hwang, S.O., Yoon, H.R., Yoon, Y.R.: Development of heart rate monitoring for mobile telemedicine using smartphone. In: 13th International Conference on Biomedical Engineering IFMBE Proceedings, vol. 23, pp. 1116–1119 (2009)
5. Verkasalo, H., Lopez-Nicolas, C., Bouwman, H.: Analysis of users and non-users of smartphone applications. *Telematics Inform.* **27**(3), 242–255 (2010)
6. Putzer, G.J.: The effects of innovation factors on smartphone adoption among nurses in community hospitals. *Perspect. Health Inf. Manag.* **7**(Winter), 1b (2010)
7. Chun, H., Lee, H., Kim, D.: The integrated model of smartphone adoption: hedonic and utilitarian value perceptions of smartphones among Korean College students. *Cyberpsychol. Behav. Soc. Netw.* **15**(9), 473–479 (2012)
8. Joo, J., Sang, Y.: Exploring Koreans' smartphone usage: an integrated model of the technology acceptance model and uses gratifications theory. *Comput. Hum. Behav.* **29**(6), 2512–2518 (2013)
9. Tripp, N., Hainey, K., Liu, A., Poulton, A., Peek, M., Kim, J., Nanan, R.: An emerging model of maternity care: smartphone, midwife, doctor? *Women Birth* **27**(1), 64–67 (2014)
10. Davis, F.D.: Perceived usefulness, perceived ease of use, and user acceptance of information technology. *MIS Q.* **13**(3), 319–340 (1989)
11. Siemsen, E.: Essay on Knowledge Sharing. A Dissertation, Faculty of University of North Carolina (2005)
12. Firdaus, O.M.: Efektivitas Penggunaan *Smart Phone* Dalam Mendukung Kegiatan Bisnis Pengusaha Muda di Kota Bandung Menggunakan *Technology Acceptance Model* (TAM). In: IENaCo (Industrial Engineering National Conference), Universitas Muhammadiyah Solo, 28 Mar 2013
13. Firdaus, O.M., Suryadi, K., Govindaraju, R., Ari Samadhi, T.M.A., Fuad, A., Zakiyyah, E.R.: Penggunaan Smartphone Pada Kegiatan Berbagi Pengetahuan Antar Residen Anak RSHS Bandung. *Forum Informatika Kesehatan Indonesia (FIKI)*, Semarang, 22–24 Apr 2013
14. Wijanto, S.H.: Structural Equation Modeling Dengan LISREL 8.8: Konsep & Tutorial. *Graha Ilmu*, Yogyakarta (2008)

# Chapter 60

## Development of the Remote Instrumentation Systems Based on Embedded Web to Support Remote Laboratory

F. Yudi Limpraptono and Irmalia Suryani Faradisa

**Abstract** Web-based remote instrumentation is a new innovation in the development of instrumentation equipment that can be accessed remotely over the Internet. The development of remote instrumentation has been started since the invention of internet technology and the development of the remote lab system. Most remote laboratory system architectures that have been published are computer based and usually using LabView application. Computer-based remote instrumentation system has the disadvantages that the investment costs are expensive and it requires large electrical power. In addition, there are several issues related to green computing that demands increased efficiency. To address some of these issues, this research study has developed an embedded web-based remote instrumentation to support remote laboratory system. Implementation of the embedded web-based remote instrumentation system is expected to contribute to improving efficiency and lowering the system's costs.

**Keywords** Remote instrumentation · Embedded-web · Remote laboratory

### 60.1 Introduction

At the end of the 20th century, remote lab is a very active area of research in the development of e-learning, and recently the number of universities working with remote labs has increased [1]. There are several advantages of using remote laboratories, such as laboratory performance will be better and more efficient because students can use laboratory equipment for 24 h. A remote laboratory creates

---

F.Y. Limpraptono (✉) · I.S. Faradisa  
Electrical Engineering, National Institute of Technology Malang, East Java, Indonesia  
e-mail: fyudil@yahoo.com

I.S. Faradisa  
e-mail: irmaliafaradisa@yahoo.com

autonomous learning [2], allows uses by handicapped students [3], and supports resource sharing and collaboration between laboratories. Various technologies in web programming have been employed to provide a comfortable remote lab environment, such as socket, applet, ajax, corba, labview, etc. [3] Typically the design of the remote laboratory consists of several parts: the first is remote lab management, the second is an experiment module, and the third is the instrumentation equipment [2]. Remote lab management is a web-based application that serves to manage user permission and set up the equipment module. Lab module is an experiment object that can be controlled remotely, that is equipped with IP cameras for object observation. Instrumentation equipment is a device used for measurement or signal generation in the experiment modules such as oscilloscopes, frequency generators, etc. Currently instrumentation equipment widely used for remote labs is conventional measuring instruments or virtual instrumentation based on LabVIEW. Based on the results of journal reviews, it can be inferred that most remote laboratory research projects use a desktop computer, where the investment costs of hardware, software, and maintenance are very high. Electrical energy requirements for servers, computers, monitors, and cooling systems in a computer-based remote laboratory are very significant. A desktop computer requires electrical power on average between 60 and 100 W [4]. Energy consumption for a computer contributes to the rise in greenhouse gas emissions. Every personal computer that is being used produces about one ton of carbon dioxide every year [5]. Based on the background described above, this research aims to design and implement remote instrumentation to support remote laboratory, which has efficient system specifications and is environmentally friendly. Development of remote instrumentation includes the designs of oscilloscope and signal generator that are implemented with embedded system technology, which is expected to increase the efficiency of the system and support Green IT era.

## 60.2 Remote Lab Architecture

The proposed design of the remote instrumentation based on embedded web is integrated with multiuser remote laboratory that has been developed and published in the manuscript titled “New Architecture of Remote Laboratories Multiuser based on Embedded Web Server” [6]. Block diagram of the remote lab architecture is shown in Fig. 60.1. The activities of this research project are divided into two phases. The first phase is the design and implementation of some remote instrumentation system including an oscilloscope and a signal generator; the research activities have been carried out in 2015. The second phase will be the design and implementation of a matrix switch module; the research activities will be carried out in 2016. Matrix switches are a series of switches that can be programmed to connect between the experimental modules and instrumentation equipment. Remote instrumentation design is implemented using the embedded systems based on Raspberry PI.

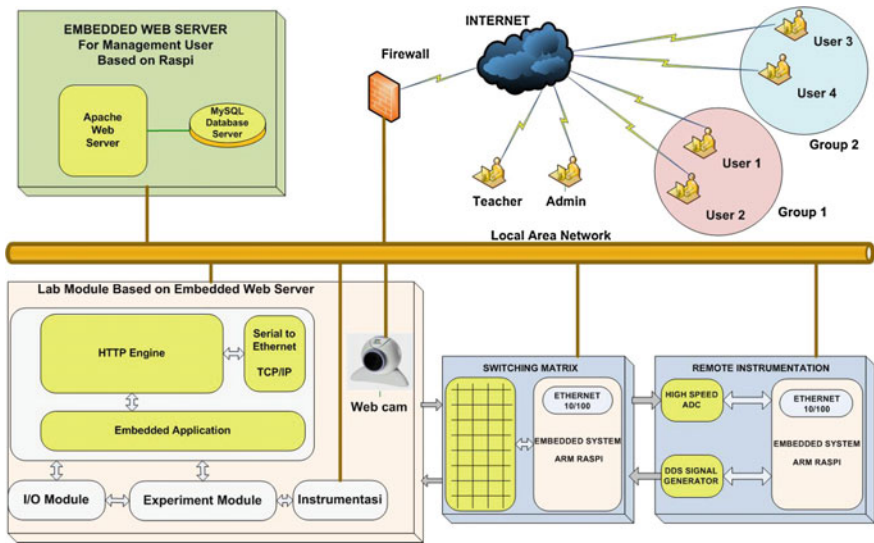


Fig. 60.1 Diagram of the remote lab architecture

### 60.3 Remote Instrumentation Design

The design of remote instrumentation, as shown in Fig. 60.2, consists of an embedded system based on Raspberry Pi, a DDS (direct digital synthesis) module based on AD9850, and a high-speed data acquisition system based on AD775. The

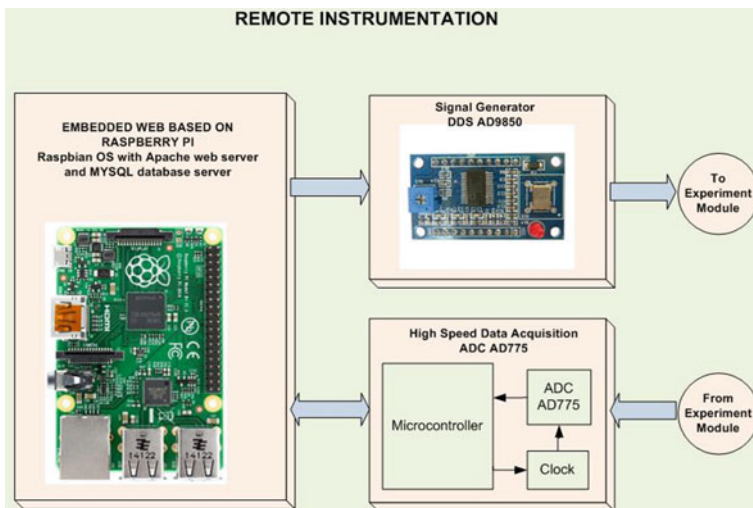


Fig. 60.2 Diagram of the remote instrumentations



Raspberry Pi embedded system functions as a web server to serve requests from the user of the remote lab and to control the DDS and the data acquisition unit. Raspberry Pi is based on the Broadcom BCM2835 system on a chip (SoC), that includes an ARM1176JZFS 700 MHz processor, 512 MB of RAM, and a storage capacity of 8 GB SD card. Raspberry Pi is also equipped with a GPIO, an Ethernet port 10/100 Mbps and a USB port [7]. The operating system used in this research project is embedded Linux Raspbian, and the installed application programs are Apache web server and MySQL database server. The design of the signal generator module uses AD9850. The AD9850 is highly integrated device that uses advanced DDS technology coupled with internal high speed, high performance digital to analog converter and comparator to form a complete, digitally programmable frequency synthesizer and clock generator function. High speed DDS AD9850 provides 32-bit frequency tuning word, which results in an output tuning resolution of 0.0291 Hz for a 125 MHz reference clock input. The AD9850 circuit allows the generation of the output frequency of up to one-half the reference clock frequency (62.5 MHz). The DDS circuitry is basically a digital frequency divider function whose incremental resolution is determined by the frequency of the reference clock divided by the  $2^N$  number of bits in the tuning word. The relationship of the output frequency, reference clock, and tuning word of the AD9850 is determined by the formula [8]:

$$f_{out} = (\Delta Phase \times CLKIN) / 2^{32} \quad (60.1)$$

wheres:

$\Delta Phase$  is the value of the 32-bit tuning word

$CLKIN$  is the input reference clock frequency in MHz

$f_{out}$  is the frequency of the output signal in MHz

The design of a digital oscilloscope uses high speed data acquisition based on AD775. The AD775 is a CMOS, low power, 8-bit data output, 20 MSPS sampling rate analog-to-digital converter (ADC). The AD775 features a built-in sampling function and on-chip reference bias resistors to provide a complete 8-bit ADC solution. The AD775 utilizes a pipelined/ping pong two-step flash architecture to provide high sampling rates (up to 35 MHz) while maintaining very low power consumption (60 mW) [9].

## 60.4 Software Design

The software of the remote instrumentation system is implemented using Python programming language, which is commonly used in embedded Linux operating systems. The following subsections will discuss the flowcharts for DDS AD9850 and data acquisition unit AD775.

### 60.4.1 Programming the DDS AD9850

The AD9850 contains a 40-bit register that is used to program the 32-bit frequency control word, the 5 bit phase modulation word, and the power down function. The interface between the DDS AD9850 with Raspberry Pi uses serial mode. In the serial mode, subsequent rising edges of W\_CLK shift 1-bit data on Pin 25 (D7) through the 40 bits of programming information. After 40 bits are shifted through, an FQ\_UD pulse is required to update the output frequency (or phase). Flowchart of the AD9850 program is shown in Fig. 60.3.

### 60.4.2 Programming the Data Acquisition

The remote oscilloscope unit consists of a data acquisition system and an embedded system based on Raspberry Pi. The data acquisition system consists of a micro-controller, a clock circuit, and ADC AD775. Raspberry Pi serves as web services for the remote oscilloscope. Acquisition process of the analog signal is performed by the data acquisition unit in real-time, and the data are stored in local memory of the oscilloscope. Periodically the data conversion results are sent serially to the

**Fig. 60.3** Flowchart of the AD9850 program

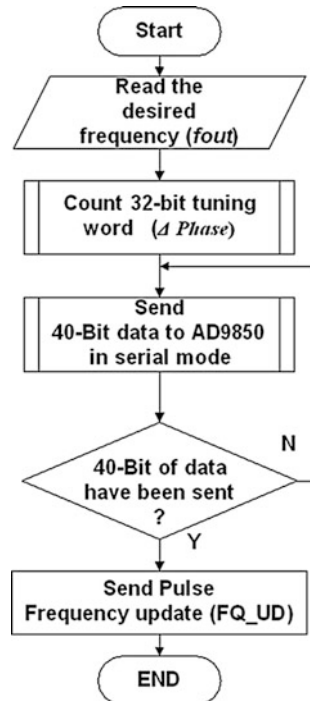
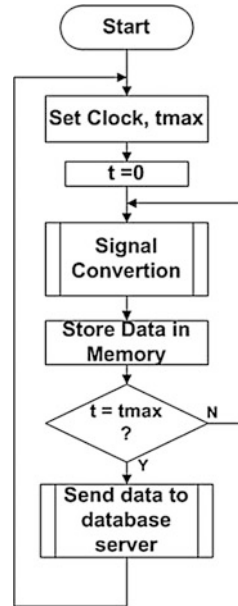


**Fig. 60.4** Flowchart of the DAQ program

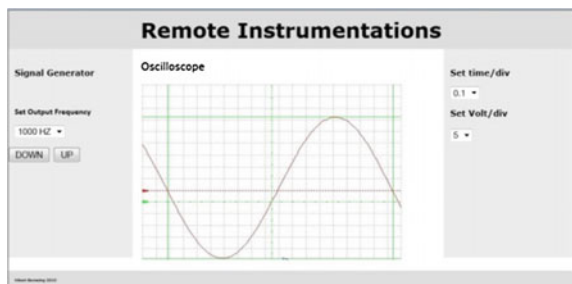


Raspberry Pi to be stored in the database server. Remote users can access the web services provided by Raspberry Pi to view the observed signals, and the signals will always be updated automatically. The flowchart of the DAQ program is shown in Fig. 60.4.

### 60.4.3 Web Application of the Remote Instrumentations

The Web-based remote instrumentation application was developed using PHP and Python programming languages. The application is used to control the hardware instrumentation, such as setting desired frequency parameters in the signal

**Fig. 60.5** Remote instrumentations web page



generator or setting parameters on the oscilloscope (time/div and volt/div), and produce graphic display on the client computer. The remote instrumentations web page is shown in Fig. 60.5.

## 60.5 Conclusion

This paper presents the development of remote instrumentation based on embedded web for supporting a remote laboratory. The aim of the research is to create a prototype of remote instrumentation—consisting of an oscilloscope and a frequency generator—that has highly efficient specifications: low cost, low power, and supporting Green IT. At the time of writing, the research project is still ongoing and the results are expected to contribute to the development of green remote instrumentation system. The instrumentations system can be integrated with the multi-user and multi-device remote laboratories that had been developed previously.

**Acknowledgments** The authors would like to thank the Indonesian Directorate General of Higher Education, which provided the funds for the remote instrumentation research project. The authors also thank the National Institute of Technology Malang, which supported our research.

## References

1. Garcia-Zubia, J., Angulo, I., Irurzun, J., Orduna, P., Ruiz, J., Hernandez, U., Castro, M., San-Cristobal, E.: Easily Integrable platform for the deployment of a remote laboratory for microcontrollers. *Int. J. Online Eng. IJOE* **6**(3), 26–31 (2010)
2. Gomes, L., Bogosyan, S.: Current trends in remote laboratories. *IEEE Trans. Ind. Electron.* **56** (12), 4744–4756 (2009)
3. Garcia-Zubia, J., Lopez-de-Ipiña, D., Orduña, P.: Evolving towards better architectures for remote laboratories: a practical case. *Int. J. Online Eng. IJOE* **1**(2), 1–11 (2005)
4. Kazandjieva, M., Heller, B., Gnawali, O., Levis, P., Kozyrakis, C.: Green enterprise computing data: assumptions and realities. In: *Green Computing Conference (IGCC), 2012 International*, pp. 1–10 (2012)
5. Murugesan, S.: Harnessing green IT: principles and practices. *IT Prof.* **10**(1), 24–33 (2008)
6. Limpraptono, F.Y., Ratna, A.A.P., Sudibyo, H.: New architecture of remote laboratories multiuser based on embedded web server. *Int. J. Online Eng. IJOE* **9**(6), 4–11 (2013)
7. Raspberry: Raspberry Pi Quick Start (2013). [www.raspberrypi.org](http://www.raspberrypi.org)
8. Analog Devices: Datasheet: 125 MHz Complete DDS Synthesizer (2004)
9. Analog Devices: Datasheet: AD775 8-Bit 20MSPS Sampling A/D Converter (1993)

# Chapter 61

## Enhancing University Library Services with Mobile Library Information System

Singgih Lukman Anggana and Stephanus Eko Wahyudi

**Abstract** An Indonesian University has to serve three main activities: Research, Teach, and Outreach. To support those activities, one of the most important facilities was library. Library has evolved from its previous original purposes to keep and preserve resources, such as books and other materials. The development of Information and Communication Technology (ICT) shifted the main library features to a broader one. However, some studies show that the end of traditional library maybe not near, as many still prefer to read printed format books instead of electronics one. Thus, it is still necessary to introduce the use of ICT to enhance the user experience of using university library service. ICT can be used to allow the user to find collection, borrow books, and many other services using mobile applications. This paper discusses the development of an Android mobile application that support the library information system, allowing the users to use the library services in a more convenient way remotely. There are number of server-side or client technologies used for the development, including: Android SDK, Laravel Framework, Laravel Dispatcher, Iron.io, Google Cloud Messaging (GCM), and Android Volley. A preliminary study carried out to gather the features needed by the prospective users, then followed by an analysis and design stages, then implemented using the aforementioned technologies. Finally, upon successful implementation stages, it was followed with a series of interviews to its prospective users, both the university's librarian as well as the prospective users. In conclusion, the developed apps met the users expectations whilst a number of improvements can also be done to boost the user experience and usability.

**Keywords** Android · Hybrid library · Library information system · Mobile apps

---

S.L. Anggana (✉) · S.E. Wahyudi  
Universitas Ciputra, UC Town, Citraland, Surabaya 60219, Indonesia  
e-mail: stephanus.eko@ciputra.ac.id

## 61.1 Introduction

The rapid development of Information and Communication Technology (ICT) also push the limit of what can be introduced to its users that support their work. Numerous applications of the technology also made possible as the number of the technology users also increasing dramatically. Based on January 2015 data, approximately 42.4 % of more than 7 billion world population are Internet users [1, 2]. Among of those figure, 45.6 % are people from Asia countries, which is approximately 1.4 billion people. In Indonesia, more than 71 million people use Internet, which is more than 28 % of its population. Those figures record a growth of 753 % compared to the year of 2000 data. Approximately 51 %—more than 3.6 billion people are unique mobile phone users. Among those, 2.7 billion people or 38 % of those are using smartphones [2].

In general, there are 3 main activities that Indonesian University should focus on—called *Tridharma*, which include: research, teach, and community service. To support these activities, a library is one of the main facilities needed. Universitas Ciputra Surabaya as one the leading universities in Surabaya also tries to improve the quality of its library service.

Digital Library is a popular terminology that has been around for more than a decade. It refers to the use of Information and Communication Technology and other services that provide a means of repositories of digital contents, including that of electronic documents and other multimedia files [3, 4]. The documents might be web pages, scanned legal documents, electronic books, or many other document types [4].

With the availability of the ICT infrastructure and digital contents that support the development of Digital Library, there is a question that the end of traditional library might be in the very near future, replaced by Digital Library. Some researches show that a physical library will stay for a very long period, as some people still prefer printed format book compared to digital format [5]. Some researches suggest that libraries should progress to hybrid library [5], a library that still maintain printed resources and start to move towards digitalizing books and collect electronic resources [8].

ICT introduces a lot of possibilities to improve the efficiency and effectiveness of traditional as well as hybrid library types. It can be used to enhance some of their main services, including book loans and returns. The availability of mobile technology should also allow them to use it to find the library collection that they need to borrow even though when they are mobile.

This paper discusses of the development of an Android mobile apps to enhance the user experience of borrowing book in a university library, especially at Universitas Ciputra.

## 61.2 Library

The definition of a library is a place where information resources, such as: books, periodicals, magazines, and other materials—including videos and musical recordings, are stored and available for people to borrow or use [6, 7]. A library usually provides a number of rooms and facilities, including collection rooms, reading rooms, audio-visual facilities, and many other facilities [7].

In the past few decades, we witness the emergence of ICT that shift of the library services and functions. Many information previously only available in printed format becoming accessible in electronic formats [8]. The original concept of library are changed, books were switched by information whereas those information are for dissemination not for preservation [8].

Libraries in this modern era should improve its facilities and functionality [8–10]. It should provide convenient and comfortable seating areas. The collection should be organized in a way that is easily to be retrieved both the printed and non-printed resources collection. It should start to digitalize its collections to allow computer to process the information contained and allow for faster information searching. It should also provide more services, both online and offline one, for examples: providing high-speed Internet terminals, a mobile app to allow the member to get information and have a virtual tour of the collections. It should organize innovative activities and learning programs in order to attract more people to come.

This paper discusses the development of a mobile application that could enhance or improve the user experience on a traditional as well as hybrid type of university library. The apps will allow them to browse collections, book or borrow books, pay late returns penalty fees, and several other services.

## 61.3 Mobile Apps Development Technologies

There are a number of mobile platforms or operating systems available in the market: IOS, Android, Windows Phone, Blackberry, and some others. Based on May 2015 market survey result [11] shown on Table 61.1, Android leads in a very significant number which is 78.0 %, compared to the 18.3 % of iOS which is the closest rival. The number is declining from 81.2 % on previous year, it still very strong for other competitors to catch up.

**Table 61.1** Smartphone OS market share, Q1 2015

Period	Android (%)	Ios (%)	Windows Phone (%)	BlackBerry OS (%)	Others (%)
Q1 2015	78.0	18.3	2.7	0.3	0.7
Q1 2014	81.2	15.2	2.5	0.5	0.7
Q1 2013	75.5	16.9	3.2	2.9	1.5
Q1 2012	59.2	22.9	2.0	6.3	9.5

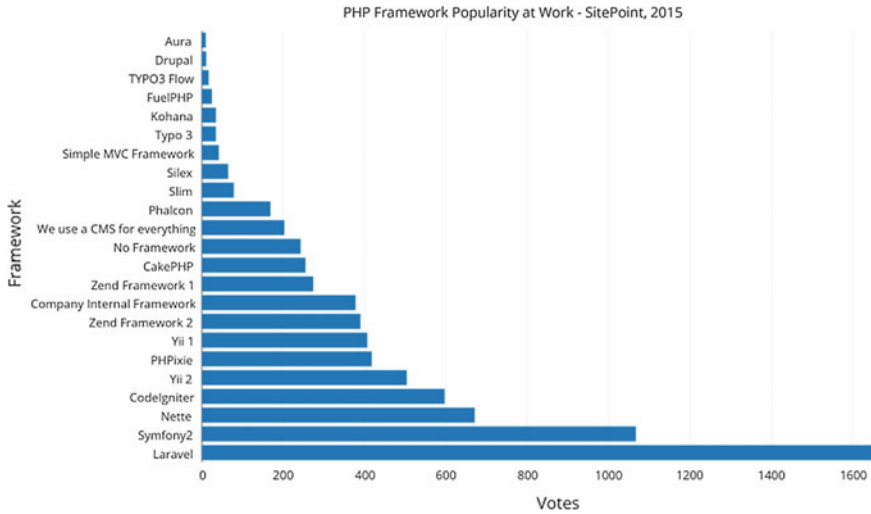


Fig. 61.1 PHP frameworks market share [12]

There are some technologies that support the development of mobile applications. There are many frameworks that support mobile apps developer to create apps in an easier and faster way. The emerging cloud technologies also a major technology that support the scalability of the backend feature.

Mobile apps usually need a backend application and database. For this purpose, there are some frameworks available in the markets that support developers for a faster development stage. Many of those frameworks are using PHP as basis the scripting language, for examples: Laravel, CodeIgniter, Symphony, Yii, and many more. Laravel is one of the most popular and widely used in the last couple of years as seen on Fig. 61.1.

Laravel is an open-source framework developed by Taylor Otwell. Laravel designed to facilitate the developers in their applications by providing features such as security, RESTful routing, queue, unit test, schema builder, and many other features. There are many advantages of using Laravel Framework, such as: a large community, easy to understand documentation, supports PHP dependency by using the composer.

There are a number of plugin that works on top of Laravel to support this project development, such as Iron.io and Laravel Dispatcher. Iron.io is a cloud-based service IaaS (Infrastructure as a Service) that provides asynchronous message queue and task. This service is useful to ease the job on the server that requires heavy work, such as: large-scale email delivery, delivery notification, date checks, and more. Dispatcher is useful for scheduling purposes that allow the application to run artisan command without the need to create cron tab configuration manually.

Another technology required in typical mobile apps is notification. For this purpose developers can use Google Cloud Messaging (GCM). GCM provide some Application Program Interface (API) that provides the interface between the





**Fig. 61.2** System design

application and the server. The cloud-based messaging services can transmit data from the server into the smartphone in real time. It handles the queue and delivery to the target device.

To improve the application networking performance, there is an HTTP Library called Volley. This library can help Android to perform efficiently and fast networking. There are many advantages of using a Volley: automatic scheduling, simultaneous multiple networks request, network demand priorities and cancellation, and the availability debugging and tracing tools.

## 61.4 Analysis and Design

The features provided in the system decided based on a study of 31 respondents of the mobile information system prospective users. Additionally, a comparison to a similar web based information system also conducted. Based on that study, the main features that should be provided in the system are: user authentication, lending system, late return penalties, notification system, loan history, collections, loan extension, and delivery system.

The mobile library information system application consists of 2 different systems: the actual Android application and web based administration application.

Figure 61.2 depicted the system architecture design where the Android apps will be able to communicate with the server using the Internet connection. The server then will be able to communicate with database server as well as to communicate with Google Cloud Messaging service that will be able to send push notifications to the Android device.

### 61.5 Results and Discussions

The application developed using variety of technologies previously mentioned. Android was chosen as the target mobile platforms due to its popularity [11]. The Android SDK was used as the basis for the Android mobile application development, whereas PHP and Laravel frameworks as the basis for the server-side scripting language and the administration application features respectively. Additionally there are some other technologies used, including: Google Cloud Messaging (GSM), Laravel Dispatcher, Iron.io, and Volley HTTP Library.

Figure 61.3 depicted some of the mobile application interfaces: the main interface for user authentication (a), navigation drawer (b), book collection (c), and book details (d). The interfaces were designed using the latest Flat UI theme found on the latest Android versions.

Figure 61.4 shows the front page of administration applications upon successful login attempt to the system. The administration dashboard was developed using responsive web technology. The page also uses of flat color scheme to introduce the modern look and feel.

Upon completion of the implementation stages, a system test was conducted both on the mobile application on the client side as well as the administration application. To test the Android application for the client side, a survey was carried out to get feedback from prospective users. Another test was performed with the university's librarian for the administration application.

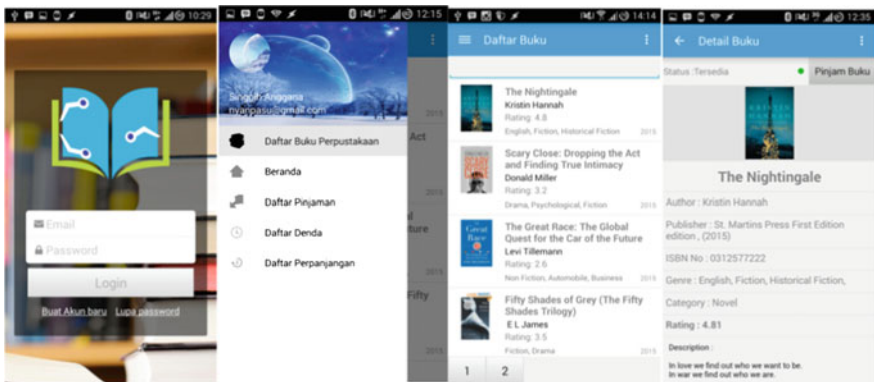


Fig. 61.3 Android mobile apps interface, left to right a, b, c and d

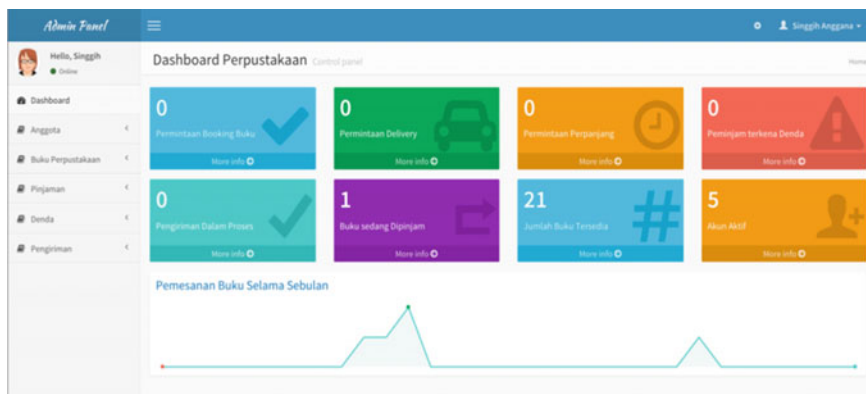


Fig. 61.4 Administration application interfaces

The users agree that this mobile application helped them to use the university library services remotely. They could find books, view loans list, book some books, borrows books, as well as to extend the loans. The use of native mobile apps also allows them to get notifications for some services.

The client side mobile application users agreed that the application was easily understood and they did not find any difficulties on using it. While some parts of the interface might need improvement in terms of usability, but in general the application was simple enough to use. They also did not have any problems on finding books from the collection, even though if there were more filter criteria provided the feature might be more helpful. Borrowing books also easily performed while they demand more information about book currently on loan.

The librarians test the administration system provided in the back-end side based on the user scenarios. The scenarios including new user account registration, book loans, lost item, late return fines, fines payment, and other scenarios. The staffs found that the application user interface was easy to use, the button arrangement as well as the naming were easy to understand. Book loans through the mobile phone were considered as an innovative feature not previously available in any similar applications. Book loan extension might needs more consideration to avoid misused. Ultimately, the challenge to use the system is the integration of the system with currently running system, the security features to ensure the data safety.

## 61.6 Conclusion

Information and Communication Technology can be used to enhance the user experience of using traditional or hybrid library services through an Android mobile application. The apps can be used to enable the user to check the book availability as well as to borrow the book without having to go to the library. The collaboration

with other services such as delivery service may also boost the user experience. The developed application works according to the intended functionality, based on features decided on the design and analysis stages. Android features such as notifications on the mobile devices also added another functionality that is not found in traditional web based information system. Future development of the system might be needed, to allow the member to access other libraries using the same application.

## References

1. Internet World Stats Website, INTERNET USAGE STATISTICS The Internet Big PictureWorld Internet Users and 2015 Population Stats [Online]. Available: <http://www.internetworldstats.com/stats.htm>
2. Kemp, S.: We Are Social—Digital, Social & Mobile Worldwide (2015). <http://wearesocial.net/blog/2015/01/digital-social-mobile-worldwide-2015/>
3. Rawat, M.K., Alam, P., Jawaid, A.H.: Digital library: infrastructure and service. In: 2nd International CALIBER-2004, New Delhi, 11–13 Feb 2004
4. Keller, M.A.: Establishing a Digital Library, White Paper. Stanford Universities (2009)
5. Liu, Z.: Print vs. electronic resources: a study of user perceptions, preferences, and use, Elsevier. *Inf. Process. Manag.* **42**, 583–592 (2006)
6. Merriam Webster, Library (2015). <http://www.merriam-webster.com/dictionary/library>
7. Dictionary, Library (2015). <http://dictionary.reference.com/browse/library>
8. Verma, M.K., Verma, N. K.: Concept of hybrid, digital and virtual library: a professional approach. In: INFOLIB, vol. 7, no. 1–4, Mar–Dec 2014
9. Korbey, H.: In the Digital Age, What Becomes of the Library? (2013). <http://ww2.kqed.org/mindshift/2013/05/31/in-the-digital-age-what-becomes-of-the-library/>
10. Matthews, S.: Why Do We Still Need “libraries”? We Don’t! (2014). <http://21stcenturylibrary.com/2014/02/03/why-do-we-still-need-libraries-we-dont/>
11. International Data Corporation (IDC), Smartphone OS Market Share, Q1 (2015). <http://www.idc.com/prodserv/smartphone-os-market-share.jsp>
12. Skvorc, B.: Best PHP Framework for 2015—SitePoint Survey Results (2015). <http://www.sitepoint.com/best-php-framework-2015-sitepoint-survey-results/>

## Chapter 62

# Multi Level Filtering to Classify and Block Undesirable Explicit Material in Website

Mohammad Iqbal, Hifshan Riesvicky, Hasma Rasjid  
and Yulia Charli

**Abstract** The growth of Internet opens wide opportunities for content production in various types of internet sites that provide information of various categories. For students or kids, ease of access to the internet site have a positive impact to provide days connectivity of user to the content that they needed for their study, but the other side, it also cause a negative impact when they accessing sites that provide undesirable explicit material such as pornographic content. During this time, pornographic content can be easy inserted through the text or images in page of internet sites. Therefore, we need a system that can filter information related to pornography and can prevent users who are not old enough to access pornographic content. To overcome this issue, we develop an online client-side filtering system that allows the user to perform a domain filtering, URL filtering, keyword filtering, and skin detection filtering. Also we proposed a hybrid skin color detection technique to overcome the failure of detecting skin when the images in close-up or scene mode. This system consist of classification using n-gram tokenizer for text and haar algorithm and skin chromaticity at HSV (Hue Saturation Value) and Normalized RGB color spaces for images. The applications created using software development tools such as flowchart and Unified Modelling Language (UML), while for the programming language using PHP, CSS, Javascript and using MySQL database.

**Keywords** Browser based filters · Domain and URL filtering · Keyword filtering · Pornography · Skin detection

---

M. Iqbal (✉) · Y. Charli  
Faculty of Computer Science and Information Technology, Gunadarma University,  
Depok, Indonesia  
e-mail: mohiqbal@staff.gunadarma.ac.id

H. Riesvicky · H. Rasjid  
Magister Management Information System Program, Gunadarma University,  
Depok, Indonesia

## 62.1 Introduction

Definition of pornography according to Merriam-Webster Dictionary [1] is the depiction of erotic behavior (as in pictures or writing) intended to cause sexual excitement, material (as books or a photograph) that depicts erotic behavior and is intended to cause sexual excitement and the depiction of acts in a sensational manner so as to arouse a quick intense emotional reaction (the pornography of violence).

There is a large number of undesirable explicit material (Pornography) available in the Internet. Pornography materials such as texts, images or any documents are easy to access using any public search engine such as Google or Yahoo. Online pornography's have a wide effects on adults work and family lives, but even more about its impact on children and teens. So, in this time, controlling access to the Internet by means of filtering software has become a growth industry around the world [2]. The formulation of the problem to be pointed as the research material consists of several questions as follows:

1. How to design and implement a pornographic content websites classification by applying tokenization method, filtering method, face detection and skin detection?
2. Is the N-gram algorithm, haar algorithm and skin chromaticity detection can be arranged and used to support the classification process pornographic content websites such as texts and images?

## 62.2 Research Method

The main contributions of our work are as follows:

1. Design and implementation of a pornographic content recognition system which achieves and provides information of classification pornographic content websites to the user with clear information.
2. Block a user who is not old enough to access pornographic websites that will be addressed.

The research method used in this study are:

1. Descriptive analysis of previous research publications. This method is implemented by analyzing the results of previous research publications, in order to integrate these findings and get a clear explicit material patterns in website and how to filtering it. We use a descriptive analysis to determine the characteristics of a variety of research consisting of:

- (a) Conventional or mechanical filtering aspects: Process building two lists of either URLs or IP addresses, first list is called blacklist which consists of forbidden web sites to access, and Whitelist is made up for allowed websites. When a new request come to access a new web page, the analysis is made by the matching the result.
  - (b) Text-based filtering aspect: Generally, it works on sensitive texts which consists of specific words or phrases related to pornographic terms such as “adult” or “sex”. Then, we try to extract keywords from texts using many classification methods.
  - (c) Image-based filtering aspect: In this step, we study the image processing and pattern recognition fields [3] to find a novel way to filter images with pornographic sensitive in web pages.
2. Design of the prototype system, includes: Design of web application using design tools flowchart and Unified Modelling Language (UML) tools, while for the programming language using PHP, CSS, Javascript and using MySQL database, and doing a black box testing.

## 62.3 Descriptive of Data Mining and Image Registration Technique

### 62.3.1 N-Gram Algorithm

There are wide varieties of texts classification or any other further processing techniques. One of them is an N-Gram extraction that include intermediate step in the process of classification or clustering. In the previous research, N-Grams can be a lightweight method, instead of using grammatical phases alike Non Polynomial (NP) in indexing the texts, or even can improve Named Entity Recognition (NER) [4]. N-Gram methods are general, there are two type of N-Grams: Character N-Grams (word substrings), usually used in language identification, and word/token N-Grams (sequences of words/tokens), used in many text classification/clustering tasks. In this research, we use N-Gram Tokenizer. The “N” is can unigram, bigrams or trigrams for some applications, but we try the max size for a particular task. The number N-grams sequences is related to the performance accuracy and efficiency. Regarding to the performance, the size “N” of the N-Grams depend on the whole classification/clustering task. Regarding to the efficiency, the big size “N” can cause slow system (for finding the N-Grams and for using them).

N-Grams can reduce input data size. Clustering and classification of the N-Grams is in the next step. In this situation, N-Gram method can be faster than Named Entity Extraction, since NER requires training on NLP extracted Noun Phrases of interest. The use of N-Gram techniques to perform URL filtering, domain filtering, and keyword filtering related to the pornographic content can be

seen in the following illustration. N-grams are pieces of  $n$  characters in a given string or piece of  $n$  words in a given sentence. For example, the word “teknik” n-grams will be obtained as shown in Table 62.1.

Blank character “\_” is used to represent space in front and at the end of the word and for the word-based n-gram example is as follows. Sentence: “*N-gram adalah potongan n karakter dalam suatu string tertentu*”. It can be seen in Tables 62.1 and 62.2.

The next step after pre-processing of the documents in the training set, is learning it documents. Step-by-step of learning is carried out as follows:

1. The obtained features (token) are transformed into the form of n-grams with  $n = 2, 3,$  and  $4$ .
2. Enter each obtained n-gram in the hash table as a counter to count the frequency of n-grams in the document. The hash table using conventional duplication handling mechanism ensure that every n-gram has its counters respectively.
3. When appears n-gram “TE” again, then the frequency (counter) “TE” plus 1, no longer add a new row in the hash table. So that duplication can be avoided.
4. Once everything is calculated, remove all n-grams and the amount appearance.
5. Sort N-Gram in reverse order based on the number of occurrence.

The end result of the above process is the *N-gram frequency profile* of the document (for each category in the training set). For testing this result, we can measure a distance profile with the profile category of the documents that will be known category [5].

**Table 62.1** Example cutting N-gram-based on character

Name	N-gram Character
Uni-gram	T, E, K, N, I, K
Bi-gram	_T, TE, EK, KN, NI, IK, K_
Tri-gram	_TE, TEK, EKN, KNI, NIK, IK_, K_ _
Quad-gram	_TEK, TEKN, EKNI, KNIK, NIK_, IK_ _, K_ _ _
etc...	

**Table 62.2** Sample cutting N-gram-based on words

Name	N-gram Words
Uni-gram	<i>n-gram, adalah, potongan, n, karakter, dalam, suatu, sring, tertentu</i>
Bi-gram	<i>n-gram adalah, adalah potongan, potongan n, n karakter, karakter dalam, dalam suatu, suatu string, string tertentu</i>
Tri-gram	<i>n-gram adalah potongan, adalah potongan n, potongan n karakter, n karakter dalam, karakter dalam suatu, dalam suatu string, suatu string tertentu</i>
etc...	



### 62.3.2 Weighting Using *tf-idf*

Term Frequency (*tf*) factor is a factor to determine the weight of a term in a document based on the amount it appears in the document. A number of occurrences of a word (term frequency) assigning to weighting to the word. Greater occurrences number of a term (*high tf*) in the document have a meaning of greater document weight or it will provide greater suitability values.

Inverse Document Frequency (*idf*) factor is the reduction of the dominate term which often appear in various documents. This factor is necessary because the terms that have appeared in various area of documents can be considered as a common term, and can be specified as un-important value. Instead, the factors rarely appear of word (*scarcity*) in a collection of documents should be considered in assigning weights [6, 7].

The *tf-idf* method is a term weighting method that is widely used as a method of comparison to the new weighting method. In this method, the calculation of the weight of term *t* in a document is done by multiplying the value of the *term frequency* with *inverse document frequency*. On the *term Frequency (tf)*, there are several types of formulas that can be used which are:

1. *Binary tf*, checking whether a word exists or not in the document. If it is found, it will be rated with one, if not, it is given a zero value.
2. *Raw tf*, *tf* value is given by the number of occurrences of word in a document. For instance, if a word appears five times then the word will be rated five.
3. *Logarithmic tf*, this formula is used to avoid the dominance of documents that contain little word in the query, but has a high frequency.

$$tf = 1 + \log(tf) \quad (62.1)$$

4. *Normalization tf*, using a comparison between the frequencies of a word with the total number of words in the document.

$$tf = 0.5 + 0.5 \times tf / \max tf \quad (62.2)$$

Inverse Document Frequency (*idf*) is calculated using equation:

$$idf_j = \log(D/df_j) \quad (62.3)$$

where:

*D* is the sum of all the documents in the collection

*df<sub>j</sub>* is the number of documents that contain *term t<sub>j</sub>*

In the research [6], the equation to be used for the calculation of term frequency (*tf*) is *raw tf*. Thus the general formula for the *tf-idf* is the incorporation of raw

calculation formula *tf-idf* formula (Eq. 62.3) by multiplying the value of term frequency (*tf*) with inverse document frequency (*idf*):

$$\begin{aligned} w_{ij} &= tf_{ij} \times idf_j \\ w_{ij} &= tf_{ij} \times \log(D/idf_j) \end{aligned} \quad (62.4)$$

where:

$w_{ij}$  is term weight  $t_j$  against document  $d_i$

$tf_{ij}$  is sum of term  $t_j$  in the document  $d_i$

D is sum of all documents in the database

$idf_j$  is sum of documents is containing term  $t_j$  (at least one word that is *term*  $t_j$ ).

### 62.3.3 Skin Detection

Skin detection technique perform by assuming skin color in certain range of values in some coordinates of a color space. This algorithm develops a skin color model that have a low false positive rate and high detection rate. It is mean, the skin detection algorithm can minimize the amount of non-skin pixels classified as skin, while detect most skin pixels. In the previous research in computer vision field, several studies have been made to detect the behavior of skin chromaticity at different color spaces such as RGB Color Space [8], the HSV (Hue Saturation Value) color Space, YUV and Normalized RGB Color Space, [9–11]. The research of [12], by using combination of YUV and YIQ color spaces, the results are more robust than other color spaces. The Duan et al. method fails to detect skin, when the background of image contains similar pixels to human skin pixels ( $20 \leq \text{intensity} \leq 90$ ) and it is not belong to the skin region. This drawbacks can be solved by Girgis et al. [13] using the saturation parameter. Research with another approach was found by using wavelet transform to initial processing and image sharpening result to detect a pornographic image recognition on the content of the information [14]. The success rate of pornographic image recognition using wavelet transform is 67.02 %.

In this research, we implement the simplest algorithms for detecting and extracting skin regions from images, with additional step to perform face detection in 3 region of deep (near to camera, medium and far away to camera). After face detection process using Haar detect object function, the next process is finding coordinates of the face object. Afterward, the system create X1 and Y1 variables that contain the value of the X and Y rectangle positions. The system also create X2 variable that contains the sum of X1 variable with the width of the rectangle, and also create Y2 variable that contains the sum of X1 variable with the height of the rectangle. These variables can be used as a reference to know the images in a close-up mode or in a scene mode. When the images known as scene modes, then we can run skin detection algorithm.

The algorithm of this technique can be described as follows:

1. Extract Images found in the website homepage.
2. Execute the Haar-like to detect a face [15].
3. Execute the Skin Detection Algorithm: Locate skin regions based on the detected skin pixels based on Girgis at 2002 [13].
4. Analyze the skin regions for clues of Pornography Decision as follows:
  - a. If skin color pixels are between 5 and 20 % it indicates a human being is most probably in the image.
  - b. If the percentage of skin pixels are between 20 and 25 %, it indicates more than likely Pornography image.
  - c. If the percentage of skin pixels are more than 25 %, it indicates a Pornography image.

### 62.4 Design of Prototype System

Flowchart in Fig. 62.1 illustrates the flow of the application process for website classification. The interface design is distinguished because there is a difference in function between user groups and admin group (illustration can be seen in Fig. 62.2). There are some activities that exist in the program flow:

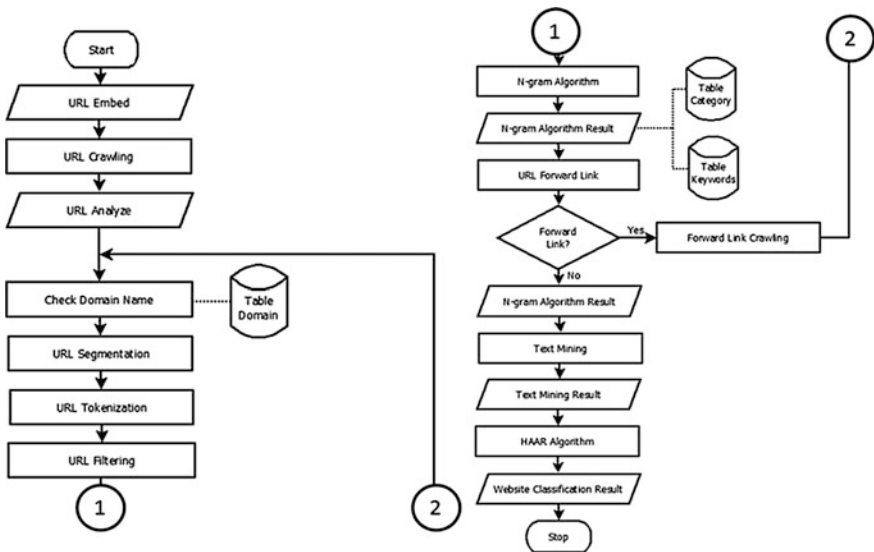
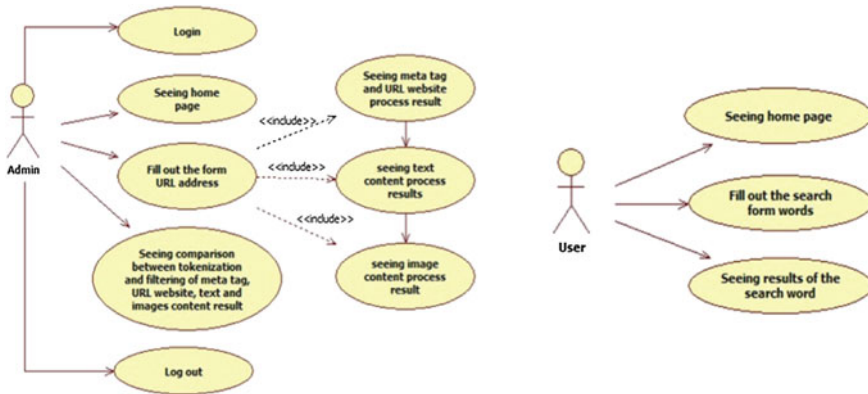


Fig. 62.1 Application program flowchart



**Fig. 62.2** Use case diagram for admin (*left*) and Use case diagram for general user (*right*)

1. Embed URL, is the process of entering the URL of the website that will check the results of the classification.
2. Crawling URL, is the process of making the entire URL of the website in questions.
3. Analyze URL, is the process of analysis of all URLs obtained from the process of crawling URLs.
4. Check Domain Name, is the process of checking the domain name in the URL of the website that will be matched with the domain Table.
5. URL Segmentation, is a segmentation process between the domain name, document path and document name are distinguished by a slash (/).
6. URL Tokenization, is the process of transforming into a piece of word segmentation result.
7. URL Filtering, is the process of removing all that is not associated with words such as removing the top level domain (.co.id, .web.id, .com, .net, etc.), remove the special characters (:, /, ., -, etc.) and remove common words (www, http or https, .html, etc.).
8. N-gram algorithm, is the cutting process of letter word that starts from 3 to 8 letters and the results will be displayed in the output.
9. Forward URL links, is the process of reading out the URL of the website. If there is a forward link, then the process is done the same as the process of checking the website URL in the input and results will be displayed in the output.
10. Text Mining, is the process of checking the word-based content from the website URL in the input and the results will be displayed in the output.
11. Haar algorithm, is the process of reading face detection and the skin detection of an existing image on the website URL in the input.
12. The classification process will be completed if there are no word, text and images processed. The end result will show that the website URL in the input will come in the type of classification.

Designing a database on a web application consists of a database that is db\_cindex. There are 8 kinds of tables consisting of table\_index, table\_cat\_index, table\_keywords, table\_url, table\_url\_status, table\_meta, table\_http\_code and table\_user.

### 62.5 Implementation and Evaluation

All modules in the website classification pornographic content on the user and admin group have been through the process of testing. Functional testing will be explained as follows:

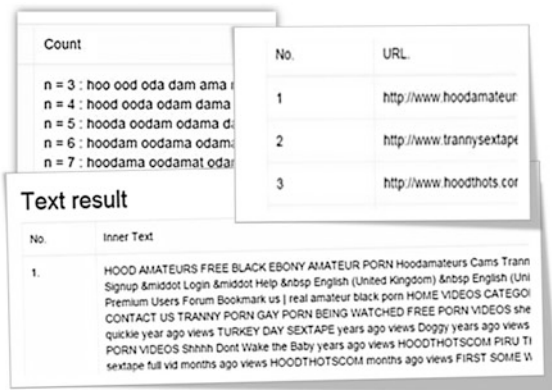
1. Testing User Interface Admin and General User Login/logout Form, Search Words Result Page and home Page.
2. Testing Admin interface: Meta Tag and URL Website Result Process, text Content Result Process, Image Content Result Process and Meta Tag, URL Website, Text and Image Comparison Result Process.

First testing is to answer how to display the correct results of the tokenization and filtering process from the URL website in the input. The results are displayed in the form of a table containing the words and the weight of each word. Weights will be used to add up the whole word. The stages of process of analysis pornography sites is illustrated in Fig. 62.3.

The search using the N-gram performed up to the value of N = 5 by considering the time needed to completed the search. When there is no more words or images processed, the classification results will be incorporated into the domain table, the table and the category table as a reference search keywords in the future.

To detect the skin, we add before face detection step to determine the presence in the region where the person is based on the z-axis by a large fraction of the rectangle marker face (Fig. 62.4).

**Fig. 62.3** N-gram segmentation (*top-left*), forward link (*top-right*) and text mining of pornography website N-gram result page



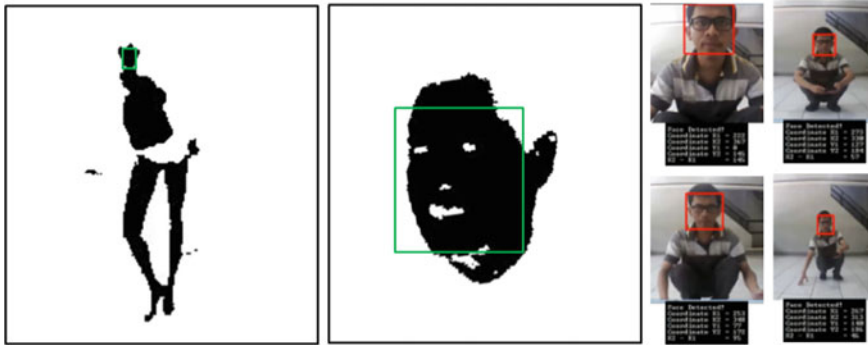


**Fig. 62.4** Illustration problem in skin detection (*left and center images*) [16] and face detection to solve misclassified of skin detection in center image (*right image*)

## 62.6 Conclusion

This paper presents an online client-side filtering application that allows the user to perform multi level combination of pornographic filtering techniques such as domain and URL filtering, keyword filtering and skin detection filtering. We implement some established skin detection techniques for color images and combine it with haar-like features for face detection as reference to find skin area, as well as markers of the object in the image in the mode close up/macro or in the scene modes. The experimental results show that our proposed filtering system is working as planned. For future research, this system can be developed to discover text content more details into internal links that exist in a website, because in this study, keyword search performed on the first level of a website only (in homepage). Moreover, it is still possible to improve run time efficiency in face recognition and skin detection using other algorithms.

## References

1. Anonim: <http://www.merriam-webster.com/dictionary/pornography>
2. Sholeh, M.: Analisis Pencegahan Akses Website Kategori Dilarang. *Jurnal Teknologi* **2**(2), 117–123 (2009)
3. Cao, L., Li, X., Yu, M., Liu, Z.: Naked people retrieval based on adaboost learning. In: *Proceedings of IEEE International Conference on Machine learning and Cybernetics*, 4–5 Nov 2002
4. Tandon, N., De Melo, G.: Information extraction from web-scale N-gram data. In: *SIGIR 2010 Web N-Gram Workshop* (2010)
5. Ramos, J.: Using TF-IDF to Determine Word Relevance in Document Queries, Technical report, Department of Computer science. Rutgers University (2000)
6. Wu, H., Luk, R., Wong, K., Kwok, K.: Interpreting TF-IDF term weights as making relevance decisions. *ACM Trans. Inf. Syst.* **26**(3), 13 (2008)

7. Zafikri, A.: Implementasi Metode Term Frequency Inverse Document Frequency (TF-IDF) pada Sistem Temu Kembali Informasi, Univesitas Sumatera Utara (2008)
8. Kakumanu, P., Makrogiannis, S., Bourbakis, N.: A survey of skin-color modeling and detection methods. *Pattern Recogn.* **40**, 1106–1122 (2007)
9. Albiol, A., Torres, L., Delp, E.J.: Optimum color spaces for skin detection. In: *Proceedings of the IEEE International Conference on Image Processing*, pp. 122–124 (2001)
10. Jayaram, S., Schmugge, S., Shin, M.C., Tsap, L.V.: Effect of color space transformation, the illuminance component, and color modeling on skin detection. In: *Proceedings of the 2004 IEEE Computer Society Conference on Computer Vision and Pattern Recognition*, vol. 2, pp. 813–818 (2004)
11. Jedynak, B., Zheng, H., Daoudi, M.: Statistical models for skin detection. In: *IEEE Workshop on Statistical Analysis in Computer Vision, CVPR 2003 Madison, Wisconsin* (2003)
12. Duan, L., Cui Gao, G.W., Zhang, H.: Adult image detection method base-on skin color model and support vector machine. In: *Asian Conference on Computer Vision*, pp. 797–800, Melbourne, Australia (2002)
13. Girgis, M.R., Mahmoud, T.M., Abd-El-Hafeez, T.: An approach to image extraction and accurate skin detection from web pages. *Int. J. Comput. Sci. Eng.* **1**, 367–375 (2007)
14. Wijaya, G.P.S., Widiartha, I.B.K.: Pengenalan Citra Porno Berbasis Kandungan Informasi Citra (Image Content). *Jurnal Teknik Elektro* **4**(2), 80–86 (2004)
15. Jones, V.: Rapid object detection using a boosted cascade of simple features. In: *Computer Vision and Pattern Recognition* (2001)
16. Jones, M.J., Rehg, J.M.: Statistical color models with application to skin detection. *Int. J. Comput. Vis.* **46**, 1 (2002)

# Chapter 63

## Query Rewriting and Corpus of Semantic Similarity as Encryption Method for Documents in Indonesian Language

Detty Purnamasari, Rini Arianty, Diana Tri Susetianingtias  
and Reni Diah Kusumawati

**Abstract** Encryption and decryption can be used to the security of data or important documents. Many methods have been developed to perform encryption and decryption. In this article, the research is conducted to develop a corpus of semantic similarity in Indonesian, and query rewriting technique that is used as one method of encryption and decryption. Corpus of semantic similarity is used to find a new query that will form a new document encryption, and the technique that is developed in this study is to secure documents in Indonesian. Encrypted document is using query rewriting techniques and corpus of semantic similarity, it will be a document with a good sentence structure, so it looks like the original document and is not expected to attract the attention of hackers. The categorization of documents was also performed on the stage of the encryption.

**Keywords** Corpus · Document · Encryption · Security · Semantic similarity · Query rewriting

### 63.1 Introduction

Delivery of data or documents in text form is becoming increasingly easy without knowing the distance and time, since technology and science have been developing. E-mail was one of example from the technology that give the easy way to send an important document.

Advances in technology of internet is accompanied also by the crimes committed by this technology, as it is known among them is the term hacker. Hacker is

---

D. Purnamasari (✉) · R. Arianty  
Information System Department, Gunadarma University, Jakarta, Indonesia  
e-mail: detty@staff.gunadarma.ac.id

D.T. Susetianingtias  
Computer System Department, Gunadarma University, Jakarta, Indonesia

R.D. Kusumawati  
Management Department, Gunadarma University, Jakarta, Indonesia



someone who goes into a computer system without permission and usually over a network/internet to commit crimes such as identity theft, and theft of intellectual property [1].

One way that can be used to secure the data/documents from hackers is to encrypt a document. Encryption is the process of securing the information to make that information cannot be read without the aid of special knowledge, while Decryption is the reverse of encryption is the process of converting encrypted data that has been returned to the original data, so it can be read or understood back. Two keys are used, namely: the public key used for encryption and private key used for decryption [4].

A study on the security of file transmissions using the RSA algorithm has been modified with a public key of an asymmetric method [5]. Text watermarking which combines images and text to encrypt documents can also be done to maintain the security of data as it is done by Jaseena et al. [6].

In this article the query rewriting techniques are developed by using a corpus of semantic similarity in Indonesian language. This technique is used as a method of encryption and decryption of the document in Indonesian language.

Query rewriting is the stage of the information search process in which the initial query statement users enhanced by adding the term [9].

Query rewriting is used as a technique to perform encryption and decryption assisted with the corpus of semantic similarity in Indonesian language, and in this article also described the steps being taken to build the corpus.

Semantics Similarity is a method to perform a search equivalence meaning of concepts/words. Semantics Similarity provides rules for interpreting the syntax that does not give meaning directly but limits the possible interpretations of what is stated [3].

Encryption method using query rewriting technique provides results in the form of encrypted document was still good, so it is not known that in fact the document has been encrypted.

## **63.2 Research Methods**

### ***63.2.1 Stage for Developing of Corpus Semantic Similarity***

Corpus is a collection of words that arranged systematically. Research on the corpus by using semantic similarity ever undertaken, and this corpus in English [7].

In this research, the corpus of semantic similarity is the corpus that contain the words in Indonesian and contain the value of its semantic similarity. Measurement of semantic similarity between two words is done by using the method of Jiang and Conrath, since the calculation of semantic similarity with Jiang and Conrath (JNC) showed the best results [2, 10].

**Fig. 63.1** Stages to developing of corpus

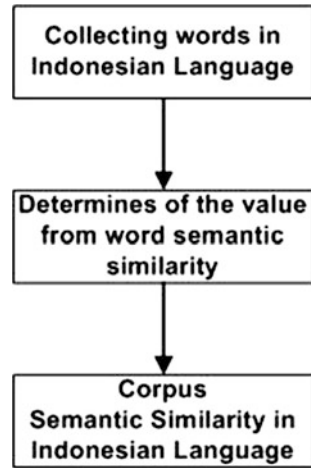


Figure 63.1 is general stages to develop of the corpus of semantic similarity in Indonesian.

General stages to develop of the corpus in this research as shown in Fig. 63.1 are:

1. Collection of words in Indonesian by using Indonesian thesaurus dictionary official printed by Eko Endarmoko and published 2006 by Gramedia Pustaka Utama (GPU). In this step, it is grouped based on similar meaning words.
2. Based on the words collected in step 1, then the value of semantic similarity is looked for using the method of Jiang and Conrath.
3. Input the words and the value of semantic similarity to the corpus.

The corpus be equipped with the value of semantic similarity, because this value will be used at the time of the query rewriting to perform encryption and decryption of the document in Indonesian language.

### ***63.2.2 Query Rewriting as Encryption Method***

Query rewriting in this article for the encryption method is as follows:

1. Reading of the text/document.
2. Determinate category for theme/content of the document based on the number of words contained in the document.
3. Separate the sentence in paragraph.
4. Separate the sentence structure.
5. Create a public key by look from the category that has been done in step 2 and look at the value of semantic similarity in the corpus.

6. Rewrite a new query into a new document which is the result of encryption. This document already contains a new query based on a formula obtained in step 6.
7. Create a private key to restore the encrypted document into the original document.

Document does not only contain one sentence, but more than one sentence. Therefore, step 2 takes categorization for theme/content of the document. This is done, in order to document the results of encryption consists of sentences that compose a new document that is encrypted to keep in touch between sentences.

Categorization in step 2 of this research was created by counting the number of words that appear in most documents.

Separation sentence in step 3 is conducted by the following method [8]:

1. Position to read the document starts from the beginning of the document character.
2. If punctuation characters beside the point (“.”) is found, then the character will be deleted, and if reading documents find the character dot (“.”) or a question mark (?) Or an exclamation mark (!), then separate sentences of position initial reading of the document until the character point/question mark/exclamation points are found and saved to a temporary database.
3. After separating the sentence, then move the starting position and read documents on the initial character of the next sentence.
4. Back to step (2) and step (3) and continue this separation sentence, until the end of the document or until characters in the document are no longer found.

Separation of sentence structure in step 4 of this research is done by determining word as the subject, predicate, object, preposition, and adverb.

Text documents is a series of paragraphs that consists of many sentences. The sentence itself is a series of words that can express their ideas, thoughts, or feelings. The sentence is the smallest unit of language that expresses a complete thought, either by writing or verbally. In the sentence should have at least the ‘Subjek/S’ (subject) and a ‘predikat/P’ (predicate). If it does not have a subject and a predicate, it is not called the sentence but called phrases. Elements of sentences in Indonesian is the ‘Subjek/S’ (subject), ‘Predikat/P’ (predicate), ‘Objek/O’ (Object), and ‘Keterangan/K’ (adverb) [8].

Elements of the sentence has been known, so that the preprocessing created database containing (i) prepositions, (ii) subject, (iii) object, and (iv) adverb, and (v) predicate

A public key to change the original document into a document that has been encrypted by looking at the categories, and refers to the value of semantic similarity in Indonesian corpus.

A public key can be created by the user to determine the value of semantic similarity that will be used based on the desired level of closeness meaning. Once the desired value has been determined, then the query rewriting as a result of the encryption is done.

Documents that have been encrypted can be returned into the original document (the decryption process) by creating the complement from a public key.

## 63.3 Results and Discussion

### 63.3.1 Corpus of Semantic Similarity

Creating corpus of semantic similarity is done by studying the Indonesian language syntax and semantics in Indonesian. The value of semantic similarity is done with reference to the thesaurus dictionary that has been officially published, and based on the dictionary.

For the examples of words that will be included in corpus is the word ‘politik’ (politics). Based on the thesaurus dictionary, the word ‘politik’ (politics) have the same meaning with three words, namely:

1. Word ‘*Garis haluan*’ (outline)
2. Word ‘*Kebijakan*’ (wisdom)
3. Word ‘*Strategi*’ (strategy)

Then calculating the value of semantic similarity by using the method of Jiang & Congrath and WordNet similarity [11], which is conducted between 2 words found in the dictionary thesaurus (presented in Table 63.1).

After the value of semantic similarity is found, then the words and the value is stored into the corpus.

The categories in step 2 is used in the encryption methods to produce a document that contains the encryption result interconnected constituent sentences.

The categories are also set in advance as preprocessing of this research. Documents can be categorized for example:

1. categorized ‘*politik*’ (politics)
2. categorized ‘*teknologi informasi*’ (information technology)
3. categorized ‘*ekonomi*’ (economics)

**Table 63.1** Example for the value of word semantic similarity

No	Word 1	Word 2	Value
1	‘Politik’ (politics)	‘GarisHaluan’ (outline)	0.066
2	‘Politik’ (politics)	‘Kebijakan’ (wisdom)	0.077
3	‘Politik’ (politics)	‘Strategi’ (strategy)	0.087

### 63.3.2 Encryption and Decryption

In the encryption process, paragraphs of a document is separated between the sentence. The following is an example of a sentence in Indonesian:

*Alat untuk e-counting dapat disimpan di kantor desa.*

(Tools for e-counting can be stored in the village office)

The example above is a sentence that will be separated by the word, and 8 words are found. Each word will be checked into a database that has been prepared in preprocessing to determine its position in the sentence structure, whether as a subject, predicate, object, adverb, preposition. The words are:

(1) “Alat” (tools) as a ‘subjek’ (subject), (2) “Untuk” (for) as a ‘kata depan’ (preposition), (3) “E-counting” as a ‘keterangan’ (adverb), (4) “Dapat” (can be) as a ‘keterangan’ (adverb), (5) “Disimpan” (stored) as a ‘predikat’ (predicate), (6) “Di” (in) as a ‘kata depan’ (preposition), (7) “Kantor” (office) as a ‘keterangan’ (adverb), (8) “Desa” (village) as a ‘keterangan’ (adverb).

Once it is separated by the structure of the sentence, look for a new query from the word of the original document by using a corpus of semantic similarity. Steps to find a new query that will be used to prepare encrypted documents are as follows:

1. Define categories of documents as a result of encrypted document.
2. Determine the value of semantic similarity by user to be encrypted document.
3. The new query is obtained by the value of the semantic similarity.
4. New Query will be rewriting into a new sentence in accordance with the order of appearance of the word in a sentence.

Encrypted documents will be back to an original document (the decryption process) by reversing (create complement) of semantic similarity values from the public key.

### 63.4 Conclusions

Developing the corpus of semantic similarity in Indonesian is done by looking at the Indonesian thesaurus dictionary that has been published officially and the value of semantic similarity obtained using the method of Jiang and Conrath.

Query rewriting is a technique that used to create a new document from the new query by using a corpus of semantic similarity. Methods of encryption and decryption by using this technique remains to form a document into a series of words/phrases to be a good structure.

Further research can be done by designing a method to enrich the corpus of semantic similarity, and developing methods to separate Indonesian complex sentence structure. Implementation of the query rewriting techniques as the method of encryption and decryption is also can be done to continue this research.

**Acknowledgments** This work is partially supported by Gunadarma University, and Study Center of Information System Technology at Gunadarma University Jakarta Indonesia.

## References

1. Ashoor, A.S., Gore, S.: What is the difference between Hackers and Intruders. *Int. J. Sci. Eng. Res.* **2**(7), 1–3 (2011)
2. Budanitsky, A., Hirst, G.: Evaluating wordnet-based measures of lexical semantic relatedness. *J. Comput. Linguist.* **32**, 13–47 (2006)
3. Euzenat, J.: Towards a Principled Approach to Semantic Interoperability. INRIA Rhône-Alpes, Montbonnot Saint-Martin (France) (2001)
4. Goyal, S.: A survey on the application of cryptography. *Int. J. Sci. Technol.* **1**, 3 (2012)
5. Jamgekar, R.S., Joshi, G.S.: File encryption and decryption using secure RSA. *Int. J. Emerg. Sci. Eng.* **1**, 4 (2013)
6. Jaseena, K.U., John, A.: Text watermarking using combined image and text for authentication and protection. *Int. J. Comput. Appl.* **20**, 4 (2011)
7. Mihalcea, R., Corley, C., Strapparava, C.: Corpus-based and knowledge-based measures of text semantic similarity. In: *Proceedings of the 21st National Conference on Artificial Intelligence*, vol. 1, pp. 775–780 (2006)
8. Purnamasari, D., Wicaksana, I.W.S., Anissa, L.R., Anneke, A.P.S., Gustin, H.: Penerapan Semantic Similarity pada Kriptografi Suatu Dokumen Teksdalam Bahasa Indonesia. In: *Proceeding Seminar Nasional Kommit* (2014)
9. Shiri, A., Revie, C.: Query expansion behavior within a thesaurus-enhanced search environment: a user-centered evaluation. *J. Am. Soc. Inf. Sci. Technol.* **57**, 4 (2006)
10. Sridhara, G., Hill, E., Pollock, L., Vijay, S.K.: Identifying word relations in software: a comparative study of semantic similarity tools. In: *Proceedings of the 16th IEEE International Conference on Program Comprehension*, pp. 123–132 (2008)
11. Wordnet Similarity: <http://marimba.d.umn.edu/cgi-bin/similarity/similarity.cgi>. Accessed 01 Apr 2015

# Chapter 64

## Securing Client-Server Application Design for Information System Inventory

Ibnu Gunawan, Djoni Haryadi Setiabudi, Agustinus Noertjahyana and Yongky Hermawan

**Abstract** This paper will discuss how to design a client server application for the building supply store located at 3 different locations along with the networking system design as well as how to secure it. Santoso Building Stores is a company engaged in the sale of construction materials. The current system for the inventory in the store is still done manually, making frequent errors in the data and the resulting delay in presenting information. Based on these problems, the company needed a system to record the inventory through purchase and sale transactions, so that the report can be presented quickly. In order to meet these needs, it developed an application to support the activities of the company so that all inventory record scan be performed quickly and report scan also be presented in real time. Applications are developed using Microsoft Visual Basic 2010 and SQL Server 2008 R2 includes SQL Encryption feature. The experiments results showed that the application was able to meet the needs of the company, inventory system that is accurate, fast and safe.

**Keywords** Client-server · Encryption · Inventory · SQL server · Visual basic

### 64.1 Introduction

The company carries out business activities by recording the sales process, purchasing, etc. manually. The company carries out recording by using paper. Activity recording the purchase and sale transaction has experienced an error. Staff often makes mistakes in the calculation process, causing the company losses. In the sales process, the staff simply records the transaction in a note. When it goes on sale in

---

I. Gunawan (✉) · D.H. Setiabudi · A. Noertjahyana · Y. Hermawan  
Faculty of Industrial Technology, Department of Informatics Engineering,  
Petra Christian University, Surabaya, Indonesia 60236  
e-mail: ibnu@petra.ac.id

small quantities and the customer does not ask for a receipt, the staff did not report these sales transactions.

In the process of purchase, owners often order goods that are still in stock. This happens because the inventory can't be calculated precisely. When the ordered items arrive, the owner did not record the details of goods coming and when the due payment of goods. This causes frequent delays in the payment process.

In the process of inventory of goods also take a long time, because it does not have data on the number of stock. The company is still conducting an inventory manually so it takes a long time to complete. Owner of the company had plans to open branches in different locations. Certainly each branch must have accurate information about inventory, either from a warehouse or center. Given these problems, it is suitable for the company to use Client-server platform as similar as a system built by Kumar [1].

The server will be placed at the head office and branches can access directly via the connected network. The process is the server receives a client request and will respond with the right result. In the client-server system design has not forgotten aspects of data security. While sending data from the server to the client, the data must first be encrypted so it can't be read by unauthorized parties [2]. Applications developed will help the staff to keep records of all sales and purchases, as well as perform automatic inventory adjustment, so that errors in the calculation of stock can be minimized. Reports can also be directly presented to owner and accurately.

## 64.2 Client Server System

Client/server system usually runs at least two different computer systems. One computer acts as a client and the other as the server. But the client and server can reside on a single computer system. A server usually serves multiple client computer. Although there may be also that only serve one client only. This server functions normally performed by a file server, except when maximum performance is required it is used a special server that the client is usually in the form of a desktop computer that is connected to the network.

If the user wants to retrieve or store information, part of the client application will issue a demand that would send (usually over a network) to the server. The server then run the query and sends the information back to the client. A database cannot replace the client/server system, although the system is a client/server often use the database server to perform the activity. Applications designed to use Microsoft Access, Microsoft FoxPro, Paradox, or other database program is not a client/server system (even if the database is in network server). All are examples of network database application because all processing is done by the client [3].



### 64.3 Encryption in SQL Server 2008

Encryption demands have increased over the past few years. For instance, there has been a demand for the ability to store encryption keys “off-the-box” physically separate from the database and the data it contains. Also there is a recognized requirement for legacy databases and applications to take advantage of encryption without changing the existing code base. To address these needs SQL Server 2008 adds the following features to its encryption arsenal:

- *Transparent Data Encryption (TDE)*: Allows you to encrypt an entire database, including log files and tempdb database, in such way that it is transparent to client application.
- *Extensible Key Management (EKM)*: Allows you to store and manage your encryption keys on an external device known as a hardware security module (HSM).
- Cryptographic random number generation functionality.
- Additional cryptography— related catalog views and dynamic management views.
- SQL Language extensions to support the new encryption functionality.

SQL Server 2008 represents the most advanced SQL Server encryption capability to date, and you can leverage even more encryption functionality using other tools. For example, you can encrypt an entire hard drive with SQL Server database on it via Windows BitLocker technology. You can also use SSL to encrypt your SQL Server communication, protecting your data in transit [4]. We can see the architecture of SQL server 2008 encryption in Fig. 64.1

### 64.4 System Analysis

This section will discuss one business process to be analyzed as purchase returns. Purchase returns process happened when the goods are received in damaged condition or disability. If the goods are defective or damaged, it can be returns back. If the goods are damaged, then also the number of items in the original sales notes and its duplicate copies will be reduced, according to the quantity of goods with damaged or defective condition. The store owner could only exchange goods with the same type and size. Document flowchart purchase returns process can be seen in Fig. 64.2.

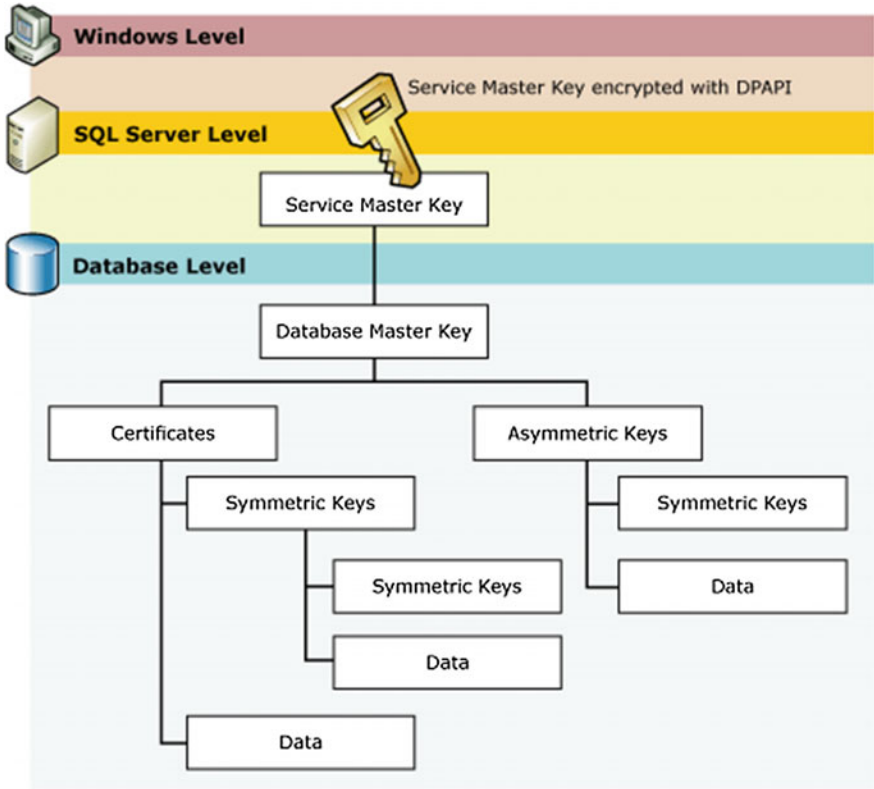


Fig. 64.1 SQL server 2008 encryption architecture

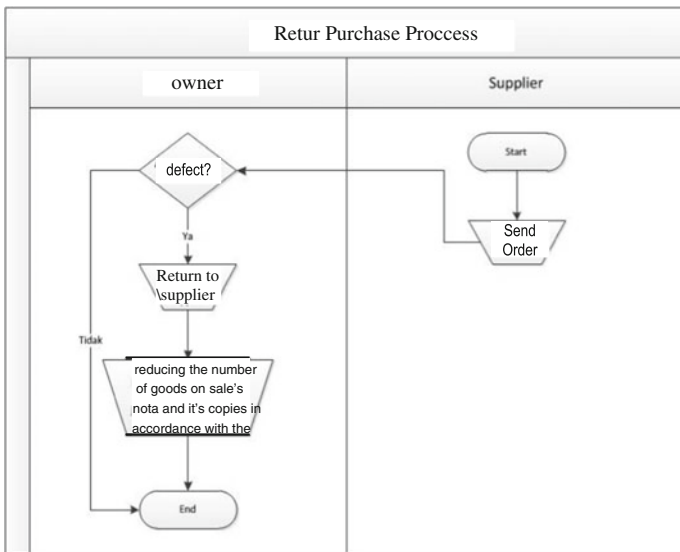


Fig. 64.2 Purchase return process

### 64.5 System Design

As we stated earlier in this paper, we will make a client server application for the building supply store located at 3 different locations along with the networking system design as well as how to secure it. Firstly, we designed a context diagram to show the whole process of the system. Context diagram on the buyer's side describes the process of purchasing data and payment, as well as the purchase invoice and payment. The supplier side shows purchasing data and payment process, order, and data charges for purchases and payments. The last side is owner who can look at reports such as purchasing reports, sales reports, report card stock and income statement. The context diagram is presented in Fig. 64.3.

Secondly, we attempt to encrypt the feature for SQL Server 2008 encryption by using the symmetric keys. For example, we create the sales.customer table using this syntax as in Fig. 64.4. Finally, we encrypt the data as in Fig. 64.5 and while it is on the client, we can see the syntax for decrypting the data. It can be seen in Fig. 64.6.

### 64.6 System Testing

In this paper, we present one of many screens since the program was built in Indonesian language. One of them is a program user interface of sale screen that we can see in Fig. 64.7.

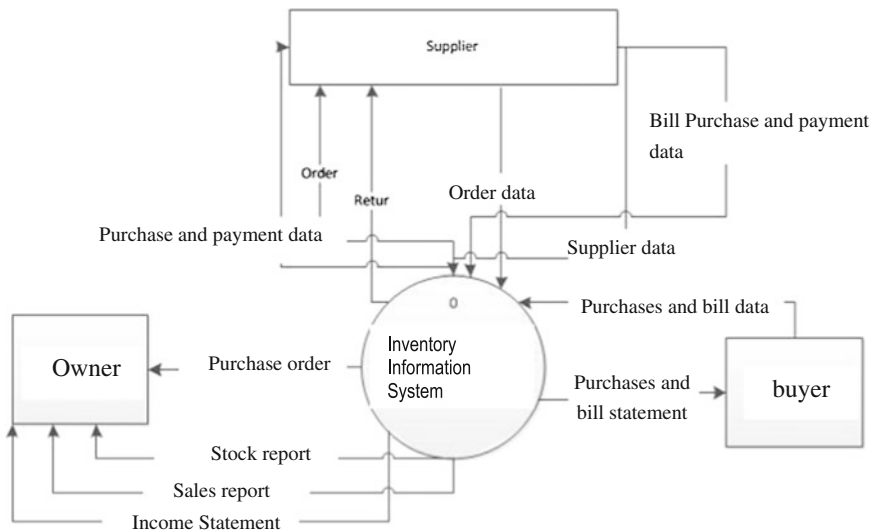


Fig. 64.3 Context diagram

**Fig. 64.4** Creating sales.customer table

```

CREATE TABLE SalesLT.EncryptedCustomer
(
  CustomerID int NOT NULL PRIMARY KEY,
  FirstName varbinary(200),
  MiddleName varbinary(200),
  LastName varbinary(200),
  EmailAddress varbinary(200),
  Phone varbinary(150),
  rowguid uniqueidentifier
);
GO

CREATE CERTIFICATE Cert1_Sales
WITH SUBJECT = N'Sales Certificate',
START_DATE = N'2009 -01-01',
EXPIRY_DATE = N'2018 -12-31';
GO
CREATE SYMMETRIC KEY SymKey1_Sales
WITH ALGORITHM = AES_256,
IDENTITY_VALUE = N'Barbarians at the Gate',
KEY_SOURCE = N'We will leave the light on for you'
ENCRYPTION BY CERTIFICATE Cert1_Sales;
GO

```

**Fig. 64.5** Encrypting the data

```

-- First wipe out the target table
TRUNCATE TABLE SalesLT.EncryptedCustomer;
GO
-- Open the key that's protected by certificate
OPEN SYMMETRIC KEY SymKey1_Sales
DECRYPTION BY CERTIFICATE Cert1_Sales;
GO
-- Encrypt the data
INSERT INTO SalesLT.EncryptedCustomer
(
  CustomerID,
  FirstName,
  MiddleName,
  LastName,
  EmailAddress,
  Phone,
  rowguid
)
SELECT
  CustomerID,
  EncryptByKey(Key_Guid(N'SymKey1_Sales'), FirstName),
  EncryptByKey(Key_Guid(N'SymKey1_Sales'), MiddleName),
  EncryptByKey(Key_Guid(N'SymKey1_Sales'), LastName),
  EncryptByKey(Key_Guid(N'SymKey1_Sales'), EmailAddress),
  EncryptByKey(Key_Guid(N'SymKey1_Sales'), Phone),
  rowguid
FROM SalesLT.Customer;
GO
-- Close the key
CLOSE SYMMETRIC KEY SymKey1_Sales;
GO

```

```
– Open the key that's protected by certificate
OPEN SYMMETRIC KEY SymKey1_Sales
DECRYPTION BY CERTIFICATE Cert1_Sales;
GO
– Decrypt the data
SELECT
    CustomerID,
    CAST(DecryptByKey(FirstName) AS nvarchar(100)) AS DecryptedFirstName,
    FirstName
FROM SalesLT.EncryptedCustomer;
GO
– Close the key
CLOSE SYMMETRIC KEY SymKey1_Sales;
GO
```

Fig. 64.6 Decrypting the data

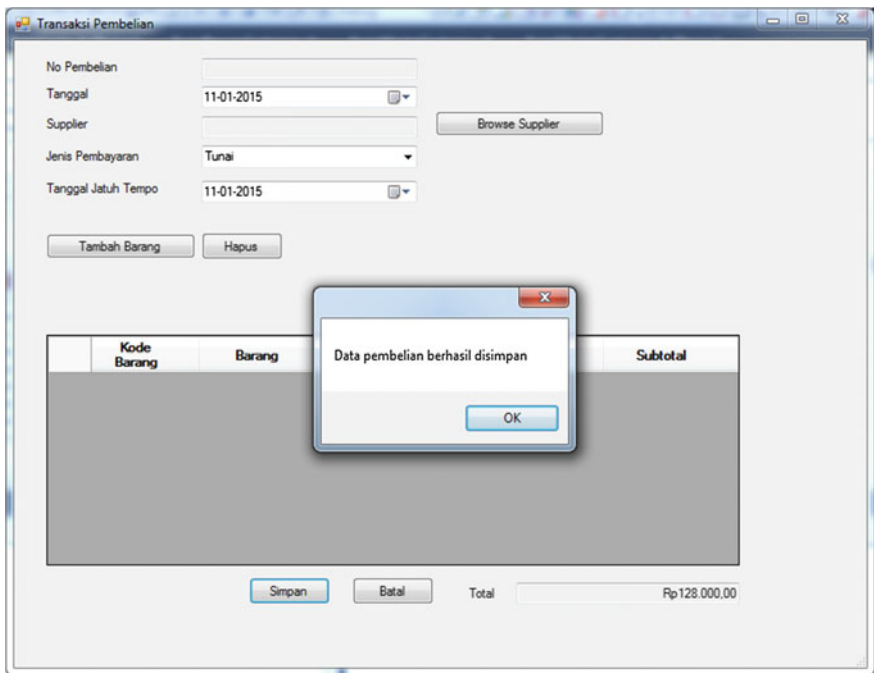


Fig. 64.7 Sales program screen

### 64.7 Conclusion

Based on the results and system test, we conclude as follows:

- Store 2 as the branch can connect to the database server is like being in one central store network.
- The application can generate reports so as to facilitate the user for getting the needed information, such as reports purchasing, sales, inventory and others.

## References

1. Kumar, A.: Thin client web-based campus information systems for Fiji National University. *Int. J. Softw. Eng. Appl. (IJSEA)* **2**, 1 (2011)
2. Qureshi, D., Desmukh, D.: Transparent data encryption—solution for security of database contents. *Int. J. Adv. Comput. Sci. Appl. (IJACSA)* **2**, 3 (2011)
3. Corporation, I.S.: *Information Systems Essentials*, 2nd edn. InterBase Software Corporation, California (1998)
4. Landrum, R., Coles, M.: *Expert SQL Server 2008 Encryption*. Apress, New York (2009)

**Part VI**  
**Technology Innovation in Information,  
Modelling and Mobile Applications**

# Chapter 65

## Analyzing Humanitarian Logistic Coordination for Disaster Relief in Indonesia

Tanti Octavia, I. Gede Agus Widyadana and Herry Christian Palit

**Abstract** Humanitarian logistics have been given an attention in recent years since logistic is one of important factors in effective disaster response and disaster relief. There are few researches on humanitarian logistic in Indonesia. In this paper, we aim to map and analyze humanitarian logistic in Indonesia. Therefore, deep interview method has been done to interview some institutions in humanitarian logistic system. We analyze the coordination of humanitarian logistic system using RASIC method. The finding of the deep interview reveals the private sector actively participates in disaster relief. In particular, it is also found the private sector actively participates in disaster relief but they do not collaborate with BNPB. It can be concluded the private sectors are able to take on the role in Indonesia humanitarian logistic system under supervision of BNPB. We finally proposed the RASIC model involving the private sector for Indonesia humanitarian logistic.

**Keywords** Humanitarian logistic · RASIC · Indonesia

### 65.1 Introduction

Humanitarian relief environments engage many organizations such as government, local and regional relief organizations, military, and private companies. Each organization has different interest, mandates capacity and logistics [1]. Logistic is one of important part in humanitarian relief, so it is important to make it efficient and effective. Therefore, some researches focus on humanitarian logistic. Liberatore et al. [3] tried to make a model for distributing emergency goods to population affected by disaster. They applied the model in Haiti earthquake case in 2010 and

---

T. Octavia (✉) · I.G.A. Widyadana · H.C. Palit  
Industrial Engineering Department, Petra Christian University,  
Jl. Siwalankerto 121-131, Surabaya 60236, Indonesia  
e-mail: tanti@petra.ac.id



concluded that coordinating recovery and distribution operations are important. Ozdamar and Ertem [4] showed that information technology should be integrated in humanitarian logistic to make humanitarian logistic more effective. They got the conclusion by applying survey.

According data from *Badan Nasional Penanggulangan Bencana Indonesia* (BNPB), number of disasters in Indonesia in 2015 until June are 1116 events where dominant in flood (32.1 %), landslide (33.2 %) and waterspout (28.5 %). Due to the disaster frequency, Indonesia needs an efficient and effective humanitarian logistics. However there are few researches on humanitarian logistic in Indonesia. In this research humanitarian logistic in Indonesia is evaluated, and improved by engaging private companies.

## 65.2 Research Method

In this research, functions of each organization in humanitarian logistics in Indonesia are evaluated using RASIC scheme that is developed by Kaynak and Tuger [2]. RASIC is a tool to set roles of every organization. The benefits of RASIC are developing a clear relation between activities and resources, defining clear responsibility for every resource, and giving suggestion for communication planning. RASIC is an acronym which stands for Responsible, Approves, Support, Informed, and Consulted. Responsible is related to the organization that is ultimately responsible for completing the activity. Approves is related to the organization that has responsibility and authority to take an action. The organization that provides resources or can help responsible organization is defined as supported. Informed is defined as an organization that has to know result of implementation to the activities. Consulted is defined as an organization that contributes the implementation suggestions for making it smoothly.

Data are conducted by interviewing *Badan Penanggulangan Bencana Daerah Jawa Timur* (BPBD), Indonesian Red Cross (IRC) East Java branch, public health office, public social office and survey through email with a logistics company which is DHL international.

## 65.3 Result

RASIC chart is used for showing the role of each organization in Indonesia humanitarian logistic. The organization includes government, social and private institution. Government institution in humanitarian logistics is *Badan Nasional Penanggulangan Bencana Daerah* (BPBD), public social office and public health office. BPBD is a non-department government institution, which has planning and

operational function in disaster management, and emergency. BNPB was formed according to Indonesian law in year 2007 number 24. Scope of BNPB includes pre-disaster, disaster response and post disaster. BPBD is part of BNPB that has smaller scope which is in provinces or towns. Public health office has a unit to handle health aspects of disaster management. The unit is called *Pusat Penanggulangan Krisis Kesehatan (PPKK Kemkes)*. The unit has the responsibility for providing medicines and medical personnel for disaster response phase. Public social office has responsibility on preparing, giving technical guidance, and supervising the implementation the preparedness' activity, mitigation, response and rehabilitation for natural disaster victims. The Indonesia Red Cross (IRC) has responsibility to prepare temporary distribution points based on the input of local government and assessment. The Indonesia Red Cross works on preparedness, response and rehabilitation phases.

RASIC chart shows the role of every organization in every activity today. We seek to analyze the role of each institution in each activity. Recent RASIC chart is shown in Fig. 65.1.

Where:

- R : Responsible
- A : Approved
- S : Supported
- I : Informed
- C : Consulted

No	Job	Institution			
		BPBD	IRC	Public Social Office	Health Social Office
<b>Preparedness</b>					
1	Community training	RA	RA	RA	RA
2	Information sharing and coordination	RA	I	I	I
3	Collaboration with private sector	RA	I	I	I
4	Provide funding	RA	S	R	R
5	Develop relief standardization	RA		RA	RA (medicines)
6	Prepare buffer stock	RA		RA	
<b>Response</b>					
1	Assessment	RA	RA	RA	RA
2	Coordination with government	RA	I	I	I
3	Sends aid	RA	S	R	R (medicines)
4	To get aid from donator	RA			
5	Providing staffs	RA	R	R	R
6	Operating soup kitchens	S	S	RA	
7	Distributing logistic aids	RA	S		RA
8	Distributing health aids	S	S	S	

Fig. 65.1 The existing RASIC chart

### 65.4 RASIC Analysis

In the vertical RASIC analysis, BPBD as a coordinator has responsibility for humanitarian logistic in Indonesia in preparedness and response phases. Instead of as a coordinator, BPBD also acts as a decision maker for most of critical activities. For preparing temporary distribution points and giving quick response in limited areas, BPBD is supported by IRC. IRC has responsibility in some activities such as community training, assessment and preparing field staffs. Public social office has activities in most area and responsibility in soup kitchen sector. Public health office focuses on health sector and has responsibility in this area.

Figure 65.1 shows that private sector is not part of humanitarian logistics in Indonesia, although some private sectors have actively participated in disaster relief programs. One of private sector that actively participates in disaster relief program is DHL. DHL is a postal and logistics industry and encompass on three divisions: DHL Express, DHL Global Forwarding, Freight and DHL Supply Chain. DHL is present in over 220 countries. DHL has two humanitarian logistic programs which are Get Airport Ready for Disaster (GARD) and Disaster Response Team (DRT). GARD was developed by cooperation between DHL and United Nations Development Programme (UNDP). GARD program goal is preparing an airport to

No	Job	Institution				
		BPBD	IRC	Public Social Office	Health Social Office	Private Sector
<b>Preparedness</b>						
1	Community training	S	R	S	S	
2	Information sharing and coordination	RI	SI	SI	SI	SI
3	Collaboration with private sector	RA	I	I	I	
4	Provides funding	RA	S	S	S	S
5	Develop relief standardization	RA	I	I	I	I
6	Prepare buffer stock	RA	NA	NA	R (medicines)	S
<b>Response</b>						
1	Assessment	C	RA	I	I	
2	Coordination with government	R	I	I	I	I
3	Sending aid	RA	S	R	R (medicines)	R
4	To get aid from donator	RA	I	I	I	
5	Providing transportation	R	R	S	S	R
6	Providing staffs	S	R	S	S	S
7	First aid operation	S	R	S	S	
8	Operating soup kitchens	S	S	RA		
9	Organizing posts disaster	S	S		RA	
10	Distribute logistic aids	S	S	R		
11	Distribute health aids		S	NA	R	

Fig. 65.2 The proposed RASIC model with private sector

handle escalation of disaster aids. GARD programme has been applied in more than 29 local airports such as airport In Armenia, Bangladesh, Nepal and Indonesia. GARD training was conducted in Indonesia in 2009 and 2011 such as Medan, Aceh, Middle of Sulawesi, Makassar, Bali and Kupang. DRT was developed by cooperation between DHL and *United Nations Office for the Coordination of Humanitarian Affairs* (OCHA). DRT supports on distribution relief including cargo airplane, warehousing and distributing for disaster relief institution. DRT network has more than 400 volunteers who are ready in less than 72 h. DRT has involved helping earthquake disaster in Padang in 2004. They worked for 1 week to organize escalation of aids in Padang airport. DRT also involved helping earthquake disaster relief in Yogyakarta in 2006. The RASIC model including private sector can be seen in Fig. 65.2.

## 65.5 Conclusion

We study the recent humanitarian logistic systems in Indonesia that involves some institutions such as BPBD and IRC. BPBD acts as a coordinator of other institutions such as IRC, health department and social department. It is found that private sectors have a contribution in humanitarian logistics but it does not include in humanitarian logistics system in Indonesia. One of them is DHL through GARD and DRT program. RASIC method is applied to show the relation between humanitarian logistic in Indonesia and to analyze the role of private sector when it is included in the system. In this research we conclude that private sector can be one of role institution in humanitarian logistic in Indonesia under supervision of BPBD. Second, we change some institution roles such as BPBD should act as coordinator in standardization, assessment, and funding. However, funding can be collected by any institutions under supervision of BNPB. In this research we only show the main model of humanitarian logistic in Indonesia. This research can be developed by detailing the roles of each institution considering their strength, weakness, opportunity and threat and use the strength of one institution to cover the weakness of other institutions. Future research can also be done by integrating an information system between each institution to make the humanitarian logistic system more efficient.

## References

1. Balciik, B., Beamon, B.M., Krejci, C.C., Muramatsu, K.M., Ramirez, M.: Coordination in humanitarian relief chains: practices, challenges, and opportunities. *Int. J. Prod. Econ.* **126**, 22–34 (2010)
2. Kaynak, R., Tuger, A.T.: Coordination and collaboration functions of disaster coordination centers for humanitarian logistics. *Procedia—Soci. Behav. Sci.* **109**, 432–437 (2014)

3. Liberatore, R., Ortuno, M.T., Tirado, G., Vitoriano, B.: Scaoarra, a hierarchical compromise model for the joint optimization of recovery operations and distribution of emergency goods in humanitarian logistics. *Comput. Oper. Res.* **42**, 3–13 (2014)
4. Ozdamar, L., Ertem, M.L.: Models, solutions and enabling technologies in humanitarian logistics. *Eur. J. Oper. Res.* **244**, 55–65 (2015)

# Chapter 66

## Surakarta Cultural Heritage Management Based on Geographic Information Systems

Ery Dewayani and M. Viny Christanti

**Abstract** Tangible cultural heritage is the legacy of physical artifacts from past generation in a nation. Indonesia is a nation which is rich in cultural heritage. Surakarta is a city that has a lot of historic buildings and other physical cultural heritage. Preservation of the cultural heritage of Surakarta can be done in various ways. One way to preserve it is to create an integrated documentation and renewable. In this research, we try to build Geographical Information System (GIS) based on web. The making of GIS of Surakarta cultural heritage, intended to facilitate the inventory, monitoring, follow-up and can be used as a reference for determining policy related to the cultural heritage conservation. Surakarta GIS is complemented with a function to register the historical heritage. Registration can be done by either the local community or the manager of the historical heritage. This function can also assist the government in obtaining the data of other historical heritages that have not been registered, so that the heritage can be protected by the government. The system is built using MapServer and PostgreSQL to manage spatial data.

**Keywords** Geographic information system · Mapserver · Postgresql · Surakarta · Tangible cultural heritage

### 66.1 Introduction

Indonesia is a nation that has a lot of cultural heritage. Surakarta is one of the cities that have a history of high heritage value and become the city's identity, so that the building and the region must be preserved [1]. Surakarta have many physical cultural heritage, especially physically immovable cultural heritage. National culture is something that must be preserved as a heritage and that preservation was done for the sustainability of this nation. Preservation of culture can be done in

---

E. Dewayani · M. Viny Christanti (✉)  
Faculty of Information Technology, Tarumanegara University,  
Jl. Letjen. S. Parman no. 1, Jakarta, Indonesia  
e-mail: viny@untar.ac.id

different ways. From maintaining, promoting and pass them from generation to generation. The cultural heritage itself can consist of two major categories i.e. tangible cultural heritage and intangible cultural heritage [2]. While on The World Heritage Convention article 1, tangible cultural heritage consist of 3 categories, i.e. monument, groups of buildings and sites [3].

Preserving means maintain for a very long time, because it can be imagined if 5 or 10 years again, the cultural heritage may no longer exist or have changed into another form. For example in Italy, the criteria and the aims of protection have changed, so that it does not tend only to preserve and manage the existing assets as well as to proceed with legal and administrative measures, but also to exploit the assets through a more complete knowledge of them [4]. Preservation effort is a maintenance effort for a very long time. Therefore, it is necessary to develop conservation as a sustained effort.

Computers can be used as a place of gathering, archiving, management, analysis and generate output geographic shape [5]. The use of these technologies can enable people to access and disseminate information. One of the ideas that can be developed is the manufacture of GIS for mapping the physical cultural heritage in Surakarta and surrounding region. The system built implemented for: (a) the acquisition and verification of data, (b) the compilation of data, (c) the storage of data, (d) changes or updating of data, (e) management and data exchange, (g) access and data presentation.

Geographic Information System (GIS) will map each activity related to spatial data and associated with the local geography. Hopefully, this mapping can give an idea or information on activities occurring graphically linked with the condition of the cultural heritage in Surakarta and surrounding areas. The purpose of this system is to provide information that can be used by public and private agencies designated to protect and utilize the cultural heritage (such as architects, archaeologists, historians and others). Moreover, it can also be used by ordinary people who are interested in cultural heritage.

In this study, the collaboration process has been conducted with the Department of Spatial Planning (*Dinas Tata Ruang Kota*) and the Department of Tourism (*Dinas Pariwisata*) of Surakarta. This collaboration has been established for 2 years. Data collection and data analysis is done intensively in 2014. Based on interview with some of managers of historical tourism destination and Head Section of Maintenance and Protection Zone and Heritage Buildings City Hall Surakarta, they state that there are some of objects not registered as cultural heritage. So the government cannot protect this object, although the object is historical object.

### **66.1.1 Cultural Heritage**

Based on article 1 of Law No. 5 of 1992, an object can be referred to as ‘objects of cultural heritage’ is man-made objects and natural objects which are moveable or

not moveable, that are considered to have significant value for the history, science and culture [6]. While the location that containing or suspected to be the objects of cultural heritage called 'sites'. Based on world heritage in 1995, cultural heritage consist of three categories, there are monuments, groups of buildings and sites [3].

In general, people familiar with the cultural heritage is an ancient building which is protected by the government. But more broadly, cultural heritage is preserved by the local communities and the livelihoods are protected by law from the danger of extinction. Based on the analysis and field research, not the entire physical cultural heritage is protected by the government. There is some physical cultural heritage that has not been included in the cultural heritage so that the heritage is not protected by the government.

People who become owners or managers of buildings and areas of cultural heritage have rights and obligations to register the object. Once the object has been examined and declared complies with the requirements of the cultural heritage, then the object will get the sign in the form of a label that is placed near the object. Label is a sign that the object is registered in the government's decree of cultural heritage and the right to be protected.

### ***66.1.2 Surakarta Cultural Heritage***

Thomas Karsten, a Dutch architect who also designed a number of ancient buildings in Surakarta say, a process that must be done before setting Surakarta as objects of cultural heritage is mapped the historic district. There are three classes that distinguish; first class is two palace complexes in Surakarta (Mangkunegaran and Pakubuanan), class two ancient buildings around the first grade and third grade are other ancient buildings beyond first class and second class [7].

The first class of the region shall be maintained the original form of the building, for any reason in these places should not be reduced or plus building. While in the second grade covers an area around the first-class area that still has the old city structure and contains ancient buildings. This area also includes the former European residential, Pacinan, Kampung Laweyan and so on. Preservation of ancient buildings can be done through four forms of conservation, among others Preservation, Rehabilitation, Reconstruction and Revitalization [6].

The determination of the direction of preservation for potential building done by classifying potential building into two, namely the high potential and low potential [8]. Categorization of buildings into a high or low potential status can be viewed from various aspects of assessment. Aspects of the assessment can be determined based on the value of cultural meaning and condition of the building or object. The assessment process carried out beforehand by experts of cultural heritage.

At this time The Department of Spatial Planning of Surakarta not has sufficient documentation to support the Surakarta cultural information, especially regarding to



the physical cultural heritage. Therefore, we collect all the primary and secondary data. Primary data collected directly in the field to do a photo shoot and interviews with locals. While secondary data obtained from The Department of Spatial Planning in the form of printed document.

### ***66.1.3 Geographic Information System***

Geographic Information Systems (GIS) is defined as a component which consists of hardware, software, geographic data and human resources that work together effectively to capture, store, repair, update, manage, manipulate, integrate, analyze, and display data in a geographic-based information [5]. To get spatial information, GIS using a location within a particular coordinate system, as a basic reference. Therefore, GIS has the ability to connect various data at a given point on earth, combine, analyze and finally mapped the results. GIS answer some questions such as: location, condition, trends, patterns, and modeling. These abilities are exactly what differentiate GIS from other information system.

Meanwhile, according to other sources, GIS is a set of computer hardware, software, data and people are combined to address spatial-based questions and provide new ways of looking at the GIS to find solutions or make decisions [9]. Based on these GIS functions, the GIS become a tool to preserve the cultural heritage. Data can be stored cultural heritage, renewable and known by the public. Cultural heritage which has changed shape, missing or unknown can still be traced back to this system.

### ***66.1.4 Spatial and Non Spatial Database***

Building a database to GIS is divided into two parts, namely spatial and non spatial database. GIS spatial database for this culture is built based on the results of data collection has been done in the previous year's study. Layer on the base map used is sub-district, district, provincial and village. Other spatial data classification carried out in several categories. Classification layer is the stage of grouping elements of spatial data in accordance with the theme of each.

At this GIS data classification carried into five parts, namely the reserve is not a tourist, not a cultural heritage tourist attractions, heritage sites, historical buildings and tourist attractions of historic buildings [10]. The purpose of this division is to locate the physical cultural heritage that has become the reserve or not, physical cultural heritage that are well known and become tourist attractions or just a cultural heritage of historic buildings.

As for non-spatial data, compiled based on data collected in the previous year's research. This Surakarta culture heritage GIS focuses on the registration process of

**Table 66.1** Category of cultural heritage based on Surakarta Department of Spatial Planning

No	Categories	Description
1	Labeling	<i>Tugu, Tembaga, Granit</i>
2	Type of object	Traditional area: traditional and non-traditional
		Traditional house
		Colonial public building
		Worship building
		<i>Gapura, Tugu, Monumen, PerabotJalan</i>
		Open Space: <i>Makam, Park, Open Garden and Open space</i>
3	Conservation	Preservation, Rehabilitation, Revitalization, Reconstruction

cultural heritage. Heritage Surakarta divided into several categories. Data have been obtained from the study of literature, has been analyzed and can be divided into three categories: Labeling, Object Types and Forms conservation [6, 10]. In Table 66.1 we can see the contents of each category.

Next analysis is that the cultural heritage can be registered by: owner, family, business or other. This analysis done based on SK. No: 646/116/1/1997 about Determination of the buildings and the historical ancient region on Surakarta Municipality level II. People who become owners or managers of buildings and areas of cultural heritage have rights and obligations as specified in local regulations on cultural preservation. The owner of cultural heritage are entitled to legal protection in the form of a Certificate of Cultural Heritage and Status Certificate of Ownership is based on evidence, which was made by the local work unit that has tasks and functions in the field of cultural heritage.

### 66.1.5 Geographical Information System of the Surakarta Cultural Heritage

After the database is built, there should be an analysis of the needs of software and hardware to build a website. Specifications of the software that used to build a GIS divided into two sides, server side and client side. We build Surakarta GIS in Ubuntu 14.04 operating system environment. PostgreSQL with PostGIS extension is used as software for database management system. For map management and visualization, we use MapServer. At client server, user only need web browser. PostgreSQL and MapServer is open source software that support and facilitate the making of GIS [11].

GIS system is built with the main purpose to preserve the physical cultural heritage city of Surakarta. As is known physical cultural heritage can be a monument, groups of buildings and sites. This legacy can be a private, family or in open

spaces. Therefore, the government itself gave the opportunity to register the heritage to be protected by law.

In this GIS system, the data of cultural heritage is presented complete with the history, location and label of the cultural heritage. Results of this GIS will connect the process of enrollment, management and storage of data with the physical cultural heritage map of the city of Surakarta. Each user can see where the location of the physical cultural heritage. The success of this research is expected to help in the preservation of the cultural heritage, in particular the physical cultural heritage in Surakarta and surrounding region. The Department of Spatial Planning and the Department of Tourism are expecting that this research could be implemented by the Surakarta government.





## 66.2 Result and Analysis

Data collection has been carried out and managed to find 74 locations of cultural heritage, and the data obtained some 62 photos of cultural heritage, cultural heritage label and the coordinates of its location. A total of 7 label of cultural heritage is not acquired by obstacles, such as heritage label is not installed, not found the location label reserve, requires permission from the owner or location of heritage buildings are being used for an activity. At Table 66.2 we can see the example of location, coordinate data of Surakarta cultural heritage and distance between location and tourism destination.

**Table 66.2** List of cultural heritage location, complete with coordinate and distance to other destination

No	Location	Destination	Distance (km)
1	Bandara Adisucipto Yogyakarta Coordinate: S $-7^{\circ} 47.1219'$ , E $110^{\circ} 26.2233'$ address: Raya Solo KM. 9, 55282, Indonesia	Candi Sambisari	3.1
		Candi Prambanan	7.8
		Museum Prambanan	8.6
		Candi Plaosan	10.2
		Ratu Bokoh	9.7
2	Candi Sambisari Coordinate: S $07^{\circ} 45.811'$ , E $110^{\circ}26.797'$ address: Desa Sambisari Kelurahan Purwomartani Jalan Nasional 15 Depok, Sleman, Yogyakarta 55281, Indonesia	Candi Prambanan	9.2
		Museum Prambanan	10
		Candi Plaosan	11.6
		Ratu Bokoh	11.1

**Table 66.3** Example pictures of the historic heritage of Surakarta

No.	Cultural heritage name	Coordinate	Photo	Label
1	Tugu Lilin Kelurahan Penumping	S 07°34'07.2" E 110°48' 19.8"		
2	Patung Slamet Riyadi Jalan Slamet Riyadi	S 07°33'55.3" E 110°48' 19.1"		

Review the location, shooting and coordinate reserve, guided by the management staff of cultural heritage label assigned by the Department of Spatial Surakarta. In addition, based on the observation, then there are 19 historic sites are considered to be a tourist attraction. That historic place is a place most often become a tourist destination by domestic and foreign tourists. The picture of cultural heritage and its label can be seen at Table 66.3.

When collected Surakarta data is done, we analyze the data, and then we found some facts that not all the historic place is the cultural heritage. Like, Mangkunegaran palace is one of the cultural heritages listed in SK No. 646/101-F/1/2012 and also became one of the most visited tourist attractions. Whereas Prambanan temple and museum is not listed as a cultural heritage though it is tourism place. Museum Radya Pustaka is listed as a cultural heritage place, but not as tourism place.

Geographical Information System of The Surakarta Cultural Heritage has following functions: display a map, pan and zoom throughout a map, identify features on a map by pointing at them, culture heritage registration, manage all culture heritage data and others. Surakarta GIS is divided into two sides of the admin and user. Admin side is for managers of Department of Spatial Planning Surakarta. Admin has functions to add, update and manage existing data.

The user side is the public at society, especially society the city of Surakarta. User can see information, history, photo and location of culture heritage. The users can also make the registration process of the cultural heritage that has not been registered in government offices. Registered cultural heritage will be reviewed by government agencies. If it has met the requirements listed in the law then the heritage will get a decree from the government.

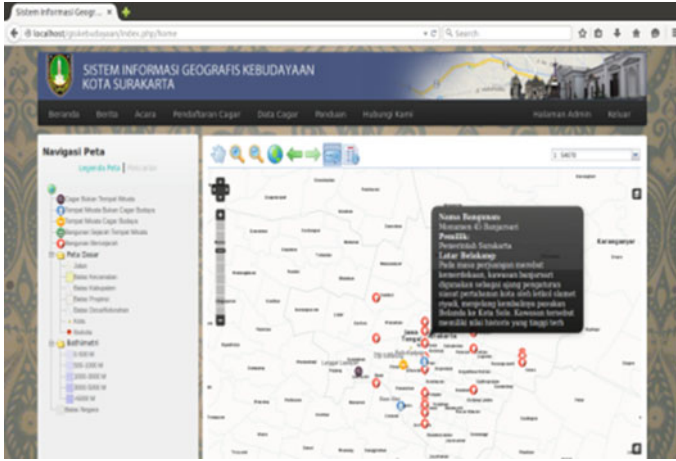


Fig. 66.1 Surakarta Map and the map legend

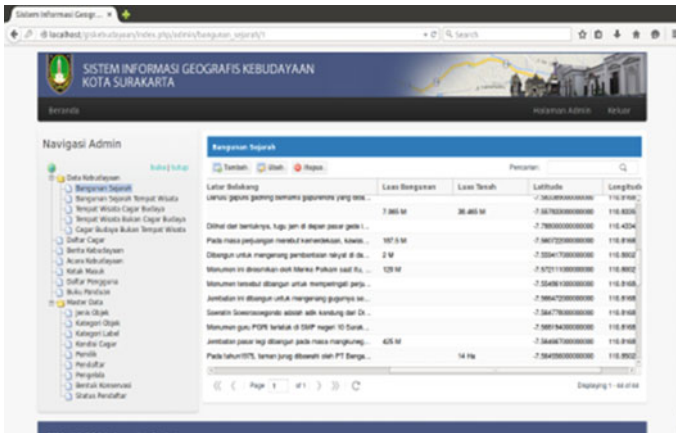


Fig. 66.2 Lists of cultural heritage

Figure 66.1 consists of a map of Surakarta and legends from one of the cultural heritage objects. Figure 66.2 is admin side that has list of cultural heritage. At Fig. 66.3 we can see categories of cultural heritage object that consist of tourism cultural heritage, tourism not cultural heritage and tourism historic building. the distribution of these categories, helping people to see the tourist attractions which have not become cultural heritage or cultural heritage which has not been promoted as a tourist or historic buildings which have not been registered as a cultural heritage. At Fig. 66.4 we can see the information of cultural heritage.

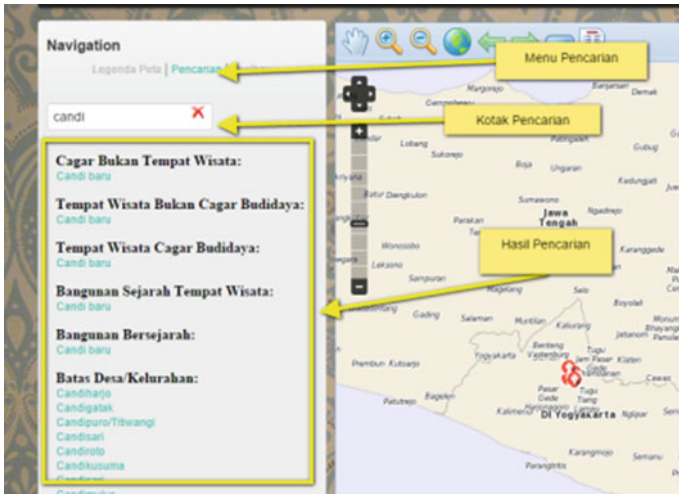


Fig. 66.3 Categories of cultural heritage



Fig. 66.4 Information of cultural heritage

### 66.3 Conclusion

This study has successfully collected data historic sites and cultural heritage is based on regulations in Surakarta. Such data has been validated directly to the informant. Researchers also managed to collect primary data and secondary data in accordance with the data recorded in the local government. The original data in the form of complete documents obtained directly from the Department of Spatial Surakarta.

Surakarta GIS is complemented with a function to register the historical heritage. Registration can be done by either the local community or the manager of the historical heritage. This function can also assist the government in obtaining the data of other historical heritage that have not been registered in order to be protected by the government.

GIS Culture Surakarta already meets the required specification data analysis. Implementation is done to Department of Spatial Planning Surakarta. Expected results of this GIS can be beneficial and improve the affection of the people of the physical cultural heritage of the city of Surakarta. Building a GIS system, is as a proof of the government's attention to the physical cultural heritage of this nation. Hopefully, this concept of GIS can be implemented for other cities.

**Acknowledgments** This research was funded by the Direktorat Jenderal Pendidikan Tinggi DP2 M Indonesia, at competitive grant (*Hibah Bersaing*). This research was developed in 2 years, from 2014 to 2015.

## References

1. Setyaningsih, W.: Potensi Spasial Fisik Kampung Kauman Surakarta sebagai Kawasan Budaya dan Religi. *GEMA TEKNIK Majalah Ilmiah Teknik* **10**(2), 119–125 (2007)
2. Galla, A.: *Guidebook for the Participation of Young People in Heritage. Conservation*. Hall and Jones Advertising, Brisbane (2001)
3. World Heritage Unit: *Australia's World Heritage*. Department of Environment, Sports and Territories, Canberra (1995)
4. Bartolotta, Michelangelo, Di Naro, S., Brutto, M., Villa, B.: Information systems for preservation of cultural heritage. *Int. Arch. Photogramm. Remote Sens.* **33**(B5/1), 864–870 (2000)
5. Bernhardsen, T.: *Geographic Information Systems—An Introduction*. Wiley, Toronto (1999)
6. Indonesia, Departemen Kebudayaan. *Undang-undang Republik Indonesia Nomor 5 Tahun 1992 Tentang Benda Cagar Budaya (Law no. 5 Concerning Cultural Object)*. Kementerian Pendidikan dan Kebudayaan, Republik Indonesia (1992)
7. Rosyid, I.: Kota Solo Diusulkan jadi Kota Cagar Budaya. *Tempo*, 13 January (2007)
8. Hariyani, S., Antariksa, Pratomo, A.S., Pelestarian Kawasan Kampung Batik Laweyan Kota Surakarta. *DIMENSI (J. Arch. Built Environ.)* **34**(2), 93–105 (2007)
9. Petrescu, F.: The use of GIS technology in cultural heritage. In: *Proceedings of the XXI International CIPA Symposium, Athens, Greece* (2007)
10. Dewayani, Ery, et al.: *Pemodelan Sistem Informasi Geografis untuk Pemetaan Warisan Budaya Fisik di Wilayah Surakarta dan Sekitarnya*. In: *Proceeding of the Digital Information System Conference 2014, Bandung, Indonesia* (2014)
11. Duran, Z., Garagon, D.A., Toz, G.: Cultural heritage preservation using internet-enabled GIS. In: *CIPA 2003 XIXth International Symposium, 30 September–October, Antalya, Turkey* (2003)

# Chapter 67

## Gray Code of Generating Tree of $n$ Permutation with $m$ Cycles

Sulistyo Puspitodjati, Henny Widowati and Crispina Pardede

**Abstract** This paper proposes a new combinatorial Gray code. Combinatorial Gray code is a method of generating combinatorial objects so that every two successive objects differ as little as possible. Combinatorial object in this paper is a set of words that associated to Puspitodjati's generating tree of  $n$ -length permutations with a given number of cycles. Nodes of the tree is labeled and then coded. The way nodes visited while traversing the tree constructs a new Gray code presented in this paper. The proof that it is a Gray code is given.

**Keywords** Combinatorial gray code · Generating tree · Permutation with cycles

### 67.1 Introduction

The term of Combinatorial Gray code originally comes from Gray code, after Frank Gray. Gray code, also known as reflected binary code, is a list of  $n$ -binary digit (bit) numbers that every two successive numbers differ in only one bit. This concept then apply to any other combinatorial class, called combinatorial Gray code. Additionally, the definition extends to as a list of combinatorial objects such that, every object in the class appears once in the list, and every two successive objects in the list differ in some small prescribed way. Sometimes, they may differ, for the first and the last word in the list in the same way. This Gray code is called cyclic or circular. How they differ as it is prescribed, depends on the objects listed, and how they are listed.

The combinatorial Gray code is a way to solve problems of generating objects in the class as exhaustively, effectively and efficiently as possible. Therefore, the objects are generated, one by one, listed in such away, so the appearance of the successive objects is only in a small way. Savage in [1] presented some

---

S. Puspitodjati (✉) · H. Widowati · C. Pardede  
Gunadarma University, Jakarta, Indonesia  
e-mail: sulisty@staff.gunadarma.ac.id



combinatorial classes that construct a combinatorial Gray codes. Some examples of the variety of ‘differ in small way’ [1] can be listed, such as: a Hamming distance one in generating  $k$ -element subset of an  $n$ -element set, differ only by the exchange of two elements (one swap) in generating permutations, differ by a single edge in generating spanning trees of a graph, etc.

Some surveys which are conducted in [1–3] said, combinatorial Gray code has many applications in diverse areas, such as signal encoding, compression, circuit testing, software testing, biology and biochemistry, and parallel computing. Therefore, there are quite a lot of researches lead to the combinatorial Gray code for some combinatorial class, for examples: avoid pattern of permutation, derangement, permutation with a fix minimum number left to right minima, P-sequence, multi set permutation, or any objects counted by Catalan numbers. They are developed through varied approached. One approach is by using their generating trees, or their ECO structures, as in Bernini [2] and Vajnovszky [4]. This paper presents a new combinatorial Gray code of new combinatorial objects. The combinatorial object of this research is motivated by Bernini’s paper [2] that object emerges based on path in generating tree of Puspitodjati’s permutation of size  $n$  with  $m$  cycles.

This paper is organized as follows. Section 67.2 explains briefly what is the generating tree and its ECO structured. Section 67.3 explains the construction of the new Gray code we offered, and the concluding remarks of this research, presented in the last section.

## 67.2 Permutation $n$ with $m$ Cycles

Permutation  $n$  in this paper means permutation on set  $S = [n] = \{1, 2, 3, \dots, n\}$ , that is a bijection  $\pi: S \rightarrow S$ . Cycles with length  $k$  in a permutation is an ordered  $e_1, e_2, \dots, e_k$  such that  $e_i = \pi(e_{i-1})$  for  $i = 2, 3, \dots, k$ , and  $e_1 = \pi(e_k)$  or  $\pi^k(e_i) = \pi(e_i)$ . Permutation  $n$  with  $m$  cycles can be expressed in their cycles product. As an example, a permutation 5 with 3 cycles, in one line notation, 2 1 3 5 4 has their cycles product

(1 2) (3) (4 5). In this paper, a cycle products of a permutation always arranged which the least element always put as the first element on a cycle, and cycles ordered in increasing order of their first element. The set of all permutation  $n$  with  $m$  cycles in this paper is denoted as  $S_{n,m}$ .

## 67.3 ECO Method and Generating Tree

Generating tree is a method to generate exhaustively combinatorial objects in certain combinatorial class. Every node in the tree is labeled and related to the object. Level of the tree is related to the size of the objects. Each object in the children is obtained from smaller objects in its parent with a local expansion.

The relation of every node with its children, formulated in rules called succession rules. This set of rules, known as “Enumerating Combinatorial Objects” (ECO) system [5].

### 67.4 Generating Tree of Permutation $n$ with $m$ Cycles

Let  $\pi_n$  or just  $\pi$  (without an index  $n$ ), is a permutation  $\pi_n: [n] \rightarrow [n]$ , while  $\pi_n(i)$ ,  $i = 1, 2, \dots, n$  to indicate an element on  $i$ -th position of permutation. Puspitodjati in [6] generate all permutation  $n$  with  $m$  cycles,  $S_{n,m}$ , using generating tree as in Fig. 67.1. Let  $s_i$  is  $i$ -th cycle of  $S_{n,m}$ , and  $s_{ij}$  is  $j$ -th element of  $s_i$ . Puspitodjati’s generation of all objects in  $S_{n,m}$  [6] was developed based on the nature proposed by Baril in [7]. According to [7]:

1. if  $\pi \in S_{n-1,m}$ ,  $n \geq 2$ ,  $1 \leq m \leq n$ , then it can be obtained  $\pi' \in S_{n,m}$ , by mapping  $\pi'(i) = n$  and  $n\pi'(n) = \pi(i)$ ,  $1 \leq i < n$ , e.g.:  $S_{3,2}(12)(3) = 213 \rightarrow S_{4,2}: 4132, 2431, 2143$ , as much 3 of  $S_{3,2}$  for  $n - 1 = 3$
2. if  $\pi \in S_{n-1,m-1}$ ,  $n \geq m \geq 2$ , then it can be obtained  $\pi'' \in S_{n,m}$ , by adding  $n$  to position  $n$ , e.g.  $S_{3,1}(123) = 231 \rightarrow S_{4,2}(123)(4) = 2314$ .

Based on those characteristics, we define a function  ${}^i\pi_n: S_{n,m} \times [n] \rightarrow S_{n+1,m}$ ,  $1 \leq m \leq n, i \in [n]$ , that map a permutation  $\pi_n \in S_{n,m}$  to a permutation  ${}^i\pi_{n+1} \in S_{n+1,m}$  as:

$${}^i\pi_{n+1}(j) = \begin{cases} \pi_n(i) & \text{for } j = n + 1 \\ n + 1 & \text{for } j = i \\ \pi_n(j) & \text{others} \end{cases} \tag{67.1}$$

Therefore, generation of all objects of permutation  $n$  with a given  $m$  cycles  $S_{n,m}$  starts with identity permutation  $(1)(2)\dots(m)$ , as a root of the generating tree. Then we generate a permutation  $m + 1$  with  $m$  cycles  $S_{m+1,m}$ , as its children, by extending them using  ${}^i\pi_{m+1}$ , for  $i \in [m]$ . Other objects are then presented by implementing the second property, that is replacing  $m$ , which this time  $m$ , with  $m + 1$  in  $m$ -th cycle, and putting  $m$  to other cycles, alternately, in other word, implementing  ${}^i\pi_m$ . The process continues by applying  ${}^i\pi_k$ , for  $k = m - 1$  to  $2$ . The process continues until the desired value of  $n$ . The node that obtained by implementating the function  ${}^i\pi_k$ , is labeled as  $o_k$ . See Fig. 67.1 as an example of the generating tree of permutation  $n$  with  $m$  cycles for the four first level. In Enumerating Combinatorial Object (ECO) system, the tree has the susccession rule as follows:

$$\Omega = \begin{cases} o_1, \text{ identity permutation} \\ o_j \mapsto (o_{j+1})^j (o_{j+2})^{j+1} \dots (o_{m+1})^{m+1-j} \end{cases} \tag{67.2}$$

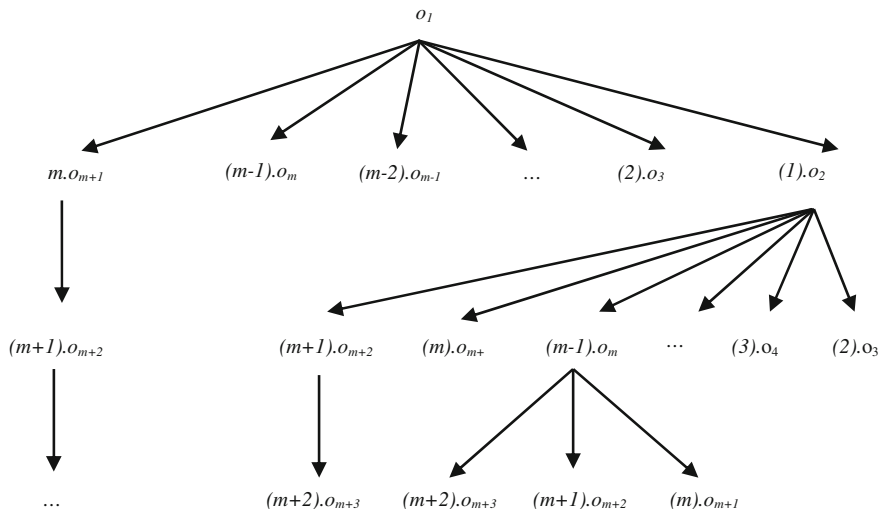


Fig. 67.1 The first four level of generating tree of a permutation  $n$  with  $m$  cycles

Motivated by [4], that constructed a combinatorial Gray code from a generating tree, we then propose a new Gray code that developed from Puspitodjati’s generating tree of permutation  $n$  with  $m$  cycles.

### 67.5 Gray Code of Generating Tree of $S_{n,m}$

Nodes in Puspitodjati’s generating tree of permutation  $n$  with  $m$  cycles, could be abbreviated by labeling each node with the sum of their children, as in Fig. 67.2. Node with label  $(j)o_{j+1}$  would have  $m + l - j$ , where  $l = n - m$  associated with level of the tree.

In order to have a Gray code, the tree rearranged using Vajnovszki’s idea as in [4]. Vajnovszki uses color-coded label. Two colors used there, they are *up* and *down*. So the label  $k$  may have two colors,  $k$  for *up* color, and  $k^R$  for *down*. The color leads to the list of its successors. The list of successors  $k^R$  is attained by reversing the list of successors of  $k$ . Therefore, to list the Puspitodjati’s generating tree of  $S_{n,m}$ , to become a Gray code, the succession rule (2) is rewritten as:

$$\Omega = \begin{cases} \varepsilon & \mapsto 1 \ 2 \ 3 \ \dots \ m, \text{ identity permutation} \\ k & \mapsto 1 \ 2^R \ 3^R \ \dots \ k^R \end{cases} \tag{67.3}$$

The generating tree as in Fig. 67.2, with the modified rules (3), becomes the new generating tree  $GTS_{n,m}$ . Figure 67.3 shows the generating tree for  $m = 4$  for the first three level.

**Fig. 67.2** Puspitodjati's generating tree of  $S_{n,m}$  with label of nodes abbreviated

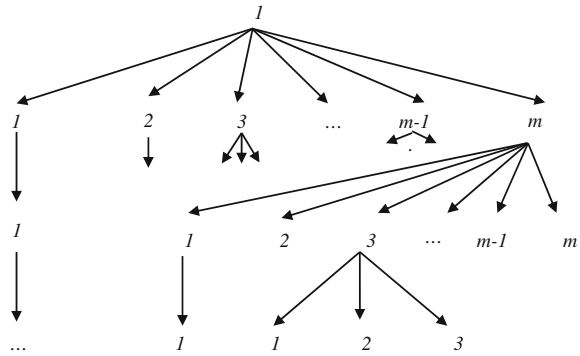
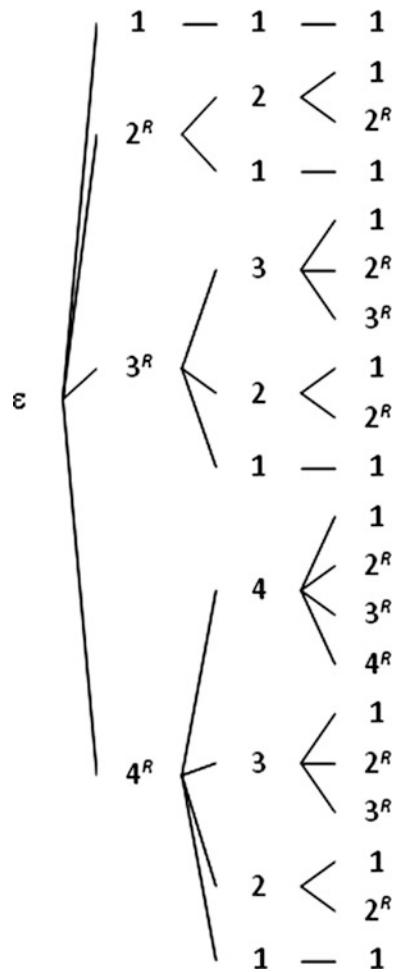


**Fig. 67.3** The generating tree  $GTS_{n,4}$  with rules as in formula (67.3)



When we visit nodes of the tree in Fig. 67.3 in a preorder way, start at 111, we then have ordered list of words formed as:

$\langle 111, 221, 222, 211, 331, 332, 333, 321, 322, \dots, 441, 442, \dots, 411 \rangle$

Notice that every two consecutive words in that list, only slightly different, with differ in at most 2 positions, even for the first (111) and the last word in the list (5111). Therefore, the Hamming distance of the two consecutive words of that list, is at most 2.

**Theorem 67.1** *The succession rule (3) gives a cyclic Gray code list with at most differ in 2 positions.*

*Proof* We prove by induction. Let  $L_d = \langle l_{d1}, l_{d2}, \dots, l_{dr_d} l_d \rangle$  is a list of the codes with length  $d$ , and  $r_d$  is the cardinality of the  $L_d$ .

**Base:** if  $d = 1$  then the theorem is true, since  $L_1 = \langle 1, 2, 3, 4, \dots, m \rangle$ , they differ in 1 position;

**Inductive hypothesis:** let us suppose that  $l_{(d-1)i}$  and  $l_{(d-1)(i+1)}$ , with  $1 \leq i \leq r_{d-1}$ , differ for at most 2 digit;

**Inductive step:** the list  $L_d$  is obtained by concatenating operation “ $\circ$ ” to every word  $l_{(d-1)i}$  in  $L_{d-1}$  with  $\langle 1, 2, \dots, last(l_{(d-1)i}) \rangle$  or with  $\langle last(l_{(d-1)i}), last(l_{(d-1)i}) - 1, \dots, 2, 1 \rangle$ , depending on the color of  $l_{(d-1)i}$  whether it is up or down. In the tree, this word extend by children of the node  $last(l_{(d-1)i})$ , so they are differ only in 1 position when the words comes in the same last sub tree with  $l_{(d-1)i}$  as its parent and up to its ancestor. Now, we will show how they differ for  $last(l_{(d-1)i}) \circ \langle 1, 2, \dots, last(l_{(d-1)i}) \rangle$  and the  $first(l_{(d-1)(i+1)}) \circ \langle 1, 2, \dots, last(l_{(d-1)(i+1)}) \rangle$ . There are two cases for two words  $l_{(d-1)i}$  and  $l_{(d-1)(i+1)}$ , they can differ one position if they come in same parent, so concatenating each, would make them differ in two positions. The second case is when  $l_{(d-1)i}$  and  $l_{(d-1)(i+1)}$ , differ in two positions, they will not in the same grandparent, therefore they both have 1 the level of grandchild, and 1 could only concatenate with 1, so they differ by two positions would be maintained.

The last to be proved is that the Gray code is cyclic. The first word of the list  $L_d$  is 1111...11, and the first letter or value of the last word of the list is  $m^R$ , therefore they would start with 1, and 1 is always concatenated with 1 again, therefore they differ in only 1 position at the beginning.

The construction of the Gray code of permutation  $n$  with given  $m$  cycles is done by concatenating every word with letter of  $\{1, 2, \dots, j\}$ , for  $1 \leq j \leq m$ , in every step, sequentially, whether, it is form 1 up to the  $j$ , or from  $j$  down to the 1. Therefore, it is from  $O(N)$  algorithm, for  $N$  the number of object in the list.

### 67.6 Conclusion

There are some papers discussed the generation of permutation with some restrictions [8–10], but not so many discussed permutation with cycles. The new Gray code offered in this paper is constructed from Puspitodjati’s generating tree of permutation with cycles. Since, words of the code related to the number of objects,

then it could be used as a new way to count the number of permutation size  $n$  with  $m$  cycles. Although, the proposed Gray code has not been transformed to the corresponding object yet, i.e. permutation with cycles, but the relabeling nodes is a function of the corresponding object. Therefore, it would be possible, to construct a Gray code of permutation with cycles with a simpler algorithm than Baril [7], that has some cases related to the size permutation and the given cycles.

## References

1. Savage, C.: A survey of combinatorial gray codes. *SIAM Rev.* **39**, 605–629 (1997)
2. Bernini, A., et al.: A general exhaustive generation algorithm for Gray structure. *Acta Informatica* **44**(5), 361–376 (2007)
3. Conflittiand, A., Mamede, R.: Gray codes and lexicographical combinatorial generation for nonnesting and sparse nonnesting set partitions. Pre-Publicacoes do Departamento de Matematica, Universidade de Coimbra, Preprint Number 13–31 (2015)
4. Vajnovzki, V.: ECO-based gray codes generation for particular classes of words. *GAS Com* 2012. <http://v.vincent.u-bourgogne.fr/0ABS/publi.html> (2012)
5. Banderier, C., et al.: Generating functions for generating trees. *Discrete Math.* **246**, 29–55 (2002)
6. Puspitodjati, S.: Exhaustive generation algorithm of permutation with fixed cycles and the size of permutation as variable. Dissertation. Doctoral Program in Information Technology. Gunadarma University, Indonesia (2010)
7. Baril, J.L.: Gray code for permutation with a fixed number of cycle. *Discrete Math.* **307**, 1559–1571 (2006)
8. Baril, J.L.: Gray code for Permutations with a fixed number of left to right minima. <http://jl.baril.u-bourgogne.fr/leftright.pdf> (2009)
9. Dukes, W.M.B., Flanagan, M.F., Mansour, T., Vajnovszki, V.: Combinatorial Gray codes for classes of pattern avoiding permutations. *Theoret. Comput. Sci.* **396**, 35–49 (2008)
10. Mansour, T., Nassar, G., Vajnovszki, V., Breckling, J.: Loop-free gray code algorithm for the e-restricted growth functions. *J. Inf. Process. Lett.* **111**(11), 541–544 (2011)

# Chapter 68

## Android and iOS Hybrid Applications for Surabaya Public Transport Information

Djoni Haryadi Setiabudi and Lady Joanne Tjahyana

**Abstract** This study is conducted to address the lack of route information of public transportation in Surabaya by creating an online guide that can be accessed by passengers to get complete information on maps and travel routes for public transportation. This guide is made interactive, simple, accessible and appropriate for transportation that is adapted to the conditions in the city of Surabaya. This research will develop an Android and iOS applications that can be used on smartphones and tablets using Android and iOS operating systems. Maps and routes are obtained from the Department of Transportation of Surabaya. Maps and route are developed using OpenStreetMap, Ajax, Javascript, XML, OpenLayer, PostgreSQL, and PostGIS. The hybrid application is compiled using PhoneGap. Passengers simply point to the destination of their journey, such as the name of the street, landmarks and public places. The system will automatically choose the alternative line of *bemo* they should choose, including the routes to reach the destination. The information includes the connecting line of a public minibus (called *bemo* in Indonesian) if the route needs to be connected by more than one *bemo* line. The information also includes the fare to be paid. From the test results, both the Android and iOS applications can adapt to a wide range of smartphones with a variety of screen sizes, from 3.5 to 5 in. smartphones and 7 in. tablets.

**Keywords** Routes · Maps · Public transportation · *Bemo* · Openstreetmaps · Android · iOS

---

D.H. Setiabudi (✉)  
Informatics Department, Petra Christian University, Surabaya, Indonesia  
e-mail: djonih@petra.ac.id

L.J. Tjahyana  
Communication Science, Petra Christian University, Surabaya, Indonesia

## 68.1 Introduction

Currently one of the mass public transportations in the city of Surabaya is the type of small and medium 1000 cc minibus commonly called *bemo* with a maximum carrying capacity of 10 persons [1]. Watkins et al. [2] in the studies of open source development of mobile transit traveler OneBusAway information system for King County Metro (KCM) in Seattle suggest that the provision of good information system for public transport passengers will increase passengers' satisfaction and increase the interest of the public transport. It would be useful to encourage people to switch from the use of private transportation to the public transportation. Setiabudi and Tjahyana [3] did a research on Surabaya public transport by using PHP language programming and MySQL database, accessed by a web browser. This application has applied website responsive technology, but each time a user will use this application s/he must be connected to the internet. Yulianto et al. [4] did a research on Jakarta public transport developed with web-based framework code igniter. However, the route map displayed was only for private cars and for public transport was only ready for one route on the map.

Furthermore, based on the observation of the initial research, there are some Android applications of Trans Jakarta Busway public transportation in Jakarta. Among them is Komutta that has the highest rating 4.6 out of 1,263 voters and has been downloaded more than 50,000 times in the Google Play Store. However, all the applications that have been created can only be running on one operating system. For instance, the application that can be used on Android cannot be used in iOS, Blackberry and Windows Mobile. Conversely the one that runs on Blackberry cannot be used in other operating systems.

As a result, not all smartphone users can take advantage of software applications that have been created. This is because all of the applications initially were developed using a native application and not with the hybrid application [5]. As a result, if an application is already developed as an Android native application, in order to make it available for iOS native application the developer must re-develop the application from the beginning, due to different programming languages that are used to develop native applications for different operating systems. If initially the applications were developed using a hybrid technology to produce cross-platform application, for example for Android, then only very minor and simple changes needed to be done when it would be developed for iOS. The idea of implementing hybrid application could be seen in the diagram of Fig. 68.1.

The head of IDC Operations of Indonesia, Sudev Bangah argued that many smartphones with varying price would be affordable for smartphone users who were on the middle segment of the market [6].

Based on the fact that market share is issued by IDC Indonesia, to increase the satisfaction of *bemo* passengers in Surabaya, this research will develop applications





Fig. 68.1 Block diagram of the system

that can be used by smartphones of Android and iOS operating systems for trip planning using bemo in Surabaya using Open Street Maps. Those applications will help the passengers plan their trips based on routes, timetables, and costs.

As shown in Fig. 68.1, the time can be shortened and costs can be saved because after developing a web-based application in the form of responsive website, it becomes a native application using PhoneGap that can then be distributed through the application store for each mobile operating system.

The applications will provide information about route guide and timetable of public transportation in Surabaya. The information will be equipped with a search feature and a trip planning using public transportation simply by typing the place of origin and destination specified by the passengers. Both the place of origin and destination can either be a street name or a landmark name and public place such as *bemo* stations, parks, rivers, shops, schools, and others.

The planned features will use a multimodal transport network that takes into account some factors such as multimodal routes, timetables, and costs to provide recommendations for the optimized route. This feature will guide the passengers to the nearest public transportation station, by giving the instruction on which public transportation they should take, to arrive at the nearest public transportation to the destination. This feature will also be equipped with an estimation of the fare for the service.

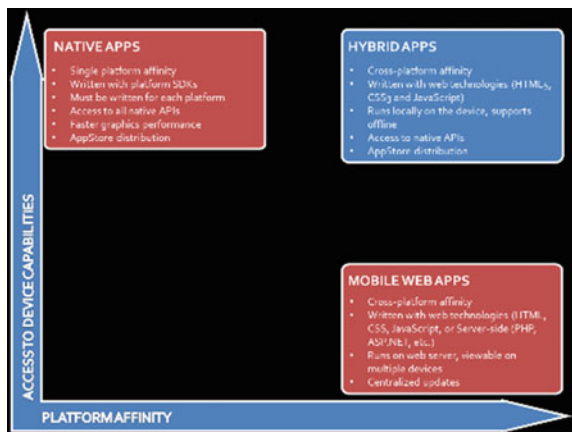
## 68.2 Hybrid Applications

There are several types of mobile application, which are Native App, Web App and Cross Platform Mobile App or Hybrid App. According to Stark [7], Native application is application installed on the phone, such as Android and iOS-based Smartphones. Native applications have access to the Smartphone hardware features such as camera, speaker, etc. developers have to use different kinds of programming language to develop native applications for different platforms. To develop Android native applications, Java programming language is needed. Objective—C is used to develop iOS native applications. Native applications are available on the official application markets such as Google PlayStore for Android and iTunes App Store for iOS.

On the contrary to the Native application, Web applications are not installed on the phone and they are not available on the official application markets such as Google PlayStore and iTunes App Store. However, they are easily accessed with the Smartphone’s web browsers and developers are only required to use HTML, CSS, and JavaScript to build Web applications. The downside for Web applications is that it cannot access certain hardware features on the smartphone [7].

Hybrid application or Cross Platform mobile application is considered to be the right solution for developer to build iOS and Android applications without mastering many programming languages and downloading any SDKs (software development kits) for each platform, but it can put the application on Google PlayStore and iTunes App Store [8]. To build a hybrid application or a cross platform mobile application both for iOS and Android, developers only need to use HTML, CSS and JavaScript to develop a web application. Next, with PhoneGap technology, the web application will be packaged into a native application for iOS, Android and other mobile platforms [7].

Fig. 68.2 Three types of applications



A graph that highlights the differences in native, hybrid and mobile web applications can be seen in Fig. 68.2. Native applications are built for a specific platform with the platform SDK, tools and languages, typically provided by the platform vendor (e.g. xCode/Objective-C for iOS, Java for Android, Visual Studio/C# for Windows Phone).

Mobile Web applications are server-side applications, built with any server-side technology (PHP, Node.js, ASP.NET) that render HTML that has been styled so that it renders well on a device form factor. Hybrid applications, like native applications, run on the device, and are written with web technologies (HTML5, CSS and JavaScript). Hybrid applications run inside a native container, and leverage the device’s browser engine to render the HTML and process the JavaScript locally. A web-to-native abstraction layer enables access to device capabilities that are not accessible in Mobile Web applications, such as the camera and local storage.

### 68.3 Research Methodology

#### 68.3.1 Fishbone Diagram

The method used in this research can be seen in Fig. 68.3. The first step includes a survey of the timetables of public transportation, the fare of travel, and the location of public places.

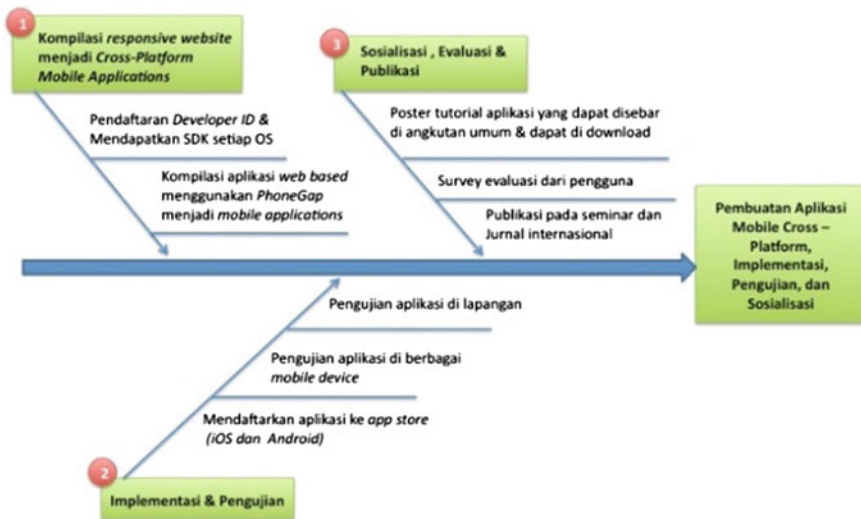


Fig. 68.3 Fishbone diagram of research methodology

The first step is to compile the responsive website that has been made to be cross-platform mobile application using Phonegap. At this stage the process will begin with registration of Developer ID in the application store for each operating system, until a developer SDK for each platform is secured. After this, the compilation of web-based applications with the SDK of each platform using phonegap, resulting in cross-platform mobile applications needs to be done. The outcomes are cross-platform mobile applications that can be used for each operating system (iOS and Android).

The second step will be the implementation and testing of applications with the following stages: Registering and uploading applications on each application store for each operating system (iOS and Android), namely AppStore for iOS and Google Play Store for Android. Testing the applications on a variety of mobile devices for each operating system with a different screen resolution size. Testing the use of applications in the real case and doing the journey planner on public transportation in Surabaya with some case studies of travel route need to be done.

The last stage or the third step will be disseminating and evaluating the applications with the following phases: Create tutorial posters about the application that will be shown at the terminal and all public transportation. Upload the tutorial posters at the Department of Transportation website and official Facebook page of the Department of Transportation. Finally evaluate the application by providing a place for criticisms and suggestions the make the application better.

### **68.3.2 System Design**

The design of the client system is shown in the flowchart in Fig. 68.4. Firstly, the users must choose what they want to do, whether they want to look all routes or directly get to the direction. If they choose to see all routes, all lists of bemo lines nearby their current position will be shown.

Furthermore, they have to pick one from the list to see the route on the map. However, if they want to get directly to their destination, they must choose one point of interest available in the server database. Then, they have to choose how the application detects their current location using GPS or manually clicking on the map. Nevertheless, the method to detect the user's location still depends on whether the GPS is available on their device or not. If the application can detect the current location of the user, then it will show the routes to go to their destination using the closest line available near their current location.

The developing process is started by preparing a source code in the form of HTML, Javascript, and CSS on the Client, while on the Server there are database and PHP script. Next, it is converted into a hybrid application by using Phonegap. For development on the Android environment, softwares Node.JS,

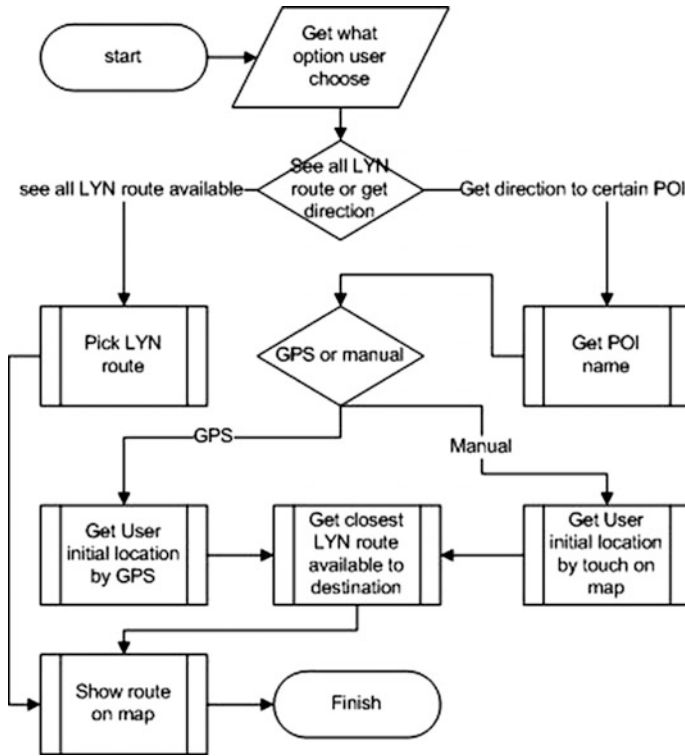


Fig. 68.4 Flowchart of the client system

Android Studio, Java Runtime Environment, JDK (Java Development Kit), and Android SDK (Software Development Kit) are needed. For development on iOS environment, softwares Node.JS, Xcode dan iOS Simulator are needed.

### 68.4 Experimental Results

The testing of the applications was done using two devices, namely 3.5 in. smartphone and 7 in. tablet, respectively for Android and iOS. The first time the applications is initialized, it will display the screen like in Fig. 68.5. There are two options to choose, namely ‘Search bemo routes to destination’ and ‘See all existing routes of bemo’.

If the user selects the option ‘See all the existing routes of *bemo*’, then the screen shows as in Fig. 68.6. If the user types a particular letter or word and presses one of the available buttons from the options, then the application will bring up a page with a map of the selected line.

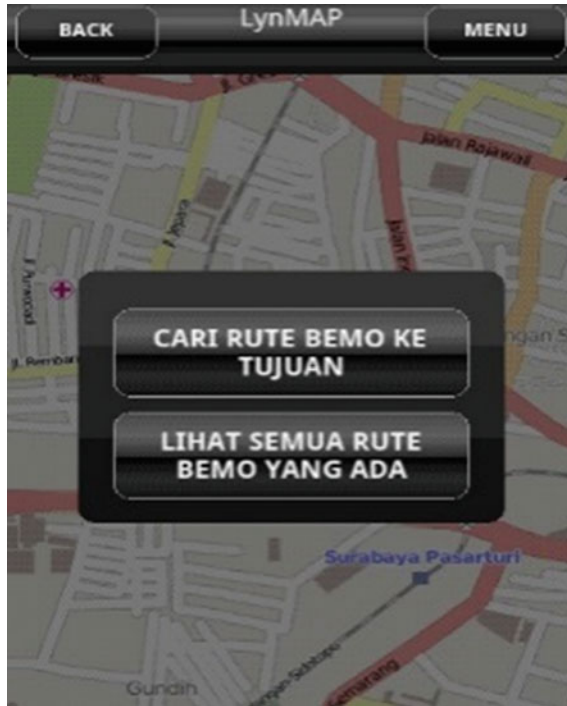


Fig. 68.5 Two options to choose

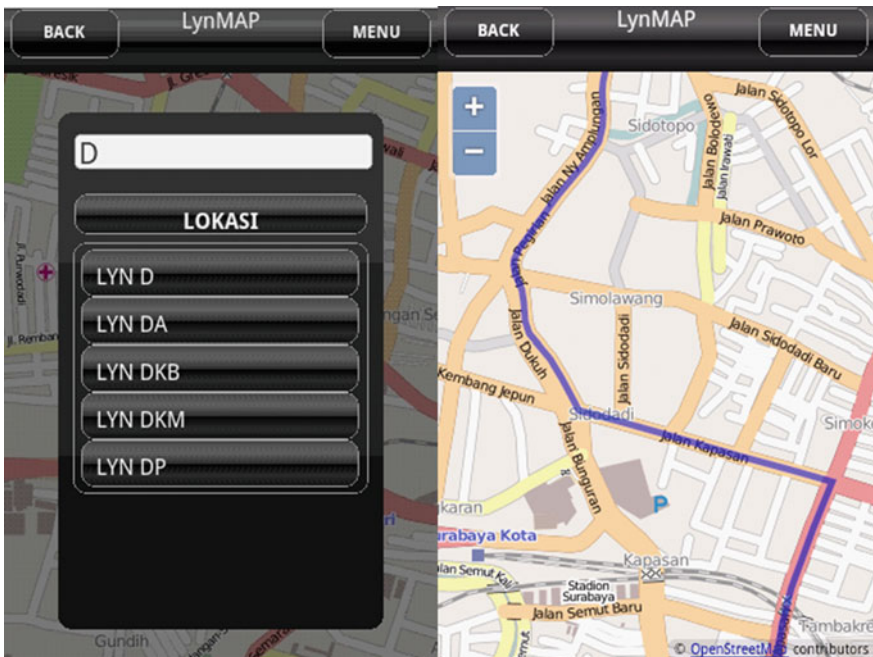
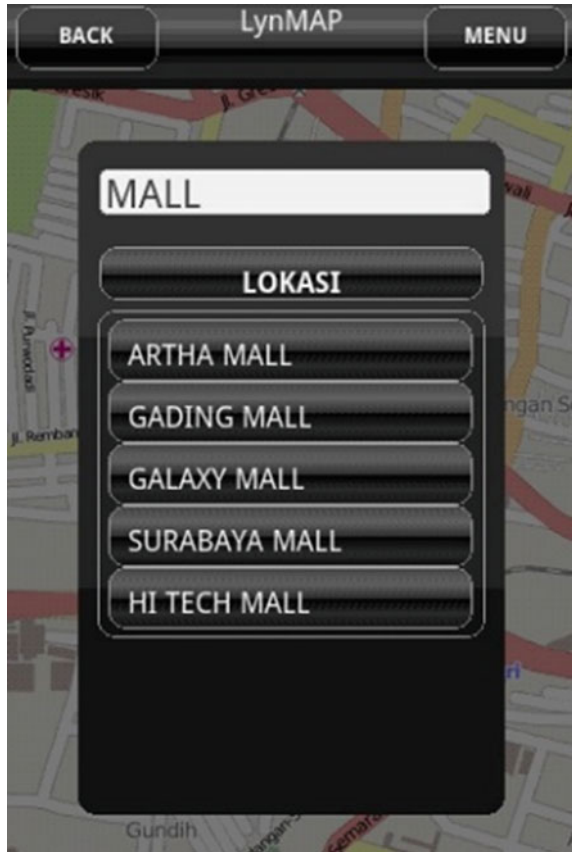


Fig. 68.6 Alternatives of Bemo routes and maps of the route

Fig. 68.7 5 Point of Interest



If in Fig. 68.5 the user selects the option ‘Point of interest’, the screen will display options as shown in Fig. 68.7. If the user types a particular word (i.e. MALL) and presses ‘ok’ button, then it will display a maximum of 5 points of interest containing the word typed by the user. Once the initial location has been determined, it will show the route to be passed and the estimated fare to be paid as in Fig. 68.8.

Figure 68.8 shows that the user originally is on Nyamplungan Street and she or he wants to travel to Ambengan Street. The first time the user is suggested to go by Line A *bemo*. On the way *s/he* should get off from the Line A *bemo* on Tambaksari Street and walk to Kapasari Street to get on Line B *bemo*. Next she or he has to get off Line B on Tambaksari Street and walk to the destination on Ambengan Street.

When the user wants to see the resulting route *s/he* can press on the ‘view map’ button, then options will appear on the display as in Fig. 68.9 on smartphone (left) and tablet (right).



Fig. 68.8 Information of routes

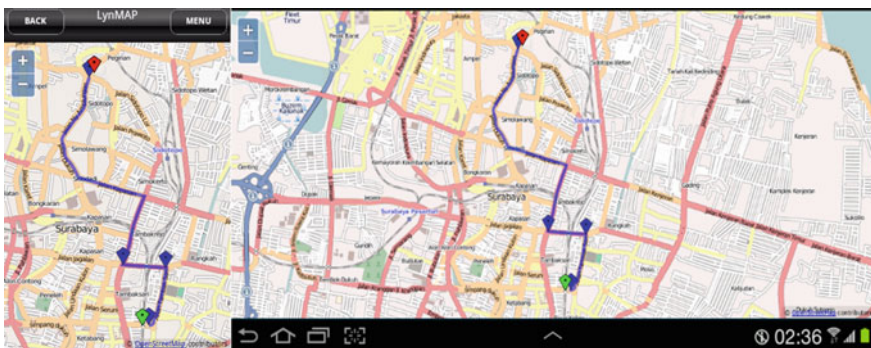


Fig. 68.9 The routes generated on the map (On Smartphone and Tablet)



## References

1. Angkutan Massal ‘Sekarat’. Available: <http://www.surabayapost.co.id/?Mnu=berita&act=view&id=0b8729fc9c2f434ea5ffb8252a78680c&jenis=b706835de79a2b4e80506f582af3676a> (2013)
2. Watkins, K., Ferris, B., Borning, A., Rutherford, S., Layton, D.: Where is My Bus? Impact of mobile real-time information on the perceived and actual wait time of transit riders. *Transp. Res. Part A* **45**, 839–848 (2011)
3. Setiabudi, D.H., Tjahyana, L.J.: Interactive map routes for public transportation in Surabaya running on smartphones and tablets. *ARPN J. Eng. Appl. Sci.* **9**(10), 1811–1816 (2014)
4. Yulianto, N., Waluyo, Tomi, B., Suryadi.: Desain Web untuk Sistem Informasi Angkutan Umum di Jakarta. *TELAHAH Jurnal Ilmu Pengetahuan dan Teknologi* 30 no. 2 (2012)
5. Kor, M., Oksma, E.: Native, HTML5, or hybrid: understanding your mobile application development options. [http://wiki.developerforce.com/page/Native,\\_HTML5,\\_or\\_Hybrid:\\_Understanding\\_Your\\_Mobile\\_Application\\_Development\\_Options](http://wiki.developerforce.com/page/Native,_HTML5,_or_Hybrid:_Understanding_Your_Mobile_Application_Development_Options) (2013)
6. Grazella, M.: Android to remain champ, Windows to pick up steam in 2013. <http://www.thejakartapost.com/news/2013/01/05/android-remain-champ-windows-pick-steam-2013.html> (2013)
7. Jonathan, S.: *Building iPhone Apps with HTML, CSS, and JavaScript*. O’Reilly Media, Inc., USA (2010)
8. Charland, A., Leroux, B.: Mobile application development: web vs native. *Commun. ACM* **54** (5), 49–53 (2011)

# Chapter 69

## Games and Multimedia Implementation on Heroic Battle of Surabaya: An Android Based Mobile Device Application

Andreas Handojo, Resmana Lim, Justinus Andjarwirawan and Sandy Sunaryo

**Abstract** Number of users of who use mobile devices and other handheld devices is rapidly increased (such as smartphones and tablet computers). This phenomena has changed the lifestyle of many people, especially in the ease of access to information. For example, access to any business information, political information, tourism information, as well as educational information. Education has also entered a new era, where books and other teaching materials, are not only presented using paper media but also in electronic form. Student can easily access that electronic information using computer/laptop or smartphone/tablet PC. So now, learning can be delivered in a more interesting and interactive media and model. It becomes new challenges for education, especially in teaching nation history, where education in paper material is no longer quite interesting. Therefore, new teaching media is required, that more interesting and interactive to the student. At this time, there are not many applications on mobile devices that explore education especially on heroic history of Indonesia. On the other hand, the education of heroic history become more necessary today, especially for young people. To answer this challenge, in this research we like to build an application software based on android mobile devices that contain education the history of the heroic battles 10 November 1945 in Surabaya. The application will provide the information of battle history, and also games and multimedia interactive such as sound, video streaming that built on android based mobile device. With this educational applications we expected that everyone especially young people can learning the knowledge about the history of the heroic battle 10 November 1945 Surabaya in the mobile device based on

---

A. Handojo (✉) · J. Andjarwirawan · S. Sunaryo  
Informatics Engineering Department, Faculty of Industrial Technology,  
Petra Christian University, Jl. Siwalankerto 121–131, Surabaya 60236, Indonesia  
e-mail: handojo@petra.ac.id

R. Lim  
Electrical Engineering Department, Faculty of Industrial Technology,  
Petra Christian University, Jl. Siwalankerto 121–131, Surabaya 60236, Indonesia

Android in interactive educational applications that provide a thorough understanding and fascinating history of the events surrounding the battle, and also exploring the historic sites in Surabaya and found fascinating city of Surabaya.

**Keywords** Android · Games · Heroism · Multimedia · Surabaya

## 69.1 Introduction

Number of users of who use mobile devices and other handheld devices is rapidly increased (such as smartphones and tablet computers). This phenomena has changed the lifestyle of many people, especially in the ease of access to information. For example, access to any business information, political information, tourism information, as well as educational information. Education has also entered a new era, where books and other teaching materials, not only presented using paper media but also in electronic form. Student can easily access that electronic information using computer/laptop or smartphone/tablet PC. So now, learning process could deliver in a more interesting and interactive media and model.

It becomes new challenges for education, especially in teaching nation history, where education in paper material is no longer quite interesting. Therefore, new teaching media is required, that more interesting and interactive to the student. Here, we saw an opportunity to present the heroic values in an application for mobile devices based on android in the interesting and interactive way. We like to present information especially related to the history of epic heroic battle in the historic events that occurred on 10 November 1945 in Surabaya. For example, the information about location of the historical battle with location photo gallery, including games (such as puzzle, quiz, finding object) and multimedia interactive implementation (such as sound, video streaming). Therefore, with this application we expect that many people would have interest to access information about the historical places in Surabaya and to explore these historic sites in Surabaya, as a memento of the heroic battle 10 November 1945.

This application builds in Indonesian and English, and enriched with multimedia content (text, sound, music, video, animation) and quiz game about historical event of 10 November 1945. With an attractive and interactive application, we expect that these applications will be widely used by mobile device users in Indonesia for teaching history lesson and provide a thorough understanding and fascinating history of the events surrounding the battle of 10 November 1945. The applications will be constructed using Java programming language, IDE Eclipse, JSON, SQL Lite database on Android, and the MySQL database on the server and using the Google Map API and GPS.

## 69.2 Related Works

Android application as an enhanced or aided learning on educational has done in many ways. Such as to deliver learning material [1, 2], to deliver test online and quiz [3, 4], class attendance report [5], etc. Another research also conduct to create computer application to enhanced learning process such as Nurazwan [6] that build 2D animation (animated multimedia) presentation to attract children's interest in learning history. This 2D animation tell story about Antenom heroism (Malay) in fighting the British army. The animation create in the website and on the compact disk that distributed on the schools.

In other hand, learning on Indonesian history and the aspects of heroism have been try to explore in the various forms of media, like comics [6] that try to visualize heroism of Pattimura that design for primary school children. Suardi [7] also tried to build 3D media on monuments building as the learning media. It shows the moments of heroic battle in the Dutch colonial period that occurred in the Bangsal Bali area. Meanwhile, Sabastian [8] tried to design an encyclopedia of 30 Indonesian independence heroes. This encyclopedia increases the value of history education for the public, especially young people to increase appreciation of the national hero. However, until now, still a few applications that explore the history of Indonesian patriotism. Such as historic heroism buildings, locations, artifacts, etc.

From the available references, we conclude that the exploration of Indonesian heroism history not yet been explored using mobile device applications as the media. Especially with interactive and educative games also with multimedia feature (text, sound, movie). So, in this research we try to create applications that run on mobile device that we hope this application might interesting for to young people.

## 69.3 Battle of 10 November 1945 in Surabaya [9, 10]

The battle of Surabaya at 10 November 1945 started when Captain Huijer, Dutch Navy arrived in Surabaya. This army have task to takeovers of Japanese army that had lost world wars 2. However, under force by Indonesian army led by Sudirman and Doel Arnowo, Japanese army handed their weapons to the Indonesian army called Badan Keamanan Rakyat (BKR). Therefore, on 1 October 1945, a fight begun to happen between Ducth Navy and Indonesian army. Indonesian begun to attack airfields on Morokrengangan and detention camp on Darmo. The Japanese army headquarters (Kempetai) also surrounded by Indonesian army. This fight ended after Captain Huijer arrested by Indonesian army. To respond this action, on 25 October 1945, allied force led by British army landed at Tanjung Perak harbor in Surabaya. This army led by Brigadier General Mallaby along with the 49th Brigade

that contained six thousand elite troops. Mallaby then send one platoon led by Captain Shaw to save Captain Huijer. Allied forces also took over the office of railways, telephone and telegraph centers, Darmo hospitals, and others vital building. The great battle was inescapable between six thousand British elite troops with around one hundred thousand soldiers and Indonesian people. Due outnumbered, Mallaby asked president Indonesia, Soekarno, to persuade Indonesian army to stop the battle. Sukarno, Hatta, and Amir Sjarifoeddin finally come to Surabaya to stop the battle. Then a cease-fire occurred between both armies.

However, an incident happened. On 30 October 1945, Buick that carrying Brigadier General Mallaby intercepted by Indonesian militia group when going to pass the Red Bridge (also known as Jembatan Merah). The incident ended with the death of Brigadier General Mallaby. Because of this incident, Lieutenant General Christinson, commander of Allied forces in the Netherlands East Indies (AFNEI) send fifth Infantry Division complete with weapon and tanks to Surabaya under the command of Major General Mansergh. This army approximately carried fifteen thousand troops. On 9 November 1945, the British issued an ultimatum to Indonesian army to surrender all their weapons at 10 November 1945. Then at 9 November 1945 23.00 PM, Soerjo, governor of Surabaya announced his decision through radio that Surabaya will fight until the end. So, on 10 November 1945 the heroic battle in Surabaya began. The battle happened on the next 3 weeks. In late November 1945, the entire city of Surabaya has fallen into the hands of Allied Force. Indonesian fighters that still alive join the refugees fled from Surabaya. The Indonesian army then created a new line of defense at West site (Mojokerto City) until East site (Sidoarjo City). This heroic battle triggered the resistance in many areas in Indonesia. Right now, this event celebrated as hero day on every 10 November.

## 69.4 Android

Android provides an open platform for developers to create their applications. Android is built using object oriented, where the constituent elements of the operating system in the form of objects that can be reused/reusable. Android also use an operating system based on Linux for mobile devices that includes an operating system, middleware and applications. The architecture of the Android Operating System and its elements can be illustrated as in Fig. 69.1. Android architecture consists of four layers of components. At the beginning, Google Inc. bought Android Inc., newcomers who make software for mobile phones/smartphones. Then to develop Android, Google formed the Open Handset Alliance, a consortium of 34 hardware, software, and telecommunications companies, including Google, HTC, Intel, Motorola, Qualcomm, T-Mobile, and Nvidia [11].

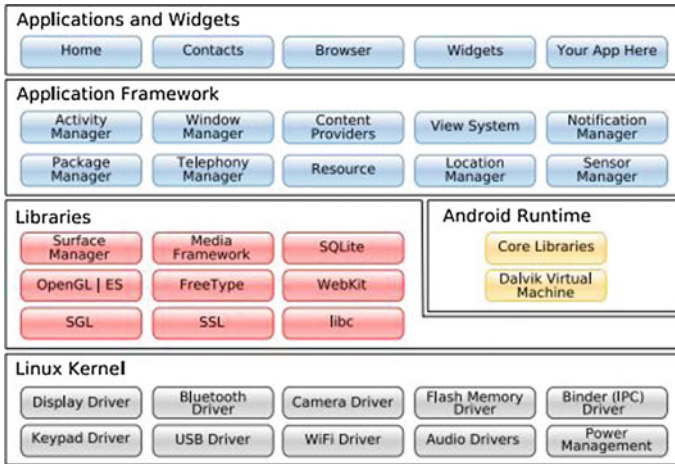


Fig. 69.1 Android architecture [11]

## 69.5 JSON (JavaScript Object Notation)

JSON or JavaScript Object Notation is a code for the exchange of mission data in XML format. The format is quite simple JSON because it will understand by people easily. JSON JavaScript programming language, ECMA-262 edition was built 3 Based on December 1999 common, CA, uses a style used by C programmers, because JSON is not affiliated in any programming language standard + C#, Java, JavaScript, Perl, Python and others [12].

## 69.6 Implementation and System Testing

The implementation and system testing of this application is apply using various types and specifications of mobile devices such as the Sony Xperia Z, Sony Xperia Arc S, LG G3, and the Samsung Galaxy Note S6 to test the reliability of applications in a wide range of devices.

The application, contain with history of battle on Surabaya and also provide with photos gallery about Surabaya battle history and also the existing Surabaya (can be seen in Fig. 69.2). User can show images and stories regarding the history of the battle of Surabaya from an existing location.

The application, also provide multimedia interactive like sound (Fig. 69.3) from history of battle on Surabaya for example like Bung Tomo (one of Great War hero on that battle) speech on 10 November 1945.

To attract and give the user an overview of the condition of the current battle this application also have movie features which will provide information (in video

Fig. 69.2 Photos gallery on Android



Fig. 69.3 Sound features on application

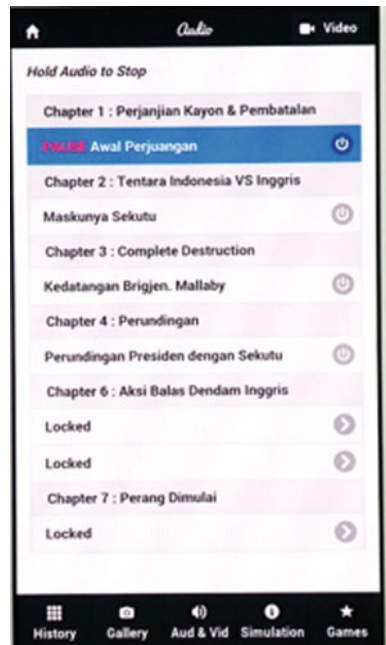


Fig. 69.4 Video multimedia on application



Fig. 69.5 Video multimedia on application





media) about the battle 10 November 1945. This video is also provide testimony from the fighters who fought at that time (as can be seen on Figs. 69.4 and 69.5).

This application also provide by games feature based on the battle story to attract user to use this application. Each of chapter will provide with mini games as can be seen on Fig. 69.6. This games is expected to attract users, especially young people to use this application. Available games such as object finding (Fig. 69.7), puzzle (Fig. 69.8), and quiz (Fig. 69.9).

We tested this application to 200 student in various age (5–17 years old) and various background of education (elementary, junior and high school). All of the respondent were very interested in sound (particularly on Bung Tomo speech). They also very interested on image and movie that are provided by this application. The respondent with age 5–10 years old have more interest in object finding game and puzzle, but respondent with age 11–17 years old have more interest in object finding game and quiz. Their opinion is that the more interactive game that they must play, the more interesting is the game. All the respondent though that this application is very interesting to learn history especially with interactive games and multimedia.

Fig. 69.6 Games on each chapter

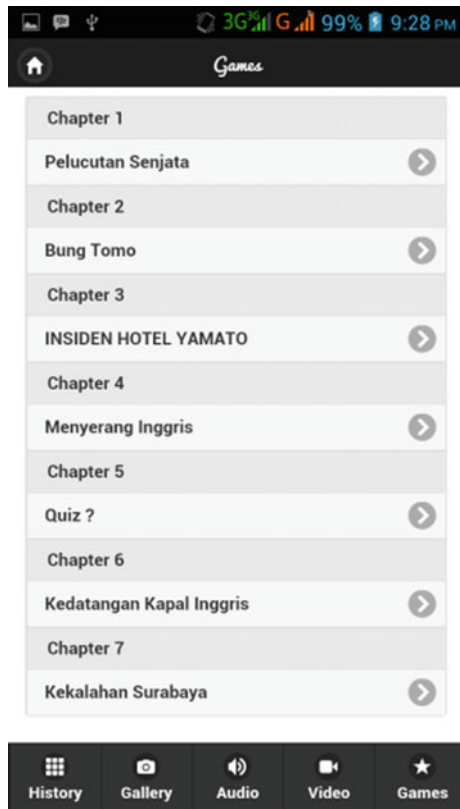




Fig. 69.7 Object finding games

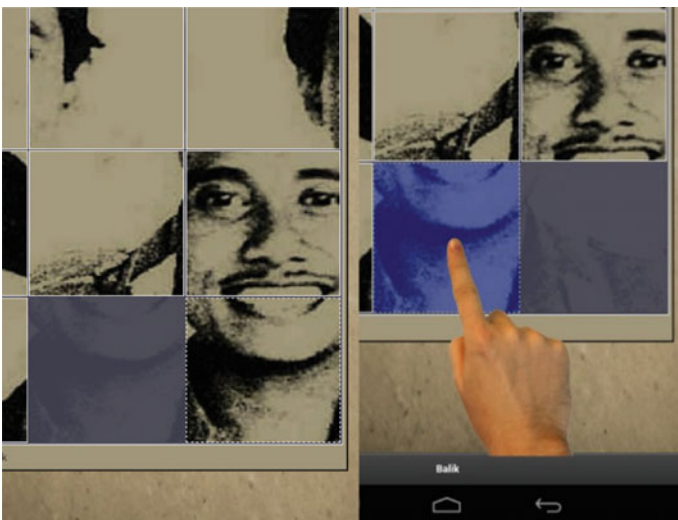


Fig. 69.8 Puzzle games

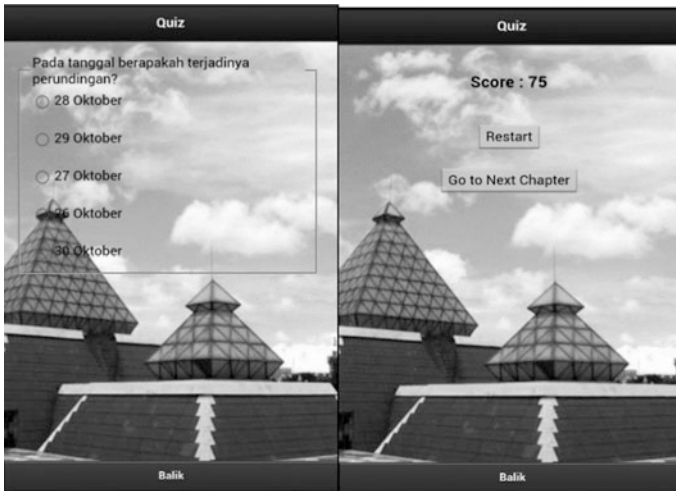


Fig. 69.9 Quiz games

## 69.7 Conclusion

The application that has been made can perform all the features such as image gallery, games, movie player, and sound player. This features also can run well on many mobile device without any technical problem. Based on testing to 200 respondents a variety of ages (5–17 years old) and educational backgrounds (elementary, junior and high school), we found that the content of Games and Multimedia on this application very interest to user especially on age 5–15 years old. We also found that 87 % of respondents have the opinion that this application is very interesting and useful for the city of Surabaya.

**Acknowledgments** This Research is funding by Directorate General of Higher Education (DIKTI) Research Grants 002/SP2H/P/K7/KM/2014.

## References

1. Chuang, Y.T.: SSCLS: A smartphone-supported collaborative learning system. *Telematics Inf.* **32** (2015)
2. Procter, P.M.: Advancing information and communication technology knowledge for undergraduate nursing students. In: 11th International Congress on Nursing Informatics (2012)
3. Handoyo, A., Leman, A., Noertjahyana, A.: Android-based test online application and website for learning process. In: RETI Conference Proceedings (2013)
4. Lim, R., Wijaya, P.S., Handoyo, A., Andjarwirawan, J., Intan, R.: Web services extension for accessing quiz on moodle mobile application. *J. Eng. Appl. Sci.* **9**(12), 2912–2915 (2014)

5. Handojo, A., Andjarwirawan, J., Wonodihardjo, J.: Presence class application with near field communication (NFC) on Android. In: Conference on Information Technology Computer and Electronic Engineering Proceedings (2013)
6. Augustine, M.N.: Pahlawan Antenom Dalam Seri Animasi. Utusan Borneo, Negeri Sabah-Malaysia (2012)
7. Suardi, P.P.E.: Pemanfaatan Monumen Perjuangan Bangsa sebagai Sumber Belajar Sejarah Bagi Generasi Muda di Desa Dalung. Badung, Jurnal Candra Sangkala **1**(1), 1–10 (2013)
8. Sebastian.: Perancangan Publikasi Ensiklopedia 30 Pahlawan Perjuangan Kemerdekaan Indonesia, Digital Repository Universitas Bina Nusantara (2012)
9. Alwi, D.: Pertempuran Surabaya November 1945, PT. Bhuana Ilmu Popoler (2012)
10. Budi, A.: Pertempuran Surabaya 10 November 1945. <http://umum.kompasiana.com/2009/11/23/pertempuran-surabaya-10-november-1945-28773.html>
11. Nazruddin, S.: Pemograman Aplikasi Mobile Smartphone dan Tablet PC Berbasis Android. Penerbit Informatika, Bandung (2012)
12. JSON.: Introducing JSON. <http://www.json.org/>

# Chapter 70

## Streamlining Business Process: A Case Study of Optimizing a Business Process to Issue a Letter of Assignment for a Lecturer in the University of Surabaya

S.T. Jimmy

**Abstract** This paper focused on revealing how a business process can be streamlined by thoroughly examined a project to optimize a business process to issue a letter of assignment in the University of Surabaya (Ubayu). The case shows evidences on how the university could successfully deliver significant benefits by utilizing IT to optimize a business process. It shows how Trkman’s success factor framework can be used as a guideline to implement a business process improvement project in a higher education institution.

**Keywords** Business process • Improvement • Success factor

### 70.1 Introduction

Business process is a system which consists of activities performed by various employees from a set of diverse units in an organization [1]. It represents how an organization works and thus, determines the organization’s performance. Efforts made to streamline business process, which also known as Business Process Re-engineering (BPR) and Business Process Management (BPM), can be considered as “the fundamental rethinking and radical redesign of business processes to achieve dramatic improvements in critical measures of performance such as cost, quality, service, and speed” [2, 3].

Such potential has lured most firms to conduct BPR [4]. Unfortunately, streamlining business process is not an easy task. Various researches suggest that BPR project are an extremely high risk project where only 30 % of those initiatives are able to successfully deliver the expected results [5–7]. Such facts suggest that

---

S.T. Jimmy (✉)

Department of Computer Science, University of Surabaya, Surabaya, Indonesia  
e-mail: jimmy@staff.ubaya.ac.id

BPR is a complex project which should be engaged carefully to harvest the expected outcomes.

This paper attempts to reveal how a business process can be streamlined by thoroughly examines a project done by Ubaya to optimize the process of issuing a letter of assignment. Other than attempting to optimize the business process, the project is also a pilot project to measure the organization's readiness towards a computer based approval system.

## 70.2 Literature Review

Prior thoroughly analyzing the case study, it is important to firstly measure the project's success since a success story offers different kind of lessons than a disastrous story. This paper will use the four dimensions model of process redesign effects [9] to measure the success level of the case study. The model compares the business process' performance before and after the improvement on four dimensions: cost, quality, time, and flexibility. Achieving maximum results on all dimensions is unlikely as each dimension might contradict other dimensions and thus often lead to trade-off that has to be made when streamlining a business process.

One way to reveal lessons behind the success story is by confirming the case with literatures regarding key success factors of business improvement project. For this purpose, Trkman [8] proposed a framework which classified the success factors into three distinct groups: contingency theory, dynamic capabilities and task-technology fit.

The contingency theory focuses on fitness between the business process and the business environment. Secondly, dynamic capabilities refer to continuous improvement to assure sustained benefits from streamlining the business process. Lastly, task-technology fit focuses on fitness between IT and the business process.

## 70.3 The Case Study

The case study is an initiative from Ubaya to streamline the process to issue letter of assignment to lecturers who want to present his/her paper in a conference. Although, this process is not a major process in the university, it plays a critical role as paper publishing is an important task that needs to be done by every lecturer in a university. The number of publication produced by a lecturer directly affects performance appraisal of the lecturer, the lecturer's department and the university.

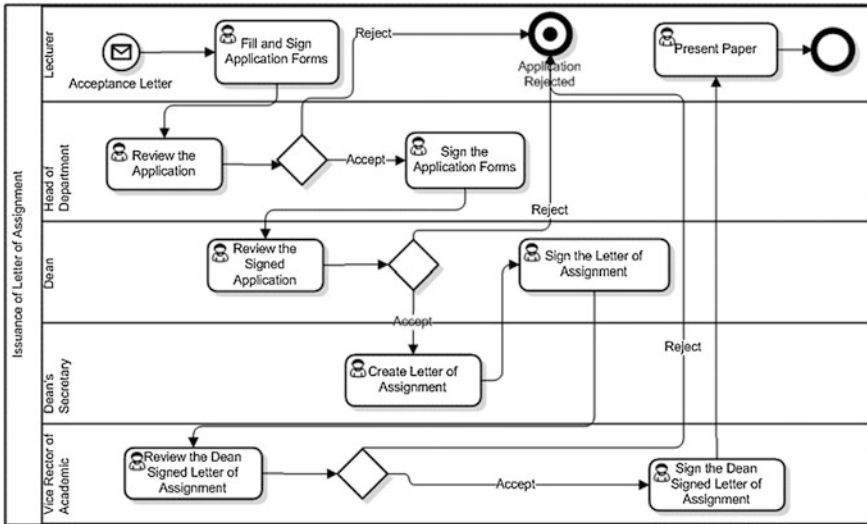


Fig. 70.1 The legacy business processes

### 70.3.1 Analysis of the Previous Process

Legacy process to issue the letter of assignment in Ubaya involves the use of traditional paper based procedures with no suffice documentation procedure. The use of paper forms has caused many redundant processes needs to be done by various stakeholders. The redundancy and the nature of paper based systems contribute to the lengthy time required to issue the letter of assignment. Figure 70.1 shows the flows of the legacy process using the BPMN (i.e. Business Process Mapping Notation).

Further, the biggest problem with the legacy system occurred after the lecturer accomplished the given assignment. Although data about published papers is required by various units, there was no clear decision towards who and how should the published paper be documented. Therefore, whenever data about publication is required, unit which requires the data will conduct survey to all lecturers to gather information about their publications. On top of that, important evidences regarding the publications often went missing with no possible way to recover it.

### 70.3.2 Implementation of the New Process

Implementation of the new process is enabled through the use of IT. Aligned with the university's policy, the new system is built on open source technologies. Database of the new system is designed using extended entity relationship diagram and is modeled using the mySql Workbench 6.0. The system itself is embedded

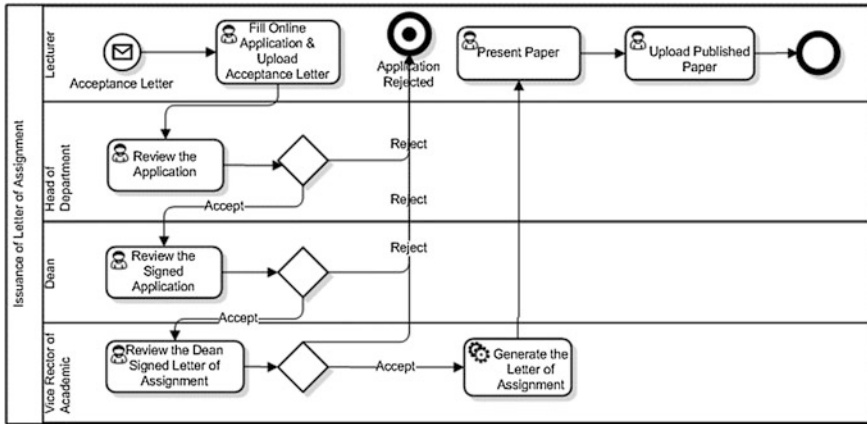


Fig. 70.2 The new business process

within the university’s portal which is developed using PHP and MySQL server as the database.

This process of optimization project was initiated by the Vice Rector of academic by gathering all stakeholders who often require the publication data and the IT department which is expected to develop the required systems. One of the most important decisions produced in the gathering is decision regarding authority of the publication data which will be held by the center of research. Another important decision is to streamline the business process using IT as a catalyst to solve various issues of the old process. Figure 70.2 shows the new business process mapping.

All tasks in the new system were designed to be done using the university’s portal including the generation of the signed letter of assignment. Signatures and stamps of all deans and the vice rector were collected, scanned, and stored in the server to be used to generate the letter of assignment. Approvers could review and decide to accept or reject the proposed assignment via internet at their convenient time and location. Further, the system also stores all necessary documentation regarding the publications. Thus, publication data along with the related documentation can be easily accessed by any authorized stakeholders.

### 70.4 Results and Discussion

This section seeks to justify the case’s success using the four dimensions as described in the literature review. Comparison of the old and new processes on each dimension is described in Table 70.1.

Table 70.1 evidently shows that the new process is better than the old process on all four dimensions. The new system is proven to be more cost effective, able to deliver better stakeholders’ experience, able to provide a better quality of publication data, more cost effective and more flexible than the old processes. Therefore,



**Table 70.1** Comparison of the old and the new processes

	Old Process	New Process
Cost	Requires application forms, Dean's secretary to write letter of assignment, and effort to collect publication data	No application forms, letter of assignment is generated by the system, easy and instant access to publication data
Quality	No clear documentation procedures, no publication database, frequent redundant questionnaires about publication irritates lecturers	Centralized publication database available conveniently for any authorized stakeholders, no publication questionnaires
Time	Days to get the letter of assignment approved, weeks to collect publication data from lecturers, hours to collect publication documentation	Head of department, Dean, and Vice Rector could approve immediately even when they are out of office, instant access to publication data
Flexibility	Requires physical contacts for approval and also physical contacts to reach lecturers to collect publication data	Instant approval via internet, publication data stored in server available for authorized users at any time

the project to optimize the business process to issue the letter of assignment can be considered as successful.

After confirming the case's success, the Trkman's framework of key success factors in business process improvement will now be used to reveal how Ubaya could successfully streamline the business process (see Table 70.2).

Table 70.2 shows that all success factors of business process improvement as suggested by Trkman have occurred in the implementation of the new business process as described in the case. This might answer how Ubaya could successfully deliver the expected benefits from changing the business process to issue the letter of assignment. Important remark to be learnt from this case is that although IT has an essential role in business process improvement, investing in IT does not automatically means guarantee performance improvements [10]. The key is to find a proper level of IT investment to support the organization's strategy.

## 70.5 Significance and Further Study

The case confirms that Trkman's success factors framework can be used as a guideline to implement a business process improvement project in a higher education institution. It is hoped that such success story could provide insight to other institutions who wish to leverage their performance.

Interesting direction for further study is measuring the necessity level of each success factor. It is likely that some factors are more important than others. Such ranking is crucial especially when it is not possible to satisfy all success factors and thus need to sacrifice some less important success factors in order to satisfy the more critical success factors.

**Table 70.2** Evidence of key success factors in the case

Contingency theory	<b>Strategic alignment:</b> Publication is critical for lecturers to leverage their carrier. The publication data is also required as a major indicator in the university’s and department’s accreditation
	<b>Level of IT investment:</b> Business owner in Ubaya should prepare a suffice amount of investment based on the Directorate of Information System advise to ensure appropriate level of IT investment
	<b>Performance measurement:</b> as described in Table 70.1
	<b>Level of employee’s specialization:</b> The new system eliminates the existence of staff that specializes in writing letter of assignment and collecting publication data.
Dynamic capabilities	<b>Organizational changes:</b> The new system does not change existing organizational structure but confirming the authority of publication data to the center of research department
	<b>Appointment of process owners:</b> All stakeholders were gathered to gain consensus on how the new process ideally works. Progresses are reported to gain feedback from all stakeholders
	<b>Implementation of proposed changes:</b> The University preferred to deliver quick wins by deploying several small projects. Project in this paper’s case is the pilot project with several other sequencing projects
	<b>Use of a continuous improvement systems:</b> Ubaya held regular cross sectional meetings to ensure any units are aware of the latest regulations and improvements
Task-Technology fit	<b>Processes standardization:</b> Business process is agreed at the university level to be applied consistently across all faculties
	<b>Informatization:</b> The new system uses less paper but still allow user to print any necessary documents when needed
	<b>Automation:</b> The new system automatically generates the letter of assignment after the Vice Rector approval
	<b>Training and employee’s empowerment:</b> The new system is introduced and trained to all representatives from faculty before officially launched

## 70.6 Conclusions

The project done in this case is considered successful as the new process able to produce significant improvements in all four dimensions: cost, quality, time, and flexibility. Further analysis shows that the business process implementation in the University of Surabaya satisfies all success factors in Trkman’s framework. Compliance to all success factors in the framework explained how Ubaya able to successfully completed the business process improvement project. Unfortunately, there is no indication on level of each factor’s influence toward the project’s success. Identification of each factor’s necessity is a good direction for further study as it is important especially when the organization unable to satisfy all factors and thus need to select the most important factors to be prioritized.

## References

1. Smimov, S., Reijers, H.A., Weske, M., Nugteren, T.: Business process model abstraction: a definition, catalog, and survey. *Distrib. Parallel Databases* **30**, 63–99 (2012)
2. Alter, S.: Information System Planning. *Information Systems: The Foundation of E-Business*, 4th edn, Chapter 11. Prentice Hall, New Jersey (2002)
3. O'Brien, J.A., Marakas, G.M.: Information Technology as a Competitive Advantage. *Enterprise Information Systems*, 13th edn, Chapter 2. McGraw-Hill, New York (2007)
4. Ranganathana, C., Dhaliwal, J.S.: A survey of business process reengineering practices in Singapore. *Inf. Manag.* **39**(2), 125–134 (2001)
5. Ahmad, H., Francis, A., Zairi, M.: Business process reengineering: critical success factors in higher education. *Bus. Process Manage. J.* **13**(3), 451–469 (2007)
6. Dennis, A.R., Carte, T.A., Kelly, G.G.: Breaking the rules: success and failure in groupware-supported business process reengineering. *Decis. Support Syst.* **36**, 31–47 (2003)
7. Malhotra, Y.: Business process redesign: an overview. *IEEE Eng. Manage. Rev.* **26**(3), 27–37 (1998)
8. Trkman, P.: The critical success factors of business process management. *Int. J. Inf. Manage.* **30**, 125–134 (2010)
9. Reijers, H.A., Mansar, S.L.: Best practices in business process redesign: an overview and qualitative evaluation of successful redesign heuristics. *Omega* **33**, 283–306 (2005)
10. Luca, M.: Business Process Reengineering. *International Conference Risk in Contemporary Economy*, 15th edn, Romania (2014)

# Chapter 71

## Design of Adventure Indonesian Folklore Game

Kartika Gunadi, Liliana and Harvey Tjahjono

**Abstract** These days traditional thing has been left behind not only by adults but also by children. One of them is folklore. It disappears because its package cannot interest the people. It needs a better package that interests a lot of people, for example game. The game took folklore theme that would teach the children about morale values. This game was made based on PC game because electronic device are increasingly in demand and with adventure game-based which is a game genre that a lot of people like including the children. This game was made by Unity3D which is can place the objects that we use easier. Besides, camera setting which is a feature of Unity3D can make the setting of the 2D graphics easier. First of all, the folklores need to be parted into the playable-part and the non-playable-part. In playable-part, the player needs to solve some tasks to play the next folklore. In non-playable-part, the game will show an animation. This folklore game can interests the children to become a better person from the morale value. But, it is hard to implement folklore into adventure game for some folklores. For example Origin of Mahakam River's Creek that has some complicated detail to express the setting of the story.

**Keywords** Folklore · Adventure game · Unity3D · Mystical crocodile of Tami River · Origin of Blue Lake · Origin of Mahakam River's Creek · Origin of Toba Lake · Timun Mas

---

K. Gunadi (✉) · Liliana · H. Tjahjono  
Petra Christian University, Surabaya, Indonesia  
e-mail: kgunadi@petra.ac.id

Liliana  
e-mail: lilian@petra.ac.id

H. Tjahjono  
e-mail: harvey.eht93@ymail.com

## 71.1 Introduction

The game is divided into two kinds, namely physical games and electronic games. Physical games are games that are often played by children, such as jumping rope, hide and seek, and so on. Electronic games are games played via electronic devices. The emergence of electronic games originated from the invention of Thomas T. Goldsmith Jr. and Estle Ray Mann [5].

One type of electronic games are computer games. There are several genres of computer games, among which is action, role-playing games, adventure. Many enthusiasts of every genre of the game, and not a few of them are still in the age of the children.

Today, children more like modern games so things that are traditional folklore are becoming obsolete or missing from the lives of children. Therefore, it will be made a game-themed folklore presented with the concept of adventure games that can be attractive and understood by children.

## 71.2 Theory

### 71.2.1 *Game*

“According to John von Neumann and Oskar Morgenstern, the game consists of a set of rules that establish competitive situation from two to several people or groups by choosing a strategy that is built to maximize its own victory or to minimize the win against” [8]. “Game is an application of the most widely used and enjoyed by the users of today’s electronic media” [6].

PC game genres there are various kinds, one of which is a adventure game. Adventure has a sense of adventure. Games in this genre focus on the game plot/storyline [2]. The important things are to be part of the adventure games include puzzles, storyline, dialogue between characters, and the purpose of the game. Making the adventure game has several steps that need to be met in making adventure game is a game writer, artist, and programmer.

Game writer is a part in making adventure games planned plot/storyline in the game. Puzzles made in the game that also need to be designed so as to fit with the storyline. In addition, game writer needs to plan the place settings, objects, characters, and conversations in the story.

Artist is a part of the audio and visual design plan that supports the course of the story in the game. Sound effects and good quality of graphics that can give satisfaction to the game players [4].

### **71.2.2 Unity 3D**

Unity 3D is a cross-platform game engine. Unity can be used to create a game. Unity can also be used to create a game that uses a web browser Unity web player plug-in. Scripting features provided, supports 2 programming language, JavaScript and C # [1, 3].

### **71.2.3 Folklore**

Folklore is a story that circulated orally and passed down from generation to generation that are traditional. In folklore contained beliefs and moral message. Folklore there from various regions in Indonesia.

### **71.2.4 Origin of Lake Toba**

Once, in North Sumatra, Indonesia, there lived a young wanderer. One day, he arrived at a place that is beautiful and fertile landscape. In the vicinity there is a clear river water. The young man was keen to settle in the place. Finally, he built a modest house not far from the river. After building a house, the young man was soon looking for a piece of land that is fertile for he planted various plants.

One day, coming home from the fields, the young man went to the river fishing. Arriving at the river, he immediately threw the fishing line to the middle of the river. He lifted and tossed back into the river fishing many times, but yet there is also a fish that eat the bait. Finally he decided to stop fishing. However, when it was about to draw his line, suddenly grabbed a fish. Quickly, he raised his fishing rather far into the land that is not released into the river. With feelings of joy, he immediately takes the fish into the basket of fish.

At home, the young man brought the fish to the kitchen. When about grilling fish, it turns firewood supply has been exhausted. He was soon out firewood underneath his house. What a surprise it after returning to the kitchen. Fish that are stored in the bin is no longer there. He was even more surprised and confused. How shocked he was when opening the door. He saw a girl. The girl also told the young man he actually was an incarnation of fish brought in by the young man from the river. He could not yet say anything, the girl spoke again to be allowed to stay in the house. The young man and eventually allow the girl was living in his house.

After a few weeks of living together, the young man proposed to her to be his wife. But the young man had to promise not to tell the origin of her as an incarnation of a fish to anybody. The young man agreed and swore. After the young man took the oath, they were married. A year later, they were blessed with a son. They care for and raise the child with attention and affection. However, due to the excessive affection, the child becomes a spoiled child and idler.

One day, the mother was feeling unwell. He also sent his son in order to deliver the packages containing rice and grilled fish for his father. At first the boy refused, but as the mother continues to force him, finally feeling annoyed with the boy that deliver food. Along the way, the boy felt hungry. He stopped and opened it. Greedily, he ate some rice and side dishes to the left just a little rice and fish meat attached to the bones. He repacked the food and proceed to the field. Arriving at the field, he immediately handed it to his father. The father was surprised when he saw the contents of the package are only remains. He also hit his son and said that her son was a child and his mother fish is an incarnation of a fish. Hearing the words of his father, the boy immediately ran back to his home crying. At home, he immediately complained to his mother. Mother was very sad to hear the complaint that her son, because her husband had violated his oath with insults which bring origin. Instantly she sent his son in ascend to the top of the hill.

Without question again, the boy immediately ran up the hill, not far from their homes. When the child was up on the hillside, the mother immediately ran towards the river. At that moment, the mother immediately jumped into the river and suddenly turned into a big fish. Not long after, the river was flooded and the water overflowed valley where the river flows. Eventually, it widespread waterlogging and eventually turns into a huge lake. By the local community, the lake was called Lake Toba [7].

### ***71.2.5 Origin Creeks Mahakam***

In the past, around the headwaters of the Mahakam River, there is a large cottage inhabited by three brothers. The oldest brother of a girl named Siluq, two brothers named Ayus, and the youngest, called Onggo. Siluq is a girl who likes to do *bebelian* (traditional rituals) and *bedewa* (worship the gods) to find the magic. Meanwhile, Ayus was a teenage boy who sloppy and meddlesome brother. Ayus have a great body and strong. While the youngest are still in their teens do not have the expertise except eating and sleeping.

On night, heavy rain fell all night, causing their roofs leak. Ayus and Onggo intends to woods to look for leaves serdang to replace their damaged roofs. Before leaving, Ayus told his brother that he would go looking for leaves serdang and asked his sister to cook. Siluq undertakes brother's request and ordered that the younger siblings do not unscrew them from the forest pot on his return later.

When Ayus and Onggo set off into the woods, Siluq immediately took a few leaves of rice to be cooked. After cleaning, the leaves of rice that she put in a pot that has been filled with water. After that, she prays to god that cooked rice leaf was turned into rice. By noon, Ayus and Onggo are back from the forest with leaves serdang. Ayus went straight into the kitchen. He immediately opened the lid of the pot. How shocked he was when he saw the pot in which there are only a few leaves of rice and some other form of rice. Fear of getting caught by his sister, he quickly closed it.

Meanwhile, Siluq just finished *bebelian*, she opened the pot lid, she saw there are still some remaining pieces of rice leaves. With the upset, she immediately approached Ayus sitting resting beside their cottage. Siluqtold her brother that she decided to stay near the center of the water so that it is free *bebelian* and *bedewa* without disturbing anyone.

Before leaving, she took her favorite magic rooster. Then, Siluq went down to the river downstream by using rafts. When looking at a raft carrying Siluq drove over a rushing river flow, hurry Ayus ran about to dissuade his sister. Ayus then took a large stone and threw it into the middle of the Mahakam River, forming a dam. Raft carrying Siluq began to slow down. When Siluq arrived near the dam, she ordered a magic male rooster crowed. Rooster powerful voice that was immediately destroyed the dam. Siluq with her raft again drove towards downstream. Ayus not to be outdone, several times he raced ahead of her sister and make the dam again even removing trees that form forest nipa in the river [7].

### **71.2.6 *Timun Mas (Golden Cucumber)***

Once, in a village in Central Java, there lived a middle-aged widow named Mbok Sрни. One night, in a dream she was visited by a giant creature who told him to go into the forest where she usually look for firewood to take a parcel under a large tree. When she awoke in the morning, Mbok Sрни hardly believe her dream last night. However, middle-aged woman was trying to ward off her doubts. Hopefully, she rushed to the place designated by the giant. Arriving in the woods, she finds a parcel under a big tree. The giant told Mbok Sрни to immediately plant cucumber seeds and Mbok Sрни will get a girl. The giant advised if the child has grown up, then Mbok Sрни must submit the child because it's going to be a giant meal. The woman was immediately planted the cucumber seeds on her farm. Hopefully, every day she took care of it with a good crop.

Two months later, the plant began to bear fruit. But strangely, the cucumber plants bear fruit only one. The color was very different, which was golden brown. When cucumber was ripe, Mbok Sрни took it home. She found a baby girl who was very pretty. She gave the name of the baby *Timun Mas*.

The next day, in the morning, set out Mbok Sрни to the mountain. Once there, she went directly to ascetics and express purpose of her arrival. Before long, the hermit was carrying four small packets and giving it to Mbok Sрни. The hermit gave four brackish each parcel that contains cucumber seeds, needles, salt and shrimp paste. The hermit explained that if the giant was chasing him, *Timun Mas* should disseminate the contents of the parcel. After receiving an explanation, Mbok Sрни brought the fourth package.

Two days later, the Giants came to collect his promise to Mbok Sрни. He already cannot wait to bring and eat meat *Timun Mas*. Before long, *Timun Mas* came out and stood beside her mother. Seeing *Timun Mas* grown, the giant was getting impatient want to eat immediately. When he tried to arrest her, *Timun Mas* the giant



was chasing her. After running away, Timun Mas began to fatigue, while the giant was getting closer. First, Timun Mas sows cucumber seeds given by her mother. Miraculously, the surrounding forest suddenly turned into a cucumber field. In an instant, cucumber stems spread and wrapped around the body of the giant. However, the giant was able to escape and return chasing Timun Mas. Cucumber Mas immediately threw the package that contains the needle. In an instant, the needle is changed into bamboo trees that are tall and spiky. However, the giant was able to pass through and continue to pursue Timun Mas, although his legs were bloody because the bamboo punctured. Seeing his efforts have not succeeded, Timun Mas unwrapped a third containing salt and spread it. Instantly, the forests that have been passed suddenly turned into a sea of vast and deep, but the giant still got through with ease. Timun Mas began to worry, because the only weapon left one. With full confidence, she threw the last bundle containing paste. Instantly, where the collapse of the shrimp paste suddenly transformed into a sea of boiling mud. As a result, the giant was plunged into it and was killed. Afterwards Timun Mas walked to her cabin to meet her mother. Seeing her girl survived, Mbok Sрни immediately says thanks to God Almighty. Since then, Mbok Sрни and Timun Mas live happily [7].

### **71.3 Design System**

At the beginning of this game, we are told of a child with a gender appropriate choice player. The child was in the library and found a book titled folk story "5 Folklore Options". Then suddenly they were sucked into the book. Then he saw a piece of paper containing an article. "Complete the journey in 5 folklore and you will be freed from this book". He also saw a gate, and he follows the command that is in the paper. After he entered the gate, will be shown a picture of the Indonesian archipelago which has 5 points in some of the islands that show 5 folklore. Not all the folk tales are open to play, but the stories should be played with a certain order.

If all the folklore that has been completed and 5 pieces of the puzzle has been obtained, the child returned to the map. It will instantly appear light and the child will be out of the book. As shown in Fig. 71.1.

### **71.4 Implementation and Testing**

Game was tested with some testing to determine the smooth course of the game, here some testing were conducted.

Testing in this section is divided into two terms. First performed on Ayus to enable obstacle on the path traversed by Siluq and Ayus movement followed by the child (Fig. 71.2). The second test conducted on Siluq running and destroy the obstacles in front of him. In the second test was initially Siluq can not eliminate

Fig. 71.1 Flowchart of game

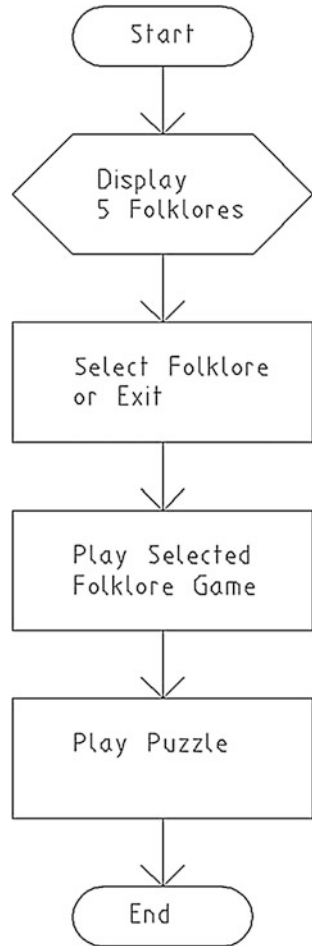


Fig. 71.2 Pursuing Siluq in river



**Fig. 71.3** Looking for wood in forest



the object in front of him because the coordinates are not exactly the same as when checking the object in front of him so that checks need to be carried out between the  $x$  coordinate object—0.1f and coordinates  $x$  object plus 0.1f.

Testing in this section initially had trouble because the player should not be allowed to take wood in the same tree. However, testing can be immediately resolved by checking on each object tree so that the tree can be seen already timber or not (Fig. 71.3).

## 71.5 Conclusion

Based on the testing, it can be concluded that the game still needs improvement in terms of making it more attractive picture. This game needs the development of interface design to make it more understandable to the user. It should be added AI in this game making it more interesting and challenging for the user. In addition there are some difficulties in the implementation of folklore into adventure games. For example the story of the Magic Crocodile River Tami content of the story is too simple that it is difficult to make a game of this story. Another story is the Origin of the Mahakam River Children who have difficulty in creating appropriate view the story as the details are complicated.

## References

1. Ae, H.K., Jae, H.B.: Development of mobile game using multiplatform (Unity3D) game engine. *Int. J. Intell. Inf. Process.* **5**(1), 29–36 (2014)
2. Hamlen, K.R.: Children's choices and strategies in video games. *Comput. Hum. Behav.* **27**, 532–539 (2011)
3. Jae, H.B., Ae, H.K.: Design and development of Unity3D game engine-based smart SNG (Social Network Game). *Int. J. Multimedia Ubiquit. Eng.* **9**(8), 261–266 (2014)
4. Moreno-Ger, P., Fuentes-Fernandez, R., Sierra-Rodriguez, J.L., Fernandez-Manjon, B.: Model-checking for adventure videogames. *Inf. Softw. Technol.* **51**, 564–580 (2009)

5. Sibero, I.C.: Langkah Mudah Membuat Game 3D. MediaKom, Yogyakarta (2009)
6. Sibero, I.C.: Membuat Game 2D Menggunakan Game Maker. MediaKom, Yogyakarta (2008)
7. Tim Penulis AdiCita Grup, 366 Cerita Rakyat Nusantara. Yogyakarta: Adicita Karya Nusa (2007)
8. Widiastuti, N.I., Setiawan, I.: Membangun Game Edukasi Sejarah Walisongo. Jurnal Ilmiah Komputer dan Informatika KOMPUTA 1(2), 41–48 (2012)

# Chapter 72

## Measuring the Usage Level of the IE Tools in SMEs Using Malcolm Baldrige Scoring System

I. Nyoman Sutapa, Togas W.S. Panjaitan and Jani Rahardjo

**Abstract** The amount of Small and Medium Enterprises (SMEs) in Indonesia is larger than large industries but possessed very low competitiveness. In many countries, SMEs have a vital role in supporting the economy so should receive more attention in order to sustain and support the economy of a country. SMEs need to implement the Industrial Engineering (IE) tools from an early stage or planning, process, and marketing that can improve customer satisfaction. Previous researches already done to develop innovative management model to improve SMEs performance using Malcolm Baldrige model but only measured some determinant factors that have the effect on performance and not measured the usage level. This study was done to get measurement models of the usage level of Industrial Engineering Tools and Methods in SMEs. Measurement is to design a scoring system of usage level at Planning and Design, Operation and Control, and Quality and Productivity Improvement. Design method was done by determining the tools in each stage and proceed with setting the usage level and score by using the Malcolm Baldrige concept.

**Keywords** Scoring system · Planning and design tools · SMEs · Malcolm Baldrige

### 72.1 Introduction

Small and Medium Enterprises (SMEs) have a crucial role for the economy of a region like East Java, Indonesia, where economic growth is contributed by this sector reached 46.37 % [1]. Small medium enterprises (SMEs), operate a major role in national economies and considered as the machine for economic growth all over the world [2]. After the local commercial become to the globalization of markets,

---

I.N. Sutapa (✉) · T.W.S. Panjaitan · J. Rahardjo  
Faculty of Industrial Technology, Department of Industrial Engineering,  
Petra Christian University, Siwalankerto 121-131, Surabaya 60236, Indonesia  
e-mail: mantapa@petra.ac.id

SMEs will have many opportunities to deal business in integration with large-scale enterprises. Based on the above data, it should be given more attention to the development of SMEs in order to provide greater impact both in terms of economic and social. SMEs are also seen to have great opportunities to increase their contribution and be able to compete with advanced or large industries.

In the process leading to such conditions, SMEs encountered some obstacles, among others, such as difficulty finding potential markets, business legality, simple packaging, lack of capital, technology is still modest, family management, standardized operation is not optimal, innovation is still weak, and the market access difficulties at international level [1]. One effort that can be done for SMEs is to use Industrial Engineering tools and technique (IE tools) in support their performance, in which large-scale industry already implemented it. An innovative management model to improve SMEs performance has already developed in Thailand using some performance measurement models, like Malcolm Baldrige model [3]. Their models only measured some determinant factors that have the effect on SMEs performance, but not measured the usage level. Therefore, it is necessary to conduct research on how to measure the usage level of IE tools in SMEs. It is intended to be able to have a guide in assessing the implementation and performance of SMEs.

## 72.2 Malcom Baldrige Scoring System

Malcolm Baldrige is one of the tools that have been widely applied in measuring the performance of an organization. In the United State of America, there are awards for the quality of performance that is named Malcolm Baldrige National Quality Award (MNBQA) [4]. Where the purpose of the application of the Malcolm Baldrige is to determine/measure the strength of which has been owned by an organization [4, 5]. The performance of each of these criteria is measured by using a score. Formulation of the score obtained from the collection of the data compiled into a detailed list of criteria that will be searched. Where the criteria by requiring qualitative answers scoring system to quantitatively determine the results [6].

The draft scoring system is divided into several stages, namely: (1) determine the types of tools that correspond to the stages to be measured, (2) the theories that support these tools, (3) the theoretical conclusions based on the entire supporting theory, (4) the operational definition, and (5) the level of usage of each tool based on the concept of Malcolm Baldrige. Usage levels using a score ranging from 0 to 4. The concept of measurement is based on the level of completeness and consistency of processes applied and the quantity and/or quality of the results. Validation of the design is done through focus group discussion (FGD).

## 72.3 Design of Industrial Engineering (IE) Tools and Methods

### 72.3.1 Product Design

IE the basic tools needed in the design of products in SMEs is Quality Function Deployment (QFD) [7, 8]. QFD is an effective management tool where consumer expectations are used to design a process or to encourage the improvement of product quality [9]. Furthermore, the stages on QFD is designing the product characteristics that fit consumer's needs, assess the characteristics that a top priority for consumers to make a miniature of a product in accordance with consumer demand, as well as conduct tests on products that have been made and improve the quality of existing design.

Product design is the stage in which the transformation of consumer demand into design quality to design a product that fits the needs of consumers, as well as testing on such products to improve design quality. The operational definition of design planning product is a product that will be produced by first researching/ensure the requirements and priorities of consumers, the presence of competitors' products, as well as the technical and economic capabilities of the company, and in addition it also conducted due diligence measures in the design of the design process. Scoring system to assess the usage level of product design implementation is presented in Table 72.1.

### 72.3.2 Planning and Inventory Control

IE the basic tools required in planning and inventory control in SMEs is Material Requirement Planning (MRP), Master Production Schedule (MPS), Bill of material (BOM), Economic Order Equation (EOQ), Reorder Point (ROP) and forecasting [10, 11] to plan production. MRP to obtain components and the appropriate amount at the right time and place. EOQ to adjust inventory to better efficiency, so that the

**Table 72.1** Scoring system for product design usage level

Score	Description
4	Have done the planning, market research, competitor research, technical and economic analysis, and test the feasibility of the design
3	Most of the activity/stage design has been done
2	Approximately half activity/stage design is not done or done
1	Most of the activity/stage design is not done
0	Without planning, market research, competitor research, technical and economic analysis, and Test the feasibility of the design. Design is completely determined by the company without regard to consumers, competitors/market

**Table 72.2** Scoring system for inventory control and planning usage level

Score	Description
4	Implement properly and consistently 5 or more tools. Examples using BOM, MRP, MPS, ROP and forecasting
3	Implement properly and consistently to four tools such as using BOM, MRP, MPS and ROP
2	Applying 3 using a tool such as BOM, MRP and ROP
1	Applying only one or two tools, among others, BOM and MRP
0	Applying only a few tools but inconsistent or no clear standards

company supplies can run well. ROP is the reorder point necessary goods. Forecasting is a technique to forecast future demand. Operational definitions for planning and inventory control are SMEs can do the planning and control of raw materials, auxiliary materials, semi-finished goods and finished goods before and after production. Usage level scores for assessment tools can be seen in Table 72.2.

### 72.3.3 *Planning and Production Control*

Operation Process chart (OPC), Process Flowchart, charts Assembly, and the scheduling method is IE the basic tools needed in the planning and production control in SMEs [11, 12]. OPC is an operation process map depicting the work steps and checks from beginning to end. Process flow chart shows the process flowchart. Assembly chart is a map that describes the steps the assembly process from beginning to end. The scheduling method is a method to set the order of job/product that will run in a system. So that an operational definition for Planning and Production Control is a production process that aims to produce a product that has stages that must be passed from the start of production until after production, where there is an inspection activity to maintain that no defective products that pass. Scoring system to assess the usage level of Planning and Production Control implementation is presented in Table 72.3.

**Table 72.3** Scoring system for planning and production control usage level

Score	Description
4	Implement properly and consistently to four tools or more. (ex. OPC, process flow and assembly chart, method of scheduling)
3	Implement properly and consistently 3 tools. (ex. OPC, process flow and assembly chart)
2	Implement properly and consistently 2 tools. (ex. using OPC, process flow charts)
1	Applying just one tool. (ex. OPC)
0	Do with inconsistent or no clear standards.



### 72.3.4 *Quality Control*

Seven tools is one of the basic tools needed IE in quality control in SMEs. Seven tool itself consists of check sheet, scatter diagrams, Pareto diagrams, fishbone diagrams, histograms, control charts, flowcharts, quality plan and sampling [11–14].

Checksheet is a tool to record every product passes and handicapped. Scatter diagram to see the correlation/cause of disability. Pareto diagram is a diagram that illustrates the main problem according to its weight. Fishbone diagram to see the potential root cause of quality problems. The histogram is a distribution diagram of disability. Control charts are charts acceptance limit. Flowchart is an overview process flow. A quality plan is planning to control the quality of the product. SMEs are also required to keep records of actual disability and examine the existing discrepancy to find the root causes of quality. Usage level scores can be seen in Table 72.4.

### 72.3.5 *Cost Control*

IE tools needed to control costs are the tools that used to determine the cost of production (HPP) [12, 15, 16]. HPP is a calculation of the total cost of a product. The costs are included in HPP production and non-production costs. Production costs include material costs, overhead costs and direct labor cost. Non-production costs include indirect labor. Operational definitions to control costs is to control operating costs in order to avoid swelling, as well as the price for each product, can be kept to a minimum. Usage level scores for assessment tools can be seen in Table 72.5.

**Table 72.4** Scoring system for quality control usage level

Score	Description
4	Has the quality characteristics, noting that the products do not fit the characteristics of quality, knowing the cause of nonconforming product, and determine the root cause
3	Do 3 points. (ex. has the quality characteristics, determine the cause of nonconforming product, and determine the root of the problem)
2	Do 2 points. (ex. quality characteristics, determine the cause of nonconforming product)
1	Doing 1 point. (ex. only has the quality characteristics)
0	Does not have the characteristics of quality, did not record a product that does not fit with the quality characteristics, not know the cause of nonconforming product and the root of the problem

**Table 72.5** Scoring System for cost control usage level

Score	Description
4	Applying standard definition cost, noting the actual production costs, comparing actual costs and standards, and can determine the cause of cost overruns
3	Just do 3 points. Ex.: Perform only standard definition cost, noting the actual production costs, comparing actual and standard
2	Just do 2 points. Ex.: Perform only standard definition cost, noting the actual production costs
1	Only 1 point. Ex.: only consider material costs alone
0	Not doing standard definition cost, does not record the actual production costs, does not compare with the actual standards, and can not know the cause of the cost overruns

### 72.3.6 Maintenance

IE the basic tools needed in the maintenance of working tools or machines in SMBs is total productive maintenance (TPM) [14, 15]. TPM is a system of maintenance and repairs on the machine or equipment. TPM is designed to prevent losses due to the cessation of production activities. The purpose of the TPM is to optimize the overall efficiency of production systems through maintenance and repair activities are organized. Operational definitions for maintenance work tools are able to reduce losses due to production activities. In addition, the improvement involving all divisions and employees up to the top management (Table 72.6).

### 72.3.7 Product Quality Improvement Tools

Quality improvement is a process that requires unity in the company to be able to develop activities and take decisions for the use of quality tools. The development of quality can be applied to several aspects, such as the quality of the products produced and the quality of the service to consumers [13, 17].

**Table 72.6** Scoring system for maintenance usage level

Score	Description
4	Identifying, recording records, analysis, planning improvements and monitor and work tools are always ready to use
3	Identifying, recording records, analysis, planning and monitoring improvement. However, sometimes working tools ready
2	Identifying, recording records, analysis. But no improvement planning and monitoring, so that the working tools are sometimes not ready
1	Identifying, recording records, analysis. But no improvement planning and monitoring, so that the working tools are often not ready
0	Just to identify it and work tools are very often not ready

IE the basic tools needed by SMEs in improving the quality of products is the method of DMAIC (define, measure, analyze, improvement, and control) [12, 14]. Define is the first step to identify problems that occur in the production process. Measure the measurement phase is to evaluate the quality level of product quality to the specified goals. Analyze is the stage of identifying the root cause of the problem is based on the measurement results. Improvement is the stage of implementation of an alternative solution to improve product quality. Control is the stage monitoring quality improvement process to fit the purpose. The operational definition of product quality improvement is to improve the quality by identifying problems, perform measurements, analyze, make improvements, and controlling. Usage level scores for assessment tools can be seen in Table 72.7.

### 72.3.8 Service Quality Improvement Tools

IE tools need basis SMEs in improving the quality of customer service is the Voice of the Customer (VOC), Importance Performance Analysis (IPA), and Service Quality [18–20].

VOC is a tool to capture preferences, reluctance, and customer expectations for a given product. IPA is a research technique to analyze the attitude of the interest or consumer satisfaction with the services received. Service Quality by Parasuraman is an empirical model to compare the performance of quality of service with customer service quality needs. The operational definition of service quality improvement is to figure out or investigate needs and customer response to the product.

These tools also perform the priority of customer needs to be based on its importance, evaluate products and make improvements. Furthermore, customers will have more confidence in the products produced, this is evidenced by the emergence of a new customer or customer loyalty. Usage level scores for assessment tools can be seen in Table 72.8.

**Table 72.7** Scoring system for product quality improvement usage level

Score	Description
4	Doing all stages ranging from determining the quality problems, disability measurements, analyze, and implement improvements, as well as control the results of the improvements made
3	Determining the quality problems, the measurement of disability, to perform the analysis of disability
2	Determining the quality problems to the measurement of disability that occurs
1	Only at the stage of determining or finding product quality problems
0	Not once did the stages of product quality improvement

**Table 72.8** Scoring system for services quality improvement usage level

Score	Description
4	Doing all stages of improving the quality of customer service (to find out, prioritizing, evaluation and improvement) by taking into account constraints or limitations that exist, such as employee salaries, facilities company, HR
3	Doing improvement by finding out the needs of consumers, carry out priority attention to the existing constraints
2	Doing improvement by finding out the needs of consumers just by observing the existing constraints
1	Doing improvement without finding out the needs of consumers
0	Do not do all the stages in an effort to improve the quality of customer service

### 72.3.9 Productivity Improvement Tools

IE the basic tools needed to increase the productivity of SMEs is the maintenance increased competence and motivation of employees [12, 14, 17]. This improvement can be done with several functions, namely: (1) the procurement function is to determine the type or quality of employees and the amount needed. (2) the function of development is to improve the technical skills, theoretical, conceptual, and morale of employees in accordance with the needs of job or position through education and training. (3) the function of compensation is to provide fringe benefits, tangible money or another reward in accordance sacrifice or employee contributions. (4) maintenance function is to maintain or improve the physical, mental, attitude of employees to remain loyal and productive work to support the achievement of corporate objectives. Increased employee productivity can be interpreted in terms of the preliminary determination to recruit, develop skills, provide compensation, and maintain the condition of the employee to support productivity. The operational definition increase employee productivity, namely the recruitment of employees in accordance with the job specification, assessing employee performance, providing special programs or incentives for employees, and provide assurance of safety of employees. Usage level scores for assessment tools can be seen in Table 72.9.

**Table 72.9** Scoring System for productivity improvement usage level

Score	Description
4	Recruiting employees in accordance job specification, assessing employee performance, providing special programs, and provide assurance of safety
3	Recruiting employees in accordance job specification, conduct performance appraisals of employees, and provide special programs for employees
2	Recruiting employees in accordance job specification and assessing employee performance
1	Only the recruitment of employees according to job specification
0	Do not do these four points at all, even without regard to recruitment job specification

## 72.4 Conclusion

This study attempted to obtain usage level assessment scheme of Industrial Engineering (IE) tools and methods at any stage or process that occurs in SMEs. Based on previous theories and researches on IE implementation, from this research can develop nine kinds of schemes like Product Design, Planning and Inventory Control, Planning and Production Control, Quality Control, Cost Control, Maintenance, Product Quality Improvement Tools, and Service Quality Improvement Tools that represent the three major stages (Planning and Design, Operation and Control, and Quality and Productivity Improvement) in the running industry especially SMEs.

## References

1. Subiyantoro, A.: UMKM Menjadi Pilar Penting Pertumbuhan Ekonomi Jawa Timur. <http://kabargress.com/2013/10/01/umkm-menjadi-pilar-penting-pertumbuhan-ekonomi-jawa-timur/>. Accessed 10 June 2015
2. Suttapong, K., Tian, Z.: Performance benchmarking for building best practice in small and medium enterprises (SMEs). *Int. J. Bus. Commer.* **1**(10), 46–60 (2012)
3. Nurach, P., Thawesaengskulthai, D., Chandrachai, A.: Innovative performance management model for SME in Thailand. *World Rev. Bus. Res.* **1**(5), 126–142 (2011)
4. Baldrige Performance Excellence Program, Criteria for Performance Excellence 2013–2014: Manufacturing, Service, Small Enterprise, and Non-Profit. National Institute of Standard and Tehnology (NIST), United States Department of Commerce (2013)
5. Sohn, S.Y., Joo, Y.G., Han, K.Y.: Structural equation model for the evaluation of national funding on R&D project of SMEs in consideration with MBNQA criteria. *Eval. Program Plann.* **30**(1), 10–20 (2007)
6. Prawira, A.S., Arijanto, S., Nugraha, C.: Sistem Perangkat Lunak untuk Internal Assessment Malcolm Baldrige Criteria for Performance Excellence (kriteria 1-kepemimpinan). *Jurnal Online Institut Teknologi Nasional*, 140–142 (2013)
7. Germani, M., Mengoni, M., Peruzzini, M.: A QFD-based method to support SMEs in benchmarking co-design tools. *Comput. Ind.* **63**(1), 12–29 (2012)
8. Marjudi, S., Sulaiman, R., Majid, N.A.A., Amran, M.F.M., Rauf, M.F.A., Kahar, S.: QFD in Malaysian SMEs food packaging CAD (PackCAD) testing. *Procedia Technol.* **11**, 518–524 (2013)
9. Besterfield, D.H., Besterfield-Michna, C., Besterfield, G.H., Besterfield-Sacre, M.: *Total Quality Management*. Pearson Prentice Hall, Upper Saddle River (2002)
10. Gel, E.S., Erkip, N., Thulaseedas, A.: Analysis of simple inventory control systems with execution errors: economic impact under correction opportunities. *Int. J. Prod. Econ.* **125**(1), 153–166 (2010)
11. Kunday, Ö., Şengüler, E.P.: A study on factors affecting the internationalization process of small and medium enterprises (SMEs). *Procedia—Soc. Behav. Sci.* **195**, 972–981 (2015)
12. Kurniawati, D., Yulianto, H.: Productivity improvement of small scale medium enterprises (SMEs) on food products: case at Yogyakarta Province, Indonesia. *Agric. Agric. Sci. Procedia* **3**, 189–194 (2012)
13. Sokovic, M., Jovanovic, J., Krivokapic, Z., Vujovic, A.: Basic quality tools in continuous improvement process. *J. Mech. Eng.* **55**(5), 333–341 (2009)

14. Mahmud, N., Hilmi, M.F.: TQM and Malaysian SMEs performance: the mediating roles of organization learning. *Procedia-Soc. Behav. Sci.* **130**, 216–225 (2014)
15. Ahmad, M.F., Zakuan, N., Jusoh, A., Takala, J.: Relationship of TQM and business performance with mediators of SPC, lean production and TPM. *Procedia-Soc. Behav. Sci.* **65**, 186–191 (2012)
16. Moro, A., Fink, M.: Loan managers' trust and credit access for SMEs. *J. Bank. Finance* **37**(3), 927–936 (2013)
17. Roghanian, P., Rasli, A., Kazemi, M., Gheysari, H.: Productivity tools: TPM and TQM. *Int. J. Fundam. Psychol. Soc. Sci.* **2**(4), 65–69 (2012)
18. Zeithaml, V.A., Parasuraman, A., Berry, L.L.: *Delivering Quality Service: Balancing Customer Perceptions and Expectations*. Free Press, New York (1990)
19. Nyeck, S., Morales, M., Ladhari, R., Pons, F.: 10 years of service quality measurement: reviewing the use of the SERVQUAL instrument. *Cuadernos de Difusion* **7**(13), 101–107 (2002)
20. Nada, N., Ali, Z.: Service value creation capability model to assess the service innovation capability in SMEs. *Procedia CIRP* **30**, 390–395 (2015)

# Chapter 73

## Enumeration and Generation Aspects of Tribonacci Strings

Maukar, Asep Juarna and Djati Kerami

**Abstract** Fibonacci string has been widely used as object of combinatorial studies by researchers. This research discusses some aspects of combinatorial Tribonacci strings, beginning with enumerating aspects that define the relationship between the length of the Tribonacci string ( $|t|$ ) and the number of Tribonacci strings with length ( $|Tn|$ ), where  $t \in Tn$ . These results are formulated in the form of recurrence relations. The next aspect is the generation to develop a formulation of recurrence relation generating Tribonacci string following lexicographical order, and identify some properties of this relation. On the enumeration aspect, the recurrence relation that describes the relationship between the number of Tribonacci strings and Tribonacci string length is generated. On the generation aspect, the recurrence relation to generate the Tribonacci string according to lexicographical order is formed. Specifically, results from the generation aspect is very useful as a basis for the formation of Gray codes and give variation to the theory of coding.

**Keywords** Enumeration · Fibonacci string · Generation · Tribonacci number · Tribonacci string · Recurrence relation

### 73.1 Introduction

Some research has associated with the Fibonacci, among others, can be seen from the writings of [1–5]. In this case, Fibonacci was viewed as a string that is the object of Combinatorics. As it known that Combinatorics is a part of mathematics which studies the structure of discrete, referred to as Combinatorial objects (or objects). Combinatorial objects are often referred to by the term Combinatorial class (or classes). Research in the field of Combinatorics has some aspects, among others: counting (counting) or enumeration (enumeration), generation or generation

---

Maukar (✉) · A. Juarna  
Gunadarma University, Depok, Indonesia  
e-mail: maukar@staff.gunadarma.ac.id

D. Kerami  
University of Indonesia, Depok, Indonesia

(generation), registration or listing, Ranking and Unranking, and the nature of the Hamiltonian.

The background of this research is the research conducted by Kenji Mikawa [6], and Vajnovszki [7–9]. The object of their research is about Fibonacci string. Fibonacci string is a string in which there is no shape or pattern of a substring 11. These research take a combinatorics class which is a family of Fibonacci, namely Tribonacci. If Fibonacci uses the involvement of 2 objects before, then Tribonacci uses the involvement 3 objects before.

Until now, there have been several studies related to the Tribonacci numbers. Among other things have done by: Jonas Siurys; Eun Mi Choi; Zhengang Li Jianghua, Wu1, and Han Zhang; Nurettin Irmak, and Murat Alp; Lexter r. Natividad, and Paola b. Policarpio; and Dumitriu. I. Their research results can be seen on the following writings [10–16].

If Fibonacci string is defined as a binary string where there is no substring or pattern form 11, then the Tribonacci string is defined as a string of binary which contains no shape or pattern substring 111. Here are examples of the Tribonacci strings: 110, 011, 00110, 10110, 011010011, and these are not Tribonacci strings 111, 0111, 010111, 1010111.

## 73.2 Methods

The scope of this research consists of two aspects, namely the aspects of enumeration and aspects of generation. On the enumeration aspects, the activities are researching how the shape of the relationship between numbers and strings of Tribonacci. Whether it can be formulated in the form of recurrence relation to describe the relationship between them. If possible, then the kind of recurrence relations was formed. On these aspects, research is managed to formulate a recurrence relations intended. Mathematically proof is done to guarantee the truth of what has been produced.

The main activities of the generation aspect is doing observation to know if the recurrence relations could be developed to generate or stir up a Tribonacci string sequence meets the criteria leksikografis. Further research is also done on some of the properties owned by the recurrence relations. All the properties that are successfully identified on this aspect have been proven mathematically to guarantee the truth of what has been produced.

## 73.3 Results and Discussion

Some of the terminologies below are used in this research:

- String  $S$  is a sequence zero or more symbol  $a$ , where  $a \in \text{alphabet } \Sigma$ . If  $\Sigma = \{0,1\}$  then called binary alphabet that form binary string.



- Strings that was formed from binary alphabet  $B \{0,1\}$ , which is not include substring 111 called Tribonacci strings.
- The variable used to determine the length of the string is  $n$ .
- The set of all strings that are formed from the binary alphabet  $\Sigma$  with length  $n$  is  $B_n$ .
- The set of Tribonacci strings with length  $n$  is  $T_n$ .
- The number of Tribonacci strings with length  $n$  is  $|T_n|$ .
- If  $t$  is a variable which represent a string, then  $t$  is element of  $T_n$  or writes  $t \in T_n$ .
- If  $t$  is a string element of  $T_n$  ( $t \in T_n$ ), then  $|t|$  is length of string  $t$ .

### 73.3.1 Enumeration Aspect

Enumeration of Tribonacci strings is conducted to know the number of Tribonacci strings with length  $n$  called  $|T_n|$ . If a binary string with length  $n$  called  $|B_n|$  and Tribonacci numbers  $n$ th called  $BT_n$ , then it can be ascertained that  $|T_n| \leq |B_n|$ , and  $|T_n| = BT_n$ . From the observations, we find:

- For  $n = 1$ , then  $B_1 = \{0,1\}$ . Because  $\forall b \in B_1, b \in T_1$ , so  $|T_1| = 2$ .
- For  $n = 2$ , then  $B_2 = \{00,01,10,11\}$ . Because  $\forall b \in B_2, b \in T_2$ , so  $|T_2| = 4$ .
- For  $n = 3$ , then  $B_3 = \{000, 001, 010, 011, 100, 101, 110, 111\}$ . Because  $\exists b \in B_3, b \in T_3$ , so  $|T_3| = 7, b = \{000, 001, 010, 011, 100, 101, 110\}$ .
- For  $n = 4$ , then  $B_4 = \{0000, 0001, 0010, 0011, 0100, 0101, 0110, 0111, 1000, 1001, 1010, 1011, 1100, 1101, 1110, 1111\}$ . Because  $\exists b \in B_4, b \in T_4$ , so  $|T_4| = 13, b = \{0000, 0001, 0010, 0011, 0100, 0101, 0110, 1000, 1001, 1010, 1011, 1100, 1101\}$ .

Recurrence relations are deduced from the results of the observation above as follows:

$$|T_n| = \begin{cases} 2 & \text{if } n = 1 \\ 4 & \text{if } n = 2 \\ 7 & \text{if } n = 3 \\ |T_{n-1}| + |T_{n-2}| + |T_{n-3}| & \text{if } n > 3 \end{cases} \tag{73.1}$$

### 73.3.2 Generation Aspect

From recurrence relation in Eq. (73.1) can be seen that, if string 0, 10, or 110 connate with  $T$  formerly, it will not generate an element that contains the substring 111. But when a string of 1110 11110 111110, 11111...0 connate with  $T$  formerly,

then it can certainly contain the substring 111 and of course it's not Tribonacci strings.

If we want to get string Tribonacci  $T_n$ , then it should be connate operation between string 0 with  $T_{n-1}$ , so the retrieved  $t \in T_n$ , and can be written:  $0 T_{n-1} = t_1$ , where  $t_1 \in T_{n-1}$ . If  $t_2 \in 0 \circ T_{n-2}$ , then  $|t_1| = |t_2|$ . The same thing can be seen if string 10 connate with  $T_{n-2}$ , and string 110 connate with  $T_{n-3}$ , and can be written as follow:  $10 \circ T_{n-2} = t_3$ , where  $t_3 \in T_{n-2}$ . If  $t_4 \in 0 \circ T_{n-2}$ , then  $|t_3| = |t_4|$ ;  $110 \circ T_{n-3} = t_5$ , where  $t_5 \in T_{n-3}$ . If  $t_6 \in 10 \circ T_{n-2}$ , then  $|t_5| = |t_6|$ . So it can be concluded that:

- i. For  $n = 1$  and  $2$ ,  $T_n = B_n$
- ii. For  $n = 3$ ,  $T_n = B_n - \{111\}$ ;  $T_3 = 0 \circ T_2 \cup 10 \circ T_1 \cup 110$ .
- iii. For  $n = 4$ ,  $T_n = B_n - \{0111, 1110, 1111\}$ ;

$$T_4 = 0 \circ T_3 \cup 10 \circ T_2 \cup 110 \circ T_1$$

Thus for  $n > 3$  can be formulated as follows:

$$T_n = 0 \circ T_{n-1} \cup 10 \circ T_{n-2} \cup 110 \circ T_{n-3} \tag{73.2}$$

Recurrence relation that was successfully developed in the enumeration aspect as follows:

$$T_n = \begin{cases} [0, 1] & \text{if } n = 1 \\ [00, 01, 10, 11] & \text{if } n = 2 \\ [000, 001, 010, 011, 100, 101, 110] & \text{if } n = 3 \\ [0 \circ T_{n-1} \cup 110 \circ T_{n-2} \cup 110 \circ T_{n-3}] & \text{if } n > 3 \end{cases} \tag{73.4}$$

Proofing of Eq. (73.4), as follows:

**Proof** Clearly that for a Tribonacci strings with length  $n \leq 3$ , recurrence relations Eq. 73.4 is true. Next to prove that recurrence relation 73.2 is true, note the process of formation of the Tribonacci strings with length  $n = 4$  is called  $T_4$ .  $T_4$  was formed from Tribonacci strings with length 3, 2 and 1, where:

- Tribonacci strings with length 3 are:  $T_3 = \{000, 001, 010, 011, 100, 101, 110\}$
- Tribonacci strings with length 2 are:  $T_2 = \{00, 01, 10, 11\}$
- Tribonacci strings with length 1 are:  $T_1 = \{0, 1\}$

So that  $T_4 = T_3 \cup T_2 \cup T_1$ .

If known set of string  $T_{4,1}$  is string 0 concated with  $T_3$ , so:

$$\begin{aligned} T_{4,1} &= 0 \circ T_3 \\ &= \{0000, 0001, 0010, 0011, 0100, 0101, 0110\} \\ &\in T_n \end{aligned}$$

Note that, if  $\forall t \in T_{4,1}$ , then  $t \in T_4$ . This indicates that all strings in  $T_{4,1}$  are Tribonacci strings with length 4. But if string 1 connotated with  $T_3$  then retrieved  $T_{4,2}$ , as follow:

$$\begin{aligned} T_{4,2} &= 1 \circ T_3 \\ &= \{1000, 1001, 1010, 1011, 1100, 1101, 1110\} \end{aligned}$$

Note that,  $\exists t \text{ not } \in T_n$ , i.e. 1110

If assumed,

$$\begin{aligned} T_{4,2,1} &= T_{4,2} - \{1110\} \\ &= \{1000, 1001, 1010, 1011, 1100, 1101\} \end{aligned}$$

Clearly that,  $\forall t \in T_{4,2,1}$ , then  $t \in T_4$ , and of course  $\forall t \in T_4$ , then  $t \in T_n$ . Note that if assumed

$$T_{4,2,2} = \{1000, 1001, 1010, 1011\}$$

It is clear that,

$$\begin{aligned} T_{4,2,2} &= 10 \circ T_2 \\ &= \{1000, 1001, 1010, 1011\} \subset T_4 \end{aligned}$$

Similarly, if it is assumed

$$T_{4,2,3} = \{1100, 1101\}$$

so it is clear that,

$$\begin{aligned} T_{4,2,3} &= 110 \circ T_1 \\ &= \{1100, 1101\} \subset T_4 \end{aligned}$$

Note that if  $\forall t_1 \in T_{4,1}$ ,  $\forall t_2 \in T_{4,2,2}$ , and  $\forall t_3 \in T_{4,2,3}$ , then  $\forall t_1, t_2, t_3 \in T_4$ . This can be shown as follows:

$$\begin{aligned} T_4 &= T_{4,1} \cup T_{4,2,2} \cup T_{4,2,3} \\ &= \{0000, 0001, 0010, 0011, 0100, 0101, 0110, 1000, 1001, 1010, 1011, 1100, 1101\}. \end{aligned}$$

Clearly visible that all of the elements  $T_4$  included in Tribonacci strings are formed by the following relation:  $T_4 = T_1 \cup T_2 \cup T_3$ . Likewise for,

$$\begin{aligned} T_5 &= 0 \circ T_4 \cup 1 \circ T_4 \\ &= 0 \circ T_4 \cup 10 \circ T_3 \cup 110 \circ T_2 \end{aligned}$$

Assuming that  $n = 3k$  is true, then it is shown that for  $n = 3k + 1$  is also true,

$$\begin{aligned}
 T_{3k+1} &= 0 \circ T_{3k} \cup 10 \circ T_{3k-1} \cup 110 \circ T_{3k-2} \\
 0 \circ T_{3k} &= 0 \circ \underbrace{\underbrace{\{000 \dots 000, \dots, 110 \dots 110\}}_{k}}_{T_\alpha} \\
 10 \circ T_{3k-1} &= 1 \circ \underbrace{\underbrace{\{000 \dots 000 \circ 000, \dots, 110 \dots 110 \circ 011\}}_{k-1}}_{T_\beta} \\
 110 \circ T_{3k-2} &= 1 \circ \underbrace{\underbrace{\{000 \dots 000 \circ 110, \dots, 110 \dots 110 \circ 101\}}_{k-1}}_{T_\gamma}
 \end{aligned}$$

It can be seen that if  $\forall t \in T_\beta$ , then  $t \in T_\alpha$ ; and if  $\forall t \in T_\gamma$ , then  $t \in T_\alpha$ . It is easily seen that  $T_\alpha = T_{3k}$ .

To conduct observations of recurrence relation 73.4, needs to be defined as follows:

If  $X \in T$  and  $X = x_1, x_2, \dots, x_n$  then,

$X^p = X_1, X_2, \dots, X_p$  and  $X_q = x_1, x_2, \dots, x_q$ , where  $p, q, n$  positif integer and  $q < n$ .

Furthermore, the results of observations against recurrence relation 73.4 have some properties as follows:

- i. Lemma: The first string generated by the recurrence relation is  $First(T_n) = (0)^n$
- ii. Lemma: The last string generated by the recurrence relation is  $Last(T_n) = (110)^{(n \div 3)} (110)_{(n \bmod 3)}$
- iii. Theorem: Recurrence relation is exhaustive (no repetition and no one is missing).

**Proof** Lemma: The first string generated by the recurrence relation is  $First(T_n) = (0)^n$ . Proofing Lemma using mathematical induction techniques. It is clear that lemma is worth right for  $n = 1$ , where  $T_1 = 0^1 = 0$ . If it is assumed that lemma is worth right for  $n = k$ , then is proofed that lemma is also true for  $n = k + 1$ . If  $n = k$  true, then  $First(T_{k+1}) = 0^{k+1} = 0^k + 0^1 = \underbrace{000 \dots 0}_k \circ \underbrace{0}_1$ .

Plain to see that the first string with length  $(3k + 1)$  is formed from the string connate operating between string with length  $3k$  and  $0$ .

**Proof** Lemma: The last string is generated by the recurrence relation is  $Last(T_n) = (110)^{(n \div 3)} (110)_{(n \bmod 3)}$ . Proofing Lemma using mathematical induction techniques. It is clear that lemma is worth right for  $n \leq 3$ . If it is assumed that lemma is worth right for  $n = 3k$ , then proofed that lemma is also true for  $n = 3k + 1$ .

If  $n = 3k$  true, then

$$\begin{aligned}
 Last(T_{3k+1}) &= (110)^{(3k+1)div3} (110)_{(3k+1)mod3} \\
 &= (110)^k (110)_1 \\
 &= \underbrace{110}_1 \circ \underbrace{110}_2 \dots \underbrace{110}_k \circ 1 \\
 &= \underbrace{110}_1 \circ \underbrace{110}_2 \dots \underbrace{110}_k \circ \underbrace{1}_1 \\
 &\qquad\qquad\qquad \underbrace{\hspace{10em}}_{3k}
 \end{aligned}$$

Certainly looks that last string with length  $(3k + 1)$  was formed from the operation connate between string with length  $3k$  and string  $1$ , i.e.  $(110)^k (110)_1$ .

**Proof Theorem:** Recurrence relation is exhaustive (no repetition and no one is missing). Note again the relation recurrence 73.2. For  $n \leq 3$  it is clear that the existing string is always different and complete. It is known that  $T_{3n} = 0T_{3n-1} \cup 10T_{3n-2} \cup 110T_{3n-3}$ . It is clear that every string that is in  $T_{3n-1}$ ,  $T_{3n-2}$ ,  $T_{3n-3}$  no repetition and no string is missing. Thus to prove that  $T_{3n}$  is the new set of strings that form has a different string and no missing, have to proof 2 interfaces, namely:

- i.  $0 \circ Last(T_{3n-1})$  and  $10 \circ First(T_{3n-2})$
- ii.  $10 \circ Last(T_{3n-2})$  and  $110 \circ First(T_{3n-3})$

The discussion started from the first interface,  $0 \circ Last(T_{3n-1})$  and  $10 \circ First(T_{3n-2})$ . Suppose  $\alpha_1 = 0 \circ Last(T_{3n-1})$  and  $\alpha_2 = 10 \circ First(T_{3n-2})$ . Note that,

$$\begin{aligned}
 \alpha_1 &= 0 \circ Last(T_{3n-1}) \\
 &= \underbrace{0}_{\alpha_{11}} \circ \underbrace{110\dots110}_{\alpha_{12}} \circ 11
 \end{aligned} \tag{73.5}$$

and,

$$\begin{aligned}
 \alpha_2 &= 10 \circ First(T_{3n-2}) \\
 &= 10 \circ \underbrace{0\dots0}_{\alpha_{21}} = 1 \circ \underbrace{0\dots0}_{\alpha_{21}} = \underbrace{1}_{\alpha_{21}} \circ \underbrace{0\dots0}_{\alpha_{22}}
 \end{aligned} \tag{73.6}$$

From Eqs. 73.5 and 73.6 can be seen that,

$$\alpha_{12} \neq \alpha_{22} \text{ and } \alpha_{11} \neq \alpha_{21}$$

Then it can be ascertained

$$\alpha_1 \neq \alpha_2$$

Further discussion for the second interface, i.e.  $10^\circ Last(T_{3n-2})$  and  $110^\circ First(T_{3n-3})$ . Suppose  $\beta_1 = 10^\circ Last(T_{3n-2})$  and  $\beta_2 = 110^\circ First(T_{3n-3})$ .

$$\begin{aligned}
 \beta_1 &= 10 \circ Last(T_{3n-2}) \\
 &= 1 \circ 0 \circ \underbrace{110 \dots 110 \circ 1}_{3n-2} \\
 &= \underbrace{1}_{\beta_{11}} \circ 0 \circ \underbrace{110 \dots 110 \circ 1}_{\beta_{12}}
 \end{aligned}
 \tag{73.7}$$

and

$$\begin{aligned}
 \beta_2 &= 110 \circ First(T_{3n-3}) \\
 &= 110 \circ \underbrace{0 \dots 0}_{3n-3} \\
 &= \underbrace{1}_{\beta_{21}} \circ \underbrace{1 \circ 0 \circ 0 \dots 0}_{\beta_{22}}
 \end{aligned}
 \tag{73.8}$$

From Eqs. 73.7 and 73.8 can be seen that,  $\beta_{12} \neq \beta_{22}$  and  $\beta_{11} \neq \beta_{21}$ . Then it can be ascertained  $\beta_1 \neq \beta_2$ . So it can be proofed that the recurrence relation is exhaustive (no repetition and no one is missing).

### 73.4 Conclusions

Some conclusions and suggestions that can be drawn from this research are as follows. On the enumeration aspect, the research successfully demonstrates the relationship between the Tribonacci numbers  $n$ th and the number of strings with strings length  $n$ , which can be formulated in the form of recurrence relation 73.1

On the generation aspect, research form recurrence relation to produce Tribonacci strings with string length  $n$ , where  $n \geq 1$ , which can be formulated in the form of recurrence relation 73.4. This aspect also successfully introduce two lemmas dan 1 theorem associated with Tribonacci strings,

This research can continued by developing recurrence relation for the establishment of Gray code for Tribonacci strings, and observing the properties of the Gray code. So the overall research can contribute to the field of coding theory.

### References

1. Baril, J.L., Vincent, V.: Minimal change list for lucas strings and some graph theoretic consequences. *Theor. Comput. Sci.* **346**, 189–199 (2005)
2. Cong, B., Zheng, S.Q., Sharma, S.: On simulation of linear arrays, rings and 2-D meshes on fibonacci cube networks. *IEEE*. 1063-7133/93, 748–751 (1993)

3. Ernastuti, Belawati, W.H.: Hamiltonicity on Interconnection Network: Extended Lucas Cube. *Proceeding of the International Conference on Soft Computing, Intelligent System, and Information Technology*, 368–371 (2007)
4. Ernastuti, Juarna, A.: On a New Family of Fibonacci Like Cubes: Extended Lucas Cube. *Proc. Int. Conf. on Graph Theory and Information Security* (2007)
5. Ernastuti, Vincent.V., Embedding of Linear Array, Rings, and 2-d Meshes on Extended Lucas Cube. *Proceeding of the International Conference on Soft Computing, Intelligent System, and Information Technology*, 368–371, (2007)
6. Mikawa, K.: Combinatorial Fibonacci Strings Constructed By Reversing Sublists. *Doctoral Thesis, Ibaraki University* (2001)
7. Juarna, A., Vajnovszki, V.: Fast Generation of Fibonacci Permutations. *CDMTCS, Research report, Auckland* (2004)
8. Juarna, A., Vajnovszki, V., Isomorphism between classes counted by Fibonacci numbers. In *Proceeding of the 5th International Conference on Word, Université du Québec à Montréal* (2005)
9. Vincent, V.: A loopless generation of bitstring without  $p$  consecutive ones. In: *Proceeding of the 3rd Discrete Mathematics and Theoretical Computer Science*, 227–239 (2001)
10. Dumitriu, I.: On generalized tribonacci sequences and additive partitions. *Discrete Math.*, Ed. **219**, 65–83 (2000)
11. Natividad, L.R., Paola, B.P.: A novel formula in solving tribonacci-like sequence. *Gen. Math. Notes* **17**(1), 82–87 (2013)
12. Irmak, N., Murap, A.: Tribonacci numbers with indices in arithmetic progression and their sums. *Miskolc Math. Notes* **14**(1), 125–133 (2013)
13. Choi, E.: Modular tribonacci numbers by matrix method. *J. Korean Soc. Math. Educ. Ser. B Pure Appl. Math.* **20**(3), 207–221 (2013)
14. Wu, J.: Extended fibonacci cubes. *IEEE Trans. Parallel Distrib. Syst.* **8**, 1203–1210 (1997)
15. Robbins, N.: On tribonacci numbers and 3-regular compositions. *Fibonacci Quart* **52**(1), 16–19 (2014)
16. Wu, Z., Jianghua, L., Han, Z.: On the smarandache-pascal derived sequences of generalized tribonacci numbers. *Adv. Differ. Equ.*, 284–292 (2013)

# Chapter 74

## A Leukocyte Detection System Using Scale Invariant Feature Transform Method

Lina and Budi Dharmawan

**Abstract** This paper describes an automatic detection and recognition system of leukocytes on a given microscopic image. The developed system detects the locations of leukocytes from a blood cell image. After the automatic detection, the system classifies each leukocyte in one of the five categories (neutrophils, eosinophils, basophils, lymphocytes, and monocytes). The system processes an input image with the Scale Invariant Feature Transform (SIFT) algorithm for leukocyte detection. Meanwhile, two different recognition methods, i.e. the Euclidean distance and the Co-occurrence matrix methods are applied for automatic recognition. The combination of detection and recognition approaches provide the optimal recognition accuracies for almost all leukocyte types.

**Keywords** Leukocyte detection · Leukocyte recognition · Microscopic image · Scale invariant feature transform

### 74.1 Introduction

Blood is a bodily fluid that delivers nutrients and oxygen to cells. The analysis of blood cells can be used to detect blood disorder or to determine the presence of infectious diseases in human body. In order to identify the hematopoietic system disorders, hematologists need to perform the blood cells identification and counting for every blood elements, such as the erythrocytes (red cells), leukocytes (white cells), and platelets [1]. Since the task is very tedious and really time consuming, an automatic blood detection and recognition system is really helpful.

Several researchers have proposed various methods to detect and recognize the blood cells, such as the Support Vector Machine method [2] and EM algorithm [3].

---

Lina (✉) · B. Dharmawan  
Faculty of Information Technology, Tarumanagara University, Jl. Letjen S. Parman no. 1,  
Jakarta 11440, Indonesia  
e-mail: lina@untar.ac.id



However, the recognition systems have not been tested for blood cells that were influenced by rotation or illumination effects after the segmentation process.

In this paper, an automatic leukocyte detection system that can detect the white blood cell locations from microscopic images is developed. The proposed system works based on the Scale Invariant Feature Transform (SIFT) method. First, the system detects the white blood cells locations using the SIFT method, then the system crops the images which contains the region of interest. After the automatic detection and cropping, the system will recognize the leukocyte type using two different recognition methods: (1) the distance based recognition system using the Euclidean distance method, and (2) the color based recognition system using the co-occurrence matrix method.

The remainder of this paper is organized as follows. In Sect. 74.2, the proposed leukocyte detection system based on SIFT algorithm is explained. Section 74.3 presents the leukocyte recognition system, while Sect. 74.4 describes the experimental setup and results. Finally, the conclusion is presented in Sect. 74.5.

## 74.2 Leukocyte Detection System

In the proposed system, the Scale Invariant Feature Transform (SIFT) method is applied to detect the leukocytes from the captured microscopic images. The SIFT algorithm, developed by Lowe [4] is an algorithm for image features generation which are invariant to image translation, scaling, rotation and partially invariant to illumination changes and affine projection. The steps for defining the SIFT image features are as follows: (1) Scale space construction, (2) Keypoint localization, (3) Orientation assignment, (4) Keypoint descriptor.

First, the system creates a scale space from the input images by calculating the Difference of Gaussian (DoG) using the Gaussian kernel. This step is necessary as an input image may consist unnecessary details for detection or recognition processes. Therefore it is important to identify locations and scales that contain only the region of interest from an image. The first step for detecting locations that are invariant to scale changes is by constructing a continuous function of scale, known as the scale space. The scale space of an image is defined as a function,  $L(x, y, \sigma) = G(x, y, \sigma) * I(x, y)$ , that is produced from the convolution of a variable-scale Gaussian  $G(x, y, \sigma)$ , with an input image  $I(x, y)$ .

To build the DoG pyramid, the input image is convolved iteratively with the Gaussian kernel. The last convolved image is down-sampled in each image direction by factor of 2, and the convolving process is repeated [4]. Each collection of images of the same size are then build together the so-called Gaussian pyramid, which is represented by a 3D function. The DoG pyramid is computed from the difference of each two nearby images in Gaussian pyramid.

The next step is to define keypoints. Keypoints are pixels from an image which have constant values for scaling, rotation, blurring, and illumination changes. Keypoint construction is done by finding the local extrema (maxima or minima) of

DoG function. The local extrema are detected by comparing each pixel with its neighbors in the scale space. If the pixel value is higher or lower than the maxima or minima, then the pixel becomes the candidate for being a keypoint. The DoG function will have a strong response along edges, even if the location along the edge is poorly determined and therefore unstable to small amounts of noise.

Further, keypoints are important to be localized. In keypoint localization, a threshold cutting is applied on simple contrast value for each keypoint. The low contrast feature points are generally less reliable than high contrast feature points. The keypoints are selected only if they are larger than all of these neighbors or smaller than all of them. To improve the stability of matching, the points that have low contrast or are poorly localized along an edge are rejected.

After the thresholding step, the system performs the corner detection process. Harris corner detection algorithm is realized by calculating each pixel's gradient [5]. If the absolute gradient values in two directions are both great, then judge the pixel as a corner. Once the SIFT feature location is determined, a main orientation is assigned to each feature based on local image gradients. For each pixel of the region around the feature location the gradient magnitude and orientation are computed using  $m(x,y)$  and  $\theta(x,y)$  [6].

Finally, the region around a keypoint is divided into  $4 \times 4$  boxes. The gradient magnitudes and orientations within each box are computed and weighted by appropriate Gaussian window, and the coordinate of each pixel and its gradient orientation are rotated relative to the keypoints orientation. Then, for each box an 8 bins orientation histogram is established. From the 16 obtained orientation histograms, a 128 dimensional vector (SIFT-descriptor) is built.

### 74.3 Leukocyte Recognition System

For the recognition system, two methods are applied to the system: (1) the distance based recognition system using the Euclidean distance method, and (2) the color based recognition system using the co-occurrence matrix method. In the Euclidean distance based recognition system, the dissimilarities between the testing and training feature vectors are calculated [7]. Meanwhile, in the color based recognition system using the co-occurrence matrix method, the co-occurrence matrix is constructed by clustering the gray-scale values of an image. Such matrix is derived from the angular relationship between the neighboring pixels as well as the distances between them. The higher the color intensity of an image, the larger size of co-occurrence matrix can be obtained. First, the probability value  $p(i,j)$  of the color frequency  $f(i,j)$  of index pair  $i$  and  $j$  is calculated. Then, the Haralick features are obtained by processing the probability values of the co-occurrence matrix. Five characteristic features are processed in the proposed system, i.e. entropy, contrast, homogeneity, energy, and correlation [7].

### 74.4 Experiments

This section describes the experiments conducted for the proposed leukocyte detection and recognition system using the Scale Invariant Feature Transform method. We developed our own database, called the FTI-Untar blood cells database, which consists of a total of 183 blood cell images with 112 neutrophils images, 37 lymphocytes images, 21 monocytes images, 10 eosinophils images, and 3 basophils images. The images were taken using a digital camera with  $1600 \times 1200$  pixels that was attached to a microscope. Figure 74.1 shows the samples of blood cell images used in the experiments.

First, we evaluated the performance of the SIFT method for detecting the leukocytes as shown in Table 74.1. Next, we tested the system with various lighting conditions. The natural lighting means the condition where images were taken with microscope standard lighting, while darken and brighten effects were done by

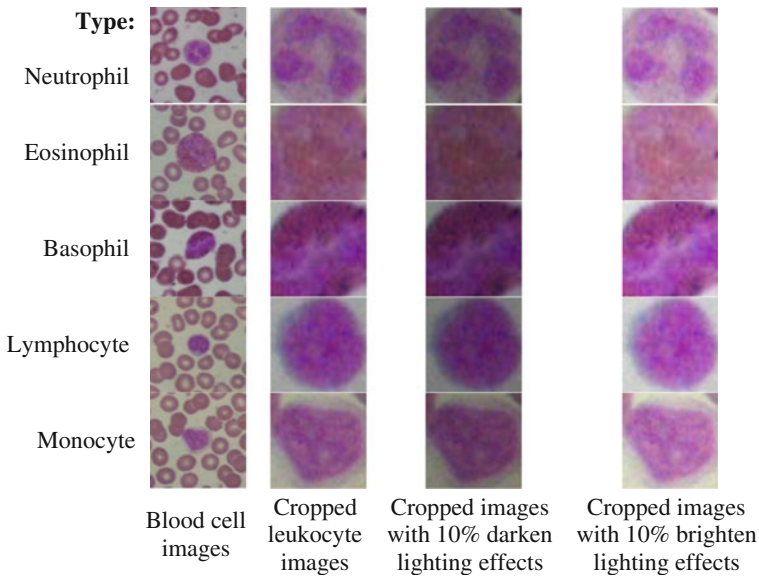


**Fig. 74.1** The image samples of white blood cells used in the experiments

**Table 74.1** The detection results using SIFT method

Blood cell type	$\Sigma$ data	$\Sigma$ training	$\Sigma$ testing	Accuracy (%)
Neutrophil	112	67	45	86.67
Eosinophil	10	6	4	100
Basophil	3	2	1	100
Lymphocyte	37	22	15	86.67
Monocyte	21	12	9	100

**Table 74.2** The detection results using SIFT method for darken lighting effects

Blood cell type	$\Sigma$ data	$\Sigma$ training	$\Sigma$ testing	Accuracy (%)	
				For darken effects	For brighten effects
Neutrophil	112	86.67	82.22	80	75.56
Eosinophil	10	100	100	75	75
Basophil	3	100	100	100	100
Lymphocyte	37	86.67	86.67	80	86.67
Monocyte	21	100	100	88.89	88.89

adjusting the contrast of the natural lighting images using a picture editing software. As shown in Table 74.2, the detection accuracies for images with brighten lighting effects were lower than that of the natural lighting and the darken effects.

We also tested various threshold values for keypoint localizations in SIFT method. Table 74.3 shows the detection results using SIFT method with three different threshold values: 0.02, 0.03, and 0.05. It is clearly seen that the detection accuracies using  $\theta = 0.03$  gave the highest results compared to the other thresholds. Finally, we conducted experiments to recognize leukocyte types from images which have fixed window sizes, both for training and testing images, i.e.  $47 \times 47$  pixels and  $57 \times 57$  pixels. These dimensions were the average size of leukocyte cells that were captured from the microscopic images. We applied two recognition methods for the leukocyte recognition system: (1) the Euclidean Distance method and (2) the Co-occurrence Matrix method. Table 74.4 shows the overall recognition accuracies

**Table 74.3** The detection results using SIFT method with various threshold values for keypoint localization

Type	$\Sigma$ data	$\Sigma$ training	$\Sigma$ testing	Accuracy (%)		
				$\theta = 0.02$	$\theta = 0.03$	$\theta = 0.05$
Neutrophil	112	67	45	77.78	86.67	93.33
Eosinophil	10	6	4	50	100	75
Basophil	3	2	1	0	100	100
Lymphocyte	37	22	15	66.67	93.33	93.33
Monocyte	21	12	9	88.89	100	100

**Table 74.4** The recognition results for leukocyte images with various cropping sizes

Type	$\Sigma$ training	$\Sigma$ testing	Accuracy (%)			
			Image size $47 \times 47$ pixels		Image size $57 \times 57$ pixels	
			Euclidean distance	Co-occurrence matrix	Euclidean distance	Co-occurrence matrix
Neutrophil	213	53	90.62	73.58	96.88	90.56
Eosinophil	100	22	83.33	63.63	77.78	59.09
Basophil	74	20	40	55	50	30
Lymphocyte	10	3	100	66.67	100	100
Monocyte	3	2	100	50	100	100

for images with  $47 \times 47$  pixels and  $57 \times 57$  pixels sizes with the Euclidean Distance method were 82.79 and 84.93 %, respectively. Meanwhile, the overall recognition accuracy for leukocyte recognition system using the Co-occurrence Matrix method was 75.93 % for images with  $47 \times 47$  pixels and 61.78 % for images with  $57 \times 57$  pixels sizes. In general, for both recognition methods, it is clearly seen that Basophil was the most difficult leukocyte type to find and to recognize.

## 74.5 Conclusion

We have presented the Scale Invariant Feature Transform method to automatically detect leukocyte areas and recognize the leukocyte types from microscopic images. The detection results of the leukocyte images using SIFT method are highly dependent on the threshold value of keypoint localization. Other parameters such as lighting condition and window size also give significant effects on the accuracy of the system. For the recognition system, the Euclidean Distance method gives a slightly better result than color based recognition, i.e. the Co-occurrence Matrix method.

In the future, we consider to develop a dynamic window model for detecting the leukocyte area, the use of other color domains, i.e. Hue, Saturation, and Value (HSV) for improving the system's accuracy.

## References

1. Lina, A.C., Mulyawan, B.: Focused color intersection for leukocyte detection and recognition system. *Int. J. Inf. Electron. Eng.* **3**(5), 498–501 (2013)
2. Markiewicz, T.: Data mining techniques for feature selection in blood cell recognition. In: *Proceedings of European Symposium on Artificial Neural Networks*, pp. 407–412 (2006)
3. Colunga, M.C., Siordia, O.S., Maybank, S.J.: Leukocyte recognition using EM-algorithm. In: *Proceedings of 8th Mexican International Conference on Artificial Intelligence*, pp. 545–555 (2009)
4. Lowe, D.G.: Distinctive image features from scale-invariant key-points. *Int. J. Comput. Vis.* **60**(2), 91–110 (2004)
5. Harris, C., Stephens, M.: A combined corner and edge detector. In: *Proceedings of the 4th Alvey Vision Conference*, pp. 147–151 (1988)
6. Chen, J., Zou, L.H., Dou, L.H.: The comparison and application of corner detection algorithms. *J. Multimedia* **4**(6), 435–441 (2009)
7. Lina, A.C., Mulyawan, B.: A combination of feature selection and co-occurrence matrix methods for leukocyte recognition system. *J. Softw. Eng. Appl.* **5**(12B), 101–106 (2012)

# Chapter 75

## The Diameter of Enhanced Extended Fibonacci Cube Interconnection Networks

Ernastuti, Mufid Nilmada and Ravi Salim

**Abstract** In this paper, we study a new cube interconnection network topology which is called *Enhanced Extended Fibonacci Cube (EEFC)*. This cube is the result of enhancing the Extended Fibonacci cube (*EFC*) where extra connections are included, linking different cube vertices, which originally form idle links left at each vertex. We construct the formulation of *EEFC* based on the extended Fibonacci cube in which any two vertices in *EEFC* are connected by an edge with the same way of the enhanced hypercube. One of the important parameters to measure the computational speed performance in a network is the diameter. The diameter of *EFC*( $n$ ) is  $n - 2$ . In this paper the size of the diameter of *EEFC* will be searched. To obtain the diameter in *EEFC* first of all should be proved that *EEFC* is a connected graph and forms an induced subgraph of the Enhanced Hypercube. Based on the analysis of the properties and the performance of *EEFC*, it has been proved that the *EEFC*( $n$ ) is a connected and an induced subgraph of the enhanced Hypercube, and the diameter of *EEFC*( $n$ ) is  $n - 3$ . The diameter of *EEFC* is decidedly smaller than the diameter of *EFC*, this means that the computational speed in *EEFC* is more efficient than in *EFC*.

**Keywords** Diameter · Enhanced hypercube · Extended fibonacci cube · Interconnection network topology

### 75.1 Introduction

Among the fundamental problems in a parallel computational system is the interconnection network design. Interconnection network is meant in order that the processors in the network be able to send messages to each other. The messages are data which are required by other processors in performing computations. Ideally each processor may send messages directly to the target without having to go

---

Ernastuti (✉) · M. Nilmada · R. Salim  
Gunadarma University, Jalan Margonda Raya 100, Depok, Indonesia  
e-mail: ernas@staff.gunadarma.ac.id

through an intermediary processor. In the last several decades, interconnection network is increasingly more important for modern technologies. So, studies of computer interconnection network topology design increases significantly. In the studies, graphs serve as models of the interconnection network topologies. Vertices in a graph represent processor elements while edges represent communication channel in the network. In many system designs such as distributed systems and multiprocessor systems, appropriate network topology selection is very important, since it determines many crucial features and consequently has overwhelming impact on the network's performance. It is crucial to speed of internode communication [1, 2]. The chosen network topology will determine the computer network system's performance ability in executing computational task. Ideally, the chosen topology should be the best possible.

However, comparing abstractly one interconnection network topology with another is a notoriously difficult task [3, 4]. Comparing advantages and/or disadvantages among interconnection network topology is highly relative, because it depends on hardware implementation technology, data flow scheme, computation workload, data/task distribution, and parameters of architecture, system, or other applications. Nowadays researchers are motivated in suggesting new network models or improvements of earlier topologies by showing their advantages, and also suggest performance evaluation in various contexts. Figure 75.1 shows several interconnection network topologies. There are ring, 2D Mesh, star, tree, linear array, tree, hypercube, and fully connected.

Network topologies are compared, by analyzing various parameters, namely for structural properties, among others: degree, diameter, radius, and center; for enumeration properties: numbers of vertices, edges, and cycles; for Hamiltonicity properties: Hamiltonian paths, and Hamiltonian cycles.; for embedding properties: linear arrays, rings, 2D Meshes, trees, and hypercube, etc.; and also for scalability; modularity, regularity, potential bottleneck; fault tolerance; recursive decomposition (Figs. 75.2, 75.3 and 75.4).

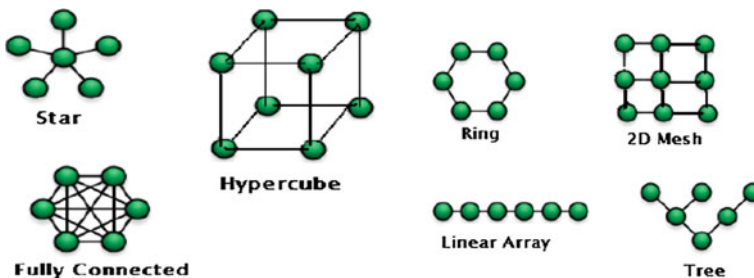


Fig. 75.1 Interconnection network topologies

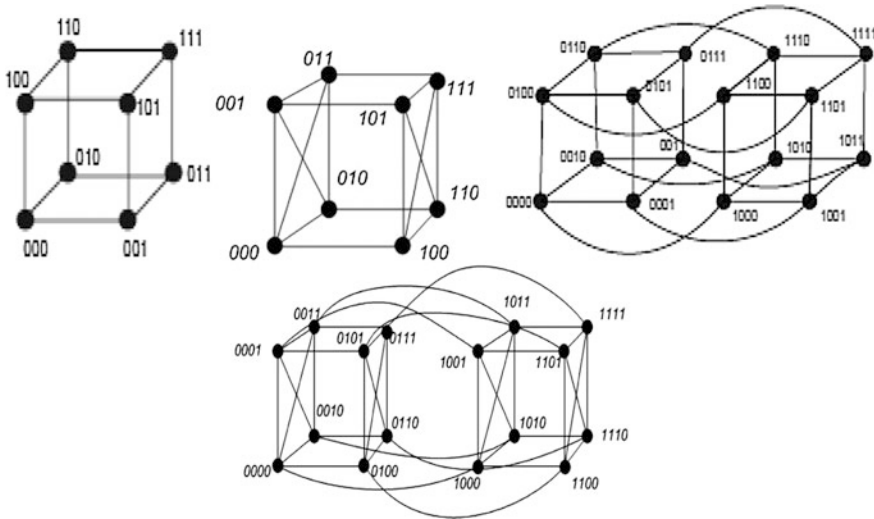


Fig. 75.2 Hypercube  $Q(3)$ ,  $Q(4)$ , and Enhanced Hypercube  $EQ(3)$ ,  $EQ(4)$

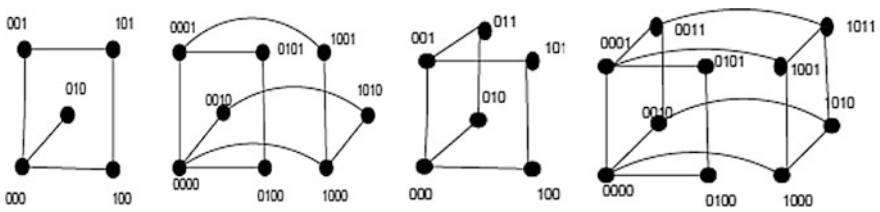


Fig. 75.3  $FC(5)$ ,  $FC(6)$ ,  $EFC(5)$ , and  $EFC(6)$

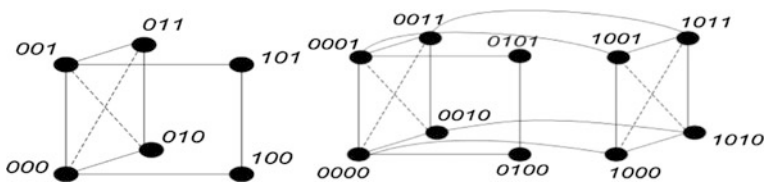


Fig. 75.4  $EEFC(5)$ , and  $EEFC(6)$

Overall, the criteria to say that a network topology being better if it is superior in efficiency, convenience, and extendibility. But on account of the many parameters that can be analyzed, there is no single network capable of handling and optimizing everyparameters at once [4]. Differently speaking, there is no single criterion for comparing network topologies, although no less than two fundamental factors exist, that must be taken into account in designing network topologies. One of them is



that usually ports that are directly connected to every processor elements are limited in number. This is due to the cost which tends to be high whenever elements are directly connected to each other. Thus the degree of each vertex tends to be small. The other one is the communication time among processors which is demanded to be short enough. Thus the diameter of the graph representing it is required to be small enough. Network topologies which have small degrees tend to have big diameters, and vice versa. Thus there should be compromised between degrees representing hardware costs, and diameters representing communication times. Thus, the multiplication of the two numbers can be introduced as a measurement criterion [5].

Common topologies of multiprocessor interconnection in current use for parallel architecture are linear array, ring, mesh, hypercube, and tree. Rich diverse properties of the hypercube networks attracts intensive researches lately. Among them are symmetries of nodes and edges, simple recursive structure, nice Hamiltonicity, and efficient embedding properties into other interconnection networks such as linear array, ring, mesh, and tree. Hence the hypercube can be viewed as ideal topologically. However for a hypercube having  $k$ -dimensions amounts to having  $2^k$  vertices. So the number of processors increases exponentially as it expands. This limits profoundly the system size where it is to be implemented.

Attempts to counterbalance this disadvantage is to consider incomplete hypercubes. Some of them retain most of the desirable properties of the hypercube, for example the Fibonacci Cube (*FC*), Extended Fibonacci Cube (*EFC*), Lucas Cube (*LC*), Extended Lucas Cube (*ELC*), respectively by Wu [6–9]. They are induced subgraphs of the hypercube. Sandi Klavzar grouped them in the family of Fibonacci cubes [10]. They have less than  $2^k$  vertices, but all the diameter of them are the same with the hypercube that is  $k$ .

Hypercube systems frequently leaves some vertices idle, since every vertex is assigned to a predetermined link number in order for the size to be maximum in the configuration. It was Ning Feng Tzeng who had an idea to add extra connections by some of the idle vertices. Thus he introduced the enhanced hypercube. These extra connections can maximize the performance measure at various traffic laden points or links. The diameter of enhanced hypercube become  $k - 1$ . It is significantly improved. So also in mean internode distance, and traffic density. It is more effective in cost minimizing if we compare it to its regular, unenhanced version [11, 12].

In this paper, we study the extended Fibonacci cube (*EFC*) with extra links are included between two vertices through otherwise unused connections left at every vertex. This cube is called *Enhanced Extended Fibonacci Cube (EEFC)*. We construct the formulation of *EEFC* based on the extended Fibonacci cube in which any two vertices in *EEFC* are connected by an edge with the same way of the enhanced hypercube. We will analyze the properties and performance of *EEFC*. The aim of this research is to find the diameter of *EEFC*. To obtain the diameter, we first prove that the *EEFC*( $n$ ) is a connected, and then prove that is an induced subgraph of enhanced Hypercube.

### 75.2 Basic Conception

For a graph  $G = (V, E)$ ,  $V$  denotes the set of its vertices, and  $E$  the set of its edges; an edge is an unordered pair  $xy = \{x, y\}$  of distinct vertices of  $G$ . To avoid ambiguity,  $V$  and  $E$  are denoted by  $V_G$  and  $E_G$ . And we denoted by  $|VG|$  and  $|EG|$  the number of vertices and edges of  $G$  [13].

**Definition 75.1** A path on a graph is a sequence  $(x_1, x_2, \dots, x_n)$  such that  $\{x_1, x_2\}, \{x_2, x_3\}, \dots, \{x_{n-1}, x_n\}$  are edges of the graph and the  $x_i$  are distinct. A closed path  $(x_1, x_2, \dots, x_n, x_1)$  on a graph is called a cycle.

**Definition 75.2** For  $x, y \in V_G$ ,  $d_G(x, y)$  or  $d(x, y)$  denotes the length of a shortest path (a path with the least number of edges) in  $G$  from  $x$  to  $y$ .

Let  $\{0, 1\}^n$  denote the set of length  $n$  binary strings. Thus,  $\{0, 1\}^n = \{x_1, x_2, \dots, x_n | x_i \in \{0,1\}, i = 1,2, \dots, n\}$ , where  $n$  is positive integer.

**Definition 75.3** The Hamming distance between two binary strings  $x, y \in \{0, 1\}^n$  denoted  $H(x, y)$ , is the number of bits where  $x$  and  $y$  differ. For example if  $x = 0010$  and  $y = 1000$ , then  $H(x, y) = 2$ .

**Definition 75.4** Let  $Q(n) = (V_Q(n), E_Q(n))$  is a graph which denote the hypercube of the order  $n$ , then  $V_Q(n) = 0, V_Q(n - 1) \cup 1, V_Q(n - 1)$ , where  $V_Q(1) = \{0,1\}$ . Two vertices  $x, y \in V_Q(n)$  are adjacent in  $Q(n)$  if and only if  $H(x, y) = 1$ .

**Definition 75.5** Let  $EQ(n) = (V_{EQ}(n), E_{EQ}(n))$  is a graph which denote the enhanced hypercube of the order  $n$ , then  $V_{EQ}(n) = 0, V_{EQ}(n - 1) \cup 1, V_{EQ}(n - 1)$ , where  $V_{EQ}(1) = \{0,1\}$ . Two vertices  $x, y \in V_{EQ}(n)$  are adjacent in  $EQ(n)$  if and only if  $H(x, y) = 1$ , or two vertices  $x, y \in V_{EEFC}$  are adjacent in  $EEFC(n)$  if  $x = (x_1, x_2, \dots, x_{n-2}, x_{n-1}, x_n)$  and  $y = (x_1, x_2, \dots, x_{n-2}, \dot{x}_{n-1}, \dot{x}_n)$ , where  $x \neq \dot{x}$ .

The symbol  $\cdot$  denotes a concatenation operation. For example  $01 \cdot \{0,1\} = \{010,011\}$ .

**Definition 75.6** Let  $FC(n) = (V_{FC}(n), E_{FC}(n))$  denote the Fibonacci cube of the order  $n$ , then  $V_{FC}(n) = 0, V_{FC}(n - 1) \cup 10, V_{FC}(n - 2)$ , where  $V_{FC}(3) = \{1,0\}$  and  $V_{FC}(4) = \{01,00,10\}$ . Two vertices in an  $FC(n)$  are connected by an edge in  $E_{FC}(n)$  if and only if their labels differ in exactly one bit position. In other words  $H(x, y) = 1$ . Remark that  $V_{FC}(n) \subseteq \{0, 1\}^n, n \geq 2$ .

**Definition 75.7** Let  $EFC(n) = (V_{EFC}(n), E_{EFC}(n))$  denote the extended Fibonacci cube of the order  $n$ , then  $V_{EFC}(n) = 0, V_{EFC}(n - 1) \cup 10, V_{EFC}(n - 2)$ , where  $V_{EFC}(3) = \{1,0\}$  and  $V_{EFC}(4) = \{01,00,10\}$ . Two vertices in an  $EFC(n)$  are connected by an edge in  $E_{EFC}(n)$  if and only if  $H(x, y) = 1, V_{EFC}(n) \subseteq \{0, 1\}^n, n \geq 2$ .

**Lemma 75.1a** [14] For any  $n \geq 5, V_{EFC}(n) = S_0(n) \cup S_1(n)$ , with  $S_0(n) = 0, S_0(n - 1) \cup 10, S_0(n - 2)$ , and  $S_1(n) = 0, S_1(n - 1) \cup 10, S_1(n - 2)$ . where  $S_0(3) = \{0\}, S_1(3) = \{1\}, S_0(4) = \{00,10\}, S_1(4) = \{01,11\}$ .

**Lemma 75.1b** [14] For every  $n \geq 4, S_0(n) = V_{FC}(n - 1) \cdot 0$  and  $S_1(n) = V_{FC}(n - 1) \cdot 1$ , where  $V_{FC}(n)$  is a set of vertices of  $FC(n)$ .

**Lemma 75.2** [5] *The diameter of  $EFC(n)$  is  $n - 2$ , for  $n \geq 4$ .*

**Definition 75.8** [15] A Fibonacci string is a binary string of length  $n$  with no two consecutive ones. There is  $w$  as follows, if  $n$  is odd then  $w = (10)^{\lfloor (n-6)/2 \rfloor}.1$ , and if  $n$  is even then  $w = (10)^{\lfloor (n-6)/2 \rfloor}$ .

**Definition 75.9**  $H(x, y)$  shows the shortest path between  $x$  and  $y$  in hypercube  $Q(n)$ .

### 75.3 Main Result

Now here we define a new cube interconnection network. This cube is called *Enhanced Extended Fibonacci Cube (EEFC)*. It is created from the extended Fibonacci cube with supplement links are included between two cube vertices through otherwise unused edges left at each vertex. We construct the formulation of *EEFC* based on the extended Fibonacci cube in which the vertices are connected with the same way of the enhanced hypercube.

**Definition 75.10** Let  $EEFC(n) = (V_{EEFC}(n), E_{EEFC}(n))$  denote the enhanced extended Fibonacci cube of the order  $n$ , then  $V_{EEFC}(n) = 0.V_{EEFC}(n - 1) \cup 10.V_{EEFC}(n - 2)$ , where  $V_{EEFC}(3) = \{1,0\}$  and  $V_{EEFC}(4) = \{01,00,10,11\}$ . Two vertices in an  $EEFC(n)$  are connected by an edge in  $E_{EEFC}(n)$  if and only if  $H(x,y) = 1$  or two vertices  $x,y \in V_{EEFC}$  are adjacent in  $EEFC(n)$  if  $x = (x_1, x_2, \dots, x_{n-2}, x_{n-1}, x_n)$  and  $y = (x_1, x_2, \dots, x_{n-2}, \hat{x}_{n-1}, \hat{x}_n)$ , where  $x \neq \hat{x}$ . Remark that  $V_{FC}(n) \subseteq \{0, 1\}^n, n \geq 2$ .

A graph is connected if we can reach any vertex from any other vertex by travelling along the edges. More formally, a graph  $G$  is said to be connected if there is at least one path between every pair of vertices in  $G$ . Otherwise,  $G$  is disconnected [16].

**Lemma 75.3** *For  $n \geq 3$ ,  $EEFC(n)$  contains two disjoint subgraphs that are isomorphic to  $EEFC(n-1)$  and  $EEFC(n-2)$ , respectively.*

*Proof* For  $n \geq 3$ ,  $V_{EEFC}(n)$  denotes the set which labels the vertices in  $EEFC(n)$ ; the interconnection of  $EEFC(n)$  are based on the Hamming distance of these codes.  $L(n)$  be a subgraph induced by  $0.V_{EEFC}(n - 1)$  and  $M(n)$  be a subgraph induced by  $10.V_{EEFC}(n - 2)$ . Clearly, both  $L(n)$  and  $M(n)$  are subgraphs of  $EEFC(n)$  which their vertices have labeled binary strings of length  $(n - 2)$  respectively. By Definition 75.8,  $V_{EEFC}(n) = 0.V_{EEFC}(n - 1) \cup 10.V_{EEFC}(n - 2)$ , where  $V_{EEFC}(n - 1)$  is a vertices set of  $EEFC(n - 1)$ , and where  $V_{EEFC}(n - 2)$  is a vertices set of  $EEFC(n - 2)$ , then clearly each vertex in  $V_{EEFC}(n - 1)$  has a labeled binary string of length  $(n - 3)$  and each vertex in  $V_{EEFC}(n - 2)$  has a labeled binary string of length  $(n - 4)$ . So,  $(s,t) \in EEFC(n - 1)$  if and only if  $(s,t) \in L(n)$ , because both  $s$  and  $t$  have the same prefix of "0" in the order  $(n - 2)$  codes which does not affect their Hamming distance. Thus,  $L(n)$  is isomorphic to  $EEFC(n - 1)$ . Similarly,  $M(n)$  is isomorphic to  $EEFC(n - 2)$ . Thus, because of each  $i \in 0.V_{EEFC}(n - 1)$  and  $j \in 10.V_{EEFC}(n - 2)$  affect  $i < j$  is viewed as integer number in binary representation, then  $L(n) \cap M(n) = \{ \}$ .

**Lemma 75.4** *EEFC(n) is a connected and an induced subgraph of enhanced hypercube EQ(n-2), n ≥ 3.*

*Proof* Definition 75.9 shows that  $V_{EEFC}(3) = \{1,0\} = V_{EQ}(1)$  and  $V_{EEFC}(4) = \{01,00,10\} = V_{EQ}(2)$ . Thus  $V_{EEFC}(n) = V_{EQ}(n-2)$ , for  $n = 3$  and  $n = 4$ . The following statements prove that  $V_{EEFC}(n) \subset V_{EQ}(n-2)$ , for  $n > 4$ . For  $n > 4$ ,  $V_{EEFC}(n) = 0. V_{EEFC}(n - 1) \cup 10. V_{EEFC}(n - 2)$ , where  $V_{EEFC}(3) = \{1,0\}$  and  $V_{EEFC}(4) = \{01,00,10,11\}$ . According to Lemma 75.3, for  $n \geq 3$ , *EEFC(n)* contains two disjoint subgraphs  $L(n)$  and  $M(n)$  that are isomorphic to *EEFC(n-1)* and *EEFC(n-2)*. We can see that  $V_{EEFC}(n-1) = V_{EEFC}(n-1)$  and  $E_{EEFC}(n-1) \subset E_{EEFC}(n-1)$ . It means if  $x, y \in EFC(n)$ , then  $x, y \in EEFC(n)$ . Due to every pairs(x, y) are connected by an edge in *EFC(n)* if and only if their labels differ exactly in one position, and *EFC(n)* is a connected graph, then *EEFC(n)* is also a connected graph.

Definition 75.5 says that *EQ(3)* has  $V_{EQ}(3) = 0. V_{EQ}(2) \cup 1. V_{EQ}(2) = 0. \{00,01,10,11\} \cup 1.\{00,01,10,11\} = \{000, 001, 010, 011, 100, 101, 110, 111\}$ . Definition 75.8 says if  $n = 5$  then *EEFC(5)* has  $V_{EEFC}(5) = 0. V_{EEFC}(4) \cup 10. V_{EEFC}(3) = \{001,000,010,011,101,100\}$ . So, it can be seen that  $V_{EEFC}(5) \subset V_{EQ}(3)$ .

$V_{EEFC}(n - 1)$  is set of binary strings of length  $(n - 3)$ . Thus  $V_L(n) = 0. V_{EEFC}(n - 1)$  is a set of length  $(n - 2)$  binary strings. Similarly,  $V_{EEFC}(n - 2)$  is set of binary strings of length  $(n - 4)$ . Thus  $V_M(n) = 10. V_{EEFC}(n - 2)$  is also a set of binary strings of length  $(n - 2)$ . Clearly  $V_L(n)$  and  $V_M(n)$  is a subset of  $V_{EQ}(n - 2)$ , respectively. Therefore  $V_{EEFC}(n) \subset V_{EQ}(n - 2)$ , for  $n > 4$ . In other words  $V_{EEFC}(n) \subseteq V_{EQ}(n - 2)$ , for  $n \geq 3$ . Definition 75.5 says that two vertices  $x,y \in V_{EQ}(n)$  are connected by an edge in *EQ(n)* if and only if their labels differ exactly in one position, or if those two vertices are  $x = (x_1, x_2, \dots, x_{n-2}, x_{n-1}, x_n)$  and  $y = (x_1, x_2, \dots, x_{n-2}, \hat{x}_{n-1}, \hat{x}_n)$ , where  $x \neq \hat{x}$ , and also Definition 75.10 says that that two vertices  $x,y \in V_{EEFC}(n)$  are connected by an edge in *EEFC(n)* if and only if their labels differ exactly in one position, or those two vertices are  $x = (x_1, x_2, \dots, x_{n-2}, x_{n-1}, x_n)$  and  $y = (x_1, x_2, \dots, x_{n-2}, \hat{x}_{n-1}, \hat{x}_n)$ , where  $x \neq \hat{x}$ . This obviously means that *EEFC(n)* is a connected and an induced subgraph of enhanced hypercube *EQ(n - 2)*,  $n \geq 3$ .

The diameter of a graph is the maximum eccentricity of any vertex in the graph. That is, it is the greatest distance between any pair of vertices. To obtain the diameter of a graph, we must find the shortest path between any two vertices at beginning. The diameter of the graph is the greatest length of any of these paths. In other words, diameter of a network having  $n$  vertices is defined as the maximum shortest paths between any two vertices in the network.

**Lemma 75.5** *Diameter of EEFC(n) is n - 3, for n ≥ 4*

*Proof* For  $n = 4$ ,  $V_{EEFC}(4) = \{00,10,11,01\}$ . Diameter of *EEFC(4)* = 1. For  $n = 5$ ,  $V_{EEFC}(5) = \{001,000,010,011,101,100\}$ . Diameter of *EEFC(5)* = 2. Thus the lemma is true for  $n = 3, 4$ , and 5.

For  $n \geq 6$ ,  $V_{EEFC}(n) = 0. V_{EEFC}(n - 1) \cup 10. V_{EEFC}(n - 2) = 0.\{0.V_{EEFC}(n - 2) \cup 10.V_{EEFC}(n - 3)\} \cup 10.\{0.V_{EEFC}(n - 3) \cup 10.V_{EEFC}(n - 4)\} = 00.V_{EEFC}(n-2) \cup 010.V_{EEFC}(n - 3) \cup 100.V_{EEFC}(n - 3) \cup 1010. V_{EEFC}(n - 4)$ .

Lemma 75.1 says that For any  $n \geq 5$ ,  $V_{EFC}(n) = S_0(n) \cup S_1(n)$ , with  $S_0(n) = 0.S_0(n-1) \cup 10.S_0(n-2)$ , and  $S_1(n) = 0.S_1(n-1) \cup 10.S_1(n-2)$ , where  $S_0(3) = \{0\}$ ,  $S_1(3) = \{1\}$ ,  $S_0(4) = \{00,10\}$ ,  $S_1(4) = \{01,11\}$ . Therefore,  $00.V_{EEFC}(n-2) \cup 010.V_{EEFC}(n-3) \cup 100.V_{EEFC}(n-3) \cup 1010.V_{EEFC}(n-4) = 00.V_{EEFC}(n-2) \cup 010.\{S_0(n-3) \cup S_1(n-3)\} \cup 100.V_{EEFC}(n-3) \cup 1010.\{S_0(n-4) \cup S_1(n-4)\}$ . Lemma 75.2 says that is  $S_0(n) = V_{FC}(n-1).0$  and  $S_1(n) = V_{FC}(n-1).1$ , for every  $n \geq 4$ , where  $V_{FC}(n)$  is a set of vertices of  $FC(n)$ .

Therefore,  $0.10.\{S_0(n-3) \cup S_1(n-3)\} = 010.\{V_{FC}(n-4).0 \cup V_{FC}(n-4).1\} = 010.V_{FC}(n-4).0 \cup 010.V_{FC}(n-4).1$ , and  $1010.\{S_0(n-4) \cup S_1(n-4)\} = 1010.\{V_{FC}(n-5).0 \cup V_{FC}(n-5).1\} = 1010.V_{FC}(n-5).0 \cup 1010.V_{FC}(n-5).1$

By Definition 75.8, a Fibonacci string is a binary string of length  $n$  with no two consecutive ones. There is  $w$  as follows, if  $n$  is odd then  $w = (10)^{\lfloor (n-6)/2 \rfloor}.1$ , and if  $n$  is even then  $w = (10)^{\lfloor (n-6)/2 \rfloor}$ . Take  $x \in 010.V_{FC}(n-4).0$ ; if  $n$  is odd, for example  $n = 7$ , then  $010.(10)^{\lfloor (n-6)/2 \rfloor}.1.0 = 010.1.0$ . Take  $y \in 1010.V_{FC}(n-5).1$ ; if  $n$  is even, for example  $n = 6$ , then  $1010.(10)^{\lfloor (n-6)/2 \rfloor}.1 = 1010.1$ .

$x$  and  $y$  above are the binary string of length 5, where  $n = 7$ . Definition 75.3 says that is: the *Hamming distance* between two binary strings  $x, y \in \{0, 1\}^n$  denoted  $H(x, y)$ , is the number of bits where  $x$  and  $y$  differ. Thus, for  $n = 7$ , Hamming distance  $H(x, y) = H(01010, 10101) = 5$ .

Definition 75.9 says that  $H(x, y)$  shows the shortest path between  $x$  and  $y$ . In other words the shortest path between  $x$  and  $y$  is a maximum length of shortest path among all vertices in  $EEFC(n)$ . This is as if the maximum length of shortest path among all vertices in  $EEFC(n)$  is  $(n - 2)$ . In fact, there is still one condition of connecting  $x$  and  $y$ , that is, two vertices  $x, y \in V_{EEFC}(n)$  are connected by an edge in  $EEFC(n)$  if those two vertices are  $x = (x_1, x_2, \dots, x_{n-2}, x_{n-1}, x_n)$  and  $y = (x_1, x_2, \dots, x_{n-2}, \hat{x}_{n-1}, \hat{x}_n)$ , where  $x \neq \hat{x}$ . Therefore diameter of  $EEFC(n) = (n - 2) - 1 = n - 3$ , for  $n \geq 4$ .

## 75.4 Conclusion

The analysis of the properties and the performance of  $EEFC$  proves that the  $EEFC$  is a connected graph, and is an induced subgraph of the enhanced Hypercube  $EQ$ . Finally, we succeeded in analyzing that the diameter of  $EEFC(n)$  is  $n - 3$ , for  $n \geq 4$ . The Lemma 75.2 says that the diameter of  $EFC(n)$  is  $n - 2$ , for  $n \geq 4$ . This means  $EEFC$  improves the speed of computation in  $EFC$ . In other words,  $EEFC$  is more efficient than  $EFC$ .

**Acknowledgments** This project is Fundamental Grant of year 2015 which supported by the Ministry of Research and Technology and Higher Education. This project is also supported by the Research Department of Gunadarma University.

## References

1. Hongmei, L.: Cycles in enhanced hypercube networks. In: International Seminar on Future Information Technology and Management Engineering, pp. 560–563 (2008)
2. Hongmei, L.: The structural features of enhanced hypercube networks. In: Fifth International Conference on Natural Computation (2009)
3. Parhami, B.: A unified formulation of honeycomb and diamond networks. *IEEE Trans. Parallel Distrib. Syst.* **12**(1), 74–80 (2001)
4. Wilkinson, B., Allen, M.: *Parallel Programming Techniques and Applications Using Networked Workstations and Parallel Computers*. Prentice Hall, New Jersey (2000)
5. Lee, H.O.: Hyper-star graph: a new interconnection network improving the network cost of the hypercube. In: Proceedings Of EurAsia-ICT (2002)
6. Wu, J.: Extended fibonacci cubes. *IEEE Trans. Parallel Distrib. Syst.* **8**(12), 1203–1210 (1997)
7. Hsu, W.J.: Fibonacci cube—a new interconnection topology. *IEEE Trans. Parallel Distrib. Syst.* **4**(1), 3–12 (1993)
8. Munarini, E.: On the Lucas Cubes. *Fibonacci Q.* **4**(39), 12–21 (2002)
9. Ernastuti, B.H.W, Kerami, D.: Extended Lucas cube: a new Hamiltonian graph. *J. Indonesian Math. Soc.* **14**(1), 25–36 (2008)
10. Klavzar, S.: On median nature and enumerative properties of Fibonacci-like cubes. *Discrete Math.* **299**, 145–153 (2005)
11. Tzeng, N.F.: Enhanced Hypercubes. *IEEE Trans. Comput.* **40**(3), 284–294 (1991)
12. Hongmei, L.: Cycles in conditional faulty enhanced hypercube networks. In: 9th International Conference on Fuzzy Systems and Knowledge Discovery (FSKD), pp. 1358–1361 (2012)
13. Ernastuti, Salim, R.A.: Complexity analysis of data routing algorithms in extended lucas cubes, web based information technologies and distributed systems. *Atlantis Ambient and Pervasive Intelligence. World Scientific Book* **2**, 25–42 (2010)
14. Ernastuti, Salim, R.A.: On enumerative properties of extended lucas cube: a new interconnection network. *Int. J. Comput. Math. Sci.* 292–297, Tokyo, Japan, WASET, (2010)
15. Baril, J.L., Vajnovzki, V.: Minimal change list for Lucas string and some theoretic consequence. *Theoret. Comput. Sci.* **316**, 189–199 (2005)
16. Deo, N.: *Graph theory with application to engineering and computer science*. PHI Learning Pvt. Ltd, New Delhi (2004)

# Chapter 76

## Prototype Design of a Realtime Monitoring System of a Fuel Tank at a Gas Station Using an Android-Based Mobile Application

Riny Sulityowati and Bayu Bhahtra Kurnia Rafik

**Abstract** Currently the fuel tank monitoring systems mostly still use conventional methods, using rulers or measuring sticks. Computers as interface media are needed to make the monitoring process easy. This research aims at facilitating the monitoring processes of a fuel tank at the public refueling gas station by implementing an Android-based mobile application. The method employed for data transmission process is wireless communication via Bluetooth and SMS gateway so that the fuel tank can be monitored directly through an application on an Android smart phone. The data of fuel volume in the fuel tank are sent and saved in the database for monitoring. The test results of the whole developed system show a success rate of 98.9 % for data transfer via Bluetooth connection and 93.33 % for data transfer via SMS gateway. Meanwhile, the accuracy rate of the ultrasonic sensor in measuring fuel volume in the tank yields an error percentage of 0–0.4 %.

**Keywords** Monitoring · Android · Fuel tank · Ultrasonic · Bluetooth

### 76.1 Introduction

The manager's jobs in the public refueling gas station, hereinafter shortened as SPBU, among others are to supervise and monitor his men at work to monitor the fuel availability in the fuel tank, and to ensure that the fuel at the SPBU is not running out of supply. These jobs are difficult to carry out simultaneously. The current monitoring systems of fuel tanks level under the ground mostly still use the conventional methods, such as using rulers or measuring sticks.

Smart phone devices such as BlackBerry, Android and iPhone can provide a lot of information for their users. In big cities like Surabaya, a lot of people use

---

R. Sulityowati (✉) · B.B.K. Rafik  
Faculty of Industrial Technology, Department of Electrical Engineering, Institute of Technology Adhi Tama Surabaya, Surabaya, Indonesia  
e-mail: riny.itats@yahoo.com

Android smart phones. This fact give us an idea to create a device that uses an Android application to monitor the fuel volume in the tank, and to help the SPBU managers and operators in doing their job. Moreover, this application can also do the monitoring process in realtime using SMS gateway.

## **76.2 Literature Review**

### **76.2.1 Previous Studies**

Water volume measurement in the container had been designed in the past using an ultrasonic sensor processed by a microcontroller and producing the output in the form of volume scale displayed on an LCD [1]. The existing design of the fuel volume measurement in the service tanks on ships was composed of two parts: one part is attached to the tank and installed with sensors, while the other is in the monitoring center. The part that was installed in the tank consisted of ultrasonic sensors, while the one at the monitoring center consisted of a personal computer connected through a serial communication cable [2, 3]. In addition, many other studies had made the design of the measurement and volume monitoring of the liquid level using ultrasonic sensors. However, the aforementioned literature still used serial communication and needed personal computers to monitor the volume or level in realtime.

### **76.2.2 Introduction to Android**

Android is a Linux-based operating system that is commonly used in smart phones or tablets that are in trend today. Around September 2007, a study reported that Google filed a mobile phone application patent, and later on Google introduced Nexus One, one of GSM smart phones employing Android as operating system. This mobile phone was manufactured by HTC.

### **76.2.3 Ultrasonic Level Sensor US-100**

The level sensor on this project uses US-100 Ultrasonic Sensors. US-100 level sensor is used to measure the distance based on the ultrasonic frequency (Fig. 76.1).

Ultrasonic sensor works on the principle of the sound wave reflection, in which the sensor produces a sound wave and catches it back, with the time difference as the basis of measurement. The time difference between the sound wave emitted and received back is directly proportional to the distance or the height of the object reflecting it. Without any contact, the distance of 2 cm to 4 m can be easily connected to a microcontroller only through one I/O pin.



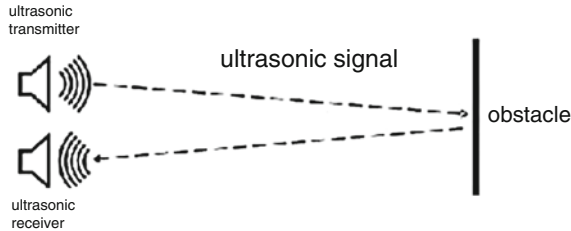


Fig. 76.1 The working principle of ultrasonic sensor [1]

### 76.2.4 Bluetooth Module HC-05

Serial Bluetooth module, hereinafter referred to as just BT module is used to send TTL serial data via Bluetooth. The main purpose of this BT module is to replace serial communication via cable. For example, if the system microcontroller is installed with slave BT module, then it can communicate with other devices such as PCs equipped with BT adapter, mobile devices, smart phones and others. Communication can immediately be carried out after both modules are paired. The connection via Bluetooth is similar to common serial communication, which requires TXD and RXD pins.

### 76.2.5 Liquid Crystal Display (LCD)

To interface between an electronic component and a microcontroller, it is necessary to know the function of each leg on the LCD. Figure 76.2 shows the LCD module with  $2 \times 16$  characters.

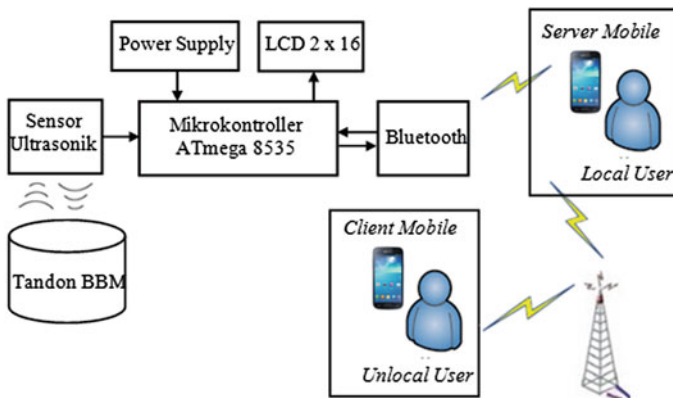


Fig. 76.2 System block diagram

### 76.2.6 ATMEGA 8535 Microcontroller

Microcontroller is an IC (Integrated Circuit) that can be programmed repeatedly, either by writing or erasing it and is normally used for automatic and manual control on electronic devices. ATMEGA 8535 is an AVR type that is equipped with an internal 8 channel ADC with fidelity or accuracy of 10 bits as many as 8 channels. In its operation mode, the ATMEGA 8535 ADC can be configured, both in single-ended and differential inputs. In addition, ATMEGA 8535 ADC has a timing configuration, reference voltage, operation mode, and very flexible noise filter capability, so it can easily be adapted to the needs of the ADC itself.

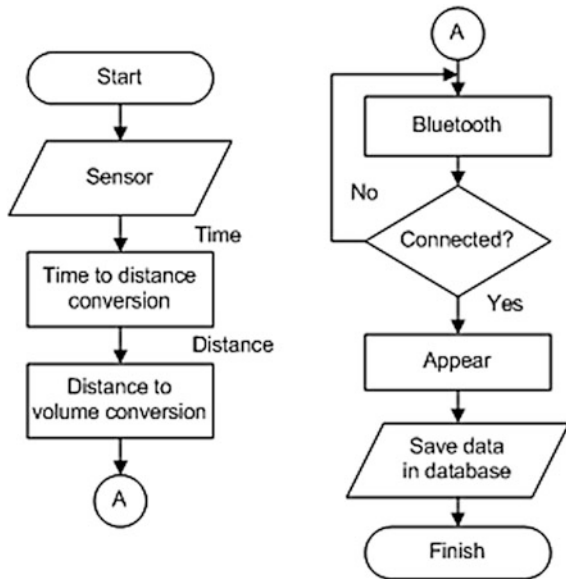
## 76.3 Research Methodology

### 76.3.1 Block Diagram System

The block diagram of a realtime monitoring system for fuel tank at SPBU based on Android Mobile Platform is composed of several electronic devices, namely ultrasonic sensor, microcontroller ATMEGA 8535 minimum system [4], Bluetooth module, power supply, LCD display and Android Smart Phone.

Android applications built on this system can be installed on the servers that are connected directly to a minimum system via Bluetooth and on a client device with SMS gateway that can monitor the data of fuel in the tank as well as store and access the database in real time (Fig. 76.3).

Fig. 76.3 System flowchart



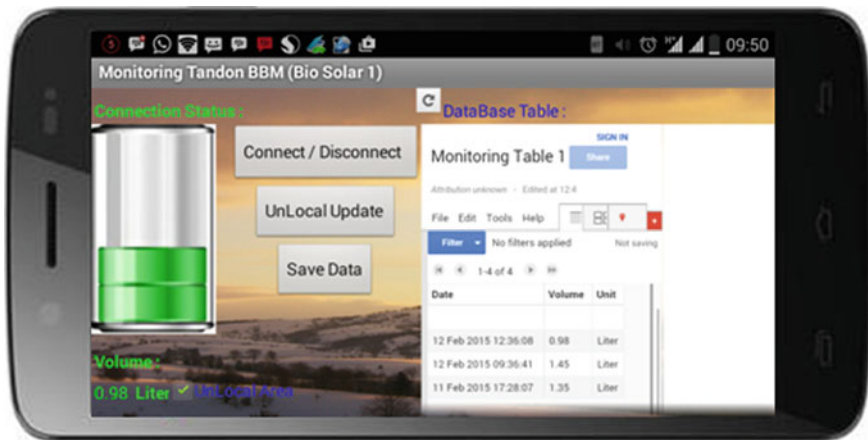


**Fig. 76.4** Main screen display of the developed Android application

### 76.3.2 *Android Smart Phone Application Making*

When developing the Smart Phone Android application, the authors chose to use the IDE APP MIT Inventor 2 software, with Kawa programming language, which is easy develop [5]. The coding method is like playing a puzzle, just drag and drop the required components in the software working window, without having to type the program code manually (Fig. 76.4).

## 76.4 Results and Discussion

### 76.4.1 *Hardware Testing*

Hardware testing was conducted to find out whether or not designed hardware is working or functioning properly as desired. The tests performed on the hardware included several blocks—hardware circuit blocks that had been designed-, and the combination of several circuit blocks. The tests on the entire blocks were conducted to find out whether the entire hardware performs well.

### 76.4.2 *Realtime Monitoring Testing*

Realtime monitoring testing was conducted to find out to what extent the Android-based mobile application that had been developed is able to display the data from the sensor readings in real time and accurately by comparing the actual

**Table 76.1** Data resulting from filling 1 L of fuel with different speeds

Experiment n-times	Filling with speed of 1 L/15 min (litre)	Filling with speed of 1 L/30 min (litre)	Filling with speed of 1 L/45 min (litre)
1	0.99	1.01	1.00
2	0.98	1.00	1.00
3	0.97	0.99	1.01
4	1.02	1.01	1.00
5	1.03	1.00	1.00
Average	0.998	1.002	1.001
Error %	0.2 %	0.19 %	0.04 %

fuel volume that was filled or reduced, being previously measured with a measuring instrument calibrated with the measuring cup.

Table 76.1 above shows the experiment results of filling 1 litre of fuel with three different filling speeds, i.e. 1 L/15 min, 1 L/30 min and 1 L/45 min with five trials for each experiment. The monitoring results were not always exactly the same as the actual volume, and thus yielded an error percentage between 0.2 and 0.4 %. This was due to bubbles or froths while filling the fuel into the tank. Thus, it can be concluded that the effective speed to be used to fill the fuel volume in this system is 1 L/45 min, with the smallest average error of 0.04 %, in order to minimize the possibility of froths/bubbles during fuel filling and reduction in the tank, so that the obtained data produce a higher level of accuracy.

### 76.4.3 Software System Testing

This software testing was done to find out to what extent the developed application that works as expected. The test was performed by experimenting on delivery

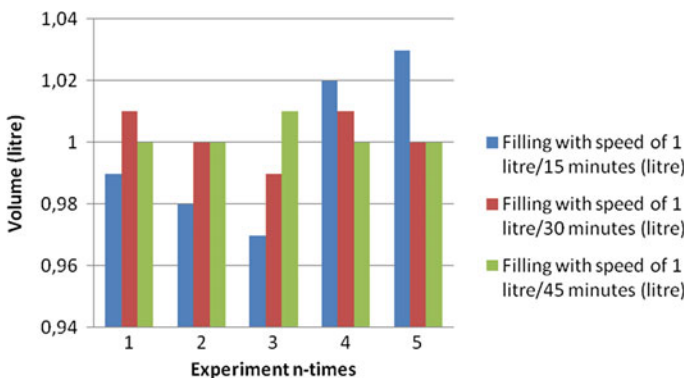


**Fig. 76.5** Comparison chart on fuel filling with 3 different speeds



**Fig. 76.6** Filling monitoring of 1 L via SMS gateway

connectivity of data obtained from the volume measurement of the fuel tank, via Bluetooth communication with some distance variations within the Bluetooth connection local area and also via SMS gateway outside the Bluetooth connection area. In data transmission testing via SMS gateway, when it was outside the Bluetooth connection area, the success rate was 90.0 % in ten trials; one experiment resulted in data pending, but the data were still sent with a time lag of more than 1 min (Figs. 76.5 and 76.6).

## 76.5 Conclusion

Based on the results of the design and testing at the end of the project, it can be concluded:

1. From the results of hardware testing, it can be concluded that the test results of the fuel volume measurement in the tank miniature are not always exactly the same as the actual volume, with the error percentage between 0.4 and 0.6 %. Apart from the sensor accuracy, the error may happen as it gets interference from other waves, and it maybe also due to the rounding-up value of ultrasonic wave travel time or the rounding-up volume in the calculation by the software.
2. After testing on the realtime monitoring, it can be concluded that the effective speed to be used to fill and reduce the fuel volume in this system is 1 L/45 min, with the smallest average error around 0–0.04 %, in order to minimize the possibility of froths/bubbles during the fuel filling and reduction in the tank, so that the obtained data produce a higher level of accuracy.

3. In the data transmission testing via SMS gateway, when it is outside the Bluetooth connection area, the success rate is 90 % for ten trials. One trial pending trial resulted in data pending, but the data were still sent with a time lag of more than 1 min.

## References

1. Gabriel, Y.: Rancang Bangun Alat Ukur Volume Air Dalam Wadah Dengan Sensor Ultrasonik Berbasis Mikrokontroler. Institut Adhi Tama Surabaya (2011)
2. Cole, M.G.: Underground Storage Tank Installation and Management. CRC Press, Washington (1991)
3. Pambudi, N.A.: Rancang Bangun Simulasi Monitoring Volume Bahan Bakar Service Tank pada Kapal Laut. Institut Teknologi Adhi Tama Surabaya (2008)
4. Teguh Arif, G.: Pengendali Pintu Gerbang Menggunakan Bluetooth Berbasis Mikrokontroler ATmega8. Informatika, Bandung (2008)
5. EMS and team: Panduan Cepat Pemrograman Android. PT Elex Media Komputindo kelompok Gramedia, Jakarta (2012)